frontiers | Research Topics

Ferroptosis: intersections, implications, and innovations in programmed cell death

Edited by
Patrice X. Petit, Bilal Çiğ and Juan Carlos Mayo

Published in
Frontiers in Cell and Developmental Biology

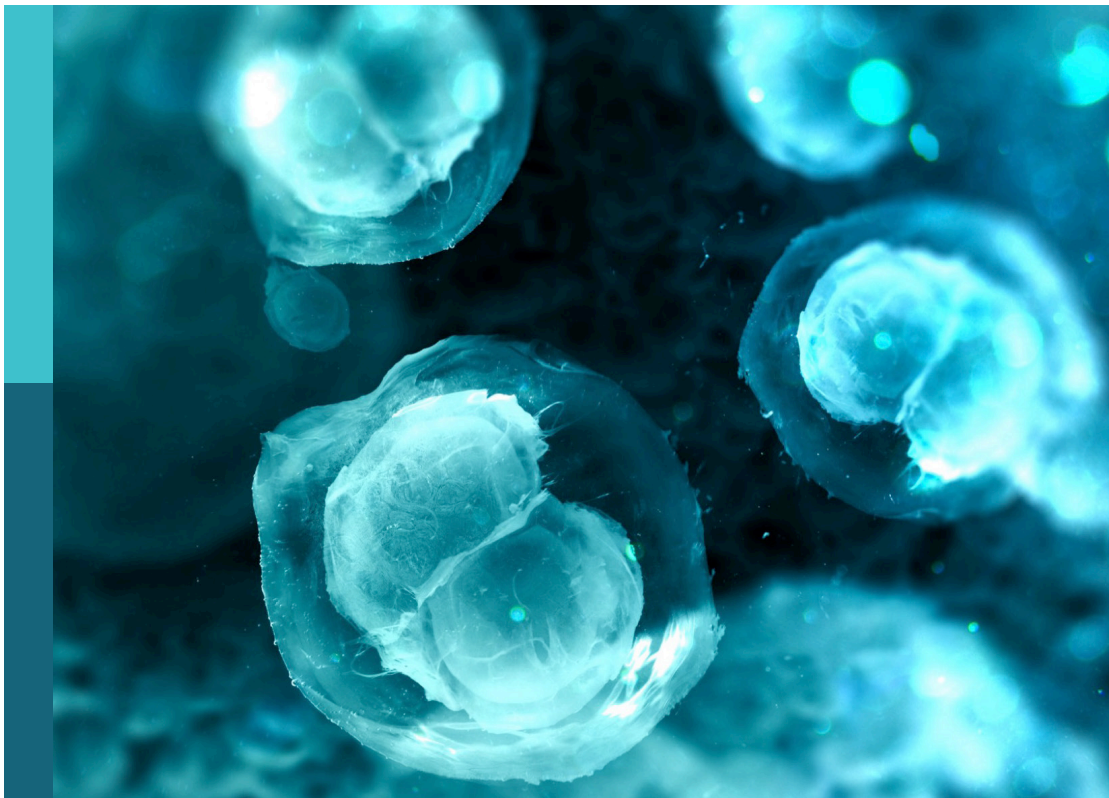

ISSN 1664-8714
ISBN 978-2-8325-6521-6
DOI 10.3389/978-2-8325-6521-6

Generative AI statement
Any alternative text (Alt text) provided alongside figures in the articles in this ebook has been generated by Frontiers with the support of artificial intelligence and reasonable efforts have been made to ensure accuracy, including review by the authors wherever possible. If you identify any issues, please contact us.

About Frontiers

Frontiers is more than just an open access publisher of scholarly articles: it is a pioneering approach to the world of academia, radically improving the way scholarly research is managed. The grand vision of Frontiers is a world where all people have an equal opportunity to seek, share and generate knowledge. Frontiers provides immediate and permanent online open access to all its publications, but this alone is not enough to realize our grand goals.

Frontiers journal series

The Frontiers journal series is a multi-tier and interdisciplinary set of open-access, online journals, promising a paradigm shift from the current review, selection and dissemination processes in academic publishing. All Frontiers journals are driven by researchers for researchers; therefore, they constitute a service to the scholarly community. At the same time, the *Frontiers journal series* operates on a revolutionary invention, the tiered publishing system, initially addressing specific communities of scholars, and gradually climbing up to broader public understanding, thus serving the interests of the lay society, too.

Dedication to quality

Each Frontiers article is a landmark of the highest quality, thanks to genuinely collaborative interactions between authors and review editors, who include some of the world's best academicians. Research must be certified by peers before entering a stream of knowledge that may eventually reach the public - and shape society; therefore, Frontiers only applies the most rigorous and unbiased reviews. Frontiers revolutionizes research publishing by freely delivering the most outstanding research, evaluated with no bias from both the academic and social point of view. By applying the most advanced information technologies, Frontiers is catapulting scholarly publishing into a new generation.

What are Frontiers Research Topics?

Frontiers Research Topics are very popular trademarks of the *Frontiers journals series*: they are collections of at least ten articles, all centered on a particular subject. With their unique mix of varied contributions from Original Research to Review Articles, Frontiers Research Topics unify the most influential researchers, the latest key findings and historical advances in a hot research area.

Find out more on how to host your own Frontiers Research Topic or contribute to one as an author by contacting the Frontiers editorial office: frontiersin.org/about/contact

Ferroptosis: intersections, implications, and innovations in programmed cell death

Topic editors

Patrice X. Petit — Centre National de la Recherche Scientifique (CNRS), France

Bilal Çiğ — Ahi Evran University Medicine Faculty Department of Physiology, Türkiye

Juan Carlos Mayo — University of Oviedo, Spain

Citation

Petit, P. X., Çiğ, B., Mayo, J. C., eds. (2025). *Ferroptosis: intersections, implications, and innovations in programmed cell death*. Lausanne: Frontiers Media SA.

doi: 10.3389/978-2-8325-6521-6

Table of contents

frontiers | Frontiers in Cell and Developmental Biology

TYPE Editorial
PUBLISHED 17 June 2025
DOI 10.3389/fcell.2025.1635046

OPEN ACCESS

EDITED AND REVIEWED BY
You-Wen He,
Duke University, United States

*CORRESPONDENCE
Bilal Cig,
bilal.cig@ahievran.edu.tr

RECEIVED 25 May 2025
ACCEPTED 06 June 2025
PUBLISHED 17 June 2025

CITATION
Cig B, Petit PX and Mayo JC (2025) Editorial: Ferroptosis: intersections, implications, and innovations in programmed cell death. *Front. Cell Dev. Biol.* 13:1635046. doi: 10.3389/fcell.2025.1635046

Editorial: Ferroptosis: intersections, implications, and innovations in programmed cell death

Bilal Cig[1]*, Patrice X. Petit[2] and Juan Carlos Mayo[3,4,5]

[1]Kirsehir Ahi Evran University School of Medicine Physiology Department, Kirsehir, Türkiye, [2]SSPIN Saints-Pères Paris Institut de Neurosciences, CNRS UMR 8003, "Mitochondria, Apoptosis and Autophagy Signalling" Université de Paris—Campus Saint-Germain, Paris, France, [3]Department of Morphology and Cell Biology, School of Medicine, University of Oviedo, Oviedo, Spain, [4]University Institute of Oncology of the Principality of Asturias (IUOPA), Oviedo, Spain, [5]Health Research Institute of the Principality of Asturias (ISPA), Avda. University Hospital, Oviedo, Spain

KEYWORDS

ferroptosis, ROS - reactive oxygen species, lipid perodixation, GSH, GPx4

Editorial on the Research Topic
Ferroptosis: intersections, implications, and innovations in programmed cell death

Ferroptosis is a series of events characterized by lipid peroxidation and disruptions in iron metabolism. Ferroptosis, first described by Dixon and colleagues in 2012 as a distinct form of regulated cell death, is morphologically and biochemically different from apoptosis, necrosis, and autophagy (Scott et al., 2012).

In this process, cell membrane damage occurs via reactive oxygen species (ROS) and lipoxygenases. Mitochondrial shrinkage, increased membrane density, and loss of crista are hallmarks of the morphological changes observed, as well as biochemical markers such as glutathione (GSH) depletion and decreased GPX4 activity. Iron metabolism imbalance leads to high levels of Fe^{2+} levels, which trigger the Fenton reaction and increases ROS production. In turn, ROS accelerate lipid peroxidation, a process driven primarily by the oxidation of polyunsaturated fatty acids (PUFAs) via lipoxygenases, positioning lipid peroxidation as a key driver of ferroptosis. The primary cellular defense mechanism against ferroptosis is the GSH-GPX4 axis, distruption of which sensitizes cells to ferroptotic death (Stockwell et al., 2017). A better understanding of ferroptosis could lead to new therapeutic strategies for the treatment of diseases such as neurodegenerative diseases, metabolic disorders and cancers.

The first article by Sun et al. reported the role of Tumor protein P73 (TAp73P) in regulating both proliferation and ferroptosis in bovine mammary epithelial cells (BMECs). Using RSL3 to inhibit GPX4 and activate ferroptotic pathways, the study shows that TAp73P suppresses cell proliferation and upregulates ferroptosis-related genes such as TFRC and PTGS2, indicating a dual functional role. In the second study, Xiong et al. present a Fe@Ba nanozyme—assembled with baicalein from traditional Chinese medicine—that effectively neutralizes ROS and suppresses ferroptosis in cisplatin-induced acute kidney injury (AKI). The nanozyme inhibits

lipid peroxidation, restores GSH levels, enhances GPX4 expression, and significantly reduces renal damage through its antioxidant capacity. Key ferroptosis-regulating axes include the GSH/GPX4 axis, GCH1/BH4/DHFR axis, and FSP1/CoQ10/NADH axis (Forcina and Dixon, 2019). In the context of non-alcoholic fatty liver disease (NAFLD), ferroptosis is strongly linked with both inflammation and disrupted lipid metabolism. Therapeutic strategies targeting ferroptosis—such as Ferrostatin-1, α-tocopherol, Lip-1, Tβ4, and ginkgolide B—along with lifestyle interventions like exercise and intermittent fasting, have shown anti-inflammatory and hepatoprotective effects (Yang et al., 2020). Li et al. highlight the mechanistic importance of ferroptosis in NAFLD, focusing on its connection to iron dysregulation and lipid peroxidation. Their work demonstrates how exercise activates antioxidant pathways (e.g., NRF2, GPX4, SLC7A11), regulates iron via ferroportin (FPN), and suppresses inflammatory responses via NF-κB and STING signaling, ultimately slowing disease progression.

A review by Zhang et al. comprehensively explores the role of SIRT1, a NAD^+-dependent histone deacetylase, in redox homeostasis, lipid peroxidation, iron metabolism, and inflammation—core biochemical processes of ferroptosis. Through modulation of pathways such as Nrf2-HO-1, p53-p21, and AMPK, SIRT1 suppresses ferroptosis and exhibits protective effects across multiple disease models, positioning it as a next-generation therapeutic target in disorders ranging from neurodegeneration to diabetes. In another review, Lu et al. underscore ferroptosis as a key contributor to osteoarthritis progression, including chondrocyte loss, synovial inflammation, and subchondral bone remodeling. By focusing on biomarkers like GPX4, TfR1, and NCOA4, the review opens the door for ferroptosis-centered diagnostic and therapeutic approaches in osteoarthritis and suggests future studies should examine combinatory therapies with ferroptosis inhibitors and immunomodulators.

A comprehensive bioinformatics and cell-based study by Ma et al. identified SOX13, a transcription factor belonging to the SOX family, as a potential prognostic biomarker and therapeutic target in ferroptosis-based interventions. In thyroid cancer (THCA) cells, SOX13 modulates ferroptosis-related genes and immune cell infiltration, thereby suppressing tumor progression and immune evasion. Li et al. explore the interaction between ferroptosis and immune response in the context of intervertebral disc degeneration (IDD). They identify seven key ferroptosis-related genes, particularly *MT1G* and *CA9*, that hold promise for diagnostic and therapeutic applications in IDD. Mitochondrial lipid peroxidation plays a crucial but not exclusive role in ferroptosis. He Huan and colleagues demonstrate that mitochondrial lipid oxidation is necessary but not sufficient for ferroptosis unless accompanied by cytosolic ROS accumulation, underscoring a dual-compartmental requirement for this death pathway.

Emerging evidence suggests that ferroptosis contributes to the pathophysiology of renal ischemia-reperfusion injury. In a study by Zhou et al., CD44 was found to be overexpressed at the gene and protein level; its blockade with anti-CD44 therapy attenuated ferroptosis and M1 macrophage infiltration, preserving kidney structure and function. A perspective by Wan Seok Yang assigns a pivotal initiating and regulatory role to the endoplasmic reticulum (ER) membrane in ferroptotic death, proposing it as a future organelle-specific therapeutic target. In a review by Su et al., ferroptosis is highlighted as a dual-edged process—enhancing tumor suppression during radiotherapy while also contributing to radiation-induced damage in healthy tissues. The final review by Liu et al. Focuses on heat shock proteins (HSPs), identifying them as bidirectional regulators of ferroptosis through iron metabolism, GSH/GPX4 signaling, and lipid peroxidation, with therapeutic implications in cancer and neurodegenerative diseases.

Together, the studies in this Research Topic provide in-depth insights into the molecular basis of ferroptosis in various pathological contexts. This information is essential for developing next-generation diagnostic tools and targeted therapeutic strategies with high translational value.

Author contributions

BC: Writing – review and editing, Writing – original draft. PP: Writing – review and editing. JM: Writing – review and editing.

Funding

The author(s) declare that no financial support was received for the research and/or publication of this article.

Conflict of interest

The authors declare that the research was conducted in the absence of any commercial or financial relationships that could be construed as a potential conflict of interest.

The author(s) declared that they were an editorial board member of Frontiers, at the time of submission. This had no impact on the peer review process and the final decision.

Generative AI statement

The author(s) declare that no Generative AI was used in the creation of this manuscript.

Publisher's note

References

Forcina, G. C., and Dixon, S. J. (2019). GPX4 at the crossroads of lipid homeostasis and ferroptosis. *Proteomics* 19 (18), e1800311. doi:10.1002/pmic.201800311

Scott, J. D., Lemberg, K. M., Lamprecht, M. R., Skouta, R., Zaitsev, E. M., Gleason, C. E., et al. (2012). Ferroptosis: an iron-dependent form of nonapoptotic cell death. *Cell* 149 (Issue 5), 1060–1072. doi:10.1016/j.cell.2012.03.042

Stockwell, B. R., Friedmann Angeli, J. P., Bayir, H., Bush, A. I., Conrad, M., Dixon, S. J., et al. (2017). Ferroptosis: a regulated cell death nexus linking metabolism, redox biology, and disease. *Cell* 171 (2), 273–285. doi:10.1016/j.cell.2017.09.021

Yang, Y., Chen, J., Gao, Q., Shan, X., Wang, J., and Lv, Z. (2020). Study on the attenuated effect of Ginkgolide B on ferroptosis in high fat diet induced nonalcoholic fatty liver disease. *Toxicology* 445, 152599. doi:10.1016/j.tox.2020.152599

frontiers | Frontiers in Cell and Developmental Biology

REVIEW
published: 11 April 2022
doi: 10.3389/fcell.2022.864635

Heat Shock Proteins and Ferroptosis

Ying Liu[1,2,3,4*†], *Lin Zhou*[1,2,3,4†], *Yunfei Xu*[1,2,3,4], *Kexin Li*[1,2,3,4], *Yao Zhao*[1,2,3,4], *Haoduo Qiao*[1,2,3,4], *Qing Xu*[1,2,3,4] *and Jie Zhao*[1*]

[1]Department of Neurosurgery, Xiangya Hospital, Central South University, Changsha, China, [2]Department of Pathophysiology, Xiangya School of Medicine, Central South University, Changsha, China, [3]Sepsis Translational Medicine Key Lab of Hunan Province, Changsha, China, [4]China-Africa Research Center of Infectious Diseases, Central South University, Changsha, China

Ferroptosis is a new form of regulatory cell death named by Dixon in 2012, which is characterized by the accumulation of lipid peroxides and iron ions. Molecular chaperones are a class of evolutionarily conserved proteins in the cytoplasm. They recognize and bind incompletely folded or assembled proteins to help them fold, transport or prevent their aggregation, but they themselves do not participate in the formation of final products. As the largest number of molecular chaperones, heat shock proteins can be divided into five families: HSP110 (HSPH), HSP90 (HSPC), HSP70 (HSPA), HSP40 (DNAJ) and small heat shock proteins (HSPB). Different heat shock proteins play different roles in promoting or inhibiting ferroptosis in different diseases. It is known that ferroptosis is participated in tumors, nervous system diseases, renal injury and ischemia-reperfusion injury. However, there are few reviews about the relationship of heat shock proteins and ferroptosis. In this study, we systematically summarize the roles of heat shock proteins in the occurrence of ferroptosis, and predict the possible mechanisms of different families of heat shock proteins in the development of ferroptosis.

Keywords: ferroptosis, heat shock proteins, ubiquitin, molecular chaperone, GPx4

OPEN ACCESS

Edited by:
Patrice X. Petit, Centre National de la Recherche Scientifique (CNRS), France

Reviewed by:
Gabriele Multhoff, Technical University of Munich, Germany
Patrick Raymond D'Silva, Indian Institute of Science (IISc), India

***Correspondence:**
Ying Liu
liu1977ying@126.com
Jie Zhao
steelzj@csu.edu.cn

†These authors have contributed equally to this work

Specialty section:
This article was submitted to Cell Death and Survival, a section of the journal Frontiers in Cell and Developmental Biology

Received: *31 January 2022*
Accepted: *23 March 2022*
Published: *11 April 2022*

Citation:
Liu Y, Zhou L, Xu Y, Li K, Zhao Y, Qiao H, Xu Q and Zhao J (2022) Heat Shock Proteins and Ferroptosis. Front. Cell Dev. Biol. 10:864635. doi: 10.3389/fcell.2022.864635

INTRODUCTION

Ferroptosis is an iron-dependent regulatory cell death mode, which is different from apoptosis, necrosis and pyrodeath in morphology, biochemistry and other aspects. Studies have found that ferroptosis is not only related to tumorigenesis, but also involved in the occurrence of a variety of nervous system diseases. What's more, it also plays an important role in many diseases such as ischemia-reperfusion injury.

The ability of cells to respond to external stress is important for homeostasis, and stress of all kinds is particularly harmful for proteins that need to fold to function (Morimoto and Cuervo, 2014). Folded proteins have very little thermodynamic stability and are susceptible to environmental changes even when cell conditions change slightly (Kim Y. E. et al., 2013). To do this, a complex network of networks formed inside the cell to cope with these stressful conditions, that is, a quality control system for proteins (Thirumalai et al., 2020). The system regulates the entire process from initial synthesis of proteins on ribosomes to final degradation of proteins. As main members of this protein quality control system, molecular chaperones play an indispensable role in maintaining protein stability. Among them, heat shock proteins (HSP) are the most abundant molecular chaperone proteins. In addition to normal expression under physiological conditions, HSPs expression increases when cells are exposed to stress conditions, such as high temperature or hypoxia (Rylander et al., 2005). According to the order of molecular weight, HSPs were classified by predecessors, including HSP110, HSP90, HSP70, HSP40 and small heat shock protein (sHSP) (Kampinga et al., 2009). What is more, there are also HSP related proteins, such as co-chaperone,

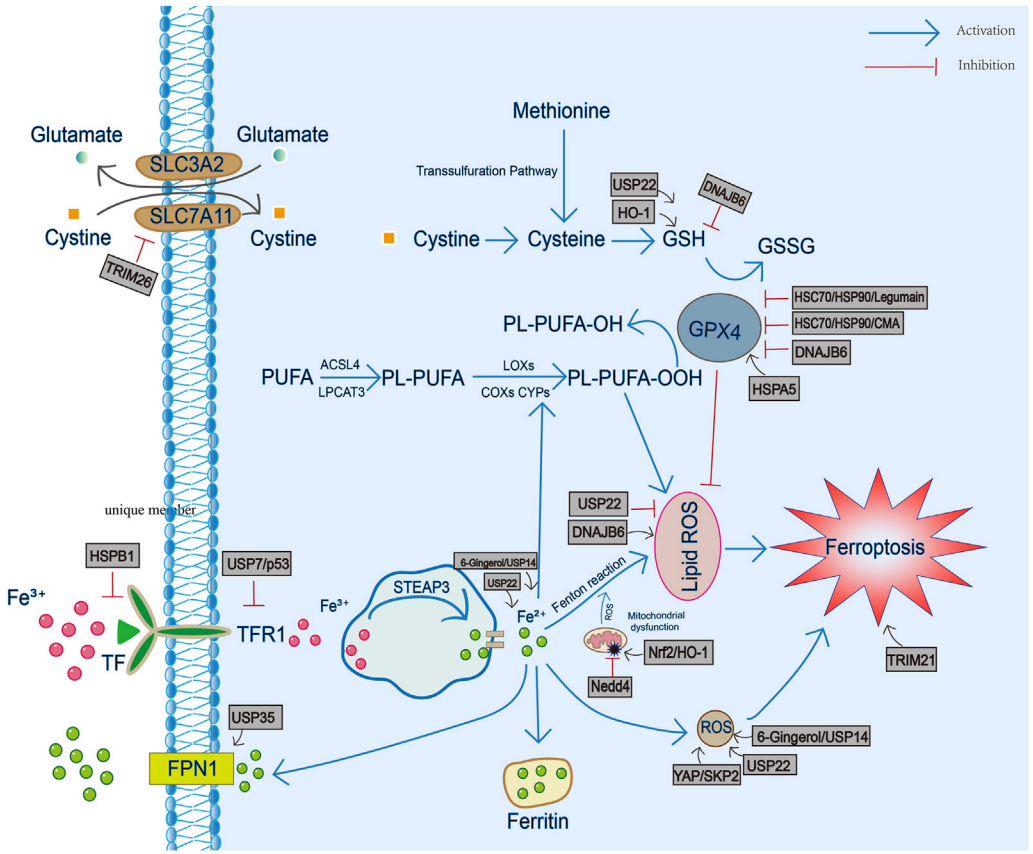

FIGURE 1 | The involvement of heat shock proteins in iron metabolism, GSH/GPX4 antioxidant pathway and production of reactive oxygen species and lipid peroxidation during ferroptosis. TF, transferrin; TFR1, transferrin receptor 1; FPN1, ferroportin1; PL-PUFA, phospholipid-bound polyunsaturated fatty acids; STEAP3, six-transmembrane epithelial antigen of prostate 3; ROS, reactive oxygen species; GSH, glutathione; GSSG, oxidized glutathione; GPX4, Glutathione peroxidase 4.

TCP-1 ring complex (TriC), protein disulfide isomerases (PDIs) and cis-trans proline isomerase, cadherin/calreticulin, etc., (Hageman and Kampinga, 2009; Kampinga et al., 2009).

In recent years, more and more studies have shown that HSPs participate in the pathophysiological process of ferroptosis. They play different roles in the process of ferroptosis in occurrence, development and regulation. Therefore, this paper makes a systematic review on the regulation of HSPs on ferroptosis, in which we focus on the important role of different HSPs in the process of ferroptosis, which may provide innovative ideas for further research on ferroptosis.

FERROPTOSIS

Regulated cell death (RCD) is an important process that maintains the metabolism and homeostasis of multicellular organisms, including apoptosis, necrosis, pyroptosis, ferroptosis and other forms of RCD (Galluzzi et al., 2018; Tang et al., 2019). Among them, ferroptosis has been revealed to be involved in more and more diseases in recent years, such as neurodegenerative diseases (Ayton et al., 2015), cancer (Chen X. et al., 2021), ischemia-reperfusion injury (IRI) (Swaminathan, 2018), intestinal diseases (Xu S. et al., 2021) and so on. Unlike apoptosis (cell atrophy, chromatin concentration, cytoskeleton disintegration and the formation of apoptotic bodies), necrosis (cell membrane rupture, organelle swelling) and pyroptosis (cell swelling, nuclear shrinkage, cell membrane rupture and content leakage), the biochemical aspects of ferroptosis are characterized by the accumulation of intracellular iron and lipid reactive oxygen. As major sites of iron utilization and master regulators of oxidative metabolism, mitochondria are the main source of reactive oxygen species (ROS) and, thus, the severity of damage to mitochondrial morphology, bioenergetics and metabolism is closely related to ferroptosis (Battaglia et al., 2020). Morphologically, when ferroptosis occurs in cells, the volume of mitochondria becomes smaller, accompanied by the increase of mitochondrial membrane density, the decrease or disappearance of cristae and the rupture of mitochondrial outer membrane, which may be caused by the dysfunction of voltage-dependent anion channels (VDCAs) and the change of mitochondrial membrane fluidity caused by lipid peroxidation products (DeHart et al., 2018). Although ferroptosis is widely involved in the pathological process of many different diseases, there is still no specific molecular detection index for it. The existence of ferroptosis can only detected by the level of lipid

peroxidation and the inhibition of ferroptosis inhibitors or iron chelators on cell death.

In recent years, the complex and unknown regulatory mechanism network of ferroptosis is slowly being revealed, including cysteine/glutamate antiporter system (system Xc^-), glutathione peroxidase (GPX), mitochondrial membrane voltage dependent anion channel, iron metabolism, ferroptosis suppressor protein 1(FSP1), GTP cyclohydrolase 1 (GCH1), p53, HO-1, p62-Keap1-Nrf2, ATG5-ATG7-NCOA4 and other related signal pathways. This paper will focus on the mechanism of ferroptosis from five aspects: iron metabolism, GSH/GPX4 antioxidant pathway, FSP1/CoQ10 antioxidant pathway, GCH1/BH4 antioxidant pathway, lipid peroxidation and the production of reactive oxygen species.

Iron Metabolism

Iron is one of the most basic life-sustaining elements and is involved in many physiological processes, such as oxygen transport, cell respiration, DNA synthesis, myelination and neurotransmitter biosynthesis. Hemoglobin in the blood contains iron, which carried by red blood cells and carries oxygen through the blood circulation to different tissues to maintain the body's blood oxygen supply (Martínková et al., 2013). Most of the iron in the human body is mainly stored in hemoglobin and myosin, the rest combined with iron storage proteins, such as ferritin, transferrin, cytochrome, etc. There is no doubt that this is necessary for normal cell and tissue physiology.

Under normal conditions, iron exists in the form of Fe^{2+} and Fe^{3+}. However, during the intracellular iron cycle, iron binds to transferrin (TF) in the form of Fe^{3+}, is absorbed into cells through transferrin receptor 1 (TFR1) and stored in endosomes. In the endosomes, Fe^{3+} is transformed into Fe^{2+} by six-transmembrane epithelial antigen of prostate 3(STEAP3) (Yan and Zhang, 2019). Then Fe^{2+} is transported from endosomes to cytosol via divalent metal transporter 1 (DMT1) (Xie et al., 2016). After that, some Fe^{2+} is stored in ferritin heavy chain 1(FTH1) and ferritin light chain (FLC) of iron storage protein complex, while others are transported out of cells through ferroportin1(FPN1). FPN1 is the only known protein that controls iron output in mammalian cells, and plays a critical role in the transport of Fe^{2+} and maintenance of intracellular iron balance (Trujillo-Alonso et al., 2019). However, based on this regulated mechanism of precise intracellular input-transport-storage or exocytosis, any process of iron uptake, transportation, storage or utilization will cause abnormal metabolism of intracellular iron ions, resulting in abnormalities in the Fe^{2+} metabolic chain, and then may lead to Fenton reaction to generate ROS (Xu et al., 2020). Then, ROS subsequently modifies and interferes with proteins, lipids and DNA, and finally induces the termination of cell life (Singh et al., 2014; Bogdan et al., 2016). It is worth noting that the release of mitochondrial ROS caused by mitochondrial damage also aggravates this process and promotes ferroptosis (Wu et al., 2021).

Glutathione/Glutathione Peroxidase 4 Antioxidant Pathway

Cells transport substances to the cells for digestion, absorption and uptake of nutrients to maintain biochemical reactions. Nutrients such as sugar, fat and amino acids cannot directly enter cells, but they must transported through specific transporters. System Xc^-, a cysteine/glutamate reverse transporter widely distributed in phospholipid bilayer, is one of these transporters. System Xc^- is a disulfide heterodimer composed of light chain subunit (SLC7A11) and heavy chain subunit (SLC3A2). It plays an important role in the upstream events of ferroptosis and is responsible for 1:1 input of cystine and excretion of glutamate (Dixon et al., 2012). Cystine transported into the cell and reduced to cysteine. In addition to relying on System Xc^-, cysteine can also enter cells through sulfur-transfer pathway. Cysteine entering cells through these two pathways and becomes the raw material for the synthesis of glutathione (GSH) and participates in the synthesis of GSH (Xu W. et al., 2021). GSH is the core substance of amino acid metabolism in the process of ferroptosis (Friedmann Angeli et al., 2014; Yang et al., 2014), which is an important antioxidant to protect cells from oxidative damage and is also the substrate of GPX4 lipid repair function. In the process of ferroptosis, GPX4 as the central regulator is an important enzyme that scavenge anaerobic free radicals from lipids (Yang et al., 2014). Once activated, GPX4 catalyzes toxic lipid hydroperoxides (L-OOH) into non-toxic lipid alcohols (L-OH) (Ursini et al., 1982). Under this catalysis, GPX4 uses two molecules of GSH as substrate to produce one molecule of oxidized glutathione (GSSG). GSSG reduced to GSH by GSH reductase in a NADPH dependent manner. Overexpression of GPX4 can inhibit ROS production and lipid peroxidation (Koppula et al., 2018), while the decrease of GPX4 activity or expression will lead to the accumulation of intracellular lipid peroxide, resulting in ferroptosis (Kim et al., 2021). Thus, the expression of GPX4 may represent the process of ferroptosis to some extent. It is worth mentioning that some studies have shown that knockout of GPX4 can also cause cell death and tissue damage by means of necrosis (Canli et al., 2016), pyroptosis (Kang et al., 2018) or apoptosis (Ran et al., 2007). Therefore, it has important pathological significance to continue to explore the role and mechanism of GPX4.

Ferroptosis Suppressor Protein 1/CoQ10 Antioxidant Pathway

Initially, the GSH/GPX4 pathway was thought to be the only ferroptosis inhibiting pathway, but later it was found that there is another parallel inhibitory pathway: in the absence of GPX4, ferroptosis suppressor protein 1 (FSP1) adequately counteracts lethal lipid peroxidation and ferroptosis (Bersuker et al., 2019; Doll et al., 2019). FSP1 is a member of the type II NADH: quinone oxidoreductase (NDH-2) family. Thus, its intrinsic role is to reduce CoQ10 using NADH (Elguindy and Nakamaru-Ogiso, 2015). During this resistance to ferroptosis, FSP1 terminates lipid autoxidation by reducing ubiquinone to ubiquinol, which in turn can directly reduce lipid free radicals. In addition, it prevents lipid peroxidation and ferroptosis by regenerating oxidized α-tocopherol radicals, the most powerful natural chain-breaking antioxidants in lipids, into non-radical forms.

GCH1/BH4 Antioxidant Pathway

As research on ferroptosis progresses more rapidly, another highly effective endogenous ferroptosis inhibitor, GTP Cyclohydrolase 1 (GCH1), was reported by Kraft in 2020 (Kraft et al., 2020). GCH1 is the rate-limiting enzyme for the synthesis of the antioxidant tetrahydrobiopterin (BH4). Like FSP1/CoQ10 axis, GCH1/BH4 pathway also blocks ferroptosis in a GPX4-independent form. In this process, BH4 needs to regenerated by reducing BH2 by dihydrofolate reductase (DHFR). What's more, BH4 converts phenylalanine to tyrosine, which in turn is converted to 4-OH-benzoate (a precursor of CoQ10) to promote the synthesis of CoQ10, thereby inhibiting ferroptosis.

Production of Reactive Oxygen Species and Lipid Peroxidation

ROS is a by-product of cellular oxygen metabolism, which is responsible for maintaining the stability of the body and participating in the signal transduction of cell normal metabolism. ROS include peroxide (H_2O_2、ROOH) superoxide (O_2^-) singlet oxygen ($^1O_2$) and free radicals (HO^-, HO_2^-, R^-, $NO^-$and NO_2^-). Under pathological conditions, excessive ROS can destroy all types of cellular components, such as nucleic acids, proteins and lipids, resulting in cell death (Imlay, 2013). Most ferroptosis related ROS come from Fenton reaction and Haber Weiss reaction (Shen et al., 2018), then ROS interacts with polyunsaturated fatty acids (PUFAs) on lipid membrane to form lipid ROS. When a large amount of lipid ROS accumulates in cells, it will cause ferroptosis (Florean et al., 2019).

Lipid peroxidation refers to the lipid oxidative degradation reaction in which lipids lose hydrogen atoms under the action of free radicals or lipid peroxidase, resulting in the oxidation, fracture and shortening of lipid carbon chain, and produce cytotoxic substances resulting in cell damage (Ayala et al., 2014). More and more studies have shown that lipid peroxide is a key mediator of many pathological states, including inflammation (Kang and Yang, 2020), cancer (Rodríguez-García et al., 2020) and neurodegenerative diseases (Zhao et al., 2021). Among them, lipid peroxides have toxic effects on cells mainly through two mechanisms: at the molecular level, lipid peroxides are further decomposed into active substances, which consume nucleic acids and proteins, leading to ferroptosis; at the structural level, lipid peroxidation leads to thinning and increased bending of the biofilm, which ultimately leads to membrane instability and micellar formation (Gaschler and Stockwell, 2017).

Before lipid peroxidation, activated long-chain acyl CoA synthase 4 (ACSl4) induced esterification of free PUFAs and incorporated into membrane phospholipids with the assistance of lysophosphatidylcholine acyltransferase 3 (LPCAT3). Therefore, the upregulation of ACSL4 generally regarded as a sign of ferroptosis. In this process, the level and location of intracellular PUFAs determine the degree of lipid peroxidation (Liu et al., 2021). It is worth noting that free PUFAs, such as arachidonic acid (AA) and adrenaline (AdA), must be esterified into phospholipids (PLs) for peroxidation (Sato et al., 1999). Subsequently, lipoxygenases (LOXs), such as cyclooxygenases (COXs) and cytochrome P450 enzymes (CYPs), catalyze PL-PUFAs to form lipid hydroperoxides (Doll and Conrad, 2017; Lei et al., 2019). As mentioned above, GPX4 reduces PL-PUFAs lipid peroxides (L-OOH) to lipid alcohols (L-OH). Excess iron ions in the cytoplasm trigger free radical induced lipid hydroperoxides that damage cells. In addition, these free radicals can transfer protons, leading to a new wave of lipid peroxidation with positive feedback.

HEAT SHOCK PROTEINS AND FERROPTOSIS

Molecular chaperones are a class of evolutionarily conserved proteins in the cytoplasm. They recognize and bind incompletely folded or assembled proteins to help them fold, transport or prevent their aggregation. However, molecular chaperones themselves do not participate in the formation of final products (Hoter et al., 2018). In cell homeostasis, molecular chaperones regulate the activity and interaction of mature proteins by assisting in the proper folding and assembly of newborn polypeptide chains, guide damaged or short-lived proteins into the degradation pathway. All these chaperones work together to maintain the mass and weight balance of protein and avoid misfolding and/or aggregation of client proteins.

Based on the naming method specified by HUGO Gene Nomenclature Committee, the HSP family divided into five subfamilies according to molecular weight: HSP110 (HSPH), HSP90 (HSPC), HSP70 (HSPA), HSP40 (DNAJ) and small HSP (HSPB). Although, the latest nomenclature contains heat shock 70 kDa proteins, DNAJ (HSP40) heat shock proteins, small heat shock proteins, heat shock 90 kDa proteins, and chaperonins.

Based on different molecular weights, different types of HSPs also have great differences in configuration. For example, the macromolecule HSP104 forms a hexameric ring and promotes unfolding through a ratchet mechanism. HSP90 forms a multi domain V-shaped structure, and its scissors like movement helps to refine the receptor protein. HSP70 and small HSP use modular "clamps" to protect the extended hydrophobic structure in the target protein. HSP60 adopts barrel "Anfinsen" cage structure for isolation and folding of target protein (Bascos and Landry, 2019).

Ferroptosis is an oxidative stress-dependent regulation of cell death related to iron accumulation and lipid peroxidation. Since it named in 2012, there are still many unexplored mechanisms (Dixon et al., 2012). Members of the HSP family play an important role in the occurrence and development of ferroptosis. However, there are few relevant reviews on the interaction between molecular chaperones and ferroptosis. In this paper, the existing research results on molecular chaperones in ferroptosis reviewed to provide clues for further revealing the unknown mechanism of ferroptosis and to clarify the potential role of molecular chaperones in ferroptosis.

HSP90 (HSPC) and Ferroptosis

HSP90 family is one of the most widely studied molecular chaperones of HSP family. It is also one of the most abundant proteins in cells, accounting for 1–2% of cellular proteins and 4–6% in stressed cells (Picard, 2002; Taipale et al., 2010).HSP90 family include cytoplasmic HSP90α and HSP90β, endoplasmic reticulum glucose regulatory protein 94 (GRP94) and mitochondrial TNF receptor associated protein 1 (TRAP1) (DeZwaan and Freeman, 2010). HSP90 have conserved domains in the process of evolution, including an amino terminal domain (NTD) and a carboxyl terminal domain (CTD) (Csermely et al., 1998). The evolutionary conservation and expression universality reflect the basic and necessary role of HSP90 in cell physiology.

As ATPase, ATP binding and hydrolysis are the key characteristics of HSP90's activity on client proteins. In addition to the hydrolysis of ATP, the function of HSP90 also regulated by its interacting co-chaperones (Sreedhar et al., 2004; Zhao et al., 2005; Prodromou, 2016). In addition, the role of HSP90 is also essential in genomic DNA. In mammalian cells, HSP90 enhances the enzymatic activity of histone methyltransferase SMYD3, which is involved in RNA polymerase II-mediated transcriptional regulation (Hamamoto et al., 2004). Moreover, *Drosophila* HSP90 also participates in the interaction with chromatin modifying enzyme trithorax protein, so as to participate in gene regulation (Tariq et al., 2009).

Compared with other HSPs, HSP90 has received more attention as a promising anticancer drug target because of its clear importance in regulating the stability and activity of many proteins involved in human cancer. It is now clear that siRNA interference with HSP90 can protect mouse nerve cells from the toxic effect of ferroptosis (Wu et al., 2019). Besides, necrotic apoptosis and ferroptosis are two different ways of necrotic cell death, there is no common regulatory mechanism. Studies have shown that HSP90 plays a complex role in necrotic apoptosis by binding and regulating the activity of RIPK1, RIPK3 or MLKL in a strictly cell environmental-dependent manner (Li et al., 2015; Jacobsen et al., 2016). However, recent studies have found that chaperone mediated autophagy (CMA) can be used as a common regulatory point to regulate necrotic apoptosis and ferroptosis (Wu et al., 2019). CMA degrades its substrate GPX4 by interacting with Lamp-2a and GPX4-HSC70-HSP90 trimers located in lysosomes. Inhibition of CMA can stabilize GPX4 and reduce ferroptosis. Furthermore, in IRI or folate-induced acute kidney injury (AKI) models, HSC70-HSP90-GPX4 interacts with legumain in the kidney to promote chaperone mediated degradation of GPX4, thereby promoting renal tubular cell ferroptosis in AKI (Chen C. A. et al., 2021).

Therefore, based on the existing scientific research results, HSP90 family may act on GPX4, inhibit the antioxidant capacity of GPX4 by inhibiting its activity (Zhou et al., 2021), then participate in the regulation of ferroptosis through GSH/GPX4 pathway and inhibite lipid peroxidation, therefore influencing ferroptosis.

HSP70 (HSPA) and Ferroptosis

The molecular chaperones of HSP70 family exist in different forms, including cytoplasmic HSP73 (also named HSC70), cytoplasmic inducible HSP72, mitochondrial HSP75/lethal protein mortalin and endoplasmic reticulum HSP78/BIP. Other variants include HSP72 and HSP70i (Kim et al., 2020).

The neuroprotective properties of HSP70 have been widely studied. In the ischemic stroke model, HSP70 plays an endogenous protective mechanism in the penumbra of the hippocampus (States et al., 1996; Weinstein et al., 2004). And HSP70 can protect cells from apoptosis, necrosis and other types of cell death (Frebel and Wiese, 2006). It is reported that HSP70 seems to improve nerve injury by blocking cell death and immune response. Besides, HSP70 is also involved in the regulation of inflammatory pathways (Kim J. Y. et al., 2013). Therefore, more and more drugs take HSP70 as a potential therapeutic target for nervous system diseases.

HSPA5, also known as GRP78 or Bip, is an important member of HSP70 family. As a receptor of endoplasmic reticulum stress, HSPA5 is responsible for regulating the folding and transport of unfolded proteins in endoplasmic reticulum, so as to maintain the homeostasis. In human pancreatic ductal adenocarcinoma cells (PDAC), HSPA5 negatively regulates ferroptosis of PDAC cells through HSPA5-GPX4 signaling pathway, and mediates resistance to ferroptosis (Zhu et al., 2017). Similarly, dihydroartemisinin (DHA) can induce ferroptosis in glioma cells. This is because DHA causes endoplasmic reticulum stress in glioma cells, which up regulates the expression of activated transcription factor 4 (ATF4) and induces the expression of HSPA5 by activating protein kinase R-like endoplasmic reticulum kinase (PERK). The upregulation of HSPA5 increases the expression and activity of GPX4, GPX4 protects glioma cells from ferroptosis by neutralizing DHA induced lipid peroxidation (Chen et al., 2019).

Thus, based on the existing research status, HSP70 family members may enhance cell resistance to ferroptosis by promoting GPX4 expression and its antioxidant activity, inhibiting the production of lipid ROS.

HSP40 (DNAJ) and Ferroptosis

In all known protein homeostasis processes, HSP70 exerts chaperone activity assisted by two types of well-defined and essential chaperones: HSP40 family and nucleotide exchange factors (NEFs) (Hartl and Hayer-Hartl, 2009). Therefore, to some extent, HSP40 and HSP70 functions are inseparable. In fact, HSP40 protein determines the activity of HSP70 by stabilizing the interaction with substrate proteins. Functionally conserved HSP40 has a J-domain that interacts with HSP70 and then referred to as a J-domain-containing protein. This domain is characterized by its conserved histidine, proline and aspartate residues (Qiu et al., 2006). The binding of J domain to HSP70 enhances the ATPase activity of HSP70, thereby regulating protein folding, translation and translocation.

Based on the unique structure and precise function of HSP40, it has been shown to be highly relevant to the development of cancer. Interestingly, HSP40 family proteins have dual properties and play different roles in anticancer and cancer promotion. For example, studies on lung cancer specimens have shown that HSP40 is highly expressed in cancerous lung tissues, detection of HSP40 level in serum of tumor patients with anti-HSP antibodies can be used for tumor diagnosis (Oka et al., 2001).

On the contrary, DNAJB4 (also known as HLJ1) is a tumor suppressor that can inhibit the proliferation and invasion of lung cancer cells. High DNAJB4 levels can slow down lung cancer cell cycle progression through the STAT1/P21 pathway (Wang et al., 2005; Zhang et al., 2011).

At present, there are few studies on the relationship between HSP40 family and ferroptosis. It is of pioneering significance to explore the regulation and occurrence of HSP40 family members and ferroptosis. Studies have confirmed that in esophageal squamous adenocarcinoma, overexpression of DNAJB6 enhances the degradation of GSH, down regulates GPX4, enhances lipid peroxidation and promotes ferroptosis. This confirmed the adverse role of HSP40 family members in regulating ferroptosis (Jiang et al., 2020).

Similarly, based on previous studies, we predict that, like DNAJB6, other HSP40 family members may promote the occurrence of ferroptosis by inhibiting GSH/GPX4 and enhancing lipid peroxidation. So, it may be of great significance to continue to explore the relationship between HSP40 family members and ferroptosis.

Small Heat Shock Protein and Ferroptosis

sHSP is usually defined as an ATP independent HSP with a subunit molecular weight of 12–43 kDa. Members of the sHSP family possess a homologous core domain, a highly conserved α-crystalline domain (ACD) consisting of 80–100 amino acids (Kriehuber et al., 2010). In the sHSP family, HO-1(HSP32), HSPB1 (HSP27), HSPB4 (αA crystal protein) and HSPB5 (αB crystal protein) have been studied and reported the most. sHSP is usually present in oligomeric complexes involving one or more family members and thus may provide cells with molecular chaperone-specific diversity. This is because the most striking feature of sHSP is its oligomerization, in which sHSP adjusts its quaternary structure through the assembly of monomers or dimers (Benesch et al., 2008). They can interact with themselves or other sHSPs to form homo or hetero oligomers containing up to 50 subunits (Garrido et al., 2012). This dynamic oligomerization process can cause rapid subunit exchange. The assembly of different substructures affects the exposure of hydrophobic surfaces, thus providing a molecular mechanism to regulate their binding activity.

Ferroptosis is a process dependent on both iron and ROS. After oxidative stress, cells respond through the inherent adaptive defense mechanism to restore healthy cell redox homeostasis. One mechanism involves the haem oxygenase enzyme system, especially its inducible isomer HO-1, a member of sHSP family. This is a kind of cell protective, anti-inflammatory and antioxidant enzyme. HO-1 expression was up-regulated in cancer cells when ferroptosis occurs (Kwon et al., 2015). For example, in human renal tubular epithelial cells, HO-1 has an important anti-ferroptosis effect. Its mechanism may be that HO-1 protects AKI from ferroptosis by promoting GSH depletion (Zhang et al., 2009; Adedoyin et al., 2018). In addition, in the pathogenesis of adriamycin induced myocardial toxicity and ischemia-reperfusion mediated ferroptosis in cardiomyopathy, Nrf2/HO-1 axis promotes the release of free iron, and excessive free iron accumulates in mitochondria, resulting in lipid peroxidation on mitochondrial membrane, mitochondrial dysfunction, and then aggravate ferroptosis (Fang et al., 2019).

HSPB1, a member of sHSP, also plays an integral role in ferroptosis. Previously, HSPB1 was considered to be a negative regulator of iron accumulation and uptake in fibroblasts or cardiac cells (Chen et al., 2006; Zhang et al., 2010). Sun et al. found that HSPB1 overexpression also inhibited erastin-induced iron uptake, while down regulating HSPB1 expression increased erastin-induced iron uptake in cancer cells (Sun et al., 2015). Therefore, when cancer cells contain abnormally elevated iron and HSPB1, if HSPB1 pathway is down regulated, cells may be prone to ferroptosis (Oesterreich et al., 1993; Torti and Torti, 2013). Inhibition of HSF1-HSPB1-PRKC pathway promotes ferroptosis in cancer cells induced by erastin (Sun et al., 2015). Besides, proteomic analysis of animal models of depression found that, the levels of alpha crystallin B (Cryab) and brain-derived neurotrophic factor (BDNF) of sHSP family members decreased, can explain the loss of some neurons during ferroptosis (Cao et al., 2021). However, the mechanism involved is unclear.

Based on the relationship and discovery of existing sHSP family members in ferroptosis, it can regulate ferroptosis through iron metabolism and GSH/GPX4 pathway. This regulation may be beneficial, such as HO-1 and HSPB1; it may also be harmful, such as Nrf2/HO-1 pathway. Therefore, in-depth study of their relationship may have some enlightenment for the research progress of ferroptosis.

Ubiquitin and Ferroptosis

Ubiquitin is a small protein with a molecular weight of 8.5 kDa and 76 amino acids. It is highly conformed in eukaryotes and named by its widespread expression in cells. There are eight amino acid sites of ubiquitin itself (Met1, Lys6, Lys11, Lys27, Lys29, Lys33, Lys48, Lys63), which can be modified by other ubiquitin molecules to form eight poly polymerized ubiquitin chains. Ubiquitin modification system is one of the most common post-translational modification (PTM) systems. It serves as a label or signal to determine the fate and/or function of its labeled substrate protein, and has complex and important physiological functions.

The process of ubiquitin modification of target protein depends on the cascade reaction catalyzed by three kinds of ubiquitin enzymes, namely, ubiquitin activase (E1) binding enzyme (E2) and ligase (E3). Firstly, E1 mediates ATP-dependent activation of ubiquitin to initiate a reaction in which E1 and the 76th amino acid glycine carboxyl group of ubiquitin converted to thiocyanates. Secondly, E2 enzyme acts on the chemical bond for thioesterification, coupling ubiquitin to cysteine residues in E2. Finally, ubiquitin attached to the lysine residue of the target protein by E3. Among them, the specificity of E3 enzyme determines the specificity of ubiquitinated substrate (Hershko and Ciechanover, 1998; Pickart and Eddins, 2004). Single ubiquitin protein can continue to link ubiquitin protein to form polymerized ubiquitin chain. The specificity of ubiquitin chain type determined by E3 enzymes and some specific E2 enzymes (Stewart et al., 2016; Swatek and Komander, 2016).

Unlike other HSPs, ubiquitin exhibits certain uniqueness in functional roles, such as protein degradation pathways (Dikic et al., 2006). As a unique member of the HSP family, ubiquitin closely related to ferroptosis. For example, ubiquitin specific protease 35(USP35) belongs to a family of de-ubiquitinase related to cell proliferation and mitosis. In lung cancer cells, USP35 interacts directly with FPN1 to maintain its protein stability and prevent iron overload and ferroptosis (Tang Z. et al., 2021). Down regulation of USP35 promotes ferroptosis and inhibits cell growth, colony formation and tumor progression. Therefore, it is a promising therapeutic target for lung cancer. 6-Gingerol improves autophagy-dependent-ferroptosis by inhibiting the expression of USP14 and increasing the contents of ROS and Fe^{2+}, which verified the protective effect of USP14 on ferroptosis (Tsai et al., 2020). In addition, overexpression of USP22 can reduce ferroptosis, accompanied by an increase in GSH and a decrease in ROS production, lipid peroxidation and iron accumulation (Ma et al., 2020). In I/R treated rat hearts, USP7, p53 and TfR1 formed a unique pathway of USP7/p53/TfR1. Inhibition of USP7 can inhibit the ubiquitination process and then activate p53, resulting in the down-regulation of TfR1, accompanied by the reduction of ferroptosis and myocardial injury (Tang L.-J. et al., 2021).

In addition to the above, different members of the E3 ligase family also play important roles in regulating ferroptosis. TRIM26 is an E3 ubiquitin ligase, which plays a role as a tumor suppressor in hepatocellular carcinoma. TRIM26 can inhibit liver fibrosis by mediating the ubiquitination of SLC7A11 and promoting the ferroptosis of hepatic stellate cells (HSCs), which can be used as a new therapeutic strategy for liver fibrosis (Zhu et al., 2021). Similarly, E3 ubiquitin ligase S-phase kinase-associated protein 2(SKP2) also plays a role in ferroptosis: YAP (Yes-associated protein 1) is the only analogue of TAZ (a regulator of the Hippo pathway, which regulates ferroptosis in renal and ovarian cancer cells), which promotes the production of ROS by regulating the SKP2 thus aggravates ferroptosis. It provides a new treatment for YAP driven tumors (Yang et al., 2021).Besides, the ubiquitin-E3 ligase TRIM21 interacts with and ubiquitinizes p62, negatively regulating the antioxidant pathway of p62-keap1-Nrf2, thereby exacerbating ferroptosis (Hou et al., 2021). Knockout of TRIM21 protects cardiomyocytes from doxorubicin-induced ferroptosis. However, from the perspective of mechanism, it should be noted that, as a ubiquitin-E3 ligase, TRIM21 can promote proteasome degradation of various proteins, and may play an anti-ferroptosis role through regulating other pathways, one of which may be regulated by the immune system (Hou et al., 2021). Similarly, as a member of the E3 ligase family, neuronal precursor cell expressed developmentally downregulated 4(Nedd4) is an important member of this family. Down-regulation Nedd4 saves erastin-induced elimination of the voltage-dependent anionic channel VDAC2/3 protein, increases the resistance of melanoma cells to erastin (Yang et al., 2020).

To sum up, ubiquitin family proteins closely related to the mechanism of ferroptosis, which may involve many cytokines or mechanisms, including GSH/GPX4 antioxidant pathway and iron metabolism, etc. The continued study of ubiquitin system has prospective significance and broad prospects for mastering the regulatory mechanism of ferroptosis.

Perspectives

In conclusion, after the above review, we summarized and predicted the mechanism of different HSP family members in ferroptosis (**Figure 1**). It seems that each HSP family has members either promote ferroptosis (such as HSP90 family, HSP40 family, partial members of sHSP family and partial ubiquitin ligases) or inhibit ferroptosis (such as HSP70 family, partial members of sHSP family and some ubiquitin ligases) by targeting the GSH/GPX4 antioxidant pathway. In addition to GSH/GPX4 axis, other antioxidant pathways, such as FSP1/CoQ10 axis and GCH1/BH4 axis, also have great exploration potential. Therefore, future studies can target these antioxidant pathways to explore the association between HSP and ferroptosis.

SUMMARY AND PROSPECT

The research on fine regulation mechanism related to ferroptosis is increasing rapidly. However, different HSP family members seem to regulate ferroptosis differently in different diseases/organ microenvironments. In this review, we summarized the effects of HSP on ferroptosis in existing studies. They may participate in the regulation of ferroptosis through iron metabolism, GSH/GPX4 axis, production of ROS and lipid peroxidation. Future research needs to determine the pathophysiological effects of HSP family in ferroptosis, especially in tumorigenesis and neurodegenerative diseases, so as to provide new ideas and strategies for defining the new mechanism of ferroptosis.

AUTHOR CONTRIBUTIONS

YL and JZ designed and directed the project. YL, LZ, YX, KL, YZ, HQ, QX, and JZ analyzed the data. All authors discussed the results and contributed to the final manuscript. YL and LZ wrote the manuscript.

FUNDING

This work was supported by National Natural Science Foundation of China (Nos. 82172147, 81571880, 81373147, 30901555, 30972870, 81360080) and Natural Science Foundation of Hunan Province (2021JJ30900, 2016JJ2157), Fundamental Research Funds for the Central Universities of Central South University (2021zzts0938) to LZ. All the funding bodies funded in the study design, collection, analysis, interpretation of data and writing the manuscript.

REFERENCES

Adedoyin, O., Boddu, R., Traylor, A., Lever, J. M., Bolisetty, S., George, J. F., et al. (2018). Heme Oxygenase-1 Mitigates Ferroptosis in Renal Proximal Tubule Cells. *Am. J. Physiology-Renal Physiol.* 314 (5), F702–F714. doi:10.1152/ajprenal.00044.2017

Ayala, A., Muñoz, M. F., and Argüelles, S. (2014). Lipid Peroxidation: Production, Metabolism, and Signaling Mechanisms of Malondialdehyde and 4-Hydroxy-2-Nonenal. *Oxid Med. Cel Longev* 2014, 360438. doi:10.1155/2014/360438

Ayton, S., Faux, N. G., and Bush, A. I. (2015). Ferritin Levels in the Cerebrospinal Fluid Predict Alzheimer's Disease Outcomes and Are Regulated by APOE. *Nat. Commun.* 6, 6760. doi:10.1038/ncomms7760

Bascos, N. A. D., and Landry, S. J. (2019). A History of Molecular Chaperone Structures in the Protein Data Bank. *Int. J. Mol. Sci.* 20 (24), 6195. doi:10.3390/ijms20246195

Battaglia, A. M., Chirillo, R., Aversa, I., Sacco, A., Costanzo, F., and Biamonte, F. (2020). Ferroptosis and Cancer: Mitochondria Meet the "Iron Maiden" Cell Death. *Cells* 9 (6), 1505. doi:10.3390/cells9061505

Benesch, J. L. P., Ayoub, M., Robinson, C. V., and Aquilina, J. A. (2008). Small Heat Shock Protein Activity Is Regulated by Variable Oligomeric Substructure. *J. Biol. Chem.* 283 (42), 28513–28517. doi:10.1074/jbc.m804729200

Bersuker, K., Hendricks, J. M., Li, Z., Magtanong, L., Ford, B., Tang, P. H., et al. (2019). The CoQ Oxidoreductase FSP1 Acts Parallel to GPX4 to Inhibit Ferroptosis. *Nature* 575 (7784), 688–692. doi:10.1038/s41586-019-1705-2

Bogdan, A. R., Miyazawa, M., Hashimoto, K., and Tsuji, Y. (2016). Regulators of Iron Homeostasis: New Players in Metabolism, Cell Death, and Disease. *Trends Biochem. Sci.* 41 (3), 274–286. doi:10.1016/j.tibs.2015.11.012

Canli, Ö., Alankuş, Y. B., Grootjans, S., Vegi, N., Hültner, L., Hoppe, P. S., et al. (2016). Glutathione Peroxidase 4 Prevents Necroptosis in Mouse Erythroid Precursors. *Blood* 127 (1), 139–148. doi:10.1182/blood-2015-06-654194

Cao, H., Zuo, C., Huang, Y., Zhu, L., Zhao, J., Yang, Y., et al. (2021). Hippocampal Proteomic Analysis Reveals Activation of Necroptosis and Ferroptosis in a Mouse Model of Chronic Unpredictable Mild Stress-Induced Depression. *Behav. Brain Res.* 407, 113261. doi:10.1016/j.bbr.2021.113261

Chen, H., Zheng, C., Zhang, Y., Chang, Y.-Z., Qian, Z.-M., and Shen, X. (2006). Heat Shock Protein 27 Downregulates the Transferrin Receptor 1-Mediated Iron Uptake. *Int. J. Biochem. Cel Biol* 38 (8), 1402–1416. doi:10.1016/j.biocel.2006.02.006

Chen, Y., Mi, Y., Zhang, X., Ma, Q., Song, Y., Zhang, L., et al. (2019). Dihydroartemisinin-Induced Unfolded Protein Response Feedback Attenuates Ferroptosis via PERK/ATF4/HSPA5 Pathway in Glioma Cells. *J. Exp. Clin. Cancer Res.* 38 (1), 402. doi:10.1186/s13046-019-1413-7

Chen, X., Kang, R., Kroemer, G., and Tang, D. (2021). Broadening Horizons: The Role of Ferroptosis in Cancer. *Nat. Rev. Clin. Oncol.* 18 (5), 280–296. doi:10.1038/s41571-020-00462-0

Chen, C. A., Wang, D., Yu, Y., Zhao, T., Min, N., Wu, Y., et al. (2021). Legumain Promotes Tubular Ferroptosis by Facilitating Chaperone-Mediated Autophagy of GPX4 in AKI. *Cell Death Dis* 12 (1), 65. doi:10.1038/s41419-020-03362-4

Csermely, P., Schnaider, T., Soti, C., Prohászka, Z., and Nardai, G. (1998). The 90-kDa Molecular Chaperone Family: Structure, Function, and Clinical Applications. A Comprehensive Review. *Pharmacol. Ther.* 79 (2), 129–168. doi:10.1016/s0163-7258(98)00013-8

DeHart, D. N., Fang, D., Heslop, K., Li, L., Lemasters, J. J., and Maldonado, E. N. (2018). Opening of Voltage Dependent Anion Channels Promotes Reactive Oxygen Species Generation, Mitochondrial Dysfunction and Cell Death in Cancer Cells. *Biochem. Pharmacol.* 148, 155–162. doi:10.1016/j.bcp.2017.12.022

DeZwaan, D. C., and Freeman, B. C. (2010). HSP90 Manages the Ends. *Trends Biochem. Sci.* 35 (7), 384–391. doi:10.1016/j.tibs.2010.02.005

Dikic, I., Crosetto, N., Calatroni, S., and Bernasconi, P. (2006). Targeting Ubiquitin in Cancers. *Eur. J. Cancer* 42 (18), 3095–3102. doi:10.1016/j.ejca.2006.05.041

Dixon, S. J., Lemberg, K. M., Lamprecht, M. R., Skouta, R., Zaitsev, E. M., Gleason, C. E., et al. (2012). Ferroptosis: An Iron-Dependent Form of Nonapoptotic Cell Death. *Cell* 149 (5), 1060–1072. doi:10.1016/j.cell.2012.03.042

Doll, S., and Conrad, M. (2017). Iron and Ferroptosis: A Still Ill-Defined Liaison. *IUBMB Life* 69 (6), 423–434. doi:10.1002/iub.1616

Doll, S., Freitas, F. P., Shah, R., Aldrovandi, M., da Silva, M. C., Ingold, I., et al. (2019). FSP1 Is a Glutathione-Independent Ferroptosis Suppressor. *Nature* 575 (7784), 693–698. doi:10.1038/s41586-019-1707-0

Elguindy, M. M., and Nakamaru-Ogiso, E. (2015). Apoptosis-Inducing Factor (AIF) and its Family Member Protein, AMID, Are Rotenone-Sensitive NADH: Ubiquinone Oxidoreductases (NDH-2). *J. Biol. Chem.* 290 (34), 20815–20826. doi:10.1074/jbc.m115.641498

Fang, X., Wang, H., Han, D., Xie, E., Yang, X., Wei, J., et al. (2019). Ferroptosis as a Target for protection against Cardiomyopathy. *Proc. Natl. Acad. Sci. U.S.A.* 116 (7), 2672–2680. doi:10.1073/pnas.1821022116

Florean, C., Song, S., Dicato, M., and Diederich, M. (2019). Redox Biology of Regulated Cell Death in Cancer: A Focus on Necroptosis and Ferroptosis. *Free Radic. Biol. Med.* 134, 177–189. doi:10.1016/j.freeradbiomed.2019.01.008

Frebel, K., and Wiese, S. (2006). Signalling Molecules Essential for Neuronal Survival and Differentiation. *Biochem. Soc. Trans.* 34 (Pt 6), 1287–1290. doi:10.1042/BST0341287

Friedmann Angeli, J. P., Schneider, M., Proneth, B., Tyurina, Y. Y., Tyurin, V. A., Hammond, V. J., et al. (2014). Inactivation of the Ferroptosis Regulator Gpx4 Triggers Acute Renal Failure in Mice. *Nat. Cel Biol* 16 (12), 1180–1191. doi:10.1038/ncb3064

Galluzzi, L., Vitale, I., Aaronson, S. A., Abrams, J. M., Adam, D., Agostinis, P., et al. (2018). Molecular Mechanisms of Cell Death: Recommendations of the Nomenclature Committee on Cell Death 2018. *Cell Death Differ* 25 (3), 486–541. doi:10.1038/s41418-017-0012-4

Garrido, C., Paul, C., Seigneuric, R., and Kampinga, H. H. (2012). The Small Heat Shock Proteins Family: The Long Forgotten Chaperones. *Int. J. Biochem. Cel Biol* 44 (10), 1588–1592. doi:10.1016/j.biocel.2012.02.022

Gaschler, M. M., and Stockwell, B. R. (2017). Lipid Peroxidation in Cell Death. *Biochem. Biophysical Res. Commun.* 482 (3), 419–425. doi:10.1016/j.bbrc.2016.10.086

Hageman, J., and Kampinga, H. H. (2009). Computational Analysis of the Human HSPH/HSPA/DNAJ Family and Cloning of a Human HSPH/HSPA/DNAJ Expression Library. *Cell Stress and Chaperones* 14 (1), 1–21. doi:10.1007/s12192-008-0060-2

Hamamoto, R., Furukawa, Y., Morita, M., Iimura, Y., Silva, F. P., Li, M., et al. (2004). SMYD3 Encodes a Histone Methyltransferase Involved in the Proliferation of Cancer Cells. *Nat. Cel Biol* 6 (8), 731–740. doi:10.1038/ncb1151

Hartl, F. U., and Hayer-Hartl, M. (2009). Converging Concepts of Protein Folding *In Vitro* and *In Vivo*. *Nat. Struct. Mol. Biol.* 16 (6), 574–581. doi:10.1038/nsmb.1591

Hershko, A., and Ciechanover, A. (1998). The Ubiquitin System. *Annu. Rev. Biochem.* 67, 425–479. doi:10.1146/annurev.biochem.67.1.425

Hoter, A., El-Sabban, M. E., and Naim, H. Y. (2018). The HSP90 Family: Structure, Regulation, Function, and Implications in Health and Disease. *Int. J. Mol. Sci.* 19 (9), 2560. doi:10.3390/ijms19092560

Hou, K., Shen, J., Yan, J., Zhai, C., Zhang, J., Pan, J.-A., et al. (2021). Loss of TRIM21 Alleviates Cardiotoxicity by Suppressing Ferroptosis Induced by the Chemotherapeutic Agent Doxorubicin. *EBioMedicine* 69, 103456. doi:10.1016/j.ebiom.2021.103456

Imlay, J. A. (2013). The Molecular Mechanisms and Physiological Consequences of Oxidative Stress: Lessons from a Model Bacterium. *Nat. Rev. Microbiol.* 11 (7), 443–454. doi:10.1038/nrmicro3032

Jacobsen, A. V., Lowes, K. N., Tanzer, M. C., Lucet, I. S., Hildebrand, J. M., Petrie, E. J., et al. (2016). HSP90 Activity Is Required for MLKL Oligomerisation and Membrane Translocation and the Induction of Necroptotic Cell Death. *Cel Death Dis* 7, e2051. doi:10.1038/cddis.2015.386

Jiang, B., Zhao, Y., Shi, M., Song, L., Wang, Q., Qin, Q., et al. (2020). DNAJB6 Promotes Ferroptosis in Esophageal Squamous Cell Carcinoma. *Dig. Dis. Sci.* 65 (7), 1999–2008. doi:10.1007/s10620-019-05929-4

Kampinga, H. H., Hageman, J., Vos, M. J., Kubota, H., Tanguay, R. M., Bruford, E. A., et al. (2009). Guidelines for the Nomenclature of the Human Heat Shock Proteins. *Cell Stress and Chaperones* 14 (1), 105–111. doi:10.1007/s12192-008-0068-7

Kang, Q., and Yang, C. (2020). Oxidative Stress and Diabetic Retinopathy: Molecular Mechanisms, Pathogenetic Role and Therapeutic Implications. *Redox Biol.* 37, 101799. doi:10.1016/j.redox.2020.101799

Kang, R., Zeng, L., Zhu, S., Xie, Y., Liu, J., Wen, Q., et al. (2018). Lipid Peroxidation Drives Gasdermin D-Mediated Pyroptosis in Lethal Polymicrobial Sepsis. *Cell Host Microbe* 24 (1), 97–108. doi:10.1016/j.chom.2018.05.009

Kim, Y. E., Hipp, M. S., Bracher, A., Hayer-Hartl, M., and Ulrich Hartl, F. (2013). Molecular Chaperone Functions in Protein Folding and Proteostasis. *Annu. Rev. Biochem.* 82, 323–355. doi:10.1146/annurev-biochem-060208-092442

Kim, J. Y., Kim, N., Zheng, Z., Lee, J. E., and Yenari, M. A. (2013). The 70 kDa Heat Shock Protein Protects against Experimental Traumatic Brain Injury. *Neurobiol. Dis.* 58, 289–295. doi:10.1016/j.nbd.2013.06.012

Kim, J. Y., Barua, S., Huang, M. Y., Park, J., Yenari, M. A., and Lee, J. E. (2020). Heat Shock Protein 70 (HSP70) Induction: Chaperonotherapy for Neuroprotection after Brain Injury. *Cells* 9 (9), 2020. doi:10.3390/cells9092020

Kim, S., Kang, S.-W., Joo, J., Han, S. H., Shin, H., Nam, B. Y., et al. (2021). Characterization of Ferroptosis in Kidney Tubular Cell Death under Diabetic Conditions. *Cel Death Dis* 12 (2), 160. doi:10.1038/s41419-021-03452-x

Koppula, P., Zhang, Y., Zhuang, L., and Gan, B. (2018). Amino Acid Transporter SLC7A11/xCT at the Crossroads of Regulating Redox Homeostasis and Nutrient Dependency of Cancer. *Cancer Commun.* 38 (1), 12. doi:10.1186/s40880-018-0288-x

Kraft, V. A. N., Bezjian, C. T., Pfeiffer, S., Ringelstetter, L., Müller, C., Zandkarimi, F., et al. (2020). GTP Cyclohydrolase 1/Tetrahydrobiopterin Counteract Ferroptosis through Lipid Remodeling. *ACS Cent. Sci.* 6 (1), 41–53. doi:10.1021/acscentsci.9b01063

Kriehuber, T., Rattei, T., Weinmaier, T., Bepperling, A., Haslbeck, M., and Buchner, J. (2010). Independent Evolution of the Core Domain and its Flanking Sequences in Small Heat Shock Proteins. *FASEB J.* 24 (10), 3633–3642. doi:10.1096/fj.10-156992

Kwon, M.-Y., Park, E., Lee, S.-J., and Chung, S. W. (2015). Heme Oxygenase-1 Accelerates Erastin-Induced Ferroptotic Cell Death. *Oncotarget* 6 (27), 24393–24403. doi:10.18632/oncotarget.5162

Lei, P., Bai, T., and Sun, Y. (2019). Mechanisms of Ferroptosis and Relations with Regulated Cell Death: A Review. *Front. Physiol.* 10, 139. doi:10.3389/fphys.2019.00139

Li, D., Xu, T., Cao, Y., Wang, H., Li, L., Chen, S., et al. (2015). A Cytosolic Heat Shock Protein 90 and Cochaperone CDC37 Complex Is Required for RIP3 Activation during Necroptosis. *Proc. Natl. Acad. Sci. U.S.A.* 112 (16), 5017–5022. doi:10.1073/pnas.1505244112

Liu, Y., Fang, Y., Zhang, Z., Luo, Y., Zhang, A., Lenahan, C., et al. (2021). Ferroptosis: An Emerging Therapeutic Target in Stroke. *J. Neurochem.* 160 (1), 64–73. doi:10.1111/jnc.15351

Ma, S., Sun, L., Wu, W., Wu, J., Sun, Z., and Ren, J. (2020). USP22 Protects against Myocardial Ischemia-Reperfusion Injury via the SIRT1-p53/SLC7A11-Dependent Inhibition of Ferroptosis-Induced Cardiomyocyte Death. *Front. Physiol.* 11, 551318. doi:10.3389/fphys.2020.551318

Martínková, M., Kitanishi, K., and Shimizu, T. (2013). Heme-based Globin-Coupled Oxygen Sensors: Linking Oxygen Binding to Functional Regulation of Diguanylate Cyclase, Histidine Kinase, and Methyl-Accepting Chemotaxis. *J. Biol. Chem.* 288 (39), 27702–27711. doi:10.1074/jbc.r113.473249

Morimoto, R. I., and Cuervo, A. M. (2014). Proteostasis and the Aging Proteome in Health and Disease. *J. Gerontol. A. Biol. Sci. Med. Sci.* 69 (Suppl. 1), S33–S38. doi:10.1093/gerona/glu049

Oesterreich, S., Weng, C. N., Qiu, M., Hilsenbeck, S. G., Osborne, C. K., and Fuqua, S. A. (1993). The Small Heat Shock Protein Hsp27 Is Correlated with Growth and Drug Resistance in Human Breast Cancer Cell Lines. *Cancer Res.* 53 (19), 4443–4448.

Oka, M., Sato, S.-i., Soda, H., Fukuda, M., Kawabata, S., Nakatomi, K., et al. (2001). Autoantibody to Heat Shock Protein Hsp40 in Sera of Lung Cancer Patients. *Jpn. J. Cancer Res.* 92 (3), 316–320. doi:10.1111/j.1349-7006.2001.tb01097.x

Picard, D. (2002). Heat-shock Protein 90, a Chaperone for Folding and Regulation. *Ell Mol. Life Sci.* 59 (10), 1640–1648. doi:10.1007/pl00012491

Pickart, C. M., and Eddins, M. J. (2004). Ubiquitin: Structures, Functions, Mechanisms. *Biochim. Biophys. Acta* 1695 (1-3), 55–72. doi:10.1016/j.bbamcr.2004.09.019

Prodromou, C. (2016). Mechanisms of Hsp90 Regulation. *Biochem. J.* 473 (16), 2439–2452. doi:10.1042/bcj20160005

Qiu, X.-B., Shao, Y.-M., Miao, S., and Wang, L. (2006). The Diversity of the DnaJ/Hsp40 Family, the Crucial Partners for Hsp70 Chaperones. *Cell. Mol. Life Sci.* 63 (22), 2560–2570. doi:10.1007/s00018-006-6192-6

Ran, Q., Liang, H., Ikeno, Y., Qi, W., Prolla, T. A., Roberts, L. J., 2nd, et al. (2007). Reduction in Glutathione Peroxidase 4 Increases Life Span through Increased Sensitivity to Apoptosis. *J. Gerontol. A. Biol. Sci. Med. Sci.* 62 (9), 932–942. doi:10.1093/gerona/62.9.932

Rodríguez-García, A., García-Vicente, R., Morales, M. L., Ortiz-Ruiz, A., Martínez-López, J., and Linares, M. (2020). Protein Carbonylation and Lipid Peroxidation in Hematological Malignancies. *Antioxidants (Basel)* 9 (12), 1212. doi:10.3390/antiox9121212

Rylander, M. N., Feng, Y., Bass, J., and Diller, K. R. (2005). Thermally Induced Injury and Heat-Shock Protein Expression in Cells and Tissues. *Ann. N.Y Acad. Sci.* 1066, 222–242. doi:10.1196/annals.1363.009

Sato, H., Tamba, M., Ishii, T., and Bannai, S. (1999). Cloning and Expression of a Plasma Membrane Cystine/Glutamate Exchange Transporter Composed of Two Distinct Proteins. *J. Biol. Chem.* 274 (17), 11455–11458. doi:10.1074/jbc.274.17.11455

Shen, Z., Liu, T., Li, Y., Lau, J., Yang, Z., Fan, W., et al. (2018). Fenton-Reaction-Acceleratable Magnetic Nanoparticles for Ferroptosis Therapy of Orthotopic Brain Tumors. *ACS Nano* 12 (11), 11355–11365. doi:10.1021/acsnano.8b06201

Singh, N., Haldar, S., Tripathi, A. K., Horback, K., Wong, J., Sharma, D., et al. (2014). Brain Iron Homeostasis: From Molecular Mechanisms to Clinical Significance and Therapeutic Opportunities. *Antioxid. Redox Signal.* 20 (8), 1324–1363. doi:10.1089/ars.2012.4931

Sreedhar, A. S., Kalmár, E., Csermely, P., and Shen, Y. F. (2004). Hsp90 Isoforms: Functions, Expression and Clinical Importance. *FEBS Lett.* 562 (1-3), 11–15. doi:10.1016/s0014-5793(04)00229-7

States, B. A., Honkaniemi, J., Weinstein, P. R., and Sharp, F. R. (1996). DNA Fragmentation and HSP70 Protein Induction in hippocampus and Cortex Occurs in Separate Neurons Following Permanent Middle Cerebral Artery Occlusions. *J. Cereb. Blood Flow Metab.* 16 (6), 1165–1175. doi:10.1097/00004647-199611000-00011

Stewart, M. D., Ritterhoff, T., Klevit, R. E., and Brzovic, P. S. (2016). E2 Enzymes: More Than Just Middle Men. *Cell Res* 26 (4), 423–440. doi:10.1038/cr.2016.35

Sun, X., Ou, Z., Xie, M., Kang, R., Fan, Y., Niu, X., et al. (2015). HSPB1 as a Novel Regulator of Ferroptotic Cancer Cell Death. *Oncogene* 34 (45), 5617–5625. doi:10.1038/onc.2015.32

Swaminathan, S. (2018). Iron Homeostasis Pathways as Therapeutic Targets in Acute Kidney Injury. *Nephron* 140 (2), 156–159. doi:10.1159/000490808

Swatek, K. N., and Komander, D. (2016). Ubiquitin Modifications. *Cel Res* 26 (4), 399–422. doi:10.1038/cr.2016.39

Taipale, M., Jarosz, D. F., and Lindquist, S. (2010). HSP90 at the Hub of Protein Homeostasis: Emerging Mechanistic Insights. *Nat. Rev. Mol. Cel Biol* 11 (7), 515–528. doi:10.1038/nrm2918

Tang, D., Kang, R., Berghe, T. V., Vandenabeele, P., and Kroemer, G. (2019). The Molecular Machinery of Regulated Cell Death. *Cel Res* 29 (5), 347–364. doi:10.1038/s41422-019-0164-5

Tang, Z., Jiang, W., Mao, M., Zhao, J., Chen, J., and Cheng, N. (2021). Deubiquitinase USP35 Modulates Ferroptosis in Lung Cancer via Targeting Ferroportin. *Clin. Transl Med.* 11 (4), e390. doi:10.1002/ctm2.390

Tang, L.-J., Zhou, Y.-J., Xiong, X.-M., Li, N.-S., Zhang, J.-J., Luo, X.-J., et al. (2021). Ubiquitin-Specific Protease 7 Promotes Ferroptosis via Activation of the p53/TfR1 Pathway in the Rat Hearts after Ischemia/reperfusion. *Free Radic. Biol. Med.* 162, 339–352. doi:10.1016/j.freeradbiomed.2020.10.307

Tariq, M., Nussbaumer, U., Chen, Y., Beisel, C., and Paro, R. (2009). Trithorax Requires Hsp90 for Maintenance of Active Chromatin at Sites of Gene Expression. *Proc. Natl. Acad. Sci. U.S.A.* 106 (4), 1157–1162. doi:10.1073/pnas.0809669106

Thirumalai, D., Lorimer, G. H., and Hyeon, C. (2020). Iterative Annealing Mechanism Explains the Functions of the GroEL and RNA Chaperones. *Protein Sci.* 29 (2), 360–377. doi:10.1002/pro.3795

Torti, S. V., and Torti, F. M. (2013). Iron and Cancer: More Ore to Be Mined. *Nat. Rev. Cancer* 13 (5), 342–355. doi:10.1038/nrc3495

Trujillo-Alonso, V., Pratt, E. C., Zong, H., Lara-Martinez, A., Kaittanis, C., Rabie, M. O., et al. (2019). FDA-Approved Ferumoxytol Displays Anti-Leukaemia Efficacy against Cells with Low Ferroportin Levels. *Nat. Nanotechnol.* 14 (6), 616–622. doi:10.1038/s41565-019-0406-1

Tsai, Y., Xia, C., and Sun, Z. (2020). The Inhibitory Effect of 6-Gingerol on Ubiquitin-Specific Peptidase 14 Enhances Autophagy-Dependent Ferroptosis

and Anti-Tumor *In Vivo* and *In Vitro*. *Front. Pharmacol.* 11, 598555. doi:10.3389/fphar.2020.598555

Ursini, F., Maiorino, M., Valente, M., Ferri, L., and Gregolin, C. (1982). Purification from Pig Liver of a Protein Which Protects Liposomes and Biomembranes from Peroxidative Degradation and Exhibits Glutathione Peroxidase Activity on Phosphatidylcholine Hydroperoxides. *Biochim. Biophys. Acta* 710 (2), 197–211. doi:10.1016/0005-2760(82)90150-3

Wang, C.-C., Tsai, M.-F., Hong, T.-M., Chang, G.-C., Chen, C.-Y., Yang, W.-M., et al. (2005). The Transcriptional Factor YY1 Upregulates the Novel Invasion Suppressor HLJ1 Expression and Inhibits Cancer Cell Invasion. *Oncogene* 24 (25), 4081–4093. doi:10.1038/sj.onc.1208573

Weinstein, P. R., Hong, S., and Sharp, F. R. (2004). Molecular Identification of the Ischemic Penumbra. *Stroke* 35 (11 Suppl. 1), 2666–2670. doi:10.1161/01.STR.0000144052.10644.ed

Wu, Z., Geng, Y., Lu, X., Shi, Y., Wu, G., Zhang, M., et al. (2019). Chaperone-Mediated Autophagy Is Involved in the Execution of Ferroptosis. *Proc. Natl. Acad. Sci. U.S.A.* 116 (8), 2996–3005. doi:10.1073/pnas.1819728116

Wu, H., Wang, F., Ta, N., Zhang, T., and Gao, W. (2021). The Multifaceted Regulation of Mitochondria in Ferroptosis. *Life (Basel)* 11 (3), 222. doi:10.3390/life11030222

Xie, Y., Hou, W., Song, X., Yu, Y., Huang, J., Sun, X., et al. (2016). Ferroptosis: Process and Function. *Cel Death Differ* 23 (3), 369–379. doi:10.1038/cdd.2015.158

Xu, Y.-Y., Wan, W.-P., Zhao, S., and Ma, Z.-G. (2020). L-Type Calcium Channels Are Involved in Iron-Induced Neurotoxicity in Primary Cultured Ventral Mesencephalon Neurons of Rats. *Neurosci. Bull.* 36 (2), 165–173. doi:10.1007/s12264-019-00424-2

Xu, S., He, Y., Lin, L., Chen, P., Chen, M., and Zhang, S. (2021). The Emerging Role of Ferroptosis in Intestinal Disease. *Cel Death Dis* 12 (4), 289. doi:10.1038/s41419-021-03559-1

Xu, W., Deng, H., Hu, S., Zhang, Y., Zheng, L., Liu, M., et al. (2021). Role of Ferroptosis in Lung Diseases. *J. Inflamm. Res.* 14, 2079–2090. doi:10.2147/jir.s307081

Yan, N., and Zhang, J.-J. (2019). The Emerging Roles of Ferroptosis in Vascular Cognitive Impairment. *Front. Neurosci.* 13, 811. doi:10.3389/fnins.2019.00811

Yang, W. S., SriRamaratnam, R., Welsch, M. E., Shimada, K., Skouta, R., Viswanathan, V. S., et al. (2014). Regulation of Ferroptotic Cancer Cell Death by GPX4. *Cell* 156 (1-2), 317–331. doi:10.1016/j.cell.2013.12.010

Yang, Y., Luo, M., Zhang, K., Zhang, J., Gao, T., Connell, D. O., et al. (2020). Nedd4 Ubiquitylates VDAC2/3 to Suppress Erastin-Induced Ferroptosis in Melanoma. *Nat. Commun.* 11 (1), 433. doi:10.1038/s41467-020-14324-x

Yang, W.-H., Lin, C.-C., Wu, J., Chao, P.-Y., Chen, K., Chen, P.-H., et al. (2021). The Hippo Pathway Effector YAP Promotes Ferroptosis via the E3 Ligase SKP2. *Mol. Cancer Res.* 19 (6), 1005–1014. doi:10.1158/1541-7786.mcr-20-0534

Zhang, D., Shen, J., Wang, C., Zhang, X., and Chen, J. (2009). GSH-Dependent iNOS and HO-1 Mediated Apoptosis of Human Jurkat Cells Induced by Nickel(II). *Environ. Toxicol.* 24 (4), 404–414. doi:10.1002/tox.20440

Zhang, X., Min, X., Li, C., Benjamin, I. J., Qian, B., Zhang, X., et al. (2010). Involvement of Reductive Stress in the Cardiomyopathy in Transgenic Mice with Cardiac-Specific Overexpression of Heat Shock Protein 27. *Hypertension* 55 (6), 1412–1417. doi:10.1161/hypertensionaha.109.147066

Zhang, L., Cai, X., Chen, K., Wang, Z., Wang, L., Ren, M., et al. (2011). Hepatitis B Virus Protein Up-Regulated HLJ1 Expression via the Transcription Factor YY1 in Human Hepatocarcinoma Cells. *Virus. Res.* 157 (1), 76–81. doi:10.1016/j.virusres.2011.02.009

Zhao, R., Davey, M., Hsu, Y.-C., Kaplanek, P., Tong, A., Parsons, A. B., et al. (2005). Navigating the Chaperone Network: An Integrative Map of Physical and Genetic Interactions Mediated by the Hsp90 Chaperone. *Cell* 120 (5), 715–727. doi:10.1016/j.cell.2004.12.024

Zhao, T., Guo, X., and Sun, Y. (2021). Iron Accumulation and Lipid Peroxidation in the Aging Retina: Implication of Ferroptosis in Age-Related Macular Degeneration. *Aging Dis.* 12 (2), 529–551. doi:10.14336/ad.2020.0912

Zhou, Y., Liao, J., Mei, Z., Liu, X., and Ge, J. (2021). Insight into Crosstalk between Ferroptosis and Necroptosis: Novel Therapeutics in Ischemic Stroke. *Oxid Med. Cel Longev* 2021, 9991001. doi:10.1155/2021/9991001

Zhu, S., Zhang, Q., Sun, X., Zeh, H. J., 3rd, Lotze, M. T., Kang, R., et al. (2017). HSPA5 Regulates Ferroptotic Cell Death in Cancer Cells. *Cancer Res.* 77 (8), 2064–2077. doi:10.1158/0008-5472.can-16-1979

Zhu, Y., Zhang, C., Huang, M., Lin, J., Fan, X., and Ni, T. (2021). TRIM26 Induces Ferroptosis to Inhibit Hepatic Stellate Cell Activation and Mitigate Liver Fibrosis Through Mediating SLC7A11 Ubiquitination. *Front. Cel Dev. Biol.* 9, 644901. doi:10.3389/fcell.2021.644901

Conflict of Interest: The authors declare that the research was conducted in the absence of any commercial or financial relationships that could be construed as a potential conflict of interest.

Publisher's Note: All claims expressed in this article are solely those of the authors and do not necessarily represent those of their affiliated organizations, or those of the publisher, the editors and the reviewers. Any product that may be evaluated in this article, or claim that may be made by its manufacturer, is not guaranteed or endorsed by the publisher.

frontiers | Frontiers in Cell and Developmental Biology

TYPE Review
PUBLISHED 13 September 2022
DOI 10.3389/fcell.2022.951116

OPEN ACCESS

EDITED BY
Bilal Çig,
Ahi Evran University Medicine Faculty Department of Physiology, Turkey

REVIEWED BY
Laurence Vernis,
Institut National de la Santé et de la Recherche Médicale (INSERM), France
Yong Liu,
Xuzhou Medical University, China

*CORRESPONDENCE
Ying Xin,
xiny@jlu.edu.cn
Xin Jiang,
jiangx@jlu.edu.cn

SPECIALTY SECTION
This article was submitted to Cell Death and Survival, a section of the journal Frontiers in Cell and Developmental Biology

RECEIVED 23 May 2022
ACCEPTED 23 August 2022
PUBLISHED 13 September 2022

CITATION
Su J, Bian C, Zheng Z, Wang H, Meng L, Xin Y and Jiang X (2022), Cooperation effects of radiation and ferroptosis on tumor suppression and radiation injury. *Front. Cell Dev. Biol.* 10:951116. doi: 10.3389/fcell.2022.951116

Cooperation effects of radiation and ferroptosis on tumor suppression and radiation injury

Jing Su[1,2,3], Chenbin Bian[1,2,3], Zhuangzhuang Zheng[1,2,3], Huanhuan Wang[1,2,3], Lingbin Meng[4], Ying Xin[5]* and Xin Jiang[1,2,3]*

[1]Jilin Provincial Key Laboratory of Radiation Oncology & Therapy, The First Hospital of Jilin University, Changchun, China, [2]Department of Radiation Oncology, The First Hospital of Jilin University, Changchun, China, [3]NHC Key Laboratory of Radiobiology, School of Public Health, Jilin University, Changchun, China, [4]Department of Hematology and Medical Oncology, Moffitt Cancer Center, Tampa, FL, United States, [5]Key Laboratory of Pathobiology, Ministry of Education, Jilin University, Changchun, China

Ferroptosis is a kind of oxidative stress-dependent cell death characterized by iron accumulation and lipid peroxidation. It can work in conjunction with radiation to increase reactive oxygen species (ROS) generation and disrupt the antioxidant system, suppressing tumor progression. Radiation can induce ferroptosis by creating ROS, depleting glutathione, activating genes linked to DNA damage and increasing the expression of acyl-CoA synthetase long-chain family member 4 (ACSL4) in tumor cells. Furthermore, ferroptosis can enhance radiosensitivity by causing an iron overload, destruction of the antioxidant system, and lipid peroxidation. Radiation can also cause ferroptosis in normal cells, resulting in radiation injury. The role of ferroptosis in radiation-induced lung, intestinal, skin, and hematological injuries have been studied. In this review, we summarize the potential mechanisms linking ferroptosis, oxidative stress and radiation; analyze the function of ferroptosis in tumor suppression and radiation injury; and discuss the potential of ferroptosis regulation to improve radiotherapy efficacy and reduce adverse effects.

KEYWORDS

ferroptosis, oxidative stress, reactive oxygen species (ROS), GPX4, SLC7A11, radiotherapy

1 Introduction

Cancer is one of the most common causes of death worldwide. About 19.3 million new cancer cases and 10.0 million cancer deaths occurred in 2020 (Sung et al., 2021). Radiotherapy is an effective strategy to treat cancer. Ionizing radiation (IR) can directly damage cellular DNA and produce double-strand breaks, resulting in death-related events such as cell cycle arrest, autophagy, and apoptosis (Delaney et al., 2005). Furthermore, radiation can ionize the cytoplasm and mitochondria, resulting in a large amount of reactive oxygen species (ROS) that interact with biological macromolecules and cause permanent damage and cell death. However, radiotherapy frequently fails to achieve the desired effect in various tumor

types (Taylor et al., 2018; Pilié et al., 2019; Huang and Zhou, 2020). Radiation resistance leads to poor prognosis and ultimately to tumor relapse and metastasis in patients with cancer (Rycaj and Tang, 2014). Therefore, safe and effective strategies must be identified to enhance radiosensitivity. Radiotherapy (RT) is a double-edged sword. Despite the continuous advancements in precision radiotherapy technology, radiation-induced damage is inevitable (De Ruysscher et al., 2019; Wei et al., 2019). Prevention of radiation damage is an urgent and serious issue.

Ferroptosis was first introduced in 2012 as a highly iron-dependent form of non-apoptotic cell death (Dixon et al., 2012). Ferroptosis differs from apoptosis, necrosis, autophagy, and pyroptosis in terms of morphology, metabolic response, and gene expression (Yagoda et al., 2007; Li et al., 2020; Bertheloot et al., 2021) (Table 1). Morphologically, ferroptosis is characterized by evident mitochondrial contraction, increased membrane density, and loss of mitochondrial crest rather than chromatin aggregation (such as apoptosis) or autophagosome production (such as autophagy) (Bertheloot et al., 2021). At the point of biochemical reaction, ferroptosis is mainly related to the peroxidation of polyunsaturated fatty acid phospholipids (PUFA-PLs). Glutathione peroxidase 4 (GPX4) is a crucial factor in ferroptosis. Inhibition of its activity results in abnormal cell metabolism, weakened antioxidant capacity, and excessive lipid ROS, leading to cell death (Li et al., 2020). Furthermore, the tumor suppressor genes P53 and BAP1 can regulate ferroptosis, but the regulatory mechanisms and effects require further investigation (Jiang et al., 2015; Zhang et al., 2018).

Recent studies have demonstrated that ferroptosis plays a crucial role in radiotherapy-induced cell death (Chen et al., 2021; Lei et al., 2021). However, further research into the exact mechanisms of ferroptosis and radiation is required. In this study, the role and mechanism of ferroptosis in radiation were examined to investigate treatment options that may improve radiotherapy efficacy and reduce radiation damage.

2 The role of ferroptosis in tumors

Ferroptosis is regulated by the iron metabolism, lipid metabolism, and antioxidant systems (Figure 1). Acyl-CoA synthetase long-chain family member 4 (ACSL4) and lysophosphatidylcholine acyltransferase 3 (LPCAT3) are the critical mediators of polyunsaturated phospholipid (PUFA-PL) synthesis. ACSL4 catalyzes the binding of free polyunsaturated fatty acids (PUFAs) to CoA to generate PUFA-CoA (Doll et al., 2017), which is then esterified by

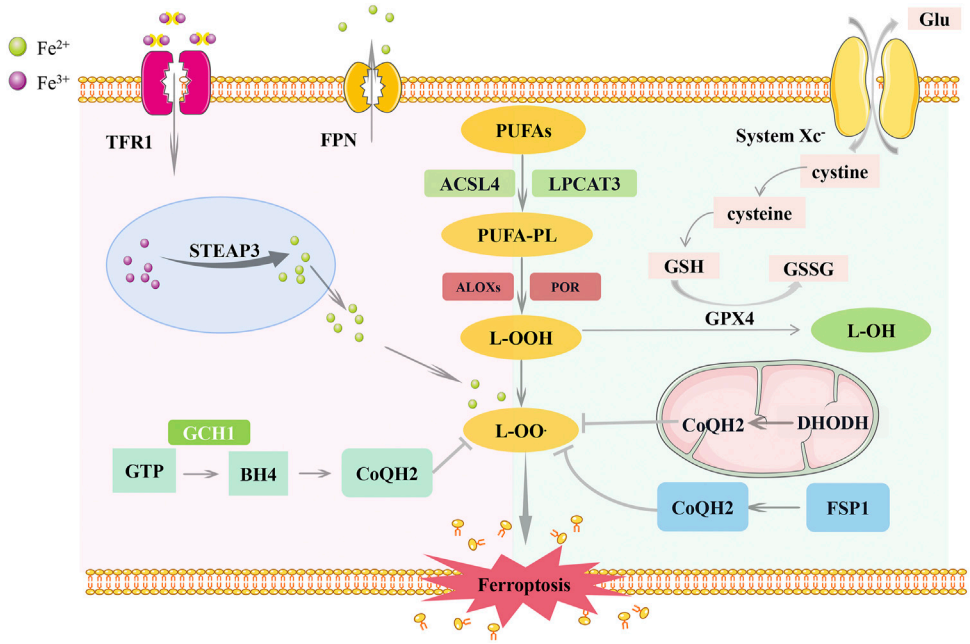

FIGURE 1
Regulatory pathways of ferroptosis. Ferroptosis is co-regulated by iron metabolism, lipid metabolism, and antioxidant systems. The inhibition of lipid peroxidation is mainly mediated by the SLC7A11-GSH-GPX4 pathway, FSP1-CoQ10-NAD (P)H pathway, GCH1-BH4-DHFR pathway and DHO-DHODH-OA pathway. Among them, the FSP1 pathway exists in the cytoplasm, the DHODH pathway exists in the mitochondria, and the GPX4 pathway plays a role in both. *SLC7A11, Cystine/glutamate antiporter solute carrier family seven member 11; GPX4, glutathione peroxidase 4; GSH, glutathione; FSP1, ferroptosis suppressor protein 1; GGH1, GTP Cyclohydrolase 1; BH4, tetrahydrobiopterin; DHFR, dihydrofolate reductase; DHO, dehydrogenation of dihydroorotate; DHODH, Dihydroorotate Dehydrogenase; OA, orotate; ACSL4, acyl-CoA synthetase long-chain family member 4; LPCAT3, lysophosphatidylcholine acyltransferase 3; ALOXs, arachidonate lipoxygenases; POR, cytochrome P450 oxidoreductase.*

LPCAT3 and linked to phospholipids to form PUFA-PLs (Dixon et al., 2015). PUFA-PLs can be oxidized by cytochrome P450 oxidoreductase (POR) and arachidonate lipoxygenases (ALOXs) to produce lipid peroxides (L-OOH) (Dixon et al., 2015; Shintoku et al., 2017; Zou et al., 2020b). Typically, L-OOH is reduced to the corresponding alcohols by GPX4 (Yang et al., 2014). However, a large amount of L-OOH reacts with Fe^{2+} to produce hydroxyl radicals (L-$OO^{\cdot}$) when Fe^{2+} and PUFAs are overloaded, or the expression of glutathione peroxidase (GPX4) and glutathione (GSH) is reduced. Accumulation of l-$OO^{\cdot}$ results in lipid peroxidation of membrane phospholipids, ultimately leading to ferroptosis (Dixon et al., 2012). Recently, ferroptosis was observed in many types of cancer, such as head and neck (Tang et al., 2021), breast (Zhang et al., 2021b), and lung cancers (Ren et al., 2021). Ferroptosis can function in cancer progression and suppression by regulating gene expression and the tumor microenvironment (TME) (Wang et al., 2020c).

P53 is one of the tumor suppressor genes that play a critical role in tumor suppression. It can reportedly regulate genes involved in ferroptosis to suppress tumor development. *P53* can downregulate the expression of cystine/glutamate antiporter solute carrier family seven member 11 (SLC7A11), a critical factor in glutathione synthesis, to inhibit GSH synthesis (Jiang et al., 2015). *P53* can also induce ferroptosis by promoting the expression of arachidonate 15-lipoxygenase (ALOX15) via its transcriptional target spermidine/spermine N1-Acetyltransferase 1 (SAT1) (Ou et al., 2016). In addition, it can act on other enzymes that control phospholipid and iron contents, such as prostaglandin-endoperoxide synthase 2 (PTGS2) and ferredoxin reductase (FDXR), to promote ROS production (Yang et al., 2014; Zhang et al., 2017). However, *P53* can also inhibit ferroptosis. Dipeptidyl peptidase 4 (DPP4) is a regulatory molecule involved in ferroptosis and lipid metabolism. It binds to nicotinamide adenine dinucleotide phosphate oxidase 1 (NOX1) to mediate ROS production. *P53* can reduce DDP4 levels and block its binding with NOX1 to inhibit ferroptosis (Xie et al., 2017). Besides, *P53* can activate cyclin-dependent kinase inhibitor 1 (CDKN1A)/p21 to increase GSH content, thus inhibiting ferroptosis (Tarangelo et al., 2018). The regulation of *P53* in ferroptosis seems to be highly dependent on the environment, although the exact mechanism remains unknown (Kang et al., 2019; Liu et al., 2020). *BAP1*, another tumor suppressor gene, has also been linked to ferroptosis. *BAP1* can reduce histone 2A ubiquitination (H2Aub) on chromatin to suppress the expression of SLC7A11, thus inducing ferroptosis (Zhang et al., 2018).

The TME refers to the internal environment closely related to tumor generation and progression. According to several researches, ferroptosis plays a crucial role in controlling immune cell function. On the one hand, the ferroptosis of immune cells reduce their number and function, impairing the immune response. On the other side, the ferroptosis of non-immune cells will cause the release of damage-associated molecular pattern (DAMP) and trigger immune responses (Wang and Lu, 2022). Zou et al. (Wang et al., 2019) found that IFN γ derived from immunotherapy-activated $CD8^+$ T cells could down-regulate SLC3A2 and SLC7A11 levels, leading to decreased cystine uptake and enhanced tumor lipid oxidation and ferroptosis. Besides, radiation can also inhibit the expression of SLC7A11, synergistic with $CD8^+$ T cells to improve tumor control (Lang et al., 2019). Thus, ferroptosis may be the focus for the development of effective combinatorial cancer therapy. In addition, ferroptosis drives the polarization of macrophages in the TME. Autophagy-dependent ferroptosis (ADF) enables the release of the $KRAS^{G12D}$ protein from cancer cells into the TME, and $KRAS^{G12D}$ induces the transformation of macrophages into an M2 phenotype, accelerating cancer development (Dai et al., 2020). However, Hsieh et al. found that Zero-valent-iron (ZVI) nanoparticle (NP) which functions like a ferroptosis inducer could efficiently repolarizes macrophages from M2 phenotype to M1 phenotype (Hsieh et al., 2021). Therefore, the relationship between ferroptosis and macrophage repolarization still deserves further discussion. Ferroptosis is also involved in the treatment of B lymphocytes immune-related diseases, such as immune deficiency disease and diffuse large B-cell lymphoma (DLBCL) (Criscitiello et al., 2020; Schmitt et al., 2021), but there is insufficient evidence showing a link between ferroptosis and tumor-infiltrating B lymphocytes. What's more, hypoxia, a well-known feature of the TME, is also involved in ferroptosis (Su et al., 2022). Hypoxia-inducible factor (HIF)-1α can prevent ferroptosis by inhibiting the expression of SLC7A11 (Jiang et al., 2017; Fan et al., 2021). However, HIF-2α can stimulate the expression of hypoxia-induced lipid droplet-associated proteins (HILPDA) and enrich the amount of polyunsaturated lipids in cells to increase their sensitivity to ferroptosis (Zou et al., 2019). In general, ferroptosis plays a vital role in the development and progression of malignancies. Additional research into its mechanisms may lead to new cancer therapy options.

3 Radiation induced ferroptosis in tumor cells

Radiation was assumed to primarily cause apoptosis; however, new studies have discovered a large amount of evidence demonstrating a strong link between radiation and ferroptosis (Lang et al., 2019; Lei et al., 2020; Ye et al., 2020) (Figure 2). Lang et al. (2019) observed that IR-induced ferroptosis is mainly associated with lipid peroxidation in tumor cells. They found that irradiation can activate the ataxia-telangiectasia mutated gene (*ATM*), inhibit the expression of SLC7A11, and cause lipid peroxidation, thereby inducing ferroptosis. Lei et al. (2020) subsequently verified this conclusion and suggested that IR significantly increases ACSL4 expression in cancer cells, with typical morphological changes in ferroptosis. However, they found that IR induced a

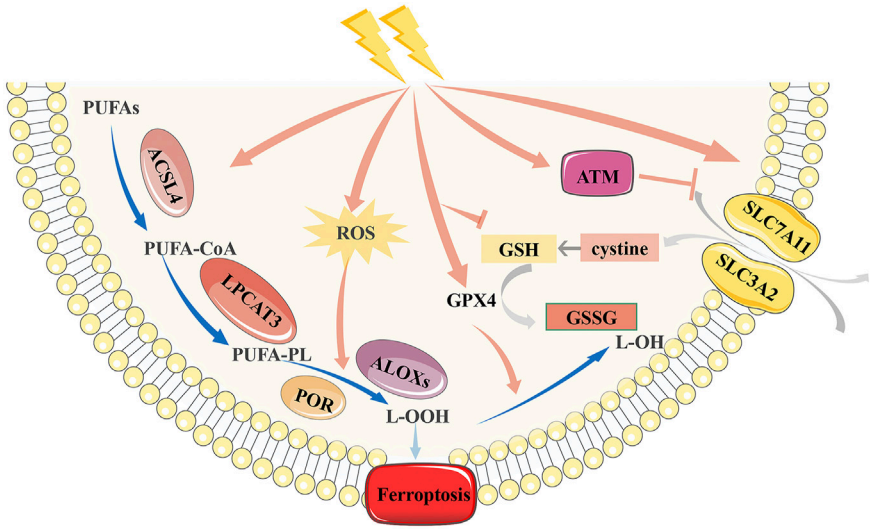

FIGURE 2
Mechanism of ferroptosis induced by radiotherapy. Radiation can inhibit the antioxidant function of SLC7A11 and GSH, and up-regulate the expression of ACSL4, thus inducing ferroptosis. However, radiation can aslo up-regulate the expression of SLC7A11 and GPX4 due to adaptive response. *SLC7A11, Cystine/glutamate antiporter solute carrier family seven member 11; GPX4, glutathione peroxidase 4; GSH, glutathione; ACSL4, acyl-CoA synthetase long-chain family member 4.*

significant upregulation of ferroptosis suppressor genes, including *SLC7A11* and *GPX4*, which may be an adaptive response. Ye et al. (2020) further refined the mechanism of IR-induced ferroptosis. GSH is a vital regulator of the antioxidant system, which can convert H_2O_2 to H_2O under the action of GPX4, thus protecting cells from external stimuli (Brigelius-Flohé, 2006). IR can consume GSH by generating a large number of ROS and limit the synthesis of GSH by inhibiting cystine uptake, finally leading to GSH depletion. And GSH shortage will impair the activity of the cellular antioxidant system and cause ferroptosis.

In addition to killing tumor cells via ROS, IR can directly damage cellular DNA and produce double-strand breaks. Various lines of evidence imply that IR-induced ferroptosis has little effect on DNA damage, whereas IR-induced DNA damage appears to affect ferroptosis through diverse mechanisms (Lei et al., 2021). Many DNA damage response (DDR) components regulate ferroptosis. For example, *ATM* activation promotes ferroptosis through the metal regulatory transcription factor 1 (MTF1) -Ferritin/FPN1 axis and SLC7A11-GSH pathway (Lang et al., 2019; Chen et al., 2020). *P53* also regulates ferroptosis by modulating DPP4, SAT1, and other factors (Ou et al., 2016; Xie et al., 2017). However, these ferroptosis-regulating target genes are not directly involved in the canonical phenotypic effects of DDR; most of them affect ferroptosis using noncanonical mechanisms. Therefore, it is reasonable to infer that ferroptosis represents a back-up death method of canonical cell death for cells with DNA damage. Further characterization of their interactions may generate new insights into tumor suppression.

To sum up, IR-induced ferroptosis is regulated by four pathways. First, IR promotes ROS production and upregulates ACSL4 expression. IR regulates the expression of SLC7A11 according to the external environment. Moreover, IR directly leads to GSH depletion and the destruction of antioxidant systems. Besides, IR-induced DNA damage also regulates the occurrence of ferroptosis. Ferroptosis accounts for a large proportion of radiation-induced cell death cases. This discovery facilitates the application of ferroptosis inducers (FINs) in radiotherapy.

4 Inducing ferroptosis enhances radiosensitivity

With the increasing application of radiotherapy, improving the radiosensitivity of tumor cells to increase its effectiveness has become an increasingly important issue. The iron, lipid, and antioxidant systems involved in regulating ferroptosis can adjust radiosensitivity (Zhang and Martin, 2014; Theriot et al., 2016; Nisticò et al., 2021). Therefore, the relationship between ferroptosis and radiosensitivity is worth investigating.

4.1 Iron metabolism and radiosensitivity

Iron is a vital component of the human body and is linked to metabolism, cell death, and the development of various diseases. Deferoxamine (DFO) was used to eliminate FIN-induced cell

death caused by FINs, implying that iron is a vital element in ferroptosis (Dixon et al., 2012). In the human body, iron absorption mainly occurs in the intestine, where Fe^{2+} can be oxidized by ceruloplasmin to Fe^{3+} and binds to transferrin (TF) on the cell membrane to form TF-Fe^{3+}. TF-Fe^{3+} can enter cells by integrating with TF receptor 1 (TFR1) (Frazer and Anderson, 2014). Fe^{3+} is then reduced to Fe^{2+} by six transmembrane epithelial antigens of prostate 3 (STEAP3) and stored in the labile iron pool and ferritin (Bogdan et al., 2016). When Fe^{2+} is overloaded, ferroptosis is induced.

In addition, iron homeostasis plays a vital role in radiotherapy. Rapidly dividing tumor cells require much more iron than normal cells; therefore, iron deprivation is a new cancer treatment option. The iron-chelating agent can reduce free Fe^{2+} content and arrest cells at the G2/M phase, thereby enhancing the radiosensitivity of cancer cells (Turner et al., 2005). In addition, Mir-7-5p could lead to ferroptosis resistance by downregulating mitoferrin and reducing Fe^{2+} content. The application of an Mir-7-5p inhibitor can reverse this effect and improve radiosensitivity (Tomita et al., 2019).

Thus, iron homeostasis serves as a link between ferroptosis and RT. Other iron-metabolizing proteins, such as heat shock protein B1 (HSPB1) (Chen et al., 2006) and iron response element-binding protein 2 (IREB2) (Mumbauer et al., 2019; Li et al., 2020), may also be potential targets for enhancing radiosensitivity.

4.2 Lipid metabolism and radiosensitivity

There is growing evidence that lipid metabolism, ferroptosis, and radiation are inextricably linked. Ferroptosis is mainly caused by the peroxidation of PUFA-PLs (Yang and Stockwell, 2016). Previously, this process was thought to be primarily catalyzed by arachidonate lipoxygenases (ALOXs). However, recent studies have shown that cytochrome P450 oxidoreductase (POR) plays a more significant role (Yan et al., 2021). Radiation can also activate ALOXs and POR to mediate lipid peroxidation (Wei et al., 2019). The radiotherapeutic efficacy in head and neck cancer has been proven to be enhanced by 15-LOX overexpression (Yang et al., 2008). However, 12-LOX has been linked to radioresistance in prostate cancer cells (Lövey et al., 2013). ACSL4 is a crucial protein involved in the formation of PUFA-PLs. ACSL4 knockout cells show superior resistance to ferroptosis (Doll et al., 2017). However, ACSL4 also negatively affects radiosensitivity in breast cancer by regulating forkhead box M1 (FOXM1) to enhance the DNA damage response and inhibit apoptosis (Kwon et al., 2021). These results demonstrated that enzymes related to phospholipids play a complex role in radiation and ferroptosis. This phenomenon is possible because they also participate in radiation-induced inflammatory responses (Kim et al., 2018). More research into these enzymes and their lipid metabolites will help us better understand the link between radiation and ferroptosis, allowing us to improve the efficacy of radiotherapy.

In addition, peroxisomes participate in ferroptosis by synthesizing ether phospholipids (Zou et al., 2020a). Ether phospholipids represent a group of phospholipids containing fatty alcohol at the stereospecific numbering (sn)-1 position. Plasmalogens appeared to be the most abundant. Its production is regulated by the fatty acyl-CoA reductase 1 (FAR1)–transmembrane 189 (TMEM189) axis (Cui et al., 2021) (Figure 3). FAR1 converts saturated fatty alcohols to unsaturated fatty alcohols and promotes the formation of alkyl ether lipids. The *TMEM189* gene encodes plasmanylethanolamine desaturase, introducing a vinyl ether double bond into alkyl ether lipids and converting alkyl-ether lipids into plasmalogens (Werner et al., 2020). Zou et al. (2020a) demonstrated that peroxisome-mediated ferroptosis is only related to unsaturated fatty acids on ether lipids but not alkyl and vinyl groups. Cui et al. (2021) suggested that vinyl groups in plasmalogens are at least partly responsible for the prevention of ferroptosis. The regulation of ferroptosis by ether glycerophospholipids is related to their content and cell localization (Balgoma and Hedeland, 2021). As a result, the differences in the above two outcomes may be caused by the different ratios of alkyl-ether phospholipids to plasmalogens in different cells. As alkyl phospholipid ether analogs have been proven to enhance the radiosensitivity of solid tumors (Elsaid et al., 2018), further research on the FAR1-TMEM189 pathway may provide new targets for radiosensitization.

4.3 Antioxidant system and radiosensitivity

Ferroptosis is strongly related to oxidative stress, and there are numerous overlapping regulation pathways. Antioxidants like superoxide dismutase (SOD), GSH, and NADPH can prevent tumor cell death by inhibiting oxidative stress. Studies have shown that ferroptosis is regulated by antioxidant systems as well. Four pathways maintain redox homeostasis during ferroptosis: the GSH/GPX4, FSP1-CoQ10-NAD (P)H, GCH1-BH4-DHFR, and DHO-DHODH-OA pathways (Bersuker et al., 2019; Doll et al., 2019; Mao et al., 2021). The radiosensitivity of tumor cells can be enhanced by adjusting these regulatory pathways (Lei et al., 2020).

4.3.1 SLC7A11-GSH-GPX4 pathway

Together, cystine uptake, GSH biosynthesis, and GPX4 activation constitute a robust defense system that keeps lipid hydroperoxides below toxicity thresholds to prevent ferroptosis. SLC7A11 (also known as xCT) is a functional subunit of system $X_{c,}^{-}$ which can exchange extracellular cystine with intracellular glutamate in a 1:1 ratio (Bannai, 1986). When cystine enters the cell, it is reduced to cysteine,

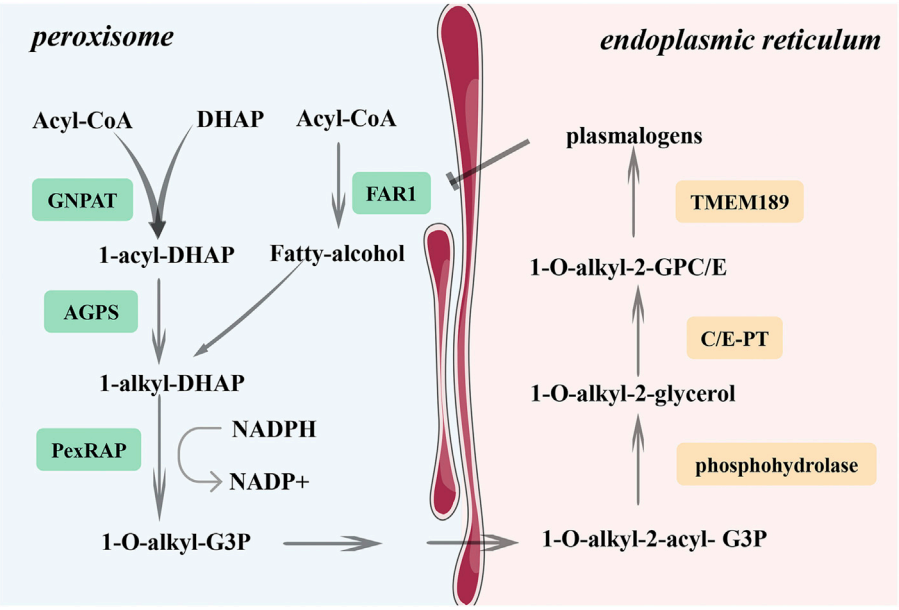

FIGURE 3
Synthesis of plasmalogens. FAR1 is a key enzyme in the synthesis of plasmalogen. It can convert saturated fatty alcohols into unsaturated fatty. The *TMEM189* gene encodes plasmanylethanolamine desaturase, which could introduce the vinyl ether double bond into plasmalogens and convert alkyl-ether lipids into plasmalogens. However, FAR1 is regulated by the negative feedback of phospholipid level, and it can be inhibited by an increase in plasmalogens content. *FAR1, fatty acyl-CoA reductase 1; GNPAT, glyceronephosphate-O-acyltransferase; AGPS, alkylglycerone phosphate synthase.*

which is the rate-limiting precursor of glutathione synthesis. GPX4 uses GSH as a cofactor to reduce PL-OOH to nontoxic PL-alcohols, thereby inhibiting ferroptosis. In addition, GPX4 maturation requires selenium. The maturation of selenocysteine tRNA is controlled by the mevalonate (MVA) pathway (Warner et al., 2000). Therefore, the regulation of the MVA pathway can also control ferroptosis.

Erastin is a classic FIN that can directly inhibit system X_c^- and thus decrease the level of glutathione (Dixon et al., 2012). Erastin increases the radiosensitivity of lung cancer cells by inducing ferroptosis (Pan et al., 2019). Studies have also confirmed that erastin can achieve radiosensitizing effects by consuming GSH and reducing antioxidant capacity *in vivo* (Shibata et al., 2019). In addition, FINs targeting GPX4, such as RSL3 and ML162, can enhance the radiosensitivity of tumor cells (Lei et al., 2020). Thus, inhibition of the SLC7A11-GSH-GPX4 pathway can achieve radiosensitization by promoting ferroptosis, and SLCA11, GPX4, and GSH should serve as targets for radiosensitization.

The genes upstream of *SLC7A11* can also regulate radiosensitivity. Nuclear factor erythroid 2-related factor 2 (*Nrf-2*) and activating transcription factor 4 (*ATF4*) can promote *SLC7A11* expression at the transcriptional level (Lewerenz and Maher, 2009). Hyperactivation of Nrf-2 leads to radiation resistance by inducing SLC7A11 expression and reducing lipid peroxidation levels *in vitro* (Feng et al., 2021a). Furthermore, RNA-binding proteins participate in the regulation of ferroptosis. Recently, the RNA-binding motif, single-stranded-interacting protein 1 (RBMS1), an RNA-binding protein, was found to directly interact with the translation initiation factor eIF3d, connecting the 3′- and 5′-UTRs of *SLC7A11*. RBMS1 ablation can sensitize radioresistant lung cancer cells to radiation by inhibiting SLC7A11 translation and inducing ferroptosis (Zhang et al., 2021c).

In addition to SLC7A11, other factors that regulate GPX4 and GSH levels can be radiation targets. 5-aminolevulinic acid (5-ALA) is a natural amino acid widely used in cancer treatment. Its radiosensitizing effect has been reported in various cancers (Yamamoto et al., 2012; Yamada et al., 2019; Tung et al., 2021). A previous study confirmed that 5-ALA promotes the synthesis of GPX4 and induces ferroptosis (Shishido et al., 2021). Transmembrane protein 27 (CLTRN, also known as TMEM27) is a type Ia transmembrane (Akpinar et al., 2005), which can be regulated by the Nrf-1/RAN/DLD protein complex to deplete GSH and enhance the radiosensitivity of hepatocellular carcinoma (HCC) cells (Yuan et al., 2021). Therefore, the SLC7A11-GSH-GPX4 pathway regulates radiosensitization, which may be related to ferroptosis.

4.3.2 Ferroptosis suppressor protein 1-CoQ10-NAD (P)H pathway

Ferroptosis suppressor protein 1 (FSP1) [also known as apoptosis-inducing factor mitochondrial 2 (AIFM2)] is a potent ferroptosis suppressor. According to one study, the FSP1-CoQ(10)-NAD(P)H pathway exists as a separate parallel system that, in conjunction with GPX4, inhibits phospholipid peroxidation and ferroptosis. FSP1 is recruited to the plasma membrane by myristoylation, where it reduces coenzyme Q10 (CoQ) to ubiquinol (CoQH2) with the help of NAD(P)H. CoQH2 then suppresses ferroptosis by capturing lipophilic free radicals (Bersuker et al., 2019; Doll et al., 2019). As a result, CoQH2 production is critical for the proper operation of the FSP1-CoQ(10)-NAD(P)H pathway.

FIN56, a special ferroptosis inducer, can bind and activate squalene synthase, leading to depletion of the endogenous antioxidant CoQ10 (Shimada et al., 2016). FIN56 can induce lipid peroxidation and significantly radiosensitize lung cancer cells (Lei et al., 2020). Statins are lipid-lowering drugs that induce ferroptosis. It can inhibit GPX4 by regulating selenoprotein and CoQ biosynthesis through the MVA pathway (Warner et al., 2000; Santoro, 2020). Statins have been confirmed to act as radiation sensitizers in various tumor cells (Hutchinson and Marignol, 2017; Jin et al., 2018; Aschenbrenner et al., 2021). In general, the FSP1-CoQ (10)-NAD(P)H pathway is closely related to radiosensitivity, with CoQ being the most critical target.

4.3.3 GTP-cyclohydrolase-1-Tetrahydrobiopterin-dihydrofolate reductase pathway

Tetrahydrobiopterin (BH4) is a redox-active cofactor that boosts CoQH2 production (Crabtree et al., 2009). The formation of BH4 and BH2 is induced by the expression of GTP-cyclohydrolase-1 (GCH1), and BH2 can be reduced to BH4 by dihydrofolate reductase (DHFR). GCH1 is the primary enzyme involved in this process. Kraft et al. 2020 observed that GCH1 overexpression protects cells against ferroptosis triggered by FINs, such as RSL3, IKE, and GPX4. The GCH1-BH4-phospholipid axis controls the endogenous production of BH4, the abundance of CoQ10, and the depletion of unusual phospholipids with two polyunsaturated fatty acyl tails. Soula et al. (2020) demonstrated that tumor cells are sensitive to RSL3, which can directly inactivate GPX4 when GCH1 is deleted or inhibited. Furthermore, inhibiting the action of DHFR with methotrexate can also increase the sensitivity of cells to ferroptosis. These findings imply that the GCH1-BH4-DHFR route, as an endogenous antioxidant pathway, inhibits ferroptosis via a mechanism unrelated to the GPX4 system.

GCH1 and DHFR are highly expressed in various cancers, and radiation can further activate BH4 metabolic enzymes to reduce radiotherapy effects, proving that BH4 metabolic enzymes are possible hallmarks and targets of radiosensitivity (Yan et al., 2020; Feng et al., 2021b). Liang et al. (2020) synthesized a series of 2,4-diaminopteridine analogs as DHFR inhibitors and demonstrated that inhibiting DHFR improves the irradiation effect on cervical cancer cells.

4.3.4 Dihydroorotate dehydrogenase-orotate pathway

Dihydroorotate dehydrogenase (DHODH) is a flavin-dependent enzyme found primarily on the inner membrane of mitochondria and is required for *de novo* pyrimidine nucleotide synthesis. It can catalyze the conversion of dihydroorotate (DHO) to orotate (OA) (Femia et al., 2021). Mao et al. (2021) found that, while DHODH oxidized DHO to OA, CoQ was reduced to CoQH2, thus inhibiting ferroptosis. DHODH works in tandem with mitochondrial GPX4 but is unaffected by cytosolic GPX4 or FSP1. Mechanistically, DHODH eliminates L-OO· through CoQH2, thus playing a synergistic role with GPX4 in inhibiting ferroptosis (Femia et al., 2021).

Pharmacological inhibition of DHODH can effectively reduce the viability of small-cell lung cancer cells (Li et al., 2019a). The relationship between DHODH and radiosensitivity remains unclear. However, ultraviolet-B (UVB) can activate DHODH, and DHODH inhibition can decrease DNA repair ability (Hosseini et al., 2019). This result proves that the relationship between DHODH and radiosensitivity is worth investigating.

Radiation can generate superfluous ROS, which destroys proteins, DNA, lipids, and other biological macromolecules in cells, leading to cell death (Wang et al., 2020b). The radiosensitivity of tumor cells can be improved by increasing ROS levels and promoting oxidative stress. However, excessive ROS can activate the antioxidant system and render radiation-resistant tumor cells. Ferroptosis is accompanied by reactive oxygen species (ROS) overload and redox imbalance.

5 Inhibition of ferroptosis can reduce radiation damage

Despite ongoing advancements in radiation technology, radiation damage to normal tissues is unavoidable (Liu et al., 2021). Overcoming the side effects of radiotherapy remains a hot research topic. Radiation can induce ferroptosis in both tumor and normal cells. Ferroptosis has been reported to play a role in the radiation-induced lung, intestinal, skin, and hematopoietic injuries. Inhibition of ferroptosis may be an effective way to alleviate radiation injury (Table 2).

TABLE 1 The difference between ferroptosis, apoptosis, autophagy, necroptosis, and pyroptosis.

	Ferroptosis	Apoptosis	Autophagy	Necroptosis	Pyroptosis
Morphology	Obvious mitochondrial contraction, increased membrane density	Cell shrinkage, chromatincon densation,	Formation of autophagosomes	Swelling of the cytoplasm and organelles, rupture of the cell membrane	Swelling of cells, rupture of the cell membrane
	reduced or disappeared mitochondrial cristae	formation of apoptotic bodies and disintegration of the cytoskeleton			
	the nuclear volume doesn't change	no significant changes in mitochondrial structure			
Biochemical reaction	Iron accumulation and plasma membrane lipid peroxidation	DNA strand breaks	Lysosomal activity is enhanced	Metabolic functions such as ion gradient and ATP production are irreversibly lost	Cell contents and pro-inflammatory cytokines release and inflammasome sensors active
Gene expression	GPX4, SLC7A11, NRF2, ATF4, P53, HSPB1, ACSL4, FSP1, DHODH, TFR1	Caspase, Bcl-2, Bax, P53, Fas	ATG5, ATG7, Beclin-1, DRAM3, TFEB, MAPLC3	RIP1, RIP3	GSDMA, GSDMC, GSDMD, GSDME

TABLE 2 Targets and mechanisms of ferroptosis inhibitors alleviating radiation injury.

Damage Type	Drugs	Target	Mechanism	References
Radiation-induced lung injury	Liproxstatin-1	GPX4	Increase GPX4 levels	(Li et al., 2019b)
	GsMTx4	PIEZO1	Inhibit PIEZO1/Ca2+/calpain pathway and increase the expression GPX4 and SLC7A11	Guo et al. (2021)
	PD151746	calpain	Inbibit calpain and increase the expression GPX4 and SLC7A11	Guo et al. (2021)
	NVP-AUY922	HSP90	Inhibit HSP90/CMA pathway and inhibit the degradation of GPX4	(Li et al., 2022)
Radiation-induced intestinal injury	Liproxstatin-1	LPCAT3	Inhibit radiation-activated LPCAT3/LOX pathway	Wang et al. (2022)
	(-)-epigallocatechin-3-gallate	Nrf-2	Increase the expression of GPX4 and SLC7A11 and reduce ROS content by activating Nrf-2	Xie et al. (2020)
Radiation-induced skin injury	NMN	NAD+	Promote the NAD+/NADH system, increase the synthesis of GSH, and enhance the resistance to ferroptosis in a GPX4-dependent manner	Feng et al. (2022)
Radiation-induced hematopoietic injury	Ferrostatin-1	GPX4	Reduce the levels of hemosiderin and liable iron pool and increase GPX4	(Zhang et al., 2021d)
Total body irradiation induced injury	Baicalein	15-LOX	Inhibit depletion of GPX4 and 15-LOX	Dar et al. (2022)
	Polycysteine	GPX4 , NOX1	Activate GPX4 and inhibit NOX1	Zhang et al. (2021a)

GPX4, glutathione peroxidase 4; HSP90, the heat shock protein 90; CAM, chaperone-mediated autophagy; LPCAT3, lysophosphatidylcholine acyltransferase 3; NMN, nicotinamide mononucleotide; LOX, lipoxygenase; Nrf-2, Nuclear factor erythroid 2-related factor 2; GSH, glutathione; NOX1, nicotinamide adenine dinucleotide phosphate oxidase.

5.1 Radiation-induced lung injury

Radiation-induced lung injury (RILI) is one of the most common and serious complications of radiotherapy for thoracic malignancies (S et al., 2019). This process is often accompanied by the upregulation of inflammatory cytokines such as interleukin-6, 10, and transforming growth factor-β1 (Szabo et al., 2010). ROS are also believed to be a key factor, and their accumulation is the basis of ferroptosis (Yin et al., 2019; Li et al., 2020). An increasing number of studies have investigated the association between ferroptosis and RILI.

In acute RILI, ferroptosis characteristics of mitochondria have been detected, together with substantial downregulation of GPX4 levels (Li et al., 2019b; Guo et al., 2021). Piezo-type mechanosensitive ion channel component 1 (PIEZO1) is a mechanically activated calcium channel highly expressed in lung tissue (Coste et al., 2010). PIEZO1/Ca^{2+}/calpain signaling mediates radiation-induced ferroptosis in pulmonary endothelial cells (Guo et al., 2021) (Figure 4). Radiation induces PIEZO1 protein overexpression, elevating intracellular Ca^{2+} levels and activating the Ca^{2+}/calpain signaling pathway. Calpain then lowered the expression of GPX4 and SLC7A11, whereas it increased the expression of

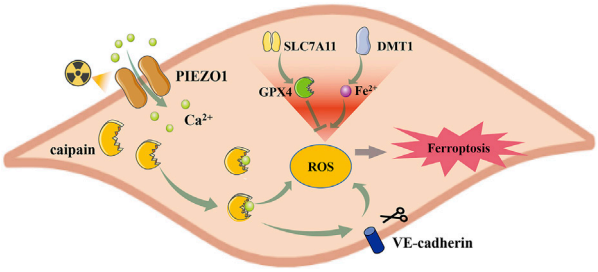

FIGURE 4
PIEZO1 regulates radiation-induced ferroptosis in lung endothelial cells. Radiation increased the expression of PIEZO1 in the lung endothelial cells, which caused the influx of Ca^{2+}. Increased intracellular Ca^{2+} activates caipain and promotes ferroptosis by regulating SLC7A11, GPX4, and DMT1 expression. Besides, the Ca2+/Caipain pathway can also promote the degradation of VE-cadherin, leading to ferroptosis. *PIEZ O 1, Piezo-type mechanosensitive ion channel component 1; SLC7A11, Cystine/glutamate antiporter solute carrier family seven member 11; GPX4, glutathione peroxidase 4; DMT1, divalent metal transporter 1.*

divalent metal transporter 1 (DMT1), which is responsible for iron uptake, induces ferroptosis, and promotes RILI. Vascular endothelial cadherin (VE-cadherin) is a calcium-dependent adhesive molecule expressed only in endothelial cells (Gory et al., 1999). Activation of the Ca^{2+}/calpain signaling pathway can promote its degradation, leading to increased ROS content and ferroptosis (Guo et al., 2021). However, the mechanism underlying VE-cadherin-induced ferroptosis has not been comprehensively investigated.

Correspondingly, inhibition of ferroptosis can alleviate RILI. Liproxstatin-1 (Lip-1), a ferroptosis inhibitor, can reduce characteristic ferroptotic changes, increase GPX4 levels, and alleviate symptoms of RILI, such as lung injury and hemorrhage. In addition, it can reduce the levels of inflammatory factors, suggesting that ferroptosis plays a role in the inflammatory microenvironment (Li et al., 2019b). Chaperone-mediated autophagy (CMA) is usually activated in response to stress, and its activation can cause the degradation of GPX4 (Yu et al., 2022). The heat shock protein 90 (HSP90) is crucial in activating CMA (Bandyopadhyay and Cuervo, 2008). NVP-AUY922, an HSP90 inhibitor, can alleviate RILI by inhibiting autophagy-dependent ferroptosis (Li et al., 2022). Therefore, ferroptosis is closely related to RILI, and ferroptosis inhibitors may play a role in RILI prevention and treatment.

5.2 Radiation-induced intestinal injuries

Radiation-induced intestinal injury (RIID) is a common complication of RT for pelvic malignancies. The clinical symptoms caused by RIID seriously affect the quality of life and even lead to death (MacNaughton, 2000). Ferroptosis regulates intestinal immune function and the occurrence of RIID (Wang et al., 2022). Radiation can cause a reduction in intraepithelial lymphocyte (IELs) count and overexpression of interferon-gamma, transforming growth factor, and other immune system changes. This effect was suppressed by Lip-1 treatment. The regulatory effect of ferroptosis on intestinal immune function may be related to the radiation-activated LPCAT3/LOX pathway (Wang et al., 2022). Epigallocatechin-3-gallate (EGCG) is a major polyphenol with a potent antioxidant activity (Zhong et al., 2012). Xie et al. (2020) observed that EGCG alleviated RIID by increasing the expression of GPX4 and SLC7A11 and inhibiting ferroptosis after radiotherapy. Therefore, regulating the ferroptosis pathway to prevent and treat RIID provides a new strategy for radiation protection.

5.3 Radiation-induced skin injury

As a result of radiotherapy, approximately 85%–95% of patients experience varying degrees of skin damage (Yang et al., 2020). Radiation-induced skin injury (RISIs) consists of both acute and chronic injuries. Acute injuries include erythema, dry and wet desquamation, edema, bleeding, and ulcers. The chronic injury involves keratosis, telangiectasias, fibrosis, and skin cancer (Hymes et al., 2006, y). Radiation-induced ROS production is closely related to RISIs, and common ROS regulatory pathways, such as the Keap1/Nrf-2 and GCH1/BH4 pathways, play a seminal role in preventing RISIs (McNeill et al., 2015; Xue et al., 2017; Wei et al., 2021). As a form of cell death caused by ROS overload, ferroptosis is also involved in RSIs. Feng et al. (Feng et al., 2022) discovered that ultraviolet (UV) exposure could induce the accumulation of lipid peroxides in human skin keratinocytes and cause intracellular Fe^{2+} overload by regulating the levels of TFRC, FTL, FTH, and the iron exporter ferroportin (FPN). Nicotinamide mononucleotide (NMN) is the precursor of NAD^+, which significantly promotes the NAD^+/NADH system, increases the synthesis of GSH, and enhances resistance to ferroptosis in a GPX4-dependent manner. The application of NMN can significantly reduce RISIs. Therefore, ferroptosis inhibitors may be an effective therapeutic approach for treating irradiation-induced skin damage. However, whether this conclusion applies to radiotherapy-induced damage remains unclear.

5.4 Radiation-induced hematopoietic injury

Radiation can inhibit the division and proliferation of hematopoietic cells in the bone marrow, causing a decline in peripheral blood images and increasing the risk of secondary infection. Studies have shown that radiation can cause ferroptosis in bone marrow mononuclear cells (BMMCs) by increasing iron and lipid peroxidation levels and depleting GPX4 and GSH. Ferrostatin-1,

a ferroptosis inhibitor, can mitigate the ferroptosis of BMMCs and increase the number of red blood cells, white blood cells, lymphocytes, and monocytes in the peripheral blood of irradiated mice (Zhang et al., 2021d). Another study showed that radiation-induced hemorrhage could induce ferroptosis in granulocyte-macrophage hematopoietic progenitor cells, and anti-ferroptosis can ameliorate hematopoietic injury (Zhang et al., 2020). Although the exact mechanism remains unknown, blocking ferroptosis can help reduce radiation-induced hematopoietic injury.

Inhibition of ferroptosis also reduced the mortality caused by radiation in mice. It was proved that *Pseudomonas aeruginosa* (PAO1) could stimulate ferroptosis by making PAO1 15-lipoxygenase (pLoxA) act on 15-LOX and GPX4 and significantly reduce the survival of irradiated mice. The application of baicalein, a lipoxygenase inhibitor, reversed this phenomenon and reduced mortality in mice exposed to total body irradiation (TBI) and PAO1 infection (Dar et al., 2022). Polycysteine can improve the survival of mice exposed to TBI and reduce radiation-induced damage by activating GPX4 and inhibiting nicotinamide adenine dinucleotide phosphate oxidase 1 (NOX1) (Zhang et al., 2021a).

The radiation-induced buildup of ROS causes oxidative stress in normal cells (Shen et al., 2018; Yahyapour et al., 2018). Ferroptosis, caused by ROS overload, is closely related to oxidative stress. Radiation injury is often accompanied by an inflammatory response. Ferroptosis is often associated with inflammatory manifestations by regulating the activity of LOXs and PTGS2 (Sun et al., 2020). Therefore, the role of ferroptosis in radiation-induced injury is essential. Radiation-mediated ferroptosis can damage normal tissues by overloading ROS and Fe^{2+}, disrupting the antioxidant systems, and inducing inflammatory responses. Its functions have been verified in multiple radiation-induced system injuries. However, it is unclear if these mechanisms apply to all systems and whether various systems have distinct specialized targets.

6 Conclusion and future perspectives

Ferroptosis, as a mode of cell death receives increasing attention, has shown great potential for cancer treatment. IR can induce ferroptosis by producing ROS, upregulating the expression of ASCL4, depleting GSH, and promoting lipid peroxidation. Besides, many DDR pathway components can also be activated by IR to affect ferroptosis through noncanonical mechanisms. Similarly, stimulating ferroptosis by regulating iron metabolism, lipid metabolism, and antioxidant systems can enhance the radiosensitivity of tumor cells, providing a new technique for increasing the efficacy of radiotherapy. FINs have not been widely used in clinical practice owing to their high toxicity, inadequate targeting, and other factors. To satisfy the therapeutic needs, new FINs that are more effective and stable should be created *in vivo*. In addition, ferroptosis is implicated in radiation-induced normal tissue damage by increasing ROS and Fe^{2+} levels, altering antioxidant systems, and generating inflammatory responses. Therefore, the question of how to promote ferroptosis in tumor cells while sparing normal cells remains unresolved.

Author contributions

YX and XJ conceived of the study and performed the funding acquisition. JS and CB participated in the design of the study and helped to draft the manuscript. CB ZZ, and HW participated in validation and investigation. LM, YX, and XJ provided writing-review and editing. All authors read and approved the final manuscript.

Funding

This research was funded by the Jilin Provincial Science and Technology Foundation (Grant Numbers. 20210509003RQ and 20210402002GH), Health Talents Special Project of the Jilin Provincial Finance Department (Grant Number JLSWSRCZX 2021-065), the Achievement Transformation Guiding Foundations of the First Hospital of Jilin University (Grant Number CGZHYD202012-029), and the Education Department Foundation of Jilin Province (Grant Number JJKH20211195KJ).

Acknowledgments

We would like to thank Editage (www.editage.cn) for English language editing.

Conflict of interest

The authors declare that the research was conducted in the absence of any commercial or financial relationships that could be construed as a potential conflict of interest.

Publisher's note

References

Akpinar, P., Kuwajima, S., Krützfeldt, J., and Stoffel, M. (2005). Tmem27: A cleaved and shed plasma membrane protein that stimulates pancreatic beta cell proliferation. *Cell Metab.* 2 (6), 385–397. doi:10.1016/j.cmet.2005.11.001

Aschenbrenner, B., Negro, G., Savic, D., Sorokin, M., Buzdin, A., Ganswindt, U., et al. (2021). Simvastatin is effective in killing the radioresistant breast carcinoma cells. *Radiol. Oncol.* 55 (3), 305–316. doi:10.2478/raon-2021-0020

Balgoma, D., and Hedeland, M. (2021). Etherglycerophospholipids and ferroptosis: Structure, regulation, and location. *Trends Endocrinol. Metab.* 32 (12), 960–962. doi:10.1016/j.tem.2021.08.005

Bandyopadhyay, U., and Cuervo, A. M. (2008). Entering the lysosome through a transient gate by chaperone-mediated autophagy. *Autophagy* 4 (8), 1101–1103. doi:10.4161/auto.7150

Bannai, S. (1986). Exchange of cystine and glutamate across plasma membrane of human fibroblasts. *J. Biol. Chem.* 261 (5), 2256–2263. doi:10.1016/s0021-9258(17)35926-4

Bersuker, K., Hendricks, J. M., Li, Z., Magtanong, L., Ford, B., Tang, P. H., et al. (2019). The CoQ oxidoreductase FSP1 acts parallel to GPX4 to inhibit ferroptosis. *Nature* 575 (7784), 688–692. doi:10.1038/s41586-019-1705-2

Bertheloot, D., Latz, E., and Franklin, B. S. (2021). Necroptosis, pyroptosis and apoptosis: An intricate game of cell death. *Cell. Mol. Immunol.* 18 (5), 1106–1121. doi:10.1038/s41423-020-00630-3

Bogdan, A. R., Miyazawa, M., Hashimoto, K., and Tsuji, Y. (2016). Regulators of iron homeostasis: New players in metabolism, cell death, and disease. *Trends biochem. Sci.* 41 (3), 274–286. doi:10.1016/j.tibs.2015.11.012

Brigelius-Flohé, R. (2006). Glutathione peroxidases and redox-regulated transcription factors. *Biol. Chem.* 387 (10-11), 1329–1335. doi:10.1515/bc.2006.166

Chen, H., Zheng, C., Zhang, Y., Chang, Y.-Z., Qian, Z.-M., and Shen, X. (2006). Heat shock protein 27 downregulates the transferrin receptor 1-mediated iron uptake. *Int. J. Biochem. Cell Biol.* 38 (8), 1402–1416. doi:10.1016/j.biocel.2006.02.006

Chen, P. H., Wu, J., Ding, C. C., Lin, C. C., Pan, S., Bossa, N., et al. (2020). Kinome screen of ferroptosis reveals a novel role of ATM in regulating iron metabolism. *Cell Death Differ.* 27 (3), 1008–1022. doi:10.1038/s41418-019-0393-7

Chen, X., Kang, R., Kroemer, G., and Tang, D. (2021). Broadening horizons: The role of ferroptosis in cancer. *Nat. Rev. Clin. Oncol.* 18 (5), 280–296. doi:10.1038/s41571-020-00462-0

Coste, B., Mathur, J., Schmidt, M., Earley, T. J., Ranade, S., Petrus, M. J., et al. (2010). Piezo1 and Piezo2 are essential components of distinct mechanically activated cation channels. *Science* 330 (6000), 55–60. doi:10.1126/science.1193270

Crabtree, M. J., Tatham, A. L., Hale, A. B., Alp, N. J., and Channon, K. M. (2009). Critical role for tetrahydrobiopterin recycling by dihydrofolate reductase in regulation of endothelial nitric-oxide synthase coupling: Relative importance of the de novo biopterin synthesis versus salvage pathways. *J. Biol. Chem.* 284 (41), 28128–28136. doi:10.1074/jbc.M109.041483

Criscitiello, M. F., Kraev, I., and Lange, S. (2020). Post-translational protein deimination signatures in serum and serum-extracellular vesicles of *Bos taurus* reveal immune, anti-pathogenic, anti-viral, metabolic and cancer-related pathways for deimination. *Int. J. Mol. Sci.* 21 (8), E2861. doi:10.3390/ijms21082861

Cui, W., Liu, D., Gu, W., and Chu, B. (2021). Peroxisome-driven ether-linked phospholipids biosynthesis is essential for ferroptosis. *Cell Death Differ.* 28 (8), 2536–2551. doi:10.1038/s41418-021-00769-0

Dai, E., Han, L., Liu, J., Xie, Y., Kroemer, G., Klionsky, D. J., et al. (2020). Autophagy-dependent ferroptosis drives tumor-associated macrophage polarization via release and uptake of oncogenic KRAS protein. *Autophagy* 16 (11), 2069–2083. doi:10.1080/15548627.2020.1714209

Dar, H. H., Epperly, M. W., Tyurin, V. A., Amoscato, A. A., Anthonymuthu, T. S., Souryavong, A. B., et al. (2022). *P. aeruginosa* augments irradiation injury via 15-lipoxygenase-catalyzed generation of 15-HpETE-PE and induction of theft-ferroptosis. *JCI Insight* 7 (4), e156013. doi:10.1172/jci.insight.156013

De Ruysscher, D., Niedermann, G., Burnet, N. G., Siva, S., Lee, A. W. M., and Hegi-Johnson, F. (2019). Radiotherapy toxicity. *Nat. Rev. Dis. Prim.* 5 (1), 13. doi:10.1038/s41572-019-0064-5

Delaney, G., Jacob, S., Featherstone, C., and Barton, M. (2005). The role of radiotherapy in cancer treatment: Estimating optimal utilization from a review of evidence-based clinical guidelines.. *Cancer* 104 (6), 1129–1137. doi:10.1002/cncr.21324

Dixon, S. J., Lemberg, K. M., Lamprecht, M. R., Skouta, R., Zaitsev, E. M., Gleason, C. E., et al. (2012). Ferroptosis: An iron-dependent form of nonapoptotic cell death. *Cell* 149 (5), 1060–1072. doi:10.1016/j.cell.2012.03.042

Dixon, S. J., Winter, G. E., Musavi, L. S., Lee, E. D., Snijder, B., Rebsamen, M., et al. (2015). Human haploid cell genetics reveals roles for lipid metabolism genes in nonapoptotic cell death. *ACS Chem. Biol.* 10 (7), 1604–1609. doi:10.1021/acschembio.5b00245

Doll, S., Freitas, F. P., Shah, R., Aldrovandi, M., Da Silva, M. C., Ingold, I., et al. (2019). FSP1 is a glutathione-independent ferroptosis suppressor. *Nature* 575 (7784), 693–698. doi:10.1038/s41586-019-1707-0

Doll, S., Proneth, B., Tyurina, Y. Y., Panzilius, E., Kobayashi, S., Ingold, I., et al. (2017). ACSL4 dictates ferroptosis sensitivity by shaping cellular lipid composition. *Nat. Chem. Biol.* 13 (1), 91–98. doi:10.1038/nchembio.2239

Elsaid, M. Y., Shahi, A., Wang, A. R., Baiu, D. C., Li, C., Werner, L. R., et al. (2018). Enhanced radiosensitivity in solid tumors using a tumor-selective alkyl phospholipid ether analog. *Mol. Cancer Ther.* 17 (11), 2320–2328. doi:10.1158/1535-7163.Mct-17-0897

Fan, Z., Yang, G., Zhang, W., Liu, Q., Liu, G., Liu, P., et al. (2021). Hypoxia blocks ferroptosis of hepatocellular carcinoma via suppression of METTL14 triggered YTHDF2-dependent silencing of SLC7A11. *J. Cell. Mol. Med.* 25 (21), 10197–10212. doi:10.1111/jcmm.16957

Femia, G., Langlois, N., Raleigh, J., Gray, B., Othman, F., Perumal, S. R., et al. (2021). Comparison of conventional autopsy with post-mortem magnetic resonance, computed tomography in determining the cause of unexplained death. *Forensic Sci. Med. Pathol.* 17 (1), 10–18. doi:10.1007/s12024-020-00343-z

Feng, L., Zhao, K., Sun, L., Yin, X., Zhang, J., Liu, C., et al. (2021a). SLC7A11 regulated by NRF2 modulates esophageal squamous cell carcinoma radiosensitivity by inhibiting ferroptosis. *J. Transl. Med.* 19 (1), 367. doi:10.1186/s12967-021-03042-7

Feng, Y., Feng, Y., Gu, L., Liu, P., Cao, J., and Zhang, S. (2021b). The critical role of tetrahydrobiopterin (BH4) metabolism in modulating radiosensitivity: BH4/NOS Axis as an angel or a devil. *Front. Oncol.* 11, 720632. doi:10.3389/fonc.2021.720632

Feng, Z., Qin, Y., Huo, F., Jian, Z., Li, X., Geng, J., et al. (2022). NMN recruits GSH to enhance GPX4-mediated ferroptosis defense in UV irradiation induced skin injury. *Biochim. Biophys. Acta. Mol. Basis Dis.* 1868 (1), 166287. doi:10.1016/j.bbadis.2021.166287

Frazer, D. M., and Anderson, G. J. (2014). The regulation of iron transport. *BioFactors* 40 (2), 206–214. doi:10.1002/biof.1148

Gory, S., Vernet, M., Laurent, M., Dejana, E., Dalmon, J., and Huber, P. (1999). The vascular endothelial-cadherin promoter directs endothelial-specific expression in transgenic mice. *Blood* 93 (1), 184–192. doi:10.1182/blood.v93.1.184

Guo, X. W., Zhang, H., Huang, J. Q., Wang, S. N., Lu, Y., Cheng, B., et al. (2021). PIEZO1 ion channel mediates ionizing radiation-induced pulmonary endothelial cell ferroptosis via Ca(2+)/calpain/VE-cadherin signaling. *Front. Mol. Biosci.* 8, 725274. doi:10.3389/fmolb.2021.725274

Hosseini, M., Dousset, L., Michon, P., Mahfouf, W., Muzotte, E., Bergeron, V., et al. (2019). UVB-induced DHODH upregulation, which is driven by STAT3, is a promising target for chemoprevention and combination therapy of photocarcinogenesis. *Oncogenesis* 8 (10), 52. doi:10.1038/s41389-019-0161-z

Hsieh, C. H., Hsieh, H. C., Shih, F. S., Wang, P. W., Yang, L. X., Shieh, D. B., et al. (2021). An innovative NRF2 nano-modulator induces lung cancer ferroptosis and elicits an immunostimulatory tumor microenvironment. *Theranostics* 11 (14), 7072–7091. doi:10.7150/thno.57803

Huang, R. X., and Zhou, P. K. (2020). DNA damage response signaling pathways and targets for radiotherapy sensitization in cancer. *Signal Transduct. Target. Ther.* 5 (1), 60. doi:10.1038/s41392-020-0150-x

Hutchinson, J., and Marignol, L. (2017). Clinical potential of statins in prostate cancer radiation therapy. *Anticancer Res.* 37 (10), 5363–5372. doi:10.21873/anticanres.11962

Hymes, S. R., Strom, E. A., and Fife, C. (2006). Radiation dermatitis: Clinical presentation, pathophysiology, and treatment 2006. *J. Am. Acad. Dermatol.* 54 (1), 28–46. doi:10.1016/j.jaad.2005.08.054

Jiang, L., Kon, N., Li, T., Wang, S. J., Su, T., Hibshoosh, H., et al. (2015). Ferroptosis as a p53-mediated activity during tumour suppression. *Nature* 520 (7545), 57–62. doi:10.1038/nature14344

Jiang, Y., Mao, C., Yang, R., Yan, B., Shi, Y., Liu, X., et al. (2017). EGLN1/c-Myc induced lymphoid-specific helicase inhibits ferroptosis through lipid metabolic gene expression changes. *Theranostics* 7 (13), 3293–3305. doi:10.7150/thno.19988

Jin, Y., Xu, K., Chen, Q., Wang, B., Pan, J., Huang, S., et al. (2018). Simvastatin inhibits the development of radioresistant esophageal cancer cells by increasing the radiosensitivity and reversing EMT process via the PTEN-PI3K/AKT pathway. *Exp. Cell Res.* 362 (2), 362–369. doi:10.1016/j.yexcr.2017.11.037

Kang, R., Kroemer, G., and Tang, D. (2019). The tumor suppressor protein p53 and the ferroptosis network. *Free Radic. Biol. Med.* 133, 162–168. doi:10.1016/j.freeradbiomed.2018.05.074

Kim, W., Son, B., Lee, S., Do, H., and Youn, B. (2018). Targeting the enzymes involved in arachidonic acid metabolism to improve radiotherapy. *Cancer Metastasis Rev.* 37 (2-3), 213–225. doi:10.1007/s10555-018-9742-0

Kraft, V. a. N., Bezjian, C. T., Pfeiffer, S., Ringelstetter, L., Müller, C., Zandkarimi, F., et al. (2020). GTP cyclohydrolase 1/tetrahydrobiopterin counteract ferroptosis through lipid remodeling. *ACS Cent. Sci.* 6 (1), 41–53. doi:10.1021/acscentsci.9b01063

Kwon, Y. S., Lee, M. G., Baek, J., Kim, N. Y., Jang, H., and Kim, S. (2021). Acyl-CoA synthetase-4 mediates radioresistance of breast cancer cells by regulating FOXM1. *Biochem. Pharmacol.* 192, 114718. doi:10.1016/j.bcp.2021.114718

Lang, X., Green, M. D., Wang, W., Yu, J., Choi, J. E., Jiang, L., et al. (2019). Radiotherapy and immunotherapy promote tumoral lipid oxidation and ferroptosis via synergistic repression of SLC7A11. *Cancer Discov.* 9 (12), 1673–1685. doi:10.1158/2159-8290.Cd-19-0338

Lei, G., Mao, C., Yan, Y., Zhuang, L., and Gan, B. (2021). Ferroptosis, radiotherapy, and combination therapeutic strategies. *Protein Cell* 12, 836–857. doi:10.1007/s13238-021-00841-y

Lei, G., Zhang, Y., Koppula, P., Liu, X., Zhang, J., Lin, S. H., et al. (2020). The role of ferroptosis in ionizing radiation-induced cell death and tumor suppression. *Cell Res.* 30 (2), 146–162. doi:10.1038/s41422-019-0263-3

Lewerenz, J., and Maher, P. (2009). Basal levels of eIF2alpha phosphorylation determine cellular antioxidant status by regulating ATF4 and xCT expression. *J. Biol. Chem.* 284 (2), 1106–1115. doi:10.1074/jbc.M807325200

Li, J., Cao, F., Yin, H.-L., Huang, Z.-J., Lin, Z.-T., Mao, N., et al. (2020). Ferroptosis: Past, present and future. *Cell Death Dis.* 11 (2), 88. doi:10.1038/s41419-020-2298-2

Li, L., Ng, S. R., Colón, C. I., Drapkin, B. J., Hsu, P. P., Li, Z., et al. (2019a). Identification of DHODH as a therapeutic target in small cell lung cancer. *Sci. Transl. Med.* 11 (517), eaaw7852. doi:10.1126/scitranslmed.aaw7852

Li, L., Wu, D., Deng, S., Li, J., Zhang, F., Zou, Y., et al. (2022). NVP-AUY922 alleviates radiation-induced lung injury via inhibition of autophagy-dependent ferroptosis. *Cell Death Discov.* 8 (1), 86. doi:10.1038/s41420-022-00887-9

Li, X., Zhuang, X., and Qiao, T. (2019b). Role of ferroptosis in the process of acute radiation-induced lung injury in mice. *Biochem. Biophys. Res. Commun.* 519 (2), 240–245. doi:10.1016/j.bbrc.2019.08.165

Liang, Y., Zeng, D., You, Y., Ma, B., Li, X., and Chen, T. (2020). Designing dihydrofolate reductase inhibitors as X-ray radiosensitizers to reverse radioresistance of cervical cancer. *ACS Med. Chem. Lett.* 11 (7), 1421–1428. doi:10.1021/acsmedchemlett.0c00105

Liu, J., Zhang, C., Wang, J., Hu, W., and Feng, Z. (2020). The regulation of ferroptosis by tumor suppressor p53 and its pathway. *Int. J. Mol. Sci.* 21 (21), 8387. doi:10.3390/ijms21218387

Liu, Z., Dong, L., Zheng, Z., Liu, S., Gong, S., Meng, L., et al. (2021). Mechanism, prevention, and treatment of radiation-induced salivary gland injury related to oxidative stress. *Antioxidants (Basel)* 10 (11), 1666. doi:10.3390/antiox10111666

Lövey, J., Nie, D., Tóvári, J., Kenessey, I., Tímár, J., Kandouz, M., et al. (2013). Radiosensitivity of human prostate cancer cells can be modulated by inhibition of 12-lipoxygenase. *Cancer Lett.* 335 (2), 495–501. doi:10.1016/j.canlet.2013.03.012

Macnaughton, W. K. (2000). Review article: New insights into the pathogenesis of radiation-induced intestinal dysfunction. *Aliment. Pharmacol. Ther.* 14 (5), 523–528. doi:10.1046/j.1365-2036.2000.00745.x

Mao, C., Liu, X., Zhang, Y., Lei, G., Yan, Y., Lee, H., et al. (2021). DHODH-mediated ferroptosis defence is a targetable vulnerability in cancer. *Nature* 593, 586–590. doi:10.1038/s41586-021-03539-7

Mcneill, E., Crabtree, M. J., Sahgal, N., Patel, J., Chuaiphichai, S., Iqbal, A. J., et al. (2015). Regulation of iNOS function and cellular redox state by macrophage Gch1 reveals specific requirements for tetrahydrobiopterin in NRF2 activation. *Free Radic. Biol. Med.* 79, 206–216. doi:10.1016/j.freeradbiomed.2014.10.575

Mumbauer, S., Pascual, J., Kolotuev, I., and Hamaratoglu, F. (2019). Ferritin heavy chain protects the developing wing from reactive oxygen species and ferroptosis. *PLoS Genet.* 15 (9), e1008396. doi:10.1371/journal.pgen.1008396

Nisticò, C., Pagliari, F., Chiarella, E., Fernandes Guerreiro, J., Marafioti, M. G., Aversa, I., et al. (2021). Lipid droplet biosynthesis impairment through DGAT2 inhibition sensitizes MCF7 breast cancer cells to radiation. *Int. J. Mol. Sci.* 22 (18), 10102. doi:10.3390/ijms221810102

Ou, Y., Wang, S. J., Li, D., Chu, B., and Gu, W. (2016). Activation of SAT1 engages polyamine metabolism with p53-mediated ferroptotic responses. *Proc. Natl. Acad. Sci. U. S. A.* 113 (44), E6806–e6812. doi:10.1073/pnas.1607152113

Pan, X., Lin, Z., Jiang, D., Yu, Y., Yang, D., Zhou, H., et al. (2019). Erastin decreases radioresistance of NSCLC cells partially by inducing GPX4-mediated ferroptosis. *Oncol. Lett.* 17 (3), 3001–3008. doi:10.3892/ol.2019.9888

Pilié, P. G., Tang, C., Mills, G. B., and Yap, T. A. (2019). State-of-the-art strategies for targeting the DNA damage response in cancer. *Nat. Rev. Clin. Oncol.* 16 (2), 81–104. doi:10.1038/s41571-018-0114-z

Ren, Z., Hu, M., Wang, Z., Ge, J., Zhou, X., Zhang, G., et al. (2021). Ferroptosis-related genes in lung adenocarcinoma: Prognostic signature and immune, drug resistance, mutation analysis. *Front. Genet.* 12, 672904. doi:10.3389/fgene.2021.672904

Rycaj, K., and Tang, D. G. (2014). Cancer stem cells and radioresistance. *Int. J. Radiat. Biol.* 90 (8), 615–621. doi:10.3109/09553002.2014.892227

Santoro, M. M. (2020). The antioxidant role of non-mitochondrial CoQ10: Mystery solved. *Cell Metab.* 31 (1), 13–15. doi:10.1016/j.cmet.2019.12.007

Schmitt, A., Xu, W., Bucher, P., Grimm, M., Konantz, M., Horn, H., et al. (2021). Dimethyl fumarate induces ferroptosis and impairs NF-κB/STAT3 signaling in DLBCL. *Blood* 138 (10), 871–884. doi:10.1182/blood.2020009404

Shen, Y., Jiang, X., Meng, L., Xia, C., Zhang, L., and Xin, Y. (2018). Transplantation of bone marrow mesenchymal stem cells prevents radiation-induced artery injury by suppressing oxidative stress and inflammation. *Oxid. Med. Cell. Longev.* 2018, 5942916. doi:10.1155/2018/5942916

Shibata, Y., Yasui, H., Higashikawa, K., Miyamoto, N., and Kuge, Y. (2019). Erastin, a ferroptosis-inducing agent, sensitized cancer cells to X-ray irradiation via glutathione starvation *in vitro* and *in vivo*. *PLoS One* 14 (12), e0225931. doi:10.1371/journal.pone.0225931

Shimada, K., Skouta, R., Kaplan, A., Yang, W. S., Hayano, M., Dixon, S. J., et al. (2016). Global survey of cell death mechanisms reveals metabolic regulation of ferroptosis. *Nat. Chem. Biol.* 12 (7), 497–503. doi:10.1038/nchembio.2079

Shintoku, R., Takigawa, Y., Yamada, K., Kubota, C., Yoshimoto, Y., Takeuchi, T., et al. (2017). Lipoxygenase-mediated generation of lipid peroxides enhances ferroptosis induced by erastin and RSL3. *Cancer Sci.* 108 (11), 2187–2194. doi:10.1111/cas.13380

Shishido, Y., Amisaki, M., Matsumi, Y., Yakura, H., Nakayama, Y., Miyauchi, W., et al. (2021). Antitumor effect of 5-aminolevulinic acid through ferroptosis in esophageal squamous cell carcinoma. *Ann. Surg. Oncol.* 28 (7), 3996–4006. doi:10.1245/s10434-020-09334-4

Soula, M., Weber, R. A., Zilka, O., Alwaseem, H., La, K., Yen, F., et al. (2020). Metabolic determinants of cancer cell sensitivity to canonical ferroptosis inducers. *Nat. Chem. Biol.* 16 (12), 1351–1360. doi:10.1038/s41589-020-0613-y

Su, J., Zhao, Q., Zheng, Z., Wang, H., Bian, C., Meng, L., et al. (2022). Prospective application of ferroptosis in hypoxic cells for tumor radiotherapy. *Antioxidants (Basel)* 11 (5), 921. doi:10.3390/antiox11050921

Sun, Y., Chen, P., Zhai, B., Zhang, M., Xiang, Y., Fang, J., et al. (2020). The emerging role of ferroptosis in inflammation. *Biomed. Pharmacother.* 127, 110108. doi:10.1016/j.biopha.2020.110108

Sung, H., Ferlay, J., Siegel, R. L., Laversanne, M., Soerjomataram, I., Jemal, A., et al. (2021). Global cancer statistics 2020: GLOBOCAN estimates of incidence and mortality worldwide for 36 cancers in 185 countries. *Ca. Cancer J. Clin.* 71 (3), 209–249. doi:10.3322/caac.21660

Szabo, S., Ghosh, S. N., Fish, B. L., Bodiga, S., Tomic, R., Kumar, G., et al. (2010). Cellular inflammatory infiltrate in pneumonitis induced by a single moderate dose of thoracic x radiation in rats. *Radiat. Res.* 173 (4), 545–556. doi:10.1667/rr1753.1

Tang, Y., Li, C., Zhang, Y. J., and Wu, Z. H. (2021). Ferroptosis-Related Long Non-Coding RNA signature predicts the prognosis of Head and neck squamous cell carcinoma. *Int. J. Biol. Sci.* 17 (3), 702–711. doi:10.7150/ijbs.55552

Tarangelo, A., Magtanong, L., Bieging-Rolett, K. T., Li, Y., Ye, J., Attardi, L. D., et al. (2018). p53 suppresses metabolic stress-induced ferroptosis in cancer cells. *Cell Rep.* 22 (3), 569–575. doi:10.1016/j.celrep.2017.12.077

Taylor, M. A., Das, B. C., and Ray, S. K. (2018). Targeting autophagy for combating chemoresistance and radioresistance in glioblastoma. *Apoptosis* 23 (11-12), 563–575. doi:10.1007/s10495-018-1480-9

Theriot, C. A., Westby, C. M., Morgan, J. L. L., Zwart, S. R., and Zanello, S. B. (2016). High dietary iron increases oxidative stress and radiosensitivity in the rat retina and vasculature after exposure to fractionated gamma radiation. *NPJ Microgravity* 2, 16014. doi:10.1038/npjmgrav.2016.14

Tomita, K., Fukumoto, M., Itoh, K., Kuwahara, Y., Igarashi, K., Nagasawa, T., et al. (2019). MiR-7-5p is a key factor that controls radioresistance via intracellular Fe(2+) content in clinically relevant radioresistant cells. *Biochem. Biophys. Res. Commun.* 518 (4), 712–718. doi:10.1016/j.bbrc.2019.08.117

Tung, F. I., Chen, L. C., Wang, Y. C., Chen, M. H., Shueng, P. W., and Liu, T. Y. (2021). Using a hybrid radioenhancer to discover tumor cell-targeted treatment for

osteosarcoma: An in vitro study. *Curr. Med. Chem.* 28 (19), 3877–3889. doi:10.2174/0929867327666201118155216

Turner, J., Koumenis, C., Kute, T. E., Planalp, R. P., Brechbiel, M. W., Beardsley, D., et al. (2005). Tachpyridine, a metal chelator, induces G2 cell-cycle arrest, activates checkpoint kinases, and sensitizes cells to ionizing radiation. *Blood* 106 (9), 3191–3199. doi:10.1182/blood-2005-03-1263

Wang, B., Wei, J., Meng, L., Wang, H., Qu, C., Chen, X., et al. (2020a). Advances in pathogenic mechanisms and management of radiation-induced fibrosis. *Biomed. Pharmacother.* 121, 109560. doi:10.1016/j.biopha.2019.109560

Wang, H., Wang, B., Wei, J., Meng, L., Zhang, Q., Qu, C., et al. (2020b). Molecular mechanisms underlying increased radiosensitivity in human papillomavirus-associated oropharyngeal squamous cell carcinoma. *Int. J. Biol. Sci.* 16 (6), 1035–1043. doi:10.7150/ijbs.40880

Wang, L., Wang, A., Fu, Q., Shi, Z., Chen, X., Wang, Y., et al. (2022). Ferroptosis plays an important role in promoting ionizing radiation-induced intestinal injuries. *Biochem. Biophys. Res. Commun.* 595, 7–13. doi:10.1016/j.bbrc.2022.01.068

Wang, P., and Lu, Y. Q. (2022). Ferroptosis: A critical moderator in the life cycle of immune cells. *Front. Immunol.* 13, 877634. doi:10.3389/fimmu.2022.877634

Wang, W., Green, M., Choi, J. E., Gijón, M., Kennedy, P. D., Johnson, J. K., et al. (2019). CD8(+) T cells regulate tumour ferroptosis during cancer immunotherapy. *Nature* 569 (7755), 270–274. doi:10.1038/s41586-019-1170-y

Wang, Y., Wei, Z., Pan, K., Li, J., and Chen, Q. (2020c). The function and mechanism of ferroptosis in cancer. *Apoptosis* 25 (11-12), 786–798. doi:10.1007/s10495-020-01638-w

Warner, G. J., Berry, M. J., Moustafa, M. E., Carlson, B. A., Hatfield, D. L., and Faust, J. R. (2000). Inhibition of selenoprotein synthesis by selenocysteine tRNA [Ser]Sec lacking isopentenyladenosine. *J. Biol. Chem.* 275 (36), 28110–28119. doi:10.1074/jbc.m001280200

Wei, J., Wang, B., Wang, H., Meng, L., Zhao, Q., Li, X., et al. (2019). Radiation-induced normal tissue damage: Oxidative stress and epigenetic mechanisms. *Oxid. Med. Cell. Longev.* 2019, 3010342. doi:10.1155/2019/3010342

Wei, J., Zhao, Q., Zhang, Y., Shi, W., Wang, H., Zheng, Z., et al. (2021). Sulforaphane-mediated Nrf2 activation prevents radiation-induced skin injury through inhibiting the oxidative-stress-activated DNA damage and NLRP3 inflammasome. *Antioxidants (Basel)* 10 (11), 1850. doi:10.3390/antiox10111850

Werner, E. R., Keller, M. A., Sailer, S., Lackner, K., Koch, J., Hermann, M., et al. (2020). The TMEM189 gene encodes plasmanylethanolamine desaturase which introduces the characteristic vinyl ether double bond into plasmalogens. *Proc. Natl. Acad. Sci. U. S. A.* 117 (14), 7792–7798. doi:10.1073/pnas.1917461117

Xie, L. W., Cai, S., Zhao, T. S., Li, M., and Tian, Y. (2020). Green tea derivative (-)-epigallocatechin-3-gallate (EGCG) confers protection against ionizing radiation-induced intestinal epithelial cell death both *in vitro* and *in vivo*. *Free Radic. Biol. Med.* 161, 175–186. doi:10.1016/j.freeradbiomed.2020.10.012

Xie, Y., Zhu, S., Song, X., Sun, X., Fan, Y., Liu, J., et al. (2017). The tumor suppressor p53 limits ferroptosis by blocking DPP4 activity. *Cell Rep.* 20 (7), 1692–1704. doi:10.1016/j.celrep.2017.07.055

Xue, J., Yu, C., Sheng, W., Zhu, W., Luo, J., Zhang, Q., et al. (2017). The nrf2/GCH1/BH4 Axis Ameliorates radiation-induced skin injury by modulating the ROS cascade. *J. Invest.. Dermatol.* 137 (10), 2059–2068. doi:10.1016/j.jid.2017.05.019

Yagoda, N., Von Rechenberg, M., Zaganjor, E., Bauer, A. J., Yang, W. S., Fridman, D. J., et al. (2007). RAS-RAF-MEK-dependent oxidative cell death involving voltage-dependent anion channels. *Nature* 447 (7146), 864–868. doi:10.1038/nature05859

Yahyapour, R., Motevaseli, E., Rezaeyan, A., Abdollahi, H., Farhood, B., Cheki, M., et al. (2018). Reduction-oxidation (redox) system in radiation-induced normal tissue injury: Molecular mechanisms and implications in radiation therapeutics. *Clin. Transl. Oncol.* 20 (8), 975–988. doi:10.1007/s12094-017-1828-6

Yamada, K., Murayama, Y., Kamada, Y., Arita, T., Kosuga, T., Konishi, H., et al. (2019). Radiosensitizing effect of 5-aminolevulinic acid in colorectal cancer *in vitro* and *in vivo*. *Oncol. Lett.* 17 (6), 5132–5138. doi:10.3892/ol.2019.10198

Yamamoto, J., Ogura, S., Tanaka, T., Kitagawa, T., Nakano, Y., Saito, T., et al. (2012). Radiosensitizing effect of 5-aminolevulinic acid-induced protoporphyrin IX in glioma cells *in vitro*. *Oncol. Rep.* 27 (6), 1748–1752. doi:10.3892/or.2012.1699

Yan, B., Ai, Y., Sun, Q., Ma, Y., Cao, Y., Wang, J., et al. (2021). Membrane damage during ferroptosis is caused by oxidation of phospholipids catalyzed by the oxidoreductases POR and CYB5R1. *Mol. Cell* 81 (2), 355–369. e10. doi:10.1016/j.molcel.2020.11.024

Yan, T., Zhang, T., Mu, W., Qi, Y., Guo, S., Hu, N., et al. (2020). Ionizing radiation induces BH(4) deficiency by downregulating GTP-cyclohydrolase 1, a novel target for preventing and treating radiation enteritis. *Biochem. Pharmacol.* 180, 114102. doi:10.1016/j.bcp.2020.114102

Yang, Q., Feng, Y., Schultz, C. J., Li, X. A., Wu, H., and Wang, D. (2008). Synergistic effect of 15-lipoxygenase 2 and radiation in killing head-and-neck cancer. *Cancer Gene Ther.* 15 (5), 323–330. doi:10.1038/cgt.2008.9

Yang, W. S., Sriramaratnam, R., Welsch, M. E., Shimada, K., Skouta, R., Viswanathan, V. S., et al. (2014). Regulation of ferroptotic cancer cell death by GPX4. *Cell* 156 (1-2), 317–331. doi:10.1016/j.cell.2013.12.010

Yang, W. S., and Stockwell, B. R. (2016). Ferroptosis: Death by lipid peroxidation. *Trends Cell Biol.* 26 (3), 165–176. doi:10.1016/j.tcb.2015.10.014

Yang, X., Ren, H., Guo, X., Hu, C., and Fu, J. (2020). Radiation-induced skin injury: Pathogenesis, treatment, and management. *Aging (Albany NY)* 12 (22), 23379–23393. doi:10.18632/aging.103932

Ye, L. F., Chaudhary, K. R., Zandkarimi, F., Harken, A. D., Kinslow, C. J., Upadhyayula, P. S., et al. (2020). Radiation-induced lipid peroxidation triggers ferroptosis and synergizes with ferroptosis inducers. *ACS Chem. Biol.* 15 (2), 469–484. doi:10.1021/acschembio.9b00939

Yin, Z., Yang, G., Deng, S., and Wang, Q. (2019). Oxidative stress levels and dynamic changes in mitochondrial gene expression in a radiation-induced lung injury model. *J. Radiat. Res.* 60 (2), 204–214. doi:10.1093/jrr/rry105

Yu, S., Li, Z., Zhang, Q., Wang, R., Zhao, Z., Ding, W., et al. (2022). GPX4 degradation via chaperone-mediated autophagy contributes to antimony-triggered neuronal ferroptosis. *Ecotoxicol. Environ. Saf.* 234, 113413. doi:10.1016/j.ecoenv.2022.113413

Yuan, Y., Cao, W., Zhou, H., Qian, H., and Wang, H. (2021). CLTRN, regulated by NRF1/RAN/DLD protein complex, enhances radiation sensitivity of hepatocellular carcinoma cells through ferroptosis pathway. *Int. J. Radiat. Oncol. Biol. Phys.* 110 (3), 859–871. doi:10.1016/j.ijrobp.2020.12.062

Zhang, K., Ping, L., Du, T., Liang, G., Huang, Y., Li, Z., et al. (2021a). A ferroptosis-related lncRNAs signature predicts prognosis and immune microenvironment for breast cancer. *Front. Mol. Biosci.* 8, 678877. doi:10.3389/fmolb.2021.678877

Zhang, W., Sun, Y., Bai, L., Zhi, L., Yang, Y., Zhao, Q., et al. (2021b). RBMS1 regulates lung cancer ferroptosis through translational control of SLC7A11. *J. Clin. Invest..* 131 (22), e152067. doi:10.1172/jci152067

Zhang, X., Tian, M., Li, X., Zheng, C., Wang, A., Feng, J., et al. (2021c). Hematopoietic protection and mechanisms of ferrostatin-1 on hematopoietic acute radiation syndrome of mice. *Int. J. Radiat. Biol.* 97 (4), 464–473. doi:10.1080/09553002.2021.1876956

Zhang, X., Xing, X., Liu, H., Feng, J., Tian, M., Chang, S., et al. (2020). Ionizing radiation induces ferroptosis in granulocyte-macrophage hematopoietic progenitor cells of murine bone marrow. *Int. J. Radiat. Biol.* 96 (5), 584–595. doi:10.1080/09553002.2020.1708993

Zhang, Y., and Martin, S. G. (2014). Redox proteins and radiotherapy. *Clin. Oncol.* 26 (5), 289–300. doi:10.1016/j.clon.2014.02.003

Zhang, Y., Qian, Y., Zhang, J., Yan, W., Jung, Y. S., Chen, M., et al. (2017). Ferredoxin reductase is critical for p53-dependent tumor suppression via iron regulatory protein 2. *Genes Dev.* 31 (12), 1243–1256. doi:10.1101/gad.299388.117

Zhang, Y., Shi, J., Liu, X., Feng, L., Gong, Z., Koppula, P., et al. (2018). BAP1 links metabolic regulation of ferroptosis to tumour suppression. *Nat. Cell Biol.* 20 (10), 1181–1192. doi:10.1038/s41556-018-0178-0

Zhong, Y., Chiou, Y. S., Pan, M. H., and Shahidi, F. (2012). Anti-inflammatory activity of lipophilic epigallocatechin gallate (EGCG) derivatives in LPS-stimulated murine macrophages. *Food Chem.* 134 (2), 742–748. doi:10.1016/j.foodchem.2012.02.172

Zou, Y., Henry, W. S., Ricq, E. L., Graham, E. T., Phadnis, V. V., Maretich, P., et al. (2020a). Plasticity of ether lipids promotes ferroptosis susceptibility and evasion. *Nature* 585 (7826), 603–608. doi:10.1038/s41586-020-2732-8

Zou, Y., Li, H., Graham, E. T., Deik, A. A., Eaton, J. K., Wang, W., et al. (2020b). Cytochrome P450 oxidoreductase contributes to phospholipid peroxidation in ferroptosis. *Nat. Chem. Biol.* 16 (3), 302–309. doi:10.1038/s41589-020-0472-6

Zou, Y., Palte, M. J., Deik, A. A., Li, H., Eaton, J. K., Wang, W., et al. (2019). A GPX4-dependent cancer cell state underlies the clear-cell morphology and confers sensitivity to ferroptosis. *Nat. Commun.* 10 (1), 1617. doi:10.1038/s41467-019-09277-9

frontiers | Frontiers in Cell and Developmental Biology

TYPE Opinion
PUBLISHED 18 May 2023
DOI 10.3389/fcell.2023.1179245

OPEN ACCESS

EDITED BY
Juan Carlos Mayo,
University of Oviedo, Spain

REVIEWED BY
Toni Petan,
Institut Jožef Stefan (IJS), Slovenia
Pedro Gonzalez-Menendez,
University of Oviedo, Spain

*CORRESPONDENCE
Wan Seok Yang,
yangw@stjohns.edu

RECEIVED 03 March 2023
ACCEPTED 25 April 2023
PUBLISHED 18 May 2023

CITATION
Yang WS (2023), Ferroptosis: whERe is the critical site of lipid peroxidation?
Front. Cell Dev. Biol. 11:1179245.
doi: 10.3389/fcell.2023.1179245

Ferroptosis: whERe is the critical site of lipid peroxidation?

Wan Seok Yang*

Department of Biological Sciences, St. John's University, New York, NY, United States

KEYWORDS

ferroptosis, endoplasmic reticulum, Raman imaging, lipid perodixation, FINO2, D-PUFA, ike, RSL3

Ferroptosis is a regulated form of cell death that is driven by a lethal accumulation of lipid peroxides in cell membranes (Dixon et al., 2012). Recent studies have revealed the involvement of ferroptosis in various physiological and pathological conditions (Stockwell, 2022). Understanding the precise mechanism of ferroptosis is necessary to explain this phenomenon in various contexts.

Following the initial observation that lipid peroxides in cell membranes "execute" ferroptotic cell death, researchers have reported a more specific biochemical nature of these peroxides. For example, a genome-wide CRISPR screening identified acyl-CoA synthetase long-chain family member 4 (ACSL4) as an essential gene for executing ferroptosis, revealing that the ACSL4-mediated loading of the PUFAs to the membrane phospholipids is a critical event for executing ferroptosis (Doll et al., 2017). Conversely, unloaded, free PUFAs within cells were found to be neutral in modulating ferroptosis sensitivity. In addition, LC-MS/MS-based lipidomics analysis showed that phosphatidylethanolamines (PEs) containing polyunsaturated fatty acids (PUFAs) were more susceptible to oxidative damage during ferroptosis compared to other phospholipids in cell membranes (Kagan et al., 2017). Later, another genome-wide CRISPR screening discovered ether-phospholipid with PUFAs as a distinct functional lipid class mediating ferroptosis (Zou et al., 2020).

Despite significant progress in identifying and refining lipid classes relevant to ferroptosis, there remined the question of whether specific subcellular locations of lipids that are more susceptible to ferroptosis initiation or play more important roles in ferroptosis execution. A recent study by von Krusenstiern and others (von Krusenstiern et al., 2023) addressed this question using fluorescence and stimulated Raman scattering (SRS) imaging techniques (Figure 1). Compared to fluorescent tags, Raman active tags offer an advantage in monitoring the subcellular location of small molecules, such as drugs or metabolites, due to their relatively tiny size (Shen et al., 2019).

The authors first examined the cellular localization of deuterated-PUFA (D-PUFA), a specific ferroptosis inhibitor (von Krusenstiern et al., 2023; Yang et al., 2016). Since deuterium is a Raman active tag, there was no need to modify D-PUFA further to visualize it within cells. SRS imaging revealed that D-PUFAs were primarily located in perinuclear regions and abundant puncta structures in the cells, and subsequent fluorescence imaging with Nile Red confirmed the puncta structures as lipid droplets. Treatment of cells with diglyceride acyltransferase (DGAT) inhibitors removed these lipid droplets. However, the absence of lipid droplets did not affect D-PUFA's anti-ferroptotic activity, suggesting that lipid droplets are not functionally relevant to ferroptosis. Further analysis using fluorescence microscopy with ER-tracker Green dye revealed that the perinuclear region was the endoplasmic reticulum (ER), indicating that the ER is another cellular location where D-PUFAs mainly reside. Unlike lipid droplets, however, there was no straightforward way to alter the surface area of ER using pharmacological or genetic reagents. For example, induction of ER-phagy (Mochida and Nakatogawa, 2022) was unsuccessful in the cell lines used in this study, despite extensive attempts. Instead, the

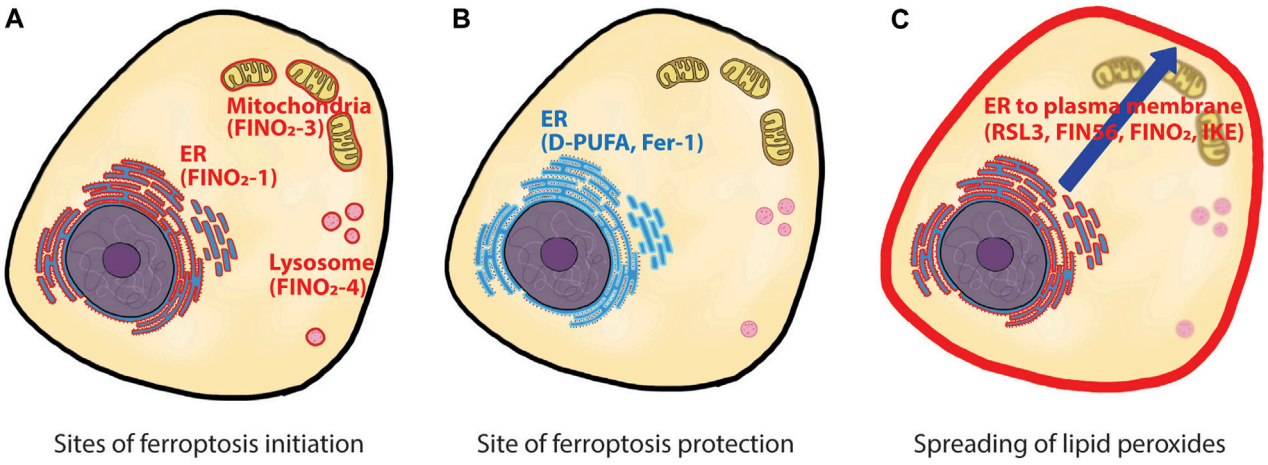

FIGURE 1
Site of action for ferroptosis initiation, protection, and spreading. **(A)** ferroptosis can be initiated from multiple sites within cells. Three ferroptosis inducers, $FINO_2$-1, $FINO_2$-3, and $FINO_2$-4 initiated ferroptosis from different locations, namely, ER, mitochondria, and lysosome. **(B)** D-PUFA and Fer-1, the two ferroptosis inhibitors, reside in ER and suppress ferroptosis initiated from all locations. **(C)** time-lapse observation of ferroptosis showed initial lipid peroxidation in ER, then a late lipid peroxidation in the plasma membrane. How the lipid peroxides spread from ER to the plasma membrane is unknown. ER: endoplasmic reticulum, D-PUFA: deuterated polyunsaturated fatty acid, Fer-1: ferrostatin-1..

authors treated cells with pro-ferroptotic PUFAs or anti-ferroptotic MUFAs and determined their cellular locations using SRS imaging. Both fatty acids were mainly located in the ER, with small percentages located in plasma membrane. The authors then overexpressed ACSL4 in the cells to increase the loading of pro-ferroptotic PUFAs or anti-ferroptotic MUFAs to the ER phospholipids. This approach demonstrated a solid correlation between the ER membrane composition and ferroptosis sensitivity, highlighting the ER as a site of ferroptosis modulation.

Next, the authors explored the site of action for $FINO_2$, a canonical ferroptosis inducer, which directly oxidizes cellular iron and indirectly inhibits GPx4 to induce ferroptosis (Gaschler et al., 2018a). Structurally, $FINO_2$ is a lipophilic compound that contains an endoperoxide moiety, allowing it to accumulate in cell membranes and induce lipid peroxidation directly at those locations. Taking advantage of this feature, the authors synthesized a series of $FINO_2$ analogs with fluorescent tags that were distributed to different cellular locations to investigate whether ferroptosis can be initiated by oxidative damage in a particular cell membrane. The original $FINO_2$ with a fluorescent tag displayed ER distribution and induced ferroptosis. Interestingly, $FINO_2$ analogs distributed to mitochondria and lysosomes also induced ferroptosis, indicating that ferroptosis can be initiated from various organelles. More importantly, cells treated with mitochondrial and lysosomal $FINO_2$ analogs were protected by ferrostatin-1 (Fer-1). A previous report demonstrated that Fer-1 primarily acted at the ER site, rather than in mitochondria and lysosomes which were dispensable to Fer-1's anti-ferroptotic activity (Gaschler et al., 2018b). These data suggest that while ferroptosis can be initiated at multiple sites, the ER is the critical site for ferroptosis protection.

Lastly, the authors examined time-dependent changes in the location of lipid peroxidation using BODIPY™-C11 dye and fluorescence microscopy. Upon treatment with ferroptosis inducers, cells underwent initial lipid peroxidation events in the ER, followed by lipid peroxidation in the plasma membrane. This time-dependent change was observed in all four classes of ferroptosis inducers (RSL3, FIN56, $FINO_2$, or IKE). These findings complement a previous study, which reported that both erastin2 and RSL3 caused intracellular lipid peroxidation before the onset of lipid peroxidation in the plasma membrane (Magtanong et al., 2022). Altogether, these data strongly point towards the ER membrane as the most critical site for inducing ferroptosis.

In summary, the findings outlined above emphasized the essential role of the ER in ferroptotic cell death. The conclusion from the current research raises several intriguing questions. First, what makes the ER so critical in executing ferroptosis? Does the ER membrane contain a higher level of ferroptosis-relevant lipids compared to other organelles? Are there any microenvironmental factors in the ER that can affect ferroptosis? A refined lipidomics analysis with subcellular fractionation samples may provide answers to these questions. Second, how is the ferroptosis signal initiated from other organelles transduced to the ER? For example, it is unclear how the lipid peroxides in mitochondria or lysosomes spread to the ER when $FINO_2$ analogs are used. This question also applies to the later stage of ferroptosis. How are the lipid peroxides in the ER transduced or transported to the plasma membrane before the onset of cell death? Could it be the conventional vesicle-mediated transport or some other mechanism? Third, can we find more specific regions within the ER, such as rough ER, smooth ER, ER lumen, or microdomains in the ER membrane, that are responsible for the initiation of ferroptosis? Lastly, what are the ER-specific genes that regulate ferroptosis? Xiaodong Wang's group recently discovered that the ER-resident oxidoreductases POR and CYB5R1 produced initial hydrogen peroxides, which subsequently induced lipid peroxidation and ferroptosis (Yan et al., 2021). Future research focused on the ER should broaden our knowledge about the natural triggers of

ferroptosis and help identify better target proteins for ferroptosis targeted therapy.

Author contributions

The author confirms being the sole contributor of this work and has approved it for publication.

Acknowledgments

The author is grateful to Katherine J. Kim (UCSD) for critical reading of the manuscript.

Conflict of interest

The author declares that the research was conducted in the absence of any commercial or financial relationships that could be construed as a potential conflict of interest.

Publisher's note

References

Dixon, S. J., Lemberg, K. M., Lamprecht, M. R., Skouta, R., Zaitsev, E. M., Gleason, C. E., et al. (2012). Ferroptosis: An iron-dependent form of nonapoptotic cell death. *Cell* 149, 1060–1072. doi:10.1016/j.cell.2012.03.042

Doll, S., Proneth, B., Tyurina, Y. Y., Panzilius, E., Kobayashi, S., Ingold, I., et al. (2017). ACSL4 dictates ferroptosis sensitivity by shaping cellular lipid composition. *Nat. Chem. Biol.* 13, 91–98. doi:10.1038/nchembio.2239

Gaschler, M. M., Andia, A. A., Liu, H., Csuka, J. M., Hurlocker, B., Vaiana, C. A., et al. (2018). FINO(2) initiates ferroptosis through GPX4 inactivation and iron oxidation. *Nat. Chem. Biol.* 14, 507–515. doi:10.1038/s41589-018-0031-6

Gaschler, M. M., Hu, F., Feng, H., Linkermann, A., Min, W., and Stockwell, B. R. (2018). Determination of the subcellular localization and mechanism of action of ferrostatins in suppressing ferroptosis. *ACS Chem. Biol.* 13, 1013–1020. doi:10.1021/acschembio.8b00199

Kagan, V. E., Mao, G., Qu, F., Angeli, J. P. F., Doll, S., Croix, C. S., et al. (2017). Oxidized arachidonic and adrenic PEs navigate cells to ferroptosis. *Nat. Chem. Biol.* 13, 81–90. doi:10.1038/nchembio.2238

Magtanong, L., Mueller, G. D., Williams, K. J., Billmann, M., Chan, K., Armenta, D. A., et al. (2022). Context-dependent regulation of ferroptosis sensitivity. *Cell Chem. Biol.* 29, 1409–1418.e6. doi:10.1016/j.chembiol.2022.06.004

Mochida, K., and Nakatogawa, H. (2022). ER-Phagy: Selective autophagy of the endoplasmic reticulum. *EMBO Rep.* 23, e55192. doi:10.15252/embr.202255192

Shen, Y., Hu, F., and Min, W. (2019). Raman imaging of small biomolecules. *Annu. Rev. Biophys.* 48, 347–369. doi:10.1146/annurev-biophys-052118-115500

Stockwell, B. R. (2022). Ferroptosis turns 10: Emerging mechanisms, physiological functions, and therapeutic applications. *Cell* 185, 2401–2421. doi:10.1016/j.cell.2022.06.003

von Krusenstiern, A. N., Robson, R. N., Qian, N., Qiu, B., Hu, F., Reznik, E., et al. (2023). Identification of essential sites of lipid peroxidation in ferroptosis *Nat. Chem. Biol.* doi:10.1038/s41589-022-01249-3

Yan, B., Ai, Y., Sun, Q., Ma, Y., Cao, Y., Wang, J., et al. (2021). Membrane damage during ferroptosis is caused by oxidation of phospholipids catalyzed by the oxidoreductases POR and CYB5R1. *Mol. Cell* 81, 355–369.e10. doi:10.1016/j.molcel.2020.11.024

Yang, W. S., Kim, K. J., Gaschler, M. M., Patel, M., Shchepinov, M. S., and Stockwell, B. R. (2016). Peroxidation of polyunsaturated fatty acids by lipoxygenases drives ferroptosis. *Proc. Natl. Acad. Sci. U. S. A.* 113, E4966–E4975. doi:10.1073/pnas.1603244113

Zou, Y., Henry, W. S., Ricq, E. L., Graham, E. T., Phadnis, V. V., Maretich, P., et al. (2020). Plasticity of ether lipids promotes ferroptosis susceptibility and evasion. *Nature* 585, 603–608. doi:10.1038/s41586-020-2732-8

frontiers | Frontiers in Immunology

TYPE Original Research
PUBLISHED 06 September 2024
DOI 10.3389/fimmu.2024.1394477

OPEN ACCESS

EDITED BY
Patrice X. Petit,
Centre National de la Recherche Scientifique (CNRS), France

REVIEWED BY
Bingcai Qi,
Capital Medical University, China
Xiaohui Liao,
Chongqing Medical University, China

*CORRESPONDENCE
Liwen Lyu
iculvliwen@163.com
LingZhang Meng
lzmeng@gxams.org.cn

†These authors have contributed equally to this work

RECEIVED 01 March 2024
ACCEPTED 22 August 2024
PUBLISHED 06 September 2024

CITATION
Zhou Y, Yang Y, Wang B, Chen W, Wei Y, Wu R, Meng L and Lyu L (2024) Discovery of ferroptosis-related genes in renal ischemia reperfusion and evaluate the potential impact on kidney transplantation.
Front. Immunol. 15:1394477.
doi: 10.3389/fimmu.2024.1394477

Discovery of ferroptosis-related genes in renal ischemia reperfusion and evaluate the potential impact on kidney transplantation

Yao Zhou[1†], Yuwei Yang[2†], Bo Wang[1†], Wan Chen[1], Yanlin Wei[1], Ruihua Wu[1], LingZhang Meng[3*] and Liwen Lyu[1*]

[1]Department of Emergency, Guangxi Academy of Medical Sciences & People's Hospital of Guangxi Zhuang Autonomous Region, Nanning, China, [2]Ruikang Hospital Affiliated to Guangxi University of Chinese Medicine, Nanning, China, [3]Institute of Cardiovascular Sciences, Guangxi Academy of Medical Sciences, & The People's Hospital of Guangxi Zhuang Autonomous Region, Nanning, China

Background: Renal ischemia reperfusion injury (IRI) is one of the pivotal event of acute kidney injury (AKI), and they are unavoidable in the process of kidney transplantation, which eventually leads to the loss of renal allograft. Ferroptosis is a newly identified programmed cell death. Recent studies have suggested that ferroptosis may participate in the pathophysiological process of renal IRI. Therefore, we aimed to determine biomarkers associated with ferroptosis during renal IRI and their impact on renal allografts.

Methods: We conducted a comprehensive bioinformatics analysis and established an IRI-AKI animal model to illustrate the critical role of ferroptosis-related hub genes (FRHGs) in IRI-AKI and their potential impact on kidney transplantation.

Results: In this study, we identified 60 ferroptosis-related genes (FRGs) in renal IRI based on the GSE148420 dataset and FerrDb database. And then we performed functional annotation analysis using Gene Ontology (GO) and Kyoto Encyclopedia of Genes and Genomes (KEGG) pathway enrichment. Protein-protein interaction (PPI) network was constructed by online tool String. EZH2, CDKN1A, PPARA, EGR1, ATF3, and CD44 were identited as six ferroptosis-related hubgenes (FRHGs) using four methods, including MMC, Degree, DMNC, and EPC. FRHGs expression level were verified by the validation sets GSE58438 and GSE126805. Protein expression level of FRHGs verified by Proteomics and Western blot. Cibersort was utilized to analyze immune cell infiltration during renal IRI as well as the correlation between FRHGs and immune cells. The GSE21374 dataset was used for renal allografts survival analysis. Finally, We induced the IRI-AKI animal model and illustrated the importance of FRGHs CD44 in ferroptosis and the accumulation of macrophages.

Conclusion: We identified 6 FRHGs. We found that FRHGs not only exhibited significant correlation with immune cells but also directly influenced the survival of transplanted kidneys in the human population. Among six FRHGs, only CD44

was overexpressed at both the gene and protein levels. Anti-CD44 exerts a protective effect by inhibiting ferroptosis and the accumulation of M1 macrophages during renal IRI. This study provided new insights into the pathogenesis of renal IRI and provided new evidence for its treatment.

KEYWORDS

acute kidney injury, ferroptosis, bioinformatics, proteomics, kidney transplantation

Introduction

Renal IRI, which can cause acute kidney injury (AKI), is a common event after kidney transplantation, increases the risk of delayed graft function (DGF), rejects the donor kidney, and leads to a long-term risk of allograft loss. Existing research has shown that metabolic imbalance and excessive generation of reactive oxygen species (ROS) during the hypoxia process, as well as inflammatory reactions during the re-oxygenation process are important pathological and physiological processes in renal IRI (1).

Ferroptosis is a novel form of programmed cell death characterized by iron-dependent phospholipid peroxidation (2). It is caused by an imbalance between oxidants and antioxidants, which is driven by the abnormal expression and activity of various oxidoreductases (3). Oxidative stress is a crucial factor in renal IRI. Recent studies have suggested that ferroptosis may play an important role in IRI (4, 5). For example, legumain has been shown to promote renal tubule ferroptosis in IRI-AKI, and this mechanism may be related to chaperone-mediated autophagy of GPX4 (6). However, further research is needed to explore how ferroptosis is involved in the development and progression of renal IRI.

In this study, we download GSE148420, GSE58438, GSE126805 and GSE21374 datasets from the Gene Expression Omnibus (GEO) database. And then we performed a systematic bioinformatic analysis based on differentially expressed ferroptosis-related genes (DEFRGs), so as to identify FRHGs involved in the renal IRI process in the kidneys and analyze their associations with immune infiltration and renal allograft survival. Finally, We performed proteomic analysis and animal experiment to further validate the expression of FRHGs and the ferroptosis-related pathways enriched during renal IRI.

Materials and methods

Data collection and acquisition of ferroptosis-related genes

The RNA expression data, which included 4 IRI groups and 4 Sham groups, were collected from GEO (http://www.ncbi.nlm.nih.gov/geo/) database with series numbers GSE148420. The GSE21374, GSE58438 and GSE126805 datasets were also obtained from the GEO database. The dataset GSE58438 contains 19 samples from 4 experimental groups, including 5 Sham group samples, five IRI 3h samples, four IRI 24h samples, and five IRI 120h samples. The dataset GSE126805 includes samples from 42 kidney transplant recipients at 4 different time points, namely before transplant, after transplant, 3 months after transplant, and 1 year after transplant. The dataset GSE21374 includes gene expression data and graft survival information from renal transplant patients, comprising 51 cases of allograft loss and 231 cases of allograft survival. These datasets cover various stages of ischemia-reperfusion injury, but unfortunately, they come from different species. Ferroptosis-related genes(FRGs), including drive, suppress, or mark gene, were obtained from the FerrDb (http://www.zhounan.org/ferrdb) database. A flowchart of this study is shown in Figure 1.

Establishment of animal models

Eighteen SPF-grade Balb/c mice were selected, aged 6-8 weeks, weighing 20-25g (purchased from Hunan SJA Laboratory Animal Co., Ltd), and were randomly divided into Sham group, IR-AKI group and IR+Anti-CD44 group. The IR+Anti-CD44 group was injected with CD44 monoclonal antibody (100ug) 30 minutes before ischemia procedure. The surgical incision was made approximately 0.5 cm to the left or right of the midline on the back of the mouse to expose the kidney. The right kidney was removed from all groups, the Sham group exposed the left kidney without clamping, and the IR group exposed the left kidney and rapidly clamped the left renal pedicle with an atraumatic microvascular clamp. Successful clamping was indicated by a rapid change in kidney color from dark red to dark purple. After 45 minutes of ischemia, releasing the clamp demonstrated a change in kidney color from purple-black back to red, indicating successful reperfusion. The reperfusion time was 24 hours. This study has been approved by the Animal Ethics Committee of Guangxi University of Chinese Medicine (Approval No.: DW20220529-216).

HE and PAS staining

Hematoxylin and eosin (HE) staining and PAS staining was used to detect pathological damage in the kidney tissue. All steps

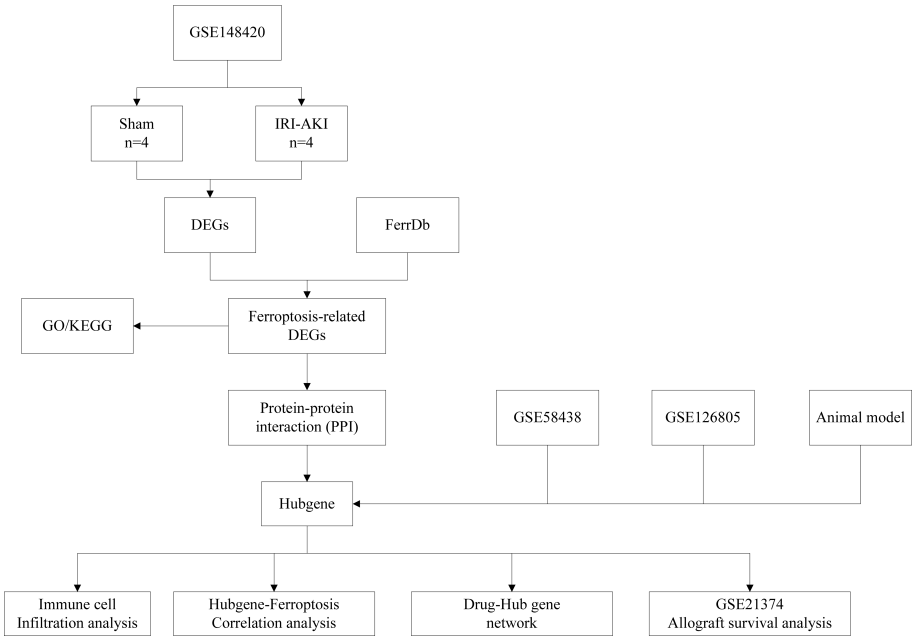

FIGURE 1
Flowchart of this study.

were performed according to manufacturer's instructions. The injury scoring was recorded with blind assessment method, with the following scores: 0, normal; 1, mild; 2, moderate; 3, severe.

Identification of differentially expressed ferroptosis-related genes

Differentially-expressed genes (DEGs) between IRI-AKI and Sham group were acquired by the "Limma" package in R software. The absolute value of Log2Fold > 1.0 and adj.P<0.05 were used as significance indicators. DEGs were visualized by volcanic maps using the "ggplot2" package in R software. The top 50 DEGs were shown by heat map based on the "pheatmap" package in R software. The intersection of DEGs and FRGs obtained in the FerrDb Database is defined as differentially expressed ferroptosis-related genes (DEFRGs). The number of DEFRGs was shown in a Venn diagram using the online tool "jvenn" (https://jvenn.toulouse.inrae.fr) (7).

Functional annotation and pathway enrichment of DEFGRs

To reveal the underlying biological functions and underlying mechanisms of DEFRGs, we used the Sangerbox (http://sangerbox.com/) online analysis tool for gene ontology (GO) and Kyoto Encyclopedia of Gene and Genes (KEGG) enrichment analysis of DEFRGs. GO enrichment analysis includes biological processes (BPs), cellular components (CCs) and molecular functions (MFs); adj. P<0.05 is the threshold for screening the main enrichment functions and pathways of DEFRGs.

Construction of protein–protein interaction network of DEFRGs

To further explore the Protein–Protein interactions(PPI) among DEFRGs, we constructed a PPI network of DEFGRs using the online tool "String" (http://www.string-db.org/) (Version 11.5) database. We set 0.4 (medium confidence) as minimum interaction score. We identified key genes in the PPI network of DEFGRs using four algorithms from the Cytohubba plug-in. The four algorithms are Degree, Density of Maximum Neighborhood Component (DMNC), Edge Percolated component (EPC) and Maximum neighborhood component (MNC). Top 10 key genes were defined as hubgenes. Then the Hubgenes obtained from the four algorithms was intersected with each other, and the intersection genes were defined as the most valuable ferroptosis-related Hub genes (FRHGs) for renal IRI.

Validation of FRHGs expression of IRI-AKI

To further validate the expression level of FRHGs in GSE148420, the external datasets GSE58438, GSE126805 were used as external validation sets. we performed a statistical analysis on the expression of the FRHGs between each group in the external validation set, and P<0.05 was considered statistically significant. Secondly, Proteomics and Western blot is used to validate the expression levels of key proteins. Proteomic sequencing is performed by Novogene Co. Ltd. Bioinformatics analysis was done with R software. An appropriate amount of liver tissue is taken and added to 500 µL of protein lysis buffer, then ground using a fully automatic cryogenic grinder. The resulting mixture is then

centrifuged at low temperature and high speed (4°C,12,000 r/min) for 10 minutes, and the supernatant is collected to obtain the extracted tissue protein solution. After quantifying the protein using the BCA method, the protein is mixed with protein loading buffer at a 4:1 ratio and boiled at 100°C for 10 minutes. 60 μg of the sample is loaded per lane, and the protein extracts are separated by polyacrylamide gel electrophoresis (PAGE) in the electrophoresis solution. The proteins are then transferred to a PVDF membrane using the "wet transfer method." The membrane is blocked with 5% skim milk at room temperature for 1 hour, followed by respective incubation with primary and secondary antibodies, and then visualized and analyzed using Imaging J.

Correlation analysis between FRHGs and immune cell infiltration

R package "Cibersort" was used to calculate the proportion of 22 different immune cells type in GSE148420 datasets (8). Spearman's correlation analysis between infiltrating immune cells and FRHGs was calculated using "Corrplot" in R software. Correlation analysis result was shown in the dot plot.

Renal graft survival analysis

We further investigated the effects of FRHGs on long-term allograft survival through the utilization of the GSE21374 dataset. The Sangerbox online tool was used to plot survival curves.

Potential drug identification of the FRHGs

We use the drug gene interactions database (DGIdb, www.dgidb.org) to predict drugs and molecular compounds that may interact with FRHGs. The Cytoscape software is used to visualize the drug-gene interaction network.

Assessment of kidney function

Renal function was evaluated through the measurement of serum creatinine(Scr) and blood urea nitrogen(BUN)levels, conducted in accordance with the manufacturer's protocol (Jiancheng, Nanjing, China).

Measurement of MDA and GSH

For the Malondialdehyde (MDA) assay, an appropriate quantity of tissue sample was weighed, thoroughly lysed, and centrifuged to yield 100 μL of supernatant. The assay was subsequently performed following the provided kit instructions (Solarbio, China), with absorbance recorded at 532 nm and 600 nm using a microplate reader. The assessment of Glutathione (GSH) was conducted in accordance with the guidance of the GSH detection kit (Solarbio, China), measuring absorbance at 412 nm. All procedures were conducted on ice to preserve sample integrity.

Immunohistochemistry and immunofluorescence detection

Tissue samples were fixed in 4% paraformaldehyde and rehydrated through a graded series of ethanol solutions. To block non-specific binding, sections were incubated at room temperature for 30 minutes in 10% goat serum. Subsequently, the sections were exposed to primary antibodies—mouse monoclonal antibodies against CD11b (EPR1344, Abcam), CD86 (EPR28721, Abcam), and GPX4 (67763-1-Ig, Proteintech)-and incubated overnight at 4°C. Following this, the samples were incubated with a secondary antibody for 30 minutes at room temperature. For immunohistochemistry (IHC), HRP-conjugated secondary antibodies were employed, while fluorescently labeled secondary antibodies were utilized for immunofluorescence (IF). Microscopic examination of the samples was conducted to assess staining.

TUNEL staining

Apoptotic cells were identified using a TUNEL Apoptosis Assay Kit (K1123, APExBIO), following the manufacturer's instructions. The average number of TUNEL-positive cells was quantified from five randomly selected fields under a fluorescence microscope (BX51, OLYMPUS, Japan) and expressed as a percentage of the total cell nuclei.

Transmission electron microscopy

Small pieces of renal cortex were excised and fixed in 2.5% glutaraldehyde. Following fixation, the samples were dehydrated and embedded. Ultra-thin sections were stained and subsequently examined using a transmission electron microscope (HITACHI HT7800, Japan).

Statistical analysis

All bioinformatics analyses were performed using R software; Statistical analyses of experimental data were processed by Prism software 9.0 (GraphPad software, La Jolla, CA). **** represents $P<0.0001$, *** represents $P<0.001$, ** represents $P<0.01$, * represents $P<0.05$.

Results

Identification of DEFRGs in IRI-AKI

In order to study the differentially expressed FRGs in IRI-AKI, 484 FRGs were extracted from FerrDb. FerrDb is a database of markers and diseases related to ferroptosis, which includes ferroptosis markers, drivers, and suppressors. Differential

expression analysis of the GSE148420 dataset showed that 2,468 genes were significantly differentially expressed in IRI-AKI group compared to sham group, with a threshold of |log2FC|≥ 1 and adj.P < 0.05 (Figure 2A). After taking the intersection of DEGs and FRGs, a total of 60 differentially expressed FRGs were defined as DEFRGs (Figure 2B), which were presented in a Venn diagram.

Functional enrichment analysis of DEFRGs

We investigated the potential biological function and pathways of DEFRGs based on GO and KEGG pathway analysis. The results were presented in a dot plot. GO-BP analysis revealed that the DEFRGs were mainly enriched in "small molecule metabolic process","response to lipid"," response to endogenous stimulus"[biological process, (BP)] (Figure 3A). GO-MF analysis revealed that the DEFRGs were mainly enriched in "oxidoreductase activity", "oxidoreductase activity acting on NADP(H)","iron ion binding" (Figure 3B). In the GO-CC, DEFRGs were mostly enriched in the "chromatin"," apical part of cell", "apical plasma membrane"," basolateral plasma membrane"," basal part of cell"," tertiary granule membrane" "chromatin silencing complex" "NADPH oxidase complex ", "perinuclear endoplasmic reticulum" [cellular component, (CC)] (Figure 3C). According to KEGG enrichment analysis, these DEFRGs were mainly enriched in the "HIF-1 signaling pathway", " Toll-like receptor signaling pathway", "NOD-like receptor signaling pathway" and "Ferroptosis" (Figure 3D).

Protein–protein interaction network construction and visualization

To explore the interactions between each DEFRG, all DEFRGs were submitted to the STING database to construct a PPI network. The DEFRGs PPI network included 59 nodes and 106 edges (Figure 4A). Subsequently, the PPI data was imported into Cytoscape, and four algorithms, namely Degree (Figure 4B), DMNC (Figure 4C), MNC (Figure 4D), and EPC (Figure 4E), were applied in Cytohubba to analyze hubgenes. The top 10 hubgenes obtained from the four algorithms were intersected, resulting in six ferroptosis-related hubgenes (FRHGs), including ATF3, EGR1, PPARA, CDKN1A, CD44, and EZH2 (Figure 4F).

Validation of FRHGs and allograft survival analysis

Through the above analysis process, we identified as EZH2, CDKN1A, PPARA, EGR1, ATF3, and CD44 as FRHGs. The datasets GSE58438 and GSE126805 were used to further confirm the expression levels of the FRHGs at different time points. In GSE58438, ATF3, EGR1, CDKN1A, and CD44 were significantly upregulated as early as 3 hours after renal IRI, where ATF3 and CD44 continued to increase for up to 120 hours. On the other hand, PPARA showed a decreasing trend at 3 hours after renal IRI, which continued to decrease for up to 120 hours. The increase in EZH2 expression was observed at around 120 hours (Figure 5A). In GSE126805, a similar trend was observed for ATF3, EGR1, and CDKN1A, whereas CD44 and EZH2 continued to increase even up to 1 year after renal IRI (Figure 5B). Interestingly, PPARA showed an increasing trend at 3 months after IR, which continued to increase for up to 1 year. To further understand the role of FRHGs in IRI-AKI, GSE21374 was utilized to analyze the relationship between FRHGs and renal allograft survival. The results showed that high expression levels of EZH2, CDKN1A, EGR1, ATF3, and CD44 were all associated with poor prognosis, while low expression of PPARA was associated with poor prognosis (Figure 5C). These experimental results indicate that EZH2, ATF3, EGR1, CDKN1A, and CD44 can be upregulated early after IR and their sustained high expression levels are associated with poor prognosis, while PPARA initially decreases in expression but can gradually recover, and its increased expression levels are associated with good prognosis.

Immune cell infiltration and correlation analysis of FRHGs and immune cells

In the GO and KEGG enrichment analysis of the DEFRGs, immune cells appear to play a crucial role in the process of renal IRI. To further confirm the role of immune cells, we conducted immune infiltration analysis and found significant differences (P<0.05) in seven immune cells between the IRI and Sham groups, namely: Dendritic cells activated, Dendritic cells resting, Macrophages M0, Macrophages M1, Macrophages M2, Monocytes, and Plasma. cells (Figures 6A, B). To better understand the role of FRHGs in immune infiltration, we used Spearman correlation analysis to determine their association with immune cell infiltration. The correlation analysis showed that EZH2, CDKN1A, PPARA, EGR1, ATF3, and CD44 were strongly correlated with all seven immune cells. Among them, EZH2 showed the strongest negative correlation with Macrophages.M0; CD44 showed strong positive correlation with Macrophages M1 and Dendritic cells resting; CDKN1A showed strong positive correlation with Macrophages M2; PPARA showed strong positive correlation with Plasma cells; and EGR1 and ATF3 showed strong positive correlation with Monocytes (Figure 6C).

Identification of potential drugs for FRHGs interactions

To further understand the interaction between FRHGs and drugs, we predicted drugs or molecular compounds that may interact with FRHGs based on the DGIDB database. A total of 87 drugs or molecular compounds that may have regulatory relationships with FRHGs were screened, of which the largest number of drugs interacting with PPARA was identified, with a total of 57 related drugs (Figure 7).

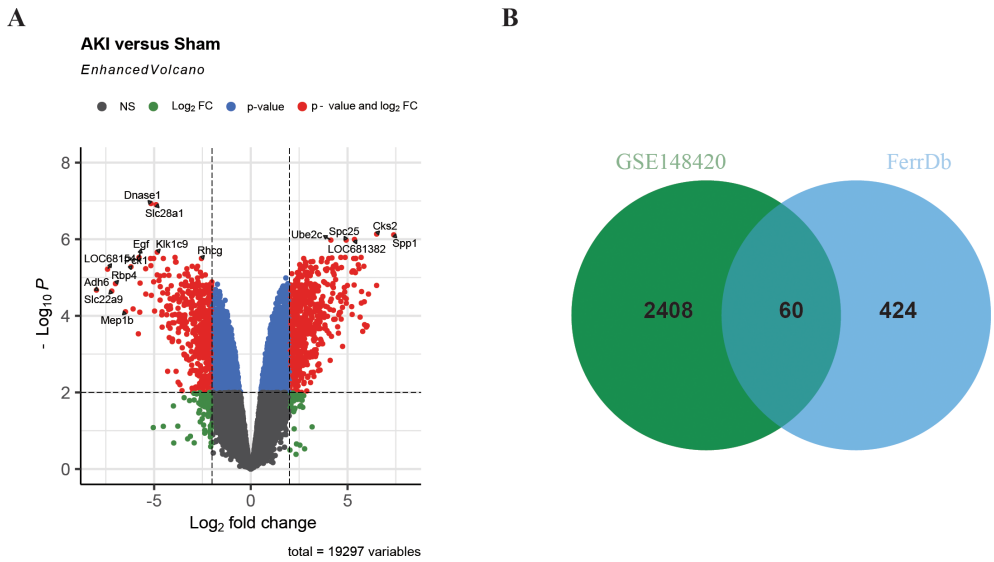

FIGURE 2
Identification of DEFRGs. **(A)** Volcano plot of differentially expressed genes in renal IRI. **(B)** Venn plot of Ferroptosis-related genes and DEGs in renal IRI.

Validation of FRHGs protein expression by proteomics and Western blot

As we all know that protein is the primary executor of gene function. In this study, Proteomics and Western blot were further used to confirm the protein expression of FRHGs. Hematoxylin and eosin (HE) staining and creatinine determination confirmed successful modeling (Figures 8A, B). Differentially expressed proteins (DEPs) between IRI-AKI and Sham groups were analyzed in R software. The results showed 88 proteins exhibiting an upregulation trend, and 198 proteins exhibiting a downregulation trend (Figure 8C). GO analysis showed that "ion transport [BP]," "membrane [CC]," "ion channel activity [MF]," and "iron ion binding [MF]" were the most significantly enriched

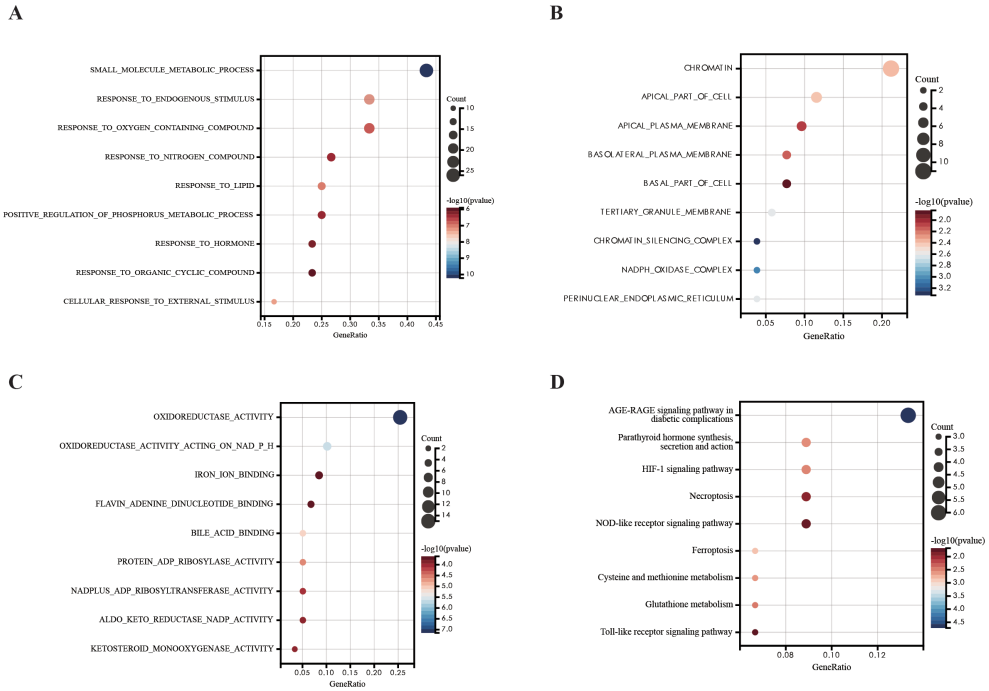

FIGURE 3
GO and KEGG pathway analysis of DEFRGs. **(A)** GO-BP analysis of DEFRGs. **(B)** GO-MF analysis of DEFRGs. **(C)** GO-CC analysis of DEFRGs. **(D)** KEGG analysis of DEFRGs.

10.3389/fimmu.2024.1394477

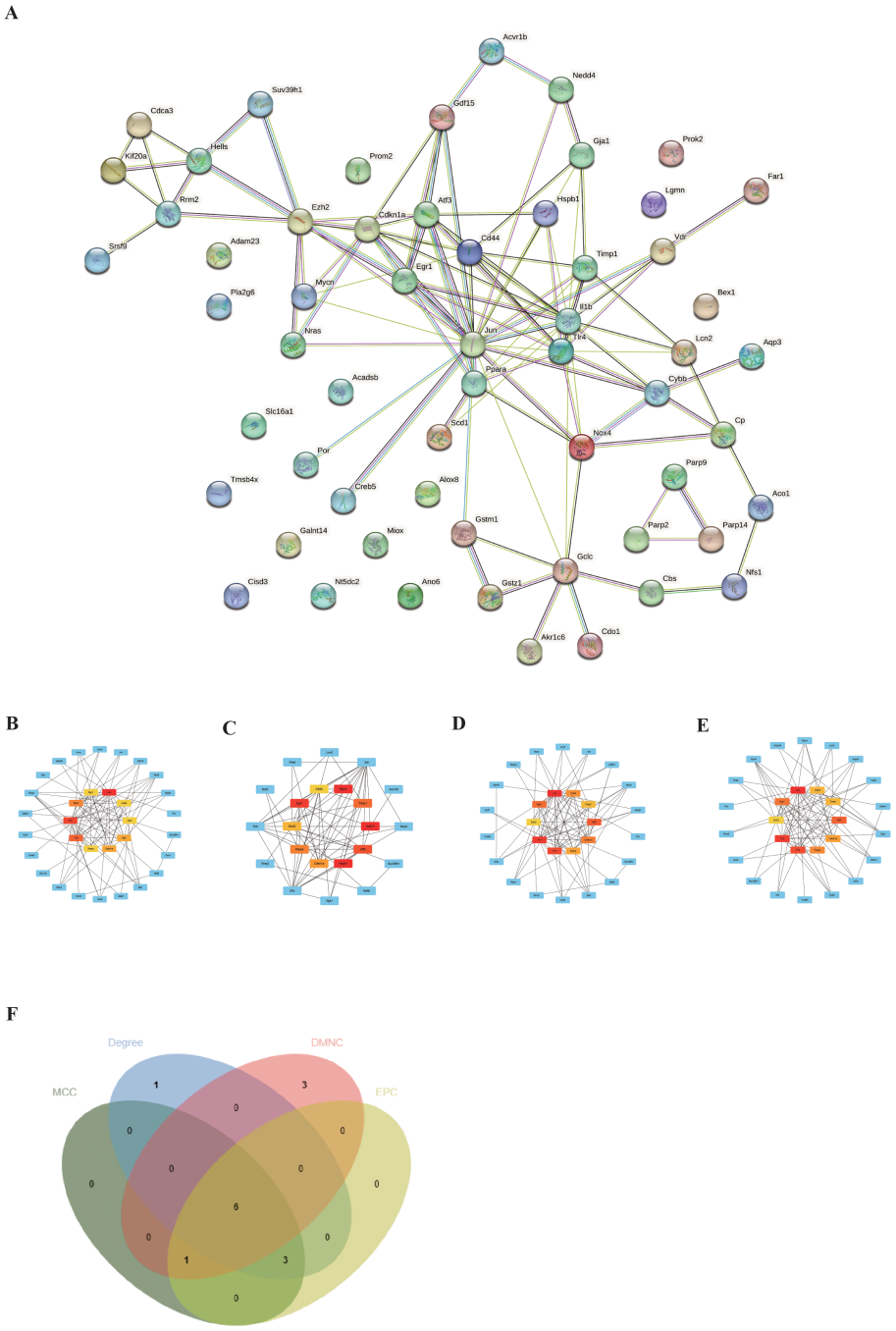

FIGURE 4
Identification of FRHGs. **(A)** PPI network of DEFRGs. **(B)** Top 10 Hubgenes identified by the Degree algorithm. **(C)** Top 10 Hubgenes identified by the DMNC algorithm. **(D)** Top 10 Hubgenes identified by the MNC algorithm. **(E)** Top 10 Hubgenes identified by the EPC algorithm. **(F)** Intersection of Hubgenes identified by all four algorithms.

biological processes (Figure 8D). In KEGG, "Arachidonic acid metabolism" was the primarily enriched pathway (Figure 8E). Among these, the iron ion binding pathway was the commonly enriched biological process between DEFRGs and DEPs. By overlapping DEFRGs with differentially expressed proteins, we identified three intersecting proteins, among which CD44 was the only FRGH with elevated expression at both the gene and protein levels (Figure 8F). Subsequently, we further validated the protein expression levels of CD44 using Western blot (Figure 8G).

Blockade of CD44 mitigates renal tissue injury following ischemia-reperfusion through inhibition of ferroptosis

To further elucidate the critical role of CD44 in IRI-AKI, we established a mouse model of IRI-AKI and administered CD44-blocking antibodies (Anti-CD44). Compared to the Sham group, the IRI-AKI group exhibited tissue damage characterized by tubular necrosis, epithelial cell shedding, and inflammatory cell infiltration

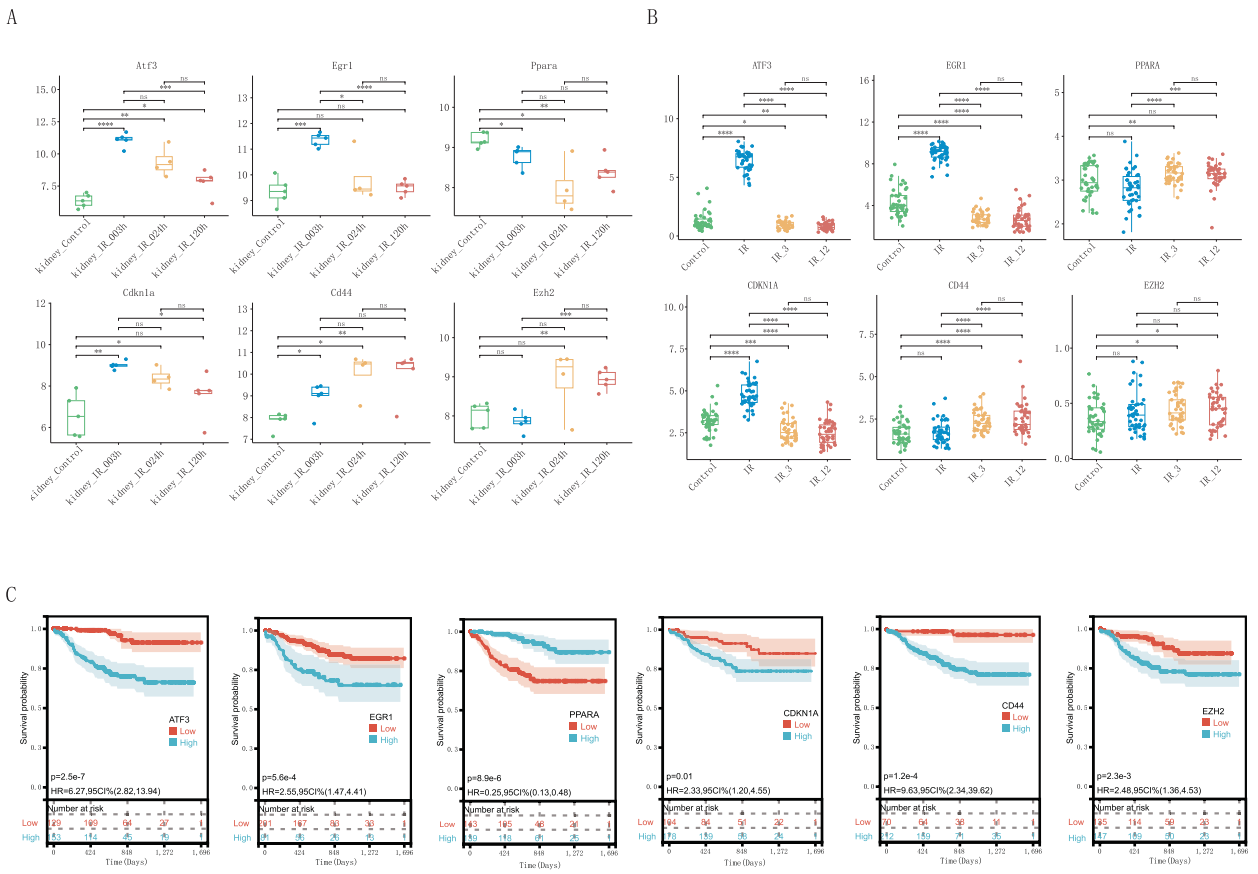

FIGURE 5
Validation and graft survival analysis of FRHGs. **(A)** FRHGs expression level in GSE58438. **(B)** FRHGs expression level in GSE126805. **(C)** The relationship between FRHGs and renal allograft survival. **** represents P<0.0001, *** represents P<0.001, ** represents P<0.01, * represents P<0.05, and ns indicates no statistical significance or no statistical difference.

(Figure 9A). Renal function assessments revealed that Scr and BUN levels were increased rapidly; however, pre-treatment with Anti-CD44 significantly mitigated histological injury and functional impairment in the kidneys (Figures 9A–C). We also investigated the role of CD44 in ferroptosis. TUNEL staining indicated high death rate in renal tissues following IRI, accompanied by significant declines in ferroptosis-related indicators such as glutathione (GSH) and GPX4, and a marked increase in MDA levels (Figures 9D–H). Transmission electron microscopy demonstrated diminished, degenerated, or absent mitochondrial cristae in the IRI-AKI group (Figure 9I). Pre-treatment with CD44 monoclonal antibodies effectively reduced ferroptosis, evidenced by a decrease in TUNEL positive cells, an increase in GSH levels, elevated GPX4 expression, and a reduction in MDA, as well as lessened mitochondrial structural damage (Figures 9D–I). These findings suggest that CD44 plays a protective role in inhibiting ferroptosis during renal IRI. Furthermore, immunohistochemical analyses indicated a significant increase in M1 macrophage accumulation during IRI, which was effectively reduced by Anti-CD44 treatment(Figure 9J). The relationship between reduced M1 macrophage accumulation and the inhibition of ferroptosis warrants further investigation.

Discussion

Acute kidney injury is a clinical syndrome characterized by a rapid decline in kidney function, such as glomerular filtration rate and endogenous creatinine clearance rate, within a short period of time. It has a high incidence and mortality rate. Although renal replacement therapy is becoming increasingly sophisticated, progress in identifying targets or treatment strategies to improve AKI outcomes has been slow. Ferroptosis is a unique form of cell death driven by iron-dependent lipid peroxidation, characterized by iron overload, accumulation of reactive oxygen species, and lipid peroxidation (2). Recent studies have shown that ferroptosis may represent a potential therapeutic target for kidney diseases, including AKI (9, 10). This study aims to identify important ferroptosis-related genes in IRI-AKI through bioinformatics analysis.

Iron accumulation and lipid peroxidation are two key signals that trigger membrane oxidative damage in the ferroptosis process (11). Iron accumulation may affect ferroptosis in three ways: the involvement of iron in the catalytic activity of metabolic enzymes LOXs and POR required for phospholipid peroxidation; iron is essential for enzymes involved in ROS generation; non-enzymatic,

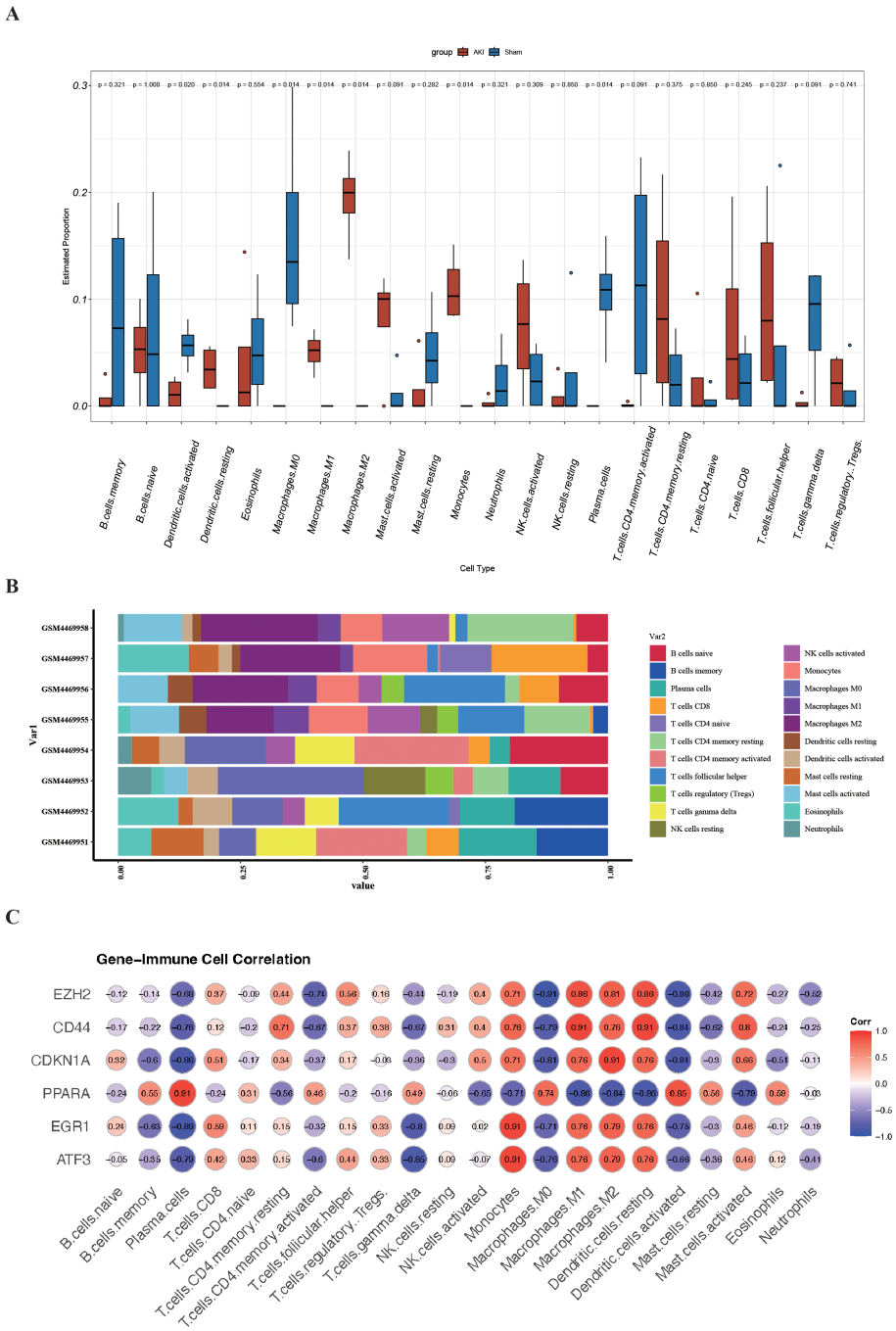

FIGURE 6
Analysis of immune cell infiltration and correlation with FRHGs in renal IRI. **(A)** Box plot shows the expression of 22 immune cells in renal IRI. **(B)** stacked plots of the expression of 22 immune cells in each sample. **(C)** correlation analysis between FRHGs and immune cells.

iron-dependent Fenton chain reactions may be necessary for ferroptosis (2). Additionally, polyunsaturated fatty acids (PUFAs), especially arachidonic acid and adrenic acid, are most susceptible to lipid peroxidation, leading to the destruction of the lipid bilayer and affecting membrane function (12, 13). In our study, we performed GO and KEGG enrichment analyses and found that DEFRGs were mainly enriched in "response to lipid (BP)", "iron ion binding (MF)", and "ferroptosis", which is interesting since lipid peroxidation is an important feature of ferroptosis. Proteins are one of the main carriers of biological functions and substance transport. Therefore, we used proteomics to explore the major changes in differential proteins in biological processes and pathways in IRI-AKI. The results showed that "ion transport (BP)", "membrane (CC)", "ion channel activity (MF)", and "iron ion binding (MF)" were the most significantly enriched biological processes. In the KEGG pathway analysis, "Arachidonic acid metabolism" was the major enriched pathway. Among them, "iron ion binding" was a common enriched biological process for

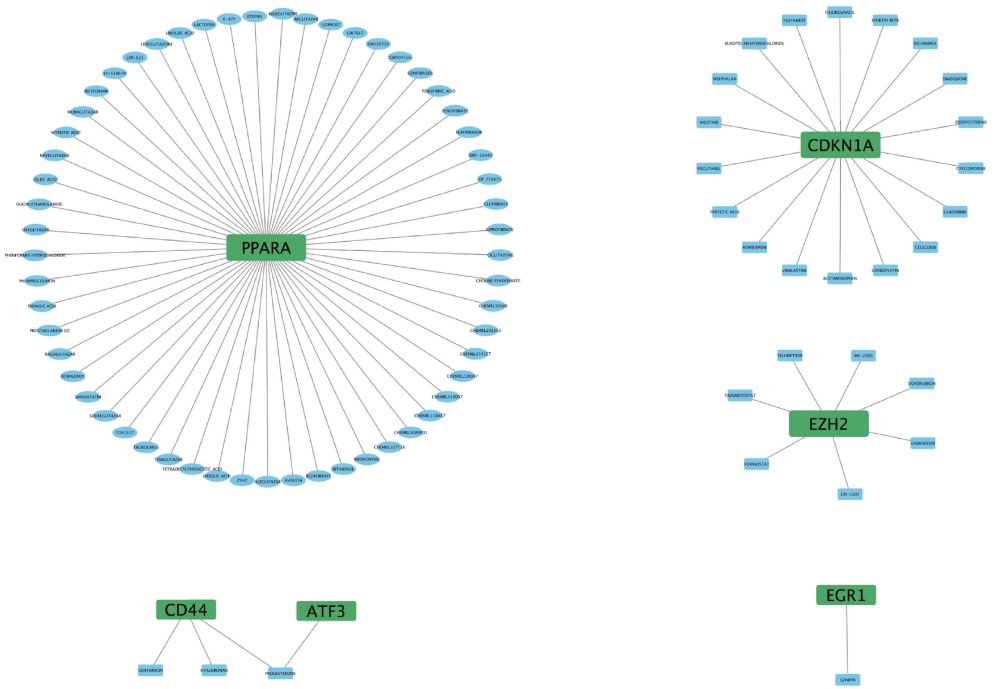

FIGURE 7
Drug interaction network with EZH2, CDKN1A, PPARA, EGR1, ATF3, and CD44 genes.

both DEFRGs and DEPs. Animal studies have shown that in IRI-AKI, STING promotes ferroptosis through NCOA4-dependent ferritinophagy (14), and inhibiting ferroptosis can alleviate drug or sepsis-induced kidney injury (15, 16). In our study, we elucidated that ferroptosis play a significant role in IRI-AKI, primarily manifested as an increase in MDA levels, a decrease in GSH levels, the reduction or disappearance of mitochondrial cristae, and a decrease in the expression of GPX4. In general, through the GO and KEGG analysis of transcriptomics and proteomics, we found multiple pathways or biological processes enriched in renal IRI related to iron transport and lipid metabolism. Through animal models, we have confirmed the occurrence of ferroptosis in IRI-AKI. Therefore, we believe that ferroptosis plays a crucial role in the process of IRI-AKI, and its mechanism may be related to iron accumulation and arachidonic acid metabolism.

Through KEGG enrichment analysis, we observed that DEFRGs were also enriched in "Toll-like receptor signaling pathway" and "NOD-like receptor signaling pathway". This suggests that ferroptosis-related genes may be involved in immune regulation and cannot be ignored in the process of renal IRI. Therefore, we performed immune infiltration analysis to further elucidate the relationship between FRGHs and immune cells. Our study suggests that PPARA is strongly positively correlated with Plasma. cells, and ATF3 and EGR1 are strongly positively correlated with Monocytes, while CD44 is strongly positively correlated with M1 Macrophages. EZH2 shows a negative correlation with M0 macrophages and a strong positive correlation with M2 macrophages. This suggests that CD44 and EZH2 may play important roles in macrophage polarization. Enhancer of zeste homolog 2 (EZH2) belongs to the family of polycomb group genes (PcGs), a crucial group of epigenetic regulators that are responsible for suppressing transcription (17). Research shows that EZH2 works as a master regulator of cell cycle progression (18), autophagy, and apoptosis (19), promotes DNA damage repair and inhibits cellular senescence (20) and plays an important role in cell lineage determination and relative signaling pathways (20). Reportedly, Targeting EZH2 protects against acute kidney injury via Raf-1/ERK1/2 pathway (21). What's more interesting, Targeted inhibition of EZH2 may improve renal fibrosis after acute kidney injury by counteracting partial EMT and blockade of M2 macrophage polarization (22). CD44, a kind of cell-surface glycoprotein, plays a role in angiogenesis, cytoskeleton rearrangement, tumor proliferation, cell adhesion, and migration (23).In recent years, studies have shown that a CD44-targeted hyaluronic acid-curcumin prodrug protects renal tubular epithelial cell survival from oxidative stress damage (24).Interestingly, CD44 contributed to the recruitment of monocyte/macrophages to the kidney following IRI (25). In our study, CD44 was the only FRGHs that was highly expressed at both the gene and protein levels. Further animal experiments confirmed that blocking CD44 inhibits ferroptosis and the accumulation of M1 macrophage, exerting a protective effect during IRI-AKI. However, the connection between M1 macrophages and ferroptosis requires further investigation.

As one of the main pathophysiological processes in kidney transplantation, IRI is closely related to the clinical prognosis of patients (26). Therefore, we investigated the impact of FRHGs on long-term graft survival. Survival analysis results showed that high expression levels of EZH2, CDKN1A, EGR1, ATF3, and CD44 were all associated with poor prognosis, while high expression of PPARA was associated with good prognosis. Among them, Early growth response 1 (EGR1) is an "immediate early" transcription factor that

10.3389/fimmu.2024.1394477

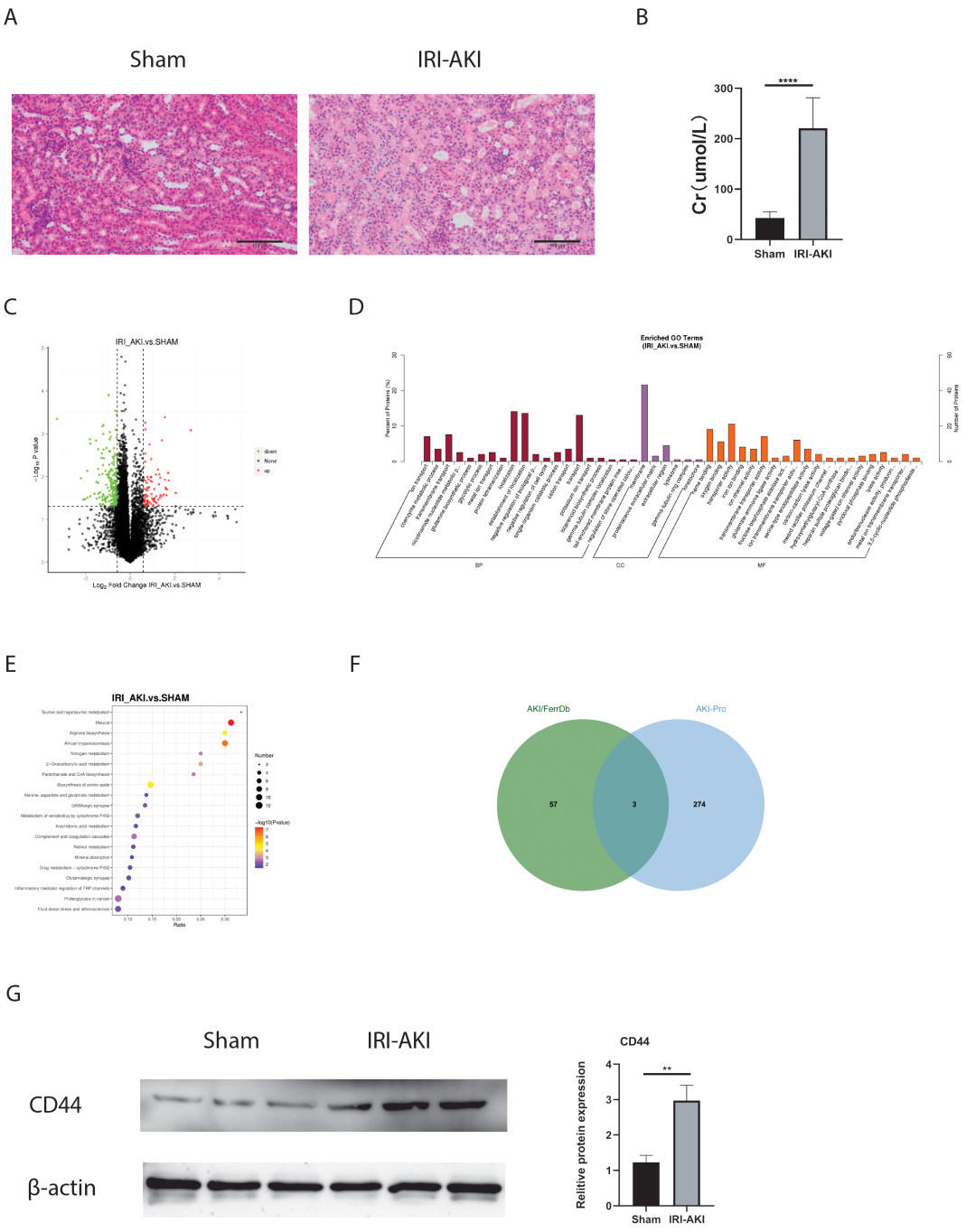

FIGURE 8
FRHGs protein expression of IRI-AKI. **(A)** The representative HE staining image of IRI-AKI. **(B)** The level of creatinine. **(C)** Volcano plot of differentially expressed proteins in IRI-AKI. **(D)** GO analysis of DEPs. **(E)** KEGG analysis of DEPs. **(F)** Intersection of FRHGs and DEPs. **(G)** CD44 proteins Level detected by Western blot. **** represents P<0.0001, ** represents P<0.01.

plays an important role in the migration of breast tumors (27). In normal adult kidneys, EGR1 expression is almost undetectable (28). EGR1 begins to rise immediately after IR and begins to decline slowly after peaking (29). ATF3 is a member of the ATF/CREB subfamily of the basic leucine zipper (BZIP) family. Previous studies have shown that ATF3 can be detected in urine within 2-24 hours in a rat model of AKI induced by ischemia reperfusion injury and is considered a novel diagnostic biomarker for AKI (30–32). PPARA has also been shown to have a protective role in IRI-AKI (33). Combined with our findings, these prognostic genes may be deeply involved in the progression of renal IRI, thereby having beneficial or harmful effects on long-term outcomes in post-transplant patients, and may serve as effective therapeutic targets. In fact, some studies have provided a theoretical basis for EGR1, ATF3, and PPARA as therapeutic targets (29, 34), and the clinical applicability needs to be further studied.

10.3389/fimmu.2024.1394477

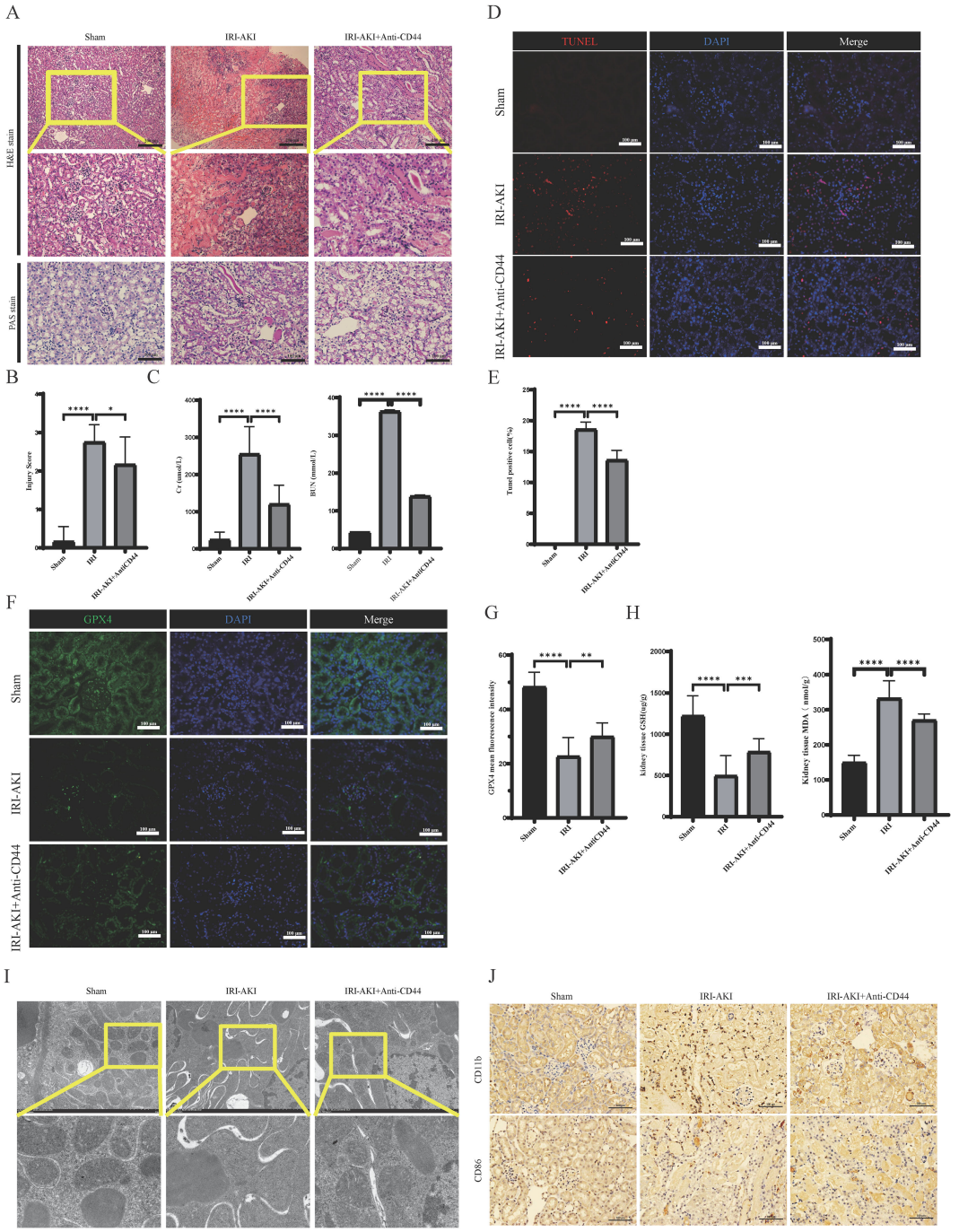

FIGURE 9
Blockade of CD44 inhibits the accumulation of macrophages and alleviates ferroptosis during the development of renal IR. **(A)** Representative image of HE and Pas staining. **(B)** Damage score of renal tubular injury; **(C)** Renal function detection; **(D)** The representative image of TUNEL staining; **(E)** The percentage of Tunel positive cell. **(F)** The representative image of immunofluorescence staining of GPX4; **(G)** Mean fluorescence intensity of GPX4. **(H)** GSH and MDA level in kidney tissue. **(I)** The representative image of transmission electron microscopy. **(J)** Macrophages infiltrated into kidney. **** represents P<0.0001, *** represents P<0.001, ** represents P<0.01, * represents P<0.05.

Finally, we predict that 87 drugs or molecular compounds may be involved in the regulation of Hub gene, which could be a potential anti-IRI-AKI drug. Many studies have already demonstrated the impact of drugs or molecular compounds on renal IRI. For example, Cyclosporine and Fenofibrate (PPARA) attenuate IRI-AKI in rat ischemia reperfusion model (35, 36). Dabrafenib alleviates kidney IRI by inhibiting cell death and suppressing inflammatory responses (37). Selective PPARA agonist GEMFIBROZIL may exert a protective role in IRI-AKI by reducing podocyte apoptosis (38); Celecoxib beneficially affects the outcome of renal IRI by reducing oxidative stress through decreasing COX-2 expression (39). These drugs or molecular compounds could be potential drugs for future treatment of IRI-AKI.

In conclusion, through bioinformatics analysis, proteomics analysis, and animal experiments, we identified six FRHGs during renal IRI: EZH2, CDKN1A, PPARA, EGR1, ATF3, and CD44. Among them, only CD44 was overexpressed at both the gene and protein levels. Anti-CD44 exerts a protective effect by inhibiting ferroptosis and the accumulation of M1 macrophages during renal IRI. However, the connection between M1 macrophages and ferroptosis requires further investigation.

The limitations of this study mainly include the following: the transcriptional data were obtained from different datasets in the GEO database, where different sequencing platforms and batch effects may affect the reliability of experimental results. Additionally, the proteomic sequencing results were self-generated data, thus potential batch effects could exist. Moreover, the sequencing data in this study included samples from both mice and humans, and insufficient consideration of inter-species differences limited the further clinical application of the study results, requiring more experiments for further validation.

Conclusions

In summary, we conducted comprehensive bioinformatics analyses of the IRI-AKI model and identified 6 ferroptosis-related Hub genes. We utilized proteomics to further validate the expression of ferroptosis-related proteins and discovered multiple pathways and biological processes related to ferroptosis were enriched in IRI-AKI. We found that ferroptosis-related hub genes not only exhibited significant correlation with immune cells but also directly influenced the survival of transplanted kidneys in the human population. Among six FRHGs, only CD44 was overexpressed at both the gene and protein levels. Anti-CD44 exerts a protective effect by inhibiting ferroptosis and the accumulation of M1 macrophages during renal IRI. The study also predicted 87 drugs that may act on IRI-AKI, some of which have been confirmed effective. These findings provide potential therapeutic targets and a deeper understanding of the mechanisms of IRI-AKI and offer novel perspectives on the diagnosis and treatment of IRI-AKI.

Data availability statement

The original contributions presented in the study are included in the article/supplementary materials. Further inquiries can be directed to the corresponding authors.

Ethics statement

The animal study was approved by the Animal Ethics Committee of Guangxi University of Chinese Medicine (Approval No.: DW20220529-216). The study was conducted in accordance with the local legislation and institutional requirements.

Author contributions

YZ: Writing – review & editing, Writing – original draft, Visualization, Formal analysis, Data curation. YY: Writing – review & editing, Writing – original draft, Visualization, Formal analysis, Data curation. BW: Writing – review & editing, Writing – original draft, Visualization, Validation. WC: Writing – review & editing, Writing – original draft. YW: Writing – review & editing, Writing – original draft, Visualization, Validation. RW: Writing – review & editing, Writing – original draft, Visualization, Validation. LM: Writing – review & editing, Writing – original draft, Supervision, Conceptualization. LL: Writing – review & editing, Writing – original draft, Supervision, Conceptualization.

Funding

The author(s) declare financial support was received for the research, authorship, and/or publication of this article. This study was funded by the Guangxi Medical and Health Appropriate Technology Development and Promotion Application Project (S2021049); Guangxi Graduate Education Innovation Program (YCSW2022338); Guangxi Natural Science Foundation (2022JJA141056, 2022JJB140644, 2023JJA141311); Guangxi Science and Technology Program (Guike AB24010174).

Acknowledgments

We acknowledge our use of R software. The results are in part based upon data derived from GEO, IMPI and FerrDB databases. We appreciate the platforms and the authors who uploaded their data.

Conflict of interest

The authors declare that the research was conducted in the absence of any commercial or financial relationships that could be construed as a potential conflict of interest.

Publisher's note

References

1. Aboutaleb N, Jamali H, Abolhasani M, Pazoki Toroudi H. Lavender oil (Lavandula angustifolia) attenuates renal ischemia/reperfusion injury in rats through suppression of inflammation, oxidative stress and apoptosis. *BioMed Pharmacother*. (2019) 110:9–19. doi: 10.1016/j.biopha.2018.11.045

2. Jiang X, Stockwell BR, Conrad M. Ferroptosis: mechanisms, biology and role in disease. *Nat Rev Mol Cell Biol*. (2021) 22:266–82. doi: 10.1038/s41580-020-00324-8

3. Tang D, Chen X, Kang R, Kroemer G. Ferroptosis: molecular mechanisms and health implications. *Cell Res*. (2021) 31:107–25. doi: 10.1038/s41422-020-00441-1

4. Li X, Ma N, Xu J, Zhang Y, Yang P, Su X, et al. Targeting ferroptosis: pathological mechanism and treatment of ischemia-reperfusion injury. *Oxid Med Cell Longev*. (2021) 2021:1587922. doi: 10.1155/2021/1587922

5. Hosohata K, Harnsirikarn T, Chokesuwattanaskul S. Ferroptosis: A potential therapeutic target in acute kidney injury. *Int J Mol Sci*. (2022) 23:6583. doi: 10.3390/ijms23126583

6. Chen C, Wang D, Yu Y, Zhao T, Min N, Wu Y, et al. Legumain promotes tubular ferroptosis by facilitating chaperone-mediated autophagy of GPX4 in AKI. *Cell Death Dis*. (2021) 12:65. doi: 10.1038/s41419-020-03362-4

7. Bardou P, Mariette J, Escudié F, Djemiel C, Klopp C. jvenn: an interactive Venn diagram viewer. *BMC Bioinf*. (2014) 15:293. doi: 10.1186/1471-2105-15-293

8. Newman AM, Steen CB, Liu CL, Gentles AJ, Chaudhuri AA, Scherer F, et al. Determining cell type abundance and expression from bulk tissues with digital cytometry. *Nat Biotechnol*. (2019) 37:773–82. doi: 10.1038/s41587-019-0114-2

9. Ni L, Yuan C, Wu X. Targeting ferroptosis in acute kidney injury. *Cell Death Dis*. (2022) 13:182. doi: 10.1038/s41419-022-04628-9

10. Feng Q, Yu X, Qiao Y, Pan S, Wang R, Zheng B, et al. Ferroptosis and acute kidney injury (AKI): molecular mechanisms and therapeutic potentials. *Front Pharmacol*. (2022) 13:858676. doi: 10.3389/fphar.2022.858676

11. Chen X, Kang R, Kroemer G, Tang D. Broadening horizons: the role of ferroptosis in cancer. *Nat Rev Clin Oncol*. (2021) 18:280–96. doi: 10.1038/s41571-020-00462-0

12. Lee JY, Nam M, Son HY, Hyun K, Jang SY, Kim JW, et al. Polyunsaturated fatty acid biosynthesis pathway determines ferroptosis sensitivity in gastric cancer. *Proc Natl Acad Sci USA*. (2020) 117:32433–42. doi: 10.1073/pnas.2006828117

13. Kagan VE, Mao G, Qu F, Angeli JPF, Doll S, Croix CS, et al. Oxidized arachidonic and adrenic PEs navigate cells to ferroptosis. *Nat Chem Biol*. (2017) 13:81–90. doi: 10.1038/nchembio.2238

14. Jin L, Yu B, Wang H, Shi L, Yang J, Wu L, et al. STING promotes ferroptosis through NCOA4-dependent ferritinophagy in acute kidney injury. *Free Radic Biol Med*. (2023) 208:348–60. doi: 10.1016/j.freeradbiomed.2023.08.025

15. Hu Z, Zhang H, Yi B, Yang S, Liu J, Hu J, et al. VDR activation attenuate cisplatin induced AKI by inhibiting ferroptosis. *Cell Death Dis*. (2020) 11:73. doi: 10.1038/s41419-020-2256-z

16. Qiongyue Z, Xin Y, Meng P, Sulin M, Yanlin W, Xinyi L, et al. Post-treatment with irisin attenuates acute kidney injury in sepsis mice through anti-ferroptosis via the SIRT1/nrf2 pathway. *Front Pharmacol*. (2022) 13:857067. doi: 10.3389/fphar.2022.857067

17. Duan R, Du W, Guo W. EZH2: a novel target for cancer treatment. *J Hematol Oncol*. (2020) 13:104. doi: 10.1186/s13045-020-00937-8

18. Nutt SL, Keenan C, Chopin M, Allan RS. EZH2 function in immune cell development. *Biol Chem*. (2020) 401:933–43. doi: 10.1515/hsz-2019-0436

19. Yao Y, Hu H, Yang Y, Zhou G, Shang Z, Yang X, et al. Downregulation of enhancer of zeste homolog 2 (EZH2) is essential for the induction of autophagy and apoptosis in colorectal cancer cells. *Genes (Basel)*. (2016) 7:83. doi: 10.3390/genes7100083

20. Ito T, Teo YV, Evans SA, Neretti N, Sedivy JM. Regulation of cellular senescence by polycomb chromatin modifiers through distinct DNA damage- and histone methylation-dependent pathways. *Cell Rep*. (2018) 22:3480–92. doi: 10.1016/j.celrep.2018.03.002

21. Zhou X, Zang X, Guan Y, Tolbert T, Zhao TC, Bayliss G, et al. Targeting enhancer of zeste homolog 2 protects against acute kidney injury. *Cell Death Dis*. (2018) 9:1067. doi: 10.1038/s41419-018-1012-0

22. Zhou X, Chen H, Hu Y, Ma X, Li J, Shi Y, et al. Enhancer of zeste homolog 2 promotes renal fibrosis after acute kidney injury by inducing epithelial-mesenchymal transition and activation of M2 macrophage polarization. *Cell Death Dis*. (2023) 14:253. doi: 10.1038/s41419-023-05782-4

23. Weng X, Maxwell-Warburton S, Hasib A, Ma L, Kang L. The membrane receptor CD44: novel insights into metabolism. *Trends Endocrinol Metab*. (2022) 33:318–32. doi: 10.1016/j.tem.2022.02.002

24. Hu JB, Li SJ, Kang XQ, Qi J, Wu JH, Wang XJ, et al. CD44-targeted hyaluronic acid-curcumin prodrug protects renal tubular epithelial cell survival from oxidative stress damage. *Carbohydr Polym*. (2018) 193:268–80. doi: 10.1016/j.carbpol.2018.04.011

25. Lau A, Rahn JJ, Chappellaz M, Chung H, Benediktsson H, Bihan D, et al. Dipeptidase-1 governs renal inflammation during ischemia reperfusion injury. *Sci Adv*. (2022) 8:eabm0142. doi: 10.1126/sciadv.abm0142

26. Nieuwenhuijs-Moeke GJ, Pischke SE, Berger SP, Sanders JSF, Pol RA, Struys MMRF, et al. Ischemia and reperfusion injury in kidney transplantation: relevant mechanisms in injury and repair. *J Clin Med*. (2020) 9:253. doi: 10.3390/jcm9010253

27. Tarcic G, Avraham R, Pines G, Amit I, Shay T, Lu Y, et al. EGR1 and the ERK-ERF axis drive mammary cell migration in response to EGF. *FASEB J*. (2012) 26:1582–92. doi: 10.1096/fj.11-194654

28. Chen J, Chen Y, Olivero A, Chen X. Identification and validation of potential biomarkers and their functions in acute kidney injury. *Front Genet*. (2020) 11:411. doi: 10.3389/fgene.2020.00411

29. Chen JW, Huang MJ, Chen XN, Wu LL, Li QG, Hong Q, et al. Transient upregulation of EGR1 signaling enhances kidney repair by activating SOX9+ renal tubular cells. *Theranostics*. (2022) 12:5434–50. doi: 10.7150/thno.73426

30. Zhou H, Cheruvanky A, Hu X, Matsumoto T, Hiramatsu N, Cho ME, et al. Urinary exosomal transcription factors, a new class of biomarkers for renal disease. *Kidney Int*. (2008) 74:613–21. doi: 10.1038/ki.2008.206

31. Panich T, Chancharoenthana W, Somparn P, Issara-Amphorn J, Hirankarn N, Leelahavanichkul A. Urinary exosomal activating transcriptional factor 3 as the early diagnostic biomarker for sepsis-induced acute kidney injury. *BMC Nephrol*. (2017) 18:10. doi: 10.1186/s12882-016-0415-3

32. Wu X, Qiu F, Jin X, Zhou J, Zang W. ATF3: a novel biomarker for the diagnosis of acute kidney injury after cardiac surgery. *Ann Transl Med*. (2021) 9:1655. doi: 10.21037/atm

33. Xu S, Lee E, Sun Z, Wang X, Ren T, Zou Z, et al. Perilipin 2 impacts acute kidney injury via regulation of PPARα. *J Immunol Res*. (2021) 2021:9972704. doi: 10.1155/2021/9972704

34. Lan YF, Chen HH, Lai PF, Cheng CF, Huang YT, Lee YC, et al. MicroRNA-494 reduces ATF3 expression and promotes AKI. *J Am Soc Nephrol*. (2012) 23:2012–23. doi: 10.1681/ASN.2012050438

35. Singh D, Chander V, Chopra K. Cyclosporine protects against ischemia/reperfusion injury in rat kidneys. *Toxicology*. (2005) 207:339–47. doi: 10.1016/j.tox.2004.09.018

36. Kaur J, Kaur T, Sharma AK, Kaur J, Yadav HN, Pathak D, et al. Fenofibrate attenuates ischemia reperfusion-induced acute kidney injury and associated liver dysfunction in rats. *Drug Dev Res*. (2021) 82:412–21. doi: 10.1002/ddr.21764

37. Liu SS, Chen YY, Wang SX, Yu Q. Protective effect of dabrafenib on renal ischemia-reperfusion injury in vivo and in *vitro*. *Biochem Biophys Res Commun*. (2020) 522:395–401. doi: 10.1016/j.bbrc.2019.11.105

38. Miglio G, Rosa AC, Rattazzi L, Grange C, Collino M, Camussi G, et al. The subtypes of peroxisome proliferator-activated receptors expressed by human podocytes and their role in decreasing podocyte injury. *Br J Pharmacol*. (2011) 162:111–25. doi: 10.1111/j.1476-5381.2010.01032.x

39. Senbel AM, AbdelMoneim L, Omar AG. Celecoxib modulates nitric oxide and reactive oxygen species in kidney ischemia/reperfusion injury and rat aorta model of hypoxia/reoxygenation. *Vascul Pharmacol*. (2014) 62:24–31. doi: 10.1016/j.vph.2014.04.004

frontiers | Frontiers in Cell and Developmental Biology

TYPE Brief Research Report
PUBLISHED 11 September 2024
DOI 10.3389/fcell.2024.1452824

OPEN ACCESS

EDITED BY
Patrice X. Petit,
Centre National de la Recherche Scientifique (CNRS), France

REVIEWED BY
Nathalie Le Floch,
Université de Versailles Saint-Quentin-en-Yvelines, France
Agnese De Mario,
University of Padua, Italy

*CORRESPONDENCE
Boris V. Chernyak,
bchernyak1@gmail.com
Konstantin G. Lyamzaev,
lyamzaev@gmail.com

RECEIVED 21 June 2024
ACCEPTED 03 September 2024
PUBLISHED 11 September 2024

CITATION
Huan H, Lyamzaev KG, Panteleeva AA and Chernyak BV (2024) Mitochondrial lipid peroxidation is necessary but not sufficient for induction of ferroptosis.
Front. Cell Dev. Biol. 12:1452824.
doi: 10.3389/fcell.2024.1452824

Mitochondrial lipid peroxidation is necessary but not sufficient for induction of ferroptosis

He Huan[1], Konstantin G. Lyamzaev[1,2]*, Alisa A. Panteleeva[1] and Boris V. Chernyak[1]*

[1]Belozersky Institute of Physico-Chemical Biology, Lomonosov Moscow State University, Moscow, Russia, [2]The "Russian Clinical Research Center for Gerontology" of the Ministry of Healthcare of the Russian Federation, Pirogov Russian National Research Medical University, Moscow, Russia

Ferroptosis, a form of regulated cell death mediated by lipid peroxidation (LPO), has become the subject of intense research due to its potential therapeutic applications in cancer chemotherapy as well as its pathophysiological role in ischemic organ injury. The role of mitochondrial lipid peroxidation (LPO) in ferroptosis remains poorly understood. We show that supplementation of exogenous iron in the form of ferric ammonium citrate (FAC) in combination with buthionine sulfoximine (BSO, an inhibitor of glutathione biosynthesis) induces mitochondrial lipid peroxidation that precedes ferroptosis in normal human fibroblasts. The mitochondrial-targeted antioxidant SkQ1 and the redox mediator methylene blue, which inhibits the production of reactive oxygen species (ROS) in complex I of the mitochondrial electron transport chain, prevent both mitochondrial lipid peroxidation and ferroptosis, but do not affect the cytosolic ROS accumulation. These data indicate that mitochondrial lipid peroxidation *is required* for ferroptosis induced by exogenous iron. FAC in the absence of BSO stimulates mitochondrial peroxidation without reducing cell viability. Glutathione depletion by BSO does not affect FAC-induced mitochondrial LPO but strongly stimulates the accumulation of ROS in the cytosol. These data allow us to conclude that mitochondrial LPO *is not sufficient* for ferroptosis and that cytosolic ROS mediates additional oxidative events that stimulate ferroptosis in conjunction with mitochondrial LPO.

KEYWORDS

ferroptosis, ferric ammonium citrate (FAC), buthionine sulfoximine (BSO), mitochondrial lipid peroxidation, mitochondrial-targeted antioxidants

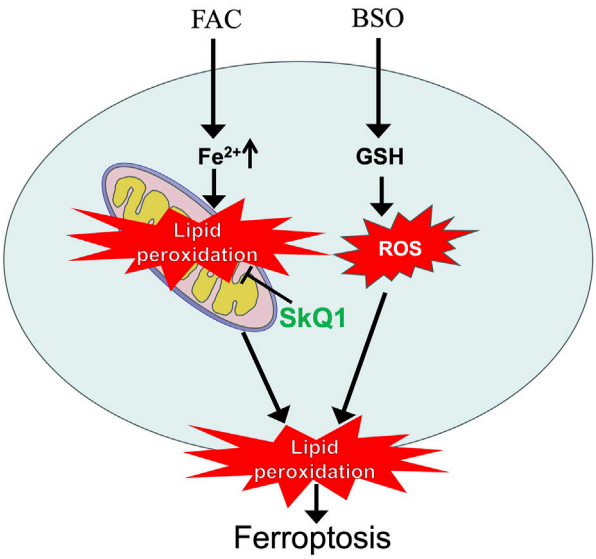

GRAPHICAL ABSTRACT

1 Introduction

The involvement of mitochondria in ferroptosis has been the subject of debate since ferroptosis has been recognized as a specific form of regulated cell death. Pioneering work by Dixon et al. (2012) reported that mitochondrial DNA depletion had no significant effect on sensitivity to ferroptosis induced by the cystine transport inhibitor erastin. A more recent study (Gao et al., 2019) showed that cells completely depleted of mitochondria by activation of mitochondria-targeted autophagy were less sensitive to ferroptosis induced by cysteine starvation, but not by inhibition of glutathione peroxidase 4 (GPx4), a lipid peroxide detoxifier. It was concluded that mitochondrial metabolism may regulate ferroptosis by modulating the level of reduced glutathione. More recently, it was shown (Gao et al., 2019) that depletion of mitochondrial DNA using the same procedure as in (Dixon et al., 2012) results in increased expression of mitochondrial GPx4 and resistance to erastin-induced ferroptosis. Studies using various mitochondria-targeted antioxidants have provided compelling evidence for the role of mitochondrial ROS in ferroptosis. Conjugates of the triphenylphosphonium cation with ubiquinol (MitoQ) or piperidine nitroxide TEMPO (MitoTEMPO) (Oh et al., 2022), as well as XJB-5-131 (TEMPO conjugated with gemigramicidin S) (Krainz et al., 2016), have been shown to inhibit ferroptosis induced by erastin or the Gpx4 inhibitor RSL3, whereas their untargeted counterparts were much less effective.

In our previous study, we analyzed lipid peroxidation (LPO) in mitochondria during ferroptosis using a novel fluorescent ratiometric probe targeting mitochondria, MitoCLox (Lyamzaev et al., 2023).The specific oxidation of MitoCLox by lipid radicals, its selective accumulation in the mitochondria of various cells and the response to mitochondrial lipid peroxidation were shown in our earlier works (Lyamzaev et al., 2019; Chernyavskij et al., 2023; Lyamzaev et al., 2024). Mitochondrial lipid peroxidation has been shown to precede cell death in models of ferroptosis induced by erastin in SV40-transformed fibroblasts and by the gamma-glutamyl cysteine synthetase inhibitor buthionine sulfoximine (BSO) in fibroblasts from the patients with Leber hereditary optic neuropathy (LHON). Mitochondrial-targeted antioxidants SkQ1 [10-(6′-plastoquinonyl) decyltriphenylphosphonium bromide] and MitoTEMPO inhibit both mitochondrial LPO and ferroptosis. The redox cycling agent methylene blue (MB), which targets mitochondria due to its positive charge, bypasses electron flow past complex I of the electron transport chain and inhibits mitochondrial ROS production, also suppresses mitochondrial LPO, and protects against ferroptosis in two models. Neither SkQ1 nor MB affects cytosolic ROS accumulation as measured by CM-H2DCFDA. These data allow us to conclude that mitochondrial LPO *is necessary* for ferroptosis (Lyamzaev et al., 2023).

In the present study, we examined oxidative stress induced by exogenous iron in normal human fibroblasts to answer the question of whether mitochondrial LPO is *sufficient* to induce ferroptosis.

2 Materials and methods

2.1 Chemicals

SkQ1 and dodecyltriphenylphosphonium bromide (C_{12}TPP) were kindly provided by the Institute of Mitoengineering, Lomonosov Moscow State University. C11-BODIPY581/591 was from Lumiprobe (Moscow, Russia), CM-H2DCFDA was from Invitrogen Life Technologies (Waltham, MA, United States). MitoCLox was synthesized from succinimidyl ester of C11-BODIPY581/591 and (5-[(4-aminobutyl) amino]-5-oxopentyl) triphenylphosphonium bromide as described in (Lyamzaev et al., 2019). MitoCLox, a ratiometric fluorescent dye that specifically reacts with lipid peroxy radicals, is addressed to mitochondria by conjugation of the fluorophore C11-BODIPY581/591 with the penetrating triphenylphosphonium cation. MitoCLox was shown

to selectively accumulates in the mitochondria of various living cells and registers mitochondrial lipid peroxidation (Lyamzaev et al., 2020; Chernyavskij et al., 2023). Other reagents, except for those indicated, were from Sigma-Aldrich (Saint Louis, MO, United States).

2.2 Cell cultures

Human primary skin fibroblasts from Common Use Center "Biobank" (Research Centre for Medical Genetics, Moscow, Russia) were cultured in DMEM (Dulbecco's modified Eagle's) medium (Gibco; Thermo Fisher Scientific, Inc., Waltham, MA, United States) supplemented with 2 mM glutamine and 10% fetal bovine serum (FBS) (HyClone, Logan, UT 84321 United States) and 100 U/mL streptomycin and 100 U/mL penicillin (all from Gibco, United States). Cells were challenged with 0.6 mM FAC alone or in combination with 1 mM BSO for 24 h or 48 h. Where indicated 0.1 mM ferrostatin-1, 0.2 mM Trolox, 10, 50 nM SkQ1, 50 nM C12TPP, or 250 nM MB were added concomitantly with FAC. Cell viability was measured using the CellTiterBlue® reagent (Promega, United States) according to the manufacturer's protocol with Fluoroskan Ascent FL Microplate Reader (Thermo Labsystems, Waltham, MA, United States).

2.3 Microscopy

Fibroblasts were plated in 35 mm glass bottom (SPL) dishes for confocal microscopy at 150,000 cells. After incubation with ferric ammonium citrate (FAC) for 24 h, cells were stained with 50 μg/mL propidium iodide and 8 μM Hoechst 33,258 for 30 min. Image acquisition was performed using a fluorescence microscope Olympus IX 83 (Japan).

2.4 Flow cytometry

Fibroblasts were stained with 100 nM MitoCLox (1 h), or 2 μM C11-BODIPY581/591 (30 min), or 1.8 μM CM-H2DCFDA (30 min). Cells were stripped with trypsin/versene, centrifuged in 1.5 mL tubes (900 g, 5 min) at 4°C and redispersed in 30 mL PBS. Flow cytometry analyses were performed using an Amnis FlowSight Imaging Flow Cytometer (Luminex Corporation, Seattle, WA, United States) with excitation at 488 nm and the detection channels 480–560 nm (Ch2) and 595–642 nm (Ch4). Channel 2 (Ch2) was used to detect autofluorescence, which indicates lipofuscin content (Malavolta et al., 2022). Each sample was measured until 4,000 events were collected. For ratiometric analysis, the Amnis IDEAS® 6.2 (Luminex, Seattle, WA, United States) image analysis software was used. Data are presented as geometric means computed using flow cytometry software.

2.5 Measurements of labile iron pool

Intracellular labile iron was measured using acetoxymethyl ester of calcein (calcein-AM) as described elsewhere (Breuer et al., 1995). This dye is initially non-fluorescent, becoming fluorescent after enzymatic modification upon penetrating the cell membrane. The fluorophore then stoichiometrically binds to iron, which quenches its green fluorescence (Tenopoulou et al., 2007). For the experiment, cells were seeded onto a 96-well plate (10×10^3 cells per vial) and incubated with varying concentrations of FAC for 48 h with or without SkQ1 (50 nM). To chelate free iron, cells were incubated with 1 mM deferroxamin (DFO) for 2 h before the addition of calcein. After this the cells were washed with serum-free medium, followed by the addition of 200 nM calcein-AM for 20 min. Post-incubation, the cells were washed three times with Hanks medium, and the fluorescence of calcein was measured using a Fluoroskan Ascent FL Microplate Reader (Thermo Labsystems, Waltham, MA, United States) with excitation/emission settings of Ex485/Em538. To normalize the cell count in each well, the CellTiterBlue® reagent (Promega, United States) was used, following the manufacturer's protocol.

2.6 Statistics

At least three repeats for each measurement were performed. Results are presented as the mean of a minimum of 3 independent replicates with standard deviation (SD). Comparisons were analyzed by one-way ANOVA. The significance was analyzed with Prism 10.0 software (GraphPad Software, LLC, California, United States); a value of $p < 0.05$(** or #) was considered to be statistically significant.

3 Results

We analyzed oxidative stress caused by iron overload supplying ferric ammonium citrate (FAC), which is a physiological form of non-transferrin-bound iron widely used as a dietary supplement. FAC has low toxicity but has been shown to sensitize HT-1080 fibrosarcoma cells to erastin-induced ferroptosis (Dixon et al., 2012). As shown in Figure 1, FAC does not induce cell death in normal human fibroblasts at concentrations up to 1.2 mM. Glutathione depletion by BSO is not toxic but strongly promotes fibroblast cell death induced by FAC (Figure 1A). Cell death induced by combination of FAC and BSO is necrotic, as detected by propidium iodide staining of nuclei (Figure 1B), and is not prevented by the pan-caspase inhibitor zVADfmk (Figure 1C), so secondary caspase-dependent necrosis is excluded. The ferroptosis inhibitor ferrostatin-1 (fer-1) and another antioxidant, the water-soluble vitamin E analogue Trolox, prevent a decrease in viability. Mitochondrial-targeted antioxidant SkQ1 protects against ferroptosis induced by the combination of FAC and BSO at very low concentrations, whereas SkQ1 analogue lacking the antioxidant moiety dodecyltriphenylphosphonium (C_{12}TPP) is ineffective (Figure 1C). Importantly, SkQ1 was shown to have no effect on the increase in intracellular labile iron pool (LIP) induced by 48 h incubation with FAC (Figure 1D). These data indicate that ROS-dependent mitochondrial processes are critical for ferroptosis induced by exogenous iron. Methylene blue (MB), which inhibits mitochondrial complex I–dependent ROS production, also protects against ferroptosis induced by combination of FAC and BSO (Figure 1C) indicating that FAC-induced mitochondrial ROS production is at least partially originated from complex I.

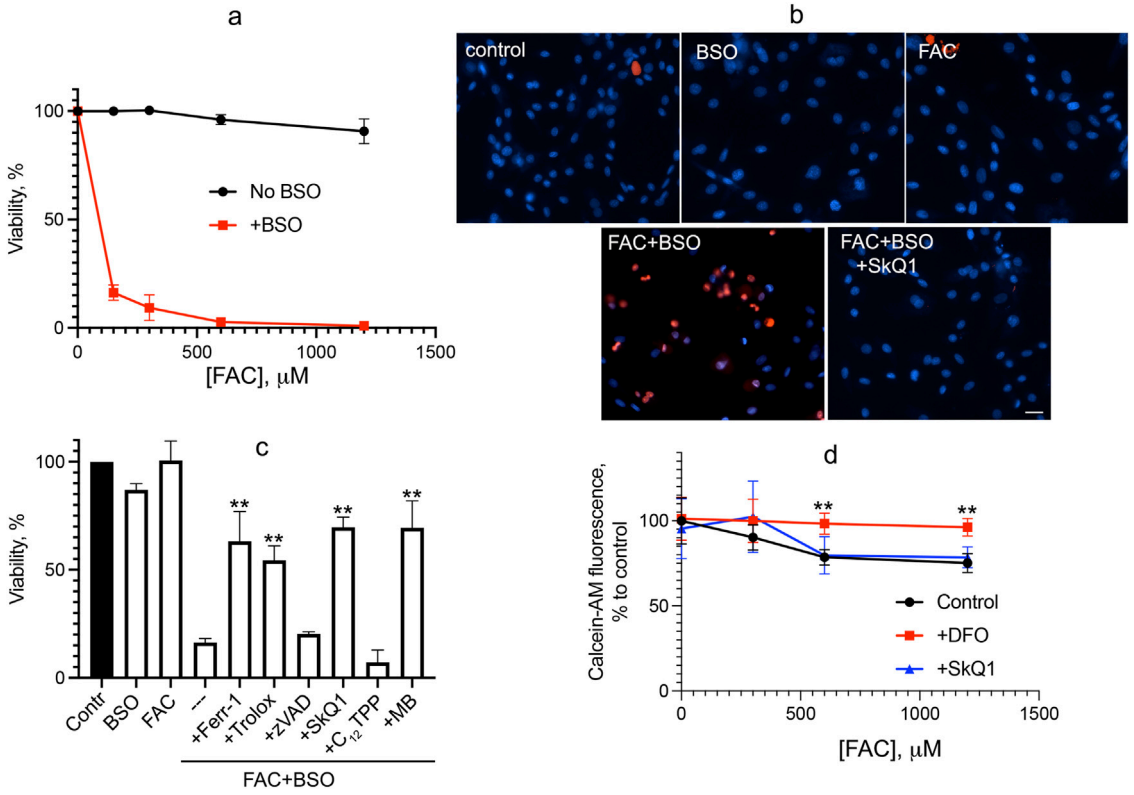

FIGURE 1
Glutathione depletion by BSO promotes ferroptosis induced by FAC in human fibroblasts. **(A)** Cells were incubated with FAC alone or in combination with 1 mM BSO for 48 h. Cell viability was measured using the CellTiterBlue reagent. **(B)** Cells were incubated with 0.6 mM FAC and 1 mM BSO separately or in combination for 48 h and stained with 50 μg/mL propidium iodide (red) and 8 μM Hoechst 33,258 (blue) for 30 min 50 nM SkQ1 was added where indicated together with FAC + BSO. Cells were analyzed using Olympus IX83 fluorescent microscope. Bar 20 μm. **(C)** Viability of cells incubated with 0.6 mM FAC alone or in combination with 1 mM BSO for 48 h. Where indicated 0.1 mM ferrostatin-1 (Ferr-1), 0.2 mM Trolox, 10 μM zVADfmk (zVAD), 50 nM SkQ1, 50 nM C_{12}TPP, 250 nM MB were added. $p < 0.05$(**)—the significance of the difference between samples treated with FAC + BSO and other samples. **(D)** Labile iron pool was measured as the quenching of intracellular calcein fluorescence after 48 h of incubation with FAC or FAC with 50 nM SkQ1. Where indicated, 1 mM deferoxamine (DFO) was added 2 h prior to calceine-AM loading. $p < 0.05$(**) - the significance of the difference between samples with DFO and other samples.

Cell death induced by FAC combined with BSO was measured after 48 h of incubation, whereas minor changes in cell viability were observed after 24 h of incubation with up to 1.2 mM FAC either alone or in combination with 1 mM BSO. This is why a 24-h incubation was chosen to measure the oxidative event preceding cell death.

Cytosolic ROS accumulation, measured by CM-H2DCFDA, is not stimulated by FAC but is significantly increased after 24-h incubation with BSO (Figure 2A). At 1 mM BSO, FAC does not affect the level of cytosolic ROS, whereas at a suboptimal concentration of BSO (0.3 mM), FAC dose-dependently stimulates the accumulation of cytosolic ROS (Figure 2B). SkQ1 and MB do not affect BSO + FAC induced H_2O_2 accumulation (Figure 2A), indicating that mitochondrial ROS do not contribute significantly to the induction of general oxidative stress in this model. Similar results were obtained previously for erastin-induced accumulation of cytosolic ROS in fibroblasts (Lyamzaev et al., 2023).

As shown in Figures 2C, D, FAC significantly stimulates mitochondrial LPO, and the addition of BSO does not affect FAC-induced LPO (or does not induce mitochondrial LPO itself). Trolox, SkQ1 (but not C_{12}TPP) and MB prevent mitochondrial lipid peroxidation induced by either FAC or FAC + BSO. Since BSO treatment appears to be critical for FAC-dependent cell death (Figure 1), it can be assumed that mitochondrial LPO is not sufficient for ferroptosis. Interestingly, similar effects are observed when measuring total lipid peroxidation using C11-BODIPY581/591 (Figure 2E). BSO does not induce total LPO and does not affect FAC-induced peroxidation. SkQ1 and MB inhibit total LPO induced by combination of FAC and BSO, indicating that (in contrast to H_2O_2 accumulation) mitochondrial ROS contribute significantly to total lipid peroxidation.

Lipofuscin, a heterogeneous complex mixture composed of highly oxidized lipids and cross-linked proteins, can be consider as a marker of severe oxidative stress (Terman and Brunk, 2004). Incubation of fibroblasts with FAC for 24 h results in accumulation of lipofuscin-like material, as evidenced by increased autofluorescence in a wide spectral range 480–560 nm (Figure 2F). As in the cases of mitochondrial and total LPO (Figures 2D, E), BSO does not induce lipofuscin accumulation and does not affect FAC-induced accumulation. SkQ1 inhibits the accumulation of lipofuscin-like material induced by combination of FAC and BSO. It is considered a

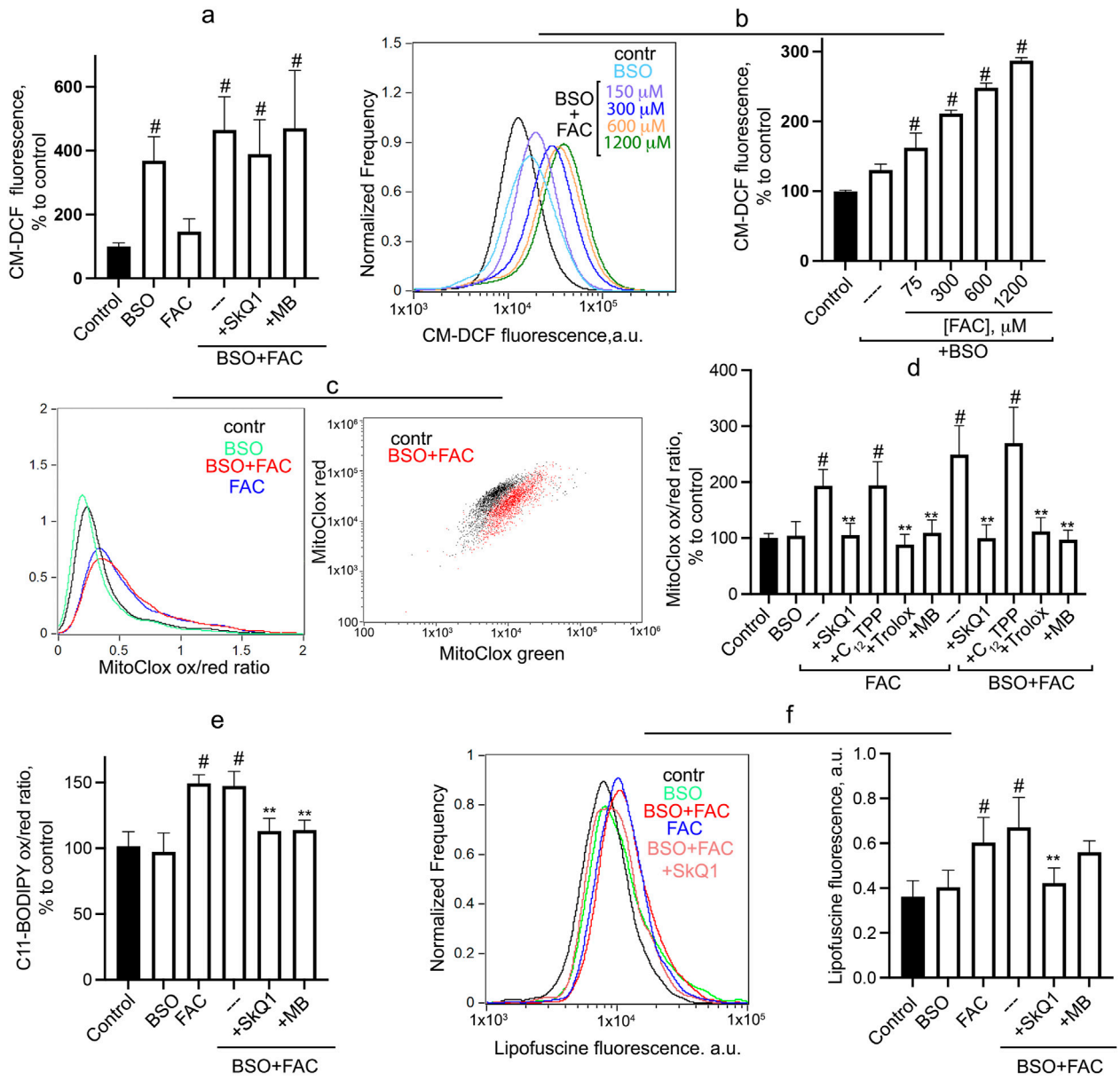

FIGURE 2
Oxidative events induced by FAC and BSO in human fibroblasts. Cells were incubated with 0.6 mM FAC, BSO (1 mM or 0.3 mM) or with their combination for 24 h **(A)** Cytosolic ROS accumulation was measured using CM-H2DCFDA. Mean values of fluorescence are presented. Cells were challenged with 1 mM BSO alone and in combination with FAC or different concentrations of FAC in combination with 0.3 mM BSO **(B)**. 50 nM SkQ1, 250 nM MB were added at the same time as BSO and FAC where indicated. **(C, D)** Mitochondrial lipid peroxidation was measured using MitoCLox. Cells were incubated with 0.6 mM FAC alone or in combination with 1 mM BSO for 24 h and stained with 100 nM MitoCLox for 1 h. Ratio of green/red fluorescence was measured. Typical histograms **(C)** and mean values **(D)** are shown. 50 nM SkQ1, 50 nM C12TPP, 250 nM MB and 0.2 mM Trolox were added where indicated. **(E)** Total lipid peroxidation was measured using C11-BODIPY581/591. Cells were incubated with 1 mM BSO and 0.6 mM FAC for 24 h and stained with 2 μM C11-BODIPY581/591 for 30 min and analyzed using flow cytometry. Ratio of green/red fluorescence was measured. Mean values are presented. 50 nM SkQ1, 50 nM C_{12}TPP, 250 nM MB and 0.2 mM Trolox were added where indicated. **(F)** FAC-induced accumulation of lipofuscin-like material was analyzed using flow cytometry without staining. Cells were incubated with 0.6 mM FAC alone and in combination 1 mM BSO for 24 h. 50 nM SkQ1, 250 nM MB were added at the same time as BSO and FAC. Mean values of fluorescence are presented. $p < 0.05$(**)—the significance of the difference between samples treated with FAC or FAC + BSO and other samples. $p < 0.05$(#)—the significance of the difference between control and other samples.

marker of organismal aging and cellular senescence and usually accumulates very slowly (von Zglinicki et al., 1995). The rapid accumulation of lipofuscin-like material in FAC-treated fibroblasts reflects lipid peroxidation and is dependent on mitochondrial ROS production.

4 Discussion

As shown in Figure 1, the mitochondria-targeted antioxidant SkQ1 and the redox agent methylene blue, which inhibits ROS production by complex I of the mitochondrial electron transport

chain, prevent ferroptosis induced by ferric ammonium citrate in combination with the glutathione biosynthesis inhibitor BSO. Data in Figure 2 show that mitochondrial lipid peroxidation precedes ferroptotic cell death and is prevented by SkQ1 and MB, whereas these mitochondria-targeting agents do not affect cytosolic ROS accumulation. These data indicate that mitochondrial LPO *is required* for ferroptosis induced by exogenous iron. This finding is entirely consistent with results obtained previously for models of ferroptosis induced by erastin in SV40-transformed fibroblasts and BSO in fibroblasts from LHON patients (Lyamzaev et al., 2023).

Evidence for the contribution of mitochondrial iron-dependent oxidative events to ferroptosis was provided also by studies in which overexpression of the mitochondrial ferritin isoform (MtFt) was shown to inhibit ferroptosis induced by erastin (Wang et al., 2016), as well as by doxorubicin or simulated ischemia/reperfusion (Chen et al., 2023). Ferritin is known to sequester labile iron, inhibiting the formation of hydroxyl radicals in the Fenton reaction and lipid peroxidation, so these data indicate an important role for mitochondrial lipid peroxidation in ferroptosis. Recently, important studies have identified the role of the natural mitochondrial lipophilic antioxidant coenzyme Q (CoQ) in protection against ferroptosis. Two enzymes localized to the inner mitochondrial membrane, dihydroorotate dehydrogenase (DHODH) (Mao et al., 2021) and glycerol-3-phosphate dehydrogenase 2 (GPD2) (Wu et al., 2022), have been reported to inhibit mitochondrial lipid peroxidation and protect against ferroptosis by reducing of CoQ to CoQH2, which can detoxify lipid peroxyl radicals in mitochondria. However, it should be noted that studies of the protective effects of DHODH have recently come under severe criticism based on experimental data (Mishima et al., 2023).

In contrast to the effects of erastin, the use of FAC allows the separation of mitochondrial lipid peroxidation and ferroptosis in fibroblasts. As shown in Figure 2, FAC stimulates mitochondrial LPO without reducing cell viability. Glutathione depletion by BSO promotes FAC-induced ferroptosis, presumably by reducing GPx4 activity and stimulating plasma membrane LPO. At the same time, BSO does not have a significant effect on FAC-induced mitochondrial LPO. These data allow us to conclude that mitochondrial LPO is *not sufficient* for ferroptosis. In contrast to FAC, BSO strongly stimulates cytosolic ROS accumulation (Figure 2A), suggesting that cytosolic ROS mediates additional oxidative events that stimulate ferroptosis in conjunction with mitochondrial LPO. SkQ1 and MB do not affect BSO-induced cytosolic H_2O_2 accumulation, so the second ferroptotic stimulus in this model is independent of mitochondrial ROS.

Interestingly, FAC induces significant total lipid peroxidation that does not lead to fibroblasts death. BSO neither induces total LPO nor stimulates FAC-induced peroxidation. Thus, general LPO, which develops in all cell membranes, cannot always be considered as a marker of ferroptosis. Different cell types have different sensitivities to FAC-induced cell death. For example, in a recent study ferroptosis was observed in islet β-cells treated with submillimolar concentrations of FAC (Deng et al., 2023). The possible role of mitochondrial LPO in ferroptosis of islet β-cells, as well as the nature of the difference in sensitivity to exogenous iron between these cells and fibroblasts, deserves further study. We also described FAC-induced ferroptosis associated with mitochondrial LPO in cardiomyocytes (Lyamzaev et al., 2024). The conclusion reached in our study concerns the basic mechanisms of ferroptosis, and it would be important to demonstrate its validity in other cell models with other ferroptosis inducers. The role of iron overload in induction of ferroptosis involved in various pathologies is well known (Chen et al., 2023; Ryan et al., 2023), while the mechanisms of ferroptosis caused by exogenous iron are still poorly understood. Since SkQ1 and MB effectively inhibit FAC-induced ferroptosis, mitochondria-targeted agents may be considered candidates for the treatment of various pathologies associated with iron overload. At the same time, our data show that mitochondrial oxidative events are not sufficient to induce ferroptosis and additional cytosolic ROS-dependent mechanisms should be taken into account.

Data availability statement

The original contributions presented in the study are included in the article/supplementary material, further inquiries can be directed to the corresponding authors.

Ethics statement

Ethical approval was not required for the studies on humans in accordance with the local legislation and institutional requirements because only commercially available established cell lines were used.

Author contributions

HH: Investigation, Methodology, Writing–review and editing. KL: Conceptualization, Formal Analysis, Funding acquisition, Investigation, Methodology, Project administration, Resources, Supervision, Writing–review and editing. AP: Investigation, Supervision, Writing–review and editing. BC: Data curation, Formal Analysis, Methodology, Supervision, Writing–original draft, Writing–review and editing.

Funding

The author(s) declare that financial support was received for the research, authorship, and/or publication of this article. This work was supported by the grant of the Russian Science Foundation No. 23-14-00061.

Acknowledgments

The authors are grateful to Patrice X. Petit (CNRS UMR 8003 Paris University, France) for his valuable advice and assistance in preparing the manuscript. We are grateful to the Moscow State University Development Program PNR5 for providing access to the Amnis Flowsight flow cytometer and to the Olympus IX83 microscope.

Conflict of interest

The authors declare that the research was conducted in the absence of any commercial or financial relationships that could be construed as a potential conflict of interest.

Publisher's note

References

Breuer, W., Epsztejn, S., and Cabantchik, Z. I. (1995). Iron acquired from transferrin by K562 cells is delivered into a cytoplasmic pool of chelatable iron(II). *J. Biol. Chem.* 270, 24209–24215. doi:10.1074/jbc.270.41.24209

Chen, Y., Guo, X., Zeng, Y., Mo, X., Hong, S., He, H., et al. (2023). Oxidative stress induces mitochondrial iron overload and ferroptotic cell death. *Sci. Rep.* 13, 15515. doi:10.1038/s41598-023-42760-4

Chernyavskij, D. A., Pletjushkina, O. Y., Kashtanova, A. V., Galkin, Ii, Karpukhina, A., Chernyak, B. V., et al. (2023). Mitochondrial oxidative stress and mitophagy activation contribute to TNF-dependent impairment of myogenesis. *Antioxidants (Basel)* 12, 602. doi:10.3390/antiox12030602

Deng, L., Mo, M. Q., Zhong, J., Li, Z., Li, G., and Liang, Y. (2023). Iron overload induces islet β cell ferroptosis by activating ASK1/P-P38/CHOP signaling pathway. *PeerJ* 11, e15206. doi:10.7717/peerj.15206

Dixon, S. J., Lemberg, K. M., Lamprecht, M. R., Skouta, R., Zaitsev, E. M., Gleason, C. E., et al. (2012). Ferroptosis: an iron-dependent form of nonapoptotic cell death. *Cell* 149, 1060–1072. doi:10.1016/j.cell.2012.03.042

Gao, M., Yi, J., Zhu, J., Minikes, A. M., Monian, P., Thompson, C. B., et al. (2019). Role of mitochondria in ferroptosis. *Mol. Cell* 73, 354–363. doi:10.1016/j.molcel.2018.10.042

Krainz, T., Gaschler, M. M., Lim, C., Sacher, J. R., Stockwell, B. R., and Wipf, P. (2016). A mitochondrial-targeted nitroxide is a potent inhibitor of ferroptosis. *ACS Cent. Sci.* 2, 653–659. doi:10.1021/acscentsci.6b00199

Lyamzaev, K. G., Huan, H., Panteleeva, A. A., Simonyan, R. A., Avetisyan, A. V., and Chernyak, B. V. (2024). Exogenous iron induces mitochondrial lipid peroxidation, lipofuscin accumulation, and ferroptosis in H9c2 cardiomyocytes. *Biomolecules* 14, 730. doi:10.3390/biom14060730

Lyamzaev, K. G., Panteleeva, A. A., Karpukhina, A. A., Galkin, Ii, Popova, E. N., Pletjushkina, O. Y., et al. (2020). Novel fluorescent mitochondria-targeted probe MitoCLox reports lipid peroxidation in response to oxidative stress *in vivo*. *Oxid. Med. Cell Longev.* 2020, 3631272. doi:10.1155/2020/3631272

Lyamzaev, K. G., Panteleeva, A. A., Simonyan, R. A., Avetisyan, A. V., and Chernyak, B. V. (2023). Mitochondrial lipid peroxidation is responsible for ferroptosis. *Cells* 12, 611. doi:10.3390/cells12040611

Lyamzaev, K. G., Sumbatyan, N. V., Nesterenko, A. M., Kholina, E. G., Voskoboynikova, N., Steinhoff, H. J., et al. (2019). MitoCLox: a novel mitochondria-targeted fluorescent probe for tracing lipid peroxidation. *Oxid. Med. Cell Longev.* 2019, 9710208. doi:10.1155/2019/9710208

Malavolta, M., Giacconi, R., Piacenza, F., Strizzi, S., Cardelli, M., Bigossi, G., et al. (2022). Simple detection of unstained live senescent cells with imaging flow cytometry. *Cells* 11, 2506. doi:10.3390/cells11162506

Mao, C., Liu, X., Zhang, Y., Lei, G., Yan, Y., Lee, H., et al. (2021). DHODH-mediated ferroptosis defence is a targetable vulnerability in cancer. *Nature* 593, 586–590. doi:10.1038/s41586-021-03539-7

Mishima, E., Nakamura, T., Zheng, J., Zhang, W., Mourao, A. S. D., Sennhenn, P., et al. (2023). DHODH inhibitors sensitize to ferroptosis by FSP1 inhibition. *Nature* 619, E9–E18. doi:10.1038/s41586-023-06269-0

Oh, S. J., Ikeda, M., Ide, T., Hur, K. Y., and Lee, M. S. (2022). Mitochondrial event as an ultimate step in ferroptosis. *Cell Death Discov.* 8, 414. doi:10.1038/s41420-022-01199-8

Ryan, S. K., Ugalde, C. L., Rolland, A. S., Skidmore, J., Devos, D., and Hammond, T. R. (2023). Therapeutic inhibition of ferroptosis in neurodegenerative disease. *Trends Pharmacol. Sci.* 44, 674–688. doi:10.1016/j.tips.2023.07.007

Tenopoulou, M., Kurz, T., Doulias, P. T., Galaris, D., and Brunk, U. T. (2007). Does the calcein-AM method assay the total cellular 'labile iron pool' or only a fraction of it? *Biochem. J.* 403, 261–266. doi:10.1042/BJ20061840

Terman, A., and Brunk, U. T. (2004). Lipofuscin. *Int. J. Biochem. Cell Biol.* 36, 1400–1404. doi:10.1016/j.biocel.2003.08.009

Von Zglinicki, T., Nilsson, E., Docke, W. D., and Brunk, U. T. (1995). Lipofuscin accumulation and ageing of fibroblasts. *Gerontology* 41 (Suppl. 2), 95–108. doi:10.1159/000213728

Wang, Y. Q., Chang, S. Y., Wu, Q., Gou, Y. J., Jia, L., Cui, Y. M., et al. (2016). The protective role of mitochondrial ferritin on erastin-induced ferroptosis. *Front. Aging Neurosci.* 8, 308. doi:10.3389/fnagi.2016.00308

Wu, S., Mao, C., Kondiparthi, L., Poyurovsky, M. V., Olszewski, K., and Gan, B. (2022). A ferroptosis defense mechanism mediated by glycerol-3-phosphate dehydrogenase 2 in mitochondria. *Proc. Natl. Acad. Sci. U. S. A.* 119, e2121987119. doi:10.1073/pnas.2121987119

frontiers | Frontiers in Cell and Developmental Biology

TYPE Original Research
PUBLISHED 16 September 2024
DOI 10.3389/fcell.2024.1416345

OPEN ACCESS

EDITED BY
Patrice X. Petit,
Centre National de la Recherche Scientifique (CNRS), France

REVIEWED BY
Xin Feng Zheng,
Shanghai Jiao Tong University, China
Xiguang Xu,
Virginia Tech, United States

*CORRESPONDENCE
Liang Wang,
liang091@aliyun.com
Zhongmin Zhang,
nfzzm@163.com

†These authors have contributed equally to this work and share first authorship

RECEIVED 12 April 2024
ACCEPTED 26 August 2024
PUBLISHED 16 September 2024

CITATION
Li C, Fei C, Le S, Lai Z, Yan B, Wang L and Zhang Z (2024) Identification and validation of ferroptosis-related biomarkers in intervertebral disc degeneration.
Front. Cell Dev. Biol. 12:1416345.
doi: 10.3389/fcell.2024.1416345

Identification and validation of ferroptosis-related biomarkers in intervertebral disc degeneration

Chenglong Li[1†], Chengshuo Fei[1†], Shiyong Le[2], Zhongming Lai[1], Bo Yan[2], Liang Wang[2*] and Zhongmin Zhang[1*]

[1]Division of Spine Surgery, Department of Orthopedics, Nanfang Hospital, Southern Medical University, Guangzhou, China, [2]Department of Orthopedics, The Third Affiliated Hospital, Southern Medical University, Academy of Orthopedics, Guangzhou, China

Introduction: Ferroptosis plays a significant role in intervertebral disc degeneration (IDD). Understanding the key genes regulating ferroptosis in IDD could reveal fundamental mechanisms of the disease, potentially leading to new diagnostic and therapeutic targets.

Methods: Public datasets (GSE23130 and GSE70362) and the FerrDb database were analyzed to identify ferroptosis-related genes (DE-FRGs) involved in IDD. Single-cell RNA sequencing data (GSE199866) was used to validate the specific roles and expression patterns of these genes. Immunohistochemistry and Western blot analyses were subsequently conducted in both clinical samples and mouse models to assess protein expression levels across different tissues.

Results: The analysis identified seven DE-FRGs, including *MT1G*, *CA9*, *AKR1C1*, *AKR1C2*, *DUSP1*, *CIRBP*, and *KLHL24*, with their expression patterns confirmed by single-cell RNA sequencing. Immunohistochemistry and Western blot analysis further revealed that *MT1G*, *CA9*, *AKR1C1*, *AKR1C2*, *DUSP1*, and *KLHL24* exhibited differential expression during the progression of IDD. Additionally, the study highlighted the potential immune-modulatory functions of these genes within the IDD microenvironment.

Discussion: Our study elucidates the critical role of ferroptosis in IDD and identifies specific genes, such as *MT1G* and *CA9*, as potential targets for diagnosis and therapy. These findings offer new insights into the molecular mechanisms underlying IDD and present promising avenues for future research and clinical applications.

KEYWORDS

intervertebral disc degeneration, ferroptosis, bioinformatics analysis, immune cell infiltration, single-cell RNA sequencing

1 Introduction

Intervertebral disc degeneration (IDD) is a leading cause of disability worldwide. It accounts for a significant proportion of lower back pain episodes globally (Andersson, 1999; Chen S. et al., 2021). A large portion of adults experience lower back pain at some point in their lives. Beyond diminishing the patient's quality of life, this affliction exerts a profound economic strain on healthcare systems and society. IDD is driven by complex mechanisms including genetic predispositions, which indicate a hereditary vulnerability; mechanical stress from activities such as heavy lifting that strain the spine; cellular apoptosis, leading to

a decline in the cells essential for disc maintenance; and obesity, which not only increases the load on the discs but also exacerbates degeneration through inflammatory and biochemical pathways. Each factor contributes uniquely to the progression of IDD. Contemporary therapeutic strategies, be they conservative or surgical, predominantly focus on palliating the associated pain but fall short in halting or reversing the degenerative process of IDD (Ma et al., 2022; Xin et al., 2022). Consequently, there's an imperative to channel research toward identifying therapeutic strategies at the molecular or cellular level for IDD. This could herald a paradigm shift in treatment modalities, not only preserving the intrinsic biological functionality of the lumbar intervertebral discs but also significantly curtailing the prevalence of lower back pain.

In recent years, ferroptosis, a distinct form of cell death linked to oxidative stress and dysregulation of iron metabolism, has received significant attention. Its involvement is recognized in numerous diseases, particularly neurodegenerative disorders and cancers (Wei et al., 2022; Masaldan et al., 2019; Ge et al., 2022). There has been marked progress in understanding the role of ferroptosis in degenerative diseases, with many such diseases confirmed as related to ferroptosis (Yang et al., 2021). Considering that IDD is a degenerative condition marked by pronounced cell death, researchers are examining the potential importance of ferroptosis in IDD progression (Yu et al., 2022; Wang et al., 2022). However, current studies on ferroptosis in IDD are still nascent, necessitating further inquiry to clarify the associated pathways in intervertebral disc cells and prospective gene-targeted treatments. Ferroptosis's interaction with the immune system is crucial for understanding IDD progression. Ferroptosis both influences and is influenced by the immune system, directly impacting the progression of IDD. For instance, macrophages play a central role in this interaction by releasing inflammatory cytokines such as TNF-α and IL-1β, which not only drive inflammation but also enhance ferroptosis, leading to increased matrix breakdown and exacerbating degeneration. Additionally, ferroptosis can activate immune regulation, where immune cells release cytotoxic substances and apoptotic signals, further promoting disc cell death and accelerating the progression of IDD. This dynamic interplay between ferroptosis and the immune system creates a feedback loop that worsens the degenerative process (Capossela et al., 2014; Ye et al., 2022; Zhang F. et al., 2023). Despite the significance of these interactions, research on immune cell infiltration during IDD progression remains limited, and the exact interplay between ferroptosis and immune infiltration in IDD has yet to be fully elucidated (Zhang et al., 2021; Wang et al., 2021).

Bioinformatics provides a powerful tool for uncovering complex disease mechanisms through the analysis of vast gene and protein databases. This approach is crucial for connecting the clinical features of IDD with their biological underpinnings. By using computational tools to study genetic and protein data, researchers can identify key biomarkers and targets for therapy, linking clinical outcomes with molecular discoveries to improve understanding and treatment options.

In our research, we used bioinformatics tools to conduct a comprehensive analysis that included Gene Ontology (GO) enrichment, KEGG pathway elucidation, and immune infiltration evaluation. The credibility of the identified DE-FRGs was rigorously tested through validation across varied datasets and Receiver Operating Characteristic (ROC) curve assessments. Subsequently, single-cell databases were employed to verify these genes and ascertain their expression in specific cell subtypes. Ultimately, the expression of these genes in clinical and mouse specimens was identified through immunohistochemistry and Western blotting, revealing key genes associated with ferroptosis in disc degeneration. These findings pave the way for novel therapeutic strategies targeting ferroptosis in IDD.

2 Materials and methods

2.1 Data collection and preprocessing

Following download and filtration processes, microarray data and platform annotation were sourced from the GEO datasets GSE23130 and GSE70362. GSE23130 was designated as the training dataset, while GSE70362 was used as an external dataset. Data analysis was conducted using the R programming language (version4.1.1).

2.2 Differential expression analysis of ferroptosis-related genes

The repeatability of the microarray data was assessed using principal component analysis. Differential analysis was executed using the "limma" package (Ritchie et al., 2015). For GSE23130, genes with |log2FC|>1 and *P*-value <0.05 were identified as differentially expressed genes (DEGs). In contrast, for GSE70362, the criteria were |Foldchange|>1.5 and *P*-value < 0.05. The "heatmap" and "ggplot2" packages (Steenwyk and Rokas, 2021) were utilized to generate heatmaps, volcano plots, and box plots. DE-FRGs were derived from the overlap between DEGs and ferroptosis-related genes (FRGs), with Venn plots illustrating the results.

2.3 Enrichment analyses

Enrichment analyses included Gene Ontology (GO) (The Gene Ontology, 2004) and Kyoto Encyclopedia of Genes and Genomes (KEGG) (Kanehisa and Goto, 2000) methodologies using the "clusterProfiler" package (Yu et al., 2012). GO enrichment delved into biological processes (BP), cellular components (CC), and molecular functions (MF), with significance defined by an adjusted P-value < 0.05. The "clusterProfiler" package also facilitated Gene Set Enrichment Analysis (GSEA) (Subramanian et al., 2005), while visualization was achieved with the "enrichplot" package. The C5 GO gene sets database (c5.all.v7.1.symbols.gmt) from the Molecular Signatures Database (MSigDB) (Liberzon et al., 2011) helped pinpoint significant biological processes between control and IDD groups. Similarly, the C2 curated gene sets (c2.all.v7.1.symbols.gmt) from MSigDB illuminated enriched signaling pathways. Significant functional enrichment was discerned with thresholds of FDR < 0.25 and $P < 0.05$.

2.4 Identification and verification of key genes

We validated the differential expression of candidate key DE-FRGs using an external dataset and identified the key DE-FRGs with specific expressions in AF and NP. In the receiver operating characteristic (ROC) analysis, we evaluated the diagnostic potential of these key DE-FRGs using the "pROC" package. Ideally, the Area Under the Curve (AUC) should fall between 0.5 and 1; an AUC approaching 1 indicates superior diagnostic quality.

2.5 Single-cell RNA-Seq data processing

The GSE199866 dataset was downloaded from the GEO database, comprising four samples including non-degenerated and degenerated NP and AF cells (NPnD, NPD, AFnD, AFD), totaling 14,001 cells. Data preprocessing and subsequent analyses were performed using the Seurat (v4.3.0) R package. Quality control parameters were set as follows: the number of features greater than 300 or less than 8,000; cells with count numbers between 500 and 60,000 were retained; cells with mitochondrial gene expression percentages over 20% and a hemoglobin proportion higher than 10% were removed. Following this, data normalization was conducted, principal component analysis (PCA) was applied for dimensionality reduction, and batch effects were mitigated using Harmony. Clustering and visualization were performed using the UMAP method with a resolution of 0.5. Clusters were identified using Seurat's Find All Clusters function. Gene Set Variation Analysis (GSVA) was utilized to analyze pathway activities in clusters from single-cell transcriptomes, utilizing "c5.go.v2023.2.Hs.symbols.gmt" gene sets from MSigDB. Pseudotime analysis and visualization were performed using Monocle2.

2.6 Clinical data acquisition and specimen collection

Following approval from our hospital's ethics committee, 24 discarded intervertebral disc tissue samples were collected from patients undergoing posterior lumbar discectomy at the Department of Spine Surgery. All participating patients were informed about the study and provided written consent.

All tissue samples were sourced from either the L4/5 or L5/S1 segments and were subjected to magnetic resonance imaging (MRI) assessments. The degree of disc degeneration was evaluated using the Pfirrmann score (Pfirrmann et al., 2001) based on pre-surgery MRI findings. In this grading system, grade I signifies no degeneration, grades 2–3 denote mild degeneration, and grades 4–5 indicate severe degeneration. For the purposes of this study, samples with grades 2–3 were categorized into the mild-IDD group, while those with grades 4–5 were grouped into the severe-IDD category.

2.7 Intervertebral disc degeneration mouse model

This study involved twenty-four 8-week-old C57 mice, used under the approval of our institution's animal experimentation committee. The mice were randomly assigned into two groups: a control group (Control) and an experimental group (IDD). The experimental protocol involved placing each mouse in a specialized device within a large cage, partially filled with 5 mm of water. This environment encouraged the mice to maintain a bipedal stance for 6 h each day over a period of 1 week. Outside of these hours, the mice were allowed free movement and access to food and water. This regimen was designed to exert significant stress on the lumbar spine, thereby inducing lumbar IDD (Ao et al., 2019). The experiment lasted for 12 weeks, after which all mice were humanely euthanized for further analysis.

2.8 Histological and immunohistochemistry studies

In the histological analysis phase, each tissue sample was initially fixed in 4% paraformaldehyde, then decalcified, embedded in paraffin, and finally sectioned into 4-μm thick slices. These prepared sections underwent deparaffinization and rehydration, followed by staining with hematoxylin and eosin (H&E), Masson's trichrome, and safranin O/Fast green (SOFG) in accordance with the manufacturer's guidelines. For the histological grading, we used the Weiler et al. (2011) scale for clinical specimens and the Tam et al. (2018) scale for mouse specimens, with three independent researchers performing the grading for each group.

The immunohistochemistry (IHC) analysis involved several key steps. After the deparaffinization and rehydration of paraffin sections, antigen retrieval was conducted by microwaving human tissue sections in EDTA buffer (pH 8) and mouse sections in citrate buffer (pH 6) for 3 min. We quenched endogenous peroxidase activity by treating the sections with 3% hydrogen peroxide for 15 min in a dark environment. To block non-specific binding, the sections were incubated with goat serum (AR0009, Boster, China) for 1 h. Following this, sections were incubated overnight at 4°C with the primary antibodies, specifically GPX4 (1:100; T56959, Abmart), MT1G (1:100; LS-B13009, BioSciences), CA9 (1:100; T55592, Abmart), DUSP1 (1:100; T56588, Abmart), AKR1C1/2 (1:100; T58076, Abmart), and KLHL24 (1:100; PU160205, Abmart). Subsequently, they were treated with goat anti-rabbit IgG (H + L) HRP secondary antibody (BF03008X, Bio-dragon) for 2 h at room temperature. Visualization was achieved using DAB (Service-Bio, Shanghai, China), and hematoxylin was used for counterstaining. The stained sections were examined under an Olympus BX63 microscope (Olympus, Tokyo, Japan), and the proportion of positive staining was quantitatively assessed using Image J software (NIH, United States).

2.9 Western blot

Clinical IVD specimens (mild-idd group: severe-idd group = 2: 2), alongside mouse IVD specimens (control group: idd group = 2: 2), were central to this study. All samples were immediately frozen in liquid nitrogen and stored at −80°C before Western blot analysis. Tissues were lysed with RIPA buffer, and proteins were resolved via SDS-PAGE, transferred to PVDF membranes, and probed with primary antibodies, including GPX4, *MT1G*, *CA9*, and GAPDH. Detection was performed using chemiluminescence, and signal quantification was facilitated by Image Lab software.

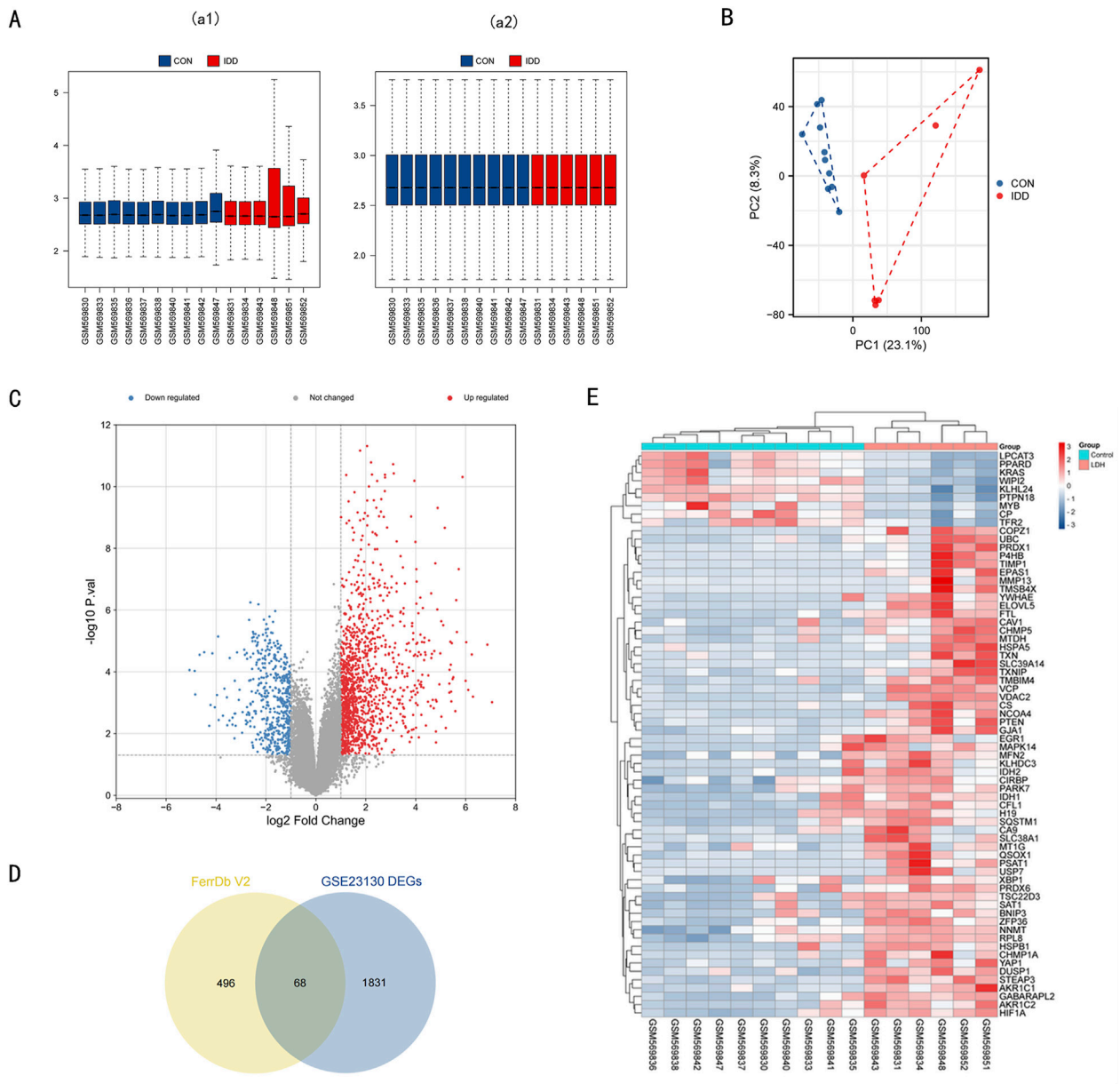

FIGURE 1
Data preprocessing of microarray data and DE-FRGs in GSE23130. **(A)** a1, The boxplot of GSE23130 before sample data standardization. a2, The boxplot of GSE23130 after sample data standardization. **(B)** Principal component analysis of the microarray data set GSE23130. **(C)** Volcano plot of GSE23130. Red refers to upregulated expression. Blue refers to downregulated ex-pression. Gray indicates no difference in expression. **(D)** Venn diagrams indicating 68 DE-FRGs. Blue indicates the 1899 DEGs. Yellow indicates the 564 FRGs. **(E)** Heatmap of the 68 DE-FRGs in Intervertebral disc.

2.10 Immune cell infiltration estimation

CIBERSORT is a specialized deconvolution method that discerns and quantifies the infiltration of 22 distinct immune cell subtypes (Newman et al., 2015). Using the CIBERSORTR script, we assessed the abundance of these 22 immune cells in the GSE23130 dataset. Visualization of results was facilitated through the "vioplot" package. To determine the correlations between infiltration rates of different immune cell types, we used the "complot" package. Spearman's correlation analysis was executed on pivotal DE-FRGs and infiltrating immune cells employing the "ggpubr" and "ggExtra" packages. Further, we utilized the Wilcoxon signed-rank test to identify the differentially infiltrated immune cells (DIICs) in the IDD group in contrast to the control group, with significance set at $P < 0.05$.

2.11 Statistical analysis

Statistical evaluations in this study were conducted using various software tools: R (version 4.1.0), SPSS 20.0 (SPSS Inc., Chicago, IL, United States), and GraphPad Prism 9.0.0 (GraphPad Software, La Jolla, CA, United States). Data representation was in the format of mean ± standard error of the mean for all the parameters measured.

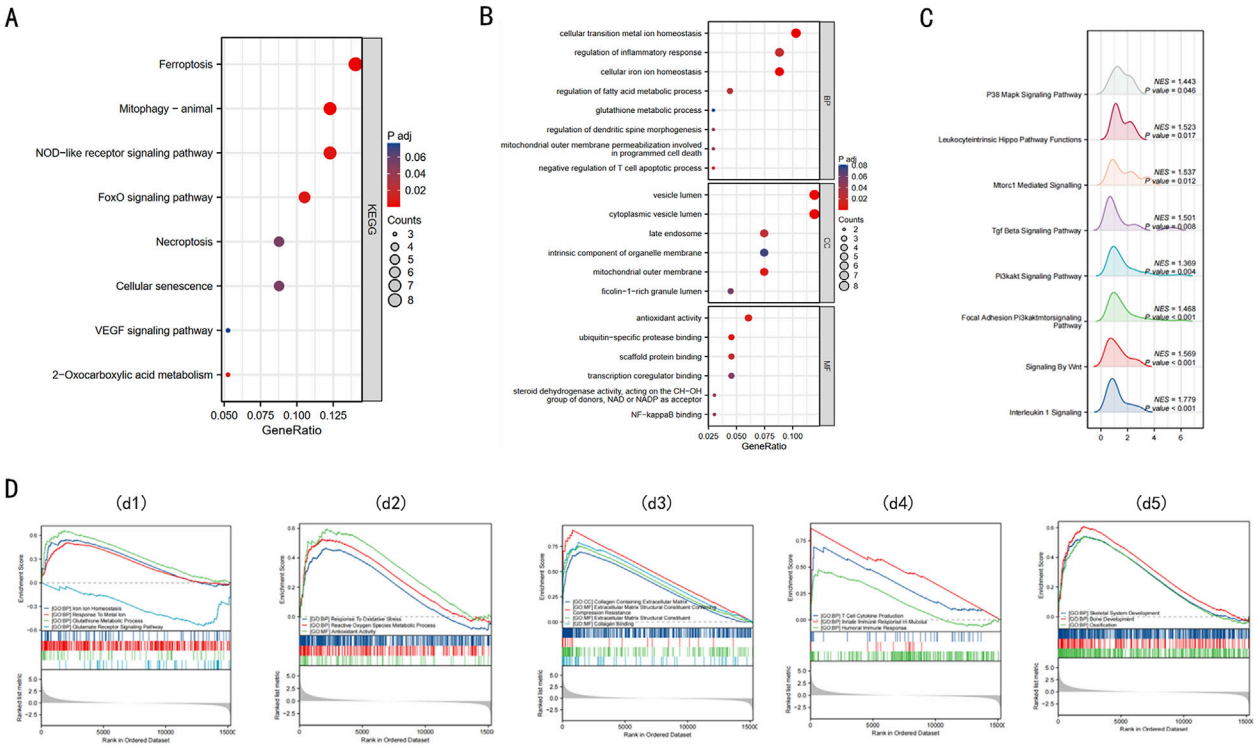

FIGURE 2
Enrichment analysis of 68 DE-FRGs in Intervertebral disc. **(A)** The bubble plot displays the gene Ontology (GO) enrichment analysis of 68 DE-FRGs in the Intervertebral disc. **(B)** The bubble plot shows the Kyoto Encyclopedia of Genes and Genomes (KEGG) analysis of 68 DE-FRGs in the Intervertebral disc. **(C)** Ridge plot of GSEA results for C2 pathway. **(D)** d1, The GSEA enrichment plot indicates that BPs relating to ferroptosis are enriched in the IDD group. d2, The GSEA enrichment plot indicates that BPs relating to ROS are enriched in the IDD group. d3, The GSEA enrichment plot indicates that BPs relating to collagen are enriched in the IDD group. d4, The GSEA enrichment plot indicates that BPs relating to immunity are enriched in the IDD group. d5, The GSEA enrichment plot indicates that BPs relating to bone development are enriched in the IDD group.

For statistical comparisons, Student's t-tests were applied, considering $P < 0.05$ as the threshold for statistical significance.

3 Results

3.1 Screening of DEGs and identification of DE-FRGs

In this section, we describe the process of identifying differentially expressed genes (DEGs) and ferroptosis-related genes (DE-FRGs) involved in intervertebral disc degeneration (IDD). Microarray data GSE23130 was sourced from the GEO database. After normalization (Figure 1A), we conducted PCA (Principal Component Analysis) as depicted in Figure 1B. Based on the PCA outcomes, we eliminated outlier samples and subsequently considered ten normal and 6 IDD samples from the dataset for further examination. The differential expression analysis revealed 1899 DEGs: 544 downregulated and 1,355 upregulated, visualized in the volcano plot (Figure 1C). Using the FerrDb V2 database, we retrieved a set of 564 FRGs. Their intersection with the 1899 DEGs yielded 68 ferroptosis-related DEGs, depicted in the heatmap (Figures 1D, E). Detailed data regarding these 68 DE-FRGs can be found in Supplementary Table 1.

3.2 Enrichment analyses of DE-FRGs

To elucidate the biological functions of the 68 DE-FRGs, we undertook KEGG and GO analyses. The KEGG analysis spotlighted significant engagement of pathways like Ferroptosis, NOD-like receptor, FOXO, and VEGF (Figure 2A) (refer to Supplementary Table 2).

The GO enrichment analysis provided insights into the functions of differentially expressed ferroptosis-related genes (DE-FRGs), highlighting their involvement in key processes that are linked to iron-induced cell death or ferroptosis. In the Biological Process (BP) category, these genes were primarily involved in maintaining cellular iron ion homeostasis, glutathione metabolism, and regulating fatty acid metabolism, all of which are crucial for controlling the iron levels and oxidative state within cells. Furthermore, they were involved in mitochondrial outer membrane permeabilization, a critical event in programmed cell death that can be triggered by iron overload and lead to cell death. In the Cellular Component (CC) category, there was notable enrichment in structures like the mitochondrial outer membrane and the late endosome, which are essential in managing cellular iron distribution and could play roles in initiating ferroptosis if dysregulated. Lastly, in the Molecular Function (MF) category, associations with antioxidant activity, NF-κB binding, and ubiquitin-specific protease binding suggest mechanisms by which

10.3389/fcell.2024.1416345

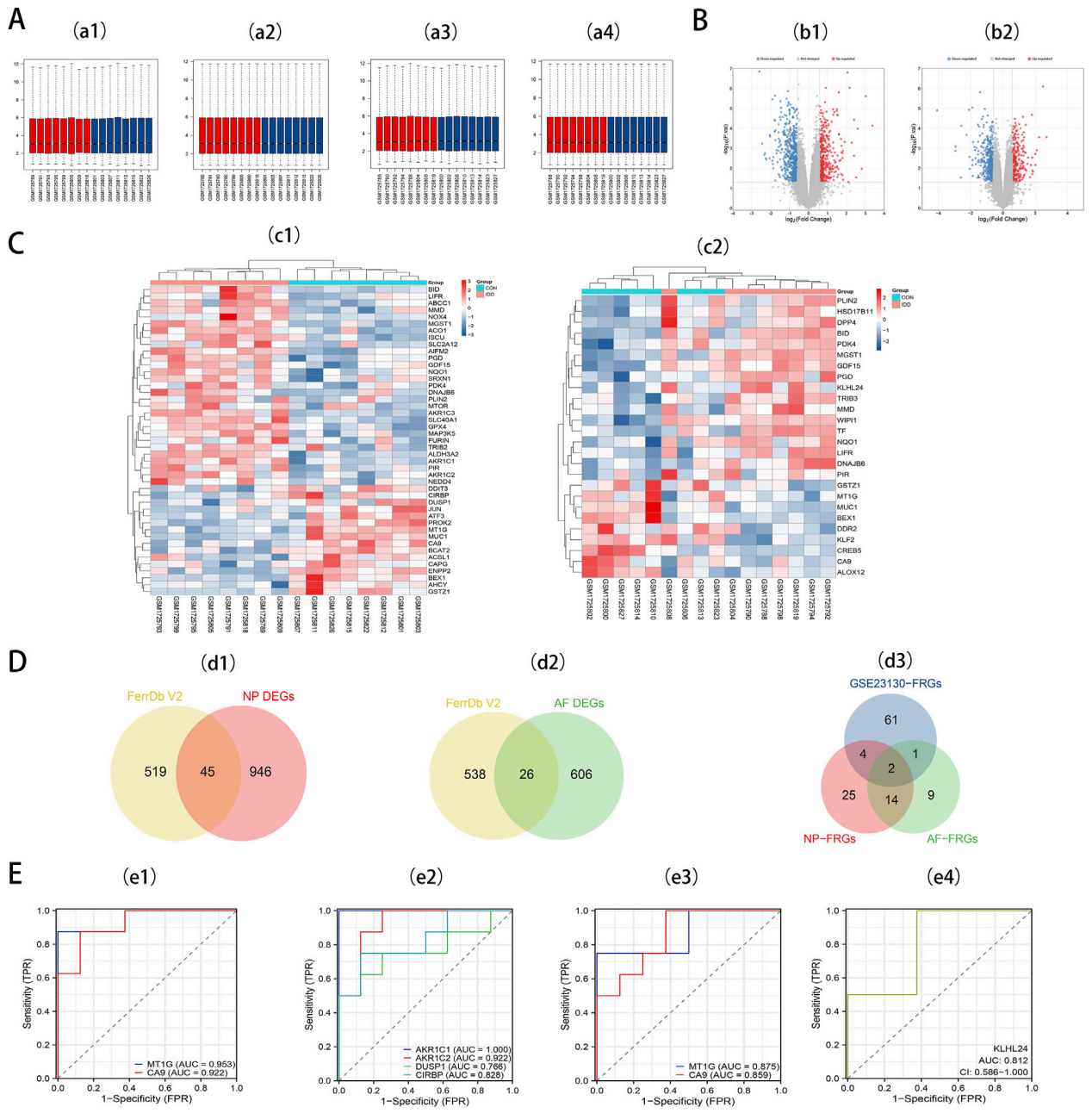

FIGURE 3
(A) a1, The boxplot of GSE70362 before AF sample data standardization. a2, The boxplot of GSE70362 after AF sample data standardization. a3, The boxplot of GSE70362 before NP sample data standardization. a4, The boxplot of GSE70362 after NP sample data standardization. **(B)** b1, Volcano plot of DEGs in AF. b2, Volcano plot of DEGs in NP. Red refers to upregulated expression. Blue refers to downregulated expression. Gray indicates no difference in expression. **(C)** c1, Heatmap of the 45 DE-FRGs for NP. c2, Heatmap of the 26 DE-FRGs for AF. **(D)** Venn diagrams indicate 45 DE-FRGs for NP and 26 DE-FRGs for AF. Blue indicates the 68 DE-FRGs derived from the Intervertebral disc dataset. Yellow indicates the 564 FRGs, Red indicates 45 DE-FRGs for NP, and Green indicates 26 DE-FRGs for AF. **(E)** e1, ROC curves of *MT1G*, and *CA9* in NP tissues. e2, ROC curves of NP-specific DE-FRGs. e3, ROC curves of *MT1G*, and *CA9* in AF tissues. e4, ROC curves of AF-specific DE-FRGs.

these genes might influence ferroptosis. Antioxidant activity is crucial in mitigating oxidative stress caused by iron, while NF-κB and ubiquitin-specific proteases could regulate the cellular response to stress and damage, including ferroptosis (Figure 2B) (details in Supplementary Table 3). These findings collectively underscore the complex interplay of molecular functions that govern iron-induced cell death, linking cellular iron management with the pathways leading to ferroptosis.

GSEA, utilizing C2 gene sets, was illustrated via a ridge plot (Figure 2C), highlighting pathways like INTERLEUKIN 1 SIGNALING, SIGNALING BY WNT, PI3KAKT SIG-NAL-ING PATHWAY, these pathways are known to be involved in inflammation, cell proliferation, and survival, which can be crucial in the context of IDD progression. Subsequent GSEA enrichment plots for GO gene sets confirmed the predominance of processes like iron ion homeostasis, response to metal ions, and glutathione

metabolism in the IDD group (Figure 2d1). These processes are directly linked to managing iron levels and detoxifying reactive oxygen species (ROS), implicating ferroptosis could significantly contribute to IDD pathology. Additionally, there were discernible enrichments related to ROS (Figure 2d2), collagen (Figure 2d3), immunity (Figure 2d4), and bone development (Figure 2d5) within the IDD group. A comprehensive summary of the GSEA findings is provided in Supplementary Table 5. Obtain seven key DE-FRGs in Nucleus Pulposus (NP) and Annulus Fibrosus (AF), these genes are essential for understanding the molecular mechanisms of IDD and how ferroptosis might be specifically managed in these tissues to potentially mitigate disease progression.

We retrieved the GSE70362 microarray expression profiling dataset from the GEO database, utilizing it as a validation set. From this, 16 fibrillar and 16 myeloid samples were chosen for normalization (Figures 3a1, 3a2). Subsequent differential expression analyses pinpointed 632 DEGs in AF and 991 DEGs in NP. For the DEGs in AF, 373 genes exhibited downregulation, while 259 showed upregulation. In contrast, the NP samples had 587 downregulated genes and 404 upregulated ones. These distributions are depicted in volcano plots (Figures 3b1, 3b2). By intersecting 564 FRGs with the identified DEGs in AF (632) and NP (991), we ascertained 26 DE-FRGs for AF (Figure 3d1) and 45 DE-FRGs for NP (Figure 3d2). The heatmaps showcasing these intersections can be observed (Figures 3c1, 3c2). More granular details on DE-FRGs in AF and NP are cataloged in Supplementary Table 5 and Supplementary Table 6, respectively.

To pinpoint diagnostic biomarkers integral to IDD, we carried out an intersection analysis on the 68 DE-FRGs derived from the Intervertebral disc dataset. This scrutiny illuminated two central DE-FRGs - *MT1G* and *CA9* - consistently expressed in both AF and NP regions. Intriguingly, *KLHL24* surfaced as a unique DE-FRG confined to AF, whereas NP revealed a distinct preference for four DE-FRGs: *AKR1C1*, *AKR1C2*, *DUSP1*, and *CIRBP* (Figure 3d3).

Seven key DE-FRGs was assessed via receiver operating characteristics (ROC) using an external dataset. In NP tissues, *MT1G* and *CA9* showcased AUC values of 0.953 and 0.922 (Figure 3e1). The ROC curve for the NP-specific DE-FRGs—*AKR1C1*, *AKR1C2*, *DUSP1*, and *CIRBP*—exhibited AUC values of 1.000, 0.922, 0.766, and 0.828, respectively (Figure 3e2). Meanwhile, in AF tissues, *MT1G* and *CA9* showcased AUC values of 0.875 and 0.859, respectively (Figure 3e3). The AF-specific DE-FRG, *KLHL24*, displayed an AUC value of 0.812 (Figure 3e4).

These enrichment analyses reveal the complex interplay of molecular functions and pathways that govern ferroptosis in IDD, offering potential targets for therapeutic intervention.

3.3 Confirmation of expression patterns of ferroptosis key genes in a single-cell dataset

To further explore the expression of key DE-FRGs at the single-cell level, we analyzed a single-cell RNA-seq dataset to identify the cell types and clusters expressing these genes in non-degenerated and degenerated intervertebral disc tissues.

Our analysis incorporated the GSE199866 single-cell RNA-seq dataset, which included 3,955 NP cells from non-degenerated discs (NPnD), 3,678 NP cells from degenerated discs (NPD), 3,226 AF cells from non-degenerated discs (AFnD), and 3,142 AF cells from degenerated discs (AFD). We analyzed the single-cell data after quality control and visualized all cells through UMAP plots (Figures 4A, B), revealing 9 clusters with distinct expression profiles, designated as clusters 0–8. This reflects the heterogeneity of intervertebral disc cell functions. These plots reveal the distinct transcriptional identities of cells in non-degenerated versus degenerated conditions, highlighting potential molecular pathways impacted by disc degeneration.

To identify the functions of each cluster and explain the role of DE-FRGs in IDD.GSVA enrichment analysis was performed on the single-cell transcriptomes, displaying the most representative metabolic pathways using a heatmap (Figure 4C). Additional results are presented in the Supplementary Table 7. Cluster 0 emphasizes the importance of cartilage and bone formation as well as the integrity of the extracellular matrix, which are vital for maintaining the structure and function of the intervertebral disc. The condensation of cartilage and the completeness of the extracellular matrix are crucial for resisting structural damage and functional loss during disc degeneration. Cluster 1 reveals the significance of protein synthesis, particularly the role of ribosomes, which is essential for repairing the extracellular matrix and combating degenerative stress in disc cells. Clusters 2 and 3, related to lipid metabolism and stress response, may be linked to the nutritional supply and cellular response mechanisms of the disc. Cluster 4 focus on cellular growth and differentiation, especially in bone and cartilage development, is significant for regenerative medicine and stem cell therapy strategies in disc research. Both Clusters 5 and 1 underscore the role of protein synthesis in restoring disc cell function and maintaining matrix integrity. Cluster 6 unveils the importance of cell division and chromosomal dynamics, potentially related to disc cell proliferation and genetic stability, which are essential for disc health and preventing degeneration. Cluster 7, involving blood coagulation and fibrinolysis, could offer insights into the inflammatory response and angiogenesis during disc degeneration. Lastly, Cluster 8 highlights the activation and regulation of specific immune cell types, unveiling potential immune-mediated mechanisms in disc degeneration, particularly in the study of disc inflammation and pain mechanisms.

In the intervertebral disc tissues, we observed an increase in the proportions of clusters 2, 3, and 7, and a decrease in clusters 0, 1, 4, and 5, potentially revealing critical biological changes and molecular mechanisms in the process of disc degeneration. The rising clusters indicate intensified inflammatory responses, heightened stress adaptation, and alterations in local microcirculation, while the declining clusters suggest a weakening in extracellular matrix synthesis and maintenance, protein synthesis, and the capacity for tissue repair and regeneration (Figure 4D).

The pseudotime analysis suggests a trajectory of cellular evolution within the degenerative process of intervertebral disc cells. The sequence or trajectory shown by cell clustering likely reflects the continuum of cell states, from healthy to degenerative stages. The proportions of cells along the principal component 1 axis (horizontal axis) align with the types of cells in disc degeneration, with clusters 0, 1, 4, and 5 representing the states of healthy or early degenerative disc cells, while clusters 2, 3, and 7 may correspond to more advanced stages of degeneration (Figures 4E, F).

10.3389/fcell.2024.1416345

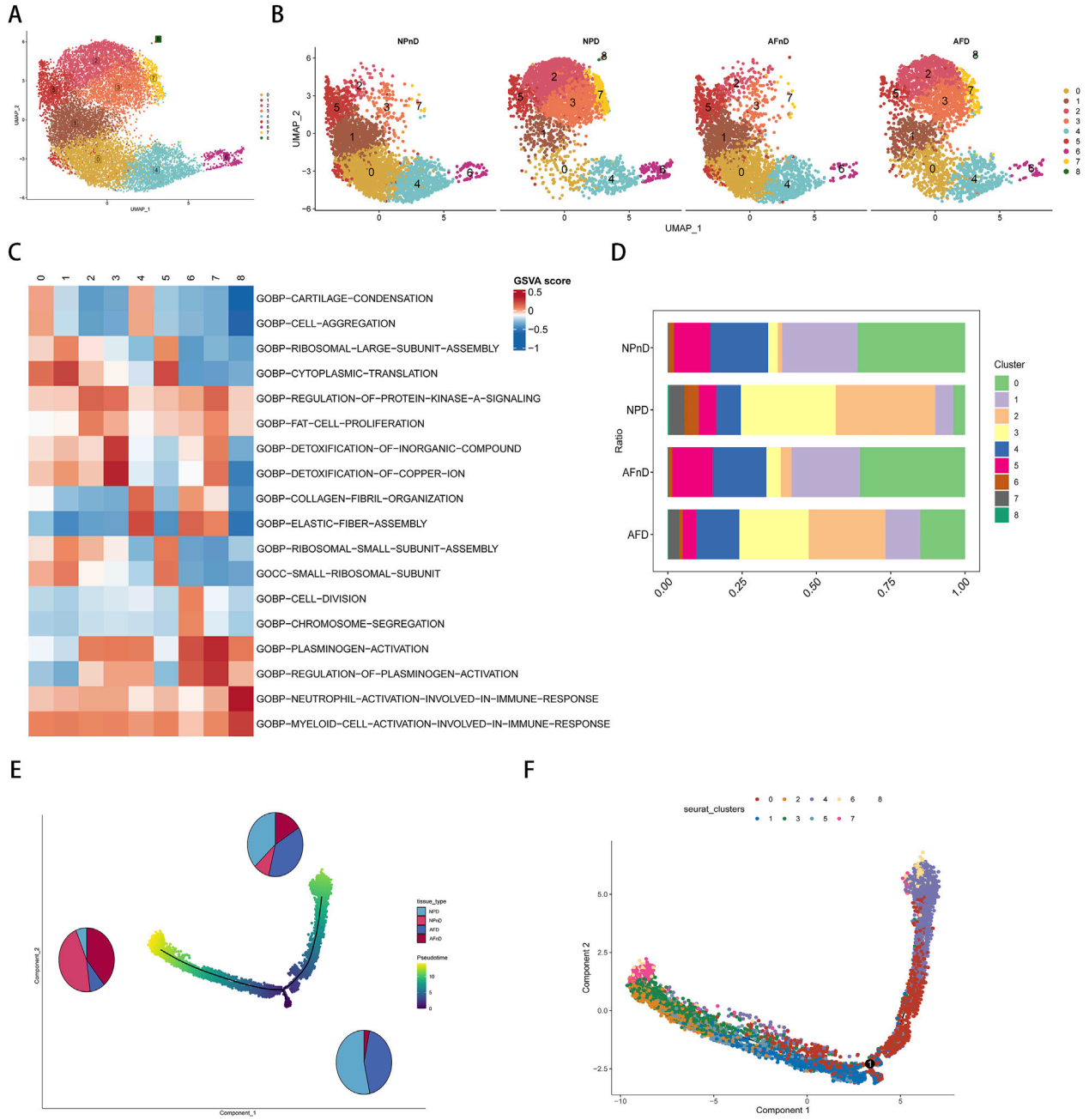

FIGURE 4
Single-cell transcriptomic landscape and pseudotime trajectory analysis of intervertebral disc cells. **(A)** Unsupervised UMAP projection representing the global transcriptional profiles of disc cells. **(B)** Unsupervised UMAP clustering showing the change in cell distribution of the 14 different clusters for NPnD, NPD, AFnD, and AFD. **(C)** GSVA enrichment analysis of the identified nine cell clusters, displaying the most representative metabolic pathways using a heatmap. **(D)** Bar chart showing the proportional representation of each cluster within the four conditions. **(E)** The pseudotime trajectory axis for tissue types along the progression of IVD degeneration, with pie charts. **(F)** The pseudotime trajectory axis for defined nine cell clusters.

The results indicate a nuanced expression pattern of key genes across different states of intervertebral disc cells, as visualized in UMAP plots (Figures 5A, B). Notably, *MT1G* and *CA9* expressions vary across clusters in both NP and AF cells, with *MT1G* generally upregulated in degenerated tissues. This suggests an adaptive cellular response to degenerative stress, potentially involving metal ion balance and oxidative stress. *CA9* upregulation in specific clusters (clusters 2, 3, 6, and 7) aligns with responses to hypoxic and acidic environments, implicating its role in disc degeneration. Box plots further quantify these expression changes (Figure 5C). The expression pattern of GPX4 is shown in Supplementary Figure 1.

The single-cell analysis highlights the specific cellular environments where ferroptosis-related changes occur, underscoring the importance of these genes and pathways in the progression of IDD.

10.3389/fcell.2024.1416345

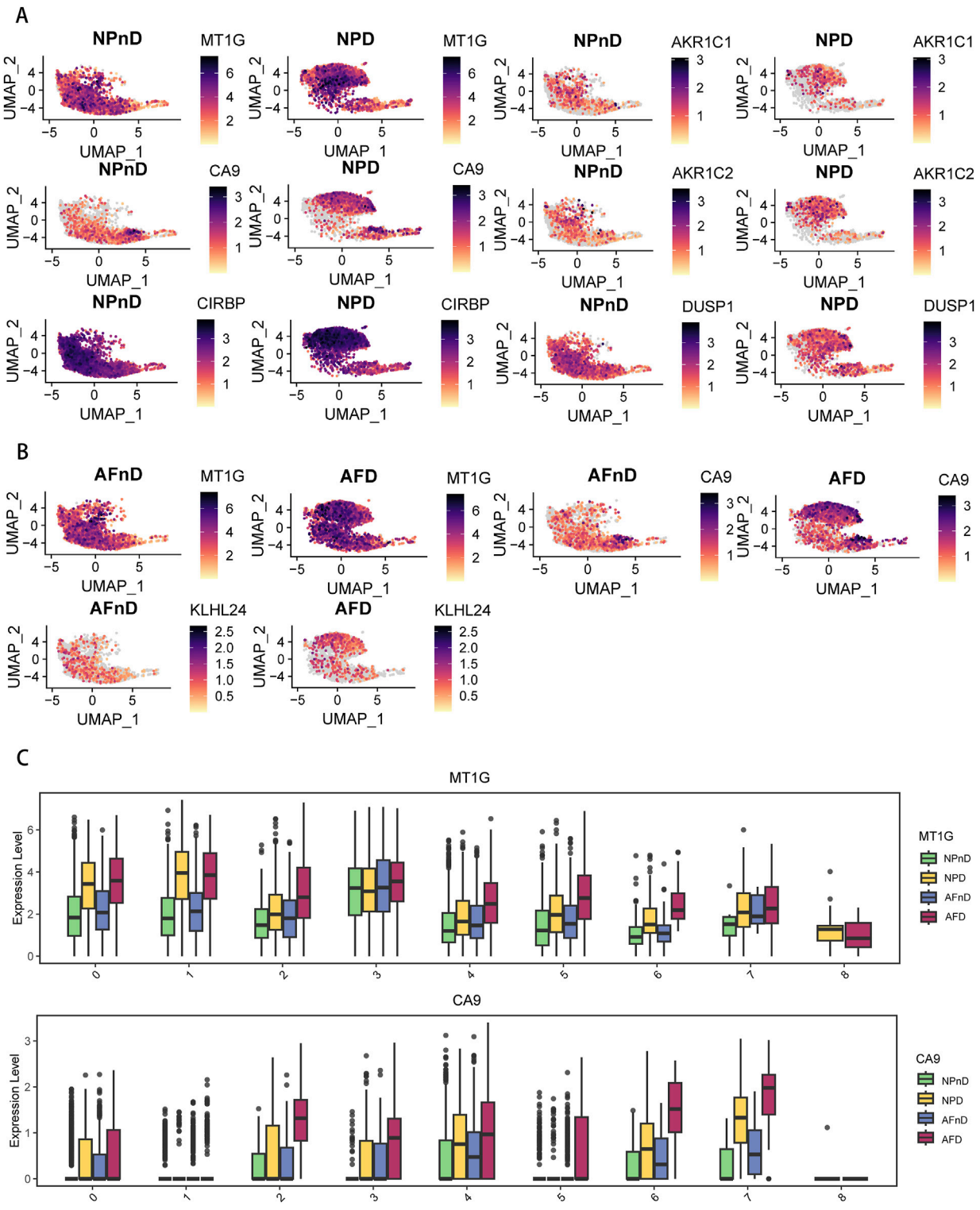

FIGURE 5
Expression of DE-FRGs in a single-cell dataset **(A)** UMAP plots demonstrate the expression levels of NP-specific DE-FRGs in NPnD versus NPD cells. **(B)** UMAP plots demonstrate the expression levels of AF-specific DE-FRGs AFnD versus AFD cells. **(C)** Box plots show the quantification of expression levels for *MT1G* and *CA9* across all clusters.

10.3389/fcell.2024.1416345

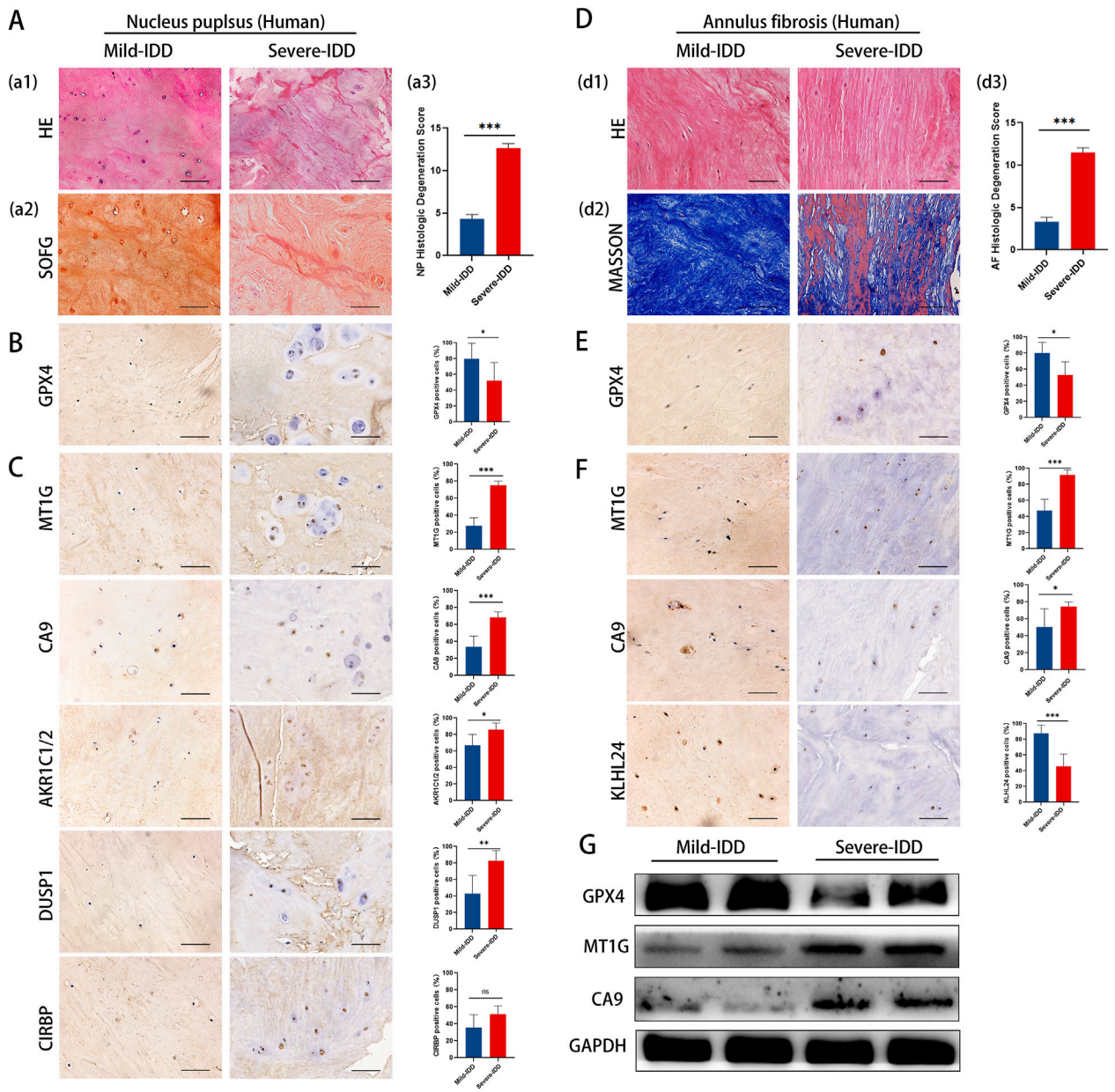

FIGURE 6
Representative histology and protein expression levels of clinical specimen. **(A)** HE staining, SOFG staining and histologic Degeneration Score of NP **(B)** Representative IHC images of GPX4 in NP. **(C)** Representative IHC images of *MT1G*, *CA9*, *AKR1C1/2*, *DUSP1*, and *CIRBP* in the NP. **(D)** HE staining, Masson staining and histologic Degeneration Score of AF. **(E)** Representative IHC images of GPX4 in AF. **(F)** Representative IHC images of *MT1GCA9*and *KLHL24* in the AF. **(G)** The protein levels of GPX4, *MT1G* and *CA9* of clinical specimen.

3.4 Validation of ferroptosis key genes in clinical specimens

To validate our findings in a clinical context, we examined the expression of key DE-FRGs in clinical specimens categorized by the degree of disc degeneration.Clinical samples were categorized by Pfirrmann grading, detailed in Supplementary Table 8. Utilizing hematoxylin and eosin (HE) staining to examine cell density and structural alterations, the analysis revealed that the NP tissues in the mild-IDD group manifested a significantly higher density of chondrocyte cells. Conversely, the severe-IDD group was characterized by a substantial decrease in cell quantity and the emergence of small-sized cellular clusters (comprising 3-7 chondrocytes), accompanied by more pronounced structural disruptions. Additionally, Safranin-O/Fast Green (SOFG) staining uncovered a striking contrast in proteoglycan distribution, with the mild-IDD group displaying a consistent red matrix, markedly diminished in the severe-IDD group (Figure 6A). Further scrutiny of the annulus fibrosus (AF) elucidated a compromised structural integrity in discs with severe degeneration, manifesting as disorganized fiber patterns. This observation was corroborated by Masson's

10.3389/fcell.2024.1416345

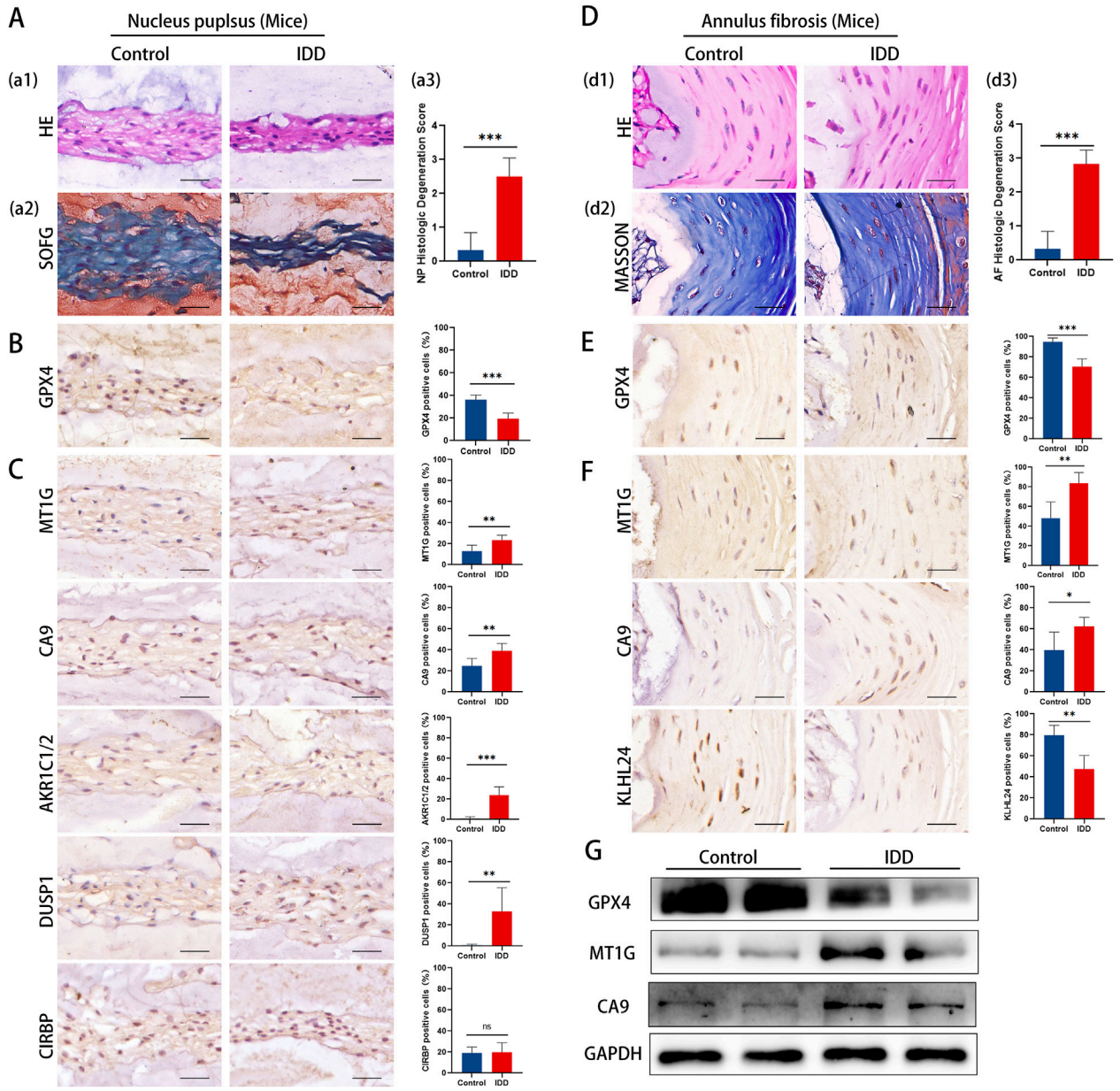

FIGURE 7
Representative histology and protein expression levels of mice specimen. **(A)** HE staining, SOFG staining and histologic Degeneration Score of NP **(B)** Representative IHC images of GPX4 in NP. **(C)** Representative IHC images of *MT1G*, *CA9*, *AKR1C1/2*, *DUSP1*, and *CIRBP* in the NP. **(D)** HE staining, Masson staining and histologic Degeneration Score of AF. **(E)** Representative IHC images of GPX4 in AF. **(F)** Representative IHC images of *MT1GCA9*and *KLHL24* in the AF. **(G)** The protein levels of GPX4, *MT1G* and *CA9* of mice specimen.

trichrome staining, which further emphasized extensive red-stained regions, indicative of advanced degeneration (Figure 6D). The variation in histological degeneration scores between the groups significantly underscored the severe degenerative alterations observed in the severe group.

To clarify the correlation between ferroptosis and IDD, we examined GPX4 expression in clinical samples with different degrees of deformation in NP and AF. Immunohistochemistry results showed that the expression of *GPX4* was decreased in both NP and AF of the highly degenerated group, and the degree of ferroptosis increased with the degree of degeneration (Figures 6B, E).

The results of immunohistochemistry staining showed that in NP, the expression of *MT1G, CA9, AKR1C1/2, DUSP1* was significantly increased, whereas *CIRBP* expression remained unchanged (Figure 6C). In AF, the expression of *MT1G* and *CA9* increased significantly, while the expression of *KLHL24* decreased significantly (Figure 6F). Western blotting results showed that *MT1G* and *CA9* protein levels were upregulated in mild-IDD specimens compared with severe-IDD specimens, while the protein levels of *GPX4* were decreased (Figure 6G).

The results from clinical specimens confirm the differential expression of key ferroptosis-related genes, reinforcing their potential role in the pathology of IDD.

10.3389/fcell.2024.1416345

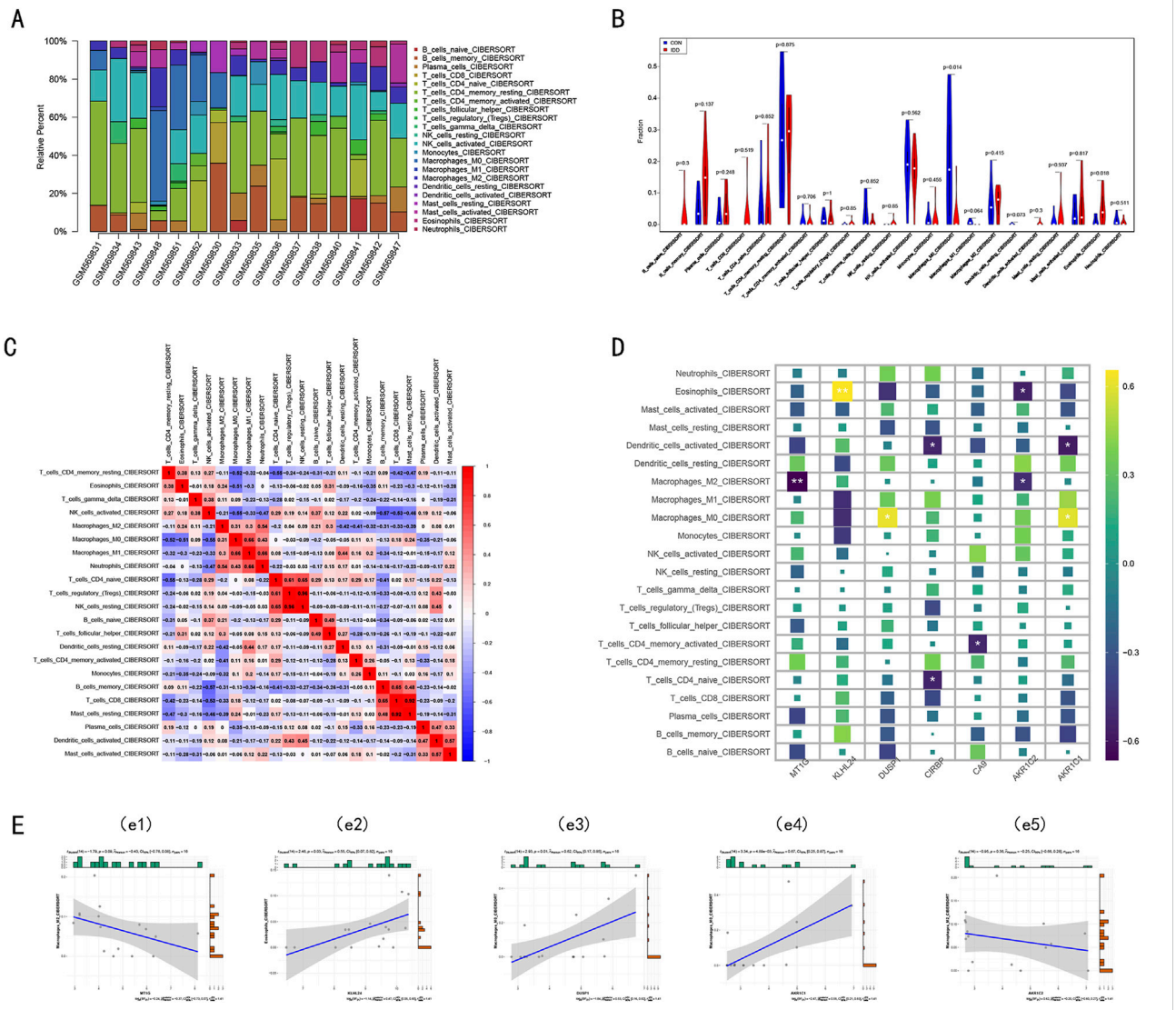

FIGURE 8
The immune infiltration landscape in the Intervertebral disc. **(A)** The stacked bar chart shows the distribution of 22 immune cells in the GSE23130 dataset, each bar represents one sample. **(B)** The violin plot demonstrates the difference in immune infiltration between intervertebral disc degenerative tissue and control tissue. **(C)** Correlation heat maps display the correlation matrix of 22 immune cell type proportions. Red: Positive correlation; Blue: Negative correlation. **(D)** Heatmap showed the correlations between the seven key DE-FRGs and 22 types of immune cells. Yellow: Upregulation; Purple: Downregulation. The depth of the colors represented the strength of the correlation. **(E)** Correlation analysis between immune cell infiltration and the expression of key DE-FRGs.

3.5 Validation of ferroptosis key genes in IDD mouse models

To further corroborate our findings, we investigated the expression of key DE-FRGs in IDD mouse models, focusing on histological and molecular changes.Histological evidence highlighted more severe degeneration in the IDD mouse group, showcasing a decrease in NP cells, extracellular matrix, and cell size (Figure 7A). Advanced degenerative changes were also noted in the annulus fibrosus (Figure 7D).

Immunohistochemistry analysis revealed a significant reduction in GPX4 expression in both NP and AF tissues (Figures 7B, E). The results aligned with clinical specimens.

The results of immunohistochemistry staining showed that in the NP, there was a notable upsurge in the expression of *MT1G*, *CA9*, *AKR1C1/2*, and *DUSP1*, whereas *CIRBP*'s expression remained largely unaltered (Figure 7C). Conversely, in the AF region, *MT1G* and *CA9*'s expression was markedly amplified, while *KLHL24*'s expression diminished significantly (Figure 7F). Western blotting confirmed these observations, showing a decrease in *GPX4* and an increase in *MT1G* and *CA9* in IDD mouse IVD tissues (Figure 7G).

The mouse model results align with our clinical findings, further supporting the involvement of ferroptosis in IDD and highlighting key DE-FRGs as potential therapeutic targets.

3.6 Immune microenvironment characteristics in IDD

The etiology of IDD is thought to involve immune dysregulation within the disc microenvironment. To explore the immune system's potential role in IDD, we analyzed immune cell infiltration in IDD samples using the GSE23130 dataset and the CIBERSORT algorithm. Our findings revealed significant differences in immune cell infiltration between IDD and control (CON) groups, underscoring the possible contribution of immune factors to the development of IDD. Specifically, there was a marked increase in the infiltration of M0 macrophages and eosinophils in the IDD group (Figures 8A, B), indicating an altered immune landscape. Further analysis using a correlation matrix of the 22 immune cell subtypes revealed a positive correlation between M0 macrophages and other inflammatory cells such as M1 and M2 macrophages, as well as neutrophils. This suggests a complex network of immune interactions contributing to inflammation and possibly disc degeneration. Conversely, there was an inverse relationship observed between resting memory CD4+ T cells, activated NK cells, and eosinophils, highlighting the diverse roles of immune cells in IDD. Interestingly, eosinophils, which were elevated in IDD, also showed positive correlations with resting memory CD4+ T cells, M2 macrophages, and T follicular helper cells (Figure 8C), further illustrating their potential role in modulating immune responses in IDD. Acknowledging the pivotal role of diverse immune components in diagnosing IDD and its underlying pathogenic mechanisms, we delved into the association between immune cell infiltration and the expression of key DE-FRGs. Notably, *DUSP1* and *AKR1C1* were found to be upregulated in M0 macrophages. In eosinophils, *KLHL24* expression was markedly elevated ($P < 0.01$), whereas *AKR1C2* displayed a declining trend ($P < 0.05$) (Figures 8D, E).

These findings suggest that specific immune cells, particularly M0 macrophages and eosinophils, may influence the expression of genes related to ferroptosis, potentially linking the immune response to iron-dependent cell death in IDD. This connection could be key in understanding the pathogenic mechanisms of IDD and could lead to targeted therapies that address these immune and molecular interactions.

4 Discussion

IDD is predominantly considered a degenerative disease and is the primary cause of chronic lower back pain (Takatalo et al., 2012; Manchikanti et al., 2009). Various pathogenic factors can disrupt the standard activity and function of both nucleus pulposus (NP) cells and annulus fibrosus (AF) cells, culminating in the deterioration of the intervertebral disc (Lotz and Ulrich, 2006; Urban, 2002). Serving as the central structural and functional component of the intervertebral disc (IVD), the NP often undergoes pathological changes early in IDD. Research has shown that cell mortality rates in degenerative human intervertebral disc samples fluctuate between 53% and 73%, particularly within the NP region. Surrounding the NP, the annulus fibrosus connects adjacent vertebral bones and faces degeneration primarily due to the loss of fibrous ring cells and imbalances in collagen fiber synthesis and metabolism (Fontana et al., 2015; Sakai and Grad, 2015; Colombini et al., 2008). Recent research has emphasized preserving IVD cell activity, with increasing interest in the potential relationship between ferroptosis and IDD (Dou et al., 2023; Ke et al., 2023; Li et al., 2023).

In this study, we explored the role of ferroptosis in the pathophysiology of IDD, specifically investigating its impact on NP and AF cells. Through bioinformatics analysis, we examined the GSE23130 dataset, pinpointing 68 potential ferroptosis-related genes (FRGs) associated with IDD. We subsequently subjected these differentially expressed FRGs to enrichment analysis to determine their possible biological roles. Our Gene Ontology (GO) examination of the FRGs identified various enrichment categories linked to ferroptosis, including macroautophagy, mitophagy, collagen protein metabolic processes, and the regulation of fibroblast proliferation. The GSEA demonstrate an increased activation of pathways involved in ferroptosis, ROS production, and immune infiltration, aligning with recent studies that underscore the multifactorial nature of IDD. This correlation supports the hypothesis that oxidative stress and immune responses play a crucial role in disc degeneration. Several signaling channels recognized through the Kyoto Encyclopedia of Genes and Genomes (KEGG) examination, like PI3K-AKT, P38 MAPK, TGF-β, and mTOR, correlate with ferroptosis. To differentiate between FRGs in the NP and the AF, we analyzed the GSE70362 dataset, cross-referencing our findings with the identified FRGs. This analysis unveiled 45 FRGs in the NP and 26 in the AF. When comparing both the GSE23130 and GSE70362 datasets, we identified seven DE-FRGs. Notably, *MT1G* and *CA9* appeared in both NP and AF datasets, *AKR1C1*, *AKR1C2*, *DUSP1*, and *CIRBP* were specific to NP, and *KLHL24* was exclusive to AF. The consistent expression of *MT1G* and *CA9* in both NP and AF tissues across different stages of IDD suggests these proteins could serve as viable biomarkers for early diagnosis and progression monitoring of the disease. Future clinical trials could explore the efficacy of targeting these markers to slow or reverse disc degeneration.

The validation of our findings through the single-cell database (GSE199866) is crucial for confirming the specificity of gene expression changes in IDD. This analysis enables us to identify the precise cell types showing ferroptosis-related alterations, adding a critical layer of validation to our bioinformatics findings. Additionally, we categorized classified clinical samples according to the lumbar intervertebral disc's Pfirrmann grading. We also developed a mouse model for IDD, closely mimicking the pathological progression of human IDD induced by mechanical stress. The IVD samples from this IDD mouse model exhibited pronounced degeneration, reflecting the pathophysiology seen in human IDD. Notably, in both the advanced degenerative clinical samples and the IDD mouse specimens, we detected a marked decline in GPX4 protein expression. This indicates a potential surge in ferroptosis as IDD progresses (Chen X. et al., 2021). Building upon our bioinformatics findings, we utilized immunohistochemistry (IHC) to validate the expression of the seven identified differentially expressed FRGs in both clinical samples and the IDD mouse model. Experimental results confirmed that *MT1G*, *CA9*, *KLHL24*, AKRC1R1, AKRC1R2, and *DUSP1* protein expression patterns aligned with our bioinformatics insights.

MT1G is a member of the Metallothionein (MTs) family (Mehus et al., 2014). This gene encodes a compact, cysteine-rich protein that play an important role in protecting cells from heavy metal toxicity, oxidative stress damage, and are involved in cell proliferation and apoptosis. *MT1G*'s specific functions include regulating the availability of metal ions, acting as an antioxidant, and potentially participating in cell signaling pathways. Recent research suggests that its dysregulation is associated with various human malignancies and can suppress ferroptosis in tumors (Sun et al., 2016). In single-cell analyses focusing on IDD, elevated *MT1G* expression was identified in IDD tissues, suggesting that *MT1G* may influence IDD by mitigating calcification (Cherif et al., 2022; Li et al., 2022). In this study, we confirmed that *MT1G* is highly expressed during IDD, and the expression of *MT1G* is upregulated across various cell clusters in degenerated tissues, reflecting an attempt by cells to protect themselves and adapt to the degenerative environment. This widespread upregulation may indicate a link between disc degeneration and imbalances in metal ion homeostasis and increased oxidative stress. Given *MT1G*'s role in resisting oxidative stress and regulating metal ion balance, enhancing its expression or function could provide protection against disc degeneration. Potential therapeutic strategies might include promoting *MT1G* expression or adjusting metal ion balance to reduce oxidative damage and promote cell survival.

CA9, commonly known as Carbonic Anhydrase IX, is a transmembrane enzyme significantly induced under hypoxic conditions and plays a vital role in regulating the cellular acid-base balance (Li et al., 2020). Research has linked *CA9* with the process of ferroptosis, suggesting it could counteract this iron-dependent form of cell death in various cancers by modifying transferrin endocytosis and stabilizing ferritin levels (Zhang C. et al., 2023; Li et al., 2019). Furthermore, *CA9* is expressed in NP cells, with increased levels observed in conditions of heightened oxygen concentration, a state contrary to the cells' naturally hypoxic environment (Silagi et al., 2018). As IDD progresses, these cells are increasingly exposed to lower pH levels and more oxygen, indicating *CA9*'s potential role in adjusting to these changes. The upregulation of *CA9* noted in our study, particularly in clusters associated with late-stage degeneration, supports its involvement in inflammatory responses, cell differentiation and growth, protein synthesis disruption, cell division, and tissue repair processes. This suggests that *CA9*'s expression might facilitate cellular adaptation to the hypoxic and acidic microenvironments during disc degeneration. Therefore, targeting *CA9* and strategies to improve the cellular micro-environment may offer new directions for the treatment of disc degeneration.

AKR1C1 and *AKR1C2* are members of the aldo-keto reductase superfamily and serve as modulators of hormone activity. These enzymes catalyze the conversion of aldehydes and ketones into their respective alcohols, employing NADH and/or NADPH as cofactors (Detlefsen, 2023). Previous studies have shown that *AKR1C1* and *AKR1C2* can efficiently degrade lipid peroxides produced by 12/15-LOX, which enhances cellular resistance to drug-induced endoplasmic reticulum-induced ferroptosis (Gagliardi et al., 2019; Wohlhieter et al., 2020). Increased levels of *AKR1C1* and *AKR1C2* may play a protective role in IDD by effectively degrading lipid peroxides to counteract ferroptosis.

DUSP1 is a dual-specific phosphatase that targets both tyrosine and serine residues (Bermudez et al., 2010). It acts on the MAP kinase MAPK1/ERK2, thereby playing a pivotal role in modulating the functions of the MAPK family, particularly in cancer cells. Recent studies suggest that *DUSP1* might curtail autophagosomes by inhibiting the phosphorylation of ULK1 or BECN1. This action establishes a feedback loop that dampens autophagy-dependent ferroptosis (Wang et al., 2016). Furthermore, investigations into the UBR3/*DUSP1* ubiquitination in IDD reveal that overexpression of UBR3 accelerates the ubiquitination and subsequent degradation of DSUP1 (Jiang et al., 2022). This degradation process results in suppressed cell growth, heightened cell apoptosis, and amplified inflammatory reactions in NP cells.

Cold-inducible RNA-binding protein (*CIRBP*) is recognized as a stress response protein that responds to a range of physiological and pathological stimuli, including hypoxia, ultraviolet radiation, glucose deprivation, heat stress, and disruptions in circadian rhythm (Zhong and Huang, 2017). In various tissues and under different stimuli, *CIRBP* plays a crucial role in attenuating cell apoptosis through pathways like p53, MAPK/ERK1/2, and the NF-κB pathway. Some research indicates that *CIRBP* can directly suppress the expression levels of p53, leading to the activation of the downstream ferroptosis pathway (Gao et al., 2022). Nonetheless, there is a lack of studies addressing *CIRBP*'s role in the framework of IDD.

KLHL24, an E3 ligase receptor responsible for substrate ubiquitination, can modulate its own ubiquitination (Cui et al., 2022). While it has been identified in tumor ferroptosis, its role in IDD remains intriguing, given the significant part ubiquitination plays during IDD progression. This positions *KLHL24* as a compelling subject for further investigation.

Due to its distinctive structure, the intervertebral disc is considered an immune-privileged organ. However, recent literature has underscored the critical influence of immune cell infiltration in IDD, with the connection between ferroptosis and this infiltration yet to be fully understood (Francisco et al., 2022). Utilizing the CiberSort method, we analyzed specific immune cell types in the intervertebral disc tissue derived from the GSE23130 dataset. Notably, the IDD group demonstrated markedly elevated M0 macrophages and eosinophils infiltration levels compared to the control group. This observation corroborates earlier findings, which posit that macrophages might amplify the immune cell recruitment to the intervertebral disc through cytokine release, thus hastening IDD progression.

Moreover, our correlation analysis between DE-FRGs and immune cells revealed increased expression of *DUSP1* and *AKR1C1* in M0 macrophages. *KLHL24* expression was heightened in eosinophils, whereas *AKR1C2* expression showed a downward trajectory within the same cell type. Past studies have suggested that *DUSP1* may modulate macrophage activation, operating as a principal downstream target protein of Ninj1, which subsequently can initiate inflammatory responses (Hu et al., 2023).

This study is accompanied by several limitations that warrant acknowledgment. Firstly, while we have ascertained the altered expression of key ferroptosis genes in IDD, we have not delved deeply into the underlying biological mechanisms linking ferroptosis to immune infiltration. Future clinical trials could

explore the efficacy of targeting these markers to slow or reverse disc degeneration Secondly, the bipedal standing mouse model for lumbar disc degeneration, though designed to replicate human lumbar disc degeneration, is not without its discrepancies when juxtaposed with actual clinical specimens. Lastly, procuring normal human intervertebral disc tissues poses a formidable challenge. Consequently, we encountered difficulties obtaining clinical samples that fall within a Pfirrmann grade of 1. Such a limitation may circumscribe our research's breadth and introduce biases or variations in our findings.

Data availability statement

The original contributions presented in the study are publicly available. This data can be found here: https://doi.org/10.6084/m9.figshare.26953588.v1.

Ethics statement

The studies involving humans were approved by The Third Affiliated Hospital, Southern Medical University. The studies were conducted in accordance with the local legislation and institutional requirements. The participants provided their written informed consent to participate in this study. The animal study was approved by Animal Care and Use Committee of Southern Medical University. The study was conducted in accordance with the local legislation and institutional requirements.

Author contributions

CL: Conceptualization, Data curation, Methodology, Software, Validation, Writing–original draft, Writing–review and editing. CF: Validation, Data curation, Visualization, Investigation, Writing–original draft, Software. SL: Data curation, Validation, Software, Writing–original draft. ZL: Writing–original draft, Visualization, Investigation, Validation. BY: Conceptualization, Funding acquisition, Supervision, Writing–review and editing. LW: Conceptualization, Funding acquisition, Supervision, Writing–review and editing. ZZ: Funding acquisition, Writing–review and editing.

Funding

The author(s) declare that financial support was received for the research, authorship, and/or publication of this article. The study was supported by National Key R&D Program of China (No.2022YFC2502904) and Natural Science Foundation of Guangdong Province (2020A1515010162).

Conflict of interest

The authors declare that the research was conducted in the absence of any commercial or financial relationships that could be construed as a potential conflict of interest.

Publisher's note

Supplementary material

The Supplementary Material for this article can be found online at: https://www.frontiersin.org/articles/10.3389/fcell.2024.1416345/full#supplementary-material

References

Andersson, G. B. (1999). Epidemiological features of chronic low-back pain. *Lancet* 354 (9178), 581–585. doi:10.1016/S0140-6736(99)01312-4

Ao, X., Wang, L., Shao, Y., Chen, X., Zhang, J., Chu, J., et al. (2019). Development and characterization of a novel bipedal standing mouse model of intervertebral disc and facet joint degeneration. *Clin. Orthop. Relat. Res.* 477 (6), 1492–1504. doi:10.1097/CORR.0000000000000712

Bermudez, O., Pagès, G., and Gimond, C. (2010). The dual-specificity MAP kinase phosphatases: critical roles in development and cancer. *Am. J. Physiol. Cell Physiol.* 299 (2), C189–C202. doi:10.1152/ajpcell.00347.2009

Capossela, S., Schläfli, P., Bertolo, A., Janner, T., Stadler, B. M., Pötzel, T., et al. (2014). Degenerated human intervertebral discs contain autoantibodies against extracellular matrix proteins. *Eur. Cell Mater* 27, 251–263. doi:10.22203/ecm.v027a18

Chen, S., Chen, M., Wu, X., Lin, S., Tao, C., Cao, H., et al. (2021a). Global, regional and national burden of low back pain 1990-2019: a systematic analysis of the Global Burden of Disease study 2019. *J. Orthop. Transl.* 32, 49–58. doi:10.1016/j.jot.2021.07.005

Chen, X., Yu, C., Kang, R., Kroemer, G., and Tang, D. (2021b). Cellular degradation systems in ferroptosis. *Cell Death Differ.* 28 (4), 1135–1148. doi:10.1038/s41418-020-00728-1

Cherif, H., Mannarino, M., Pacis, A. S., Ragoussis, J., Rabau, O., Ouellet, J. A., et al. (2022). Single-cell RNA-seq analysis of cells from degenerating and non-degenerating intervertebral discs from the same individual reveals new biomarkers for intervertebral disc degeneration. *Int. J. Mol. Sci.* 23 (7), 3993. doi:10.3390/ijms23073993

Colombini, A., Lombardi, G., Corsi, M. M., and Banfi, G. (2008). Pathophysiology of the human intervertebral disc. *Int. J. Biochem. Cell Biol.* 40 (5), 837–842. doi:10.1016/j.biocel.2007.12.011

Cui, J., Zhao, Q., Song, Z., Chen, Z., Zeng, X., Wang, C., et al. (2022). *KLHL24*-Mediated hair follicle stem cells structural disruption causes alopecia. *J. Invest Dermatol.* 142 (8), 2079–2087.e8. doi:10.1016/j.jid.2022.01.007

Detlefsen, A. J. (2023). Aldo keto-reductase family 1C members 1 through 4 recombinant enzyme purification and enzyme assay. *Methods Enzymol.* 689, 303–329. doi:10.1016/bs.mie.2023.04.007

Dou, X., Ma, Y., Luo, Q., Song, C., Liu, M., Liu, X., et al. (2023). Therapeutic potential of melatonin in the intervertebral disc degeneration through inhibiting the ferroptosis of nucleus pulpous cells. *J. Cell Mol. Med.* 27 (16), 2340–2353. doi:10.1111/jcmm.17818

Fontana, G., See, E., and Pandit, A. (2015). Current trends in biologics delivery to restore intervertebral disc anabolism. *Adv. Drug Deliv. Rev.* 84, 146–158. doi:10.1016/j.addr.2014.08.008

Francisco, V., Pino, J., González-Gay, M. Á., Lago, F., Karppinen, J., Tervonen, O., et al. (2022). A new immunometabolic perspective of intervertebral disc degeneration. *Nat. Rev. Rheumatol.* 18 (1), 47–60. doi:10.1038/s41584-021-00713-z

Gagliardi, M., Cotella, D., Santoro, C., Corà, D., Barlev, N. A., Piacentini, M., et al. (2019). Aldo-keto reductases protect metastatic melanoma from ER stress-independent ferroptosis. *Cell Death Dis.* 10 (12), 902. doi:10.1038/s41419-019-2143-7

Gao, H., Xie, R., Huang, R., Wang, C., Wang, Y., Wang, D., et al. (2022). *CIRBP* regulates pancreatic cancer cell ferroptosis and growth by directly binding to p53. *J. Immunol. Res.* 2022, 2527210. doi:10.1155/2022/2527210

Ge, H., Xue, X., Xian, J., Yuan, L., Wang, L., Zou, Y., et al. (2022). Ferrostatin-1 alleviates white matter injury via decreasing ferropto-sis following spinal cord injury. *Mol. Neurobiol.* 59, 161–176. doi:10.1007/s12035-021-02571-y

Hu, Y., Zhan, F., Wang, Y., Wang, D., Lu, H., Wu, C., et al. (2023). The ninj1/*DUSP1* Axis contributes to liver ischemia reperfusion injury by regulating macro-phage activation and neutrophil infiltration. *Cell Mol. Gastroenterol. Hepatol.* 15 (5), 1071–1084. doi:10.1016/j.jcmgh.2023.01.008

Jiang, Z., Zhao, Q., Chen, L., Luo, Y., Shen, L., Cao, Z., et al. (2022). UBR3 promotes inflammation and apoptosis via *DUSP1*/p38 pathway in the nucleus pulposus cells of patients with intervertebral disc degeneration. *Hum. Cell* 35 (3), 792–802. doi:10.1007/s13577-022-00693-6

Kanehisa, M., and Goto, S. (2000). KEGG: Kyoto Encyclopedia of genes and Genomes. *Nucleic Acids Res.* 28(1): 27–30. doi:10.1093/nar/28.1.27

Ke, W., Liao, Z., Liang, H., Tong, B., Song, Y., Li, G., et al. (2023). Stiff substrate induces nucleus pulposus cell ferroptosis via YAP and N-cadherin mediated mechanotransduction. *Adv. Healthc. Mater* 12 (23), e2300458. doi:10.1002/adhm.202300458

Li, S., Liao, Z., Yin, H., Liu, O., Hua, W., Wu, X., et al. (2023). G3BP1 coordinates lysophagy activity to protect against compression-induced cell ferroptosis during intervertebral disc degeneration. *Cell Prolif.* 56 (3), e13368. doi:10.1111/cpr.13368

Li, Z., Jiang, L., Chew, S. H., Hirayama, T., Sekido, Y., and Toyokuni, S. (2019). Carbonic anhydrase 9 confers resistance to ferroptosis/apoptosis in malignant mesothelioma under hypoxia. *Redox Biol.* 26, 101297. doi:10.1016/j.redox.2019.101297

Li, Z., Jiang, L., and Toyokuni, S. (2020). Role of carbonic anhydrases in ferroptosis-resistance. *Arch. Biochem. Biophys.* 689, 108440. doi:10.1016/j.abb.2020.108440

Li, Z., Ye, D., Dai, L., Xu, Y., Wu, H., Luo, W., et al. (2022). Corrigendum: single-cell RNA sequencing reveals the difference in human normal and degenerative nucleus pulposus tissue profiles and cellular interactions. *Front. Cell Dev. Biol.* 10, 1051707. doi:10.3389/fcell.2022.1051707

Liberzon, A., Subramanian, A., Pinchback, R., Thorvaldsdóttir, H., Tamayo, P., and Mesirov, J. P. (2011). Molecular signatures database (MSigDB) 3.0. *Bioinformatics* 27(12): 1739–1740. doi:10.1093/bioinformatics/btr260

Lotz, J. C., and Ulrich, J. A. (2006). Innervation, inflammation, and hypermobility may characterize pathologic disc degeneration: review of animal model data. *J. Bone Jt. Surg. Am.* 88 (Suppl. 2), 76–82. doi:10.2106/JBJS.E.01448

Ma, X., Su, J., Wang, B., and Jin, X. (2022). Identification of characteristic genes in whole blood of intervertebral disc degeneration Pa-tients by weighted gene coexpression network analysis (WGCNA). *Comput. Math. Methods Med.* 2022, 6609901. doi:10.1155/2022/6609901

Manchikanti, L., Singh, V., Datta, S., Cohen, S. P., Hirsch, J. A., and American Society of Interventional Pain Physicians (2009). Comprehensive review of epidemiology, scope and impact of spinal pain. *Pain Physician* 12, E35–E70.

Masaldan, S., Bush, A. I., Devos, D., Rolland, A. S., and Moreau, C. (2019). Striking while the iron is hot: iron metabolism and ferroptosis in neurodegeneration. *Free Radic. Biol. Med.* 133, 221–233. doi:10.1016/j.freeradbiomed.2018.09.033

Mehus, A. A., Muhonen, W. W., Garrett, S. H., Somji, S., Sens, D. A., and Shabb, J. B. (2014). Quantitation of human metallothionein isoforms: a family of small, highly conserved, cysteine-rich proteins. *Mol. Cell Proteomics* 13 (4), 1020–1033. doi:10.1074/mcp.M113.033373

Newman, A. M., Liu, C. L., Green, M. R., Gentles, A. J., Feng, W., Xu, Y., et al. (2015). Robust enumeration of cell subsets from tissue expression profiles. *Nat. Methods* 12 (5), 453–457. doi:10.1038/nmeth.3337

Pfirrmann, C. W., Metzdorf, A., Zanetti, M., Hodler, J., and Boos, N. (2001). Magnetic resonance classification of lumbar intervertebral disc degeneration. *Spine (Phila Pa 1976)* 26 (17), 1873–1878. doi:10.1097/00007632-200109010-00011

Ritchie, M. E., Phipson, B., Wu, D., Hu, Y., Law, C. W., Shi, W., et al. (2015). Limma powers differential expression analyses for RNA-sequencing and microarray studies. *Nucleic Acids Res.* 43(7), e47, doi:10.1093/nar/gkv007

Sakai, D., and Grad, S. (2015). Advancing the cellular and molecular therapy for intervertebral disc disease. *Adv. Drug Deliv. Rev.* 84, 159–171. doi:10.1016/j.addr.2014.06.009

Silagi, E. S., Schoepflin, Z. R., Seifert, E. L., Merceron, C., Schipani, E., Shapiro, I. M., et al. (2018). Bicarbonate recycling by HIF-1-Dependent carbonic anhydrase isoforms 9 and 12 is critical in maintaining intracellular pH and viability of nucleus pulposus cells. *J. Bone Min. Res.* 33 (2), 338–355. doi:10.1002/jbmr.3293

Steenwyk, J. L., and Rokas, A. (2021). Ggpubfigs: colorblind-friendly color palettes and ggplot2 graphic system extensions for publication-quality scientific figures. *Microbiol. Resour. Announc.* 10(44): e0087121-21. doi:10.1128/MRA.00871-21

Subramanian, A., Tamayo, P., Mootha, V. K., Mukherjee, S., Ebert, B. L., Gillette, M. A., et al. (2005). Gene set enrichment analysis: a knowledge-based approach for interpreting genome-wide expression profiles. *Proc. Natl. Acad. Sci.* 102(43): 15545–15550. doi:10.1073/pnas.0506580102

Sun, X., Niu, X., Chen, R., He, W., Chen, D., Kang, R., et al. (2016). Metallothionein-1G facilitates sorafenib resistance through inhibition of ferroptosis. *Hepatology* 64 (2), 488–500. doi:10.1002/hep.28574

Takatalo, J., Karppinen, J., Niinimäki, J., Taimela, S., Mutanen, P., Sequeiros, R. B., et al. (2012). Association of modic changes, Schmorl's nodes, spondylolytic defects, high-intensity zone lesions, disc herniations, and radial tears with low back symptom severity among young Finnish adults. *Spine (Phila Pa 1976)* 37 (14), 1231–1239. doi:10.1097/BRS.0b013e3182443855

Tam, V., Chan, W. C. W., Leung, V. Y. L., Cheah, K. S. E., Cheung, K. M. C., Sakai, D., et al. (2018). Histological and reference system for the analysis of mouse intervertebral disc. *J. Orthop. Res.* 36 (1), 233–243. doi:10.1002/jor.23637

The Gene Ontology (GO) database and informatics resource[J]. *Nucleic Acids Res.*, 2004, 32(90001): 258D - 261.

Urban, J. P. (2002). The role of the physicochemical environment in determining disc cell behaviour. *Biochem. Soc. Trans.* 30 (Pt 6), 858–864. doi:10.1042/bst0300858

Wang, J., Zhou, J. Y., Kho, D., Reiners, J. J. Jr, and Wu, G. S. (2016). Role for *DUSP1* (dual-specificity protein phosphatase 1) in the regulation of autophagy. *Autophagy* 12 (10), 1791–1803. doi:10.1080/15548627.2016.1203483

Wang, L., He, T., Liu, J., Tai, J., Wang, B., Zhang, L., et al. (2021). Revealing the immune infiltration landscape and identifying diagnostic biomarkers for lumbar disc herniation. *Front. Immunol.* 12, 666355. doi:10.3389/fimmu.2021.666355

Wang, W., Jing, X., Du, T., Ren, J., Liu, X., Chen, F., et al. (2022). Iron overload promotes intervertebral disc degeneration via inducing oxidative stress and ferroptosis in endplate chondrocytes. *Free Radic. Biol. Med.* 190, 234–246. doi:10.1016/j.freeradbiomed.2022.08.018

Wei, T., Zhang, M., Zheng, X., Xie, T., Wang, W., Zou, J., et al. (2022). Interferon-γ induces retinal pigment epithelial cell Ferroptosis by a JAK1-2/STAT1/SLC7A11 signaling pathway in Age-related Macular Degeneration. *FEBS J.* 289, 1968–1983. doi:10.1111/febs.16272

Weiler, C., Lopez-Ramos, M., Mayer, H. M., Korge, A., Siepe, C. J., Wuertz, K., et al. (2011). Histological analysis of surgical lumbar intervertebral disc tissue provides evidence for an association between disc degeneration and increased body mass index. *BMC Res. Notes* 4, 497. doi:10.1186/1756-0500-4-497

Wohlhieter, C. A., Richards, A. L., Uddin, F., Hulton, C. H., Quintanal-Villalonga, À., Martin, A., et al. (2020). Concurrent mutations in STK11 and KEAP1 promote ferroptosis protection and SCD1 dependence in lung cancer. *Cell Rep.* 33 (9), 108444. doi:10.1016/j.celrep.2020.108444

Xin, J., Wang, Y., Zheng, Z., Wang, S., Na, S., and Zhang, S. (2022). Treatment of intervertebral disc degeneration. *Orthop. Surg.* 14, 1271–1280. doi:10.1111/os.13254

Yang, R., Xu, W., Zheng, H., Zheng, X., Li, B., Jiang, L., et al. (2021). Involvement of oxidative stress-induced annulus fibrosus cell and nucleus pulposus cell ferroptosis in intervertebral disc degeneration pathogenesis. *J. Cell. Physiology* 236, 2725–2739. doi:10.1002/jcp.30039

Ye, F., Lyu, F. J., Wang, H., and Zheng, Z. (2022). The involvement of immune system in intervertebral disc herniation and degeneration. *JOR Spine* 5 (1), e1196. doi:10.1002/jsp2.1196

Yu, G., Wang, L. G., Han, Y., and He, Q. Y. (2012). clusterProfiler: an R Package for comparing biological themes among gene clusters. *OMICS A J. Integr. Biol.* 16 (5): 284–287. doi:10.1089/omi.2011.0118

Yu, X., Xu, H., Liu, Q., Wang, Y., Wang, S., Lu, R., et al. (2022). circ_0072464 shuttled by bone mesenchymal stem cell-secreted extracel-lular vesicles inhibits nucleus pulposus cell ferroptosis to relieve intervertebral disc degeneration. *Oxidative Med. Cell. Longev.* 2022, 1–21. doi:10.1155/2022/2948090

Zhang, C., Lu, X., Liu, X., Xu, J., Li, J., Qu, T., et al. (2023b). Carbonic anhydrase IX controls vulnerability to ferroptosis in gefitinib-resistant lung cancer. *Oxid. Med. Cell Longev.* 2023, 1367938. doi:10.1155/2023/1367938

Zhang, F., Cui, D., Wang, K., Cheng, H., Zhai, Y., Jiao, W., et al. (2023a). Identifification and validation of ferroptosis signatures and immune infifiltration characteristics associated with intervertebral disc degeneration. *Front. Genet.* 14, 1133615. doi:10.3389/fgene.2023.1133615

Zhang, Y., Han, S., Kong, M., Tu, Q., Zhang, L., and Ma, X. (2021). Single-cell RNA-seq analysis identifies unique chondrocyte subsets and reveals involvement of ferroptosis in human intervertebral disc degeneration. *Osteoarthr. Cartil.* 29 (9), 1324–1334. doi:10.1016/j.joca.2021.06.010

Zhong, P., and Huang, H. (2017). Recent progress in the research of cold-inducible RNA-binding protein [published correction appears in Future Sci OA. 2018 Apr 11; 4(5):FSO246]. *Future Sci. OA* 3 (4), FSO246. doi:10.4155/fsoa-2017-0077

frontiers | Frontiers in Immunology

TYPE Original Research
PUBLISHED 11 December 2024
DOI 10.3389/fimmu.2024.1478395

OPEN ACCESS

EDITED BY
Bilal Çiğ,
Ahi Evran University, Türkiye

REVIEWED BY
Barbara Maria Jarzab,
Maria Skłodowska-Curie National Research Institute of Oncology, Poland
Ekin Çelik,
Ahi Evran University, Türkiye

*CORRESPONDENCE
Ying-ying Mu
zunyi_muyingying@163.com
Wei Zhang
lawrence2013@163.com

†These authors have contributed equally to this work

RECEIVED 09 August 2024
ACCEPTED 25 November 2024
PUBLISHED 11 December 2024

CITATION
Ma Y-y, Zhou W-y, Qian Y, Mu Y-y and Zhang W (2024) SOX13 as a potential prognostic biomarker linked to immune infiltration and ferroptosis inhibits the proliferation, migration, and metastasis of thyroid cancer cells.
Front. Immunol. 15:1478395.
doi: 10.3389/fimmu.2024.1478395

SOX13 as a potential prognostic biomarker linked to immune infiltration and ferroptosis inhibits the proliferation, migration, and metastasis of thyroid cancer cells

Yan-yan Ma[1†], Wei-ye Zhou[2†], Yue Qian[3], Ying-ying Mu[4*] and Wei Zhang[2,3*]

[1]Department of Rehabilitation Medicine, Beijing Jishuitan Hospital Guizhou Hospital, Guiyang, Guizhou, China, [2]Cell Biology Department, Wuxi School of Medicine, Jiangnan University, Wuxi, Jiangsu, China, [3]Department of Pathogen Biology, Guizhou Nursing Vocational College, Guiyang, Guizhou, China, [4]Department of Pathology, Zunyi Hospital of Traditional Chinese Medicine, Zunyi, Guizhou, China

Background: SOX13 is a transcription factor belonging to the SOX family. SOX proteins are critical regulators of multiple cancer progression, and some are known to control carcinogenesis. Nevertheless, the functional and clinical significance of SOX13 in human thyroid cancer (THCA) remain largely unelucidated.

Methods: Data on SOX13 expression were obtained through The Cancer Genome Atlas together with Gene Expression Omnibus. Co-expression, differential expression, and functional analyses of genes were investigated by databases. Associations between SOX13 levels, immune infiltration, ferroptosis, and immune checkpoint gene levels were analyzed. Genetic changes in SOX13 were investigated using CBioPortal. Associations between SOX13 levels and THCA clinicopathological features were analyzed and nomogram modeling for diagnostic and prognostic prediction. The influence of SOX13 on proliferation, migration, and metastasis was determined in KTC-1 and TPC-1 cell lines.

Results: SOX13 was significantly lower in THCA tumors compared to controls. In addition, upregulated SOX13 gene mutation were evident in thyroid cancer. SOX13-associated genes exhibited differential expression in pathways associated with thyroid cancer development. Significant associations were found between SOX13 levels, immune infiltration, ferroptosis, and immune checkpoint genes in THCA tissue. SOX13 levels correlated with THCA stage, histologic grade, and primary neoplasm focus types, and independently predicted overall and progression-free intervals. SOX13 expression effectively distinguished between tumor and normal thyroid tissue. Spearman correlations highlighted a significant relationship between SOX13 and ferroptosis-associated genes. Overexpression of SOX13 enhances the inhibition of RSL3 (iron death activator) on the cell viability of TPC-1. Higher SOX13 levels in Thyroid cancer cells may lead to reduced proliferation, migration, and metastasis by regulating ferroptosis.

Conclusion: Reduced SOX13 expression inversely impacts patient prognosis. In addition, SOX13 strongly regulates cancer immunity and Ferroptosis. Hence, SOX13 has great promise as a bioindicator for both thyroid cancer prognosis and immune cell invasion.

KEYWORDS

SOX13, biomarker, THCA, genetic alterations, tumor-immune infiltration, ferroptosis

1 Introduction

Thyroid cancer is the leading endocrine cancer, and its incidence is increasing (1, 2). The disease arises from thyroid follicular epithelial cells, which constitute over 95% of thyroid malignancies. Types include papillary thyroid carcinoma (PTC), anaplastic thyroid carcinoma (ATC)/undifferentiated thyroid carcinoma (UTC), and follicular thyroid carcinoma (FTC) (3). Medullary thyroid carcinoma (MTC) derives from thyroid parafollicular cells and demonstrates a highly malignant transformation. According to 2021 data, the United States estimated 44,280 cases of thyroid cancer, comprising 12,150 males and 32,130 females (4–6). Despite 90% of patients achieving cure through standard treatment, approximately 10% experience local recurrence or distant metastasis, significantly impacting prognosis. Therefore, a comprehensive elucidation of thyroid cancer etiology and novel molecular biomarker or prognostic model identification are crucial for early detection and treatment strategies.

SOX13 is a member of the SOX family, spanning approximately 12 kb with 13 exons (7). It is expressed in humans and other animals such as mice, with the human SOX13 gene located on chromosome 1q32 (8). Research indicates that SOX13 plays crucial roles in preventing inflammation, promoting cartilage formation, neurogenesis (9, 10), limb development, and T-cell differentiation. Emerging evidences revealed that SOX13 is intricately linked to multiple cancers, namely, hepatocellular carcinoma, colorectal cancer, gastric cancer, and gliomas (11). Recent reports indicate that SOX9 plays a role in the invasiveness of thyroid cancer through the Wnt/β-catenin pathway (12). Both SOX9 and SOX13 belong to the same subfamily within the SOX gene family. However, whether SOX13 is involved in the regulation of thyroid cancer remains unexplored.

Herein, we assessed SOX13 levels and their correlation with patient prognosis in a THCA cohort. Additionally, we examined links between SOX13 content and immune cell invasion, ferroptosis, and immune status-indicating gene sets using several databases. Simultaneously, we assessed the impact of SOX13 overexpression on THCA cell proliferation, apoptosis, migration, and oncogenic signaling networks. The findings underscored the critical significance of the SOX13 gene in THCA prognosis and demonstrated its correlation with clinical outcomes in the THCA cohort, including tumor-invading immune cells.

2 Methodology

2.1 Datasets

Datasets, both clinical together with RNA-seq, from 512 THCA (TCGA-THCA) cases, together with information on 59 matched pairs of tumor/adjacent non-cancerous tissue were obtained through TCGA database. Datasets were collected within FPKM format and were subsequently converted to TPM using the following formula: $TPM = \frac{FPKM}{sum\ \ of\ \ FPKM\ \ values\ \ for\ \ all\ \ genes} \times 10^6$. RNA-seq datasets within TPM format were also obtained via UCSC Xena from the GTEx database and analyzed using the DESeq2 package, which provides tools for quality control and normalization (13). The analyses followed the guidelines of the Declaration of Helsinki, 2013 revision. Information on SOX13 mRNA was also obtained from the GEO GSE33630 and GSE65144 datasets. The HPA databaseincludes immunohistochemistry (IHC) data from 44 different types of normal tissues and 17 major types of cancers (14).

2.2 TIMER2.0 analysis

The TIMER2.0 database allows the investigation of differential gene expression between tumor and control samples using TCGA data (15, 16). Thus, TIMER2.0 was used to determine SOX13 levels in various cancers.

2.3 Survival analysis

We analyzed survival data from 512 THCA patients obtained from The Cancer Genome Atlas (TCGA) database. Kaplan-Meier plots, together with log-rank assessments, probed survival, utilizing median level of SOX13 expression as a cutoff value. The links across clinical features and survival were assessed through univariate/multivariate

Cox regression (17, 18) with major parameters (P< 0.05) from the univariate analysis employed within multivariate analysis. Forest maps were constructed using the R package "ggplot2".

2.4 Mutation analysis of SOX13 in THCA

The frequencies of SOX13 mutations in THCA were assessed using cBioPortal and the specific types of mutation were also analyzed using the Catalogue of Somatic Mutations in Cancer (COSMIC) repository.

2.5 Functional enrichment analyses

Significant SOX13-related genes were identified by GO, KEGG and GSEA. GSEA utilized the gene set 'h.all.v2022.1.Hs.symbols.gmt [Hallmarks]' (19). Significance cut-off was adjusted to false discovery rate (FDR) < 0.25 and p.adjust < 0.05.

2.6 Immune invasion

Single-sample GSEA (ssGSEA) analyses were performed through R package GSVA package to examine THCA tumor infiltration of immune cells in relation to gene expression. Twenty-four immune cell types were investigated in terms of the gene expression profiles (20). Links across SOX13 levels and subsets of infiltrating cells were examined with Spearman and Wilcoxon rank-sum tests, and Pearson correlation coefficients evaluated associations between SOX13 and immune checkpoint genomic expression distribution. Associations between SOX13 levels and immune cells were examined by analysis of chemokines and their receptors using the"chemokine" module in TISIDB.

2.7 Relationships between SOX13 levels and ferroptosis-associated genes

The potential relationships between SOX13 and ferroptosis-associated gene levels were evaluated in TCGA-THCA datasets using DESeq2 package (version 1.30.1), which was also used to assess the proportions of ferroptosis-associated genes in high- or low-SOX13 samples. The "ggboxplot" package in R was used for visualization of the results.

2.8 Cell culture and cell experiment

KTC-1 and TPC-1 cell lines were employed to assess the SOX13-mediated regulation of THCA cells. The cells were acquired from Procell Life Science & Technology Co., Ltd (CL-0103, Wuhan, China) and were maintained in DMEM with 10% fetal bovine serum, 100 U/mL penicillin, and 100 U/mL streptomycin, at 37°C with 5% CO_2 and saturated humidity in a constant temperature incubator.

2.9 Plasmid transfection

The SOX13-overexpression plasmid (OE-SOX13) and the negative control NC recombinant plasmid (NC-SOX13) (Supplementary Table S1) were constructed using Gima Gene (Shanghai, China). Plasmids and vectors were transfected into THCA cells with lipofectamine 6000 (Beyotime Biotechnology, Shanghai, China) or DNA transfection reagent (TF201201 (TF20121201), Neofect (beijing) biotech Co,.Ltd, Beijing, China) as per kit directions.

2.10 Western blot

Following KTC-1 and TPC-1 cell lysis in RIPA buffer (P0013B, Beyotime Biotechnology) containing phenylmethanesulfonyl fluoride (PMSF, ST506) and phosphatase inhibitor (PPI, P1081), proteins were electrophoresed on SDS-PAGE prior to transfer to PVDF membranes (0.45 μm; Merck Millipore, Burlington, MA, USA). Membranes underwent a 1-hour blocking in 5% BSA. Subsequently, they were treated with primary antibodies rabbit anti-SOX13 (K007627P, Solarbo, Beijing, China; 1:1000), rabbit Anti-NFE2L2 (NRF2) Polyclonal Antibody (K106685P, Solarbo, Beijing, China; 1:1000), rabbit anti-TFRC (AF8136, Beyotime Biotechnology, Beijing, China; 1:1000), rabbit anti-SLC7A11 (AF7992, Beyotime Biotechnology, Beijing, China; 1:1000), rabbit anti-GPX4 (K003083P, Solarbo, Beijing, China; 1:1000), and rabbit anti-GAPDH (GB15002, Servicebio Biotech, Wuhan, China; 1:2000), followed by secondary antibodies. Protein quantification was done with Tanon-2500B gel imaging analysis system (Tanon, Shanghai, China), and signal intensity was measured with ImageJ (V1.6, NIH, Bethesda, MD, USA) using densitometry.

2.11 Wound healing assays

KTC-1 and TPC-1 cells underwent a 48-h transfection with SOX13-overexpression plasmid. Once confluent in 6-well plates, cells were PBS-rinsed to eliminate excess. Using a 200 μl pipette tip, scratches were generated on the monolayer and the cells were kept in serum-free medium with imaging at 0, 24, and 48 h and analysis with ImageJ 2.3.0.

2.12 Cell viability assays

KTC-1 and TPC-1 cells underwent transfection with SOX13-overexpression plasmid prior to a 48-h culture or RSL3(IR1120, Beyotime Biotechnology, Beijing, China) to a 24-h culture in 96-well plates ($5x10^3$/well). Subsequently, 10 μL CCK-8 reagent (MCE,

USA) was introduced to 100 μL medium in each well, and absorbances at 450 nm were read in a Bio-Tek microplate reader (Winooski, VT, USA) following 1 h of CCK-8 treatment.

2.13 Transwell invasion assay

The Transwell upper chamber contained 3 × 10^4 cells (100 μL) in serum-free DMEM, while the lower chamber included medium with 10% FBS (600 μL). The setup was incubated at 37°C for 30 h, prior to staining of invaded cells with crystal violet staining solution (C0121, Beyotime Biotechnology) and observed under a light microscope.

2.14 Ethics statement

Ethical approval was waived by the respective committee of Guizhou Nursing Vocational College as the tissue microarrays were commercially procured.

2.15 Statistical analyses

Bioinformatics data were assessed through R version 4.0.3. Datasets reflected means ± SEM, while differences were evaluated with t-tests or one-way analysis of variance (ANOVA) for separate specimens. P< 0.05 was deemed to confer statistical significance. Relationships between SOX13 levels and patient clinicopathological features were analyzed by $\chi 2$ assessments, logistic regression, Fisher's exact, and Wilcoxon rank-sum assessments.

3 Results

3.1 SOX13 levels in THCA

We analyzed SOX13 expression across 38 cancer types using the TIMER2.0 database. SOX13 showed significant discreet expressions between tumor and normal groups across 20 types of malignancies, including THCA (P<0.001; Figure 1A). The relationships between SOX13 levels and clinical features were evaluated using TCGA data. This indicated that, in agreement with the above findings, SOX13 levels were markedly reduced in the 512 THCA tissues in comparison with the 59 controls (P< 0.01; Figure 1B). A further comparison of 59 paired THCA and normal tissues confirmed these findings, showing reduction of SOX13 in tumor tissues (P< 0.01; Figure 1C). SOX13 mRNA levels were then investigated in both TCGA and GTEx, showing marked reduction in 512 tumors compared with 338 control specimens (P< 0.001; Figure 1D).

Microarray dataset profiles GSE33630 and GSE65144 were downloaded from GEO DataSets. After normalization, probes were converted to gene symbols for series matrix files of each dataset and the gene expression data of these two datasets were merged (Figure 2A). The expressions of SOX13 in both datasets was tested and it was found that the expression level of SOX13 is

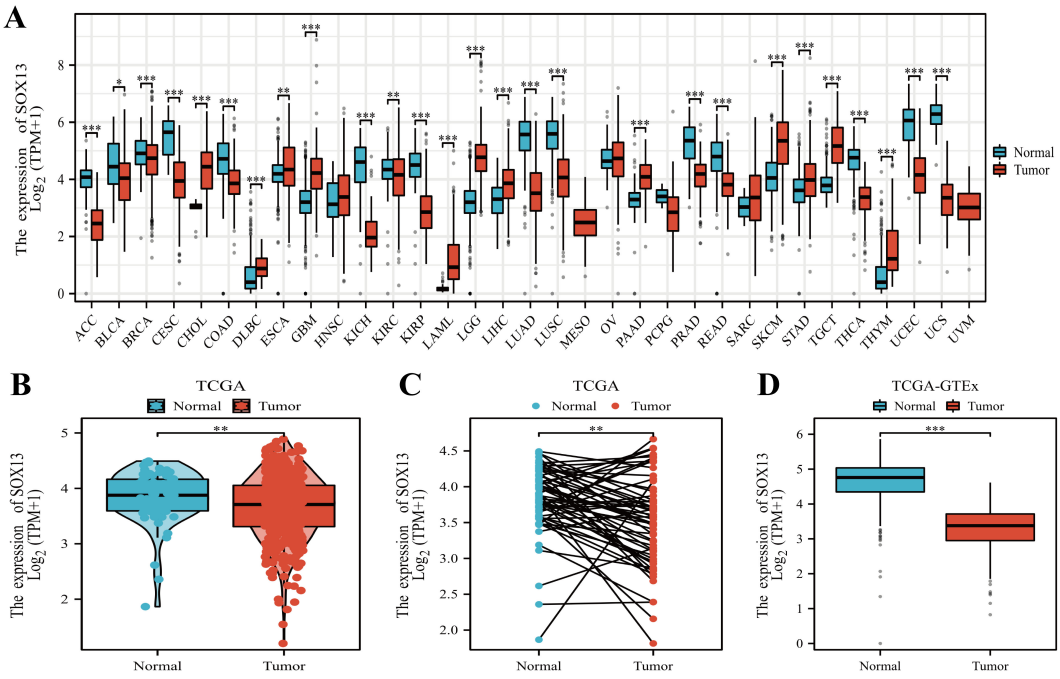

FIGURE 1
SOX13 expression profile across differing cancer models. **(A)** SOX13 levels within various tumors, determined through TIMER2.0®. **(B)** SOX13 levels across tumor/healthy specimens, from TCGA. **(C)** SOX13 levels in matched tumor and normal samples (TCGA). **(D)** Comparative analysis for SOX13 expression across GTEx and TCGA databases, evidenced by Wilcoxon rank-sum tests. *P< 0.05, **P< 0.01, ***P< 0.001.

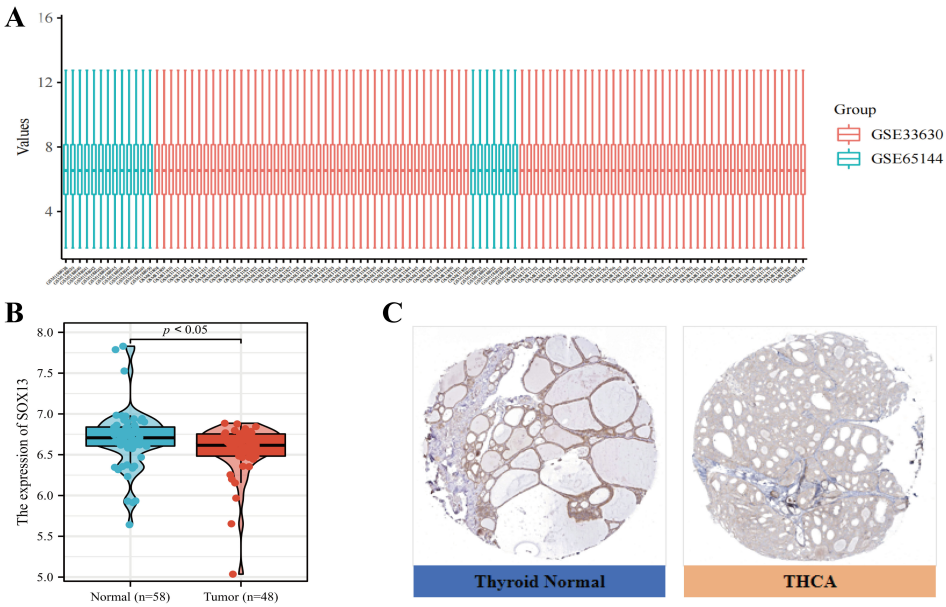

FIGURE 2
Levels of SOX13 in the GSE33630 and GSE65144 microarray datasets **(A)** Gene profile matrices were combined without inter-batch variations. **(B)** SOX13 profile scores in microarray datasets GSE33630 and GSE65144. **(C)** Immunohistochemical staining of SOX13 protein in THCA and normal thyroid tissues was performed with the HPA database.

significantly down-regulated in the 48 THCA tissues in comparison with the 58 controls (P < 0.05; Figure 2B). Furthermore, IHC staining data from HPA database indicated that medium levels of SOX13 expression were present in normal thyroid tissues, while low levels of expression were observed in THCA tissues (Figure 2C). Taken together, these results indicated that SOX13 was more highly expressed at the transcriptional and proteomic levels in normal thyroid tissues than in THCA tissues.

3.2 Analysis of prognostic factors and survival analysis of SOX13 in THCA

Clinical information and SOX13 levels in 512 THCA patients from TCGA. Associations between these parameters were examined by univariate analysis, finding a significant association between reduced SOX13 levels and T and pathological stage, and histological and primary neoplasm focus types (all P< 0.05; Figures 3A–D, Table 1). The dataset outcomes suggested THCA cases with down-regulated SOX13 had raised odds for experiencing advanced disease in comparison with those with heighter SOX13 levels.

Kaplan–Meier survival plots demonstrated that cases having reduced SOX13 had significantly reduced OS (HR=0.25, P< 0.029) (Figure 3E), together with progression-free intervals (PFI) (HR=0.49, P< 0.013) in comparison to cases having upregulated SOX13 (Figure 3F). The ROC curve analysis showed that SOX13 had a satisfactory diagnostic value and the AUC of SOX13 were 0.926 in THCA (Figure 3G). A nomogram was plotted to determine the eligibility of SOX13 in predicting survival duration of THCA patients (Figure 3H).

3.3 Mutations of SOX13 in THCA

Mutation frequencies in SOX13 were assessed using the cBioPortal online resource. All five datasets, namely, AMC, MSK, RIKEN, INSERM, and TCGA Pan-Cancer Atlas, were analyzed, comprising 1000 samples (21). The overall frequency of somatic mutations in SOX13 associated with THCA was found to be 0.2%, representing a low figure of just five mutations per 633 samples, most of which were missense mutations (Figure 4A). This indicated an absence of an association between SOX13 mutations and THCA patient prognosis (Figures 4B, C). The types of SOX13 mutations were also assessed using the COSMIC database. Figure 4 shows two pie charts illustrating the different types of mutation. Approximately 46.47% of samples contained missense mutations, with synonymous mutations seen in 16.79% (Figure 4D). Most substitutions involved C > T (36.50%), with G > A accounting for 26.62% and C > A, 10.65% (Figure 4E).

3.4 Functional annotation and pathway enrichment of SOX13-associated genes within THCA

In all, we identified 1,659 DEGs using a threshold of |log2 fold-change (FC)| > 1.0 and adjusted p-value< 0.05, comprising 1,330 highly-expressed and 329 scarcely-expressed genes (Figure 5A). Subsequently, GO and KEGG analyses (Figures 5B, D) of DEGs were conducted, revealing primary biological processes (BP) including immunoglobulin synthesis, immune response mediator formation, and humoral immune response. The cellular component (CC) exhibited marked enrichment in

10.3389/fimmu.2024.1478395

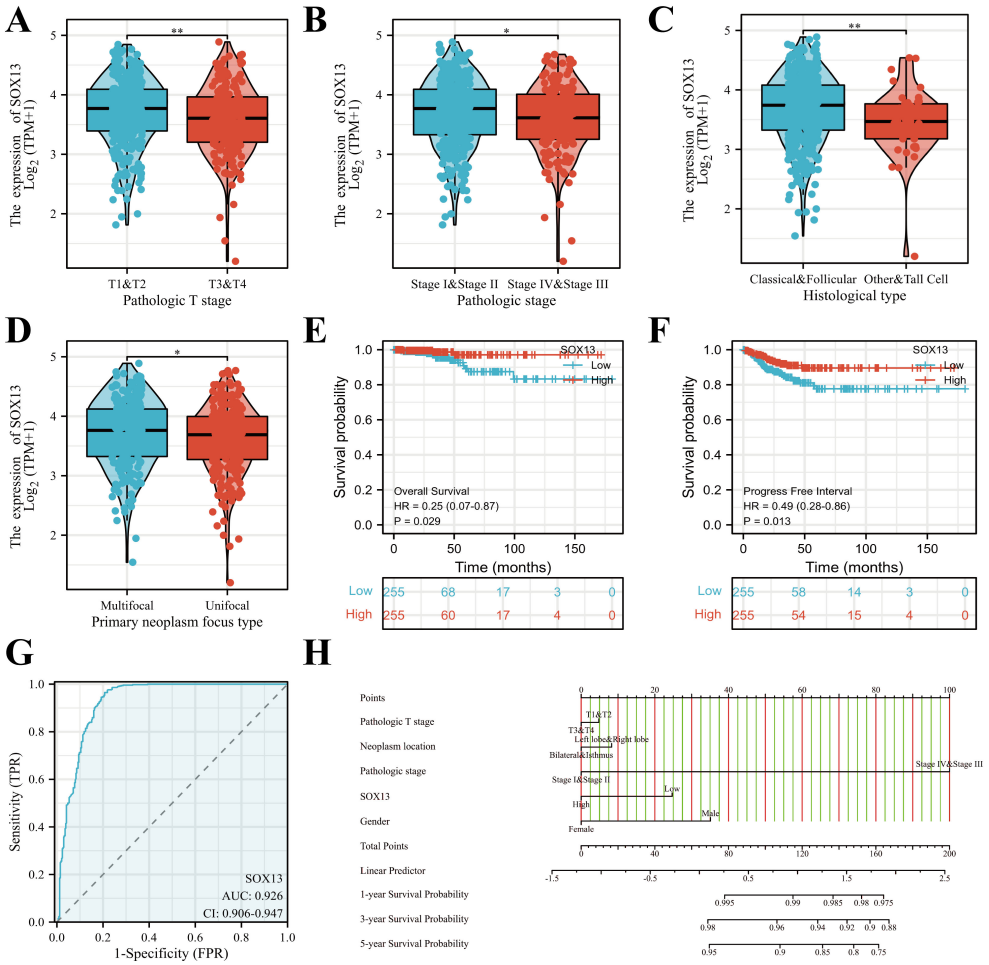

FIGURE 3
SOX13 mRNA levels in relation to clinical features and prognostic survival curve of THCA. **(A)** Relationship between SOX13 mRNA levels and T stage. **(B)** Links across SOX13 mRNA expression and pathologic stage. **(C)** Links across SOX13 mRNA levels and Histological type. **(D)** Links across SOX13 mRNA levels and Primary neoplasm focus type. **(E)** OS from the GEPIA database. **(F)** PFI from the GEPIA database. **(G)** The predictive performance of SOX13 (AUC). **(H)** Nomogram estimating the 1-, 3-, and 5-year OS of THCA patients. *P< 0.05, **P< 0.01.

the immunoglobulin complex, circulating immunoglobulin complex, and T cell receptor complex. The molecular function (MF) primarily involved antigen interaction, immunoglobulin receptor interaction, and cytokine activity. The enriched KEGG pathways were primarily related to cytokine-cytokine receptor association, Type I diabetes mellitus, and PD-L1 expression and PD-1 checkpoint. Finally, GSEA analysis was conducted on SOX13 differential genes and identified pathways, revealing enrichment in 8 pathways: reactive oxygen species, PI3K-

TABLE 1 Links across SOX13 levels and THCA clinicopathological characteristics, shown through logistic regression assessment.

Characteristics	Total (N)	OR (95% CI)	P value
Pathologic T stage (T3&T4 vs. T1&T2)	510	0.628 (0.439 - 0.900)	0.011
Pathologic N stage (N1 vs. N0)	462	0.671 (0.465 - 0.968)	0.033
Pathologic M stage (M1 vs. M0)	295	0.676 (0.178 - 2.570)	0.566
Pathologic stage (Stage III & Stage IV vs. Stage I & Stage II)	510	0.630 (0.435 - 0.914)	0.015
Neoplasm location (Left lobe & Right lobe vs. Bilateral & Isthmus)	506	0.650 (0.424 - 0.996)	0.048
Gender (Male vs. Female)	512	1.580 (1.066 - 2.342)	0.023
Histological type (Other & Tall Cell vs. Classical & Follicular)	512	0.374 (0.192 - 0.732)	0.004
Primary neoplasm focus type (Unifocal vs. Multifocal)	502	0.853 (0.600 - 1.212)	0.374
Thyroid gland disorder history (Normal & Other, specify vs. Lymphocytic Thyroiditis & Nodular Hyperplasia)	454	1.237 (0.832 - 1.841)	0.294

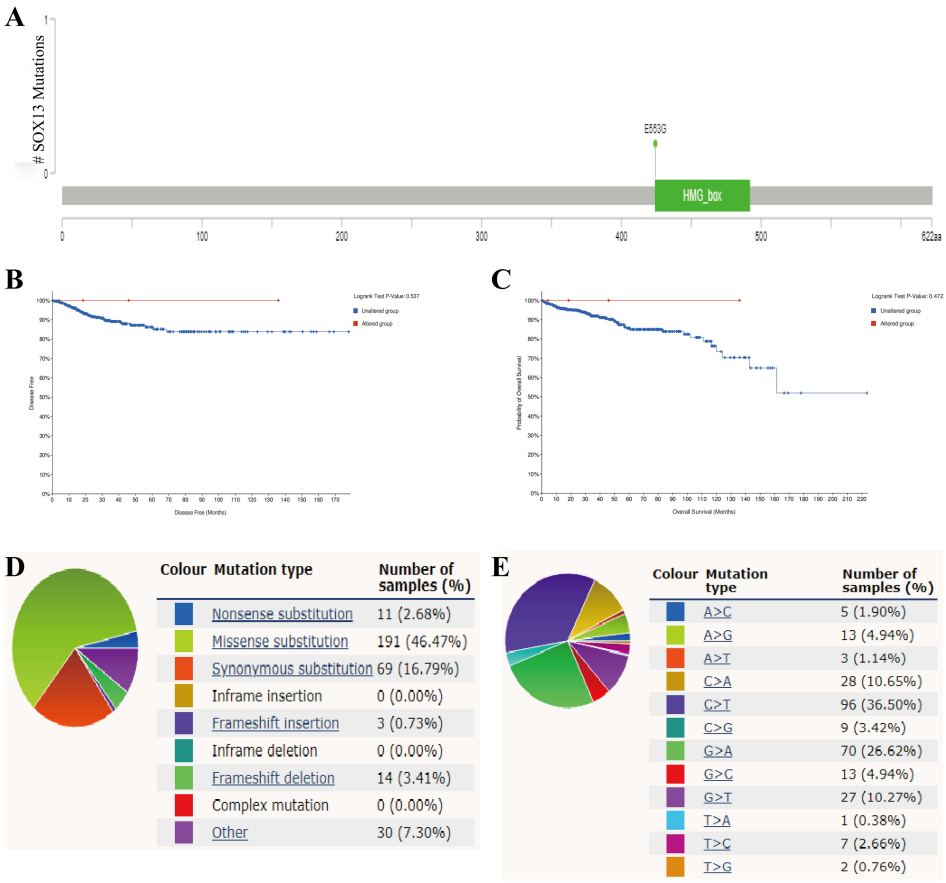

FIGURE 4
SOX13 mutations in THCA. **(A)** Schematic showing SOX13 mutations in THCA, determined by cBioPortal. **(B)** Potential association between SOX13 mutation status and disease-free survival of THCA, as evidenced by the cBioPortal tool. **(C)** Potential association between SOX13 mutation status and overall survival of THCA, as evidenced by the cBioPortal tool. **(D, E)** Types of SOX13 mutations, determined by the COSMIC.

AKT-mTOR, DNA repair, p53, oxidative phosphorylation, etc. (Figure 5C).

3.5 SOX13 is a major inverse modulator of ferroptosis in THCA

Prior investigations revealed that diminished oxidative phosphorylation and ROS contents suppress ferroptosis (22–24). Emerging reports reveal that ferroptosis suppression accelerates metastasis in clear cell renal cell carcinoma, breast cancer, and melanoma (25–27). Hence, we hypothesized that decreased SOX13 levels enables THCA metastasis via ferroptosis inhibition. To determine the association between SOX13 contents and ferroptosis, we conducted Pearson correlation analysis using GEPIA2 and TCGA-THCA datasets. This revealed a significant association between SOX13 levels and ferroptosis markers, such as SLC40A1, PTGS2, TFRC, GPX4, SLC7A11, and NFE2L2 (NRF2), with SOX13 showing the strongest link with NRF2 ($R = 0.651$, $P < 0.001$) (Figures 6A, B).

TCGA-THCA samples were stratified into reduced and elevated SOX13-expression groups, and differentially expressed ferroptosis-related genes were identified (Figure 6C). It was found that these genes, including SLC40A1, TF, TFRC, HSPB1, SLC7A11, and NFE2L2, were expressed strongly in the high-SOX13 group ($P<0.05$). Moreover, the cell viability of TPC-1 reduced markedly in correspondence with the RSL3 concentrations relative to the control (Supplementary Figure S1A). Overexpression of SOX13 enhances the inhibition of RSL3 (iron death activator) on the cell viability of TPC-1 (Supplementary Figure S1B). Thus, SOX13 may influence THCA progression and prognosis through its ability to regulate ferroptosis.

3.6 SOX13 levels and immune cell infiltration in THCA

Accumulating evidences indicate that cancer metabolism not only controls tumor development and progression but also reprograms immune cell metabolic networks, leading to dysregulated anti-tumor immune responses (28, 29). Currently, cancer metabolic regulation was shown to cooperatively augment immunotherapy in research (30). Therefore, herein, we investigated the association between SOX13 and tumor immunity, with the goal of determining its potential as an immunotherapy target. The tumor

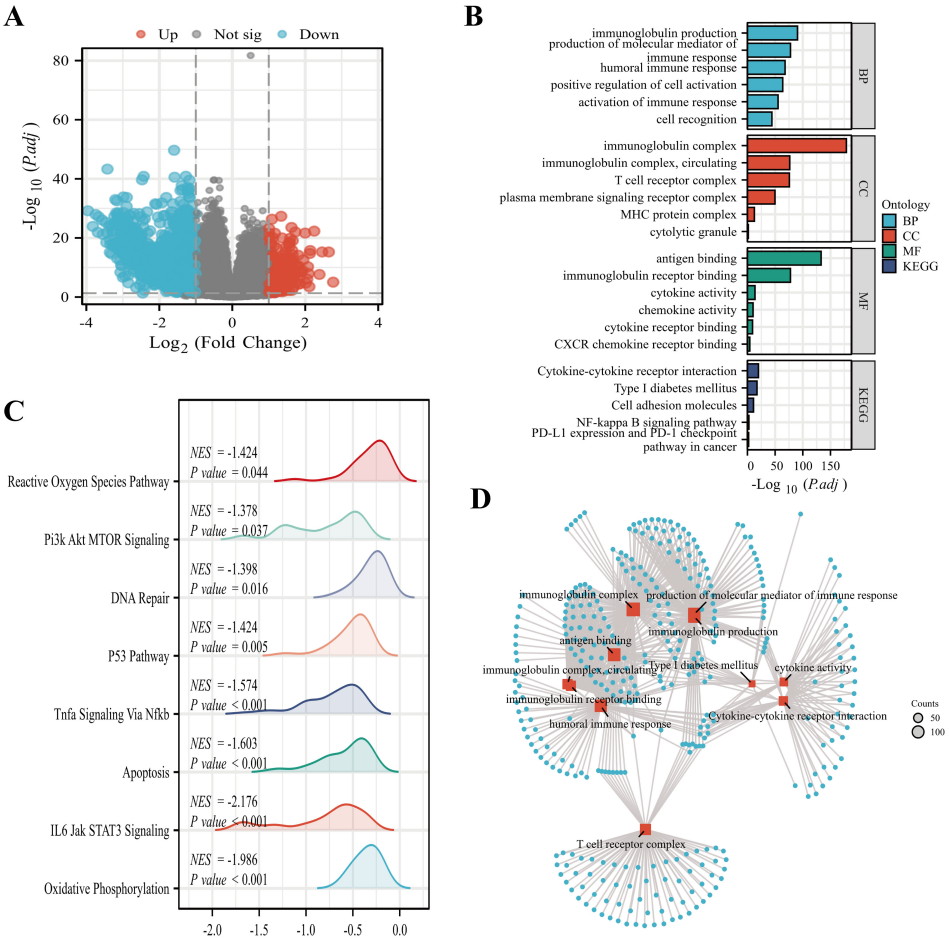

FIGURE 5
Functional enrichment analyses of SOX13-associated DEGs in THCA. **(A)** Volcano plot showing differential expression of SOX13^{high} and SOX13^{low} genes. **(B)** GO and KEGG analyses of SOX13-associated DEGs. **(C)** Analysis of the most significantly enriched networks between elevated SOX13 and reduced SOX13 samples using GSEA. **(D)** GO and KEGG analyses of SOX13-associated DEGs. *p<0.05; **p<0.01; ***p<0.001; ****p<0.0001. NS, not significant.

microenvironment (TME) is a critical modulator of tumor initiation and progression (31). In an immunosuppressive TME, dysfunctional infiltrating immune cells evade immune surveillance, leading to uncontrolled malignant cell proliferation (32–34). THCA tumor invasion by 24 immune cell types was assessed using ssGSEA, and their correlation with SOX13 levels was measured using Spearman's correlation coefficients. We revealed that SOX13 content is directly related to multiple cell types, especially NK cells (R=0.370, P< 0.001), Eosinophils (R=0.171, P<0.001), Tcm (R=0.160, P<0.001), and type 17 T helper cells (R=0.120, P<0.01), while aDC (R=-0.366, P<0.001), regulatory T cell (R=-0.353, P<0.001), cytotoxic cells (R= -0331, P< 0.001), B cells (R=-0.306, P<0.001), and T cells (R= -0.303, P<0.001) were the strongest negatively related to SOX13 (Figures 7A, B).

Immunotherapy involving inhibition of immune checkpoints has shown promising results in many cancers (35). Thus, we evaluated associations between the levels of SOX13 and those of 40 genes encoding immune checkpoints genes in patients with THCA observing correlations between 36 of the 40 genes, such as CD200, CTLA4, CD276, and TNFRSF15 (Figure 8A). CTLA4 is known to be a biomarker associated with inhibition of immune checkpoints that could be used as a therapeutic target (36). These associations indicate that SOX13 may modulate the immune response in THCA. For further investigation into SOX13 and immune cell migrative property, this investigation subsequently probed relationships across SOX13 levels together with those of various chemokines and their receptors (Figures 8B–D). These results indicated that there were positive associations between SOX13 and CXCL12 contents (r = 0.108, P=0.0151), CCL14 (r = 0.235, P =8.49e−08), and CCR10 (r = 0.123, P=0.00562) in THCA. These findings thus suggest that SOX13 levels are linked with increased invasion of certain immune cell types within TME.

3.7 Upregulation of SOX13 suppresses THCA cell proliferation, migration, and invasion

Western blotting confirmed a significant increase in SOX13 expression following transfection with the SOX13 overexpression

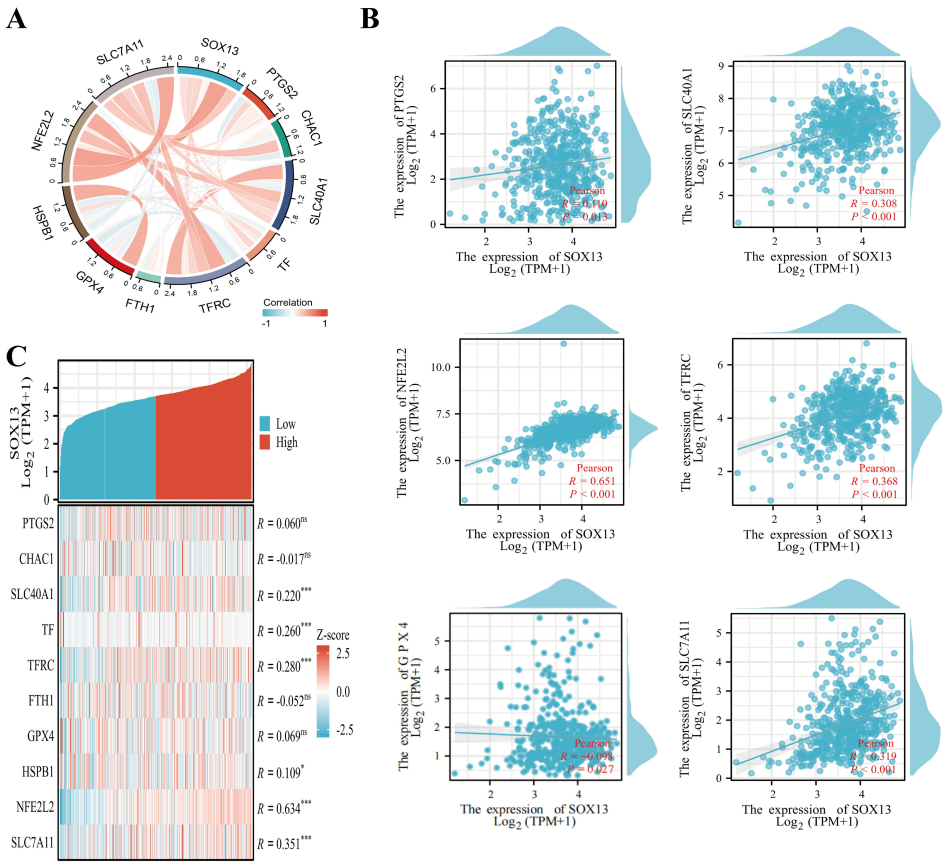

FIGURE 6
Relationships between the expression of SOX13 and that of ferroptosis-associated genes in THCA. **(A)** Correlations between SOX13 and ferroptosis markers using TCGA data. **(B)** Correlations between SOX13 and ferroptosis markers using GEPIA2 data. **(C)** Differentially expressed ferroptosis markers between the elevated- and reduced-SOX13 groups in THCA samples. *p<0.05; **p<0.01; ***p<0.001; ****p<0.0001. NS, not significant.

plasmid in both KTC-1 and TPC-1 cells (Figures 9A, B). To further evaluate SOX13-mediated ferroptosis, the effects of ferroptosis-related genes were investigated by SOX13 overexpression plasmid in TPC-1 cells. Western blotting analysis revealed a significant up-regulation of SOX13 together with down-regulation of NRF2, GPX4, and SLC7A11 (Supplementary Figure S2A–C). Subsequently, CCK-8 tests demonstrated a remarkable decline in cell proliferation upon SOX13 overexpression (Figures 9C, D). Moreover, wound healing assays revealed a substantial decrease in metastatic potential in cells with activated SOX13 expression compared to the control group over

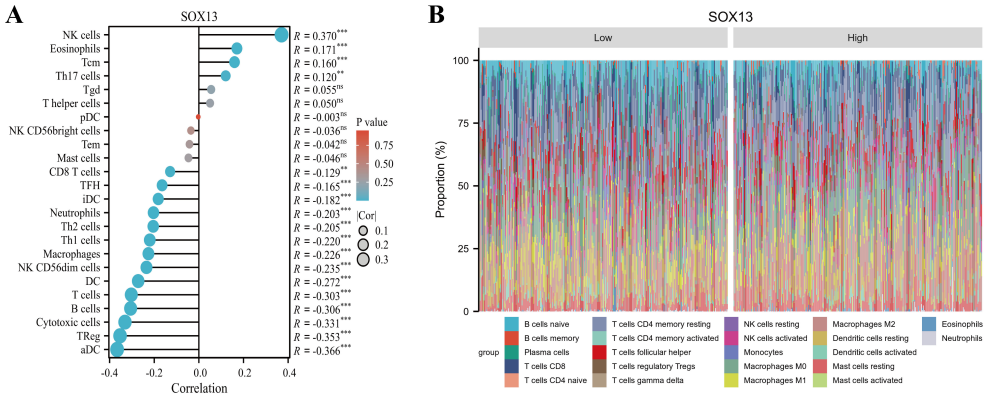

FIGURE 7
Relationships between SOX13 levels and immune cell invasion in THCA. **(A)** Correlations between 24 immune cell type invasions and SOX13 content using the ssGSEA algorithm. **(B)** Degree of 24 immune cell type invasions in elevated- and reduced-SOX13 cohorts assessed using the Cibersort algorithm.

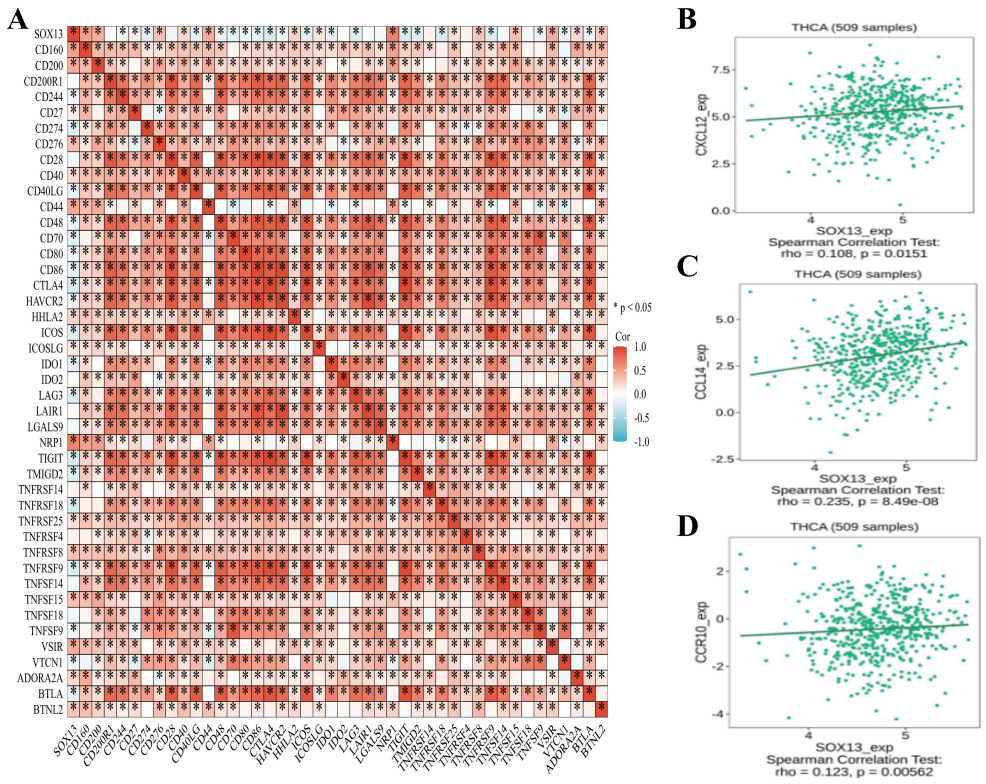

FIGURE 8
Associations between the SOX13, immune checkpoints, chemokines, and chemokine receptor contents. **(A)** Associations between levels of SOX13 and 40 immune checkpoints. **(B)** Direct relationships were seen between SOX13 and CXCL12 contents. **(C)** Direct relationships were seen between SOX13 levels and CCL14. **(D)** Positive correlations were seen between SOX13 and CCR10 contents.

the study duration (Figures 9E–H). Additionally, Transwell experiments were undertaken to assess the effects of SOX13 overexpression on cellular invasion capacity, demonstrating a significant reduction (Figures 9I, J).

4 Discussion

The SOX (SRY-related HMG-box) family was first discovered because of its highly conserved high-mobility motifs, and early studies focused on its role in embryonic development and tissue differentiation. However, the publication of numerous studies has led to an understanding of its role in tumorigenesis as well (37–39). SOX13 belongs to the D group within the SOX gene subfamily (40, 41). Within the SOXD subfamily, SOX13 was the most closely related to cancer development and progression. SOX13 critically regulates cell differentiation and stemness by modulating the Wnt/β-catenin axis (42). Emerging reports have indicated high SOX13 levels in liver cancer, with links to both metastasis and unfavorable prognosis (43). SOX13 is induced by hepatocyte growth factor through the JAK2/STAT3 signaling pathway, promoting metastasis in colorectal cancer by upregulating SNAI2 and c-MET expression (44). Additionally, research has shown high expression of SOX13 in various tumors including gastric (45), breast (46), and pancreatic cancers (47). Overall, these reports indicate that SOX13 has tumor-associated functions in multiple cancer types.

Nevertheless, there is limited information regarding SOX13 roles within THCA, whereby this investigation thus conducted a comprehensive bioinformatics-based investigation of its possible functional and diagnostic role in this context. This investigation revealed that SOX13 levels within tumor samples were markedly associated to tumor status and pathological phase, as well as survival outcomes. In addition, reduced SOX13 content was linked with worse patient prognosis and advanced tumor stages. SOX13 levels were shown by logistic regression as being markedly associated to T and pathologic stage, histological type, together with primary neoplasm focus type while Kaplan-Meier curves indicated that patient OS and PFI were markedly reduced in cases with lower SOX13 levels. Associations between SOX13 and poor prognosis have been observed in various cancer types, including liver cancer, gastric, nonsmall-cell lung cancer, and pancreatic cancers (48). Such dataset outcomes imply that SOX13 could be a prognostic biomarker within numerous cancers, including THCA.

The importance of genetic and epigenetic contributions to cancer development is well-known. For instance, mutations in the immune checkpoint gene PD-L1 influence its structure, cellular expression, and overall functioning (49). Overexpression of the JAK2/PDL1/PD-L2 pathway leads to activation and altered functioning of other immune checkpoint molecules (50, 51). However, here, it was found that SOX13 was mutated in only 0.2% of THCA tissue samples, nor were mutations linked with OS and DSS in THCA. Further investigations into possible SOX13 roles

10.3389/fimmu.2024.1478395

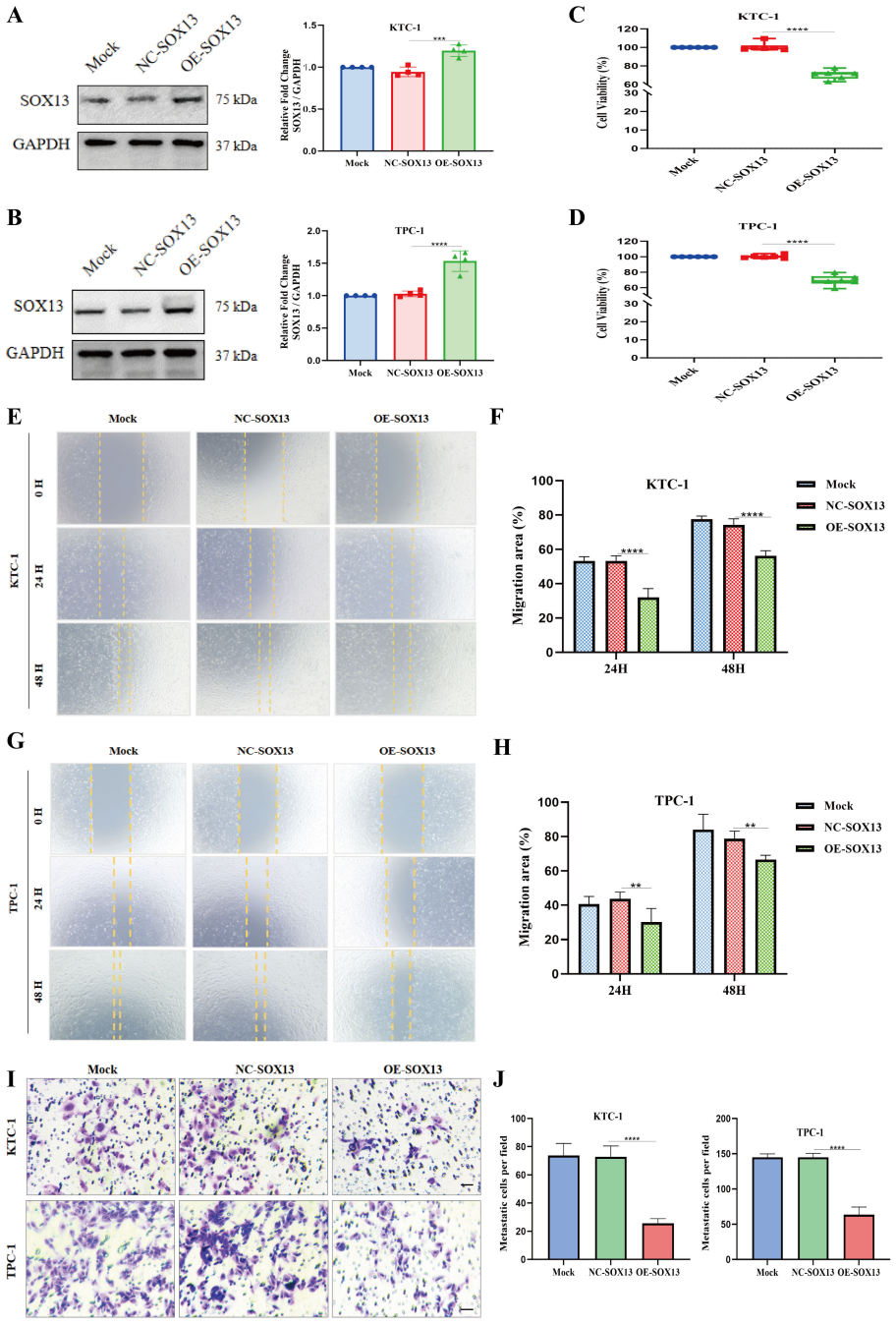

FIGURE 9
Upregulation of SOX13 reduces THCA cell proliferation, migration, and invasion. **(A, B)** SOX13 content significantly increased following SOX13 overexpression plasmid in two distinct THCA cell lines, as observed by Western blot (WB). Upregulation of SOX13 significantly inhibited proliferation **(C, D)**, migration **(E–H)**, and invasion **(I–J)** capabilities of THCA cells. Scale bar represents 50μm; **p< 0.01; ***p< 0.001;****p< 0.0001.

within THCA using annotation/pathway analyses indicated its involvement in various pathways including the activity of humoral immune response and the biology of cytokine-cytokine receptor interaction, suggesting that SOX13 may modulate immune response of tumor cells.

Targeting of ferroptosis has been suggested for treating cancer, especially for the treatment of refractory tumors (52). A number of tumor suppressor proteins, such as P53, fumarase, and BAP1, can sensitize tumor cells ferroptosis (53). Here, the relationships between SOX13 levels and ferroptosis-associated genes were investigated, observing positive correlations between them. These findings suggest that the SOX13-mediated tumorgenesis suppression is linked to the SOX13 ability to regulate ferroptosis and may reveal novel ferroptosis targeting in THCA treatment.

The TME encompasses not only tumor cells but also a diverse array of immune and stromal cells, namely fibroblasts, endothelial cells, and neurons (54). The immunogenicity of a tumor is influenced by its antigens, the extent of immune cell invasion,

and the types and levels of immunomodulatory molecules present within the TME (55). Immune cell infiltration, a significant component of the TME, has been demonstrated to critically impact the initiation and advancement of cancers (56). Here, we identified an association between infiltration and SOX13 levels, observing that SOX13 was negatively associated with the numbers of cytotoxic, regulatory T cell, and B cells in THCA tumor samples. Cytotoxic cells initiate immune responses against tumors, resulting in tumor cell lysis (57), while regulatory T cells promote recruitment of type-1 T helper cells and immune activation (58). Our study also found a direct relationship between SOX13 content and emergence of type 17 helper T cells and Tcm cells. Type 17 helper T cells have been reported to suppress the glycolysis pathway, thereby intensifying inflammatory responses and affecting the progression of tumor diseases (59). Additionally, cytokines namely IL-4 and IL-13, secreted by Th2 cells, promote cancer progression by inducing polarization of M2 macrophages (60). SOX13 levels were also found to correlate with the concentrations of multiple chemokines, chemokine receptors, and immune checkpoints in THCA tissues, indicating its potential to influence the TME through diverse mechanisms. Our findings suggest that decreased levels of SOX13 are closely linked to mechanisms that facilitate immune evasion in THCA tumor cells, thereby contributing to both tumor growth and progression.

Finally, this study utilized SOX13 overexpression plasmid transfection to upregulate SOX13 expression in two THCA cell lines. The increased expression of SOX13 resulted in reduced viability, proliferation, metastasis, and invasion capabilities of THCA cells. Overexpression of SOX13 enhanced the inhibitory effect of RSL3 on the viability of TPC-1 cells. Moreover, our study also found that the overexpression of SOX13 inhibited the expression of ferroptosis-related genes in TPC-1 cells. This discovery further supports the involvement of SOX13 in the THCA cell cycle, regulating invasion and metastasis of THCA cells through ferroptosis. These findings highlight SOX13 as a promising target for targeted therapies against tumors.

This study provides crucial preliminary findings, but its sample population is relatively small. Future verification using a larger patient population is necessary. The accuracy of prediction and diagnosis using a single biomarker remains uncertain. Therefore, future research should prioritize combinations of multiple distinct biomarkers. Furthermore, the functional role of SOX13 in modulating immune response and ferroptosis was assessed using bioinformatics and *in vitro* cell experiments. To further validate these findings, *in vivo* tumor model experiments are necessary.

5 Conclusions

In conclusion, down-regulation of SOX13 may inhibit the antitumor immune response while promoting the incidence, metastasis, and invasion of THCA. SOX13 presence correlates with and has potential to predict the occurrence of THCA. These findings will assist medical professionals in developing more patient-friendly treatment regimens.

Data availability statement

The datasets presented in this study can be found in online repositories. The names of the repository/repositories and accession number(s) can be found in the article/Supplementary Material.

Ethics statement

The manuscript presents research on animals that do not require ethical approval for their study. The Ethics Committee of the Guizhou Nursing Vocational College agreed to submit the study for review and has waived the need for ethical approval, as the data in this study are from public bioinformatics databases.

Author contributions

YaM: Data curation, Formal analysis, Investigation, Resources, Validation, Writing – original draft. WyZ: Data curation, Investigation, Methodology, Software, Writing – review & editing. YQ: Formal analysis, Investigation, Validation, Writing – review & editing. YiM: Conceptualization, Formal analysis, Investigation, Software, Visualization, Writing – review & editing. WZ: Conceptualization, Formal analysis, Funding acquisition, Investigation, Methodology, Resources, Software, Writing – original draft, Writing – review & editing.

Funding

The author(s) declare financial support was received for the research, authorship, and/or publication of this article. This work was supported by grants from Guizhou Nursing Vocational College Foundation (gzhlyj2023-04), Guizhou Nursing Vocational College Foundation (gzhlyj2021-02), and Science and Technology Foundation of Guizhou Provincial Health Committee (gzwkj2022-518).

Acknowledgments

We are grateful to all co-authors of this study.

Conflict of interest

The authors declare that the research was conducted in the absence of any commercial or financial relationships that could be construed as a potential conflict of interest.

Publisher's note

All claims expressed in this article are solely those of the authors and do not necessarily represent those of their affiliated organizations, or those of the publisher, the editors and the reviewers. Any product that may be evaluated in this article, or claim that may be made by its manufacturer, is not guaranteed or endorsed by the publisher.

Supplementary material

The Supplementary Material for this article can be found online at: https://www.frontiersin.org/articles/10.3389/fimmu.2024.1478395/full#supplementary-material

References

1. Takano T. Natural history of thyroid cancer [Review. *Endocr J*. (2017) 64:237–44. doi: 10.1507/endocrj.EJ17-0026

2. Cheng F, Xiao J, Shao C, Huang F, Wang L, Ju Y, et al. Burden of thyroid cancer from 1990 to 2019 and projections of incidence and mortality until 2039 in China: findings from global burden of disease study. *Front Endocrinol (Lausanne)*. (2021) 12:738213. doi: 10.3389/fendo.2021.738213

3. Deng Y, Li H, Wang M, Li N, Tian T, Wu Y, et al. Global burden of thyroid cancer from 1990 to 2017. *JAMA Netw Open*. (2020) 3:e208759. doi: 10.1001/jamanetworkopen.2020.8759

4. Pacini F, Castagna MG, Brilli L, Pentheroudakis G. Thyroid cancer: ESMO Clinical Practice Guidelines for diagnosis, treatment and follow-up. *Ann Oncol*. (2012) 23 Suppl 7:i110–19. doi: 10.1093/annonc/mds230

5. Cabanillas ME, McFadden DG, Durante C. Thyroid cancer. *Lancet*. (2016) 388:2783–95. doi: 10.1016/S0140-6736(16)30172-6

6. Carling T, Udelsman R. Thyroid cancer. *Annu Rev Med*. (2014) 65:125–37. doi: 10.1146/annurev-med-061512-105739

7. Argentaro A, Olsson J, Critcher R, McDowall SG, Harley VR. Genomic characterisation and fine mapping of the human SOX13 gene. *Gene*. (2000) 250:181–89. doi: 10.1016/s0378-1119(00)00157-8

8. Roose J, Korver W, de Boer R, Kuipers J, Hurenkamp J, Clevers H. The Sox-13 gene: structure, promoter characterization, and chromosomal localization. *Genomics*. (1999) 57:301–05. doi: 10.1006/geno.1999.5779

9. Demos C, Johnson J, Andueza A, Park C, Kim Y, Villa-Roel N, et al. Sox13 is a novel flow-sensitive transcription factor that prevents inflammation by repressing chemokine expression in endothelial cells. *Front Cardiovasc Med*. (2022) 9:979745. doi: 10.3389/fcvm.2022.979745

10. Baroti T, Schillinger A, Wegner M, Stolt CC. Sox13 functionally complements the related Sox5 and Sox6 as important developmental modulators in mouse spinal cord oligodendrocytes. *J Neurochem*. (2016) 136:316–28. doi: 10.1111/jnc.13414

11. Diawara M, Martin LJ. Regulatory mechanisms of SoxD transcription factors and their influences on male fertility. *Reprod Biol*. (2023) 23:100823. doi: 10.1016/j.repbio.2023.100823

12. Huang J, Guo L. Knockdown of SOX9 inhibits the proliferation, invasion, and EMT in thyroid cancer cells. *Oncol Res*. (2017) 25:167–76. doi: 10.3727/096504016X14732772150307

13. Zhang W, Qian Y, Jin X, Wang Y, Mu L, Jiang Z. SIRT7 is a prognostic biomarker in kidney renal clear cell carcinoma that is correlated with immune cell infiltration. *Int J Gen Med*. (2022) 15:3167–82. doi: 10.2147/IJGM.S353610

14. Liu K, Ma J, Ao J, Mu L, Wang Y, Qian Y, et al. The oncogenic role and immune infiltration for CARM1 identified by pancancer analysis. *J Oncol*. (2021) 2021:2986444. doi: 10.1155/2021/2986444

15. Zhang W, Qiao XY, Li Q, Cui C, Qiao CM, Shen YQ, et al. Comprehensive pan-cancer analysis of TRPM8 in tumor metabolism and immune escape. *Front Oncol*. (2022) 12:914060. doi: 10.3389/fonc.2022.914060

16. Zhang W, Dao JJ, Li Q, Liu C, Qiao CM, Cui C, et al. Neuregulin 1 mitigated prolactin deficiency through enhancing TRPM8 signaling under the influence of melatonin in senescent pituitary lactotrophs. *Int J Biol Macromol*. (2024) 275:133659. doi: 10.1016/j.ijbiomac.2024.133659

17. Lin WW, Ou GY, Dai HF, Zhao WJ. Neuregulin 4 (Nrg4) cooperates with melatonin to regulate the PRL expression *via* ErbB4/Erk signaling pathway as a potential prolactin (PRL) regulator. *J Cell Biochem*. (2024) 125:e30551. doi: 10.1002/jcb.30551

18. Zhao WJ, Ou GY, Lin WW. Integrative analysis of neuregulin family members-related tumor microenvironment for predicting the prognosis in gliomas. *Front Immunol*. (2021) 12:682415. doi: 10.3389/fimmu.2021.682415

19. Lin WW, Ou GY, Zhao WJ. Mutational profiling of low-grade gliomas identifies prognosis and immunotherapy-related biomarkers and tumour immune microenvironment characteristics. *J Cell Mol Med*. (2021) 25:10111–25. doi: 10.1111/jcmm.16947

20. Ou GY, Lin WW, Zhao WJ. Construction of long noncoding RNA-associated ceRNA networks reveals potential biomarkers in alzheimer's disease. *J Alzheimers Dis*. (2021) 82:169–83. doi: 10.3233/JAD-210068

21. Ahn SM, Jang SJ, Shim JH, Kim D, Hong SM, Sung CO, et al. Genomic portrait of resectable hepatocellular carcinomas: implications of RB1 and FGF19 aberrations for patient stratification. *Hepatology*. (2014) 60:1972–82. doi: 10.1002/hep.27198

22. Liu W, Chakraborty B, Safi R, Kazmin D, Chang CY, McDonnell DP. Dysregulated cholesterol homeostasis results in resistance to ferroptosis increasing tumorigenicity and metastasis in cancer. *Nat Commun*. (2021) 12:5103. doi: 10.1038/s41467-021-25354-4

23. Nagpal A, Redvers RP, Ling X, Ayton S, Fuentes M, Tavancheh E, et al. Neoadjuvant neratinib promotes ferroptosis and inhibits brain metastasis in a novel syngeneic model of spontaneous HER2(+ve) breast cancer metastasis. *Breast Cancer Res*. (2019) 21:94. doi: 10.1186/s13058-019-1177-1

24. Lu Y, Qin H, Jiang B, Lu W, Hao J, Cao W, et al. KLF2 inhibits cancer cell migration and invasion by regulating ferroptosis through GPX4 in clear cell renal cell carcinoma. *Cancer Lett*. (2021) 522:1–13. doi: 10.1016/j.canlet.2021.09.014

25. Alvarez SW, Sviderskiy VO, Terzi EM, Papagiannakopoulos T, Moreira AL, Adams S, et al. NFS1 undergoes positive selection in lung tumours and protects cells from ferroptosis. *Nature*. (2017) 551:639–43. doi: 10.1038/nature24637

26. Miess H, Dankworth B, Gouw AM, Rosenfeldt M, Schmitz W, Jiang M, et al. The glutathione redox system is essential to prevent ferroptosis caused by impaired lipid metabolism in clear cell renal cell carcinoma. *Oncogene*. (2018) 37:5435–50. doi: 10.1038/s41388-018-0315-z

27. Ubellacker JM, Tasdogan A, Ramesh V, Shen B, Mitchell EC, Martin-Sandoval MS, et al. Lymph protects metastasizing melanoma cells from ferroptosis. *Nature*. (2020) 585:113–18. doi: 10.1038/s41586-020-2623-z

28. Bagchi S, Yuan R, Engleman EG. Immune checkpoint inhibitors for the treatment of cancer: clinical impact and mechanisms of response and resistance. *Annu Rev Pathol*. (2021) 16:223–49. doi: 10.1146/annurev-pathol-042020-042741

29. Derer A, Frey B, Fietkau R, Gaipl US. Immune-modulating properties of ionizing radiation: rationale for the treatment of cancer by combination radiotherapy and immune checkpoint inhibitors. *Cancer Immunol Immunother*. (2016) 65:779–86. doi: 10.1007/s00262-015-1771-8

30. Kunz M, Holzel M. The impact of melanoma genetics on treatment response and resistance in clinical and experimental studies. *Cancer Metastasis Rev*. (2017) 36:53–75. doi: 10.1007/s10555-017-9657-1

31. Doroshow DB, Bhalla S, Beasley MB, Sholl LM, Kerr KM, Gnjatic S, et al. PD-L1 as a biomarker of response to immune-checkpoint inhibitors. *Nat Rev Clin Oncol*. (2021) 18:345–62. doi: 10.1038/s41571-021-00473-5

32. Garman B, Jiang C, Daouti S, Kumar S, Mehta P, Jacques MK, et al. Comprehensive immunophenotyping of solid tumor-infiltrating immune cells reveals the expression characteristics of LAG-3 and its ligands. *Front Immunol*. (2023) 14:1151748. doi: 10.3389/fimmu.2023.1151748

33. Ye L, Zhang T, Kang Z, Guo G, Sun Y, Lin K, et al. Tumor-infiltrating immune cells act as a marker for prognosis in colorectal cancer. *Front Immunol*. (2019) 10:2368. doi: 10.3389/fimmu.2019.02368

34. Domingues P, Gonzalez-Tablas M, Otero A, Pascual D, Miranda D, Ruiz L, et al. Tumor infiltrating immune cells in gliomas and meningiomas. *Brain Behav Immun*. (2016) 53:1–15. doi: 10.1016/j.bbi.2015.07.019

35. Zappasodi R, Serganova I, Cohen IJ, Maeda M, Shindo M, Senbabaoglu Y, et al. CTLA-4 blockade drives loss of T(reg) stability in glycolysis-low tumours. *Nature*. (2021) 591:652–58. doi: 10.1038/s41586-021-03326-4

36. Van Coillie S, Wiernicki B, Xu J. Molecular and cellular functions of CTLA-4. *Adv Exp Med Biol*. (2020) 1248:7–32. doi: 10.1007/978-981-15-3266-5_2

37. Lefebvre V. The SoxD transcription factors–Sox5, Sox6, and Sox13–are key cell fate modulators. *Int J Biochem Cell Biol*. (2010) 42:429–32. doi: 10.1016/j.biocel.2009.07.016

38. Akiyama H. Sox family regulate chondrogenesis. *Clin Calcium*. (2006) 16:368–72.

39. Jiang T, Hou CC, She ZY, Yang WX. The SOX gene family: function and regulation in testis determination and male fertility maintenance. *Mol Biol Rep*. (2013) 40:2187–94. doi: 10.1007/s11033-012-2279-3

40. Du F, Li X, Feng W, Qiao C, Chen J, Jiang M, et al. SOX13 promotes colorectal cancer metastasis by transactivating SNAI2 and c-MET. *Oncogene*. (2020) 39:3522–40. doi: 10.1038/s41388-020-1233-4

41. Noto M, Noguchi N, Ishimura A, Kiyonari H, Abe T, Suzuki T, et al. Sox13 is a novel early marker for hair follicle development. *Biochem Biophys Res Commun*. (2019) 509:862–68. doi: 10.1016/j.bbrc.2018.12.163

42. Jin X, Shao X, Pang W, Wang Z, Huang J. Sex-determining Region Y-box transcription factor 13 promotes breast cancer cell proliferation and glycolysis by activating the tripartite motif containing 11-mediated Wnt/beta-catenin signaling pathway. *Bioengineered*. (2022) 13:13033–44. doi: 10.1080/21655979.2022.2073127

43. Liu A, Han N, Munoz-Muriedas J, Bender A. Deriving time-concordant event cascades from gene expression data: A case study for Drug-Induced Liver Injury (DILI). *PloS Comput Biol*. (2022) 18:e1010148. doi: 10.1371/journal.pcbi.1010148

44. Aksoy I, Jauch R, Eras V, Chng WB, Chen J, Divakar U, et al. Sox transcription factors require selective interactions with Oct4 and specific transactivation functions to mediate reprogramming. *Stem Cells*. (2013) 31:2632–46. doi: 10.1002/stem.1522

45. Yang H, Li Q, Chen X, Weng M, Huang Y, Chen Q, et al. Targeting SOX13 inhibits assembly of respiratory chain supercomplexes to overcome ferroptosis resistance in gastric cancer. *Nat Commun*. (2024) 15:4296. doi: 10.1038/s41467-024-48307-z

46. Gao T, Jiang B, Zhou Y, He R, Xie L, Li Y. SOX13 is a novel prognostic biomarker and associates with immune infiltration in breast cancer. *Front Immunol*. (2024) 15:1369892. doi: 10.3389/fimmu.2024.1369892

47. Nelson SR, Roche S, Cotter M, Garcia PA, Reitmeier D, Zollbrecht E, et al. Genomic Profiling and Functional Analysis of let-7c miRNA-mRNA Interactions Identify SOX13 to Be Involved in Invasion and Progression of Pancreatic Cancer. *J Oncol*. (2020) 2020:2951921. doi: 10.1155/2020/2951921

48. Zhang L, Peng H, Xu Z, Yang Q, Wang Y, Wang H, et al. Circular RNA SOX13 promotes Malignant behavior and cisplatin resistance in non-small cell lung cancer through targeting microRNA-3194-3p/microtubule-associated protein RP/EB family member 1. *Bioengineered*. (2022) 13:1814–27. doi: 10.1080/21655979.2021.1997223

49. Fukushima Y, Someya M, Nakata K, Hori M, Kitagawa M, Hasegawa T, et al. Influence of PD-L1 expression in immune cells on the response to radiation therapy in patients with oropharyngeal squamous cell carcinoma. *Radiother Oncol*. (2018) 129:409–14. doi: 10.1016/j.radonc.2018.08.023

50. Pichler R, Heidegger I, Fritz J, Danzl M, Sprung S, Zelger B, et al. PD-L1 expression in bladder cancer and metastasis and its influence on oncologic outcome after cystectomy. *Oncotarget*. (2017) 8:66849–64. doi: 10.18632/oncotarget.19913

51. Xu SB, Wang MY, Shi XZ, Wang Q, Yu M, Zhang W, et al. Influence of PD-1/PD-L1 on immune microenvironment in oral leukoplakia and oral squamous cell carcinoma. *Oral Dis*. (2023) 29:3268–77. doi: 10.1111/odi.14332

52. Wang Y, Lv MN, Zhao WJ. Research on ferroptosis as a therapeutic target for the treatment of neurodegenerative diseases. *Ageing Res Rev*. (2023) 91:102035. doi: 10.1016/j.arr.2023.102035

53. Jiang L, Kon N, Li T, Wang SJ, Su T, Hibshoosh H, et al. Ferroptosis as a p53-mediated activity during tumour suppression. *Nature*. (2015) 520:57–62. doi: 10.1038/nature14344

54. Hinshaw DC, Shevde LA. The tumor microenvironment innately modulates cancer progression. *Cancer Res*. (2019) 79:4557–66. doi: 10.1158/0008-5472.CAN-18-3962

55. Banerjee A, Chabria Y, Kanna NRR, Gopi J, Rowlo P, Sun XF, et al. Role of tumor specific niche in colon cancer progression and emerging therapies by targeting tumor microenvironment. *Adv Exp Med Biol*. (2021) 1341:177–92. doi: 10.1007/5584_2019_355

56. Cachot A, Bilous M, Liu YC, Li X, Saillard M, Cenerenti M, et al. Tumor-specific cytolytic CD4 T cells mediate immunity against human cancer. *Sci Adv*. (2021) 7. doi: 10.1126/sciadv.abe3348

57. Walch M, Dotiwala F, Mulik S, Thiery J, Kirchhausen T, Clayberger C, et al. Cytotoxic cells kill intracellular bacteria through granulysin-mediated delivery of granzymes. *Cell*. (2014) 157:1309–23. doi: 10.1016/j.cell.2014.03.062

58. Sakaguchi S, Mikami N, Wing JB, Tanaka A, Ichiyama K, Ohkura N. Regulatory T cells and human disease. *Annu Rev Immunol*. (2020) 38:541–66. doi: 10.1146/annurev-immunol-042718-041717

59. Krebs CF, Schmidt T, Riedel JH, Panzer U. T helper type 17 cells in immune-mediated glomerular disease. *Nat Rev Nephrol*. (2017) 13:647–59. doi: 10.1038/nrneph.2017.112

60. Bernstein ZJ, Shenoy A, Chen A, Heller NM, Spangler JB. Engineering the IL-4/IL-13 axis for targeted immune modulation. *Immunol Rev*. (2023) 320:29–57. doi: 10.1111/imr.13230

frontiers | Frontiers in Cell and Developmental Biology

TYPE Review
PUBLISHED 18 December 2024
DOI 10.3389/fcell.2024.1510390

OPEN ACCESS

EDITED BY
Patrice X. Petit,
Centre National de la Recherche Scientifique (CNRS), France

REVIEWED BY
Márcio Simão,
University of Algarve, Portugal
Fangyang Fan,
Beijing University of Chinese Medicine, China

*CORRESPONDENCE
Junping Zhen,
harrygin@163.com

RECEIVED 12 October 2024
ACCEPTED 04 December 2024
PUBLISHED 18 December 2024

CITATION
Lu S, Liu Z, Qi M, Wang Y, Chang L, Bai X, Jiao Y, Chen X and Zhen J (2024) Ferroptosis and its role in osteoarthritis: mechanisms, biomarkers, and therapeutic perspectives.
Front. Cell Dev. Biol. 12:1510390.
doi: 10.3389/fcell.2024.1510390

Ferroptosis and its role in osteoarthritis: mechanisms, biomarkers, and therapeutic perspectives

Shanyu Lu[1,2,3], Zhenyu Liu[1,2,3], Meiling Qi[1,2,3], Yingchao Wang[1,2], Le Chang[1,2], Xiaolong Bai[1,2], Yingguang Jiao[1,2], Xinyao Chen[1,2] and Junping Zhen[1,2,4]*

[1]College of Medical Imaging, Shanxi Medical University, Taiyuan, Shanxi, China, [2]Department of Imaging, Second Hospital of Shanxi Medical University, Taiyuan, Shanxi, China, [3]Shanxi Key Laboratory for Immunomicroecology, Taiyuan, Shanxi, China, [4]Molecular Imaging Laboratory, Second Hospital of Shanxi Medical University, Taiyuan, Shanxi, China

Osteoarthritis (OA) is one of the leading causes of disability worldwide, characterized by a complex pathological process involving cartilage degradation, synovial inflammation, and subchondral bone remodeling. In recent years, ferroptosis, a form of programmed cell death driven by iron-dependent lipid peroxidation, has been recognized as playing a critical role in the onset and progression of OA. Investigating the molecular mechanisms of ferroptosis and its involvement in OA may offer novel strategies for diagnosing and treating this disease. This review first outlines the core mechanisms of ferroptosis, with a particular focus on the roles of critical molecules such as Glutathione Peroxidase 4 (GPX4), Transferrin Receptor 1 (TfR1), and Nuclear Receptor Coactivator 4 (NCOA4). Subsequently, this study examines the specific impacts of ferroptosis on the pathophysiology of OA. Building on this, the potential of ferroptosis-related biomarkers for OA diagnosis and treatment is highlighted, along with proposed therapeutic strategies targeting ferroptosis regulation. This review aims to deepen the understanding of ferroptosis mechanisms and advance the clinical application of regulatory therapies for OA.

KEYWORDS

osteoarthritis, ferroptosis, molecular mechanisms, biomarkers, therapeutic strategies

1 Introduction

Osteoarthritis (OA) is a highly prevalent and destructive degenerative joint disease, affecting approximately 7.6% of the global population, with over 595 million cases in 2020 alone (GBD, 2021 Osteoarthritis Collaborators, 2023). Its incidence is expected to approach 1 billion by 2050, driven by the aging population (GBD, 2021 Osteoarthritis Collaborators, 2023). This rising prevalence poses a significant public health challenge (Martel-Pelletier et al., 2016; Grandi and Bhutani, 2020). The pathological features of OA include cartilage degeneration, synovial inflammation, subchondral bone remodeling, and joint space narrowing, among others (Barnett, 2018; Zhou et al., 2024). Traditionally, OA has been attributed primarily to excessive mechanical load; however, recent research indicates that it is a multifactorial process involving inflammation, metabolic imbalance, and impacts on various joint structures (Barnett, 2018; Hunter and Bierma-Zeinstra, 2019;

Zhou et al., 2024). Despite extensive studies revealing some molecular mechanisms and risk factors associated with OA, the exact pathogenesis remains unclear, and effective treatments to halt or slow disease progression are lacking (Henrotin, 2022; Salman et al., 2023). Clinically, OA management predominantly focuses on symptom relief and surgical intervention, underscoring the urgent need to explore its underlying mechanisms and identify new therapeutic targets (Hunter et al., 2020; Kolasinski et al., 2020; Cho et al., 2021; Loughlin, 2022; Mobasheri et al., 2023).

With advancements in the study of cell death mechanisms, ferroptosis—a form of cell death distinctly different from traditional apoptosis and necrosis—has been identified (Dixon and Pratt, 2023; Wahida and Conrad, 2023; Berndt et al., 2024). Ferroptosis involves iron-dependent lipid peroxidation, leading to disrupted iron homeostasis, excess ROS production, and increased lipid peroxidation byproducts (Chen et al., 2023; Deng et al., 2023; von Krusenstiern et al., 2023; Bell et al., 2024; Dixon and Olzmann, 2024). Ferroptosis, discovered in 2012, is now recognized as a key factor in various diseases, including neurodegenerative disorders, cancer, and ischemia-reperfusion injury (Dixon et al., 2012; Deng et al., 2023; Fang et al., 2023; Graham et al., 2023; Miao et al., 2023; Yao et al., 2023; Ahola and Langer, 2024; Levi et al., 2024). Initial research indicates that ferroptosis could be a primary mechanism responsible for OA's death of chondrocytes and synoviocytes (Miao et al., 2022; He Q et al., 2023). Increased intra-articular iron levels, lipid peroxidation, and weakened antioxidant defenses promote ferroptosis, worsening cartilage degeneration, and joint function loss (Chen J et al., 2024). This finding provides fresh insight into the pathogenesis of OA and presents potential for developing new therapeutic approaches aimed at targeting ferroptosis.

Although research on the precise mechanisms and clinical relevance of ferroptosis in OA is still in its infancy, the volume of related studies is growing swiftly (Yang et al., 2021; Ohnishi et al., 2022; Wang et al., 2023). A thorough review of the molecular pathological mechanisms, potential physiological functions, and therapeutic possibilities of ferroptosis in OA is thus essential. This review systematically outlines the core mechanisms of ferroptosis and its specific impacts on OA, explores the potential of ferroptosis-related biomarkers as diagnostic and therapeutic targets, and discusses the challenges and opportunities for clinical translation.

2 Biological mechanisms of ferroptosis

2.1 Overview of ferroptosis

Ferroptosis is a distinct type of programmed cell death, setting itself apart from conventional forms like apoptosis, necrosis, and autophagy. Its uniqueness lies in its dependence on iron accumulation, which triggers lipid peroxidation (Dixon et al., 2012; Chen et al., 2016; Zhang et al., 2018; Frank and Vince, 2019; Stockwell and Jiang, 2020; Liu et al., 2022; Tang et al., 2024). Morphologically, ferroptosis is characterized by alterations in mitochondrial structure, such as increased mitochondrial membrane density, diminished or missing cristae, and overall mitochondrial shrinkage (Wang et al., 2017; Fang et al., 2019; Deng et al., 2023; Mao et al., 2023). Biochemically, ferroptosis is indicated by the inhibition of cystine/glutamate antiporter (System Xc^-), the depletion of glutathione (GSH), decreased activity of glutathione peroxidase 4 (GPX4), accumulation of lipid peroxides (LOOH), and a decline in mitochondrial membrane potential (Mao et al., 2021; Wang and Min, 2021). These changes result in excessive intracellular iron accumulation, triggering oxidative stress and cellular damage (Ingold et al., 2018; Bersuker et al., 2019; Zheng and Conrad, 2020).

Current research on the mechanisms of ferroptosis focuses on three primary signaling axes: dysregulated iron metabolism, lipid peroxidation, and the System Xc^--GSH-GPX4 axis. Dysfunctions in these pathways can lead to cellular iron overload. To maintain iron homeostasis, cells employ intricate regulatory mechanisms, including iron uptake via the transferrin receptor (TFR1), storage of iron in ferritin, and ferritinophagy to mitigate the toxic effects of iron overload (Kakhlon and Cabantchik, 2002; Gammella et al., 2015; Anderson and Frazer, 2017; Feng et al., 2020). GPX4 plays a critical role in counteracting ferroptosis by mitigating lipid peroxidation, while other factors like nicotinamide adenine dinucleotide phosphate (NADPH) and coenzyme Q10 (CoQ10) also contribute to ferroptosis regulation (Bersuker et al., 2019).

In addition to these well-characterized mechanisms, recent studies have highlighted alternative ferroptosis surveillance pathways that operate independently of GPX4. Enzymes such as FSP1 and MBOAT1/2 have been identified as important contributors to these pathways, suggesting a broader and more complex regulatory network of ferroptosis beyond the conventional System Xc^--GSH-GPX4 axis (Liang et al., 2023). The complex biological network governing ferroptosis highlights its central role in cellular homeostasis and disease progression. This understanding provides a crucial foundation for exploring ferroptosis-driven mechanisms in osteoarthritis. Figure 1 offers a comprehensive depiction of the critical molecular mechanisms underpinning ferroptosis.

2.1.1 Iron metabolism

Iron metabolism and regulation are crucial for maintaining normal cellular functions (Ward et al., 2014; Zheng and Conrad, 2020; Simao and Cancela, 2021). Transferrin receptor 1 (TfR1) mediates the endocytosis of iron-bound transferrin (TF) (Aisen et al., 1978; Johnsen et al., 2019). TF, a natural chelator abundant in plasma, possesses two high-affinity iron-binding sites. Once TF binds to Fe^{3+} to form holo-TF, it associates with TfR1 on the cell surface and is internalized. In the acidic environment of endosomes, the lowered pH facilitates the release of Fe^{3+} from the Tf-TfR1 complex, allowing TfR1 and apotransferrin (apoTF) to be recycled back to the cell surface (Klausner et al., 1983; Zhou et al., 2021). During this process, divalent metal transporter 1 (DMT1) is crucial for the transmembrane transport of iron, primarily responsible for transporting iron ions from the extracellular space or organelles into the cytoplasm. Metalloreductase six-transmembrane epithelial antigen of prostate 3 (STEAP3) possesses ferrireductase activity, reducing Fe^{3+} to Fe^{2+}, which is then released into the cytoplasm via DMT1, contributing to an unstable iron pool (Pantopoulos, 2004; Feng et al., 2020; Koike et al., 2020). Excess iron is stored in ferritin or exported extracellularly through ferroportin 1 (FPN1) (Kakhlon and Cabantchik, 2002).

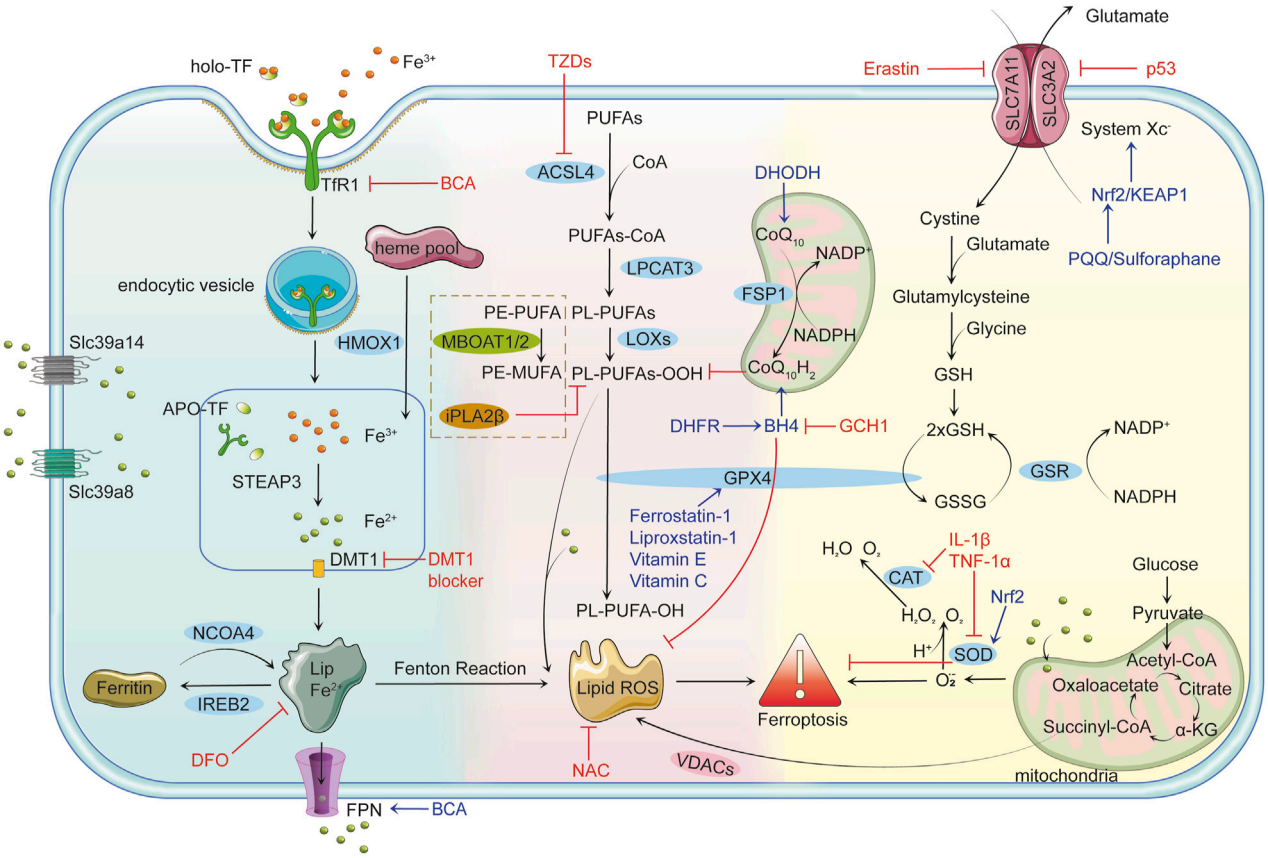

FIGURE 1
Mechanisms of Ferroptosis Iron Metabolism and Ferroptosis: Cells uptake iron-bound transferrin (TF) through transferrin receptor 1 (TFR1). Iron enters the cell in the Fe^{3+} form via endocytosis and is reduced to Fe^{2+} by six-transmembrane epithelial antigen of prostate 3 (STEAP3) in the endosome, subsequently transported to the cytoplasm by divalent metal transporter 1 (DMT1). Non-transferrin-bound iron (NTBI) uptake, mediated by solute carrier family 39 member 14 (Slc39a14) and solute carrier family 39 member 8 (Slc39a8), further contributes to intracellular iron overload. Free Fe^{2+} can participate in the Fenton reaction, producing highly reactive hydroxyl radicals (●OH) that trigger lipid peroxidation and lead to the accumulation of lipid reactive oxygen species (Lipid ROS). Ferritin alleviates iron toxicity by storing iron, while Nuclear Receptor Coactivator 4 (NCOA4) mediates ferritin degradation, releasing iron ions and enhancing ferroptosis. Lipid Peroxidation and Ferroptosis: Polyunsaturated fatty acids (PUFAs) are catalyzed by long-chain fatty acid-CoA ligase 4 (ACSL4) to form PUFAs-CoA, which are then integrated into the lipid bilayer by lysophosphatidylcholine acyltransferase 3 (LPCAT3), producing phospholipid PUFAs (PL-PUFAs). Lipoxygenases (LOXs) further oxidize PL-PUFAs into phospholipid peroxides (PL-PUFA-OOH), and the accumulated lipid ROS triggers ferroptosis. Voltage-dependent anion channels (VDACs) facilitate the accumulation of lipid ROS, accelerating cell death. Glutathione peroxidase 4 (GPX4)-independent pathways, such as iPLA2β (a calcium-independent phospholipase A2 family member) and membrane-bound O-acyltransferase 1/2 (MBOAT1/2), provide additional defense against ferroptosis by reducing peroxidized lipids and remodeling phospholipids, respectively. Antioxidant Defense Mechanisms and Ferroptosis: GPX4 is the primary inhibitor of ferroptosis, reducing PL-PUFA-OOH to non-toxic phospholipids (PL-PUFA-OH) using reduced glutathione (GSH) to prevent lipid ROS accumulation. GSH synthesis depends on System Xc^-, which consists of solute carrier family seven member 11 (SLC7A11) and solute carrier family three member 2 (SLC3A2) and facilitates the transmembrane exchange of cystine and glutamate. Inhibition of System Xc^- decreases GSH production, leading to lipid peroxidation and ferroptosis. Key Regulatory Factors and Drug Actions: p53 limits GSH synthesis by inhibiting System Xc^-, promoting ferroptosis. The nuclear factor erythroid 2-related factor 2 (Nrf2)/kelch-like ech-associated protein 1 (KEAP1) pathway enhances cellular antioxidant capacity and inhibits ferroptosis. Tetrahydrobiopterin (BH4), synthesized by gtp cyclohydrolase 1 (GCH1), boosts antioxidant defenses and suppresses lipid peroxidation. Ferroptosis suppressor protein 1 (FSP1) participates in antioxidant reactions through coenzyme Q10 (CoQ10), inhibiting ferroptosis. Erastin promotes ferroptosis by suppressing System Xc^- and reducing GSH levels. Ferrostatin-1 and Liproxstatin-1 prevent ferroptosis by inhibiting lipid peroxidation, while deferoxamine (DFO) chelates free iron to prevent ferroptosis by blocking the Fenton reaction. N-acetylcysteine (NAC) enhances antioxidant capacity by increasing GSH synthesis. Thiazolidinediones (TZDs) reduce lipid peroxide formation by inhibiting ACSL4 activity. Connection between Ferroptosis and Inflammatory Responses: Pro-inflammatory factors such as interleukin-1β (IL-1β) and tumor necrosis factor-alpha (TNF-α) can induce ROS production, facilitating ferroptosis. Concurrently, ferroptosis can activate inflammatory responses, exacerbating cellular damage. Role of Mitochondria in Ferroptosis: Mitochondria produce energy via oxidative phosphorylation and the tricarboxylic acid (TCA) cycle while generating superoxide (O_2●$^-$), which is converted to H_2O_2 by superoxide dismutase (SOD). H_2O_2 reacts with Fe^{2+} to form OH●, further aggravating lipid peroxidation. Additionally, mitochondria release ROS through VDACs, closely linking this process to ferroptosis. Dihydroorotate dehydrogenase (DHODH) regulates ferroptosis by influencing mitochondrial redox reactions.

Intracellular iron overload is a key driver of ferroptosis, facilitated by increased iron uptake and ferritin degradation through ferritinophagy. In ferroptosis-sensitive cells, TfR1 expression is upregulated, enhancing iron uptake, while ferritin heavy chain (FTH1) and ferritin light chain (FTL) undergo selective degradation via ferritinophagy (Santana-Codina and Mancias, 2018; Li et al., 2024). This process is regulated by nuclear receptor coactivator 4 (NCOA4), a critical mediator of intracellular iron homeostasis. NCOA4 recognizes and binds to ferritin, transporting it to lysosomes for degradation (Latunde-

Dada, 2017). This releases stored iron, increasing the pool of bioavailable iron (Mancias et al., 2015). Upregulation of NCOA4 significantly elevates intracellular iron levels, further promoting lipid peroxidation and ferroptosis (Masaldan et al., 2018). Additionally, research has found a close interplay between NCOA4 and other ferroptosis-related signaling pathways. For instance, NCOA4-mediated ferritinophagy may impact the activity of glutathione peroxidase 4 (GPX4), as increased iron levels can deplete intracellular antioxidants like glutathione, indirectly inhibiting GPX4 function and thereby facilitating ferroptosis (Mancias et al., 2014).

Additionally, iron overload in ferroptosis is further modulated by key metal ion transporters, including solute carrier family 39 member 14 (Slc39a14) and solute carrier family 39 member 8 (Slc39a8) (Aierken et al., 2024). Slc39a14 primarily facilitates the uptake of non-transferrin-bound iron (NTBI), significantly contributing to intracellular iron accumulation (Aierken et al., 2024). Likewise, Slc39a8 also has a similar function, enhancing iron import and increasing intracellular iron levels (Aierken et al., 2024). Upregulation of these transporters promotes iron overload, lipid peroxidation, and ferroptosis. Conversely, inhibiting Slc39a14 or Slc39a8 has alleviated ferroptosis by reducing intracellular iron levels and mitigating oxidative stress (Aierken et al., 2024).

Together, the processes of ferritinophagy, mediated by NCOA4, and enhanced iron import via Slc39a14 and Slc39a8 synergistically increase intracellular iron levels, solidifying their roles as critical factors in regulating ferroptosis.

2.1.2 Lipid peroxidation

Lipid peroxidation, a central driving process of ferroptosis, is a key distinguishing feature from other forms of cell death (Liang et al., 2022). It occurs when reactive oxygen species (ROS) attack polyunsaturated fatty acids (PUFAs) in cellular membranes. ROS, highly reactive molecules derived from molecular oxygen, include superoxide anions, hydrogen peroxide, and hydroxyl radicals. They are primarily generated through enzymatic reactions involving NADPH oxidases (NOXs), cytochrome P450 reductase (POR), and NADH-cytochrome b5 reductase (CYB5R1), with the mitochondrial electron transport chain (mETC) serving as another significant source (Ai et al., 2021; Yan et al., 2021). PUFAs, with their multiple double bonds, are particularly vulnerable to oxidative attack, leading to the formation of lipid peroxidation products (L-OOH) such as malondialdehyde (MDA) and 4-hydroxy-trans-2-nonenal (4-HNE) (Barrera et al., 2015). These toxic byproducts compromise membrane integrity, increase permeability, cause leakage of intracellular components, and trigger inflammatory responses, exacerbating cellular damage (Yang and Stockwell, 2016). Additionally, iron plays a critical role as a cofactor in the biosynthesis of lipoxygenases (LOXs) and cytochrome P450 enzymes, which are central to the generation of ROS during ferroptosis (Zou et al., 2020). Iron metabolism promotes lipid peroxidation through the Fenton reaction ($Fe^{2+} + H_2O_2 \rightarrow Fe^{3+} + \cdot OH + OH^-$), which produces hydroxyl radicals that amplify oxidative stress and accelerate lipid peroxidation, as well as the Haber–Weiss reaction (Dixon et al., 2012).

ROS-driven lipid peroxidation proceeds through three main stages: initiation, propagation, and termination. ROS, such as hydroxyl radicals, abstract allylic hydrogen atoms from PUFAs during initiation, generating lipid radicals (L·). In tell as the Haber–Weiss reaction (Dixon et al., 2012), adjacent lipids produce more lipid radicals and lipid hydroperoxides (L-OOH), thus sustaining the chain reaction (Hermetter et al., 2012; Volinsky and Kinnunen, 2013; Que et al., 2018). This process leads to severe oxidative damage if left unchecked, compromising membrane integrity and ultimately triggering ferroptosis.

Notably, the specific composition of membrane phospholipids, particularly the levels of phosphatidylethanolamine (PE) containing polyunsaturated fatty acids (PE-PUFAs), plays a crucial role in determining ferroptosis sensitivity (Kagan et al., 2017). Higher PE-PUFA content increases the susceptibility of cells to lipid peroxidation, thereby elevating the risk of ferroptosis (Kagan et al., 2017). Acyl-CoA synthetase long-chain family member 4 (ACSL4) catalyzes the conversion of PUFAs into PUFA-CoA derivatives, which are then incorporated into PE by lysophosphatidylcholine acyltransferase 3 (LPCAT3) (Kagan et al., 2017). This process enhances membrane susceptibility to oxidative damage, accelerating lipid peroxidation and ferroptosis.

However, lipid peroxidation is not entirely uncontrollable, as multiple regulatory mechanisms exist within cells. Glutathione peroxidase 4 (GPX4), a key inhibitor of ferroptosis, uses glutathione (GSH) as a cofactor to reduce phospholipid hydroperoxides to their corresponding alcohols, thereby protecting cells and membranes from oxidative damage. In addition to the pivotal role of GPX4, recent studies have identified several GPX4-independent pathways that regulate lipid peroxidation and ferroptosis, providing multilayered protection against oxidative stress. Membrane-bound O-acyltransferase 1/2 (MBOAT1/2) is a ferroptosis suppressor (Liang et al., 2023). As a member of the lysophospholipid acyltransferase (LPLAT) family, MBOAT1/2 transfers monounsaturated fatty acids (MUFA) from MUFA-CoA to lysophosphatidylethanolamine (lyso-PE), thereby competitively reducing the incorporation of PUFA-CoA into lyso-PE (Liang et al., 2023). This modification alters the cellular phospholipid profile by increasing PE-MUFA levels while decreasing PE-PUFA levels, the latter being the preferred substrate for lipid peroxidation and a key determinant of ferroptosis sensitivity (Liang et al., 2023). Thus, this selective remodeling decreases the pool of peroxidation-prone phospholipids, offering an alternative pathway to suppress ferroptosis independently of GPX4 and FSP1 (Liang et al., 2023). Moreover, iPLA2β, a member of the calcium-independent phospholipase A2 family, functions independently of glutathione by cleaving oxidized fatty acid chains from phospholipids, directly removing peroxidized products, effectively detoxifying damaged lipids, and maintaining membrane integrity (Chen et al., 2021). This activity is particularly crucial under conditions where GPX4 is absent or impaired, significantly suppressing lipid peroxidation and ferroptosis. Studies have also shown that iPLA2β reduces oxidized phospholipid levels mediated by ALOX12, thereby limiting the accumulation of lipid peroxidation products (Chen et al., 2021). This detoxification mechanism works synergistically with the lipid remodeling functions of MBOAT1 and MBOAT2, forming a multi-layered defense system against ferroptosis.

In summary, lipid peroxidation is central in ferroptosis, driven by ROS-mediated oxidative damage to PUFAs in cellular

membranes. While GPX4 is a key regulator in detoxifying lipid peroxides, several GPX4-independent mechanisms, such as lipid remodeling by MBOAT1 and MBOAT2 and lipid detoxification by iPLA2β, provide additional layers of protection. These interconnected mechanisms further illuminate the complexity of ferroptosis regulation and underscore the essential role of lipid peroxidation in its execution.

2.1.3 Collapse of antioxidant defense mechanisms

The antioxidant defense System in cells is critically dependent on glutathione peroxidase 4 (GPX4), a crucial metabolic enzyme that uses glutathione (GSH) to convert lipid peroxides into non-toxic alcohols, thereby minimizing harmful lipid peroxidation and safeguarding cells from ferroptosis. The activity of GPX4 is highly reliant on sufficient intracellular GSH levels, which are synthesized via the cystine/glutamate antiporter System Xc^-. Comprising the subunits solute carrier family seven member 11 (SLC7A11) and solute carrier family three member 2 (SLC3A2), System Xc^- is a vital antioxidant System, facilitating the 1:1 exchange of cystine and glutamate across the cell membrane (Dixon et al., 2014). The imported cystine is reduced to cysteine within the cell, contributing to GSH synthesis (Dixon et al., 2014). GPX4 converts GSH to oxidized glutathione while reducing toxic lipid peroxides (L-OOH) to their corresponding alcohols (L-OH), thus lowering ROS production (Yang and Stockwell, 2016; Zheng and Conrad, 2020). Under normal physiological conditions, reduced GSH is present in concentrations 10 to 100 times greater than oxidized GSH (GSSG), making the GSH/GSSG ratio a common measure of cellular oxidative stress (Em et al., 2013; Lei et al., 2015; Hambright et al., 2017; Tang et al., 2021). Therefore, maintaining adequate GSH levels and GPX4 activity is crucial for cellular antioxidant defense; any disruption to this mechanism can lead to increased oxidative stress and subsequent cellular damage.

The function of GPX4 is precisely regulated by nuclear factor E2-related factor 2 (NRF2), a key transcription factor that activates the expression of various antioxidant genes, including those encoding GSH synthetase and superoxide dismutase (SOD), facilitating the clearance of excess ROS (Xie et al., 2016; Tang et al., 2021). Under normal conditions, NRF2 is tightly suppressed by Kelch-like ECH-associated protein 1 (KEAP1), which mediates NRF2 degradation through ubiquitination (Kobayashi et al., 2004). However, under oxidative stress, KEAP1 undergoes a conformational change that relieves its suppression, allowing NRF2 to stabilize and upregulate antioxidant gene expression (Sun et al., 2016).

In addition to GPX4 and NRF2, cells employ various antioxidant mechanisms, including SOD, catalase (CAT), and vitamins C and E, to combat oxidative stress (Chen et al., 2016). SOD effectively catalyzes the conversion of superoxide radicals into water and oxygen, serving as the first line of antioxidant defense, while CAT further decomposes hydrogen peroxide to prevent harmful hydroxyl radical formation (Yuewei et al., 2014; Baker et al., 2023). Vitamins C and E enhance cellular antioxidant capacity through their hydrophilic and lipophilic properties, respectively (Tm et al., 2019; Hu Q et al., 2021). However, inflammatory factors such as interleukin-1β (IL-1β) and tumor necrosis factor-alpha (TNF-α) can significantly inhibit SOD and CAT activity, reduce levels of vitamins C and E, and activate the nuclear factor-kappa B (NF-κB) pathway, exacerbating oxidative stress and stimulating inflammatory responses, thereby creating a vicious cycle (Ueda and Takasawa, 2018).

Additionally, the NADPH/FSP1/CoQ10 pathway, through the action of FSP1, reduces CoQ10 with NADPH, further inhibiting lipid peroxidation and ferroptosis (Frei et al., 1990). Research also indicates that the gtp cyclohydrolase 1/Tetrahydrobiopterin/dihydrofolate reductase (GCH1/BH4/DHFR) pathway, particularly DHFR, suppresses ferroptosis by promoting BH4 synthesis; inhibiting DHFR leads to decreased BH4 production, thereby enhancing lipid peroxidation (Soula et al., 2020; Fanet et al., 2021).

Mitochondria, as central organelles for iron, calcium, lipid, and amino acid metabolism, have limited iron content. However, elevated iron levels can disrupt mitochondrial iron homeostasis (Beckman and Ames, 1998). Research has demonstrated that inhibiting mitochondrial tricarboxylic acid cycles or electron transport chains can lower mitochondrial membrane hyperpolarization and lipid peroxidation, underscoring the critical role of mitochondrial pathways in ferroptosis (Steiner and Lang, 2017; Haileselassie et al., 2019).

In summary, the ferroptosis-related biological components discussed above are presented in Table 1 and Figure 1. Figure 1 was created using Adobe Illustrator 2019 (Adobe Inc., San Jose, CA, USA). The design of the signaling pathways related to iron metabolism, the Fenton reaction, lipid peroxidation, and antioxidant pathways was inspired by the overall concepts and graphical elements from the literature to ensure scientific accuracy and rigor (An et al., 2023).

3 The role of ferroptosis in osteoarthritis

Osteoarthritis (OA) is characterized by pathological changes affecting the entire joint structure, with degenerative alterations in articular cartilage being the primary manifestation (Findlay and Atkins, 2014). These pathological changes are accompanied by bone spur formation, subchondral bone sclerosis, and synovitis. Under abnormal biomechanical and biochemical stimuli, the balance between anabolic and catabolic processes in chondrocytes is disrupted, leading to the characteristic phenotypic changes associated with OA and promoting disease progression. For example, hypertrophic chondrocytes release matrix degradation products and pro-inflammatory mediators, which aggravate cartilage damage and trigger the proliferation of nearby synovial cells and inflammatory responses (Hunter and Bierma-Zeinstra, 2019; Singh et al., 2019). In turn, these proliferating synovial cells release pro-inflammatory mediators that stimulate the expression of matrix-degrading enzymes and other catabolic factors (Hunter and Bierma-Zeinstra, 2019; Singh et al., 2019). The formation of bone spurs at the joint margins is closely linked to cartilage formation and ossification, a process influenced by inflammatory factors and joint overload (Hsia et al., 2018). Additionally, changes in subchondral bone contribute to cartilage destruction, primarily through an imbalance between osteoblastic and osteoclastic activity (Hu Y et al., 2021).

TABLE 1 Ferroptosis-related biological components in osteoarthritis.

Biological components	Mechanism or intervention target	Function	Reference
TfR1	Cellular iron uptake	Mediates endocytosis of transferrin-bound iron	Aisen et al. (1978), Johnsen et al. (2019)
DMT1	Iron transmembrane transport	Transports iron ions into the cytoplasm	Pantopoulos (2004), Feng et al. (2020), Koike et al. (2020)
STEAP3	Iron reduction	Reduces $Fe3^+$ to $Fe2^+$ for cytoplasmic iron pool	Pantopoulos (2004), Feng et al. (2020), Koike et al. (2020)
FPN1	Transmembrane iron export	Exports excess iron out of the cell	Kakhlon and Cabantchik (2002)
NCOA4	Ferritin autophagy	Regulates intracellular iron levels by ferritin degradation	Latunde-Dada (2017)
GPX4	Antioxidant enzyme activity	Protects cells from oxidative damage and ferroptosis by reducing lipid peroxides	Mancias et al. (2014)
System Xc^-	Cystine/glutamate exchange	Mediate's cystine uptake for GSH synthesis	Dixon et al. (2014)
NRF2	Antioxidant gene expression	Regulates antioxidant gene expression under oxidative stress	Xie et al. (2016), Tang et al. (2021)
SOD	Superoxide radicals	Catalyzes the dismutation of superoxide radicals	Cheng et al. (2022)
CAT	Hydrogen peroxide	Decomposes hydrogen peroxide to water and oxygen	Baker et al. (2023)
NADPH	CoQ10 reduction	Reduces CoQ10 to inhibit lipid peroxidation	Frei et al. (1990)
FSP1	NADPH-dependent CoQ10 reduction	Catalyzes NADPH reduction of CoQ10	Frei et al. (1990)
GCH1	BH4 synthesis	Promotes BH4 synthesis to inhibit ferroptosis	Soula et al. (2020), Fanet et al. (2021)
DHFR	BH4 synthesis	Promotes BH4 synthesis, reducing lipid peroxidation	Soula et al. (2020), Fanet et al. (2021)
ACSL4	Promotes lipid peroxidation	Accelerates lipid peroxidation	Kagan et al. (2017)

Recent studies have identified iron overload as a risk factor for osteoarthritis. While research on the relationship between ferroptosis and OA is limited, emerging evidence suggests that ferroptosis plays a crucial role in regulating chondrocyte activity, extracellular matrix degradation, and synovial inflammation, thereby influencing OA progression (Feng et al., 2020; Yao et al., 2021). Elevated iron levels in OA patients' joint tissues may trigger chondrocyte ferroptosis by enhancing oxidative stress and lipid peroxidation (Feng et al., 2020). In elderly female OA patients, higher iron storage levels may be associated with increased iron burden due to estrogen deficiency. Patients with significantly elevated ferritin levels are more prone to severe joint complications, and this increase correlates positively with the severity of arthritis (Morales-Ivorra et al., 2018; Jing et al., 2021a). However, some studies propose a biphasic effect of iron status on OA progression, where iron overload and deficiency increase OA risk (Kennish et al., 2014). This article will explore how ferroptosis impacts various pathological processes in OA, aiming to provide new insights into its prevention and treatment (Figure 2). Figure 2 was created using Adobe Illustrator 2019 (Adobe Inc., San Jose, CA, USA).

3.1 Cartilage degeneration and ferroptosis

A prominent feature of OA is the degeneration and degradation of articular cartilage, closely linked to the metabolic balance of chondrocytes (Zheng et al., 2021). Chondrocytes, the only cellular component of cartilage, maintain the dynamic equilibrium of the extracellular matrix (ECM) through precise regulation of collagen type II and matrix-degrading enzyme secretion (Chang et al., 2022). However, this balance is disrupted during the pathological progression of OA, leading to metabolic imbalances in chondrocytes and consequent cartilage degradation. Ferroptosis is crucial in the loss of chondrocytes associated with this process.

In mouse models of OA, typical characteristics of ferroptosis have been observed in chondrocytes, including abnormal iron metabolism, lipid peroxidation, and mitochondrial dysfunction (Sun et al., 2021). These alterations impair normal chondrocyte function and exacerbate apoptosis and ECM degradation (Sun et al., 2021). Under iron overload conditions, catabolic pathways in chondrocytes are activated, while anabolic pathways are suppressed, destroying the cartilage matrix and progression of OA. In OA models induced by interleukin-1 beta (IL-1β) and ferric ammonium citrate (FAC), hallmark ferroptosis markers such as glutathione peroxidase 4 (GPX4) and solute carrier family seven member 11 (SLC7A11) exhibit significant downregulation, whereas expression levels of the tumor suppressor gene p53 and acyl-CoA synthetase long-chain family member 4 (ACSL4) are elevated (Yao et al., 2021). These findings further corroborate the involvement of ferroptosis in chondrocytes, indicating mechanisms related to lipid peroxidation and oxidative stress imbalance.

Recent studies have highlighted the mediating role of hypoxia-inducible factor 2 alpha (HIF-2α) in chondrocyte ferroptosis, promoting lipid storage and accumulation of lipid peroxidation products. Overexpression of HIF-2α decreases GPX4 levels and facilitates the activity of carnitine palmitoyltransferase 1A

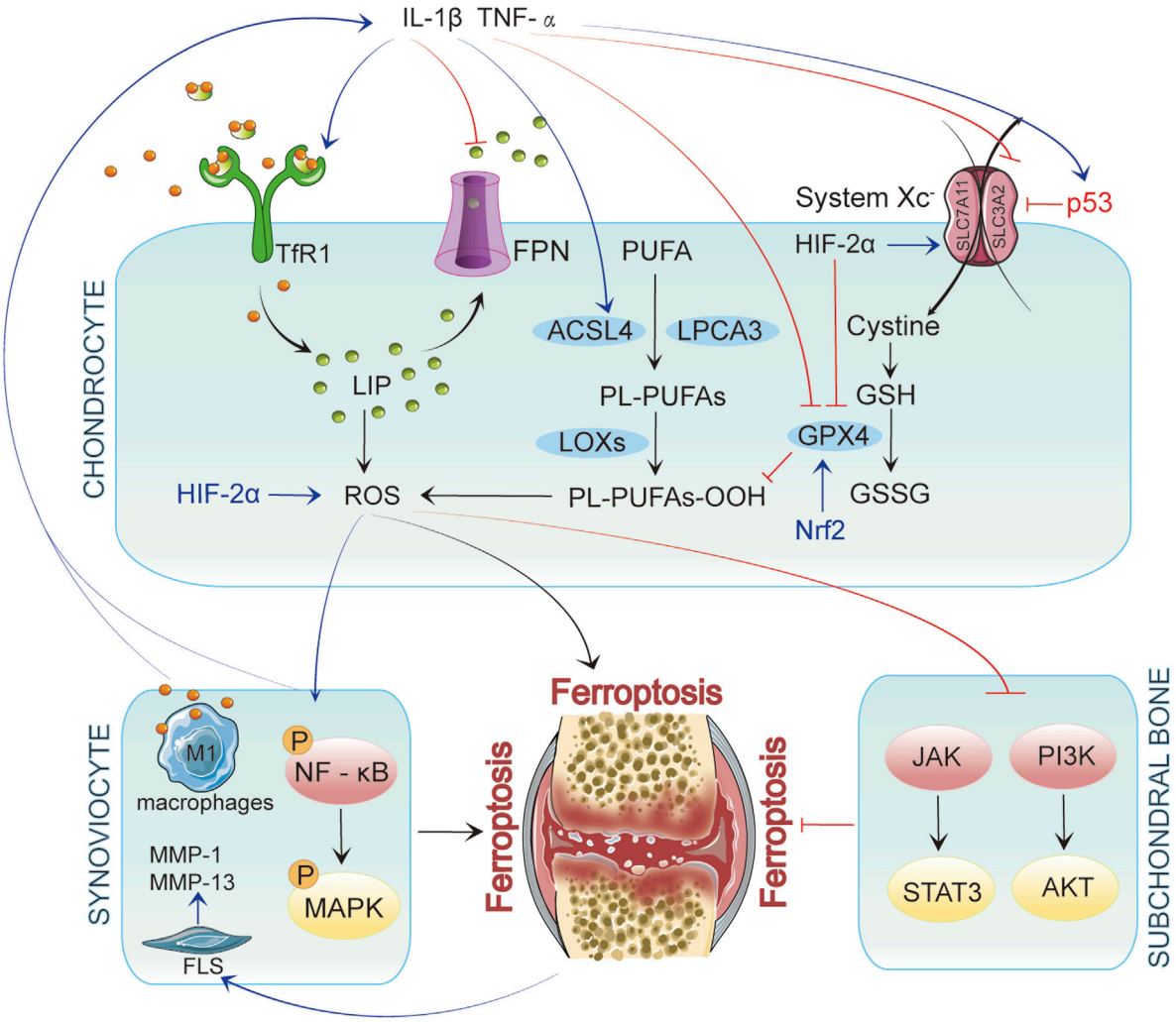

FIGURE 2
In Chondrocytes, ferroptosis is initiated by iron accumulation and lipid peroxidation. When p53 is upregulated, it inhibits System Xc⁻, leading to decreased glutathione levels and reduced GPX4 activity, ultimately resulting in ferroptosis. Inflammatory factors such as IL-1β and TNF-α enhance the generation of reactive oxygen species (ROS) by activating TfR1 and ACSL4 while upregulating p53 expression, further promoting ferroptosis. These inflammatory mediators affect chondrocytes and interact with synovial cells and their microenvironment, exacerbating inflammation in OA. In synovial cells, inflammatory signaling pathways activate NF-κB and MAPK, promoting ferroptosis. Concurrently, iron overload polarizes synovial macrophages to the classical M1 type, leading to increased secretion of inflammatory mediators. This activation of inflammation further drives ferroptosis, which activates fibroblast-like synoviocytes (FLSs) to produce matrix metalloproteinases (MMP-1 and MMP-13), intensifying synovitis and creating a vicious cycle. In subchondral bone, ferroptosis is similarly regulated by multiple signaling pathways, particularly the JAK/STAT3 and PI3K/AKT axes.

(CPT1A), which transports fatty acids into the mitochondrial matrix for β-oxidation, thus aggravating cartilage degeneration (Zhou et al., 2021).

Moreover, inflammatory cytokines have been found to disrupt iron homeostasis in chondrocytes by upregulating transferrin receptor 1 (TfR1) and downregulating the iron transporter ferroportin (FPN), contributing to iron overload (Jing et al., 2020). In OA, This iron overload is closely related to disease progression, as it not only directly induces chondrocyte apoptosis but also accelerates cartilage degradation by upregulating matrix-degrading enzyme expression (Jing et al., 2021a). For instance, iron overload induced by ferric ammonium citrate significantly enhances chondrocyte apoptosis and increases the expression of matrix metalloproteinases (MMP3, MMP13) (Jing et al., 2021a). Furthermore, downregulation of nuclear factor E2-related factor 2 (Nrf2) leads to reduced GPX4 expression, thereby intensifying ferroptosis (Ni et al., 2020; Lu et al., 2022; Yang et al., 2022b). As a key antioxidant transcription factor, Nrf2's interaction with ferroptosis illustrates its critical role in regulating oxidative stress and cellular fate.

Beyond directly disrupting iron homeostasis, ferroptosis further contributes to the pathological progression of OA through additional mechanisms. The roles of HIF-2α, GPX4, and lipid peroxidation in ferroptosis are particularly critical. Ferroptosis damages chondrocytes directly and exacerbates joint injury by inducing local inflammatory responses. For instance, iron overload can enhance chondrocyte catabolism through overactivated NLRP3 inflammasomes, promoting MMP expression and exacerbating cartilage degeneration (Li S et al., 2023).

Recent studies have established a close relationship between ferroptosis and ECM degradation (Wilkinson et al., 2019). The ECM, composed of proteoglycans, collagen, and minerals, is essential for maintaining the biomechanical properties of articular cartilage. However, as chondrocyte function declines, tissue hydration decreases, leading to progressive ECM damage. In the early stages of OA, proliferating chondrocytes disrupt ECM composition, resulting in reduced proteoglycan synthesis and altered matrix permeability and mechanical compliance (Sun et al., 2012). Inflammatory factors and proteases play pivotal roles in ECM degradation. Evidence suggests that iron regulates ECM deposition and remodeling via oxidative stress, indicating its critical role in ECM integrity (Maldonado and Nam, 2013; Wilkinson et al., 2019). Additionally, mechanical injuries, such as joint wear, trigger inflammatory responses in cartilage and synovium, further upregulating the expression of matrix-degrading proteins, accelerating ECM degradation, and promoting OA progression (Maldonado and Nam, 2013). Studies have shown that iron can enhance IL-1β-induced expression of MMP-3 and MMP-13, further facilitating ECM degradation (Maldonado and Nam, 2013). This association with iron accumulation in chondrocytes is characterized by IL-1β upregulating TfR1 and DMT1 while downregulating FPN1, which exacerbates iron overload, disrupts ECM balance, and ultimately leads to cartilage damage (Jing et al., 2020; Jing et al., 2021). While the negative impact of iron overload on ECM has been established, the specific mechanisms by which ferroptosis contributes to ECM degradation remain underexplored. Given that ECM degradation involves inflammation and oxidative stress—key components of ferroptosis—a complex relationship between ferroptosis and ECM degradation warrants further investigation.

In recent years, the roles of oxidative stress and mitochondrial dysfunction in the progression of OA have garnered significant attention (Blanco et al., 2011; Suantawee et al., 2013; Ansari et al., 2020; Wang et al., 2020; Zheng et al., 2021). Excessive iron can induce mitochondrial dysfunction in chondrocytes by producing reactive oxygen species (ROS), thereby promoting the expression of OA catabolic markers (Jing et al., 2021a). However, the implications of iron-induced mitochondrial dysfunction on chondrocyte metabolism require deeper exploration (Jing et al., 2021b). Additionally, studies suggest that the mitochondrial membrane potential in chondrocytes decreases significantly impacts mitochondrial structure and function (Jing et al., 2021b). Under IL-1β stimulation, chondrocyte mitochondrial membrane potential decreases substantially, closely correlating with mitochondrial dysfunction (Chen B. Y et al., 2024). The interconnections among ferroptosis, oxidative stress, and mitochondrial dysfunction in OA cartilage degeneration collectively influence chondrocyte metabolism, ECM balance, and the progression of OA. Nonetheless, these three elements' specific regulatory networks and mechanisms require further elucidation.

3.2 Synovial inflammation and ferroptosis

Synovial inflammation is another critical feature in the pathological progression of OA and may even precede cartilage degeneration (Scanzello and Goldring, 2012). Synovial changes are closely linked to symptoms such as pain and functional impairment. Research suggests that iron homeostasis in synovial tissue is regulated by iron regulatory proteins, revealing a strong link between synovitis, synovial hyperplasia, and iron deposition (Nieuwenhuizen et al., 2013). For instance, in patients with hemophilia, significant deposits of hemosiderin in the periosteum can stimulate fibroblast proliferation, leading to hemophilic synovitis (Wen et al., 2002; Nieuwenhuizen et al., 2013). Synovial lesions mainly impact areas near cartilage degeneration and are marked by synovial lining cell hyperplasia, infiltration of inflammatory cells, neovascularization, and fibrin deposition (Sellam and Berenbaum, 2010).

Recent research progressively highlights the potential role of ferroptosis in synovial cells as a major factor contributing to synovial inflammation. Compared to healthy individuals, OA patients exhibit significantly elevated levels of iron ions in synovial fluid, alongside observable iron deposits in synovial tissue (Yazar et al., 2005). Under conditions of iron overload, macrophages in the synovium polarize into classically activated M1 macrophages (Hakobyan et al., 2004; Nieuwenhuizen et al., 2013; Zhou et al., 2018; Wu et al., 2020). This process is closely associated with ROS production induced by iron overload and p53 acetylation (Stockwell et al., 2017). M1 macrophages secrete pro-inflammatory cytokines such as IL-1β, IL-6, and TNF-α, which trigger further inflammatory responses in the synovium and contribute to cartilage destruction and osteophyte formation, thus exacerbating OA progression (Marchev et al., 2017; Ansari et al., 2020). Ferroptosis induced by iron overload may also disrupt the synovial microenvironment, impairing the function of fibroblast-like synoviocytes (FLS). Ferroptosis can trigger a non-specific immune response, leading to the release of IL-1β, which activates FLS to produce MMP-1 and MMP-13—proteins closely associated with synovial inflammatory responses (Ni et al., 2018; Jing et al., 2021a). Additionally, IL-1β promotes the expression of cyclooxygenase-2 (COX-2) in FLS, enhancing the secretion of prostaglandin E2 (PGE2) and further aggravating synovial inflammation (Tsai et al., 2017).

The release of lipid peroxidation products and oxidative stress signals during ferroptosis activates inflammatory pathways in synovial cells, such as the NF-κB and MAPK pathways, resulting in the release of additional inflammatory factors and creating a vicious cycle (Kumar et al., 2019; Tm et al., 2019; Liu et al., 2022; Lv et al., 2022; Miao et al., 2022). ACSL4 is highly expressed in OA synovial tissue, while the key antioxidant enzyme GPX4 expression is significantly reduced. ACSL4 influences the oxidative-antioxidative balance within cells, promoting ferroptosis, whereas the deficiency of GPX4 exacerbates ferroptosis and associated inflammatory responses (He W et al., 2023; Zheng et al., 2024).

Moreover, an imbalance in the exchange of glutamate and cystine in the System Xc^- transport system inhibits its function, leading to glutathione depletion and indirect suppression of GPX4 activity, thus facilitating ferroptosis. Glutamate may also induce intra-articular inflammatory responses and abnormal pain in OA patients by activating N-methyl-D-aspartic acid (NMDA) receptors, further advancing OA progression (Piepoli et al., 2009).

TABLE 2 Ferroptosis-related biological components in osteoarthritis.

Biological components	Intervention target	Function	Reference
SLC7A11	Antioxidant enzyme system	Inhibits oxidative stress and lipid peroxidation	Yao et al. (2021)
CPT1A	Facilitates fatty acid β-oxidation	Increases lipid oxidation	Zhou et al. (2021)
MMP-1	synovial	Related to synovitis and inflammation	Ni et al. (2018), Jing et al. (2021a)
MMP-13	synovial	Related to synovitis and inflammation	Ni et al. (2018), Jing et al. (2021a)
COX-2	arachidonic acid	Increases prostaglandin E2 secretion	Tsai et al. (2017)
NMDA receptor	OA joint	Triggers inflammation and pain in OA progression	Piepoli et al. (2009)
ROS	Osteoblasts and Osteoclasts	Disrupts bone cell function, leading to abnormal bone remodeling	Stockwell et al. (2017)
HIF-1α	Cartilage Cells (Chondrocytes)	Critical for the growth and survival of chondrocytes, influencing subchondral bone	Fan et al. (2018), Lin et al. (2022)
LncRNA PMAN	SLC7A11 mRNA	Maintains the stability of ferroptosis-regulating gene SLC7A11 mRNA, inhibiting ferroptosis	Fan et al. (2018), Lin et al. (2022)
FOXO3	NF-κB/MAPK signaling pathway	Upregulates antioxidant genes, reduces lipid peroxidation and iron accumulation, protects chondrocytes and ECM	Zhao et al. (2023)
BoNT/A	SLC7A11/GPX4 anti-ferroptosis system	Reduces ROS and iron ion accumulation, restores mitochondrial function	Zeng et al. (2024)

3.3 Subchondral bone remodeling and ferroptosis

Subchondral bone remodeling is a hallmark pathological feature in advanced stages of OA, typically characterized by bone sclerosis and osteophyte formation. Research indicates a close interplay between articular cartilage and subchondral bone. On the one hand, abnormal remodeling and angiogenesis in subchondral bone can destroy articular cartilage. On the other hand, chondrocytes can regulate subchondral bone remodeling through the RANK-RANKL-OPG signaling pathway (Hu Y et al., 2021). Mechanistically, the core of bone remodeling lies in the balance between osteoblasts' bone-forming activity and osteoclasts' bone-resorbing activity (Simao and Cancela, 2021). The death of chondrocytes and the cartilage matrix's degradation can disrupt the cartilage-bone interface's structure, consequently affecting osteoblasts' and osteoclast activity (Miao et al., 2022). In this process, ferroptosis plays several critical roles (Miao et al., 2022).

Studies have shown that iron overload elevates intracellular ROS levels, triggering lipid peroxidation, disrupting redox balance, and altering the bone marrow microenvironment (Cen et al., 2018). This process blocks the JAK/STAT3 and PI3K/AKT signaling pathways, activates the p38-MAPK pathway, and induces G1 cell cycle arrest and autophagy in osteoblasts (Cen et al., 2018). Elevated ROS also promotes osteoclast differentiation via NF-κB, JNK, and ERK signaling, driving abnormal bone remodeling and OA progression (Wang et al., 2018). Furthermore, iron overload can directly impair osteoblasts' and osteoclast functions and alter the bone matrix's composition and structure, facilitating bone sclerosis and osteophyte formation. This abnormal bone remodeling further increases the mechanical burden on the joint, exacerbating OA symptoms (Hu Y et al., 2021).

Additionally, hypoxia-inducible factor 1 (HIF-1) is a key regulator of chondrocyte growth and survival, significantly influencing the state of subchondral bone. Research indicates that HIF-1α-induced long non-coding RNA (lncRNA) PMAN can regulate ferroptosis by maintaining the mRNA stability of the ferroptosis-related gene SLC7A11, inhibiting ferroptosis and contributing to subchondral bone remodeling (Fan et al., 2018; Lin et al., 2022). This interaction affects the progression of osteoarthritis. However, the specific roles of ferroptosis-related genes and miRNAs remain to be explored further, representing a potential direction for future research into ferroptosis.

In conclusion, the biological molecules of ferroptosis involved in this part are shown in Tables 1, 2.

4 Biomarkers related to ferroptosis and clinical prospects in osteoarthritis

Progressive joint pain is a hallmark of osteoarthritis (OA), and treatments aim to alleviate pain and improve joint function. Conventional treatments encompass lifestyle changes, physical therapy, medication, and surgical interventions, with effectiveness depending on disease severity and duration, highlighting the need for individualized treatment. New therapies such as nerve blocks, mesenchymal stem cell injections, platelet-rich plasma injections, and osteoporosis medications like strontium ranelate offer additional options for OA management. However, due to the incomplete understanding of OA's pathogenesis, recognized effective treatment methods remain limited.

Iron homeostasis imbalance, leading to iron overload and subsequent ferroptosis, can damage the synovium, cartilage, and extracellular matrix (ECM), playing a crucial role in OA progression.

Key proteins and genes involved in iron metabolism, lipid peroxidation, and associated signaling pathways may be potential therapeutic targets for OA. Ferroptosis-related molecular biomarkers hold great potential for diagnosing OA, monitoring disease progression, and guiding personalized treatment strategies. The following sections will delve into biomarkers associated with ferroptosis, iron metabolism, lipid peroxidation, and antioxidant defenses, analyzing their clinical application prospects in OA.

4.1 Iron metabolism-related biomarkers and osteoarthritis

4.1.1 Transferrin receptor 1 (TfR1)

TfR1 expression is elevated in OA patients' synovial tissue and chondrocytes, making it a potential early diagnostic marker that reflects disease progression. Its integration with imaging techniques can enhance diagnostic accuracy, facilitating timely intervention. Research on TfR1 has identified several therapeutic interventions. For example, ferristatin II promotes the degradation of TfR1, disrupting Tf-mediated iron delivery and intervening in the pathological processes of OA (Yuewei et al., 2014). Additionally, Biochanin A (BCA) can reduce intracellular iron levels by suppressing TfR1 activity and enhancing the expression of ferroportin (FPN), thereby alleviating mitochondrial damage and chondrocyte apoptosis induced by iron overload (He Q et al., 2023).

Iron chelators represent an effective intervention for patients with excessive TfR1 expression, binding circulating and intracellular iron for excretion via urine or bile, thereby reducing ferroptosis (Di Maggio and Maggio, 2017). Commonly used iron chelators include deferoxamine (DFO), deferiprone (DFP), and deferasirox (DFS) (Rodrigues de Morais and Gambero, 2019). *In vitro* studies have demonstrated that DFO can inhibit the degradation of type II collagen in osteoarthritis cartilage while also reducing the expression of inflammatory factors such as MMP-1, MMP-13, IL-1β, and TNF-α (Tchetina et al., 2016). Furthermore, DFO can restore ferritin levels by inhibiting NCOA4 expression and chelating excess iron to regulate iron homeostasis. These findings indicate that iron chelators regulate iron levels and contribute to managing inflammation associated with OA.

However, existing iron chelators exhibit side effects in clinical applications, including gastrointestinal discomfort, hepatotoxicity, and nephrotoxicity (Guo et al., 2024). Thus, developing novel iron chelators, particularly nanoscale formulations, may represent a future direction to reduce side effects while maintaining or enhancing therapeutic efficacy (Kalanaky et al., 2016). Additionally, the compound White Cardamonin (CAR), derived from Vitex negundo, protects cartilage by mitigating iron overload-induced chondrocyte damage and apoptosis (Li S et al., 2023). CAR activates the SIRT1 pathway and inhibits the p38 MAPK signaling pathway, reducing NLRP3 inflammasome production and alleviating inflammation and cartilage degeneration (Li S et al., 2023). It also reverses the reduction in type II collagen expression and the elevation of MMPs caused by iron overload, thereby mitigating chondrocyte degeneration (Li S et al., 2023).

Based on TfR1-mediated iron uptake and ferroptosis mechanisms, researchers are exploring possibly delaying OA progression by intervening in ferroptosis. Inhibiting TfR1 expression may reduce chondrocyte ferroptosis and diminish synovial inflammation, slowing OA advancement. Currently, ferroptosis inhibitors such as Ferrostatin-1 and Liproxstatin-1 have entered clinical trials, potentially leading to precision treatment strategies that integrate TfR1 detection techniques (Li S et al., 2023).

Despite the promising clinical prospects of TfR1 in OA, challenges remain in its practical application. Future research should further validate the specificity and sensitivity of TfR1 as an early diagnostic marker and develop cost-effective detection technologies. Moreover, multi-omics analyses could help elucidate the interactions between TfR1 and other ferroptosis regulatory molecules, such as GPX4, providing a comprehensive perspective to support personalized treatment strategies.

4.1.2 Divalent metal ion transporter 1 (DMT1)

DMT1 plays a crucial role in the transport of iron ions, and its abnormal expression in OA patients is closely associated with disease progression. Research has shown that the upregulation of DMT1 results in excessive iron accumulation within chondrocytes, increasing the risk of cellular damage (Li S et al., 2023). Research indicates that DMT1 is critical in the progression of osteoarthritis (OA) driven by iron overload; inhibiting DMT1 alleviates IL-1β-induced inflammatory responses and extracellular matrix degradation by significantly suppressing the MAPK and PI3K/AKT/NF-κB signaling pathways (Liu et al., 2024). This finding suggests that regulating the activity of the iron transporter DMT1 could offer a novel therapeutic target for OA.

Implementing DMT1 inhibitors as an intervention strategy demonstrates significant therapeutic potential (Jing et al., 2020). Additionally, multi-target combination strategies are gaining attention. For instance, combining DMT1 inhibitors with antioxidants can yield synergistic effects across multiple pathways. This approach reduces iron ion accumulation, suppresses ferroptosis, and enhances antioxidant defense mechanisms, thereby protecting chondrocytes from oxidative stress damage and effectively slowing OA progression.

4.1.3 Ferritin

Ferritin consists of heavy chain ferritin (FTH1) and light chain ferritin (FTL), and it primarily functions to store intracellular iron, preventing excessive accumulation of free iron and reducing cellular iron toxicity (Arosio et al., 2017). In OA patients, alterations in ferritin expression and stability lead to elevated levels of free iron, heightening the risk of ferroptosis. Studies have shown that in models of iron overload and destabilization of the medial meniscus (DMM)-induced OA, FTH1 expression is significantly elevated, accompanied by increased ferritin levels in the synovial tissue (Yuan et al., 2024). Thus, monitoring changes in both FTH1 and FTL may provide new insights for early OA diagnosis.

Combining the detection of ferritin with other ferroptosis biomarkers, such as TfR1, DMT1, and GPX4, holds promise for enhancing diagnostic sensitivity and accuracy, thereby offering stronger support for early intervention. Additionally, variations in ferritin levels may serve as auxiliary indicators for evaluating the efficacy of antioxidant treatments (Arosio et al., 2017). The concurrent use of antioxidants, such as N-acetylcysteine (NAC),

may improve treatment precision and reduce adverse effects (de Andrade et al., 2015; Li et al., 2022).

Furthermore, ferritin plays a dual role in iron metabolism imbalance; while it helps sequester excess free iron, it may also act as a source of free iron during ferroptosis (Bauckman et al., 2015; Bellelli et al., 2016). Research has identified YL-939, a ferroptosis inhibitor targeting prohibitin 2 (PHB2), which can reduce iron levels in the labile iron pool (LIP) by modulating ferritin expression and uptake (Yang et al., 2022a). Consequently, in future developments of ferroptosis inhibitors, ferritin is anticipated to be a potential target. Its combination with iron chelators and agents that regulate ferritin could further enhance intervention strategies for ferroptosis, providing new avenues for OA treatment.

4.1.4 Ferroportin (FPN)

FPN is mammalian cells' sole iron exporter, pivotal in maintaining intracellular iron homeostasis. Recent studies have highlighted the significance of FPN in regulating ferroptosis. The degradation of FPN, mediated by the E3 ubiquitin ligase RNF217, leads to intracellular iron accumulation, thereby increasing susceptibility to ferroptosis (Jiang et al., 2021). Therefore, maintaining proper FPN function is crucial for preventing iron overload and subsequent ferroptotic cell death in joint tissues.

Therapeutic approaches to prevent FPN degradation may hold promise for mitigating OA progression. For instance, targeting the RNF217-mediated degradation pathway of FPN could help preserve its function, thereby reducing intracellular iron accumulation and the risk of ferroptosis. Additionally, combining such approaches with antioxidants or ferroptosis inhibitors might synergize in protecting chondrocytes and synovial cells from iron-induced damage (Jiang et al., 2021).

Further research is needed to elucidate the precise role of FPN in OA and to develop targeted therapies that modulate its expression or activity. Understanding the interplay between iron metabolism, FPN regulation, and ferroptosis will be essential in devising effective interventions for OA and other iron-related pathologies.

4.1.5 Hepcidin and NCOA4

Hepcidin and NCOA4 play crucial roles in regulating iron homeostasis and ferroptosis, and their abnormal expression is closely linked to the progression of OA (Bellelli et al., 2016; Wang and Babitt, 2019). Hepcidin, a central regulatory hormone in iron metabolism, promotes the degradation of FPN, leading to decreased extracellular iron export and subsequent intracellular iron overload (Wang and Babitt, 2019). This mechanism exacerbates chondrocyte damage associated with ferroptosis in OA patients. Concurrently, NCOA4 mediates the autophagy of ferritin, releasing stored iron and further increasing free iron levels within cells (Bellelli et al., 2016). This process induces oxidative stress and lipid peroxidation, accelerating ferroptosis and driving the progression of OA.

Targeting these mechanisms by inhibiting the activity of hepcidin and NCOA4 offers new therapeutic avenues for OA. Recently, a class of ferroptosis inhibitors that target NCOA4 has been identified. These compounds bind to NCOA4, disrupting its interaction with FTH1 and inhibiting NCOA4-dependent ferritin autophagy, thereby reducing intracellular free iron (Fe^{2+}) levels and suppressing ferroptosis (Fang et al., 2021).

4.2 Lipid peroxidation-related biomarkers and OA

4.2.1 Malondialdehyde (MDA) and 4-Hydroxynonenal (4-HNE)

MDA and 4-HNE are key end products of lipid peroxidation and significant markers of ferroptosis. Their levels are markedly elevated in OA patients' synovial fluid, cartilage, and serum and positively correlate with disease severity. Thus, MDA and 4-HNE are considered effective biomarkers for reflecting the progression of OA (Shah et al., 2005; Mas-Bargues et al., 2021). Studies show that MDA levels significantly increase in IL-1β- or erastin-induced OA mouse models, while 4-HNE and its protein adducts rise in the synovial fluid and chondrocytes of OA patients, underscoring the critical role of lipid peroxidation in OA pathology (Grigolo et al., 2003; Shah et al., 2005; Gladkova, 2022).

Targeting this mechanism, antioxidants like astaxanthin exhibit potential therapeutic effects (Wang et al., 2022a). Astaxanthin mitigates the downregulation of ferroptosis-related proteins induced by IL-1β by downregulating p53 expression, effectively inhibiting chondrocyte ferroptosis (Wang et al., 2022a). Forkhead Box O3 (FOXO3), an important transcription factor, reduces lipid peroxidation and intracellular iron accumulation by upregulating antioxidant genes and inhibiting the NF-κB/MAPK signaling pathway, thereby lessening chondrocyte ferroptosis and ECM degradation (Zhao et al., 2023). *In vitro* experiments indicate that stimulating FOXO3 expression significantly decreases the generation of ferroptosis-related markers like MDA, suggesting its potential to suppress OA progression (Zhao et al., 2023).

Moreover, Tanshinone IIA (Tan IIA) can inhibit lipopolysaccharide (LPS)-induced iron hypersensitivity by lowering iron, reactive oxygen species, and MDA levels while increasing glutathione (GSH) levels (Xu J et al., 2023). These findings suggest that Tan IIA may demonstrate potential clinical value in OA treatment by improving oxidative stress conditions. Recent studies show that naringin (NAR), an active component of grapefruit, possesses significant anti-inflammatory and antioxidant properties (Pan et al., 2022). *In vitro*, NAR has been found to reduce intracellular MDA levels and ROS accumulation while upregulating the antioxidant gene NRF2, indicating its ability to alleviate oxidative stress and chondrocyte damage induced by iron overload (Pan et al., 2022).

As terminal products of lipid peroxidation, MDA and 4-HNE directly reflect the extent of lipid oxidative damage within cells. Therefore, monitoring these biomarkers can aid in the early diagnosis of OA and serve for disease monitoring and prognostic assessment, facilitating the development of more targeted treatment strategies.

4.2.2 Glutathione peroxidase 4 (GPX4)

GPX4 is a crucial enzyme inhibiting ferroptosis, protecting cell membranes from oxidative damage by reducing lipid peroxides. A decline in GPX4 function directly increases the risk of ferroptosis, making its expression changes in OA a significant marker for assessing this risk. Clinically, monitoring GPX4 levels in articular cartilage can enhance the accuracy of early OA diagnosis.

Recent studies have explored therapeutic strategies targeting the GPX4 axis to suppress ferroptosis. For example, icariin (ICA) can

upregulate GPX4 expression, reducing MDA levels and iron content in synovial cells, thereby activating the System Xc^-/GPX4 axis to inhibit ferroptosis and alleviate synovial inflammation (Wang et al., 2016; Xiao et al., 2024). Such research opens possibilities for developing GPX4-based OA treatments (Xiao et al., 2024). Additionally, thiazolidinedione (TZD) drugs selectively inhibit ACSL4 activity, significantly reducing lipid peroxidation and ferroptosis (Doll et al., 2017).

Combining GPX4 with iron chelators, antioxidants, or free radical scavengers such as Fer-1, Lip-1, vitamin E, or edaravone can further enhance its protective effects, reducing lipid oxidative damage and slowing OA progression (Kagan et al., 2017; Homma et al., 2019). Studies indicate that in mild OA patients, using ferroptosis inhibitors like Ferrostatin-1 (Fer-1) can significantly upregulate GPX4 and SLC7A11 expression while downregulating ACSL4 expression, suggesting the potential for early intervention with these inhibitors (Y. Xu Y et al., 2023). However, this regulatory effect weakens in moderate to severe OA patients, indicating that early treatment may be more effective, with additional therapies needed in later stages for optimal results (Xu Y et al., 2023).

In clinical practice, selecting ferroptosis inhibitors or antioxidants based on GPX4 level changes can substantially improve patient outcomes. For patients with markedly reduced GPX4 expression, antioxidants like NAC could enhance antioxidant capacity and delay disease progression. Although GPX4's potential in OA treatment is evident, further validation as a therapeutic target is necessary. Future research should explore GPX4's specific roles in different OA subtypes, developing personalized treatments based on GPX4.

4.2.3 Membrane-bound O-Acyltransferase 1/2 (MBOAT1/2)

MBOAT1/2, as critical membrane-bound O-acyltransferases, functions by incorporating monounsaturated fatty acids (MUFA) into phospholipids, thereby reducing polyunsaturated fatty acids (PUFA) levels. This mechanism decreases the proportion of peroxidation-prone phospholipids, thereby enhancing cellular resistance to ferroptosis. These enzymes have demonstrated potential therapeutic value in mitigating lipid peroxidation and ferroptosis (Liang et al., 2023). Studies have shown that these enzymes are transcriptionally regulated by sex hormone receptors—estrogen receptor (ER) and androgen receptor (AR)—which mediate ferroptosis surveillance independent of GPX4 and FSP1 (Liang et al., 2023).

Postmenopausal women experience a significant decline in estrogen levels, associated with an increased incidence of OA (Parazzini and Progretto Menopausa Italia Study Group, 2003; Herndon, 2004; Høegh-Andersen et al., 2004). Researchers using an ovariectomized rat model found that the decline in estrogen levels significantly increased the metabolic activity of subchondral bone, leading to frequent microdamage and remodeling. This process resulted in increased subchondral bone stiffness, which subsequently altered the local biomechanical environment of the joint, exacerbating cartilage damage and accelerating the progression of OA (Sowers et al., 1996; Wu et al., 2019; Xu et al., 2019; Ziemian et al., 2021). Given the pivotal role of MBOAT1/2 in suppressing oxidative stress and ferroptosis, strategies aimed at restoring their functions may offer therapeutic benefits in addressing joint damage associated with sex hormone deficiencies (Liang et al., 2023). For instance, hormone replacement therapy (HRT) or pharmacological agents mimicking estrogen may enhance the protective role of MBOAT1, thereby inhibiting ferroptosis and lipid peroxidation (Liang et al., 2023).

Targeted therapeutic strategies that regulate MBOAT1/2 activity, particularly for hormone-deficient populations, could serve as a promising approach to delay OA progression. Combining MBOAT1/2-enhancing interventions with antioxidants or ferroptosis inhibitors may yield synergistic effects. Future research should focus on elucidating the specific mechanisms of hormone-MBOAT1/2 interactions in OA treatment and further validating their clinical applications in personalized therapies.

4.2.4 Lipid reactive oxygen species (Lipid-ROS)

Lipid-ROS are reactive oxygen species produced during lipid peroxidation, and their accumulation is a core feature of ferroptosis. In OA, elevated levels of Lipid-ROS are closely linked to chondrocyte death and cartilage degradation. Monitoring Lipid-ROS levels can aid in assessing OA progression and provide a basis for dynamically adjusting treatment strategies.

In the context of ferroptosis regulation, inhibiting Lipid-ROS generation is a crucial therapeutic approach for OA. Ferroptosis inhibitors like Fer-1 and Liproxstatin-1 (Lip-1) effectively reduce the accumulation of Lipid-ROS, thereby inhibiting chondrocyte ferroptosis and delaying OA progression (Skouta et al., 2014; Shah et al., 2017; Guo et al., 2022). While both Lip-1 and Fer-1 operate through similar mechanisms, Lip-1 possesses better pharmacokinetic properties, allowing it to inhibit ferroptosis effectively at lower doses (Wang et al., 2022c). However, these compounds have limitations in solubility and half-life, necessitating further optimization to enhance clinical applicability.

Melatonin has emerged as an important adjunct in combating OA due to its suppressing oxidative stress caused by iron overload (Yang et al., 2017). It inhibits ROS accumulation and protects stem cell osteogenic differentiation and proliferation by modulating signaling pathways like p53, ERK, and p38 (Yang et al., 2017). Other antioxidants also show potential in protecting cartilage by inhibiting Lipid-ROS. For instance, metformin reduces OA cartilage damage by inhibiting lipid peroxidation (Li et al., 2020); NAC prevents osteoblast apoptosis by inhibiting ROS production (Tian et al., 2016); resveratrol effectively reduces bone loss due to its potent antioxidant capabilities (Zhao et al., 2015); and tea polyphenols promote bone formation while reducing bone resorption through their antioxidant and anti-inflammatory properties (Shen et al., 2013). While these antioxidants hold great promise for OA treatment, further studies are required to validate their safety and efficacy before clinical application. Future therapeutic directions should focus on developing more targeted Lipid ROS inhibitors and utilizing advanced imaging techniques to monitor real-time dynamic changes in Lipid ROS levels.

4.3 Antioxidant defense-related biomarkers

4.3.1 Nuclear factor E2-Related factor 2 (Nrf2)

Nrf2 is a key transcription factor that regulates the expression of antioxidant genes, directly influencing a cell's antioxidant capacity.

In OA, one of the core mechanisms of ferroptosis is the imbalance between lipid peroxidation and the antioxidant defense system. Nrf2 can effectively inhibit lipid peroxidation and mitigate cellular damage by regulating the expression of antioxidant enzymes such as GPX4. Therefore, activating Nrf2 offers a potential therapeutic strategy for intervening in ferroptosis in OA.

Studies have shown that Nrf2 activators, such as sulforaphane (SFN), can significantly reduce the generation of lipid peroxidation products by increasing GPX4 levels, thereby alleviating ferroptosis-induced damage to chondrocytes (Calabrese and Kozumbo, 2021; Mahn and Castillo, 2021). As a potent antioxidant, Pyrroloquinoline quinone (PQQ) may also reduce lipid peroxidation, though its direct impact on GPX4 regulation remains further elucidated (Li J et al., 2023). Additionally, ergosterol (ER) has been found to enhance Nrf2 activity, inhibiting molecules related to ferroptosis, such as MMP-9 and MMP-13, which strengthens the cell's resistance to oxidative stress and protects chondrocytes from damage (Cai et al., 2021). Preclinical studies have validated the safety of Nrf2 activators, laying the groundwork for their clinical application in OA.

4.3.2 Superoxide dismutase (SOD) and catalase (CAT)

SOD and CAT are essential enzymes in the antioxidant defense system. SOD converts superoxide anions (O_2^-) into hydrogen peroxide (H_2O_2), which is then decomposed by CAT into water and oxygen, thereby alleviating oxidative stress. In osteoarthritis (OA), the inhibition of the Nrf2 pathway leads to decreased activity levels of SOD and CAT, impairing the antioxidant defense system's ability to eliminate reactive ROS and increasing the risk of ferroptosis effectively. Since SOD and CAT neutralize excess ROS, their reduced activity directly reflects weakened antioxidant capacity and exacerbated ferroptosis.

Therefore, monitoring the activity levels of SOD and CAT can serve as supplementary indicators for assessing the antioxidant defense status and ferroptosis risk in OA patients. The significant roles of SOD and CAT in antioxidant defense and ferroptosis suppression also highlight the therapeutic potential of combining antioxidants with ferroptosis inhibitors. Employing a multi-target intervention strategy that includes anti-inflammatory drugs, antioxidants, and ferroptosis inhibitors can more effectively control oxidative stress and the ferroptosis process.

In terms of personalized treatment, adjusting therapeutic strategies based on the activity levels of SOD and CAT can optimize the suppression of ferroptosis according to the patient's antioxidant capacity. Future research should focus on exploring the regulatory mechanisms of SOD and CAT, particularly on how to restore antioxidant defense capabilities when the Nrf2 pathway is inhibited in order to halt the progression of OA.

4.3.3 Hypoxia-inducible factor - 2α (HIF-2α)

HIF-2α plays a significant role in the progression of OA, particularly in regulating the sensitivity of chondrocytes to ferroptosis. Studies indicate that HIF-2α, upon stimulation by inflammatory factors such as IL-1β, leads to a decrease in GSH levels, thereby increasing chondrocytes' sensitivity to lipid peroxidation and ferroptosis. This process weakens the cellular antioxidant defense, accelerating chondrocyte death and the progression of OA pathology. Research has also shown that supplementing D-mannose can reverse this change, restoring GSH levels and enhancing the expression of GPX4 and SLC7A11, which reduces the occurrence of ferroptosis (Zhou et al., 2021).

The weakening of cellular antioxidant defenses caused by reduced GSH levels accelerates chondrocyte death and drives the progression of OA pathology. Future therapeutic strategies targeting HIF-2α-related pathways to modulate chondrocyte ferroptosis responses may effectively inhibit OA progression. Additionally, the potential of combining HIF-2α with other ferroptosis inhibitors warrants further exploration. By regulating oxidative stress responses within cartilage, combination therapies could more effectively address the sensitivity issues associated with HIF-2α-mediated ferroptosis and suppress OA deterioration. Clinical research should further validate the potential application of HIF-2α in personalized treatment, alongside ferroptosis markers like GPX4, to precisely regulate the survival environment of chondrocytes, advancing and refining OA treatment.

4.3.4 Mitochondrial ferritin (FtMt)

FtMt, localized in mitochondria, is essential for maintaining iron homeostasis by reducing free iron ions and mitigating oxidative stress, thereby inhibiting ferroptosis (Wang et al., 2022b). FtMt deficiency has been shown to cause mitochondrial iron overload and oxidative stress, triggering ferroptosis through enhanced mitophagy (Wang et al., 2022b). In OA, these processes may contribute to cellular damage and disease progression. Ferroptosis inhibitors, such as Fer-1, have demonstrated the potential to alleviate oxidative stress, restore mitochondrial integrity, and reduce lipid peroxidation damage (Chen J et al., 2024). Additionally, significant rescue of IL-1β-induced loss of mitochondrial membrane potential is achieved by inhibiting hypoxia-inducible factor 1α (HIF-1α) or TfR1, indicating that protecting mitochondrial function plays a crucial role in preventing chondrocyte ferroptosis and degeneration (Chen B. Y. et al., 2024). Research has shown that Catalpol, an active component of traditional medicine, can promote mitochondrial biogenesis by inducing the expression of key regulators like PGC-1α, NRF1, and TFAM (Chen et al., 2022). It also enhances the expression of mitochondrial and nuclear DNA, increasing mitochondrial respiration rates and ATP production (Chen et al., 2022). These findings suggest that Catalpol may alleviate oxidative stress and ferroptosis by enhancing mitochondrial function, which could positively influence OA progression. Recent studies indicate that astragalus polysaccharides (APS) can significantly mitigate the damage caused by iron overload to the function of bone marrow mesenchymal stem cells by suppressing ROS levels within mitochondria (F. Yang et al., 2016). These findings further support the therapeutic potential of improving chondrocyte health in OA through mitochondrial function regulation.

In addition to conventional antioxidant and iron regulation strategies, botulinum toxin type A (BoNT/A) has emerged as a promising therapeutic approach for alleviating osteoarthritis (OA) by inhibiting chondrocyte ferroptosis. The mechanisms of BoNT/A include reducing reactive oxygen species (ROS) and iron ion accumulation, restoring mitochondrial function, and activating the SLC7A11/GPX4 anti-ferroptotic pathway (Zeng et al., 2024). Furthermore, the successful application of BoNT/A

TABLE 3 Ferroptosis-related small molecules and drugs in osteoarthritis.

Small molecules or drugs	Intervention target	Function	Reference
Malondialdehyde (MDA)	Cell membrane lipids	Toxic product that damages cell membrane integrity and increases permeability	Grigolo et al. (2003), Shah et al. (2005), Gladkova (2022)
4-Hydroxy-trans-2-nonenal (4-HNE)	Cell membrane lipids	Toxic product that damages cell membrane integrity and increases permeability	Grigolo et al. (2003), Shah et al. (2005), Gladkova (2022)
CoQ10	Mitochondrial respiratory chain, liposomal membranes	Inhibits lipid peroxidation	Frei et al. (1990)
BH4	liposomal membranes	Inhibits lipid peroxidation	Soula et al. (2020), Fanet et al. (2021)
Ferric Ammonium Citrate (FAC)	Cellular iron metabolism and cartilage homeostasis	Enhances iron-induced cell death and cartilage degradation	Yao et al. (2021)
PGE2	FLS	Enhances inflammation response	Tsai et al. (2017)
Ferristatin II	TfR1	Promotes TfR1 degradation and interferes with Tf-mediated iron delivery, intervening in OA pathology	(Cheng et al., 2022)
Biochanin A (BCA)	TfR1, FPN	Inhibits TfR1, promotes FPN expression, reduces intracellular iron concentration, alleviates mitochondrial damage and apoptosis in chondrocytes caused by iron overload	(He Q et al., 2023)
Deferoxamine (DFO)	Iron ions, MMP-1, MMP-13, IL-1β, TNF-α, NCOA4	Inhibits Type II collagen degradation, downregulates inflammatory cytokines, and restores iron homeostasis by chelating excess iron	Tchetina et al. (2016)
Deferiprone (DFP)	Iron ions	Chelates iron to reduce iron levels and prevent ferroptosis	Rodrigues de Morais and Gambero (2019)
Deferasirox (DFS)	Iron ions	Chelates iron to reduce iron levels and prevent ferroptosis	Rodrigues de Morais and Gambero (2019)
White Cardamonin (CAR)	SIRT1, p38MAPK, NLRP3 inflammasome, Type II collagen, MMP	Protects cartilage by reversing iron overload-induced chondrocyte damage and inhibiting apoptosis, reduces cartilage degradation and inflammation	(Li S et al., 2023)
YL-939	PHB2 (Prohibitin 2)	Regulates ferritin expression and phagocytosis to reduce intracellular free iron levels	Yang et al. (2022a)
Astaxanthin	p53 expression	Downregulates p53 expression and reduces ferroptosis-related protein expression	Wang et al. (2022a)
Tanshinone IIA (Tan IIA)	Oxidative stress (iron, ROS, MDA levels)	Reduces iron, ROS, and MDA levels, increases GSH levels, and improves oxidative stress status	(Xu J et al., 2023)
Naringin (NAR)	NRF2 expression	Reduces MDA and ROS accumulation, upregulates NRF2, mitigates oxidative stress	Pan et al. (2022)
Icariin (ICA)	GPX4	Upregulates GPX4 expression, reducing MDA and iron levels, activating System Xc^-/GPX4 axis, inhibiting ferroptosis	(Wang et al., 2016; Xiao et al., 2024)
Thiazolidinedione (TZD)	ACSL4	Selective inhibition of ACSL4 activity, significantly inhibiting lipid peroxidation	Doll et al. (2017)
Ferrostatin-1 (Fer-1)	GPX4, Mitochondrial structure	Inhibits ferroptosis, upregulating GPX4 and SLC7A11, downregulating ACSL4 in mild OA\Restores mitochondrial structure	(Xu Y et al., 2023)
Liproxstatin-1 (Lip-1)	GPX4	Antioxidant enhancing GPX4 protective effects, reducing lipid peroxidation	(Skouta et al., 2014; Shah et al., 2017; Guo et al., 2022)
Vitamin E	GPX4	Antioxidant enhancing GPX4 protective effects, reducing lipid peroxidation	(Kagan et al., 2017; Homma et al., 2019)

(Continued on following page)

TABLE 3 (*Continued*) Ferroptosis-related small molecules and drugs in osteoarthritis.

Small molecules or drugs	Intervention target	Function	Reference
Edaravone	GPX4	Antioxidant enhancing GPX4 protective effects, reducing lipid peroxidation	(Kagan et al., 2017; Homma et al., 2019)
N-acetylcysteine (NAC)	GPX4	Antioxidant enhancing GPX4 protective effects, delaying disease progression	Tian et al. (2016)
Melatonin	p53/ERK/p38	Blocks ROS accumulation and p53/ERK/p38 activation to protect against iron overload-induced osteogenic differentiation dysfunction and senescence	Yang et al. (2017)
Metformin	AMPK	Increased the expression of phosphorylated and total AMPK in articular cartilage tissue	Li et al. (2020)
Resveratrol	FOXO1, OPG/RANKL	Reverses the reduction of Runx2, OCN, and type I collagen caused by excess iron. Upregulates the level of FOXO1. Maintains the antioxidant/prooxidant equilibrium. Reduces the ratio of OPG/RANKL to inhibit osteoclastogenesis	(Zhao et al., 2015)
Tea polyphenols	Runx2, Wnt\caspase-3, RANKL	Promote bone formation by upregulating factors like Runx2 and Wnt, and inhibit bone resorption by reducing caspase-3 and RANKL	Shen et al. (2013)
Pyrroloquinoline quinone (PQQ)	Nrf2	Increases GPX4 levels, reduces lipid peroxidation, and mitigates ferroptosis damage to chondrocytes	(Li J et al., 2023)
Sulforaphane	Nrf2/ARE	Increases GPX4 levels, reduces lipid peroxidation, and mitigates ferroptosis damage to chondrocytes	(Calabrese and Kozumbo, 2021; Mahn and Castillo, 2021)
Ergosterol (ER)	Nrf2	Upregulates Nrf2 activity inhibits ferroptosis-related molecules such as MMP-9 and MMP-13, enhances oxidative stress resistance, and protects chondrocytes	Cai et al. (2021)
D-Mannose	HIF-2β	Restores GSH levels, increases GPX4 and SLC7A11 expression, reducing ferroptosis in chondrocytes	Zhou et al. (2021)
Catalpol	Mitochondrial biogenesis (PGC-1α, NRF1, TFAM)	Promotes mitochondrial DNA and nuclear DNA expression, enhances mitochondrial respiration rate and ATP production	Chen et al. (2022)
Astragalus Polysaccharides (APS)	Mitochondrial ROS levels	Mitigates iron overload-induced damage in bone marrow mesenchymal stem cells	Yang and Stockwell (2016)

in experimental models offers valuable insights into its potential clinical translation in OA treatment. Future studies exploring the detailed mechanisms and long-term effects of BoNT/A may pave the way for precision OA therapy targeting ferroptosis regulation.

In summary, the ferroptosis-related biological molecules discussed in this section are presented in Table 2, while the small molecules and drugs are listed in Table 3.

5 Discussion and perspectives

Osteoarthritis (OA) is a common degenerative condition, marked by gradual progression and associated with high rates of disability, resulting from complex etiological factors that limit effective treatment options. Abnormal iron metabolism significantly impacts bone and joint health, highlighting the importance of maintaining iron homeostasis for the integrity of joint structures. Ferroptosis, a novel form of cell death associated with iron imbalance, reactive oxygen species (ROS) accumulation, and mitochondrial membrane damage, is closely linked to the progression of OA. However, the mechanisms underlying ferroptosis remain complex and not fully elucidated. Extensive research has identified key molecules and pathways in ferroptosis, such as GPX4, iron metabolism, and lipid peroxidation. However, modulating these mechanisms in the complex OA microenvironment across various cell types and tissues remains challenging.

Currently, ferroptosis primarily influences the pathological progression of OA indirectly through iron overload. Future research should focus more on its direct mechanisms. Past studies have predominantly concentrated on cartilage tissue, yet cartilage lacks nerve distribution; thus, pain is more likely associated with vascular and neural invasion in subchondral bone and synovial

inflammation. Future investigations could explore novel therapeutic avenues from the synovium and subchondral bone perspectives.

Current ferroptosis inhibitors like GPX4 agonists and iron chelators show promise in experiments and clinical trials. However, targeting specific cells or tissues remains a challenge. Non-specific treatments may lead to side effects or impair other physiological functions, limiting clinical applicability. Therefore, precisely regulating ferroptosis targets without compromising normal cell functions is a critical challenge for future therapies. Employing multi-omics technologies to identify ferroptosis-related molecular biomarkers, coupled with large-scale clinical trials, will aid in validating the efficacy of ferroptosis inhibitors and promote their clinical application.

Innovative therapeutic strategies targeting ferroptosis are essential. Developing novel ferroptosis inhibitors and intervention methods, such as small molecule drugs, gene therapy, and cell therapy, may offer more effective treatment options for OA in the context of ferroptosis. Embracing the concept of precision medicine through personalized treatment approaches will also be a significant future direction to enhance efficacy and safety. Comprehensive treatment strategies that integrate various therapeutic modalities may yield improved outcomes. Future studies should investigate the combined use of ferroptosis inhibitors with other therapies, such as anti-inflammatory drugs and immunomodulators, to enhance treatment effectiveness.

This review elucidates the molecular mechanisms of ferroptosis in OA and its critical role in disease progression, exploring the impacts of iron metabolism dysregulation, lipid peroxidation, and the collapse of antioxidant defense systems on cartilage degeneration, synovial inflammation, and subchondral bone remodeling. It highlights the potential of key molecules like GPX4, TfR1, and NCOA4 as diagnostic and therapeutic targets. However, this review has limitations, notably its inability to comprehensively cover the specific molecular mechanisms of ferroptosis across different OA subtypes, and it provides limited discussion on the interactions between ferroptosis and other forms of cell death. Future research should deepen the understanding of ferroptosis in various OA subtypes, identify additional key regulatory factors and signaling pathways, and explore the interactions between ferroptosis and other cell death modalities, such as apoptosis and necrosis. Overall, the study of ferroptosis in OA presents vast potential. Through ongoing research and exploration, we anticipate achieving precise regulation of ferroptosis, developing more effective treatment methods, and ultimately providing new solutions for managing OA, thereby improving patients' quality of life and health outcomes.

Author contributions

SL: Conceptualization, Methodology, Visualization, Writing–original draft, Writing–review and editing. ZL: Methodology, Writing–original draft, Writing–review and editing. MQ: Methodology, Writing–original draft, Writing–review and editing. YW: Visualization, Writing–review and editing. LC: Visualization, Writing–review and editing. XB: Writing–review and editing. YJ: Writing–review and editing. XC: Writing–review and editing. JZ: Funding acquisition, Methodology, Project administration, Resources, Supervision, Writing–review and editing.

Funding

The author(s) declare that financial support was received for the research, authorship, and/or publication of this article. This work was supported by a grant from the National Natural Science Foundation of China (No. 82172011).

Acknowledgments

We thank the members of Zhen's research group for providing feedback and help preparing the manuscript.

Conflict of interest

The authors declare that the research was conducted in the absence of any commercial or financial relationships that could be construed as a potential conflict of interest.

Generative AI statement

The author(s) declare that no Generative AI was used in the creation of this manuscript.

Publisher's note

References

Ahola, S., and Langer, T. (2024). Ferroptosis in mitochondrial cardiomyopathy. *Trends Cell Biol.* 34 (2), 150–160. doi:10.1016/j.tcb.2023.06.002

Ai, Y., Yan, B., and Wang, X. (2021). The oxidoreductases POR and CYB5R1 catalyze lipid peroxidation to execute ferroptosis. *Mol. Cell Oncol.* 8 (2), 1881393. doi:10.1080/23723556.2021.1881393

Aierken, Y., He, H., Li, R., Lin, Z., Xu, T., Zhang, L., et al. (2024). Inhibition of Slc39a14/Slc39a8 reduce vascular calcification via alleviating iron overload induced ferroptosis in vascular smooth muscle cells. *Cardiovasc Diabetol.* 23 (1), 186. doi:10.1186/s12933-024-02224-z

Aisen, P., Leibman, A., and Zweier, J. (1978). Stoichiometric and site characteristics of the binding of iron to human transferrin. *J. Biol. Chem.* 253 (6), 1930–1937. doi:10.1016/s0021-9258(19)62337-9

An, F., Zhang, J., Gao, P., Xiao, Z., Chang, W., Song, J., et al. (2023). New insight of the pathogenesis in osteoarthritis: the intricate interplay of ferroptosis and autophagy

mediated by mitophagy/chaperone-mediated autophagy. *Front. Cell Dev. Biol.* 11, 1297024. doi:10.3389/fcell.2023.1297024

Anderson, G. J., and Frazer, D. M. (2017). Current understanding of iron homeostasis. *Am. J. Clin. Nutr.* 106, 1559S-1566S–1566S. doi:10.3945/ajcn.117.155804

Ansari, M. Y., Ahmad, N., and Haqqi, T. M. (2020). Oxidative stress and inflammation in osteoarthritis pathogenesis: role of polyphenols. *Biomed. Pharmacother.* 129, 110452. doi:10.1016/j.biopha.2020.110452

Arosio, P., Elia, L., and Poli, M. (2017). Ferritin, cellular iron storage and regulation. *IUBMB Life* 69 (6), 414–422. doi:10.1002/iub.1621

Baker, A., Lin, C.-C., Lett, C., Karpinska, B., Wright, M. H., and Foyer, C. H. (2023). Catalase: a critical node in the regulation of cell fate. *Free Radic. Biol. Med.* 199, 56–66. doi:10.1016/j.freeradbiomed.2023.02.009

Barnett, R. (2018). Osteoarthritis. *Lancet* 391 (10134), 1985. doi:10.1016/S0140-6736(18)31064-X

Barrera, G., Pizzimenti, S., Ciamporcero, E. S., Daga, M., Ullio, C., Arcaro, A., et al. (2015). Role of 4-hydroxynonenal-protein adducts in human diseases. *Antioxid. Redox Signal* 22 (18), 1681–1702. doi:10.1089/ars.2014.6166

Bauckman, K. A., Owusu-Boaitey, N., and Mysorekar, I. U. (2015). Selective autophagy: xenophagy. *Methods* 75, 120–127. doi:10.1016/j.ymeth.2014.12.005

Beckman, K. B., and Ames, B. N. (1998). The free radical theory of aging matures. *Physiol. Rev.* 78 (2), 547–581. doi:10.1152/physrev.1998.78.2.547

Bell, H. N., Stockwell, B. R., and Zou, W. (2024). Ironing out the role of ferroptosis in immunity. *Immunity* 57 (5), 941–956. doi:10.1016/j.immuni.2024.03.019

Bellelli, R., Federico, G., Matte', A., Colecchia, D., Iolascon, A., Chiariello, M., et al. (2016). NCOA4 deficiency impairs systemic iron homeostasis. *Cell Rep.* 14 (3), 411–421. doi:10.1016/j.celrep.2015.12.065

Berndt, C., Alborzinia, H., Amen, V. S., Ayton, S., Barayeu, U., Bartelt, A., et al. (2024). Ferroptosis in health and disease. *Redox Biol.* 75, 103211. doi:10.1016/j.redox.2024.103211

Bersuker, K., Hendricks, J. M., Li, Z., Magtanong, L., Ford, B., Tang, P. H., et al. (2019). The CoQ oxidoreductase FSP1 acts parallel to GPX4 to inhibit ferroptosis. *Nature* 575 (7784), 688–692. doi:10.1038/s41586-019-1705-2

Blanco, F. J., Rego, I., and Ruiz-Romero, C. (2011). The role of mitochondria in osteoarthritis. *Nat. Rev. Rheumatol.* 7 (3), 161–169. doi:10.1038/nrrheum.2010.213

Cai, D., Yan, H., Liu, J., Chen, S., Jiang, L., Wang, X., et al. (2021). Ergosterol limits osteoarthritis development and progression through activation of Nrf2 signaling. *Exp. Ther. Med.* 21 (3), 194. doi:10.3892/etm.2021.9627

Calabrese, E. J., and Kozumbo, W. J. (2021). The phytoprotective agent sulforaphane prevents inflammatory degenerative diseases and age-related pathologies via Nrf2-mediated hormesis. *Pharmacol. Res.* 163, 105283. doi:10.1016/j.phrs.2020.105283

Cen, W.-J., Feng, Y., Li, S.-S., Huang, L.-W., Zhang, T., Zhang, W., et al. (2018). Iron overload induces G1 phase arrest and autophagy in murine preosteoblast cells. *J. Cell Physiol.* 233 (9), 6779–6789. doi:10.1002/jcp.26405

Chang, X., Kang, Y., Yang, Y., Chen, Y., Shen, Y., Jiang, C., et al. (2022). Pyroptosis: a novel intervention target in the progression of osteoarthritis. *J. Inflamm. Res.* 15, 3859–3871. doi:10.2147/JIR.S368501

Chen B. Y, B. Y., Pathak, J. L., Lin, H. Y., Guo, W. Q., Chen, W. J., Luo, G., et al. (2024). Inflammation triggers chondrocyte ferroptosis in TMJOA via HIF-1α/TFRC. *J. Dent. Res.* 103 (7), 712–722. doi:10.1177/00220345241242389

Chen, D., Chu, B., Yang, X., Liu, Z., Jin, Y., Kon, N., et al. (2021). iPLA2β-mediated lipid detoxification controls p53-driven ferroptosis independent of GPX4. *Nat. Commun.* 12 (1), 3644. doi:10.1038/s41467-021-23902-6

Chen, D., Guo, J., and Li, L. (2022). Catalpol promotes mitochondrial biogenesis in chondrocytes. *Arch. Physiol. Biochem.* 128 (3), 802–808. doi:10.1080/13813455.2020.1727927

Chen J, J., Deng, X., Lin, T., Huang, J., Yang, Y., and Lian, N. (2024). Ferrostatin-1 reversed chronic intermittent hypoxia-induced ferroptosis in aortic endothelial cells via reprogramming mitochondrial function. *Nat. Sci. Sleep.* 16, 401–411. doi:10.2147/NSS.S442186

Chen, X., He, W.-T., Hu, L., Li, J., Fang, Y., Wang, X., et al. (2016). Pyroptosis is driven by non-selective gasdermin-D pore and its morphology is different from MLKL channel-mediated necroptosis. *Cell Res.* 26 (9), 1007–1020. doi:10.1038/cr.2016.100

Chen, Y., Fang, Z.-M., Yi, X., Wei, X., and Jiang, D.-S. (2023). The interaction between ferroptosis and inflammatory signaling pathways. *Cell Death Dis.* 14 (3), 205. doi:10.1038/s41419-023-05716-0

Cheng, Y., Qu, W., Li, J., Jia, B., Song, Y., Wang, L., et al. (2022). Ferristatin II, an iron uptake inhibitor, exerts neuroprotection against traumatic brain injury via suppressing ferroptosis. *ACS Chem. Neurosci.* 13 (5), 664–675. doi:10.1021/acschemneuro.1c00819

Cho, Y., Jeong, S., Kim, H., Kang, D., Lee, J., Kang, S.-B., et al. (2021). Disease-modifying therapeutic strategies in osteoarthritis: current status and future directions. *Exp. Mol. Med.* 53 (11), 1689–1696. doi:10.1038/s12276-021-00710-y

de Andrade, K. Q., Moura, F. A., dos Santos, J. M., de Araújo, O. R. P., de Farias Santos, J. C., and Goulart, M. O. F. (2015). Oxidative stress and inflammation in hepatic diseases: therapeutic possibilities of N-acetylcysteine. *Int. J. Mol. Sci.* 16 (12), 30269–30308. doi:10.3390/ijms161226225

Deng, L., He, S., Guo, N., Tian, W., Zhang, W., and Luo, L. (2023). Molecular mechanisms of ferroptosis and relevance to inflammation. *Inflamm. Res.* 72 (2), 281–299. doi:10.1007/s00011-022-01672-1

Di Maggio, R., and Maggio, A. (2017). The new era of chelation treatments: effectiveness and safety of 10 different regimens for controlling iron overloading in thalassaemia major. *Br. J. Haematol.* 178 (5), 676–688. doi:10.1111/bjh.14712

Dixon, S. J., Lemberg, K. M., Lamprecht, M. R., Skouta, R., Zaitsev, E. M., Gleason, C. E., et al. (2012). Ferroptosis: an iron-dependent form of nonapoptotic cell death. *Cell* 149 (5), 1060–1072. doi:10.1016/j.cell.2012.03.042

Dixon, S. J., and Olzmann, J. A. (2024). The cell biology of ferroptosis. *Nat. Rev. Mol. Cell Biol.* 25 (6), 424–442. doi:10.1038/s41580-024-00703-5

Dixon, S. J., Patel, D. N., Welsch, M., Skouta, R., Lee, E. D., Hayano, M., et al. (2014). Pharmacological inhibition of cystine-glutamate exchange induces endoplasmic reticulum stress and ferroptosis. *Elife* 3, e02523. doi:10.7554/eLife.02523

Dixon, S. J., and Pratt, D. A. (2023). Ferroptosis: a flexible constellation of related biochemical mechanisms. *Mol. Cell* 83 (7), 1030–1042. doi:10.1016/j.molcel.2023.03.005

Doll, S., Proneth, B., Tyurina, Y. Y., Panzilius, E., Kobayashi, S., Ingold, I., et al. (2017). ACSL4 dictates ferroptosis sensitivity by shaping cellular lipid composition. *Nat. Chem. Biol.* 13 (1), 91–98. doi:10.1038/nchembio.2239

Em, H., Jr, G., C, B., C, H., and Ch, L. (2013). Thioredoxins, glutaredoxins, and peroxiredoxins--molecular mechanisms and health significance: from cofactors to antioxidants to redox signaling. *Antioxidants and redox Signal.* 19 (13), 1539–1605. doi:10.1089/ars.2012.4599

Fan, X., Yuan, J., Xie, J., Pan, Z., Yao, X., Sun, X., et al. (2018). Long non-protein coding RNA DANCR functions as a competing endogenous RNA to regulate osteoarthritis progression via miR-577/SphK2 axis. *Biochem. Biophys. Res. Commun.* 500 (3), 658–664. doi:10.1016/j.bbrc.2018.04.130

Fanet, H., Capuron, L., Castanon, N., Calon, F., and Vancassel, S. (2021). Tetrahydrobioterin (BH4) pathway: from metabolism to neuropsychiatry. *Curr. Neuropharmacol.* 19 (5). doi:10.2174/1570159X18666200729103529

Fang, X., Ardehali, H., Min, J., and Wang, F. (2023). The molecular and metabolic landscape of iron and ferroptosis in cardiovascular disease. *Nat. Rev. Cardiol.* 20 (1), 7–23. doi:10.1038/s41569-022-00735-4

Fang, X., Wang, H., Han, D., Xie, E., Yang, X., Wei, J., et al. (2019). Ferroptosis as a target for protection against cardiomyopathy. *Proc. Natl. Acad. Sci. U.S.A.* 116 (7), 2672–2680. doi:10.1073/pnas.1821022116

Fang, Y., Chen, X., Tan, Q., Zhou, H., Xu, J., and Gu, Q. (2021). Inhibiting ferroptosis through disrupting the NCOA4-FTH1 interaction: a new mechanism of action. *ACS Cent. Sci.* 7 (6), 980–989. doi:10.1021/acscentsci.0c01592

Feng, H., Schorpp, K., Jin, J., Yozwiak, C. E., Hoffstrom, B. G., Decker, A. M., et al. (2020). Transferrin receptor is a specific ferroptosis marker. *Cell Rep.* 30 (10), 3411–3423. doi:10.1016/j.celrep.2020.02.049

Findlay, D. M., and Atkins, G. J. (2014). Osteoblast-chondrocyte interactions in osteoarthritis. *Curr. Osteoporos. Rep.* 12 (1), 127–134. doi:10.1007/s11914-014-0192-5

Frank, D., and Vince, J. E. (2019). Pyroptosis versus necroptosis: similarities, differences, and crosstalk. *Cell Death Differ.* 26 (1), 99–114. doi:10.1038/s41418-018-0212-6

Frei, B., Kim, M. C., and Ames, B. N. (1990). Ubiquinol-10 is an effective lipid-soluble antioxidant at physiological concentrations. *Proc. Natl. Acad. Sci. U. S. A.* 87 (12), 4879–4883. doi:10.1073/pnas.87.12.4879

Gammella, E., Recalcati, S., Rybinska, I., Buratti, P., and Cairo, G. (2015). Iron-induced damage in cardiomyopathy: oxidative-dependent and independent mechanisms. *Oxidative Med. Cell. Longev.* 2015, 230182. doi:10.1155/2015/230182

GBD 2021 Osteoarthritis Collaborators (2023). Global, regional, and national burden of osteoarthritis, 1990-2020 and projections to 2050: a systematic analysis for the Global Burden of Disease Study 2021. *Lancet Rheumatol.* 5 (9), e508–e522. doi:10.1016/S2665-9913(23)00163-7

Gladkova, E. V. (2022). Role of imbalance of lipid peroxidation and articular cartilage remodeling in the pathogenesis of early primary and post-traumatic gonarthrosis in rats. *Bull. Exp. Biol. Med.* 172 (4), 415–418. doi:10.1007/s10517-022-05405-6

Graham, F. J., Pellicori, P., Kalra, P. R., Ford, I., Bruzzese, D., and Cleland, J. G. F. (2023). Intravenous iron in patients with heart failure and iron deficiency: an updated meta-analysis. *Eur. J. Heart Fail* 25 (4), 528–537. doi:10.1002/ejhf.2810

Grandi, F. C., and Bhutani, N. (2020). Epigenetic therapies for osteoarthritis. *Trends Pharmacol. Sci.* 41 (8), 557–569. doi:10.1016/j.tips.2020.05.008

Grigolo, B., Roseti, L., Fiorini, M., and Facchini, A. (2003). Enhanced lipid peroxidation in synoviocytes from patients with osteoarthritis. *J. Rheumatol.* 30 (2), 345–347.

Guo, Z., Lin, J., Sun, K., Guo, J., Yao, X., Wang, G., et al. (2022). Deferoxamine alleviates osteoarthritis by inhibiting chondrocyte ferroptosis and activating the Nrf2 pathway. *Front. Pharmacol.* 13. doi:10.3389/fphar.2022.791376

Guo, Z., Lin, Y., Liu, H., Guo, J., Hou, L., Zhang, X., et al. (2024). Deferoxamine alleviates chondrocyte senescence and osteoarthritis progression by maintaining iron homeostasis. *Int. Immunopharmacol.* 139, 112619. doi:10.1016/j.intimp.2024.112619

Haileselassie, B., Mukherjee, R., Joshi, A. U., Napier, B. A., Massis, L. M., Ostberg, N. P., et al. (2019). Drp1/Fis1 interaction mediates mitochondrial dysfunction in septic cardiomyopathy. *J. Mol. Cell Cardiol.* 130, 160–169. doi:10.1016/j.yjmcc.2019.04.006

Hakobyan, N., Kazarian, T., Jabbar, A. A., Jabbar, K. J., and Valentino, L. A. (2004). Pathobiology of hemophilic synovitis I: overexpression of mdm2 oncogene. *Blood* 104 (7), 2060–2064. doi:10.1182/blood-2003-12-4231

Hambright, W. S., Fonseca, R. S., Chen, L., Na, R., and Ran, Q. (2017). Ablation of ferroptosis regulator glutathione peroxidase 4 in forebrain neurons promotes cognitive impairment and neurodegeneration. *Redox Biol.* 12, 8–17. doi:10.1016/j.redox.2017.01.021

He Q, Q., Yang, J., Pan, Z., Zhang, G., Chen, B., Li, S., et al. (2023). Biochanin A protects against iron overload associated knee osteoarthritis via regulating iron levels and NRF2/System xc-/GPX4 axis. *Biomed. Pharmacother.* 157, 113915. doi:10.1016/j.biopha.2022.113915

He W, W., Lin, X., and Chen, K. (2023). Specificity protein 1-mediated ACSL4 transcription promoted the osteoarthritis progression through suppressing the ferroptosis of chondrocytes. *J. Orthop. Surg. Res.* 18 (1), 188. doi:10.1186/s13018-023-03673-0

Henrotin, Y. (2022). Osteoarthritis in year 2021: biochemical markers. *Osteoarthr. Cartil.* 30 (2), 237–248. doi:10.1016/j.joca.2021.11.001

Hermetter, A., Kinnunen, P., and Spickett, C. (2012). Oxidized phospholipids-their properties and interactions with proteins. *Biochim. Biophys. Acta* 1818 (10), 2373. doi:10.1016/j.bbamem.2012.06.009

Herndon, J. H. (2004). Osteoarthritis in women after menopause. *Menopause* 11 (5), 499–501. doi:10.1097/01.gme.0000135244.19596.30

Høegh-Andersen, P., Tankó, L. B., Andersen, T. L., Lundberg, C. V., Mo, J. A., Heegaard, A.-M., et al. (2004). Ovariectomized rats as a model of postmenopausal osteoarthritis: validation and application. *Arthritis Res. Ther.* 6 (2), R169–R180. doi:10.1186/ar1152

Homma, T., Kobayashi, S., Sato, H., and Fujii, J. (2019). Edaravone, a free radical scavenger, protects against ferroptotic cell death *in vitro*. *Exp. Cell Res.* 384 (1), 111592. doi:10.1016/j.yexcr.2019.111592

Hsia, A. W., Emami, A. J., Tarke, F. D., Cunningham, H. C., Tjandra, P. M., Wong, A., et al. (2018). Osteophytes and fracture calluses share developmental milestones and are diminished by unloading. *J. Orthop. Res.* 36 (2), 699–710. doi:10.1002/jor.23779

Hu, Q., Zhang, Y., Lou, H., Ou, Z., Liu, J., Duan, W., et al. (2021). GPX4 and vitamin E cooperatively protect hematopoietic stem and progenitor cells from lipid peroxidation and ferroptosis. *Cell death and Dis.* 12 (7). doi:10.1038/s41419-021-04008-9

Hu, Y., Chen, X., Wang, S., Jing, Y., and Su, J. (2021). Subchondral bone microenvironment in osteoarthritis and pain. *Bone Res.* 9 (1), 20. doi:10.1038/s41413-021-00147-z

Hunter, D. J., and Bierma-Zeinstra, S. (2019). Osteoarthritis. *Lancet* 393 (10182), 1745–1759. doi:10.1016/S0140-6736(19)30417-9

Hunter, D. J., March, L., and Chew, M. (2020). Osteoarthritis in 2020 and beyond: a lancet commission. *Lancet* 396 (10264), 1711–1712. doi:10.1016/S0140-6736(20)32230-3

Ingold, I., Berndt, C., Schmitt, S., Doll, S., Poschmann, G., Buday, K., et al. (2018). Selenium utilization by GPX4 is required to prevent hydroperoxide-induced ferroptosis. *Cell* 172 (3), 409–422. doi:10.1016/j.cell.2017.11.048

Jiang, L., Wang, J., Wang, K., Wang, H., Wu, Q., Yang, C., et al. (2021). RNF217 regulates iron homeostasis through its E3 ubiquitin ligase activity by modulating ferroportin degradation. *Blood* 138 (8), 689–705. doi:10.1182/blood.2020008986

Jing, X., Du, T., Li, T., Yang, X., Wang, G., Liu, X., et al. (2021a). The detrimental effect of iron on OA chondrocytes: importance of pro-inflammatory cytokines induced iron influx and oxidative stress. *J. Cell Mol. Med.* 25 (12), 5671–5680. doi:10.1111/jcmm.16581

Jing, X., Lin, J., Du, T., Jiang, Z., Li, T., Wang, G., et al. (2020). Iron overload is associated with accelerated progression of osteoarthritis: the role of DMT1 mediated iron homeostasis. *Front. Cell Dev. Biol.* 8, 594509. doi:10.3389/fcell.2020.594509

Jing, X., Wang, Q., Du, T., Zhang, W., Liu, X., Liu, Q., et al. (2021b). Calcium chelator BAPTA-AM protects against iron overload-induced chondrocyte mitochondrial dysfunction and cartilage degeneration. *Int. J. Mol. Med.* 48 (4), 196. doi:10.3892/ijmm.2021.5029

Johnsen, K. B., Burkhart, A., Thomsen, L. B., Andresen, T. L., and Moos, T. (2019). Targeting the transferrin receptor for brain drug delivery. *Prog. Neurobiol.* 181, 101665. doi:10.1016/j.pneurobio.2019.101665

Kagan, V. E., Mao, G., Qu, F., Angeli, J. P. F., Doll, S., Croix, C. S., et al. (2017). Oxidized arachidonic and adrenic PEs navigate cells to ferroptosis. *Nat. Chem. Biol.* 13 (1), 81–90. doi:10.1038/nchembio.2238

Kakhlon, O., and Cabantchik, Z. I. (2002). The labile iron pool: characterization, measurement, and participation in cellular processes. *Free Radic. Biol. Med.* 33 (8), 1037–1046. doi:10.1016/S0891-5849(02)01006-7

Kalanaky, S., Hafizi, M., Safari, S., Mousavizadeh, K., Kabiri, M., Farsinejad, A., et al. (2016). TLc-A, the leading nanochelating-based nanochelator, reduces iron overload *in vitro* and *in vivo*. *Int. J. Hematol.* 103 (3), 274–282. doi:10.1007/s12185-015-1932-8

Kennish, L., Attur, M., Oh, C., Krasnokutsky, S., Samuels, J., Greenberg, J. D., et al. (2014). Age-dependent ferritin elevations and HFE C282Y mutation as risk factors for symptomatic knee osteoarthritis in males: a longitudinal cohort study. *BMC Musculoskelet. Disord.* 15, 8. doi:10.1186/1471-2474-15-8

Klausner, R. D., Ashwell, G., van Renswoude, J., Harford, J. B., and Bridges, K. R. (1983). Binding of apotransferrin to K562 cells: explanation of the transferrin cycle. *Proc. Natl. Acad. Sci. U. S. A.* 80 (8), 2263–2266. doi:10.1073/pnas.80.8.2263

Kobayashi, A., Kang, M.-I., Okawa, H., Ohtsuji, M., Zenke, Y., Chiba, T., et al. (2004). Oxidative stress sensor Keap1 functions as an adaptor for Cul3-based E3 ligase to regulate proteasomal degradation of Nrf2. *Mol. Cell Biol.* 24 (16), 7130–7139. doi:10.1128/MCB.24.16.7130-7139.2004

Koike, N., Kota, R., Naito, Y., Hayakawa, N., Matsuura, T., Hishiki, T., et al. (2020). 2-Nitroimidazoles induce mitochondrial stress and ferroptosis in glioma stem cells residing in a hypoxic niche. *Commun. Biol.* 3 (1), 450. doi:10.1038/s42003-020-01165-z

Kolasinski, S. L., Neogi, T., Hochberg, M. C., Oatis, C., Guyatt, G., Block, J., et al. (2020). 2019 American college of rheumatology/arthritis foundation guideline for the management of osteoarthritis of the hand, hip, and knee. *Arthritis Care Res. Hob.* 72 (2), 149–162. doi:10.1002/acr.24131

Kumar, S., Adjei, I. M., Brown, S. B., Liseth, O., and Sharma, B. (2019). Manganese dioxide nanoparticles protect cartilage from inflammation-induced oxidative stress. *Biomaterials* 224, 119467. doi:10.1016/j.biomaterials.2019.119467

Latunde-Dada, G. O. (2017). Ferroptosis: role of lipid peroxidation, iron and ferritinophagy. *Biochim. Biophys. Acta Gen. Subj.* 1861 (8), 1893–1900. doi:10.1016/j.bbagen.2017.05.019

Lei, P., Ayton, S., Appukuttan, A. T., Volitakis, I., Adlard, P. A., Finkelstein, D. I., et al. (2015). Clioquinol rescues Parkinsonism and dementia phenotypes of the tau knockout mouse. *Neurobiol. Dis.* 81, 168–175. doi:10.1016/j.nbd.2015.03.015

Levi, S., Ripamonti, M., Moro, A. S., and Cozzi, A. (2024). Iron imbalance in neurodegeneration. *Mol. Psychiatry* 29 (4), 1139–1152. doi:10.1038/s41380-023-02399-z

Li, J., Zhang, B., Liu, W.-X., Lu, K., Pan, H., Wang, T., et al. (2020). Metformin limits osteoarthritis development and progression through activation of AMPK signalling. *Ann. Rheum. Dis.* 79 (5), 635–645. doi:10.1136/annrheumdis-2019-216713

Li J, J., Zhang, J., Xue, Q., Liu, B., Qin, R., Li, Y., et al. (2023). Pyrroloquinoline quinone alleviates natural aging-related osteoporosis via a novel MCM3-Keap1-Nrf2 axis-mediated stress response and Fbn1 upregulation. *Aging Cell* 22 (9), e13912. doi:10.1111/acel.13912

Li, J.-Y., Feng, Y.-H., Li, Y.-X., He, P.-Y., Zhou, Q.-Y., Tian, Y.-P., et al. (2024). Ferritinophagy: a novel insight into the double-edged sword in ferritinophagy-ferroptosis axis and human diseases. *Cell Prolif.* 57 (7), e13621. doi:10.1111/cpr.13621

Li, Q., Liao, J., Chen, W., Zhang, K., Li, H., Ma, F., et al. (2022). NAC alleviative ferroptosis in diabetic nephropathy via maintaining mitochondrial redox homeostasis through activating SIRT3-SOD2/Gpx4 pathway. *Free Radic. Biol. Med.* 187, 158–170. doi:10.1016/j.freeradbiomed.2022.05.024

Li S, S., He, Q., Chen, B., Zeng, J., Dou, X., Pan, Z., et al. (2023). Cardamonin protects against iron overload induced arthritis by attenuating ROS production and NLRP3 inflammasome activation via the SIRT1/p38MAPK signaling pathway. *Sci. Rep.* 13 (1), 13744. doi:10.1038/s41598-023-40930-y

Liang, D., Feng, Y., Zandkarimi, F., Wang, H., Zhang, Z., Kim, J., et al. (2023). Ferroptosis surveillance independent of GPX4 and differentially regulated by sex hormones. *Cell* 186 (13), 2748–2764.e22. doi:10.1016/j.cell.2023.05.003

Liang, D., Minikes, A. M., and Jiang, X. (2022). Ferroptosis at the intersection of lipid metabolism and cellular signaling. *Mol. Cell* 82 (12), 2215–2227. doi:10.1016/j.molcel.2022.03.022

Lin, Z., Song, J., Gao, Y., Huang, S., Dou, R., Zhong, P., et al. (2022). Hypoxia-induced HIF-1α/lncRNA-PMAN inhibits ferroptosis by promoting the cytoplasmic translocation of ELAVL1 in peritoneal dissemination from gastric cancer. *Redox Biol.* 52, 102312. doi:10.1016/j.redox.2022.102312

Liu, H., Chi, R., Xu, J., Guo, J., Guo, Z., Zhang, X., et al. (2024). DMT1-mediated iron overload accelerates cartilage degeneration in Hemophilic Arthropathy through the mtDNA-cGAS-STING axis. *Biochim. Biophys. Acta Mol. Basis Dis.* 1870 (4), 167058. doi:10.1016/j.bbadis.2024.167058

Liu, X., Wang, T., Wang, W., Liang, X., Mu, Y., Xu, Y., et al. (2022). "Emerging potential therapeutic targets of ferroptosis in skeletal diseases," in *Oxidative medicine and cellular longevity*. Editor L. Luo, 1–19. doi:10.1155/2022/3112388

Loughlin, J. (2022). Translating osteoarthritis genetics research: challenging times ahead. *Trends Mol. Med.* 28 (3), 176–182. doi:10.1016/j.molmed.2021.12.007

Lu, H., Xiao, H., Dai, M., Xue, Y., and Zhao, R. (2022). Britanin relieves ferroptosis-mediated myocardial ischaemia/reperfusion damage by upregulating GPX4 through activation of AMPK/GSK3β/Nrf2 signalling. *Pharm. Biol.* 60 (1), 38–45. doi:10.1080/13880209.2021.2007269

Lv, M., Cai, Y., Hou, W., Peng, K., Xu, K., Lu, C., et al. (2022). The RNA-binding protein SND1 promotes the degradation of GPX4 by destabilizing the HSPA5 mRNA and suppressing HSPA5 expression, promoting ferroptosis in osteoarthritis chondrocytes. *Inflamm. Res.* 71 (4), 461–472. doi:10.1007/s00011-022-01547-5

Mahn, A., and Castillo, A. (2021). Potential of sulforaphane as a natural immune system enhancer: a review. *Molecules* 26 (3), 752. doi:10.3390/molecules26030752

Maldonado, M., and Nam, J. (2013). The role of changes in extracellular matrix of cartilage in the presence of inflammation on the pathology of osteoarthritis. *Biomed. Res. Int.* 2013, 284873. doi:10.1155/2013/284873

Mancias, J. D., Pontano Vaites, L., Nissim, S., Biancur, D. E., Kim, A. J., Wang, X., et al. (2015). Ferritinophagy via NCOA4 is required for erythropoiesis and is regulated by iron dependent HERC2-mediated proteolysis. *Elife* 4, e10308. doi:10.7554/eLife.10308

Mancias, J. D., Wang, X., Gygi, S. P., Harper, J. W., and Kimmelman, A. C. (2014). Quantitative proteomics identifies NCOA4 as the cargo receptor mediating ferritinophagy. *Nature* 509 (7498), 105–109. doi:10.1038/nature13148

Mao, C., Liu, X., Zhang, Y., Lei, G., Yan, Y., Lee, H., et al. (2021). DHODH-mediated ferroptosis defence is a targetable vulnerability in cancer. *Nature* 593 (7860), 586–590. doi:10.1038/s41586-021-03539-7

Mao, X., Liu, K., Shen, S., Meng, L., and Chen, S. (2023). Ferroptosis, a new form of cell death: mechanisms, biology and role in gynecological malignant tumor. *Am. J. Cancer Res.* 13 (7), 2751–2762.

Marchev, A. S., Dimitrova, P. A., Burns, A. J., Kostov, R. V., Dinkova-Kostova, A. T., and Georgiev, M. I. (2017). Oxidative stress and chronic inflammation in osteoarthritis: can NRF2 counteract these partners in crime? *Ann. N. Y. Acad. Sci.* 1401 (1), 114–135. doi:10.1111/nyas.13407

Martel-Pelletier, J., Barr, A. J., Cicuttini, F. M., Conaghan, P. G., Cooper, C., Goldring, M. B., et al. (2016). Osteoarthritis. *Nat. Rev. Dis. Prim.* 2, 16072. doi:10.1038/nrdp.2016.72

Masaldan, S., Clatworthy, S. A. S., Gamell, C., Meggyesy, P. M., Rigopoulos, A.-T., Haupt, S., et al. (2018). Iron accumulation in senescent cells is coupled with impaired ferritinophagy and inhibition of ferroptosis. *Redox Biol.* 14, 100–115. doi:10.1016/j.redox.2017.08.015

Mas-Bargues, C., Escrivá, C., Dromant, M., Borrás, C., and Viña, J. (2021). Lipid peroxidation as measured by chromatographic determination of malondialdehyde. Human plasma reference values in health and disease. *Arch. Biochem. Biophys.* 709, 108941. doi:10.1016/j.abb.2021.108941

Miao, R., Fang, X., Zhang, Y., Wei, J., Zhang, Y., and Tian, J. (2023). Iron metabolism and ferroptosis in type 2 diabetes mellitus and complications: mechanisms and therapeutic opportunities. *Cell Death Dis.* 14 (3), 186. doi:10.1038/s41419-023-05708-0

Miao, Y., Chen, Y., Xue, F., Liu, K., Zhu, B., Gao, J., et al. (2022). Contribution of ferroptosis and GPX4's dual functions to osteoarthritis progression. *EBioMedicine* 76, 103847. doi:10.1016/j.ebiom.2022.103847

Mobasheri, A., Thudium, C. S., Bay-Jensen, A.-C., Maleitzke, T., Geissler, S., Duda, G. N., et al. (2023). Biomarkers for osteoarthritis: current status and future prospects. *Best. Pract. Res. Clin. Rheumatol.* 37 (2), 101852. doi:10.1016/j.berh.2023.101852

Morales-Ivorra, I., Romera-Baures, M., Roman-Viñas, B., and Serra-Majem, L. (2018). Osteoarthritis and the mediterranean diet: a systematic review. *Nutrients* 10 (8), 1030. doi:10.3390/nu10081030

Ni, R., Song, G., Fu, X., Song, R., Li, L., Pu, W., et al. (2020). Reactive oxygen species-responsive dexamethasone-loaded nanoparticles for targeted treatment of rheumatoid arthritis via suppressing the iRhom2/TNF-α/BAFF signaling pathway. *Biomaterials* 232, 119730. doi:10.1016/j.biomaterials.2019.119730

Ni, S., Li, C., Xu, N., Liu, X., Wang, W., Chen, W., et al. (2018). Follistatin-like protein 1 induction of matrix metalloproteinase 1, 3 and 13 gene expression in rheumatoid arthritis synoviocytes requires MAPK, JAK/STAT3 and NF-κB pathways. *J. Cell Physiol.* 234 (1), 454–463. doi:10.1002/jcp.26580

Nieuwenhuizen, L., Schutgens, R. E. G., van Asbeck, B. S., Wenting, M. J., van Veghel, K., Roosendaal, G., et al. (2013). Identification and expression of iron regulators in human synovium: evidence for upregulation in haemophilic arthropathy compared to rheumatoid arthritis, osteoarthritis, and healthy controls. *Haemophilia* 19 (4), e218–e227. doi:10.1111/hae.12208

Ohnishi, T., Iwasaki, N., and Sudo, H. (2022). Causes of and molecular targets for the treatment of intervertebral disc degeneration: a review. *Cells* 11 (3), 394. doi:10.3390/cells11030394

Pan, Z., He, Q., Zeng, J., Li, S., Li, M., Chen, B., et al. (2022). Naringenin protects against iron overload-induced osteoarthritis by suppressing oxidative stress. *Phytomedicine* 105, 154330. doi:10.1016/j.phymed.2022.154330

Pantopoulos, K. (2004). Iron metabolism and the IRE/IRP regulatory system: an update. *Ann. N. Y. Acad. Sci.* 1012, 1–13. doi:10.1196/annals.1306.001

Parazzini, F., and Progretto Menopausa Italia Study Group (2003). Menopausal status, hormone replacement therapy use and risk of self-reported physician-diagnosed osteoarthritis in women attending menopause clinics in Italy. *Maturitas* 46 (3), 207–212. doi:10.1016/s0378-5122(03)00193-2

Piepoli, T., Mennuni, L., Zerbi, S., Lanza, M., Rovati, L. C., and Caselli, G. (2009). Glutamate signaling in chondrocytes and the potential involvement of NMDA receptors in cell proliferation and inflammatory gene expression. *Osteoarthr. Cartil.* 17 (8), 1076–1083. doi:10.1016/j.joca.2009.02.002

Que, X., Hung, M.-Y., Yeang, C., Gonen, A., Prohaska, T. A., Sun, X., et al. (2018). Oxidized phospholipids are proinflammatory and proatherogenic in hypercholesterolaemic mice. *Nature* 558 (7709), 301–306. doi:10.1038/s41586-018-0198-8

Rodrigues de Morais, T., and Gambero, A. (2019). Iron chelators in obesity therapy - old drugs from a new perspective? *Eur. J. Pharmacol.* 861, 172614. doi:10.1016/j.ejphar.2019.172614

Salman, L. A., Ahmed, G., Dakin, S. G., Kendrick, B., and Price, A. (2023). Osteoarthritis: a narrative review of molecular approaches to disease management. *Arthritis Res. Ther.* 25 (1), 27. doi:10.1186/s13075-023-03006-w

Santana-Codina, N., and Mancias, J. D. (2018). The role of NCOA4-mediated ferritinophagy in health and disease. *Pharm. (Basel)* 11 (4), 114. doi:10.3390/ph11040114

Scanzello, C. R., and Goldring, S. R. (2012). The role of synovitis in osteoarthritis pathogenesis. *Bone* 51 (2), 249–257. doi:10.1016/j.bone.2012.02.012

Sellam, J., and Berenbaum, F. (2010). The role of synovitis in pathophysiology and clinical symptoms of osteoarthritis. *Nat. Rev. Rheumatol.* 6 (11), 625–635. doi:10.1038/nrrheum.2010.159

Shah, R., Margison, K., and Pratt, D. A. (2017). The potency of diarylamine radical-trapping antioxidants as inhibitors of ferroptosis underscores the role of autoxidation in the mechanism of cell death. *ACS Chem. Biol.* 12 (10), 2538–2545. doi:10.1021/acschembio.7b00730

Shah, R., Raska, K., and Tiku, M. L. (2005). The presence of molecular markers of *in vivo* lipid peroxidation in osteoarthritic cartilage: a pathogenic role in osteoarthritis. *Arthritis Rheum.* 52 (9), 2799–2807. doi:10.1002/art.21239

Shen, C.-L., Chyu, M.-C., and Wang, J.-S. (2013). Tea and bone health: steps forward in translational nutrition. *Am. J. Clin. Nutr.* 98 (6 Suppl. l), 1694S-1699S–1699S. doi:10.3945/ajcn.113.058255

Simao, M., and Cancela, M. L. (2021). Musculoskeletal complications associated with pathological iron toxicity and its molecular mechanisms. *Biochem. Soc. Trans.* 49 (2), 747–759. doi:10.1042/BST20200672

Singh, P., Marcu, K. B., Goldring, M. B., and Otero, M. (2019). Phenotypic instability of chondrocytes in osteoarthritis: on a path to hypertrophy. *Ann. N. Y. Acad. Sci.* 1442 (1), 17–34. doi:10.1111/nyas.13930

Skouta, R., Dixon, S. J., Wang, J., Dunn, D. E., Orman, M., Shimada, K., et al. (2014). Ferrostatins inhibit oxidative lipid damage and cell death in diverse disease models. *J. Am. Chem. Soc.* 136 (12), 4551–4556. doi:10.1021/ja411006a

Soula, M., Weber, R. A., Zilka, O., Alwaseem, H., La, K., Yen, F., et al. (2020). Metabolic determinants of cancer cell sensitivity to canonical ferroptosis inducers. *Nat. Chem. Biol.* 16 (12), 1351–1360. doi:10.1038/s41589-020-0613-y

Sowers, M. F., Hochberg, M., Crabbe, J. P., Muhich, A., Crutchfield, M., and Updike, S. (1996). Association of bone mineral density and sex hormone levels with osteoarthritis of the hand and knee in premenopausal women. *Am. J. Epidemiol.* 143 (1), 38–47. doi:10.1093/oxfordjournals.aje.a008655

Steiner, J. L., and Lang, C. H. (2017). Etiology of alcoholic cardiomyopathy: mitochondria, oxidative stress and apoptosis. *Int. J. Biochem. Cell Biol.* 89, 125–135. doi:10.1016/j.biocel.2017.06.009

Stockwell, B. R., Friedmann Angeli, J. P., Bayir, H., Bush, A. I., Conrad, M., Dixon, S. J., et al. (2017). Ferroptosis: a regulated cell death nexus linking metabolism, redox biology, and disease. *Cell* 171 (2), 273–285. doi:10.1016/j.cell.2017.09.021

Stockwell, B. R., and Jiang, X. (2020). The chemistry and biology of ferroptosis. *Cell Chem. Biol.* 27 (4), 365–375. doi:10.1016/j.chembiol.2020.03.013

Suantawee, T., Tantavisut, S., Adisakwattana, S., Tanavalee, A., Yuktanandana, P., Anomasiri, W., et al. (2013). Oxidative stress, vitamin e, and antioxidant capacity in knee osteoarthritis. *J. Clin. Diagn Res.* 7 (9), 1855–1859. doi:10.7860/JCDR/2013/5802.3333

Sun, K., Guo, Z., Hou, L., Xu, J., Du, T., Xu, T., et al. (2021). Iron homeostasis in arthropathies: from pathogenesis to therapeutic potential. *Ageing Res. Rev.* 72, 101481. doi:10.1016/j.arr.2021.101481

Sun, X., Ou, Z., Chen, R., Niu, X., Chen, D., Kang, R., et al. (2016). Activation of the p62-Keap1-NRF2 pathway protects against ferroptosis in hepatocellular carcinoma cells. *Hepatology* 63 (1), 173–184. doi:10.1002/hep.28251

Sun, Y., Mauerhan, D. R., Kneisl, J. S., James Norton, H., Zinchenko, N., Ingram, J., et al. (2012). Histological examination of collagen and proteoglycan changes in osteoarthritic menisci. *Open Rheumatol. J.* 6, 24–32. doi:10.2174/1874312901206010024

Tang, D., Chen, X., Kang, R., and Kroemer, G. (2021). Ferroptosis: molecular mechanisms and health implications. *Cell Res.* 31 (2), 107–125. doi:10.1038/s41422-020-00441-1

Tang, Y., Zhuang, Y., Zhao, C., Gu, S., Zhang, J., Bi, S., et al. (2024). The metabolites from traditional Chinese medicine targeting ferroptosis for cancer therapy. *Front. Pharmacol.* 15, 1280779. doi:10.3389/fphar.2024.1280779

Tchetina, E. V., Markova, G. A., Poole, A. R., Zukor, D. J., Antoniou, J., Makarov, S. A., et al. (2016). Deferoxamine suppresses collagen cleavage and protease, cytokine, and

COL10A1 expression and upregulates AMPK and krebs cycle genes in human osteoarthritic cartilage. *Int. J. Rheumatol.* 2016, 6432867. doi:10.1155/2016/6432867

Tian, Q., Wu, S., Dai, Z., Yang, J., Zheng, J., Zheng, Q., et al. (2016). Iron overload induced death of osteoblasts *in vitro*: involvement of the mitochondrial apoptotic pathway. *PeerJ* 4, e2611. doi:10.7717/peerj.2611

Tm, S., B, P., and M, C. (2019). Role of GPX4 in ferroptosis and its pharmacological implication. *Free Radic. Biol. and Med.* 133, 144–152. doi:10.1016/j.freeradbiomed.2018.09.014

Tsai, M.-H., Hsu, L.-F., Lee, C.-W., Chiang, Y.-C., Lee, M.-H., How, J.-M., et al. (2017). Resveratrol inhibits urban particulate matter-induced COX-2/PGE2 release in human fibroblast-like synoviocytes via the inhibition of activation of NADPH oxidase/ROS/NF-κB. *Int. J. Biochem. Cell Biol.* 88, 113–123. doi:10.1016/j.biocel.2017.05.015

Ueda, N., and Takasawa, K. (2018). Impact of inflammation on ferritin, hepcidin and the management of iron deficiency anemia in chronic kidney disease. *Nutrients* 10 (9), 1173. doi:10.3390/nu10091173

Volinsky, R., and Kinnunen, P. K. J. (2013). Oxidized phosphatidylcholines in membrane-level cellular signaling: from biophysics to physiology and molecular pathology. *FEBS J.* 280 (12), 2806–2816. doi:10.1111/febs.12247

von Krusenstiern, A. N., Robson, R. N., Qian, N., Qiu, B., Hu, F., Reznik, E., et al. (2023). Identification of essential sites of lipid peroxidation in ferroptosis. *Nat. Chem. Biol.* 19 (6), 719–730. doi:10.1038/s41589-022-01249-3

Wahida, A., and Conrad, M. (2023). Ferroptosis: under pressure. *Curr. Biol.* 33 (7), R269–R272. doi:10.1016/j.cub.2023.03.009

Wang, C.-Y., and Babitt, J. L. (2019). Liver iron sensing and body iron homeostasis. *Blood* 133 (1), 18–29. doi:10.1182/blood-2018-06-815894

Wang, F., and Min, J. (2021). DHODH tangoing with GPX4 on the ferroptotic stage. *Signal Transduct. Target Ther.* 6 (1), 244. doi:10.1038/s41392-021-00656-7

Wang, F.-S., Kuo, C.-W., Ko, J.-Y., Chen, Y.-S., Wang, S.-Y., Ke, H.-J., et al. (2020). Irisin mitigates oxidative stress, chondrocyte dysfunction and osteoarthritis development through regulating mitochondrial integrity and autophagy. *Antioxidants (Basel)* 9 (9), 810. doi:10.3390/antiox9090810

Wang, H., An, P., Xie, E., Wu, Q., Fang, X., Gao, H., et al. (2017). Characterization of ferroptosis in murine models of hemochromatosis. *Hepatology* 66 (2), 449–465. doi:10.1002/hep.29117

Wang, P., Zhang, F., He, Q., Wang, J., Shiu, H. T., Shu, Y., et al. (2016). Flavonoid compound icariin activates hypoxia inducible factor-1α in chondrocytes and promotes articular cartilage repair. *PLoS One* 11 (2), e0148372. doi:10.1371/journal.pone.0148372

Wang, X., Chen, B., Sun, J., Jiang, Y., Zhang, H., Zhang, P., et al. (2018). Iron-induced oxidative stress stimulates osteoclast differentiation via NF-κB signaling pathway in mouse model. *Metabolism* 83, 167–176. doi:10.1016/j.metabol.2018.01.005

Wang, X., Liu, T., Qiu, C., Yu, S., Zhang, Y., Sheng, Y., et al. (2023). Characterization and role exploration of ferroptosis-related genes in osteoarthritis. *Front. Mol. Biosci.* 10, 1066885. doi:10.3389/fmolb.2023.1066885

Wang, X., Liu, Z., Peng, P., Gong, Z., Huang, J., and Peng, H. (2022a). Astaxanthin attenuates osteoarthritis progression via inhibiting ferroptosis and regulating mitochondrial function in chondrocytes. *Chemico-Biological Interact.* 366, 110148. doi:10.1016/j.cbi.2022.110148

Wang, X. D., Ma, H., Sun, J., Zheng, T., Zhao, P., Li, H., et al. (2022b). Mitochondrial ferritin deficiency promotes osteoblastic ferroptosis via mitophagy in type 2 diabetic osteoporosis. *Biol. Trace Elem. Res.* 200 (1), 298–307. doi:10.1007/s12011-021-02627-z

Wang, Y., Zhang, M., Bi, R., Su, Y., Quan, F., Lin, Y., et al. (2022c). ACSL4 deficiency confers protection against ferroptosis-mediated acute kidney injury. *Redox Biol.* 51, 102262. doi:10.1016/j.redox.2022.102262

Ward, R. J., Zucca, F. A., Duyn, J. H., Crichton, R. R., and Zecca, L. (2014). The role of iron in brain ageing and neurodegenerative disorders. *Lancet Neurology* 13 (10), 1045–1060. doi:10.1016/S1474-4422(14)70117-6

Wen, F.-Q., Jabbar, A. A., Chen, Y.-X., Kazarian, T., Patel, D. A., and Valentino, L. A. (2002). c-myc proto-oncogene expression in hemophilic synovitis: *in vitro* studies of the effects of iron and ceramide. *Blood* 100 (3), 912–916. doi:10.1182/blood-2002-02-0390

Wilkinson, H. N., Upson, S. E., Banyard, K. L., Knight, R., Mace, K. A., and Hardman, M. J. (2019). Reduced iron in diabetic wounds: an oxidative stress-dependent role for STEAP3 in extracellular matrix deposition and remodeling. *J. Invest Dermatol* 139 (11), 2368–2377. doi:10.1016/j.jid.2019.05.014

Wu, C.-L., Harasymowicz, N. S., Klimak, M. A., Collins, K. H., and Guilak, F. (2020). The role of macrophages in osteoarthritis and cartilage repair. *Osteoarthr. Cartil.* 28 (5), 544–554. doi:10.1016/j.joca.2019.12.007

Wu, Y., Kadota-Watanabe, C., Ogawa, T., and Moriyama, K. (2019). Combination of estrogen deficiency and excessive mechanical stress aggravates temporomandibular joint osteoarthritis *in vivo*. *Arch. Oral Biol.* 102, 39–46. doi:10.1016/j.archoralbio.2019.03.012

Xiao, J., Luo, C., Li, A., Cai, F., Wang, Y., Pan, X., et al. (2024). Icariin inhibits chondrocyte ferroptosis and alleviates osteoarthritis by enhancing the SLC7A11/GPX4 signaling. *Int. Immunopharmacol.* 133, 112010. doi:10.1016/j.intimp.2024.112010

Xie, Y., Hou, W., Song, X., Yu, Y., Huang, J., Sun, X., et al. (2016). Ferroptosis: process and function. *Cell Death Differ.* 23 (3), 369–379. doi:10.1038/cdd.2015.158

Xu J, J., Zhi, X., Zhang, Y., and Ding, R. (2023). Tanshinone IIA alleviates chondrocyte apoptosis and extracellular matrix degeneration by inhibiting ferroptosis. *Open Life Sci.* 18 (1), 20220666. doi:10.1515/biol-2022-0666

Xu, X., Li, X., Liang, Y., Ou, Y., Huang, J., Xiong, J., et al. (2019). Estrogen modulates cartilage and subchondral bone remodeling in an ovariectomized rat model of postmenopausal osteoarthritis. *Med. Sci. Monit.* 25, 3146–3153. doi:10.12659/MSM.916254

Xu Y, Y., Yang, Z., Dai, T., Xue, X., Xia, D., Feng, Z., et al. (2023). Characteristics and time points to inhibit ferroptosis in human osteoarthritis. *Sci. Rep.* 13 (1), 21592. doi:10.1038/s41598-023-49089-y

Yan, B., Ai, Y., Sun, Q., Ma, Y., Cao, Y., Wang, J., et al. (2021). Membrane damage during ferroptosis is caused by oxidation of phospholipids catalyzed by the oxidoreductases POR and CYB5R1. *Mol. Cell* 81 (2), 355–369.e10. doi:10.1016/j.molcel.2020.11.024

Yang, F., Yan, G., Li, Y., Han, Z., Zhang, L., Chen, S., et al. (2016). Astragalus polysaccharide attenuated iron overload-induced dysfunction of mesenchymal stem cells via suppressing mitochondrial ROS. *Cell Physiol. Biochem.* 39 (4), 1369–1379. doi:10.1159/000447841

Yang, F., Yang, L., Li, Y., Yan, G., Feng, C., Liu, T., et al. (2017). Melatonin protects bone marrow mesenchymal stem cells against iron overload-induced aberrant differentiation and senescence. *J. Pineal Res.* 63 (3). doi:10.1111/jpi.12422

Yang, J., Hu, S., Bian, Y., Yao, J., Wang, D., Liu, X., et al. (2021). Targeting cell death: pyroptosis, ferroptosis, apoptosis and necroptosis in osteoarthritis. *Front. Cell Dev. Biol.* 9, 789948. doi:10.3389/fcell.2021.789948

Yang, W., Mu, B., You, J., Tian, C., Bin, H., Xu, Z., et al. (2022a). Non-classical ferroptosis inhibition by a small molecule targeting PHB2. *Nat. Commun.* 13 (1), 7473. doi:10.1038/s41467-022-35294-2

Yang, W., Wang, Y., Zhang, C., Huang, Y., Yu, J., Shi, L., et al. (2022b). Maresin1 protect against ferroptosis-induced liver injury through ROS inhibition and Nrf2/HO-1/GPX4 activation. *Front. Pharmacol.* 13, 865689. doi:10.3389/fphar.2022.865689

Yang, W. S., and Stockwell, B. R. (2016). Ferroptosis: death by lipid peroxidation. *Trends Cell Biol.* 26 (3), 165–176. doi:10.1016/j.tcb.2015.10.014

Yao, F., Peng, J., Zhang, E., Ji, D., Gao, Z., Tang, Y., et al. (2023). Pathologically high intraocular pressure disturbs normal iron homeostasis and leads to retinal ganglion cell ferroptosis in glaucoma. *Cell Death Differ.* 30 (1), 69–81. doi:10.1038/s41418-022-01046-4

Yao, X., Sun, K., Yu, S., Luo, J., Guo, J., Lin, J., et al. (2021). Chondrocyte ferroptosis contribute to the progression of osteoarthritis. *J. Orthop. Transl.* 27, 33–43. doi:10.1016/j.jot.2020.09.006

Yazar, M., Sarban, S., Kocyigit, A., and Isikan, U. E. (2005). Synovial fluid and plasma selenium, copper, zinc, and iron concentrations in patients with rheumatoid arthritis and osteoarthritis. *Biol. trace Elem. Res.* 106 (2), 123–132. doi:10.1385/BTER:106:2:123

Yuan, Z., Yang, L., Li, Y., Li, X., Peng, C., Pan, J., et al. (2024). FTH1 protects against osteoarthritis by MAPK pathway inhibition of extracellular matrix degradation. *BMC Musculoskelet. Disord.* 25 (1), 282. doi:10.1186/s12891-024-07411-3

Yuewei, S., Isabel, A., De, C., Mj, M., Af, M., M, T., et al. (2014). Superoxide dismutases and superoxide reductases. *Chem. Rev.* 114 (7), 3854–3918. doi:10.1021/cr4005296

Zeng, L., Liu, Y., Wang, Q., Wan, H., Meng, X., Tu, P., et al. (2024). Botulinum toxin A attenuates osteoarthritis development via inhibiting chondrocyte ferroptosis through SLC7Al1/GPX4 axis. *Biochim. Biophys. Acta Mol. Basis Dis.* 1870 (5), 167215. doi:10.1016/j.bbadis.2024.167215

Zhang, Y., Chen, X., Gueydan, C., and Han, J. (2018). Plasma membrane changes during programmed cell deaths. *Cell Res.* 28 (1), 9–21. doi:10.1038/cr.2017.133

Zhao, C., Sun, G., Li, Y., Kong, K., Li, X., Kan, T., et al. (2023). Forkhead box O3 attenuates osteoarthritis by suppressing ferroptosis through inactivation of NF-κB/MAPK signaling. *J. Orthop. Transl.* 39, 147–162. doi:10.1016/j.jot.2023.02.005

Zhao, L., Wang, Y., Wang, Z., Xu, Z., Zhang, Q., and Yin, M. (2015). Effects of dietary resveratrol on excess-iron-induced bone loss via antioxidative character. *J. Nutr. Biochem.* 26 (11), 1174–1182. doi:10.1016/j.jnutbio.2015.05.009

Zheng, J., and Conrad, M. (2020). The metabolic underpinnings of ferroptosis. *Cell Metab.* 32 (6), 920–937. doi:10.1016/j.cmet.2020.10.011

Zheng, L., Zhang, Z., Sheng, P., and Mobasheri, A. (2021). The role of metabolism in chondrocyte dysfunction and the progression of osteoarthritis. *Ageing Res. Rev.* 66, 101249. doi:10.1016/j.arr.2020.101249

Zheng, Z., Shang, X., Sun, K., Hou, Y., Zhang, X., Xu, J., et al. (2024). P21 resists ferroptosis in osteoarthritic chondrocytes by regulating GPX4 protein stability. *Free Radic. Biol. Med.* 212, 336–348. doi:10.1016/j.freeradbiomed.2023.12.047

Zhou, R., Fu, W., Vasylyev, D., Waxman, S. G., and Liu, C.-J. (2024). Ion channels in osteoarthritis: emerging roles and potential targets. *Nat. Rev. Rheumatol.* 20 (9), 545–564. doi:10.1038/s41584-024-01146-0

Zhou, X., Smith, Q. R., and Liu, X. (2021). Brain penetrating peptides and peptide-drug conjugates to overcome the blood-brain barrier and target CNS diseases. *Wiley Interdiscip. Rev. Nanomed Nanobiotechnol* 13 (4), e1695. doi:10.1002/wnan.1695

Zhou, X., Zheng, Y., Sun, W., Zhang, Z., Liu, J., Yang, W., et al. (2021). D-mannose alleviates osteoarthritis progression by inhibiting chondrocyte ferroptosis in a HIF-2α-dependent manner. *Cell Prolif.* 54 (11), e13134. doi:10.1111/cpr.13134

Zhou, Y., Que, K.-T., Zhang, Z., Yi, Z. J., Zhao, P. X., You, Y., et al. (2018). Iron overloaded polarizes macrophage to proinflammation phenotype through ROS/acetyl-p53 pathway. *Cancer Med.* 7 (8), 4012–4022. doi:10.1002/cam4.1670

Ziemian, S. N., Ayobami, O. O., Rooney, A. M., Kelly, N. H., Holyoak, D. T., Ross, F. P., et al. (2021). Low bone mass resulting from impaired estrogen signaling in bone increases severity of load-induced osteoarthritis in female mice. *Bone* 152, 116071. doi:10.1016/j.bone.2021.116071

Zou, Y., Li, H., Graham, E. T., Deik, A. A., Eaton, J. K., Wang, W., et al. (2020). Cytochrome P450 oxidoreductase contributes to phospholipid peroxidation in ferroptosis. *Nat. Chem. Biol.* 16 (3), 302–309. doi:10.1038/s41589-020-0472-6

frontiers | Frontiers in Cell and Developmental Biology

TYPE Review
PUBLISHED 05 March 2025
DOI 10.3389/fcell.2025.1525294

OPEN ACCESS

EDITED BY
Patrice X. Petit,
Centre National de la Recherche Scientifique (CNRS), France

REVIEWED BY
Adrianna Skoneczna,
Polish Academy of Sciences, Poland
Jing Liu,
University of Pennsylvania, United States
Márcio Simão,
University of Algarve, Portugal

*CORRESPONDENCE
Sixi Zhang,
sixi@jlu.edu.cn

RECEIVED 09 November 2024
ACCEPTED 14 February 2025
PUBLISHED 05 March 2025

CITATION
Zhang Y, Kong F, Li N, Tao L, Zhai J, Ma J and Zhang S (2025) Potential role of SIRT1 in cell ferroptosis.
Front. Cell Dev. Biol. 13:1525294.
doi: 10.3389/fcell.2025.1525294

Potential role of SIRT1 in cell ferroptosis

Yueming Zhang[1], Fanxiao Kong[2], Nan Li[1], Lina Tao[3], Jinghui Zhai[1], Jie Ma[1] and Sixi Zhang[1]*

[1]Department of Clinical Pharmacy, The First Hospital of Jilin University, Jilin, China, [2]State Key Laboratory of Bioactive Substance and Function of Natural Medicines, Institute of Materia Medica, Chinese Academy of Medical Sciences and Peking Union Medical College, Beijing, China, [3]Department of Pharmacy, The First Hospital of Jilin University, Jilin, China

Ferroptosis is a novel form of cell death that uniquely requires iron and is characterized by iron accumulation, the generation of free radicals leading to oxidative stress, and the formation of lipid peroxides, which distinguish it from other forms of cell death. The regulation of ferroptosis is extremely complex and is closely associated with a spectrum of diseases. Sirtuin 1 (SIRT1), a NAD + -dependent histone deacetylase, has emerged as a pivotal epigenetic regulator with the potential to regulate ferroptosis through a wide array of genes intricately associated with lipid metabolism, iron homeostasis, glutathione biosynthesis, and redox homeostasis. This review provides a comprehensive overview of the specific mechanisms by which SIRT1 regulates ferroptosis and explores its potential therapeutic value in the context of multiple disease pathologies, highlighting the significance of SIRT1-mediated ferroptosis in treatment strategies.

KEYWORDS

SIRT1, ferroptosis, molecular mechanisms, therapeutic strategies, various diseases

1 Introduction

Ferroptosis, first identified in 2012, is a unique form of regulated cell death that is distinct from traditional apoptosis, necroptosis, and senescence (Dixon et al., 2012). Cells undergoing ferroptosis typically display shrunken mitochondria, increased mitochondrial membrane density, loss of mitochondrial cristae, reduced mitochondrial membrane potential, and rupture of the outer mitochondrial membrane (Li et al., 2024a; Shan et al., 2024; Lin et al., 2024a). The occurrence of ferroptosis is intricately linked to several critical biochemical processes, including the disruptions in iron homeostasis, limited synthesis of glutathione (GSH), and the accumulation of lipid peroxides (Tian et al., 2024; Cai et al., 2024; Li et al., 2024b; Yang et al., 2024). Excess iron is typically stored in ferritin to prevent it from catalyzing the formation of hydroxyl radicals, which can react with polyunsaturated fatty acids in the cell and plasma membranes. This reaction leads to the generation of a significant amount of lipid reactive oxygen species (ROS), contributing to the cellular demise that is characteristic of ferroptosis. The system XC is pivotal in sustaining cellular GSH levels by mediating the cellular uptake of cystine. GSH acts as a cofactor for antioxidant enzymes such as GPX4, which play a role in the elimination of ROS. These pathways form an interconnected network that safeguards cells against ferroptosis by maintaining a delicate balance between antioxidant defense and the production of reactive species. Ferroptosis s closely related to the occurrence and development of a variety of diseases, such as nervous system diseases,

heart diseases, liver diseases, gastrointestinal diseases, lung diseases, kidney diseases, pancreatic diseases tumors, kidney injury, tumor, etc. By targeting the key components of ferroptosis, disease progression can be slowed, offering promising treatment strategies for many diseases.

Sirtuins (SIRTs), a subset of NAD + -dependent histone deacetylases, are evolutionarily conserved and consist of seven isoforms. Among these, SIRT1-3 have been implicated in the regulation of ferroptosis, with SIRT1 being the most extensively studied. SIRT1 is widely expressed across tissues and organs such as the brain, heart, liver, kidneys, and skeletal muscle, with particularly high expression in tissues vulnerable to oxidative stress and those with high metabolic activity. SIRT1 exhibits diverse subcellular localizations, being found in the nucleus, cytoplasm, or both, depending on the cell type (Sgadari et al., 2023). Structurally, it is composed of 747 amino acid (aa) residues, with both C- and N-terminal domains contributing to its structure and function. The C-terminal domain, comprising 25 aa residues, is crucial for SIRT1's catalytic activity. It forms a hairpin that interacts with the β-sheet of the NAD + -binding domain, while the N-terminal domain enhances the enzyme's activity (Davenport et al., 2014). As a central modulator of ferroptosis, SIRT1 modulates key ferroptosis-related proteins through deacetylation, thereby enhancing cellular resilience against ferroptotic cell death. Its regulatory role has significant implications for the treatment and management of diseases associated with oxidative stress and ferroptosis. Recent studies have highlighted SIRT1's potential in inhibiting ferroptosis by influencing pathways related to glutathione synthesis, antioxidant mechanisms, and the metabolism of lipids and iron. Despite the growing evidence of SIRT1's involvement in ferroptosis, a comprehensive understanding of the regulatory interplay between SIRT1 and ferroptosis signaling pathways is yet to be fully elucidated (Dang et al., 2022; Wang et al., 2021; Qiongyue et al., 2022). In this review, we delve into the current evidence of the functions of SIRT1 in regulating ferroptosis and therapeutic potential in various diseases. We aim to consolidate current understanding and explore the therapeutic implications of targeting SIRT1-mediated ferroptosis, offering insights into its promise as an innovative pathway for developing treatment strategies.

2 Regulation of SIRT1 on ferroptosis

2.1 Redox homeostasis

Reactive oxygen species (ROS) are central to the process of ferroptosis, as they facilitate lipid peroxidation and damage cell membranes. Therefore, regulating ROS levels may be an important strategy for controlling ferroptosis and related diseases. The System XC and GPX4 are vital in maintaining intracellular GSH levels, which are essential for ROS removal. Notably, SIRT1 functions as a sensor of redox changes and plays a critical protective role against ferroptosis by regulating redox homeostasis via Nuclear factor erythroid 2-related factor 2 (Nrf2) and p53 (Liang et al., 2023).

2.1.1 Role of SIRT1- Nrf2 in ferroptosis

Nuclear factor erythroid 2-related factor 2 (Nrf2) is a key transcription factor that maintains redox balance and protects cells from oxidative damage. Accumulating evidence points that Nrf2 upregulation can suppress the initiation of ferroptosis (Bellezza et al., 2012; Sun et al., 2016; Wang et al., 2023a; Lv et al., 2021). SIRT1 modulates various components within the antioxidant system, such as Heme Oxygenase-1(HO-1), glutathione (GSH), catalase (CAT), superoxide dismutase 1(SOD1) and SOD2 through deacetylation of Nrf2 (Zhang et al., 2018; Abukhalil et al., 2025; Xia et al., 2023). Recent studies have illustrated the role of the SIRT1-Nrf2-HO-1 pathway in the regulation of ferroptosis. Wang *et al.* have shown that SIRT1-Nrf2-HO-1 activation attenuated lipid peroxide accumulation and inhibited ferroptosis (Wang et al., 2023a). Another study demonstrated that SIRT1 activation positively regulates the Nrf2/HO-1 pathway, reducing mitochondrial damage and ferroptosis. Furthermore, HO-1 may play a role in modulating GPX4 levels (Xie et al., 2022). Dang et al. pointed that SIRT1 activation may mediate the upregulation of GPX4 levels by Nrf2-HO-1 axis in the alleviation of neuronal injury. Significant strides have been made in recent years to elucidate the protective effects of SIRT1-Nrf2 activation against ferroptosis (Xia et al., 2023; Xie et al., 2022), and further exploration of the underlying regulatory mechanisms is warranted.

2.1.2 Role of SIRT1-p53 in ferroptosis

p53 is a multifunctional protein that plays a crucial role in regulating intracellular levels of reactive oxygen species (ROS) and modulating ferroptosis through targeting downstream molecules (Latunde-Dada, 2017). The complex interplay between SIRT1 and p53 is crucial in managing ferroptosis activation, primarily through inhibition of p53's pro-ferroptotic activity and promotion of p21 and GSH synthesis. First, overexpression of SIRT1 has been shown to repress p53 transcriptional activity, increasing SLC7A11 levels and inhibiting ferroptosis (Ma et al., 2020). Zhao et al. reported that SIRT1 participates in the development of gastric cancer by targeting p53 to regulate ferroptosis (Zhao et al., 2023a). In gastric cancer cells, silencing SIRT1 leads to upregulation of p53 and downregulation of SLC7A11, indicating that SIRT1 suppression promotes ferroptosis. Second, p21, a downstream target of p53, can form a complex with p53 and influence its transcriptional activity. SIRT1 enhances p21 expression by modulating p53 activity, which may contribute to cellular redox balance and ferroptosis resistance by mitigating oxidative stress. Through this pathway, SIRT1 indirectly supports antioxidant defenses, including GSH synthesis, further reducing ferroptosis susceptibility (Gu et al., 2022; Wang et al., 2025). While these findings highlight SIRT1's protective role in ferroptosis regulation via the p53/p21 axis, further research is needed to elucidate its context-specific effects across different disease models.

2.2 Iron homeostasis

Iron homeostasis is crucial for maintaining normal cellular and physiological metabolism. When iron supply is abundant, iron storage protein ferritin synthesis increases to store the excess. Iron (Fe^{2+}) can be oxidized to Fe^{3+} by the ferroxidase hephaestin (Heph) and bind to transferrin (TF) on cell membranes, forming the TF-Fe^{3+} complex, which is facilitated by the presence of apo-Tf. Apo-Tf acts as an iron acceptor molecule, enhancing iron (Fe^{2+}) efflux from cells via ferroportin (FPN1), and thus enhancing iron

export and absorption (Weichhart, 2024). Most intracellular iron is either found in heme-containing and mitochondrial proteins or stored by ferritin as $Fe3^{+}$, preventing iron overload that could lead to oxidative stress. Ferritin plays a vital role in preserving iron balance by storing and releasing iron. However, excessive iron levels can increase the labile iron pool (LIP), elevate intracellular reactive oxygen species (ROS), and lead to the accumulation of lipid peroxides, ultimately promoting ferroptosis. SIRT1 has been shown to influence ferroptosis by regulating iron metabolism. Activation of the SIRT1/Nrf2 pathway, such as by alpha lipoic acid, can modulate iron metabolism and mitigate ferroptosis by up-regulating ferritin and ferritin heavy chain 1 (FTH1), and down-regulating the iron import protein divalent metal transporter 1 (DMT1) (Zheng et al., 2023). Lv et al. demonstrated that suppression of the SIRT1/Nrf2/HO-1/GPX4 pathway and FTH1 protein can exacerbate ferroptosis, underscoring the significance of the SIRT1-Nrf2 signaling pathway in iron metabolism and ferroptosis (Lv et al., 2024). Additionally, SIRT1 activation is linked to altered hepcidin production and increased ferritinophagy, which can suppress ferroptosis and prevent the detrimental effects of elevated cytosolic iron (Su et al., 2021; Tziastoudi et al., 2023). However, Zhou et al. noted an exception to the inhibitory effect of SIRT1 on ferroptosis, where intestinal SIRT1 deficiency improves iron metabolism in ethanol-induced hepatic injury in mice by ameliorating iron dysfunction and alleviating ferroptosis in hepatocytes. This suggests that the role of SIRT1 can be context-dependent (Zhou et al., 2020). In summary, SIRT1 plays a multifaceted role in regulating iron metabolism and influencing ferroptosis. Modulating SIRT1 can protect against ferroptosis by influencing key iron-related proteins and pathways. However, the specific outcomes of SIRT1's actions can vary depending on the cellular context and the type of stress involved. Further research is needed to fully understand the complex interactions between SIRT1, iron metabolism, and ferroptosis, which could potentially lead to the development of novel therapeutic strategies for iron-related diseases.

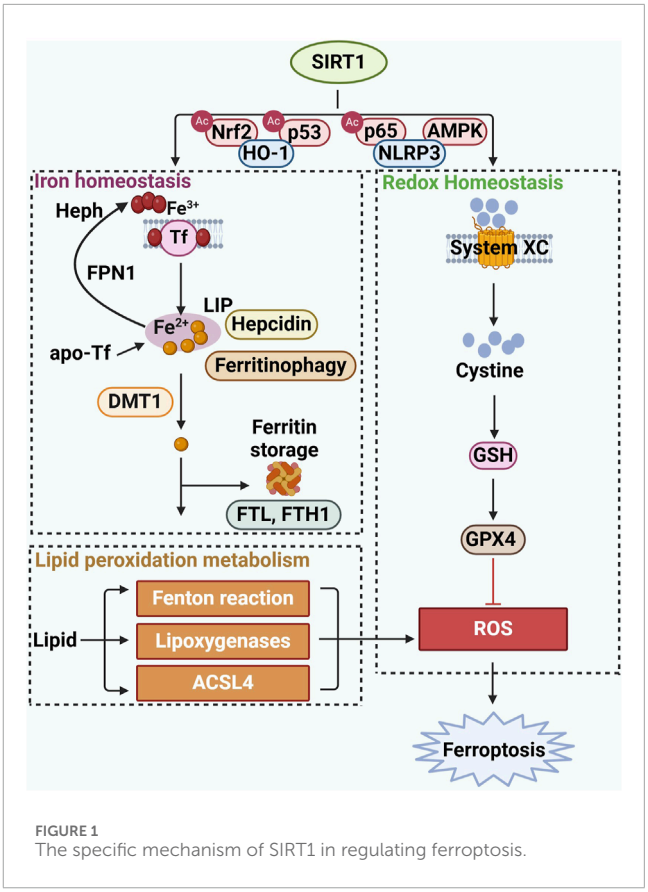

FIGURE 1
The specific mechanism of SIRT1 in regulating ferroptosis.

2.3 Lipid peroxidation metabolism

Iron can exacerbate the accumulation of lipid peroxides by catalyzing Fenton reaction, which in turn disrupts the intracellular redox balance, leading to an attack on biomolecules and ultimately culminating in ferroptosis. SIRT1, a key metabolic factor in energy regulation, can stimulate various endocrine signals related to lipid metabolism. and an increasing number of studies have shown that SIRT1 is involved in endocrine and metabolic diseases (Lu et al., 2023). The long-chain fatty acyl CoA synthetase (ACSLs) family of enzymes, which significantly contributes to lipid metabolism, has been recognized as a crucial regulator in the process of ferroptosis (Dixon et al., 2015). Emerging research suggests that SIRT1 activation may reduce ACSL4 expression levels, potentially alleviating the effects of ferroptosis (Majeed et al., 2021; Wang et al., 2020; Yu et al., 2023a). The work by Chen et al. provides compelling evidence that overexpression of SIRT1 can inhibit lipid peroxidation and decrease malondialdehyde (MDA) levels, a marker of lipid peroxidation. Furthermore, SIRT1 overexpression can reverse the typical upregulation of ACSL4 and acetylated p53, and the downregulation of SLC7A11 and GPX4 observed in ferroptosis, thus inhibiting ferroptotic cell death (Chen et al., 2022a). These findings underscore SIRT1's potential in modulating lipid metabolism and its protective role against ferroptosis. However, the precise mechanisms by which SIRT1 interacts with ACSL4 to regulate ferroptosis remain to be fully understood, indicating a need for further research in this area. This research could pave the way for developing novel therapeutic strategies that target the SIRT1-ACSL4 axis to combat diseases associated with ferroptosis (Figure 1).

2.4 Inflammation

Inflammation and ferroptosis are closely interconnected, with inflammation often promoting ferroptosis through the release of pro-inflammatory cytokines and the induction of oxidative stress. Nuclear Factor kappa B (NF-κB), a key transcription factor, is involved in the regulation of both inflammation and oxidative stress. Upon activation, NF-κB translocates to the nucleus, where it induces the expression of pro-inflammatory and pro-ferroptotic genes, promote iron accumulation and reactive ROS production, leading to lipid peroxidation and ferroptosis (Chen et al., 2024a). By deacetylating the p65 subunit of NF-κB at lysine 310, SIRT1 inhibits its nuclear translocation and transcriptional activity, thereby reducing inflammation, decreasing ROS production and lipid peroxidation, ultimately inhibiting ferroptosis and alleviating cell injury (Min et al., 2025). Conversely, the downregulation of SIRT1 has been shown to activate the NLRP3 inflammasome, leading to the release of pro-inflammatory cytokines like IL-1β and the

subsequent disruption of iron homeostasis. This disruption is characterized by increased lipid peroxidation, and the depletion of key antioxidants such as GPX4 and GSH, further weakening the cellular defense against oxidative stress and rendering cells more susceptible to ferroptosis (Hacioglu, 2024). Additionally, under pathological conditions, SIRT1 activation by adenosine 5′-monophosphate (AMP)-activated protein kinase (AMPK), a key energy sensor that regulates cellular metabolism and stress responses, further attenuates inflammatory signaling. Activation of the AMPK/SIRT1 signaling pathway alleviates the degradation of GSH, thus inhibiting ferroptosis. Selective inhibition of SIRT1 weakens the protective effect of the AMPK/SIRT1 signaling pathway against endoplasmic reticulum stress and ferroptosis (Xu et al., 2023). Restoring the activity of AMPK and SIRT1 can effectively inhibit ferroptosis, providing a potential therapeutic strategy for treating related diseases. Interestingly, SIRT1 inhibition subsequently affects the phosphorylation of AMPK, leading to downstream activation of acetyl-CoA carboxylase, promotes the synthesis of polyunsaturated fatty acids, which serve as substrates for lipid peroxidation and ferroptosis induction (Zhang et al., 2023a). Taken together, these findings underscore the critical role of SIRT1 in modulating inflammation-driven ferroptosis through NF-κB, NLRP3 and AMPK signaling. Enhancing SIRT1 activity could serve as a potential therapeutic strategy for mitigating ferroptosis-associated diseases by reducing inflammation, preserving antioxidant defenses, and regulating lipid metabolism. Further studies are warranted to fully elucidate the therapeutic potential of targeting the SIRT-mediated inflammation in ferroptosis-related pathologies.

3 SIRT1-mediated ferroptosis and disease

3.1 Neuro diseases

Studies have delineated the neuroprotective role of SIRT1 in various pathological conditions, including early brain injury following subarachnoid hemorrhage. SIRT1's role in ferroptosis within brain injury is primarily through the regulation of cellular oxidative stress and iron metabolic balance. By deacetylating a variety of key proteins, SIRT1 enhances the antioxidant capacity of cells, reduces the production of ROS, and inhibits lipid peroxidation, thus alleviating the damage caused by ferroptosis to nerve cells (Hao et al., 2022; Conde et al., 2023; Xie et al., 2022; Liang et al., 2023; Guo et al., 2022). SIRT1 activation also helps to maintain homeostasis of intracellular iron ions, prevent Fenton reaction induced by excess iron ions, and reduce oxidative DNA damage and protein degeneration. Furthermore, SIRT1 inhibits ferroptosis and protects nerve cells from oxidative stress by promoting the expression of antioxidant enzymes like glutathione peroxidase 4 (GPX4) and activating pathways such as Nrf2/HO-1 and ferroptosis suppressor protein 1 (FSP1), playing a vital role in neuroprotection and repair post-brain injury (Liu et al., 2023; Yuan et al., 2022; Chen et al., 2024b; Zhang et al., 2024a). Additionally, SIRT1-mediated ferroptosis is significant in neurodegenerative diseases and cognitive disorders, with activation of the SIRT1/Nrf2 pathway shown to inhibit oxidative stress and ferroptosis, improving cognitive function (Chen et al., 2023a). Treatments such as propofol, ketogenic diets, mesenchymal stem cell-derived exosomes, and components like ferulate acid from traditional Chinese medicine have demonstrated potential in reducing hippocampal neuron ferroptosis and improving cognitive function by enhancing the SIRT1/Nrf2/GPX4 pathway (Wen et al., 2024; Yang et al., 2022; Liu et al., 2022; Wang et al., 2023b; Yan et al., 2024). miR-30a-5p also regulates ferroptosis by targeting SIRT1, affecting cognitive dysfunction in conditions like chronic cerebral hypoperfusion (Wang et al., 2024a). In neurodegenerative diseases such as Friedreich's ataxia and Parkinson's disease, SIRT1 activation helps maintain cellular iron balance, reducing oxidative stress and lipid peroxidation via Nrf2, GPX4 and FTH1, thereby protecting neurons from damage caused by ferroptosis (Lv et al., 2024; Zheng et al., 2023; Sanz-Alcázar et al., 2024). The therapeutic potential of targeting the SIRT1/Nrf2/HO-1/GPX4 pathway is further supported by research indicating that edaravone, a widely used anesthetic, mitigates depression and anxiety by inhibiting ferroptosis through this pathway (Dang et al., 2022; Shen et al., 1826). In gliomas, SIRT1-mediated ferroptosis plays a key role by finely regulating intracellular iron metabolism, redox balance, and autophagy processes. Activation of SIRT1 can enhance the antioxidant capacity of cells by deacetylating key proteins such as Nrf2 and p53, reduce the production of ROS, and inhibit lipid peroxidation, protecting nerve cells from the damage caused by ferroptosis by regulating proteins related to iron metabolism and antioxidant defense mechanisms such as Nrf2, GPX4, and FTH1. Moreover, SIRT1 activates transcription factor activating transcription factor 3 (ATF3) through its interaction with active regulator and regulation of NAD + levels, thereby inhibiting the expression of SLC7A11 and GPX4, promoting the accumulation of iron ions and lipid peroxides in cells, and aggravating ferroptosis (Chen et al., 2024c; Sun et al., 2022). Collectively, targeting SIRT1 in neuro diseases offers promising therapeutic avenues. SIRT1 activators such as resveratrol, SRT1720, and SRT2104 have been shown to alleviate neurodegenerative disease symptoms by reducing oxidative stress, enhancing autophagy flux, and promoting neuronal survival (Su et al., 2021; Zhu et al., 2022; Bai et al., 2023; Rao et al., 2024). In addition, propofol, ketogenic diet, mesenchymal stem cell-derived exosomes, and the traditional Chinese medicine were able to reduce ferroptosis in hippocampal neurons and improve cognitive function (Wen et al., 2024; Yang et al., 2022; Liu et al., 2022; Wang et al., 2023b; Yan et al., 2024). These findings underscore the multifaceted role of SIRT1 in the regulation of ferroptosis and highlight its therapeutic potential value in the treatment of neuro diseases, providing a scientific basis for the development of new therapies targeting SIRT1-mediated ferroptosis (Figure 2).

3.2 Liver diseases

SIRT1 is a pivotal regulator of ferroptosis in liver disease, playing a crucial role in maintaining hepatic health. In human acute liver failure tissue, SIRT1 levels are diminished, however, its activation can mitigate cell damage by modulating the ferroptosis and pyroptosis processes in hepatocytes through the regulation of the p53/GPX4/GSDMD and Nrf2/p53 signaling pathway, thereby

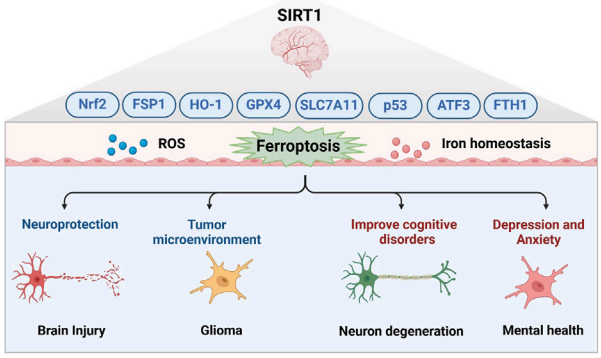

FIGURE 2
The potential of SIRT1-mediated ferroptosis in neuroprotection and disease treatment.

exerting a protective effect on the liver (Zhou et al., 2024a). In a mouse model of sepsis-induced liver failure, the upregulation of SIRT1 indicates a potential role in safeguarding hepatocytes from ferroptosis, lessening liver damage, and enhancing the clinical prognosis for liver failure (Chen et al., 2022b). Furthermore, SIRT1 activators such as salidroside and ulinastatin, as well as therapeutic agents like rosa rugosa and dihydroquercetin, have been shown to significantly ameliorate liver pathological changes associated with ferroptosis by reducing oxidative stress and inflammatory responses, thus safeguarding liver cells (Wang et al., 2021; Xu et al., 2023; Lei et al., 2023; Zeng et al., 2024a). In the pathogenesis of non-alcoholic steatohepatitis (NASH), SIRT1 expression levels inversely correlate with disease progression, hinting at a significant regulatory function in ferroptosis. Activation of SIRT1 has been shown to boost the expression of antioxidant genes by deacetylating and activating Nrf2, subsequently mitigates cell damage caused by oxidative stress and dysregulated iron metabolism. SIRT1 may also curb ferroptosis in NASH by modulating other molecular pathways associated with ferroptosis, such as inhibiting lipid peroxidation and fostering iron metabolic equilibrium, offering new potential targets for NASH treatment (He et al., 2023; Yang et al., 2023). Interestingly, contrary to the hepatoprotective effects of SIRT1 activation, the loss of intestinal SIRT1 in mice shields them from ethanol-induced inflammation and liver damage by reducing liver ferroptosis. Targeting intestinal SIRT1 or alleviating ferroptosis signals in the liver may offer promising avenues for the treatment of human alcoholic liver disease (Zhou et al., 2020). Collectively, SIRT1 activation has emerged as a key therapeutic strategy. SIRT1 activators such as salidroside, ulinastatin, rosa rugosa and dihydroquercetin, have been shown to significantly improve liver pathological changes associated with ferroptosis by reducing oxidative stress and inflammatory responses (Wang et al., 2021; Xu et al., 2023; Lei et al., 2023; Zeng et al., 2024a). Interestingly, targeting intestinal SIRT1 has also been proposed as a novel approach for treating alcoholic liver disease by reducing liver ferroptosis. The findings above indicate that SIRT1-targeted therapies could serve as innovative approaches for treating various liver diseases by modulating ferroptosis pathways.

3.3 Lung diseases

Studies have shown that SIRT1-mediated ferroptosis plays a key role in lung injury. In acute lung injury (ALI) caused by heat attack, activation of SIRT1 has been shown to ameliorate ferroptosis in alveolar epithelial cells under heat stress. This activation alleviates the damage to the alveolar capillary barrier and maintains the barrier function of pulmonary microvascular endothelial cells, suggesting that the SIRT1/p53 axis plays a crucial role in regulating ferroptosis in ALI (Chen et al., 2022a). In lipopolysaccharide (LPS) -induced ALI, activation of SIRT1 by Meteorin-like/Meteorin-β and fibroblast growth factor (FGF) reduces ferroptosis and protects lung tissue by inhibiting p53 acetylation and Nrf2 (Chen et al., 2023b; Lin et al., 2024b). In ALI induced by sepsis, SIRT1 plays a role in inhibiting ferroptosis by activating the NADPH oxidase 4 signaling pathway, which reduces the production of ROS and the level of lipid peroxidation, and maintains the balance of iron metabolism in cells. The overexpression of growth differentiation factor 11 (GDF11) further inhibits ferroptosis by promoting the activity of SIRT1, providing a new molecular target and therapeutic strategy for treating sepsis related ALI (Wu et al., 2024). Moreover, quercetin has shown the potential to inhibit ferroptosis and alleviate ALI by activating SIRT1/Nrf2/GPX4 signaling pathway, providing a new strategy for the treatment of ALI (Deng et al., 2023). The role of SIRT1 in ALI is mainly realized by regulating oxidative stress and iron metabolism balance. By activating SIRT1, iron death can be effectively inhibited, inflammatory response and lung tissue injury can be alleviated. In addition, activation of SIRT1 by small molecule compounds, natural products, Meteorin-like/Meteorin-β, or upregulation of GDF11 may be potential strategies for the treatment of ALI. These studies provide an important scientific basis for the development of novel therapies for ALI.

3.4 Heart diseases

Bioinformatics analysis has identified SIRT1 as a key gene associated with myocardial infarction, with its role in ferroptosis being particularly significant (Jiang et al., 2022). During myocardial ischemia-reperfusion, SIRT1 activation can inhibit ferroptosis and reduce cardiac cell death, thereby protecting cardiac function. SIRT1 also interacts with Nicotinamide phosphoribosyltransferase (NAMPT) and PTEN-induced putative kinase 1 (PINK1)/Parkinson disease protein 2 (Parkin) signaling pathways to maintain mitochondrial homeostasis and promote mitochondrial autophagy, which is critical for preventing ferroptosis and myocardial damage (Ma et al., 2020; Liao et al., 2023; Ju et al., 2023). In patients with sepsis-induced cardiomyopathy (SIC), lower serum levels of GPX4 and SIRT1, along with higher levels of Creatine Kinase-Muscle/Brain (CK-MB), cardiac troponin I (cTnI), tumor necrosis factor-alpha (TNF-α), and interleukin-6 (IL-6), have been observed. Experiments showed that quercetin can reduce intracellular $Fe2^{+}$ and prostaglandin-endoperoxide synthase 2 (PTGS2) levels, decrease the apoptosis rate, and upregulate GPX4 and ferritin levels by activating the SIRT1/p53/SLC7A11 signaling pathway. This action inhibits ferroptosis in H9C2 cells *in vitro* and alleviates SIC *in vivo* in a dose-dependent manner, suggesting a potential treatment strategy for SIC (Lin et al., 2023). In doxorubicin (DOX)-induced

cardiomyopathy models, SIRT1 downregulation exacerbates ferroptosis in cardiomyocytes, while its activation reduces oxidative stress and inhibits ferroptosis by increasing the expression of antioxidant enzymes such as GPX4. Furthermore, SIRT1 enhances cellular antioxidant response through activation of Nrf2/Kelch-like ECH-associated protein 1(Keap1) signaling pathway, thus protecting cardiomyocytes from DOX-induced damage (Wang et al., 2023a; Abdel-Rahman et al., 2022; Yarmohammadi et al., 2024). SIRT1 also inhibits ferroptosis through p53-SLC7A11/GPX4 pathway, protects cardiomyocytes, and improves cardiac function in Type 1 Diabetes Mellitus (Tang et al., 2024). Icariin has been shown to protect against ethanol-induced atrial remodeling by activating the SIRT1 signaling pathway, reducing atrial ferroptosis, and inhibiting atrial fibrosis and oxidative stress. However, the protective effect of icariin is countered by the ferroptosis activator erastin and the SIRT1 inhibitor EX527 (Yu et al., 2023a). In heart failure models, SIRT1-mediated ferroptosis plays a crucial role in the pathogenesis, with AKG improving cardiac dysfunction through mitochondrial autophagy and ferroptosis inhibition mediated by the NAD + -SIRT1 signaling pathway (Yu et al., 2024). SIRT1 activation has been shown to inhibit ferroptosis in cardiomyocytes by reducing the acetylation of p53 protein, maintaining the stability of SLC7A11 protein, and increasing intracellular GSH and GPX4 levels, thereby reducing oxidative stress and lipid peroxidation (Tang et al., 2024). Natural compounds such as resveratrol and pterostilbene have shown inhibition of ferroptosis in cardiomyocytes via the SIRT1/p53 and SIRT1/Glycogen Synthase Kinase-3β (GSK-3β)/GPX4 signaling pathways, improving cardiac function and reducing cardiac remodeling in heart failure models (Zhang et al., 2023b; Zhang et al., 2024b). Natural compounds such as quercetin, icariin, resveratrol and pterostilbene reduce oxidative stress, inhibit ferroptosis of cardiomyocytes, and improve heart function by activating the SIRT1 signaling pathway (Lin et al., 2023; Yu et al., 2023a; Zhang et al., 2023b; Zhang et al., 2024b). Therefore, the regulation of SIRT1 and its associated signaling pathways not only provides insight into the molecular mechanisms of various heart diseases, but also provides potential targets for the development of new therapeutic strategies (Figure 3).

3.5 Kidney disease

Recent studies have highlighted the key role of SIRT1-mediated ferroptosis in multiple kidney diseases. In contrast induced nephropathy (CIN), SIRT1 activated by calorie restriction was able to reduce kidney damage via the modulation GPX4 (Fang et al., 2021). In sepsis associated acute kidney injury (SA-AKI), the exercise hormone irisin mitigates ferroptosis and kidney damage through the SIRT1/Nrf2 signaling pathway (Qiongyue et al., 2022). In Polymyxin B (PMB) -induced acute kidney injury, baicalein activated SIRT1 by reducing p53 acetylation level, thereby inhibiting ferroptosis (Yu et al., 2023b). In cisplatin-induced renal toxicity, gastrodin inhibits ferroptosis through SIRT1/FOXO3A/GPX4 signaling pathway and protects the kidney from damage (Qiu et al., 2024). The water extract of earthworms alleviates oxidative stress-induced renal cell death by enhancing SIRT1/Nrf2 signaling pathways and improving mitochondrial function (Shu et al., 2024). Baicalein, gastrodin and extract of earthworms alleviates renal cell ferroptosis induced by oxidative stress by enhancing SIRT1/Nrf2 signaling pathway and improving mitochondrial function (Yu et al., 2023b; Qiu et al., 2024; Shu et al., 2024). These researches suggest that ferroptosis can be effectively inhibited by regulating SIRT1 and its associated signaling pathways, providing a new therapeutic strategy for the treatment of kidney diseases caused by different causes.

3.6 Bone health

SIRT1 plays an important role in maintaining bone health by regulating ferroptosis. In disc degeneration, the SIRT1-autophagy axis may protect disc cells by inhibiting ferroptosis caused by oxidative stress (Zhou and Ruan, 2022). Moreover, in primary osteoporosis, SIRT1 is recognized as a pivotal gene linked to ferroptosis, with its expression levels potentially influencing bone metabolism and the viability of bone cells (Xia et al., 2022). Consequently, SIRT1's role extends to Type 2 diabetic osteoporosis, where vitamin K2 promotes bone mass by activating the adenosine monophosphate-activated protein kinase (AMPK)/SIRT1 signaling pathway to suppress ferroptosis. Similarly, in postmenopausal osteoporosis, the Chinese herbal ingredient icariin is believed to have therapeutic benefits by targeting multiple ferroptosis-related pathways, including the modulation of SIRT1 (Huang et al., 2024; Wang et al., 2024b; Jin et al., 2023; Jing et al., 2019; Schluesener and Schluesener, 2014). In osteoarthritis, by deacetylating key proteins, SIRT1 activates the antioxidant response element (ARE), thereby upregulating the expression of antioxidant genes such as Nrf2, HO-1, and GPX4. This activation enhances the cellular defense against oxidative stress and suppresses the iron-mediated ROS production, which are pivotal in the pathogenesis of osteoarthritis. Consequently, the SIRT1/Nrf2 signaling axis emerges as a critical pathway in maintaining chondrocyte integrity and attenuating the degenerative processes in the joint, offering a potential therapeutic strategy for managing osteoarthritis (Zhan et al., 2023; Zhang et al., 2024c; Sun et al., 2023; Ruan et al., 2023). Together, SIRT1 activation has shown potential in maintaining bone health by inhibiting ferroptosis. Vitamin K2 and icariin have been demonstrated to promote bone mass and protect bone cells from oxidative damage by activating the AMPK/SIRT1 and SIRT1/Nrf2 pathways, respectively (Jin et al., 2023; Jing et al., 2019; Schluesener and Schluesener, 2014). These findings highlight SIRT1's central role in regulating ferroptosis, protecting bone cells from oxidative damage, and maintaining bone health.

3.7 Cancer

SIRT1-mediated ferroptosis is increasingly recognized as a pivotal factor in diverse cancer treatment strategies. Bioinformatics analysis has revealed a significant association between SIRT1 and ferroptosis in both hepatocellular carcinoma (HCC), gastric cancer and Ewing's sarcoma, highlighting its potential as a therapeutic target in these diseases (Sui et al., 2019; Niu et al., 2023; Jiao et al., 2023). In HCC, SIRT1 inhibition by protocadherin 20 promotes ferroptosis via reducing the expression of SLC7A11, GPX4 and GSH, while increasing MDA, ROS and intracellular iron levels,

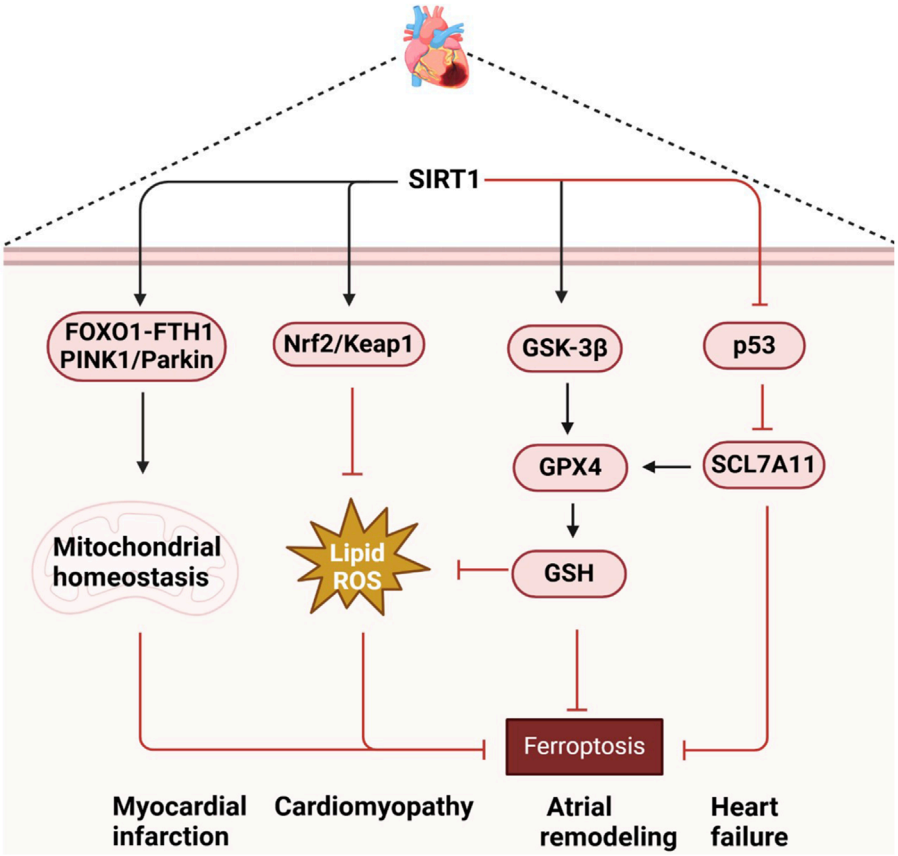

FIGURE 3
Mechanistic insights and therapeutic implications of SIRT1-mediated ferroptosis in cardiac diseases.

resulting in a significant decrease in cell viability, colony-forming ability, and the growth and size of tumor (Jun et al., 2023). In the context of gastric cancer, SIRT1 collaborates with APE1 to stimulate cancer cell ferroptosis by repressing p53, thereby curbing cancer cell proliferation (Zhao et al., 2023a). Furthermore, the loss of long non-coding RNA DACT3-AS1 in exosomes derived from cancer-associated fibroblasts (CAFs) promotes gastric tumor malignant transformation and oxaliplatin resistance by affecting the miR-181a-5p/SIRT1 axis, a process involved in the regulation of ferroptosis (Qu et al., 2023). In addition, in colorectal cancer, ropivacaine enhances cisplatin sensitivity by inhibiting SIRT1 expression, an effect achieved in part by promoting ferroptosis (Zeng et al., 2024b). In melanoma studies, ubiquitin specific peptidase 22 controls melanoma metastasis and sensitivity to ferroptosis through the SIRT1/phosphatase and tensin homolog deleted on chromosome 10 (PTEN)/phosphoinositol-3 kinase (PI3K) signaling pathway, suggesting that activation of the SIRT1 pathway may enhance melanoma cells' sensitivity to ferroptosis (Sun et al., 2024). In the study of lung adenocarcinoma, high doses of β-nicotinamide mononucleotide promote ferroptosis and inhibit lung cancer cell growth through the excess nicotinamide-mediated SIRT1/AMPK/acetyl-coA carboxylase (ACC) signaling pathway (Zhang et al., 2023a). In head and neck cancer, the activation of SIRT1 facilitates the epithelial-mesenchymal transition (EMT), thereby enhancing cancer cells' susceptibility to ferroptosis. Conversely, the inhibition of SIRT1 diminishes ferroptosis. Additionally, SIRT1 plays a role in governing ferroptosis by modulating the expression of GPX4, SLC7A11, and SLC3A2 (Lee et al., 2020). In paclitaxel-tolerant persister head and neck cancer (HNC) cell lines, SIRT1 activation promotes ferroptosis by increasing mitochondrial fatty acid oxidation via facilitating the dispersion and localization of lipid droplets on mitochondria (You et al., 2021). In addition, in studies of chronic lymphocytic leukemia (CLL), activation or inhibition of SIRT1 influenced the sensitivity of CLL cells to ferroptosis, suggesting a potential role for SIRT1 in regulating ferroptosis in CLL cells (Pan et al., 2022). These results underscore the potential of SIRT1 modulators (activators or inhibitors) and the ferroptosis pathway it regulates, as a novel therapeutic strategy for cancer treatment. Future research will further explore the specific mechanisms of action of SIRT1 modulators in different types of cancer, providing a scientific basis for the development of more effective cancer therapies.

3.8 Inflammatory disease

SIRT1-mediated ferroptosis plays an important role in the pathological process of mastitis. The activation of SIRT1 can inhibit the activation of inflammasome and the release of inflammatory

cytokines, and reduce the inflammatory response. At the same time, SIRT1 deacetylates multiple transcription factors, such as Nrf2, promotes its entry into the nucleus and activates the expression of antioxidant stress genes, such as HO-1 and GPX4, the activation of which helps mitigate cell damage caused by ferroptosis. In mastitis, SIRT1 activation helps to reduce intracellular iron content and inhibit lipid peroxidation, thereby reducing ferroptosis and protecting breast tissue from damage (Zhou et al., 2024b; Zhao et al., 2023b; Zhao et al., 2023c). Natural compounds and small-molecule activators that enhance SIRT1 activity could be developed as novel therapeutics for mitigating inflammatory responses and protecting tissue from ferroptosis-induced damage.

3.9 Diabetes

In diabetes mellitus, SIRT1-mediated ferroptosis plays an important role in islet β-cell dysfunction. Research has shown that hyperglycemia inhibits the expression of SIRT1 in islet β-cells, leading to decreased levels of the antioxidant enzyme GPX4 and increased expression of the ferroptosis-related protein TFR1. This weakens the cells' antioxidant capacity, making them more susceptible to oxidative stress and ultimately resulting in ferroptosis. Stabilizing SIRT1 activity alleviates ferroptosis in islet β-cells, improves insulin secretion, and mitigates hyperglycemia symptoms (Zhang et al., 2022). SIRT1 is also involved in the development of diabetic complications through its regulation of ferroptosis. Under high-glucose conditions, SIRT1 activity is reduced, leading to increased ferroptosis. Activating SIRT1 can inhibit ferroptosis and reduce pathological damage in diabetic complications. For example, in diabetic retinopathy (DR), SIRT1 suppresses inflammation and retinal vascular damage by regulating HMGB1 deacetylation and inhibiting ferroptosis (Peng et al., 2025). Inhibition of SIRT1 reduces Nrf2 activity, decreases the expression of antioxidant-related molecules, and exacerbates ferroptosis. Astragaloside-IV can enhance SIRT1 and Nrf2 activity, boost cellular antioxidant capacity, reduce hyperglycemia-induced ferroptosis, and protect retinal pigment epithelial (RPE) cells from damage, offering a potential therapeutic strategy for DR (Tang et al., 2022). Flavanones can increase SIRT1 activity, inhibit ferroptosis through the FOXO3a and Nrf2 signaling pathways, and alleviate renal tubular epithelial cell injury induced by high glucose (Zhou et al., 2025). Additionally, activating the SIRT1/Nrf2/p62 pathway can promote the healing of diabetic foot ulcers, possibly mediated by autophagy-dependent ferroptosis (Han et al., 2024). In diabetic peripheral neuropathy (DPN), inactivation of SIRT1 promotes the production of mitochondrial ROS, leading to dysfunction and ferroptosis in Schwann cells. Activation of the AMPK/SIRT1/PGC-1α signaling pathway by honokiol alleviates hyperglycemia-induced oxidative stress and ferroptosis, thereby improving cell function (Liang et al., 2023; Hu et al., 2023). These findings suggest that SIRT1 and its regulation of ferroptosis are crucial in diabetic complications and may represent a novel therapeutic target for these conditions.

Together, the diverse roles of SIRT1 across multiple disease types underscore its significance as a promising therapeutic target. A variety of therapeutic agents have been explored for modulating SIRT1 in ferroptosis-related diseases. Table 1 summarizes key SIRT1-targeted interventions, their mechanisms, and potential clinical applications across various pathological conditions. This consolidated information provides a reference for ongoing research and potential translational applications in ferroptosis-associated diseases (Table 1).

4 Future research directions and prospects

The role of SIRT1 in the regulation of ferroptosis has emerged as a promising area of research with significant therapeutic potential in a multiple of diseases. While significant progress has been made in understanding the role of SIRT1 in ferroptosis, there are still many challenges to overcome. The integration of new technologies and the pursuit of innovative research directions will be instrumental in advancing the field and unlocking the therapeutic potential of targeting SIRT1 and ferroptosis. Future research should focus on elucidating the precise molecular mechanisms by which SIRT1 regulates ferroptosis. This includes investigating the full spectrum of SIRT1 targets, the epigenetic changes it induces, and how these contribute to the susceptibility of target cells to ferroptosis. Research could focus on identifying SIRT1-dependent gene regulatory networks that modulate ferroptosis. Investigating the interplay between SIRT1 and other cellular pathways, such as autophagy and the unfolded protein response, will also be crucial for a comprehensive understanding of ferroptosis regulation. What's more, the development of small molecules that specifically target SIRT1 or its regulatory pathway is a promising avenue. This includes the design of more potent and selective SIRT1 modulators and the evaluation of their efficacy in preclinical models of diseases characterized by ferroptosis, such as kidney diseases, neurodegenerative disorders, and cancer. Moreover, the development of predictive biomarkers for ferroptosis sensitivity is crucial. Future studies should aim to identify and validate biomarkers that can predict a patient's response to ferroptosis-inducing therapies, allowing for personalized treatment strategies. Translational research efforts should be directed towards the design of clinical trials assessing the safety and efficacy of SIRT1-targeted ferroptosis induction in patients. Notably, long-term studies are needed to assess the safety and efficacy of SIRT1 modulation in inducing ferroptosis.

Through the diligent exploration of these research avenues, the scientific community can potentially unlock the therapeutic potential of SIRT1 and ferroptosis as novel strategies in human disease. This advancement may provide renewed hope for patients who have exhausted conventional treatment options and are in dire need of innovative therapeutic interventions.

5 Discussion

Our review underscores the multifaceted role of SIRT1 in modulating ferroptosis, highlighting its potential as a therapeutic target. The intricate interplay between SIRT1 and the molecular machinery governing ferroptosis offers a rich avenue for therapeutic intervention. SIRT1's ability to deacetylate and thereby activate

TABLE 1 Therapeutic strategies targeting SIRT1 in ferroptosis-associated diseases.

Disease type	SIRT1 regulation	Therapeutic strategies	Mechanism	Clinical potential	Ref
Neurological Diseases	Activation	Resveratrol, SRT1720, SRT2104, Propofol, Ketogenic diet, Ferulic acid	Enhance Nrf2/GPX4, reduces oxidative stress, mitigates lipid peroxidation	Protect neurons from ferroptosis in neurodegenerative disorders and cognitive decline	Wen et al. (2024), Yang et al. (2022), Liu et al. (2022), Wang et al. (2023b), and Yan et al. (2024)
Liver Diseases	Activation	Salidroside, Ulinastatin, Rosa rugosa, Dihydroquercetin	Regulate p53/GPX4/GSDMD and Nrf2/p53, decreases oxidative stress	Protect against liver failure, sepsis, and NASH	Wang et al. (2021), Xu et al. (2023), Lei et al. (2023), and Zeng et al. (2024a)
Lung Diseases	Activation	Meteorin-like, Meteorin-β, FGF, GDF11, Quercetin	Suppress p53 acetylation, activate SIRT1/Nrf2/GPX4, maintains iron homeostasis	Alleviate ALI	Chen et al. (2022a), Chen et al. (2023b), Lin et al. (2024b), Wu et al. (2024), and Deng et al. (2023)
Cardiovascular Diseases	Activation	Quercetin, Resveratrol, Icariin, Pterostilbene,	Activate Nrf2/Keap1, SIRT1/p53/SLC7A11, inhibit ferroptosis in cardiomyocytes	Protect against myocardial infarction, ischemia-reperfusion injury, and doxorubicin-induced cardiotoxicity	Lin et al. (2023), Wang et al. (2023a), Abdel-Rahman et al. (2022), Yarmohammadi et al. (2024), Tang et al. (2024), Yu et al. (2023a), Yu et al. (2024), Zhang et al. (2023b), and Zhang et al. (2024b)
Kidney Diseases	Activation	Baicalein, Gastrodin, Earthworm extract	Enhance SIRT1/Nrf2, reduce oxidative stress	Mitigates acute kidney injury	Yu et al. (2023b), Qiu et al. (2024), and Shu et al. (2024)
Bone Health	Activation	Vitamin K2, Icariin	Activate AMPK/SIRT1, inhibit oxidative stress-induced ferroptosis	Prevent osteoporosis and osteoarthritis	Jin et al. (2023), Jing et al. (2019), and Schluesener and Schluesener (2014)
Cancer	Activation or Inhibition	Protocadherin 20, Ropivacaine, β-nicotinamide mononucleotide	Regulate SIRT1/AMPK, PTEN/PI3K, modulate ferroptosis sensitivity in tumors	Enhances ferroptosis-based strategies in HCC, colorectal cancer, melanoma, and lung adenocarcinoma	Jun et al. (2023), Zeng et al. (2024b), Sun et al. (2024), and Zhang et al. (2023a)
Mastitis	Activation	Schisandrin B, saikosaponin A, diosmetin	Regulate SIRT1/p53/SLC7A11, Nrf2, GPX4	Alleviate mastitis	Zhou et al. (2024b), Zhao et al. (2023b), and Zhao et al. (2023c)
Diabetes	Activation	Astragaloside-IV, Flavanones, Honokiol	Enhance FOXO3a/NRF2, preserve β-cell function	Ameliorate diabetes and its complications	Tang et al. (2022), Zhou et al. (2025), Han et al. (2024), Liang et al. (2023), and Hu et al. (2023)

key proteins involved in ferroptosis, such as GPX4 and FOXO3A, positions it as a nodal point in the regulation of this cell death process. By maintaining cellular redox balance and influencing iron homeostasis, SIRT1 contributes to the cellular resistance against ferroptosis. The therapeutic potential of SIRT1 in modulating ferroptosis is vast and spans a range of diseases, including neurodegenerative disorders, cancer, and kidney diseases. The activation of SIRT1 has been shown to ameliorate ferroptosis-associated cell death in various models, suggesting its utility in developing protective strategies against diseases where ferroptosis plays a pathogenic role. However, the field faces challenges, including the need for a deeper understanding of the molecular

underpinnings of SIRT1's role in ferroptosis and the development of targeted therapies that can effectively harness this enzyme's activity. In conclusion, the regulation of ferroptosis by SIRT1 represents a burgeoning frontier in cellular biology with significant therapeutic implications. As we continue to unravel the complexities of this process, we edge closer to a future where the modulation of ferroptosis through SIRT1 activation may offer novel treatment strategies for a host of diseases. Our review establish a foundation for future research and pave the way for novel therapeutic strategies that could harness the potential of ferroptosis in biological and medical contexts.

Author contributions

YZ: Writing–original draft, Funding acquisition. FK: Visualization, Writing–original draft. NL: Supervision, Writing–review and editing. LT: Supervision, Writing–review and editing. JZ: Conceptualization, Writing–review and editing. JM: Conceptualization, Writing–review and editing. SZ: Conceptualization, Writing–review and editing.

Funding

The author(s) declare that financial support was received for the research, authorship, and/or publication of this article. This study was supported by the Department of Science and Technology of Jilin Province (grant No. YDZJ202201ZYTS068 to Lina Tao), the Department of Education of Jilin Province (grant No. JJKH20221106KJ to Yueming Zhang), Jilin Provincial Health Commission (grant No. J2023JC006 to Jie Ma) and the Department of Science and Technology of Jilin Province (grant No. 20210401091YY to Sixi Zhang).

Conflict of interest

The authors declare that the research was conducted in the absence of any commercial or financial relationships that could be construed as a potential conflict of interest.

Generative AI statement

The author(s) declare that no Generative AI was used in the creation of this manuscript.

Publisher's note

References

Abdel-Rahman, A., Soliman, E., Testai, L., Sun, Z., Yu, L., Xu, C., et al. (2022). Fisetin attenuates doxorubicin-induced cardiomyopathy *in vivo* and *in vitro* by inhibiting ferroptosis through SIRT1/nrf2 signaling pathway activation. *Front. Pharmacol.* 12. doi:10.3389/fphar.2021.808480

Abukhalil, M. H., Al-Alami, Z., Alfwuaires, M. A., Imran, M. R., Aladaileh, S. H., and Althunibat, O. Y. (2025). Taxifolin protects against 5-fluorouracil-induced cardiotoxicity in mice through mitigating oxidative stress, inflammation, and apoptosis: possible involvement of sirt1/Nrf2/HO-1 signaling. *Cardiovasc Toxicol.* doi:10.1007/s12012-025-09962-w

Bai, X., Ye, D., Shi, Y., Fan, M., Lu, P., Feng, Y., et al. (2023). Neuroprotection of SRT2104 in murine ischemia/reperfusion injury through the enhancement of Sirt1-mediated deacetylation. *Invest. Ophthalmol. Vis. Sci.* 64, 31. doi:10.1167/iovs.64.4.31

Bellezza, I., Tucci, A., Galli, F., Grottelli, S., Mierla, A. L., Pilolli, F., et al. (2012). Inhibition of NF-κB nuclear translocation via HO-1 activation underlies α-tocopheryl succinate toxicity. *J. Nutr. Biochem.* 23, 1583–1591. doi:10.1016/j.jnutbio.2011.10.012

Cai, M., Fu, T., Zhu, R., Hu, P., Kong, J., Liao, S., et al. (2024). An iron-based metal-organic framework nanoplatform for enhanced ferroptosis and oridonin delivery as a comprehensive antitumor strategy. *Acta Pharm. Sin. B* 14, 4073–4086. doi:10.1016/j.apsb.2024.05.015

Chen, H., Lin, X., Yi, X., Liu, X., Yu, R., Fan, W., et al. (2022a). SIRT1-mediated p53 deacetylation inhibits ferroptosis and alleviates heat stress-induced lung epithelial cells injury. *Int. J. Hyperth.* 39, 977–986. doi:10.1080/02656736.2022.2094476

Chen, J., Chen, P., Song, Y., Wei, J., Wu, F., Sun, J., et al. (2024a). STING upregulation mediates ferroptosis and inflammatory response in lupus nephritis by upregulating TBK1 and activating NF-κB signal pathway. *J. Biosci.* 49, 9. doi:10.1007/s12038-023-00381-z

Chen, J., Xiao, L., Chen, Y., Li, W., Liu, Y., Zhou, Y., et al. (2023a). YT521-B homology domain containing 1 ameliorates mitochondrial damage and ferroptosis in sleep deprivation by activating the sirtuin 1/nuclear factor erythroid-derived 2-like 2/heme oxygenase 1 pathway. *Brain Res. Bull.* 197, 1–12. doi:10.1016/j.brainresbull.2023.03.008

Chen, L., Xu, H., Zhang, C., He, J., and Wang, Y. (2024b). Semaglutide alleviates early brain injury following subarachnoid hemorrhage by suppressing ferroptosis and neuroinflammation via SIRT1 pathway. *Am. J. Transl. Res.* 16, 1102–1117. doi:10.62347/IZGJ1332

Chen, Q., Liu, L., and Ni, S. (2022b). Screening of ferroptosis-related genes in sepsis-induced liver failure and analysis of immune correlation. *PeerJ* 10, e13757. doi:10.7717/peerj.13757

Chen, X., Wang, Z., Li, C., Zhang, Z., Lu, S., Wang, X., et al. (2024c). SIRT1 activated by AROS sensitizes glioma cells to ferroptosis via induction of NAD+ depletion-dependent activation of ATF3. *Redox Biol.* 69, 103030. doi:10.1016/j.redox.2024.103030

Chen, Z., Li, J., Peng, H., Zhang, M., Wu, X., Gui, F., et al. (2023b). Meteorin-like/Meteorin-β protects LPS-induced acute lung injury by activating SIRT1-P53-SLC7A11 mediated ferroptosis pathway. *Mol. Med.* 29, 144. doi:10.1186/s10020-023-00714-6

Conde, M. A., Alza, N. P., Funk, M. I., Maniscalchi, A., Benzi Juncos, O. N., Berge, I., et al. (2023). α-Synuclein attenuates maneb Neurotoxicity through the modulation of redox-Sensitive transcription factors. *Oxidative Med. Cell. Longev.* 2023, 5803323–5803415. doi:10.1155/2023/5803323

Dang, R., Wang, M., Li, X., Wang, H., Liu, L., Wu, Q., et al. (2022). Edaravone ameliorates depressive and anxiety-like behaviors via Sirt1/Nrf2/HO-1/Gpx4 pathway. *J. Neuroinflammation* 19, 41. doi:10.1186/s12974-022-02400-6

Davenport, A. M., Huber, F. M., and Hoelz, A. (2014). Structural and functional analysis of human SIRT1. *J Mol Biol* 426 (3), 526–41. doi:10.1016/j.jmb.2013.10.009

Deng, S., Li, J., Li, L., Lin, S., Yang, Y., Liu, T., et al. (2023). Quercetin alleviates lipopolysaccharide-induced acute lung injury by inhibiting ferroptosis via the Sirt1/Nrf2/Gpx4 pathway. *Int. J. Mol. Med.* 52, 118. doi:10.3892/ijmm.2023.5321

Dixon, S. J., Lemberg, K. M., Lamprecht, M. R., Skouta, R., Zaitsev, E. M., Gleason, C. E., et al. (2012). Ferroptosis: an iron-dependent form of Nonapoptotic cell death. *Cell* 149, 1060–1072. doi:10.1016/j.cell.2012.03.042

Dixon, S. J., Winter, G. E., Musavi, L. S., Lee, E. D., Snijder, B., Rebsamen, M., et al. (2015). Human Haploid cell Genetics reveals roles for lipid metabolism genes in Nonapoptotic cell death. *ACS Chem. Biol.* 10, 1604–1609. doi:10.1021/acschembio.5b00245

Fang, D., Wang, Y., Zhang, Z., Yang, D., Gu, D., He, B., et al. (2021). Calorie restriction protects against contrast-induced nephropathy via SIRT1/GPX4 activation. *Oxid Med Cell Longev*. 9846101. doi:10.1155/2021/2999296

Gu, X., Zhang, G., Qin, Z., Yin, M., Chen, W., Zhang, Y., et al. (2022). Safinamide protects against amyloid β (Aβ)-induced oxidative stress and cellular senescence in M17 neuronal cells. *Bioengineered* 13, 1921–1930. doi:10.1080/21655979.2021.2022262

Guo, J., Xue, H., Zhong, H., Sun, W., Zhao, S., Meng, J., et al. (2022). Involvement of LARP7 in activation of SIRT1 to inhibit NF-κB signaling protects microglia from Acrylamide-induced neuroinflammation. *Neurotox. Res.* 40, 2016–2026. doi:10.1007/s12640-022-00624-1

Hacioglu, C. (2024). Long-term exposure of sucralose induces neuroinflammation and ferroptosis in human microglia cells via SIRT1/NLRP3/IL-1β/GPx4 signaling pathways. *Food Sci. and Nutr.* 12, 9094–9107. doi:10.1002/fsn3.4488

Han, Q., Gu, Y., and Qian, Y. (2024). Study on the mechanism of activating SIRT1/Nrf2/p62 pathway to mediate autophagy-dependent ferroptosis to promote healing of diabetic foot ulcers. *Schmiedeb. Arch. Pharmacol.* doi:10.1007/s00210-024-03400-4

Hao, R., Ge, J., Song, X., Li, F., Sun-Waterhouse, D., and Li, D. (2022). Cadmium induces ferroptosis and apoptosis by modulating miR -34a-5p/Sirt1axis in PC12 cells. *Environ. Toxicol.* 37, 41–51. doi:10.1002/tox.23376

He, L., Wang, J., Tao, B., Zhu, R., Li, C., and Ning, B. (2023). Identification of ferroptosis-related genes in the progress of NASH. *Front. Endocrinol.* 14, 1184280. doi:10.3389/fendo.2023.1184280

Hu, M., Jiang, W., Ye, C., Hu, T., Yu, Q., Meng, M., et al. (2023). Honokiol attenuates high glucose-induced peripheral neuropathy via inhibiting ferroptosis and activating AMPK/SIRT1/PGC -1α pathway in Schwann cells. *Phytotherapy Res.* 37, 5787–5802. doi:10.1002/ptr.7984

Huang, C., Li, Y., Li, B., Liu, X., Luo, D., Liu, Y., et al. (2024). Identifying potential ferroptosis key genes for diagnosis and treatment of postmenopausal osteoporosis through competitive endogenous RNA network analysis. *Heliyon* 10, e23672. doi:10.1016/j.heliyon.2023.e23672

Jiang, Y.-H., Wu, S.-Y., Wang, Z., Zhang, L., Zhang, J., Li, Y., et al. (2022). Bioinformatics analysis identifies ferroptosis-related genes in the regulatory mechanism of myocardial infarction. *Exp. Ther. Med.* 24, 748. doi:10.3892/etm.2022.11684

Jiao, X., Li, Q., and Xu, X. (2023). Prognostic implication of a ferroptosis-related gene signature associates with immunity in Ewing's sarcoma. *Electron. J. Biotechnol.* 64, 42–58. doi:10.1016/j.ejbt.2023.01.004

Jin, C., Tan, K., Yao, Z., Lin, B., Zhang, D., Chen, W.-K., et al. (2023). A novel anti-osteoporosis mechanism of VK2: Interfering with ferroptosis via AMPK/SIRT1 pathway in type 2 diabetic osteoporosis. *J. Agric. Food Chem.* 71, 2745–2761. doi:10.1021/acs.jafc.2c05632

Jing, X., Du, T., Chen, K., Guo, J., Xiang, W., Yao, X., et al. (2019). Icariin protects against iron overload-induced bone loss via suppressing oxidative stress. *J. Cell Physiol.* 234, 10123–10137. doi:10.1002/jcp.27678

Ju, J., Li, X.-M., Zhao, X.-M., Li, F.-H., Wang, S.-C., Wang, K., et al. (2023). Circular RNA FEACR inhibits ferroptosis and alleviates myocardial ischemia/reperfusion injury by interacting with NAMPT. *J. Biomed. Sci.* 30, 45. doi:10.1186/s12929-023-00927-1

Jun, L., Chen, W., Han, L., Yanmin, L., Qinglei, Z., and Pengfei, Z. (2023). Protocadherin 20 promotes ferroptosis by suppressing the expression of Sirtuin 1 and promoting the acetylation of nuclear factor erythroid 2-related factor 2 in hepatocellular carcinoma. *Int. J. Biochem. and Cell Biol.* 156, 106363. doi:10.1016/j.biocel.2023.106363

Latunde-Dada, G. O. (2017). Ferroptosis: role of lipid peroxidation, iron and ferritinophagy. *Biochim. Biophys. Acta Gen. Subj.* 1861, 1893–1900. doi:10.1016/j.bbagen.2017.05.019

Lee, J., You, J. H., Kim, M.-S., and Roh, J.-L. (2020). Epigenetic reprogramming of epithelial-mesenchymal transition promotes ferroptosis of head and neck cancer. *Redox Biol.* 37, 101697. doi:10.1016/j.redox.2020.101697

Lei, Y., Lei, X., Zhu, A., Xie, S., Zhang, T., Wang, C., et al. (2023). Ethanol extract of rosa rugosa ameliorates acetaminophen-induced liver injury via upregulating Sirt1 and subsequent Potentiation of LKB1/AMPK/Nrf2 cascade in hepatocytes. *Molecules* 28, 7307. doi:10.3390/molecules28217307

Li, C., Cui, K., Zhu, X., Wang, S., Yang, Q., and Fang, G. (2024a). 8-weeks aerobic exercise ameliorates cognitive deficit and mitigates ferroptosis triggered by iron overload in the prefrontal cortex of APP Swe/PSEN 1dE9 mice through Xc-/GPx4 pathway. *Front. Neurosci.* 18, 1453582. doi:10.3389/fnins.2024.1453582

Li, R., Yuan, H., Zhang, C., Han, D., Wang, Y., and Feng, L. (2024b). Induced ferroptosis pathway by regulating cellular lipid peroxidation with Peroxynitrite generator for reversing "Cold" tumors. *"Cold" Tumors, Small* 20, e2404807. doi:10.1002/smll.202404807

Liang, Z., Zhang, N., Wang, X., Zhang, J., Li, K., and Lei, T. (2023). Epothilone B inactivation of Sirtuin1 promotes mitochondrial reactive oxygen species to induce dysfunction and ferroptosis of Schwann cells. *Eur. J. Pharm. Sci.* 181, 106350. doi:10.1016/j.ejps.2022.106350

Liao, Y., Ke, B., Long, X., Xu, J., and Wu, Y. (2023). Abnormalities in the SIRT1-SIRT3 axis promote myocardial ischemia-reperfusion injury through ferroptosis caused by silencing the PINK1/Parkin signaling pathway. *BMC Cardiovasc Disord.* 23, 582. doi:10.1186/s12872-023-03603-2

Lin, L., Yang, L., Wang, N., Chen, S., Du, X., Chen, R., et al. (2024b). FGF10 protects against LPS-induced epithelial barrier injury and inflammation by inhibiting SIRT1-ferroptosis pathway in acute lung injury in mice. *Int. Immunopharmacol.* 127, 111426. doi:10.1016/j.intimp.2023.111426

Lin, X., Zhao, X., Chen, Q., Wang, X., Wu, Y., and Zhao, H. (2023). Quercetin ameliorates ferroptosis of rat cardiomyocytes via activation of the SIRT1/p53/SLC7A11 signaling pathway to alleviate sepsis-induced cardiomyopathy. *Int. J. Mol. Med.* 52, 116. doi:10.3892/ijmm.2023.5319

Lin, Y.-S., Tsai, Y.-C., Li, C.-J., Wei, T.-T., Wang, J.-L., Lin, B.-W., et al. (2024a). Overexpression of NUDT16L1 sustains proper function of mitochondria and leads to ferroptosis insensitivity in colorectal cancer. *Redox Biol.* 77, 103358. doi:10.1016/j.redox.2024.103358

Liu, J., Huang, J., Zhang, Z., Zhang, R., Sun, Q., Zhang, Z., et al. (2022). Mesenchymal stem cell-derived exosomes ameliorate Delayed Neurocognitive Recovery in aged mice by inhibiting Hippocampus ferroptosis via activating SIRT1/Nrf2/HO-1 signaling pathway. *Oxidative Med. Cell. Longev.* 2022, 3593294–3593322. doi:10.1155/2022/3593294

Liu, Q., Liu, Y., Li, Y., Hong, Z., Li, S., and Liu, C. (2023). PUM2 aggravates the neuroinflammation and brain damage induced by ischemia–reperfusion through the SLC7A11-dependent inhibition of ferroptosis via suppressing the SIRT1. *Mol. Cell Biochem.* 478, 609–620. doi:10.1007/s11010-022-04534-w

Lu, C., Zhao, H., Liu, Y., Yang, Z., Yao, H., Liu, T., et al. (2023). Novel role of the SIRT1 in endocrine and metabolic diseases. *Int. J. Biol. Sci.* 19, 484–501. doi:10.7150/ijbs.78654

Lv, Q.-K., Tao, K.-X., Yao, X.-Y., Pang, M.-Z., Cao, B.-E., Liu, C.-F., et al. (2024). Melatonin MT1 receptors regulate the Sirt1/Nrf2/Ho-1/Gpx4 pathway to prevent α-synuclein-induced ferroptosis in Parkinson's disease. *J. Pineal Res.* 76, e12948. doi:10.1111/jpi.12948

Lv, Z., Wang, F., Zhang, X., Zhang, X., Zhang, J., and Liu, R. (2021). Etomidate attenuates the ferroptosis in myocardial ischemia/reperfusion rat model via Nrf2/HO-1 pathway. *Shock* 56, 440–449. doi:10.1097/SHK.0000000000001751

Ma, S., Sun, L., Wu, W., Wu, J., Sun, Z., and Ren, J. (2020). USP22 protects against myocardial ischemia–reperfusion injury via the SIRT1-p53/SLC7A11–dependent inhibition of ferroptosis–induced cardiomyocyte death. *Front. Physiol.* 11, 551318. doi:10.3389/fphys.2020.551318

Majeed, Y., Halabi, N., Madani, A. Y., Engelke, R., Bhagwat, A. M., Abdesselem, H., et al. (2021). SIRT1 promotes lipid metabolism and mitochondrial biogenesis in adipocytes and coordinates adipogenesis by targeting key enzymatic pathways. *Sci. Rep.* 11, 8177. doi:10.1038/s41598-021-87759-x

Min, X., Shi, Y., Xu, Y., Li, Y., Dong, Y., Chen, F., et al. (2025). Mechanism of sirtuin1-mediated deacetylation of p65-mediated ferroptosis of hippocampal neurons in cerebral injury after Cardiopulmonary Resuscitation in rats. *Neurochem. Res.* 50, 66. doi:10.1007/s11064-024-04297-4

Niu, J., Guo, W., Lu, A., Han, G., Wang, G., Peng, B., et al. (2023). Comparison with gastric cancer-associated genes reveals the role of ferroptosis-related genes in eosinophils of asthma patients: a bioinformatic study. *Medicine* 102, e35002. doi:10.1097/MD.0000000000035002

Pan, B., Li, Y., Xu, Z., Miao, Y., Yin, H., Kong, Y., et al. (2022). Identifying a novel ferroptosis-related prognostic score for predicting prognosis in chronic lymphocytic leukemia. *Front. Immunol.* 13, 962000. doi:10.3389/fimmu.2022.962000

Peng, Y., Hu, L., Xu, H., Fang, J., and Zhong, H. (2025). Resveratrol alleviates reactive oxygen species and inflammation in diabetic retinopathy via SIRT1/HMGB1 pathway-mediated ferroptosis. *Toxicol. Appl. Pharmacol.* 495, 117214. doi:10.1016/j.taap.2024.117214

Qiongyue, Z., Xin, Y., Meng, P., Sulin, M., Yanlin, W., Xinyi, L., et al. (2022). Post-treatment with irisin attenuates acute kidney injury in sepsis mice through anti-ferroptosis via the SIRT1/Nrf2 pathway. *Front. Pharmacol.* 13, 857067. doi:10.3389/fphar.2022.857067

Qiu, C.-W., Chen, B., Zhu, H.-F., Liang, Y.-L., and Mao, L.-S. (2024). Gastrodin alleviates cisplatin nephrotoxicity by inhibiting ferroptosis via the SIRT1/FOXO3A/GPX4 signaling pathway. *J. Ethnopharmacol.* 319, 117282. doi:10.1016/j.jep.2023.117282

Qu, X., Liu, B., Wang, L., Liu, L., Zhao, W., Liu, C., et al. (2023). Loss of cancer-associated fibroblast-derived exosomal DACT3-AS1 promotes malignant transformation and ferroptosis-mediated oxaliplatin resistance in gastric cancer. *Drug Resist. Updat.* 68, 100936. doi:10.1016/j.drup.2023.100936

Rao, Y. L., Ganaraja, B., Suresh, P. K., Joy, T., Ullal, S. D., Manjrekar, P. A., et al. (2024). Outcome of resveratrol and resveratrol with donepezil combination on the β-amyloid plaques and neurofibrillary tangles in Alzheimer's disease. *3 Biotech.* 14, 190. doi:10.1007/s13205-024-04034-2

Ruan, Q., Wang, C., Zhang, Y., and Sun, J. (2023). Brevilin A attenuates cartilage destruction in osteoarthritis mouse model by inhibiting inflammation and ferroptosis via SIRT1/Nrf2/GPX4 signaling pathway. *Int. Immunopharmacol.* 124, 110924. doi:10.1016/j.intimp.2023.110924

Sanz-Alcázar, A., Portillo-Carrasquer, M., Delaspre, F., Pazos-Gil, M., Tamarit, J., Ros, J., et al. (2024). "Deciphering the ferroptosis pathways in dorsal root ganglia of Friedreich ataxia models," in *The role of LKB1/AMPK, KEAP1, and GSK3β in the impairment of the NRF2 response*. doi:10.1101/2024.05.10.593481

Schluesener, J. K., and Schluesener, H. (2014). Plant polyphenols in the treatment of age-associated diseases: revealing the pleiotropic effects of icariin by network analysis. *Mol. Nutr. Food Res.* 58, 49–60. doi:10.1002/mnfr.201300409

Sgadari, M., Cacciola, N. A., Power, K., Martano, M., and Restucci, B. (2023). Sirtuin 1 expression in canine Mammary tumors: a Pilot study. *Anim. (Basel)* 13, 2609. doi:10.3390/ani13162609

Shan, H., Gao, L., Zhao, S., Dou, Z., and Pan, Y. (2024). Bone marrow mesenchymal stem cells with PTBP1 knockdown protect against cerebral ischemia-reperfusion injury by inhibiting ferroptosis via the JNK/P38 pathway in rats. *Neuroscience* S0306-4522 (24), 130–142. doi:10.1016/j.neuroscience.2024.09.038

Shen, J., Hao, C., Yuan, S., Chen, W., Tong, T., Chen, Y., et al. (1826). Acupuncture alleviates CUMS-induced depression-like behaviors of rats by regulating oxidative stress, neuroinflammation and ferroptosis. *Brain Res.* 1826, 148715. doi:10.1016/j.brainres.2023.148715

Shu, G., Wang, C., Song, A., Zheng, Z., Zheng, S., Song, Y., et al. (2024). Water extract of earthworms mitigates kidney injury triggered by oxidative stress via activating intrarenal Sirt1/Nrf2 cascade and ameliorating mitochondrial damage. *J. Ethnopharmacol.* 335, 118648. doi:10.1016/j.jep.2024.118648

Su, G., Yang, W., Wang, S., Geng, C., and Guan, X. (2021). SIRT1-autophagy axis inhibits excess iron-induced ferroptosis of foam cells and subsequently increases IL-1B and IL-18. *Biochem. Biophysical Res. Commun.* 561, 33–39. doi:10.1016/j.bbrc.2021.05.011

Sui, S., Zhang, J., Xu, S., Wang, Q., Wang, P., and Pang, D. (2019). Ferritinophagy is required for the induction of ferroptosis by the bromodomain protein BRD4 inhibitor (+)-JQ1 in cancer cells. *Cell Death Dis.* 10, 331. doi:10.1038/s41419-019-1564-7

Sun, H., Meng, Y., Yao, L., Du, S., Li, Y., Zhou, Q., et al. (2024). Ubiquitin-specific protease 22 controls melanoma metastasis and vulnerability to ferroptosis through targeting SIRT1/PTEN/PI3K signaling. *MedComm* 5, e684. doi:10.1002/mco2.684

Sun, J., Zhang, Y., Wang, C., and Ruan, Q. (2023). Kukoamine A protects mice against osteoarthritis by inhibiting chondrocyte inflammation and ferroptosis via SIRT1/GPX4 signaling pathway. *Life Sci.* 332, 122117. doi:10.1016/j.lfs.2023.122117

Sun, W., Yan, J., Ma, H., Wu, J., and Zhang, Y. (2022). Autophagy-dependent ferroptosis-related signature is closely associated with the prognosis and tumor immune Escape of patients with glioma. *IJGM* 15, 253–270. doi:10.2147/IJGM.S343046

Sun, X., Ou, Z., Chen, R., Niu, X., Chen, D., Kang, R., et al. (2016). Activation of the p62-Keap1-NRF2 pathway protects against ferroptosis in hepatocellular carcinoma cells. *Hepatology* 63, 173–184. doi:10.1002/hep.28251

Tang, X., Li, X., Zhang, D., and Han, W. (2022). Astragaloside-IV alleviates high glucose-induced ferroptosis in retinal pigment epithelial cells by disrupting the expression of miR-138-5p/Sirt1/Nrf2. *Bioengineered* 13, 8240–8254. doi:10.1080/21655979.2022.2049471

Tang, Y., Zhang, Z., Yan, T., Chen, K., Xu, G., Xiong, S., et al. (2024). Irisin attenuates type 1 diabetic cardiomyopathy by anti-ferroptosis via SIRT1-mediated deacetylation of p53. *Cardiovasc Diabetol.* 23, 116. doi:10.1186/s12933-024-02183-5

Tian, Y., He, X., Yuan, Y., Zhang, S., Wang, C., Dong, J., et al. (2024). TME-responsive nanoplatform with glutathione depletion for enhanced tumor-specific Mild Photothermal/gene/ferroptosis Synergistic Therapy. *Int. J. Nanomedicine* 19, 9145–9160. doi:10.2147/IJN.S475698

Tziastoudi, M., Pissas, G., Golfinopoulos, S., Filippidis, G., Dousdampanis, P., Eleftheriadis, T., et al. (2023). Sodium-glucose transporter 2 (SGLT2) inhibitors and iron deficiency in heart failure and chronic kidney disease: a Literature review. *Life (Basel)* 13, 2338. doi:10.3390/life13122338

Wang, C., Liu, T., Tong, Y., Cui, R., Qu, K., Liu, C., et al. (2021). Ulinastatin protects against acetaminophen-induced liver injury by alleviating ferroptosis via the SIRT1/NRF2/HO-1 pathway. *Am. J. Transl. Res.* 13, 6031–6042.

Wang, L., Li, M., Liu, B., Zheng, R., Zhang, X., and Yu, S. (2024a). miR-30a-5p mediates ferroptosis of hippocampal neurons in chronic cerebral hypoperfusion-induced cognitive dysfunction by modulating the SIRT1/NRF2 pathway. *Brain Res. Bull.* 212, 110953. doi:10.1016/j.brainresbull.2024.110953

Wang, M., Huang, J., Zou, J., Xu, Z., Yang, A., Liu, Z., et al. (2025). Electroacupuncture regulates SIRT1/p53/p21 signaling pathway to prevent stress-induced premature senescence of nucleus pulposus cells in degenerative intervertebral discs. *Int. Immunopharmacol.* 148, 114114. doi:10.1016/j.intimp.2025.114114

Wang, W., Li, X., Ding, N., Teng, J., Zhang, S., Zhang, Q., et al. (2020). miR-34a regulates adipogenesis in porcine intramuscular adipocytes by targeting ACSL4. *BMC Genet.* 21, 33. doi:10.1186/s12863-020-0836-7

Wang, W., Zhong, X., Fang, Z., Li, J., Li, H., Liu, X., et al. (2023a). Cardiac sirtuin1 deficiency exacerbates ferroptosis in doxorubicin-induced cardiac injury through the Nrf2/Keap1 pathway. *Chem-Biol Interact.* 377, 110469. doi:10.1016/j.cbi.2023.110469

Wang, X., Shao, N., Zhang, X., Chen, H., Chang, Z., Xie, D., et al. (2023b). Ferulic acid activates SIRT1-mediated ferroptosis signaling pathway to improve cognition dysfunction in Wilson's disease. *NDT* 19, 2681–2696. doi:10.2147/NDT.S443278

Wang, X., Wei, K., Wang, M., and Zhang, L. (2024b). Identification of potential key ferroptosis- and autophagy-related genes in myelomeningocele through bioinformatics analysis. *Heliyon* 10, e29654. doi:10.1016/j.heliyon.2024.e29654

Weichhart, T. (2024). Transferrin: the iron transporter takes control. *Blood* 144, 9–10. doi:10.1182/blood.2024024731

Wen, Y., Zhang, W., Wang, D., and Lu, M. (2024). Propofol ameliorates cognitive deficits following splenectomy in aged rats by inhibiting ferroptosis via the SIRT1/Nrf2/GPX4 pathway. *NeuroReport* 35, 846–856. doi:10.1097/WNR.0000000000002074

Wu, Z., Xi, Q., Zhao, Q., and Zhu, S. (2024). GDF11 overexpression alleviates sepsis-induced lung microvascular endothelial barrier damage by activating SIRT1/NOX4 signaling to inhibit ferroptosis. *Shock* 62, 245–254. doi:10.1097/SHK.0000000000002391

Xia, Y., Li, S., Wang, X., Zhao, B., Chen, S., Jiang, Q., et al. (2023). Astilbin targeted Sirt1 to inhibit acetylation of Nrf2 to alleviate grass carp hepatocyte apoptosis caused by PCB126-induced mitochondrial kinetic and metabolism dysfunctions. *Fish and Shellfish Immunol.* 141, 109000. doi:10.1016/j.fsi.2023.109000

Xia, Y., Zhang, H., Wang, H., Wang, Q., Zhu, P., Gu, Y., et al. (2022). Identification and validation of ferroptosis key genes in bone mesenchymal stromal cells of primary osteoporosis based on bioinformatics analysis. *Front. Endocrinol.* 13, 980867. doi:10.3389/fendo.2022.980867

Xie, R., Zhao, W., Lowe, S., Bentley, R., Hu, G., Mei, H., et al. (2022). Quercetin alleviates kainic acid-induced seizure by inhibiting the Nrf2-mediated ferroptosis pathway. *Free Radic. Bio Med.* 191, 212–226. doi:10.1016/j.freeradbiomed.2022.09.001

Xu, J., Zhao, L., Zhang, X., Ying, K., Zhou, R., Cai, W., et al. (2023). Salidroside ameliorates acetaminophen-induced acute liver injury through the inhibition of endoplasmic reticulum stress-mediated ferroptosis by activating the AMPK/SIRT1 pathway. *Ecotoxicol. Environ. Saf.* 262, 115331. doi:10.1016/j.ecoenv.2023.115331

Yan, C., Yang, S., Shao, S., Zu, R., Lu, H., Chen, Y., et al. (2024). Exploring the anti-ferroptosis mechanism of Kai-Xin-San against Alzheimer's disease through integrating network pharmacology, bioinformatics, and experimental validation strategy *in vivo* and *in vitro*. *J. Ethnopharmacol.* 326, 117915. doi:10.1016/j.jep.2024.117915

Yang, J., Zhang, M., Zhang, X., Zhou, Y., Ma, T., Liang, J., et al. (2024). Glioblastoma-derived exosomes promote lipid accumulation and induce ferroptosis in dendritic cells via the NRF2/GPX4 pathway. *Front. Immunol.* 15, 1439191. doi:10.3389/fimmu.2024.1439191

Yang, M., Xia, L., Song, J., Hu, H., Zang, N., Yang, J., et al. (2023). Puerarin ameliorates metabolic dysfunction-associated fatty liver disease by inhibiting ferroptosis and inflammation. *Lipids Health Dis.* 22, 202. doi:10.1186/s12944-023-01969-y

Yang, Y., Wang, X., Xiao, A., Han, J., Wang, Z., and Wen, M. (2022). Ketogenic diet prevents chronic sleep deprivation-induced Alzheimer's disease by inhibiting iron dyshomeostasis and promoting repair via Sirt1/Nrf2 pathway. *Front. Aging Neurosci.* 14, 998292. doi:10.3389/fnagi.2022.998292

Yarmohammadi, F., Wallace Hayes, A., and Karimi, G. (2024). Molecular mechanisms involved in doxorubicin-induced cardiotoxicity: a bibliometrics analysis by VOSviewer. *Naunyn. Schmiedeb. Arch. Pharmacol.* 397, 1971–1984. doi:10.1007/s00210-023-02773-2

You, J. H., Lee, J., and Roh, J. (2021). PGRMC1-dependent lipophagy promotes ferroptosis in paclitaxel-tolerant persister cancer cells. *J. Exp. Clin. Cancer Res.* 40, 350. doi:10.1186/s13046-021-02168-2

Yu, H., Gan, D., Luo, Z., Yang, Q., An, D., Zhang, H., et al. (2024). α-Ketoglutarate improves cardiac insufficiency through NAD+-SIRT1 signaling-mediated mitophagy and ferroptosis in pressure overload-induced mice. *Mol. Med.* 30, 15. doi:10.1186/s10020-024-00783-1

Yu, L.-M., Dong, X., Huang, T., Zhao, J.-K., Zhou, Z.-J., Huang, Y.-T., et al. (2023a). Inhibition of ferroptosis by icariin treatment attenuates excessive ethanol consumption-induced atrial remodeling and susceptibility to atrial fibrillation, role of SIRT1. *Apoptosis* 28, 607–626. doi:10.1007/s10495-023-01814-8

Yu, M., Li, H., Wang, B., Wu, Z., Wu, S., Jiang, G., et al. (2023b). Baicalein ameliorates polymyxin B-induced acute renal injury by inhibiting ferroptosis via regulation of SIRT1/p53 acetylation. *Chemico-Biological Interact.* 382, 110607. doi:10.1016/j.cbi.2023.110607

Yuan, B., Zhao, X.-D., Shen, J.-D., Chen, S.-J., Huang, H.-Y., Zhou, X.-M., et al. (2022). Activation of SIRT1 alleviates ferroptosis in the early brain injury after subarachnoid hemorrhage. *Oxidative Med. Cell. Longev.* 2022, 9069825–9069919. doi:10.1155/2022/9069825

Zeng, L., Zhao, W., Han, T., Qing, F., He, Z., Zhao, Q., et al. (2024b). Ropivacaine prompts ferroptosis to enhance the cisplatin-sensitivity of human colorectal cancer through SIRT1/Nrf2 signaling pathway. *Chemico-Biological Interact.* 400, 111163. doi:10.1016/j.cbi.2024.111163

Zeng, Y., He, Y., Wang, L., Xu, H., Zhang, Q., Wang, Y., et al. (2024a). Dihydroquercetin improves experimental acute liver failure by targeting ferroptosis and mitochondria-mediated apoptosis through the SIRT1/p53 axis. *Phytomedicine* 128, 155533. doi:10.1016/j.phymed.2024.155533

Zhan, Y., Yang, Z., Zhan, F., Huang, Y., and Lin, S. (2023). SIRT1 is transcriptionally repressed by YY1 and suppresses ferroptosis in rheumatoid arthritis. *Adv. Rheumatol.* 63, 9. doi:10.1186/s42358-023-00289-0

Zhang, F., Zeng, Z., Zhang, J., Li, X., Yang, W., Wei, Y., et al. (2024b). Pterostilbene attenuates heart failure by inhibiting myocardial ferroptosis through SIRT1/GSK-3β/GPX4 signaling pathway. *Heliyon* 10, e24562. doi:10.1016/j.heliyon.2024.e24562

Zhang, J., Zhu, Q., Peng, Z., Li, X.-J., Ding, P.-F., Gao, S., et al. (2024a). Menaquinone-4 attenuates ferroptosis by upregulating DHODH through activation of SIRT1 after subarachnoid hemorrhage. *Free Radic. Biol. Med.* 210, 416–429. doi:10.1016/j.freeradbiomed.2023.11.031

Zhang, M., Cui, J., Chen, H., Wang, Y., Kuai, X., Sun, S., et al. (2023a). High-dosage NMN promotes ferroptosis to suppress lung adenocarcinoma growth through the NAM-mediated SIRT1–AMPK–ACC pathway. *Cancers* 15, 2427. doi:10.3390/cancers15092427

Zhang, S., Liu, X., Wang, J., Yuan, F., and Liu, Y. (2022). Targeting ferroptosis with miR-144-3p to attenuate pancreatic β cells dysfunction via regulating USP22/SIRT1 in type 2 diabetes. *Diabetol. Metab. Syndr.* 14, 89. doi:10.1186/s13098-022-00852-7

Zhang, W., Qian, S., Tang, B., Kang, P., Zhang, H., and Shi, C. (2023b). Resveratrol inhibits ferroptosis and decelerates heart failure progression via Sirt1/p53 pathway activation. *J. Cell. Mol. Medi* 27, 3075–3089. doi:10.1111/jcmm.17874

Zhang, X., Wu, Q., Lu, Y., Wan, J., Dai, H., Zhou, X., et al. (2018). Cerebroprotection by salvianolic acid B after experimental subarachnoid hemorrhage occurs via Nrf2-and SIRT1-dependent pathways. *Free Radic. Biol. Med.* 124, 504–516. doi:10.1016/j.freeradbiomed.2018.06.035

Zhang, Z., Zhang, N., Li, M., Ma, X., and Qiu, Y. (2024c). Sappanone a alleviates osteoarthritis progression by inhibiting chondrocyte ferroptosis via activating the SIRT1/Nrf2 signaling pathway. *Schmiedeb. Arch. Pharmacol.* 397, 8759–8770. doi:10.1007/s00210-024-03179-4

Zhao, H., Ding, Y., and Zhang, L. (2023a). SIRT1/APE1 promotes the viability of gastric cancer cells by inhibiting p53 to suppress ferroptosis. *Open Med-Warsaw* 18 (1), 20220620. doi:10.1515/med-2022-0620

Zhao, L., Jin, L., and Yang, B. (2023b). Saikosaponin A alleviates *Staphylococcus aureus* -induced mastitis in mice by inhibiting ferroptosis via SIRT1/Nrf2 pathway. *J. Cell. Mol. Medi* 27, 3443–3450. doi:10.1111/jcmm.17914

Zhao, L., Jin, L., and Yang, B. (2023c). Diosmetin alleviates S. aureus-induced mastitis by inhibiting SIRT1/GPX4 mediated ferroptosis. *Life Sci.* 331, 122060. doi:10.1016/j.lfs.2023.122060

Zheng, Q., Ma, P., Yang, P., Zhai, S., He, M., Zhang, X., et al. (2023). Alpha lipoic acid ameliorates motor deficits by inhibiting ferroptosis in Parkinson's disease. *Neurosci. Lett.* 810, 137346. doi:10.1016/j.neulet.2023.137346

Zhou, D., Sun, L., Li, J., and Yang, Y. (2024b). Schisandrin B inhibits inflammation and ferroptosis in S.aureus-induced mastitis through regulating SIRT1/p53/SLC7A11 signaling pathway. *Int. Immunopharmacol.* 137, 112430. doi:10.1016/j.intimp.2024.112430

Zhou, Q., and Ruan, D. (2022). SIRT1-autophagy axis may inhibit oxidative stress-induced ferroptosis in human nucleus pulposus cells. *Med. Hypotheses* 159, 110757. doi:10.1016/j.mehy.2021.110757

Zhou, X.-N., Zhang, Q., Peng, H., Qin, Y.-J., Liu, Y.-H., Wang, L., et al. (2024a). Silent information regulator sirtuin 1 ameliorates acute liver failure *via* the p53/glutathione peroxidase 4/gasdermin D axis. *World J. Gastroenterol.* 30, 1588–1608. doi:10.3748/wjg.v30.i11.1588

Zhou, Y., Hu, T., Zeng, H., Lin, L., Xie, H., Lin, R., et al. (2025). Naringenin inhibits ferroptosis in renal tubular epithelial cells of diabetic nephropathy through SIRT1/FOXO3a signaling pathway. *Drug Dev. Res.* 86, e70044. doi:10.1002/ddr.70044

Zhou, Z., Ye, T. J., DeCaro, E., Buehler, B., Stahl, Z., Bonavita, G., et al. (2020). Intestinal SIRT1 deficiency protects mice from ethanol-induced liver injury by mitigating ferroptosis. *Am. J. Pathol.* 190, 82–92. doi:10.1016/j.ajpath.2019.09.012

Zhu, H., Huang, J., Chen, Y., Li, X., Wen, J., Tian, M., et al. (2022). Resveratrol pretreatment protects neurons from oxygen-glucose deprivation/reoxygenation and ischemic injury through inhibiting ferroptosis. *Biosci. Biotechnol. Biochem.* 86, 704–716. doi:10.1093/bbb/zbac048

frontiers | Frontiers in Medicine

TYPE Review
PUBLISHED 26 March 2025
DOI 10.3389/fmed.2025.1462145

OPEN ACCESS

EDITED BY
Juan Carlos Mayo,
University of Oviedo, Spain

REVIEWED BY
Pedro Gonzalez-Menendez,
University of Oviedo, Spain
Yao Luo,
Sichuan University, China
Zilong Zhao,
University of Texas MD Anderson Cancer Center, United States

*CORRESPONDENCE
Yufei Liu
✉ liuyufei@hebipe.edu.cn
Lin Xu
✉ xulin@hebipe.edu.cn

RECEIVED 09 July 2024
ACCEPTED 14 March 2025
PUBLISHED 26 March 2025

CITATION
Li C, Deng D, Jiang Q, Shi J, Xu L and Liu Y (2025) Ferroptosis in NAFLD: insights and the therapeutic potential of exercise. *Front. Med.* 12:1462145. doi: 10.3389/fmed.2025.1462145

Ferroptosis in NAFLD: insights and the therapeutic potential of exercise

Chang Li[1], Dongkun Deng[1], Qingfeng Jiang[1], Jiaming Shi[1], Lin Xu[2]* and Yufei Liu[2]*

[1]Graduate School, Harbin Sport University, Harbin, Heilongjiang, China, [2]College of Human Sport Science, Harbin Sport University, Harbin, Heilongjiang, China

Ferroptosis, a distinct form of non-apoptotic cell death driven by iron accumulation, has garnered significant attention in recent years. Emerging evidence suggests that ferroptosis in hepatocytes may serve as a pivotal trigger in the pathogenesis of non-alcoholic fatty liver disease (NAFLD). Importantly, inhibiting ferroptosis has shown promising potential in slowing the progression of NAFLD. Concurrently, exercise, a cornerstone in the prevention and management of chronic diseases, plays a critical role in regulating disease progression. As such, the modulation of ferroptosis through exercise represents a promising avenue for developing innovative therapeutic strategies. This review aims to systematically elucidate the conceptual framework and molecular mechanisms underlying ferroptosis, with particular emphasis on its pathophysiological role in NAFLD. We have systematically summarized the effects of exercise on ferroptosis regulation through multiple molecular mechanisms, including upregulation of antioxidant defense systems via activation of NRF2, GPX4, and SLC7A11 signaling pathways; and modulation of iron metabolism through FPN-mediated iron homeostasis regulation. These findings not only provide valuable insights into the molecular basis of exercise-induced protection against ferroptosis-mediated cellular damage but also offer novel perspectives for future investigations into exercise-based interventions for NAFLD management. This work thereby contributes to the advancement of therapeutic strategies in the field of metabolic liver diseases.

KEYWORDS

ferroptosis, non-alcoholic fatty liver disease, cell death, exercise, mechanism

1 Introduction

Non-alcoholic fatty liver disease (NAFLD) has become one of the most prevalent and serious chronic liver diseases worldwide, and represents a leading cause of liver disease globally, significantly impairing patients' quality of life and, in severe cases, leading to life-threatening complications such as cirrhosis and hepatocellular carcinoma. According to research employing Markov models to forecast the epidemiology of diseases over the coming decades, the burden of advanced liver diseases (1), such as cirrhosis and hepatocellular carcinoma, caused by NAFLD is projected to more than double globally from 2016 to 2030, reflecting an exponential increase in the disease burden. The ongoing global rise in obesity and type 2 diabetes rates is a major driver of the increasing incidence of NAFLD,

thereby imposing a substantial economic and healthcare burden on individuals and society, highlighting the urgent need for effective interventions. Effective management of NAFLD requires a deeper understanding of its pathogenesis and the development of mechanism-based therapeutic strategies. Currently, ferroptosis, a recently discovered form of regulated cell death, has gained significant attention in diverse fields such as life sciences, medicine, and chemistry, and has been implicated in the pathogenesis of various major diseases, including cancers, neurodegenerative disorders, and metabolic diseases (2–5).

2 Ferroptosis

In 2012, Dixon et al. first described ferroptosis (6), a novel form of regulated cell death characterized by its distinct mechanisms and morphological features, setting it apart from necrosis, apoptosis, and autophagy. The morphological hallmarks of ferroptosis are predominantly observed in mitochondria, which display characteristic changes such as shrinkage, increased membrane density, and a marked reduction or complete loss of mitochondrial cristae. The biological hallmarks of ferroptosis include the depletion of glutathione (GSH) and the subsequent reduction in the activity of glutathione peroxidase 4 (GPX4), a key enzyme responsible for lipid peroxide detoxification. In the absence of GSH, the activity of enzymes such as NADPH oxidase (NOX) may be upregulated. NOX is a key enzymatic source of reactive oxygen species (ROS) within cells (7), and its increased activity leads to elevated ROS levels, which subsequently trigger ferroptosis. A comparison of the key features of different forms of programmed cell death, including ferroptosis, apoptosis, necrosis, and autophagy, is summarized in Table 1.

2.1 The sequential mechanism of ferroptosis

2.1.1 Iron metabolism

Iron is a vital trace element essential for numerous biological processes, including oxygen transport, energy production, DNA synthesis, and cellular respiration (8). Disruptions in iron metabolism can impair normal physiological functions and are implicated in the pathogenesis of various diseases, including anemia, neurodegenerative disorders, and cancer. Iron metabolism is tightly regulated by a sophisticated control system that maintains iron homeostasis through precise regulation of iron absorption, storage, and excretion (9). Under conditions of iron overload, iron regulatory proteins (IRPs) play a central role in modulating the expression of genes involved in iron import, storage, and export, thereby maintaining cellular iron homeostasis (10). Under physiological conditions, transferrin (TRF) binds and transports iron primarily in its ferric form (Fe^{3+}) to various tissues and cells. Transferrin-bound iron (TBI) is internalized via binding to transferrin receptor 1 (TFR1) on the cell surface. Following internalization, Fe^{3+} is reduced to Fe^{2+} by six-transmembrane epithelial antigen of the prostate 3 (STEAP3) and subsequently transported into the cytoplasm by divalent metal transporter 1 (DMT1). The released iron can be utilized for cellular processes, stored in the labile iron pool (LIP), or exported to the extracellular space via ferroportin (FPN), the only known mammalian iron exporter (10). However, persistently elevated Fe^{2+} levels can trigger the Fenton reaction, in which Fe^{2+} reacts with hydrogen peroxide to generate highly reactive hydroxyl radicals, leading to the accumulation of reactive oxygen species (ROS) and enhanced lipid peroxidation (11). Additionally, iron is a cofactor for lipoxygenases (LOXs), enzymes that catalyze the oxidation of polyunsaturated fatty acids, leading to the production of lipid ROS, such as lipid hydroperoxides. The resulting lipid peroxidation causes extensive damage to cellular and mitochondrial membranes, ultimately triggering ferroptosis (12) (Figure 1).

2.1.2 Lipid peroxidation

Lipid peroxidation, a process driven by the oxidation of polyunsaturated fatty acids (PUFAs) in cellular membranes, is the primary driver of ferroptosis. Lipid hydroperoxides, generated primarily through the activity of lipoxygenases (LOXs), are key mediators of cellular dysfunction and death (13). Thus, LOXs are critically involved in the induction of ferroptosis by catalyzing the production of lipid hydroperoxides. Pharmacological inhibition of LOXs has been demonstrated to attenuate ferroptosis, highlighting the enzyme's central role in this cell death pathway (14). Genetic knockout of 12/15-LOX or pharmacological inhibition with baicalein has been shown to protect mice from traumatic brain injury and improve neurological outcomes, further supporting the role of LOXs in ferroptosis (15, 16). These findings underscore the significant role of LOXs in ferroptosis. The extent of ferroptosis is directly influenced by the degree of lipid peroxidation, which is largely determined by the abundance and oxidation susceptibility of polyunsaturated fatty acids (PUFAs) in cellular membranes. Ferroptosis is driven by the peroxidation of specific phospholipid membranes, a process that requires the incorporation of PUFAs into membrane phospholipids. This incorporation renders membranes susceptible to lipid peroxidation through enzymatic (e.g., LOXs) and non-enzymatic (e.g., Fenton reaction) mechanisms, ultimately leading to cell death via the accumulation of toxic peroxidation products (17). Pre-treatment of cells with deuterated PUFAs (D-PUFAs), which are resistant to oxidation due to the kinetic isotope effect, effectively prevents lipid peroxidation and inhibits ferroptosis (18). Future research may explore therapeutic strategies targeting PUFA metabolism, such as inhibiting their incorporation into phospholipid membranes or developing compounds that block their oxidation, as potential approaches to prevent ferroptosis.

2.1.3 Antioxidant system

2.1.3.1 System Xc-/GSH/GPX4 axis

The cystine/glutamate antiporter (System Xc-), glutathione (GSH), and glutathione peroxidase 4 (GPX4) form a critical antioxidant axis that plays a central role in regulating ferroptosis. System Xc- is a heterodimeric complex composed of the light chain SLC7A11 and the heavy chain SLC3A2, which mediates the 1:1 exchange of extracellular cystine for intracellular glutamate (19). Following uptake, cystine is reduced to cysteine by thioredoxin reductase 1 (TrxR1) (20), a critical step for glutathione synthesis. Dysregulation of System Xc- impairs cystine uptake, leading to cysteine and GSH depletion, and consequently increasing cellular

TABLE 1 Comparison of programmed cell death modes.

Programmed cell death pathways	Morphological features	Biochemical characteristics
Apoptosis	Cellular shrinkage, preserved plasma membrane integrity, nuclear condensation, fragmentation of nuclear DNA	Members of the BCL-2 family, activation of caspases, ROS production
Necroptosis	Cellular swelling, rupture of the plasma membrane, lysis of the nucleus	Activation of RIPK1, RIPK3, and MLKL;ROS production, Release of DAMP
Ferroptosis	Mitochondrial atrophy, increased mitochondrial membrane density, and reduced or absent mitochondrial cristae	GSH depletion, GPX4 activity reduction, ROS accumulation, lipid peroxidation
Necrosis	Nuclear swelling, dissolution of the nuclear membrane and cytoplasmic granule membrane, and rupture of the cell membrane	HSPs release, ATP release, inflammasome activation, pro-inflammatory factor release
Pyroptosis	Cell membrane rupture, cell swelling, intact nucleus, nuclear DNA fragmentation	Caspase, caspase-3, caspase-1 activation Pro-inflammatory factors IL-1β and IL-18 release
Autophagy	Cell membrane intact, cytoplasmic vacuolization, chromatin not aggregated	The conversion from LC3-I to LC3-II and the increase in autophagic flux.

BCL-2, B-cell lymphoma-2; caspase, cysteine-aspartic proteases; ROS, reactive oxygen species; RIPK1, receptor-interacting serine/threonine-protein kinase 1; RIPK3, receptor-interacting serine/threonine-protein kinase 3; MLKL, mixed lineage kinase domain-like pseudokinase; DAMPs, damage-associated molecular patterns; GSH, glutathione; GPX4, glutathione peroxidase 4; HSPs, heat shock proteins; IL-1β, interleukin-1 beta; IL-18, interleukin-18; LC3-I/LC3-II, microtubule-associated proteins 1A/1B light chain 3 (autophagy markers).

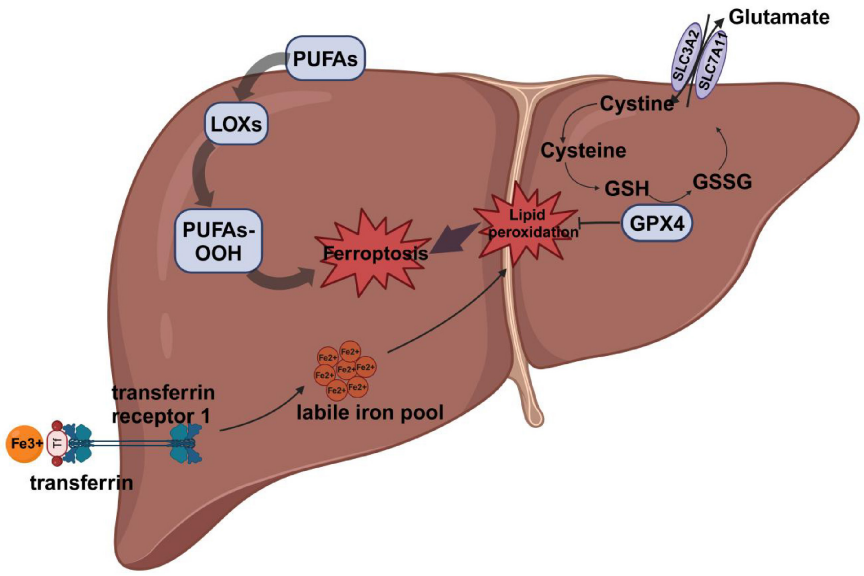

FIGURE 1
The main mechanism of ferroptosis. Iron Uptake and Metabolism:Fe^{3+} binds to TF and is transported into the cell via TFR1. Fe^{3+} is released from TF and reduced to Fe^{2+} by lysosomal reductases. Fe^{2+} enters the LIP, where it catalyzes ROS production via the Fenton reaction. Lipid Peroxidation: PUFAs are incorporated into membrane phospholipids. LOXs or Fe^{2+}-catalyzed ROS oxidize PUFAs to form PUFA-PLOOH, driving membrane damage. System Xc?/GSH/GPX4 Axis:System Xc? imports cystine in exchange for glutamate, supporting GSH synthesis. GSH is required for GPX4 activity, which reduces PLOOH to non-toxic lipid alcohols, preventing ferroptosis. Inhibition of System Xc? depletes GSH, inactivates GPX4, and leads to lipid peroxidation and ferroptosis. TF, transferrin;TFR1, transferrin receptor 1; LIP, labile iron pool; PUFAs, polyunsaturated fatty acids; LOXs, lipoxygenases; GSH, glutathione; GPX4, glutathione peroxidase 4; ROS, reactive oxygen species; SLC3A2, solute carrier family 3 member 2; SLC7A11, solute carrier family 7 member 11;GSSG, glutathione disulfide.

susceptibility to ferroptosis. GSH, a key cellular antioxidant, serves as an essential cofactor for GPX4 activity, enabling the enzyme to neutralize lipid hydroperoxides. GPX4 specifically reduces phospholipid hydroperoxides, protecting cell membranes from oxidative damage and playing a pivotal role in regulating ferroptosis. By converting lipid hydroperoxides into non-toxic alcohols, GPX4 mitigates lipid peroxidation toxicity and maintains the integrity of the lipid bilayer (Figure 2). Aegul et al. demonstrated that genetic ablation of GPX4 in mice leads to acute renal failure and renal tubular ferroptosis, highlighting the enzyme's critical role in preventing ferroptosis (21). Erastin, a ferroptosis inducer, depletes GSH levels, thereby reducing GPX4 activity, increasing ROS accumulation, and triggering ferroptosis (22). Erastin induces ferroptosis by inhibiting System Xc-. In contrast, Erastin2 not only selectively inhibits System Xc- but also independently suppresses mTOR and activates the GCN2/ATF4 pathway, enhancing its ferroptosis-inducing effects (23). Thus, Erastin2 exhibits superior potency in inducing ferroptosis through

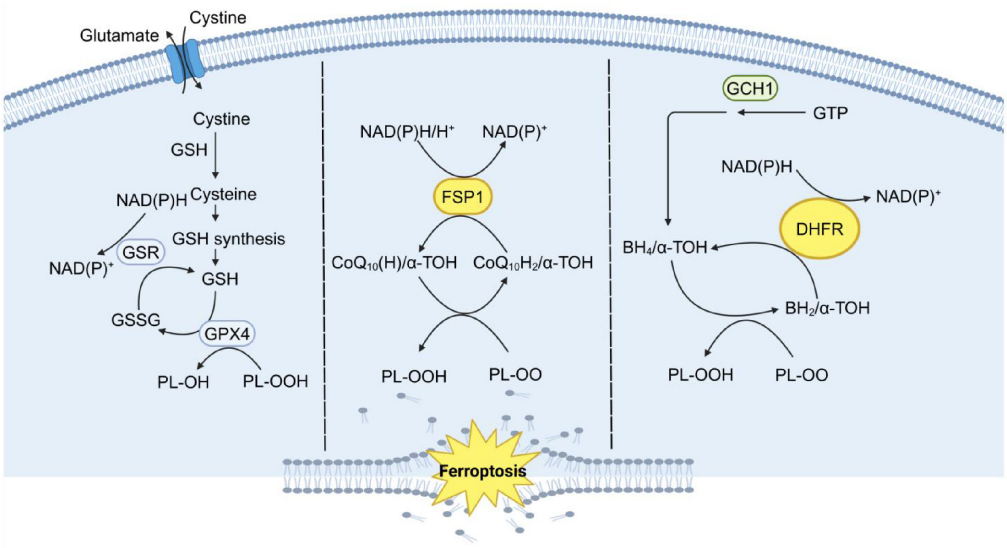

FIGURE 2
The three major systems that control ferroptosis. Ferroptosis is regulated by three major antioxidant axes: the System Xc-/GSH/GPX4 axis, the GCH1/BH4/DHFR axis, and the FSP1/CoQ10/NADH axis, all of which are driven by NADPH. System Xc-/GSH/GPX4 Axis: This axis relies on the cystine-glutamate antiporter system Xc-, which imports cystine for GSH synthesis. GSH is a critical substrate for GPX4, an enzyme that reduces PLOOH to non-toxic lipid alcohols, thereby preventing lipid peroxidation and ferroptosis. GCH1/BH4/DHFR Axis: This axis involves GCH1, which catalyzes the production of BH4, a potent antioxidant. BH4 helps regenerate reduced forms of cofactors and scavenges ROS. DHFR further supports this pathway by maintaining BH4 levels, thus enhancing cellular antioxidant capacity. FSP1/CoQ10/NADH Axis: FSP1 utilizes NADH to reduce CoQ10 to CoQ10H2, a potent lipophilic antioxidant. CoQ10H2 directly neutralizes lipid PLOO and inhibits lipid peroxidation, independent of the GPX4 pathway. This axis is supported by the mevalonate pathway, which generates CoQ10. These three parallel metabolic pathways work synergistically to suppress phospholipid peroxidation, a hallmark of ferroptosis, by maintaining redox homeostasis and protecting cellular membranes from oxidative damage. GSH, glutathione; GSR, glutathione reductase; GSSG, glutathione disulfide; GPX4,glutathione peroxidase 4; FSP1, ferroptosis-suppressor protein 1; CoQ10, ubiquinone; CoQ10H2, ubiquinol; α-TOH, α-tocopherol; GTP, guanosine triphosphate; GCH1, guanosine triphosphate cyclohydrolase 1; BH2, dihydrobiopterin; BH4, tetrahydrobiopterin; DHFR, dihydrofolate reductase; PLOO, peroxyl radical; PLOOH, phospholipid hydroperoxides.

dual targeting of System Xc- and mTOR/GCN2 pathways; however, its efficacy is context-dependent and may vary across cell types and experimental settings. RSL3, another ferroptosis inducer, directly inhibits GPX4 activity, leading to ferroptosis in colorectal cancer cells (24). Targeting ferroptosis as a therapeutic strategy has spurred the development of numerous pharmacological inducers and inhibitors, which are being actively investigated for their potential in treating various diseases (Table 2).

2.1.3.2 The GCH1/BH4/DHFR axis

Guanosine triphosphate (GTP) cyclohydrolase 1 (GCH1) catalyzes the initial step in the biosynthesis of tetrahydrobiopterin (BH4), a process that also involves 6-pyruvyl tetrahydrobiopterin synthase (PTPS) and sepiapterin reductase (SPR). BH4 is regenerated from its oxidized form by dihydrofolate reductase (DHFR), ensuring its availability as a cofactor. GCH1, the rate-limiting enzyme in BH4 biosynthesis, catalyzes the first and key regulatory step of this pathway (25). As an essential cofactor, BH4 plays a critical role in numerous physiological and pathological processes, including the modulation of oxidative stress and inflammatory responses (26). Treatment with the ferroptosis inducer Erastin led to a significant reduction in BH4 levels, whereas RSL4 treatment did not induce any notable changes in BH4 levels. Elevated GCH1 mRNA expression was observed in colorectal cancer, suggesting a potential link between GCH1 activity and oxidative stress-induced cell death. Erastin treatment suppressed GCH1 expression, correlating with the observed reduction in BH4 levels. The GCH1/BH4 pathway is implicated in Erastin-induced ferroptosis, with its deficiency exacerbating lipid peroxidation in colorectal cancer cells (27). Furthermore, following GPX4 ablation, BH4 levels were elevated, and GCH1 overexpression resulted in a modest increase in free thiols and glutathione levels, even in the presence of the glutathione synthesis inhibitor L-Buthionine-sulfoximine (L-BSO). These findings align with data from GPX4 ablation studies, including those involving BH4 supplementation. Thus, the GCH1/BH4 pathway represents an endogenous antioxidant mechanism that operates independently of the GPX4/GSH axis and plays a critical role in modulating ferroptosis (28).

2.1.3.3 FSP1 CoQ10/NADH axis

Ferroptosis-suppressor protein 1 (FSP1), coenzyme Q10 (CoQ10), and nicotinamide adenine dinucleotide (NADH) constitute a parallel antioxidant system that functions independently of GPX4 to suppress ferroptosis. FSP1, a key resistance factor against ferroptosis, functions as a plasma membrane-associated redox enzyme that utilizes NADH to reduce CoQ10, thereby generating antioxidants and inhibiting lipid peroxidation. Loss of FSP1 does not affect System Xc- or glutathione synthesis but, even in the presence of functional GPX4, results in elevated phospholipid oxidation (29). Coenzyme Q10 (CoQ10), a lipophilic molecule, is predominantly localized

TABLE 2 A summary of some inducers and inhibitors of ferroptosis.

Compound	Mechanism of action	References
Inducer		
Erastin	System xc−inhibitor	(21, 26)
Erastin2	System xc−inhibitor	(22)
BSO	γGCS inhibitor, depletion of GSH	(27)
RSL3	GPX4 inhibitor	(23)
Inhibitor		
Fer-1	Catalytic RTA, prevention of lipid peroxidation	(36–39)
Tβ4	Alleviate oxidative stress, enhance GPX4 activity	(40–42)
GB	Prevent lipid peroxidation, activate Nrf2	(43, 44)
Lip-1	Catalytic RTA, prevention of lipid peroxidation	(37, 45–47)
α-tocotrienol	Prevent lipid peroxidation, enhance antioxidant capacity	(48–51)

BSO, buthionine sulfoximine; RSL3, RAS-selective lethal 3; Fer-1, ferrostatin-1; Tβ4, thymosin β4; GB, ginkgolide B; Lip-1, liproxstatin-1; γGCS, γ-glutamylcysteine synthetase; GSH, glutathione;GPX4, glutathione peroxidase 4; Nrf2, nuclear factor erythroid 2-related factor 2; RTA, radical trapping antioxidant.

in the inner mitochondrial membrane, where it plays a critical role in electron transport and antioxidant defense. The reduced form of CoQ10 (CoQ10H2) acts as a potent antioxidant by scavenging free radicals, thereby preventing lipid peroxidation. Additionally, CoQ10H2 can indirectly promote the generation of α-tocotrienol, which further inhibits ferroptosis through its radical-scavenging activity (30). CoQ2, a key enzyme in the CoQ10 biosynthesis pathway, catalyzes the initial step in the synthesis of coenzyme Q10. Genetic knockout or pharmacological inhibition of CoQ2, even in the context of FSP1 overexpression, fails to prevent ferroptosis. In contrast, soluble analogs of coenzyme Q10 effectively inhibit ferroptosis and lipid peroxidation, highlighting the therapeutic potential of targeting this pathway (29, 31). These findings demonstrate that the FSP1/CoQ10 axis functions as a parallel antioxidant system to GPX4, playing a critical role in regulating ferroptosis.

2.1.3.4 Other molecular mechanisms

In addition to GPX4, several regulatory pathways, including the PERK-NRF2-HO-1, AMPK/GSK-3β/NRF2, and HSF1-HSPB1 axes, play critical roles in modulating ferroptosis independently of the GPX4 system. In colorectal cancer, the ER stress inhibitor 4-PBA effectively suppresses erastin-induced ferroptosis and downregulates the expression of nuclear factor E2-related factor 2 (NRF2) and heme oxygenase-1 (HO-1). NRF2 is directly phosphorylated by protein kinase R-like ER kinase (PERK), a key mediator of the NRF2-HO-1 signaling pathway activation in response to erastin. Erastin triggers ferroptosis in colorectal cancer cells by activating the PERK-NRF2-HO-1 signaling pathway, thereby exerting potent anti-tumor effects (32). Under conditions of glucose deprivation, AMPK is activated, initiating a protective energy stress response that mitigates ferroptosis by impairing the synthesis of polyunsaturated fatty acids (PUFAs), essential drivers of lipid peroxidation (33). This mechanism has been demonstrated in the context of myocardial ischemia-reperfusion injury (MIRI), where AMPK activation plays a protective role against ferroptosis. Dexmedetomidine protects against MIRI-induced ferroptosis by activating NRF2 through the AMPK/GSK-3β signaling pathway, which involves the phosphorylation of AMP-activated protein kinase (AMPK) and subsequent NRF2 activation (34). Heat shock protein β-1 (HSPβ-1) functions as a negative regulator of ferroptosis in iron-dependent cancer cells by mitigating iron-mediated oxidative stress. Knockdown of HSF1 and HSPβ-1 sensitizes cells to Erastin-induced ferroptosis, whereas protein kinase C-mediated phosphorylation of HSPβ-1 exerts a protective effect by reducing iron-dependent ROS accumulation, thereby inhibiting ferroptosis (35).

3 Ferroptosis and NAFLD

3.1 Ferroptosis and inflammation

Globally, the prevalence of NAFLD continues to rise, encompassing a spectrum of conditions from simple steatosis to NASH, fibrosis, and cirrhosis (40). To investigate therapeutic strategies for NAFLD, researchers have established a high-fat diet-induced rat model, which recapitulates key features of the disease, including lipid accumulation and inflammation. Administration of Tβ4 has been shown to significantly improve lipid metabolism and reduce pro-inflammatory markers, such as TNF-α and IL-6, in high-fat diet-fed rats. This protective effect is mediated through the upregulation of GPX4, a key regulator of ferroptosis that mitigates lipid peroxidation and cellular damage. In contrast, the ferroptosis inducer Erastin exacerbates liver inflammation, while the iron chelator Ferrostatin-1 (Fer-1) attenuates inflammatory responses. Silencing GPX4 expression using small interfering RNA (siRNA) not only induced ferroptosis but also altered the expression of apoptosis-related factors, leading to exacerbated liver injury (45). In a separate study (52), a high-fat diet-induced mouse model was employed to evaluate the effects of ferroptosis inhibitors on NAFLD progression. These inhibitors suppressed key ferroptosis markers, such as ACSL4 and ALOX15, improving lipid metabolism, insulin sensitivity, and reducing liver inflammation. Notably, the iron chelator deferoxamine demonstrated pronounced anti-inflammatory and anti-ferroptotic effects, significantly mitigating liver injury. Bone morphogenetic protein 4 (BMP4), traditionally recognized for its role in bone and cartilage development (53), has recently been implicated in the pathogenesis of NAFLD. Elevated serum BMP4 levels have been observed in patients with obesity and metabolic syndrome, correlating closely with visceral adipose tissue accumulation (54). In both NAFLD mouse models and FFA-induced hepatocyte models, BMP4 upregulation enhances GPX4 expression at both the gene and protein levels, suggesting a protective role against ferroptosis. These findings indicate that BMP4 attenuates hepatic steatosis and inflammation by modulating ferroptosis pathways. *In vitro*, BMP2 overexpression reduced oxidative stress markers, including ROS and malondialdehyde (MDA), alleviating ferroptosis and attenuating liver inflammation (36). Enoyl coenzyme A hydratase 1 (ECH1), a key enzyme in mitochondrial β-oxidation, plays a critical role in mitigating

inflammation and oxidative stress. ECH1 overexpression reduces inflammatory and oxidative stress markers, while its silencing diminishes these protective effects. Notably, Ferrostatin-1 (Fer-1) treatment significantly ameliorated NASH symptoms in ECH1 knockdown mice, highlighting the role of ferroptosis in disease progression (43). These findings suggest that ECH1 attenuates inflammation and NASH progression by suppressing ferroptosis (43). In summary, ferroptosis is intricately linked to liver inflammation, and targeting ferroptosis pathways holds promise for reducing inflammation and slowing NAFLD progression.

3.2 Ferroptosis and lipid metabolism

Ferroptosis, a recently discovered form of regulated cell death characterized by iron-dependent lipid peroxidation, has emerged as a major focus in biological research due to its implications in various diseases. Emerging evidence highlights the critical role of ferroptosis in modulating lipid metabolism, particularly in the context of metabolic disorders such as NAFLD (45). To elucidate the relationship between ferroptosis and lipid metabolism, researchers established both *in vivo* (mouse) and *in vitro* (hepatocyte) models, enabling comprehensive analysis of ferroptosis-related mechanisms (55). Analysis of ferroptosis-related protein expression revealed that ginkgolide B (GB) treatment significantly upregulated NRF2, a key regulator of ferroptosis, in both liver tissue and hepatocyte models. These findings suggest that NRF2 activation exerts protective effects against ferroptosis by reducing lipid accumulation and oxidative stress, thereby mitigating NAFLD progression. This provides direct evidence linking ferroptosis to the regulation of lipid metabolism. GPX4, a key enzyme in ferroptosis regulation, not only neutralizes polyunsaturated fatty acid hydroperoxides but also mitigates oxidized cholesterol and its esters, highlighting its dual role in ferroptosis and hepatic steatosis (22). Overexpression of GPX4 counteracts the detrimental effects of TRIM59 in NAFLD, while TRIM59 inhibition has been shown to alleviate hepatic steatosis, further underscoring the interplay between these pathways. *In vitro* studies have confirmed that GPX4 overexpression reduces lipid accumulation in hepatocytes, supporting its protective role against steatosis. These findings highlight GPX4's pivotal role in modulating both ferroptosis and hepatic steatosis. TRIM59 promotes hepatic steatosis and ferroptosis by enhancing GPX4 ubiquitination, leading to its degradation and subsequent loss of antioxidant activity (56). In NAFLD models, upregulation of FMO1 and ferroptosis markers contributes to hepatic lipid accumulation, disrupting lipid metabolism and accelerating disease progression (57). These findings provide deeper insights into the intricate interplay between ferroptosis and lipid metabolism in NAFLD pathogenesis. To explore therapeutic strategies targeting ferroptosis, researchers utilized iron inhibitors and demonstrated that Liproxstatin-1 (Lip-1) significantly reduces hepatic lipid deposition, highlighting its potential for improving lipid metabolism (52). This discovery opens new avenues for developing therapeutic strategies targeting ferroptosis in metabolic diseases such as NAFLD. Fatty acid metabolism, a central process in NAFLD development and progression, has emerged as a key area of research due to its role in lipid homeostasis and disease pathogenesis. Excessive fatty acids overwhelm mitochondrial β-oxidation capacity, leading to mitochondrial dysfunction and the accumulation of toxic lipid intermediates. Unmetabolized fatty acids accumulate as lipid droplets or lipotoxic lipids, inducing endoplasmic reticulum (ER) stress and further exacerbating cellular dysfunction. ER stress triggers the generation of ROS, which exacerbate lipid peroxidation and drive ferroptosis (58). This highlights the intricate connection between ferroptosis and dysregulated fatty acid metabolism in NAFLD pathogenesis. In summary, ferroptosis is a key regulator of lipid metabolism, with its dysregulation contributing significantly to NAFLD progression. Further exploration of ferroptosis mechanisms and pathways may yield novel therapeutic strategies for lipid metabolism-related diseases, including NAFLD.

4 Potential effective therapies targeting ferroptosis for NAFLD

4.1 Ferroptosis inhibitors

Fer-1 is a selective and potent inhibitor of ferroptosis, known for its ability to scavenge lipid radicals and prevent lipid peroxidation. By reducing lipid hydroperoxides in the presence of ferrous iron, Fer-1 prevents lipid membrane damage and exerts potent anti-ferroptotic effects (37). In a methionine-choline-deficient (MCD) diet-induced NASH mouse model, Fer-1 treatment effectively inhibits ferroptosis by neutralizing lipid ROS, leading to significant reductions in inflammation, fibrosis, and liver injury (38). Fer-1 also reverses hepatotoxicity associated with lipid metabolism disorders by restoring GPX4 activity and inhibiting lipid hydroperoxide accumulation, thereby preventing NAFLD progression (39). Recent studies have demonstrated that Fer-1 treatment not only suppresses lipid ROS accumulation but also protects against mitochondrial dysfunction, further highlighting its therapeutic potential (59).

Tβ4, a G-actin sequestering peptide, plays a pivotal role in regulating actin polymerization and is implicated in a wide range of critical biological processes, including cell migration, wound healing, and inflammation (41). Previous studies have demonstrated that Tβ4 exerts anti-apoptotic and antioxidant effects by inhibiting ROS production and enhancing cellular survival pathways (42). Tβ4 levels are inversely correlated with inflammation and fibrosis in patients with chronic hepatitis B and NAFLD, suggesting a protective role in liver disease progression (44). These findings suggest that Tβ4 may attenuate liver inflammation and fibrosis by suppressing ROS generation and alleviating oxidative stress, thereby protecting against liver injury. Recent studies have confirmed this hypothesis, showing that Tβ4 treatment reduces inflammation, enhances antioxidant defenses, and upregulates GPX4 expression in high-fat diet (HFD)-induced NAFLD rats. These effects collectively inhibit ferroptosis and improve liver function (45).

GB, a terpenoid compound derived from Ginkgo biloba leaves and root bark, is one of the key bioactive constituents known for its therapeutic properties (60). GB exhibits potent anti-inflammatory, antioxidant, and free radical scavenging activities,

making it a promising candidate for mitigating oxidative stress-related diseases (46). Recent studies have demonstrated that GB significantly modulates oxidative stress and ferroptosis markers, highlighting its potential role in regulating cellular redox balance (60). GB treatment significantly inhibits lipid peroxidation and oxidative stress in both HFD-induced NAFLD mice and palmitic acid (PA)/oleic acid (OA)-treated HepG2 cells, with a pronounced effect on ferroptosis pathways. This protective effect is mediated through the activation of the Nrf2 pathway, which upregulates key antioxidant proteins, including GPX4, HO-1, TFR1, and FTH1, thereby mitigating ferroptosis (55).

Lip-1, a spiroquinoxaline derivative, exhibits potent and selective inhibitory effects on iron-dependent lipid peroxidation pathways, making it a promising candidate for targeting ferroptosis. Lip-1 exerts its effects by disrupting iron ion metabolism, mitigating lipid peroxidation-induced cellular damage, and demonstrating neuroprotective properties in cellular models (47). Given its ability to inhibit lipid peroxidation, Lip-1 has garnered significant interest for its potential therapeutic applications in metabolic diseases, including NAFLD and NASH. Lip-1 treatment alleviates hypertriglyceridemic pancreatitis by modulating lipid metabolism, inhibiting ferroptosis, and mitigating ER stress (61). In liver disease models linked to metabolic syndrome, Lip-1 reduces hepatic steatosis and mitochondrial ROS dysfunction, thereby slowing disease progression (52). Similarly, in NASH models, prophylactic Lip-1 supplementation significantly reduces hepatic steatosis and improves liver histology (38).

α-Tocopherol, also known as vitamin E, is a potent natural antioxidant that also functions as a ferroptosis inhibitor, effectively attenuating cellular lipid peroxidation and inhibiting ferroptosis (62). The anti-ferroptosis activity of α-tocopherol is mediated by Alox15, a key enzyme responsible for the generation of 4-hydroxy-2-nonenal (4-HNE), one of the final products of lipid peroxidation (63, 64). Previous studies have shown that 4-HNE protein adducts are significantly elevated in the livers of NAFLD patients, indicating elevated levels of lipid peroxidation (48). In a mouse model of MCD-induced liver injury, supplementation with α-tocopherol attenuated the MCD-induced increase in hepatic lipid peroxidation and restored the levels of GSH and SOD (49, 50). Recent research suggests that α-tocopherol supplementation reduces intracellular iron accumulation, attenuates lipid peroxidation, upregulates GPX4 expression, and restores mitochondrial membrane potential, thereby mitigating hepatotoxicity. This protective effect is mediated through the upregulation of Nrf2 expression (51). Similarly, oral supplementation of α-tocopherol in mice inhibits iron accumulation and modulates Nrf2 expression, leading to the depletion of hepatic iron stores and enhanced iron efflux through FPN, further strengthening the antioxidant response (65). However, the molecular mechanisms underlying the protective effects of α-tocopherol in ferroptosis-associated NAFLD remain poorly understood, offering an exciting direction for future research.

Despite their potent anti-ferroptotic effects, these inhibitors face significant challenges in clinical translation, primarily due to pharmacokinetic and physicochemical limitations. Fer-1 suffers from poor water solubility, which severely limits its bioavailability and hinders its therapeutic potential (66). These physicochemical properties impair its distribution and absorption, while also rendering it prone to oxidation and conferring a short half-life (67, 68). These pharmacokinetic challenges undermine its sustained efficacy, and the need for frequent dosing may elevate the risk of adverse effects, further limiting its clinical utility. Similarly, Tβ4 has a short biological half-life, requiring frequent dosing to maintain therapeutic levels, which diminishes its clinical practicality (69). Moreover, Tβ4 has a narrow therapeutic window, where both excessive and insufficient doses can result in suboptimal therapeutic outcomes or adverse effects, further complicating its clinical application (70).

Despite its potent antioxidant properties, the clinical utility of GB is hindered by poor bioavailability and inefficient delivery to target tissues, limiting its therapeutic efficacy (71). Lip-1 is rapidly metabolized and exhibits a short elimination half-life, which may compromise its therapeutic efficacy and reduce patient compliance due to the need for frequent dosing (21). Notably, most preclinical studies have relied on parenteral administration rather than oral formulations, indicating potential challenges in achieving adequate oral bioavailability and limiting its clinical applicability.

While high-dose α-tocopherol supplementation may exert therapeutic effects in specific contexts, the current evidence on the safety profile of high-dose α-tocopherol supplementation is still inconclusive. The recommended daily intake of 1,073 milligrams of RRR-α-tocopherol or its esters is currently recommended, yet the safety implications of exceeding this dosage warrant further investigation (72). Moreover, notable differences in bioavailability are observed between natural and synthetic α-tocopherol isoforms, with the natural form exhibiting superior biological activity. These limitations collectively hinder the clinical translation of ferroptosis inhibitors.

4.2 Intermittent fasting and time-restricted eating

Intermittent fasting (IF) and time-restricted feeding (TRF) are two widely studied dietary interventions, with IF involving strict caloric restriction within a limited time window, and TRF typically restricting caloric intake to specific hours of the day, commonly implemented as the 16:8 protocol. The protective effects of fasting have been extensively documented in a wide range of organisms, spanning from simple model organisms, such as yeast, nematodes, and fruit flies, to mammalian models, including mice and primates. These organisms have exhibited significantly extended lifespans under conditions of fasting or nutrient deprivation (73, 74). Fasting induces a metabolic shift from glucose utilization to fatty acid oxidation and ketone body production as primary energy sources. Additionally, ketone bodies act as potent signaling molecules, activating downstream protective pathways that modulate metabolic disorders, such as NAFLD and NASH. These pathways are mediated by factors like PPARγ coactivator 1α (PGC-1α) and fibroblast growth factor 21 (FGF21) (75). To explore the association between fasting and NASH, researchers established a NASH mouse model induced by a high-sugar, high-fat diet. Their results demonstrated that TRF significantly attenuated liver injury, decreased hepatic iron accumulation, and suppressed ferroptosis, thereby ameliorating NASH pathology. Moreover, ferroptosis was implicated in the

pathogenesis of NASH, particularly through the inhibition of PPARα signaling. The study also identified a significant association between the circadian rhythm gene Per2 and ferroptosis, with hepatocyte-specific knockout of Per2 markedly suppressing hepatic ferroptosis (76).

5 Exercise regulates ferroptosis

Ferroptosis is a critical pathophysiological mechanism closely associated with the pathogenesis and progression of multiple diseases. Exercise, as a multifaceted health-promoting intervention, plays a pivotal role in the prevention and management of chronic diseases by modulating lipid metabolism, mitigating oxidative stress, and suppressing inflammatory responses (77). Furthermore, exercise can reduce an organism's susceptibility to ferroptosis, providing novel insights into the prevention and therapeutic strategies for ferroptosis-related diseases (Table 3). Studies have demonstrated that moderate-intensity aerobic exercise can restore oxidative stress homeostasis by augmenting endogenous antioxidant defenses. This exercise-induced activation of various antioxidant pathways significantly decreases intracellular ROS levels, thereby inhibiting ferroptosis and ameliorating conditions such as osteoarthritis (78). Recent findings indicate that moderate-intensity exercise can suppress synovial ferroptosis through the upregulation of lipoxin A4 (LXA4) levels, thus alleviating knee osteoarthritis damage. This therapeutic effect is partially mediated by the activation of estrogen receptor β (ERβ) (79). Furthermore, exercise modulates bone health by promoting the release of irisin from bone cells. Under mechanical stimulation from exercise, increased irisin levels facilitate the removal of excess iron ions from bone cells, thereby preventing ferroptosis and preserving bone structural integrity. This discovery offers a novel theoretical basis for the prevention and management of osteoporosis (80). Moreover, studies have shown that ferroptosis is associated with cardiac dysfunction and mitochondrial structural abnormalities. However, exercise has been proven to enhance cardiac function by upregulating the activity of myocardial oxidative stress-related enzymes, thereby increasing the expression of two key ferroptosis biomarkers, GPX4 and PTGS2, and inhibiting myocardial ferroptosis (81, 82). This finding provides further evidence supporting the cardiovascular benefits of exercise. In cerebral ischemia/reperfusion injury, the expression of ferroptosis-related proteins is markedly downregulated. However, exercise can counteract this effect by upregulating ferroptosis-related protein expression, thereby inhibiting ferroptosis (83, 84). Notably, in some cases, such as when SLC7A11 is downregulated by Erastin, the neuroprotective effects of exercise may be partially attenuated (83). After traumatic brain injury, a decrease in GPX4 expression and an increase in lipid peroxidation are indicators of ferroptosis. However, these ferroptosis-related features are significantly mitigated by exercise intervention (85). Additionally, research has shown that 8 weeks of aerobic exercise can suppress lipid peroxidation through the Xc-/GPX4 axis in neurodegenerative diseases, thereby reducing neuronal sensitivity to ferroptosis and improving spatial cognition, learning, and memory in mice (86).

In summary, exercise modulates ferroptosis through multiple interconnected molecular pathways. The key mechanisms involve: (1) enhancement of antioxidant defense systems via the activation of NRF2, GPX4, and SLC7A11; (2) regulation of iron metabolism through FPN-mediated iron homeostasis; (3) suppression of lipid peroxidation via the ACSL4 and SLC7A11 pathways; (4) inhibition of inflammatory responses and cell death signaling through the NF-κB and STING pathways; and (5) improvement of mitochondrial function (Figure 3). These synergistic mechanisms collectively highlight exercise as a potent intervention against ferroptosis-induced cellular damage, thereby providing therapeutic potential for a range of ferroptosis-associated diseases. However, current research on the effects of exercise on ferroptosis is still limited, with the majority of studies concentrating on aerobic exercise interventions. Future studies should broaden their scope to investigate the impact of other exercise modalities on ferroptosis inhibition. Additionally, further research is required to elucidate the precise mechanisms underlying exercise-induced inhibition of ferroptosis, to comprehensively understand its biological underpinnings and clinical implications. The role of exercise in modulating ferroptosis is summarized in Table 3.

TABLE 3 The use of exercise in ferroptosis.

Modes of exercise	Disease	Mechanism of action and targets	References
Aerobic exercise	Osteoarthritis	Upregulate NRF2, GPX4, SLC7A11, and inhibit NF-κB.	(78)
Aerobic exercise	Knee osteoarthritis	Upregulate LXA4 and NRF2 expression	(79)
Aerobic exercise	Osteoporosis	Upregulate NRF2 and FPN expression	(80)
Aerobic exercise	High-fat induced myocardial injury	Enhance the expression of NRF2 and GPX4	(81)
Aerobic exercise	Azithromycin-induced myocardial injury	Increase the expression of GPX4 and PTGS2	(82)
Aerobic exercise	Ischemia/reperfusion	Enhance the expression of NRF2, SLC7A11, GPX4.	(83)
Aerobic exercise	Ischemic brain injury	Upregulate GPX4 and SLC7A11 expression, downregulate ACSL4 expression.	(84)
Aerobic exercise	Traumatic brain injury	Upregulate GPX4 expression, inhibit STING expression	(85)
Aerobic exercise	Alzheimer's disease	Upregulate Xc- and GPX4 expression	(86)

NRF2, nuclear factor erythroid 2-related factor 2; GPX4, glutathione peroxidase 4; SLC7A11, solute carrier family 7 member 11; FPN, ferroportin; ACSL4, Acyl-CoA synthetase long-chain family member 4; NF-κB, nuclear factor kappa B; STING, stimulator of interferon genes; PTGS2, prostaglandin-endoperoxide synthase 2; LXA4, lipoxin A4.

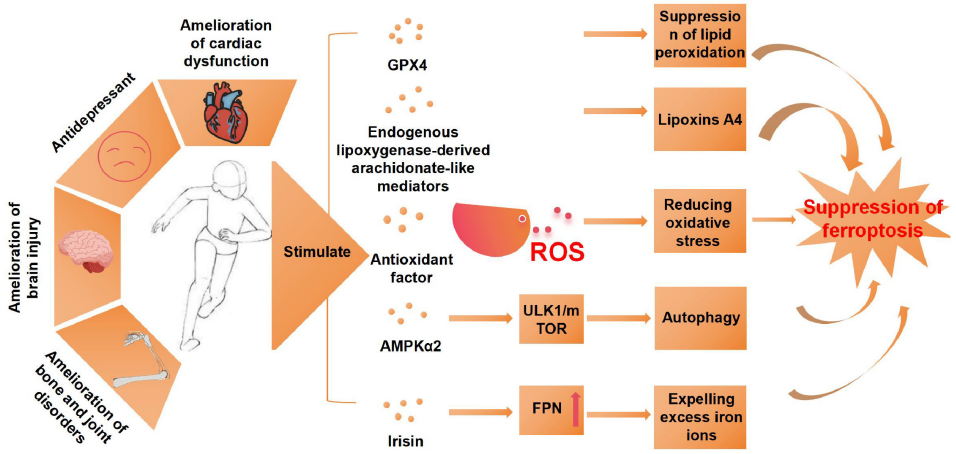

FIGURE 3
Exercise mitigates the effects of ferroptosis and its underlying mechanisms. AMPKα2, protein kinase AMP-activated catalytic subunit alpha 2; ULK1, unc-51-like kinase 1; mTOR, mammalian target of rapamycin; FPN, ferroportin; ROS, reactive oxygen species.

6 Conclusion

Ferroptosis, a recently discovered form of regulated cell death, is driven by iron-dependent lipid peroxidation and involves intricate molecular mechanisms. Emerging evidence has established a strong link between ferroptosis and the pathogenesis and progression of non-alcoholic fatty liver disease (NAFLD). This association is mediated through dysregulated iron metabolism, lipid peroxidation, and key signaling pathways, including the System Xc-/GSH/GPX4 axis, GCH1/BH4/DHFR pathway, and FSP1/CoQ10/NADH system. These findings highlight the potential of targeting ferroptosis as a novel therapeutic strategy for NAFLD, offering new avenues for disease management. This review also underscores the potential of exercise to inhibit ferroptosis, thereby modulating NAFLD progression and offering a non-pharmacological therapeutic option. Further research is essential to elucidate the dynamic interplay between exercise, ferroptosis, and NAFLD, providing a solid theoretical basis and practical guidelines for exercise-based interventions targeting ferroptosis inhibition. Despite promising findings, research on exercise interventions targeting ferroptosis in NAFLD is still in its infancy, with many unanswered questions and challenges. Key questions regarding optimal exercise modalities, intensities, and mechanisms of action remain to be addressed. While current studies have primarily focused on aerobic exercise, the effects of HIIT, resistance training, and combined exercise modalities on ferroptosis regulation are largely unexplored. Additionally, the differential effects of exercise intensity and training load on ferroptosis pathways remain poorly understood, representing a critical research gap. Nevertheless, exercise-based interventions targeting ferroptosis hold significant promise and may provide a novel, effective, and accessible therapeutic strategy for NAFLD patients.

Author contributions

CL: Writing – original draft, Writing – review and editing. DD: Writing – original draft. QJ: Investigation, Writing – review and editing. JS: Investigation, Writing – review and editing. LX: Funding acquisition, Resources, Supervision, Writing – original draft, Writing – review and editing. YL: Writing – original draft, Writing – review and editing, Funding acquisition, Resources, Supervision.

Funding

The author(s) declare that financial support was received for the research and/or publication of this article. This work was supported by Natural Science Foundation of Heilongjiang Province (LH2022C051), and Basic Research Expenses for Undergraduate Universities in Heilongjiang Province (2022KYYWF-FC04).

Acknowledgments

We acknowledge the contributions of specific colleagues, institutions, or agencies that aided the efforts of the authors. The figures were created with BioRender software (BioRender.com).

Conflict of interest

The authors declare that the research was conducted in the absence of any commercial or financial relationships that could be construed as a potential conflict of interest.

Publisher's note

References

1. Estes, C, Anstee Q, Arias-Loste M, Bantel H, Bellentani S, Caballeria J, et al. Modeling NAFLD disease burden in China,France, Germany, Italy, Japan, Spain, United Kingdom, and United States for the period 2016-2030. *J Hepatol.* (2018) 69:896–904. doi: 10.1016/j.jhep.2018.05.036

2. Zhou Q, Meng Y, Li D, Yao L, Le J, Liu Y, et al. Ferroptosis in cancer: From molecular mechanisms to therapeutic strategies. *Signal Transduct Target Ther.* (2024) 9:55. doi: 10.1038/s41392-024-01769-5

3. Xiang Y, Song X, Long D. Ferroptosis regulation through Nrf2 and implications for neurodegenerative diseases. *Arch Toxicol.* (2024) 98:579–615. doi: 10.1007/s00204-023-03660-8

4. Tsurusaki S, Tsuchiya Y, Koumura T, Nakasone M, Sakamoto T, Matsuoka M, et al. Hepatic ferroptosis plays an important role as the trigger for initiating inflammation in nonalcoholic steatohepatitis. *Cell Death Dis.* (2019) 10:449. doi: 10.1038/s41419-019-1678-y

5. Cheng Z, Chu H, Zhu Q, Yang L. Ferroptosis in non-alcoholic liver disease: Molecular mechanisms and therapeutic implications. *Front Nutr.* (2023) 10:1090338. doi: 10.3389/fnut.2023.1090338

6. Dixon S, Lemberg K, Lamprecht M, Skouta R, Zaitsev E, Gleason C, et al. Ferroptosis: an iron-dependent form of nonapoptotic cell death. *Cell.* (2012) 149:1060–72. doi: 10.1016/j.cell.2012.03.042

7. Su L, Zhang J, Gomez H, Kellum J, Peng Z. Mitochondria ROS and mitophagy in acute kidney injury. *Autophagy.* (2023) 19:401–14. doi: 10.1080/15548627.2022.2084862

8. Lu J, Hayashi K, Awai M. Transferrin receptor expression in normal, iron-deficient and iron-overloaded rats. *Acta Pathol Jpn.* (1989) 39:759–64.

9. Vela D. Keeping heart homeostasis in check through the balance of iron metabolism. *Acta Physiol (Oxf).* (2020) 228:e13324. doi: 10.1111/apha.13324

10. Chifman J, Laubenbacher R, Torti SV. A systems biology approach to iron metabolism. *Adv Exp Med Biol.* (2014) 844:201–25.

11. Huang L, Bian M, Zhang J, Jiang L. Iron metabolism and ferroptosis in peripheral nerve injury. *Oxid Med Cell Longev.* (2022) 2022:5918218.

12. Xie L, Fefelova N, Pamarthi S, Gwathmey J. Molecular mechanisms of ferroptosis and relevance to cardiovascular disease. *Cells.* (2022) 11:2726. doi: 10.3390/cells11172726

13. Gaschler M, Stockwell B. Lipid peroxidation in cell death. *Biochem Biophys Res Commun.* (2017) 482:419–25.

14. Stockwell B, Friedmann Angeli J, Bayir H, Bayir H, Bush A, Conrad M, et al. Ferroptosis: A regulated cell death nexus linking metabolism redox biology, and disease. *Cell.* (2017) 171:273–85. doi: 10.1016/j.cell.2017.09.021

15. van Leyen K, Kim H, Lee S, Jin G, Arai K, Lo E, et al. Baicalein and 12/15-lipoxygenase in the ischemic brain. *Stroke.* (2006) 37:3014–8. doi: 10.1161/01.STR.0000249004.25444.a5

16. Kenny E, Fidan E, Yang Q, Anthonymuthu T, New L, Meyer E, et al. Ferroptosis contributes to neuronal death and functional outcome after traumatic brain injury. *Crit Care Med.* (2019) 47:410–8. doi: 10.1097/CCM.0000000000003555

17. Qiu B, Zandkarimi F, Bezjian C, Reznik E, Soni R, Gu W, et al. Phospholipids with two polyunsaturated fatty acyl tails promote ferroptosis. *Cell.* (2024) 187:1177–1190.e18. doi: 10.1016/j.cell.2024.01.030.

18. Yang W, Kim K, Gaschler M. Peroxidation of polyunsaturated fatty acids by lipoxygenases drives ferroptosis. *Proc Natl Acad Sci U S A.* (2016) 113:E4966–75.

19. Koppula P, Zhuang L, Gan B. Cystine transporter SLC7A11/xCT in cancer: ferroptosis, nutrient dependency, and cancer therapy. *Protein Cell.* (2021) 12:599–620. doi: 10.1007/s13238-020-00789-5

20. Mandal P, Seiler A, Perisic T, Kölle P, Banjac Canak A, et al. System x(c)- and thioredoxin reductase 1 cooperatively rescue glutathione deficiency. *J Biol Chem.* (2010) 285:22244–53. doi: 10.1074/jbc.M110.121327

21. Friedmann Angeli J, Schneider M, Proneth B, Tyurina Y, Tyurin V, Hammond V, et al. Inactivation of the ferroptosis regulator Gpx4 triggers acute renal failure in mice. *Nat Cell Biol.* (2014) 16:1180–91. doi: 10.1038/ncb3064

22. Forcina G, Dixon S. GPX4 at the crossroads of lipid homeostasis and ferroptosis. *Proteomics.* (2019) 19:e1800311. doi: 10.1002/pmic.201800311

23. Conlon M, Poltorack C, Forcina G, Armenta D, Mallais M, Perez M, et al. compendium of kinetic modulatory profiles identifies ferroptosis regulators. *Nat Chem Biol.* (2021) 17:665–74. doi: 10.1038/s41589-021-00751-4

24. Sui X, Zhang R, Liu S, et al. RSL3 drives ferroptosis through GPX4 inactivation and ROS production in colorectal cancer. *Front Pharmacol.* (2018) 9:1371. doi: 10.3389/fphar.2018.01371

25. Xu J, Wu Y, Song P, Zhang M, Wang S, Zou M. Proteasome-dependent degradation of guanosine 5'-triphosphate cyclohydrolase I causes tetrahydrobiopterin deficiency in diabetes mellitus. *Circulation.* (2007) 116:944–53.

26. Fanet H, Capuron L, Castanon N, Calon F, Vancassel S. Tetrahydrobioterin (BH4) pathway: From metabolism to neuropsychiatry. *Curr Neuropharmacol.* (2021) 19:591–609.

27. Hu Q, Wei W, Wu D, Huang F, Li M, Li W, et al. Blockade of GCH1/BH4 axis activates ferritinophagy to mitigate the resistance of colorectal cancer to erastin-induced ferroptosis. *Front Cell Dev Biol.* (2022) 10:810327. doi: 10.3389/fcell.2022.810327

28. Kraft V, Bezjian C, Pfeiffer S, Ringelstetter L, Müller C, Zandkarimi F, et al. GTP cyclohydrolase 1/tetrahydrobiopterin counteract ferroptosis through lipid remodeling. *ACS Cent Sci.* (2020) 6:41–53. doi: 10.1021/acscentsci.9b01063

29. Bersuker K, Hendricks J, Li Z, Magtanong L, Ford B, Tang P, et al. The CoQ oxidoreductase FSP1 acts parallel to GPX4 to inhibit ferroptosis. *Nature.* (2019) 575:688–92. doi: 10.1038/s41586-019-1705-2

30. Crane F. Discovery of ubiquinone (coenzyme Q) and an overview of function. *Mitochondrion.* (2007) 7:S2–7. doi: 10.1016/j.mito.2007.02.011

31. Doll S, Freitas F, Shah R, Aldrovandi M, da Silva M, Ingold I, et al. FSP1 is a glutathione-independent ferroptosis suppressor. *Nature.* (2019) 575:693–8. doi: 10.1038/s41586-019-1707-0

32. Wei R, Zhao Y, Wang J, Yang X, Li S, Wang Y, et al. Tagitinin C induces ferroptosis through PERK-Nrf2-HO-1 signaling pathway in colorectal cancer cells. *Int J Biol Sci.* (2021) 17:2703–17. doi: 10.7150/ijbs.59404

33. Kagan V, Mao G, Qu F, Angeli J, Doll S, Croix C, et al. Oxidized arachidonic and adrenic PEs navigate cells to ferroptosis. *Nat Chem Biol.* (2017) 13:81–90. doi: 10.1038/nchembio.2238

34. Wang Z, Yao M, Jiang L, Wang L, Yang Y, Wang Q, et al. Dexmedetomidine attenuates myocardial ischemia/reperfusion-induced ferroptosis via AMPK/GSK-3β/Nrf2 axis. *Biomed Pharmacother.* (2022) 154:113572. doi: 10.1016/j.biopha.2022.113572

35. Sun X, Ou Z, Xie M, Kang R, Fan Y, Niu X. HSPB1 as a novel regulator of ferroptotic cancer cell death. *Oncogene.* (2015) 34:5617–25. doi: 10.1038/onc.2015.32

36. Wang X, Ma B, Wen X, You H, Sheng C, Bu L, et al. Bone morphogenetic protein 4 alleviates nonalcoholic steatohepatitis by inhibiting hepatic ferroptosis [published correction appears. *Cell Death Discov.* (2022) 8:463. doi: 10.1038/s41420-022-01011-7

37. Miotto G, Rossetto M, Di Paolo M, Orian L, Venerando R, Roveri A, et al. Insight into the mechanism of ferroptosis inhibition by ferrostatin-1. *Redox Biol.* (2020) 28:101328. doi: 10.1016/j.redox.2019.101328

38. Li X, Wang T, Huang X, Li Y, Sun T, Zang S, et al. Targeting ferroptosis alleviates methionine-choline deficient (MCD)-diet induced NASH by suppressing liver lipotoxicity. *Liver Int.* (2020) 40:1378–94. doi: 10.1111/liv.14428

39. Sun M, Sun Q, Li T, Ren X, Xu Q, Sun Z, et al. Silica nanoparticles induce liver lipid metabolism disorder via ACSL4-mediated ferroptosis. *Environ Pollut.* (2024) 359:124590. doi: 10.1016/j.envpol.2024.124590

40. Rinella M, Neuschwander-Tetri B, Siddiqui M, Siddiqui M, Abdelmalek M, Caldwell S, et al. AASLD practice guidance on the clinical assessment and management of nonalcoholic fatty liver disease. *Hepatology.* (2023) 77:1797–835. doi: 10.1097/HEP.0000000000000323

41. Jiang Y, Han T, Zhang Z, Li M, Qi F, Zhang Y, et al. Potential role of thymosin beta 4 in the treatment of nonalcoholic fatty liver disease. *Chronic Dis Transl Med.* (2017) 3:165–8. doi: 10.1016/j.cdtm.2017.06.003

42. Li Y, Zhu X, Liu X, Du A, Yu B. miR-200a mediates protection of thymosin β-4 in cardiac microvascular endothelial cells as a novel mechanism under hypoxia-reoxygenation injury. *J Cell Biochem.* (2019) 120:19098–106. doi: 10.1002/jcb.29237

43. Liu B, Yi W, Mao X, Yang L, Rao C. Enoyl coenzyme A hydratase 1 alleviates nonalcoholic steatohepatitis in mice by suppressing hepatic ferroptosis. *Am J Physiol Endocrinol Metab.* (2021) 320:E925–37.

44. Liang J, Cai W, Han T, Jing L, Ma Z, Gao Y. The expression of thymosin β4 in chronic hepatitis B combined nonalcoholic fatty liver disease. *Medicine (Baltimore).* (2016) 95:e5763. doi: 10.1097/MD.0000000000005763

45. Zhu Z, Zhang Y, Huang X, Can L, Zhao X, Wang Y, et al. Thymosin beta 4 alleviates non-alcoholic fatty liver by inhibiting ferroptosis via up-regulation of GPX4. *Eur J Pharmacol.* (2021) 908:174351. doi: 10.1016/j.ejphar.2021.174351

46. Chen J, Ou Z, Gao T, Yang Y, Shu A, Xu H, et al. Ginkgolide B alleviates oxidative stress and ferroptosis by inhibiting GPX4 ubiquitination to improve diabetic nephropathy. *Biomed Pharmacother.* (2022) 156:113953. doi: 10.1016/j.biopha.2022.113953

47. Chen J, Chen Z, Yu D, Yan Y, Hao X, Zhang M, et al. Neuroprotective effect of hydrogen sulfide subchronic treatment against tbi-induced ferroptosis and cognitive deficits mediated through Wnt signaling pathway. *Cell Mol Neurobiol.* (2023) 43:4117–40. doi: 10.1007/s10571-023-01399-5

48. Podszun M, Chung J, Ylaya K, Kleiner D, Hewitt S, Rotman Y. 4-HNE immunohistochemistry and image analysis for detection of lipid peroxidation in

human liver samples using Vitamin E treatment in NAFLD as a proof of concept. *J Histochem Cytochem.* (2020) 68:635–43. doi: 10.1369/0022155420946402

49. Presa N, Clugston R, Lingrell S, Kelly S, Merrill A, Jana S, et al. Vitamin E alleviates non-alcoholic fatty liver disease in phosphatidylethanolamine N-methyltransferase deficient mice. *Biochim Biophys Acta Mol Basis Dis.* (2019) 1865:14–25. doi: 10.1016/j.bbadis.2018.10.010

50. Nan Y, Wu W, Fu N, Liang B, Wang R, Li L, et al. Antioxidants vitamin E and 1-aminobenzotriazole prevent experimental non-alcoholic steatohepatitis in mice. *Scand J Gastroenterol.* (2009) 44:1121–31. doi: 10.1080/00365520903114912

51. Sen Gupta P, Karmakar S, Biswas I, Ghosal J, Banerjee A, Roy S, et al. Vitamin E alleviates chlorpyrifos induced glutathione depletion, lipid peroxidation and iron accumulation to inhibit ferroptosis in hepatocytes and mitigate toxicity in zebrafish. *Chemosphere.* (2024) 359:142252. doi: 10.1016/j.chemosphere.2024.142252

52. Tong J, Lan X, Zhang Z, Liu Y, Sun D, Wang X, et al. Ferroptosis inhibitor liproxstatin-1 alleviates metabolic dysfunction-associated fatty liver disease in mice: potential involvement of PANoptosis. *Acta Pharmacol Sin.* (2023) 44:1014–28. doi: 10.1038/s41401-022-01010-5

53. Zhao M, Harris S, Horn D, Geng Z, Nishimura R, Mundy G, et al. Bone morphogenetic protein receptor signaling is necessary for normal murine postnatal bone formation. *J Cell Biol.* (2002) 157:1049–60. doi: 10.1083/jcb.200109012

54. Son J, Kim M, Park Y, Baek K, Yoo S, Song K, et al. Association of serum bone morphogenetic protein 4 levels with obesity and metabolic syndrome in non-diabetic individuals. *Endocr J.* (2011) 58:39–46. doi: 10.1507/endocrj.k10e-248

55. Yang Y, Chen J, Gao Q, Shan X, Wang J, Lv Z. Study on the attenuated effect of Ginkgolide B on ferroptosis in high fat diet induced nonalcoholic fatty liver disease. *Toxicology.* (2020) 445:152599.

56. Zhang J, Xie H, Yao J, Jin W, Pan H, Pan Z, et al. TRIM59 promotes steatosis and ferroptosis in non-alcoholic fatty liver disease via enhancing GPX4 ubiquitination. *Hum Cell.* (2023) 36:209–22. doi: 10.1007/s13577-022-00820-3

57. Zou L, Shi Q, Li Y, Yuan Z, Peng L, Lu J, et al. FMO1 promotes nonalcoholic fatty liver disease progression by regulating PPARα activation and inducing ferroptosis. *Discov Med.* (2023) 35:612–22. doi: 10.24976/Discov.Med.202335177.60

58. Bailey A, Koster G, Guillermier C, Hirst E, MacRae J, Lechene C, et al. Antioxidant role for lipid droplets in a stem cell niche of drosophila. *Cell.* (2015) 163:340–53. doi: 10.1016/j.cell.2015.09.020

59. Cai W, Wu S, Ming X, Li Z, Pan D, Yang X, et al. IL6 derived from macrophages under intermittent hypoxia exacerbates NAFLD by promoting ferroptosis via MARCH3-Led ubiquitylation of GPX4. *Adv Sci (Weinh).* (2024) 11:e2402241. doi: 10.1002/advs.202402241

60. Yang Y, Wu Q, Shan X, Zhou H, Wang J, Hu Y, et al. Ginkgolide B attenuates cerebral ischemia-reperfusion injury via inhibition of ferroptosis through disrupting NCOA4-FTH1 interaction. *J Ethnopharmacol.* (2024) 318:116982. doi: 10.1016/j.jep.2023.116982

61. Xiang X, Xu M, Liu L, Meng N, Lei Y, Feng Y, et al. Liproxstatin-1 attenuates acute hypertriglyceridemic pancreatitis through inhibiting ferroptosis in rats. *Sci Rep.* (2024) 14:9548. doi: 10.1038/s41598-024-60159-7

62. Hu Q, Zhang Y, Lou H, Liu J, Duan W, Wang H, et al. GPX4 and vitamin E cooperatively protect hematopoietic stem and progenitor cells from lipid peroxidation and ferroptosis. *Cell Death Dis.* (2021) 12:706. doi: 10.1038/s41419-021-04008-9

63. Wenzel S, Tyurina Y, Zhao J, St Croix C, Dar H, Mao G, et al. PEBP1 wardens ferroptosis by enabling lipoxygenase generation of lipid death signals. *Cell.* (2017) 171:628–641.e26. doi: 10.1016/j.cell.2017.09.044.

64. Tomita K, Takashi Y, Ouchi Y, Kuwahara Y, Igarashi K, Nagasawa T, et al. Lipid peroxidation increases hydrogen peroxide permeability leading to cell death in cancer cell lines that lack mtDNA. *Cancer Sci.* (2019) 110:2856–66. doi: 10.1111/cas.14132

65. Baratz E, Protchenko O, Jadhav S, Zhang D, Violet P, Grounds S, et al. Vitamin E induces liver iron depletion and alters iron regulation in mice. *J Nutr.* (2023) 153:1866–76. doi: 10.1016/j.tjnut.2023.04.018

66. Wang K, Jiang L, Zhong Y, Zhang Y, Yin Q, Li S, et al. Ferrostatin-1-loaded liposome for treatment of corneal alkali burn via targeting ferroptosis. *Bioeng Transl Med.* (2021) 7:e10276. doi: 10.1002/btm2.10276

67. Hofmans S, Vanden Berghe T, Devisscher L, Hassannia B, Lyssens S, Joossens J, et al. Novel ferroptosis inhibitors with improved potency and ADME properties. *J Med Chem.* (2016) 59:2041–53. doi: 10.1021/acs.jmedchem.5b01641

68. Devisscher L, Van Coillie S, Hofmans S, Van Rompaey D, Goossens K, Meul E, et al. Discovery of novel, drug-like ferroptosis inhibitors with in vivo efficacy. *J Med Chem.* (2018) 61:10126–40. doi: 10.1021/acs.jmedchem.8b01299

69. Mora C, Baumann C, Paino J, Goldstein A, Badamchian M. Biodistribution of synthetic thymosin beta 4 in the serum, urine, and major organs of mice. *Int J Immunopharmacol.* (1997) 19:1–8. doi: 10.1016/s0192-0561(97)00005-2

70. Ruff D, Crockford D, Girardi G, Zhang YA. randomized, placebo-controlled, single and multiple dose study of intravenous thymosin beta4 in healthy volunteers. *Ann N Y Acad Sci.* (2010) 1194:223–9. doi: 10.1111/j.1749-6632.2010.05474.x

71. Liu Y, Zhang C, Cheng L, Wang H, Lu M, Xu H. Enhancing both oral bioavailability and anti-ischemic stroke efficacy of ginkgolide B by preparing nanocrystals self-stabilized Pickering nano-emulsion. *Eur J Pharm Sci.* (2024) 192:106620. doi: 10.1016/j.ejps.2023.106620

72. Hathcock J, Azzi A, Blumberg J, Bray T, Dickinson A, Frei B, et al. Vitamins E and C are safe across a broad range of intakes. *Am J Clin Nutr.* (2005) 81:736–45. doi: 10.1093/ajcn/81.4.736

73. Longo V, Mattson M. Fasting: Molecular mechanisms and clinical applications. *Cell Metab.* (2014) 19:181–92. doi: 10.1016/j.cmet.2013.12.008

74. Redman L, Smith S, Burton J, Martin C, Il'yasova D, Ravussin E. Metabolic slowing and reduced oxidative damage with sustained caloric restriction support the rate of living and oxidative damage theories of aging. *Cell Metab.* (2018) 27:805–815.e4. doi: 10.1016/j.cmet.2018.02.019.

75. Marjot T, Tomlinson J, Hodson L, Ray D. Timing of energy intake and the therapeutic potential of intermittent fasting and time-restricted eating in NAFLD. *Gut.* (2023) 72:1607–19. doi: 10.1136/gutjnl-2023-329998

76. Shu Y, Gao W, Chu H, Yang L, Pan X, Ye J. Attenuation by time-restricted feeding of high-fat and high-fructose diet-induced NASH in mice is related to Per2 and ferroptosis. *Oxid Med Cell Longev.* (2022) 2022:8063897. doi: 10.1155/2022/8063897

77. Angulo J, El Assar M, Álvarez-Bustos A, Rodríguez-Mañas L. Physical activity and exercise: Strategies to manage frailty. *Redox Biol.* (2020) 35:101513. doi: 10.1016/j.redox.2020.101513

78. Han J, Zhan LN, Huang Y, Guo S, Zhou X, Kapilevich L, et al. Moderate mechanical stress suppresses chondrocyte ferroptosis in osteoarthritis by regulating NF-κB p65/GPX4 signaling pathway. *Sci Rep.* (2024) 14:5078. doi: 10.1038/s41598-024-55629-x

79. Hu Z, Chen L, Zhao J, Zhang W, Jin Z, Sun Y, et al. Lipoxin A4 ameliorates knee osteoarthritis progression in rats by antagonizing ferroptosis through activation of the ESR2/LPAR3/Nrf2 axis in synovial fibroblast-like synoviocytes. *Redox Biol.* (2024) 73:103143. doi: 10.1016/j.redox.2024.103143

80. Tao L, Wang J, Wang K, Liu Q, Li H, Xu S, et al. Exerkine FNDC5/irisin-enriched exosomes promote proliferation and inhibit ferroptosis of osteoblasts through interaction with Caveolin-1. *Aging Cell.* (2024):23:e14181. doi: 10.1111/acel.14181

81. Wang L, Qiao Y, Yu J, Wang Q, Wu X, Cao Q, et al. Endurance exercise preconditioning alleviates ferroptosis induced by doxorubicin-induced cardiotoxicity through mitochondrial superoxide-dependent AMPKα2 activation. *Redox Biol.* (2024) 70:103079.

82. Gao Y, Ling Y, Wu H, Zhang P, Zhou J, Gu H, et al. Swimming training attenuates doxorubicin induced cardiomyopathy by targeting the mir-17-3p/KEAP1/NRF2 axis. *Biochem Biophys Res Commun.* (2024) 739:150568. doi: 10.1016/j.bbrc.2024.150568

83. Liu T, Cui Y, Dong S, Kong X, Xu X, Wang Y, et al. Treadmill training reduces cerebral ischemia-reperfusion injury by inhibiting ferroptosis through activation of SLC7A11/GPX4. *Oxid Med Cell Longev.* (2022) 2022:8693664.

84. Huang M, Cheng S, Li Z, Chen J, Wang C, Li J, et al. Preconditioning exercise inhibits neuron ferroptosis and ameliorates brain ischemia damage by skeletal muscle-derived exosomes via regulating miR-484/ACSL4 Axis. *Antioxid Redox Signal.* (2024) 28:769–92.

85. Chen J, Zhu T, Yu D, Yan B, Zhang Y, Jin J, et al. Moderate Intensity of treadmill exercise rescues TBI-induced ferroptosis, neurodegeneration, and cognitive impairments via suppressing STING pathway. *Mol Neurobiol.* (2023) 60:4872–96.

86. Li C, Cui K, Zhu X, Wang S, Yang Q, Fang G. 8-weeks aerobic exercise ameliorates cognitive deficit and mitigates ferroptosis triggered by iron overload in the prefrontal cortex of APPSwe/PSEN1dE9 mice through Xc-/GPx4 pathway. *Front Neurosci.* (2024) 18:1453582. doi: 10.3389/fnins.2024.1453582

frontiers | Frontiers in Pharmacology

TYPE Original Research
PUBLISHED 01 April 2025
DOI 10.3389/fphar.2025.1535969

OPEN ACCESS

EDITED BY
Patrice X. Petit,
Centre National de la Recherche Scientifique (CNRS), France

REVIEWED BY
Hongwei Cheng,
University of Macau, China
Dong-Yang Zhang,
Guangzhou Medical University, China

*CORRESPONDENCE
Yang Zhu,
zhuyang@mail.ustc.edu.cn
Lixin Wei,
lixinwei66@fjmu.edu.cn

†These authors have contributed equally to this work

RECEIVED 28 November 2024
ACCEPTED 24 March 2025
PUBLISHED 01 April 2025

CITATION
Xiong Y, Kang H, Rao Y, Huang X, Zhu Y and Wei L (2025) Metal-phenolic nanozyme as a ferroptosis inhibitor for alleviating cisplatin-induced acute kidney injury.
Front. Pharmacol. 16:1535969.
doi: 10.3389/fphar.2025.1535969

Metal-phenolic nanozyme as a ferroptosis inhibitor for alleviating cisplatin-induced acute kidney injury

Yunfeng Xiong[1†], Huimin Kang[2†], Yanping Rao[1], Xiayu Huang[1], Yang Zhu[3*] and Lixin Wei[1,4*]

[1]Department of Nephrology, Fujian Medical University Union Hospital, Fuzhou, China, [2]Department of Pediatrics, Fujian Medical University Union Hospital, Fuzhou, China, [3]CAS Key Laboratory of Soft Matter Chemistry, Department of Chemistry, University of Science and Technology of China, Hefei, China, [4]Fujian Institute of Clinical Immunology, Fuzhou, China

Introduction: Cisplatin-induced acute kidney injury (AKI) is primarily caused by oxidative stress from reactive oxygen species (ROS) accumulation. Developing ROS scavengers presents promising opportunities for preventing and treating this condition by targeting oxidative stress mechanisms.

Methods: This study involves the fabrication of a metal-polyphenol self-assembled nanozyme (Fe@Ba) designed to inhibit ferroptosis through synergistic catalytic actions and antioxidant properties. The nanozyme is constructed using metal-polyphenol coordination-driven nanoprecipitation techniques. Its performance is evaluated *in vitro* using MTEC cells and *in vivo* within an AKI model, with assessments of catalytic activities, ROS depletion efficacy, antioxidant effects, and anti-ferroptotic mechanisms.

Results: The Fe@Ba nanozyme demonstrates significant catalase (CAT) and superoxide dismutase (SOD)-like activities upon internalization by MTEC cells, effectively reducing high ROS levels in the AKI model. Baicalein (Ba), a traditional Chinese medicine component in the nanozyme, exhibits strong antioxidant properties, inhibits lipid peroxidation (LPO), upregulates reductive glutathione (GSH), and promotes glutathione peroxidase 4 (GPX4) expression, thereby inhibiting ferroptosis. Fluorescence imaging confirms effective renal accumulation of Cy5.5-labeled Fe@Ba nanozyme. *In vivo* experiments show the nanozyme reduces inflammation and significantly enhances survival rates in AKI models.

Discussion: This study validates the concept of self-assembling nanozymes for AKI treatment and offers new insights into nanomedicine applications. The Fe@Ba nanozyme's ability to counteract inflammation-related damage and inhibit ferroptosis through multiple mechanisms highlights its therapeutic potential. The successful integration of traditional Chinese medicine components with nanotechnology represents an innovative approach to addressing cisplatin-induced AKI, suggesting broader applications for metal-polyphenol nanozymes in oxidative stress-related kidney diseases.

KEYWORDS

nanozyme, acute kidney injury, ferroptosis, cisplatin, reactive oxygen species

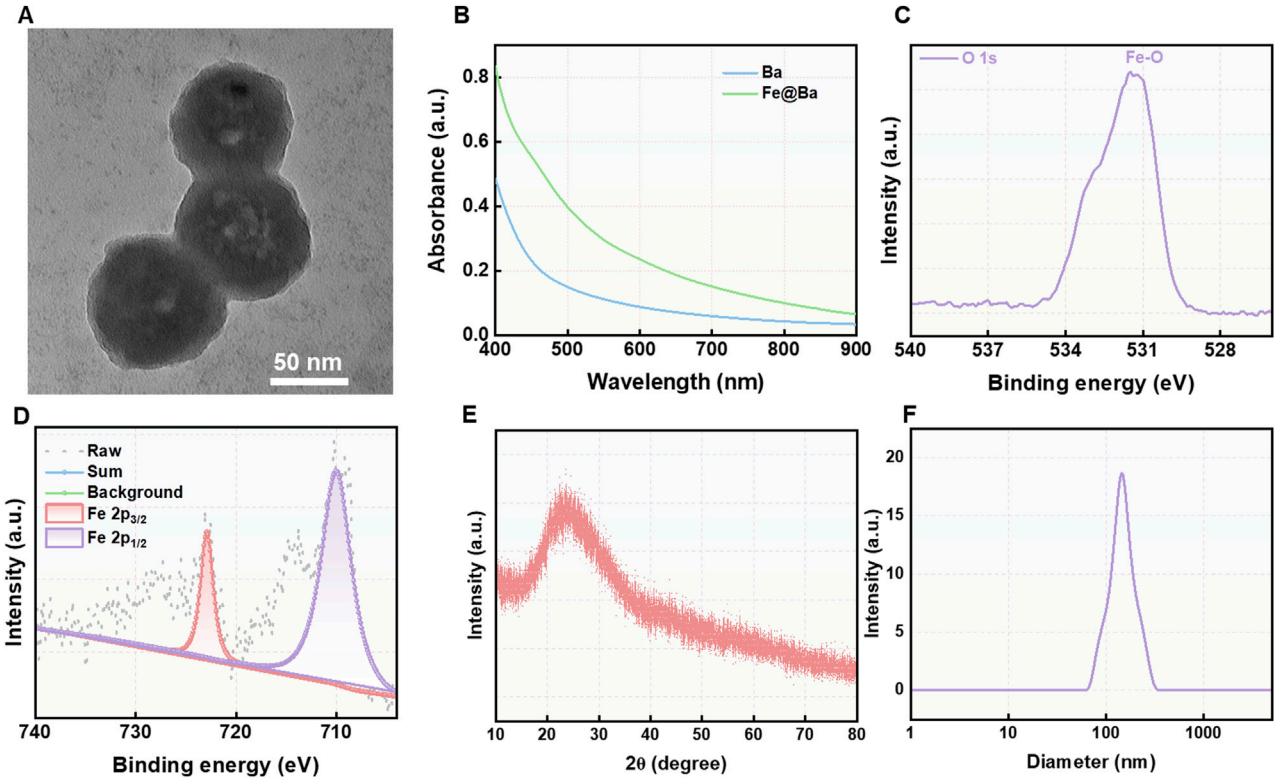

FIGURE 1
(A) TEM image of Fe@Ba nanozyme. **(B)** The DLS results of Fe@Ba nanozyme. **(C)** XPS spectrum of O 1s in Fe@Ba nanozyme. **(D)** High-resolution XPS spectrum of Fe 2p. **(E)** XRD spectrum of Fe@Ba nanozyme. **(F)** The UV-vis spectra of BDP and Fe@Ba nanozyme.

Introduction

Acute kidney injury (AKI) is a critical global health issue that rapidly impairs kidney function, often resulting in tubular cell death and inflammation (Li et al., 2023; Jiang et al., 2024; Liu et al., 2020). It is frequently associated with severe illnesses and can be intensified by conditions such as reduced blood flow, sepsis, low blood pressure, and the overuse of certain antibiotics and chemotherapy drugs, including cisplatin (DDP) (Tang et al., 2023; Li et al., 2021a; Zhang et al., 2021a; Li et al., 2021b). DDP-induced AKI is a major clinical complication, and its development is closely tied to the buildup of reactive oxygen species (ROS) (Li et al., 2021a; Dai et al., 2020), which overwhelms the body's antioxidant defenses (Zhao et al., 2021; Meng et al., 2018; Zhang et al., 2021b). These ROS can damage essential cellular components like lipids (Zhu et al., 2024a; Liu et al., 2015), nucleic acids (Zhu et al., 2023a; Liu et al., 2021), and proteins (Pan et al., 2024; Huang et al., 2024), leading to kidney dysfunction. While treatments like N-acetylcysteine are employed to counteract ROS and mitigate cisplatin-induced AKI, they are swiftly cleared by the immune system (Magner et al., 2022). In addition, antioxidant enzymes such as catalase (CAT) and superoxide dismutase (SOD) are promising candidates for clinical treatment of ROS-induced diseases (Chen et al., 2023; Scholz et al., 2021). Consequently, exploring artificial enzyme systems to address the challenges of scavenging ROS generation, and inhibiting ferroptosis, ultimately preventing cisplatin-induced kidney damage remains a substantial challenge.

Nanozymes, nanomaterials that mimic the functions of enzymes, are gaining recognition as a viable substitute for natural enzymes (Zhang et al., 2022; Zhu et al., 2023b; Jiang et al., 2019; Huang et al., 2019). Their appeal stems from their affordability, customizable catalytic properties, and enhanced stability (Chen and Arnold, 2020; Peng et al., 2024; Zhu et al., 2022; Zhu et al., 2021). Nanozymes have emerged as promising alternatives to natural enzymes, effectively bridging the unique intersection of nanotechnology and biomedicine (Zhu et al., 2023c; Xu et al., 2024; Zhu et al., 2024b). Metal-polyphenol nanozymes have been widely exploited in recent years (Liang et al., 2024a; Liang et al., 2024b). Previous studies have reported that various nanozymes with CAT- and SOD-like activities have been proven effective in treating AKI by neutralizing harmful ROS, which aids in the recovery of kidney function (Wang et al., 2022; Zhang et al., 2021c). While the potential of nanozymes in treating cisplatin-induced AKI is encouraging, several challenges remain (Li et al., 2024). Firstly, their relatively low catalytic efficiency hinders their effectiveness in treating AKI. Secondly, the ongoing process of ROS scavenging by nanozymes is not as effective as needed. Consequently, it is crucial to develop new nanozymes that are highly catalytically efficient and can continuously eliminate ROS, to address the issue of AKI in cancer patients treated with cisplatin.

Herein, we have developed a metal-polyphenol nanozyme, Fe@Ba, which is formed by the interaction of ferric ions (Fe^{3+}) and the antioxidant compound baicalein (Ba) from traditional Chinese medicine. The polyphenol contains phenolic hydroxyl groups, which have more lone pair electrons, while the trivalent iron ion

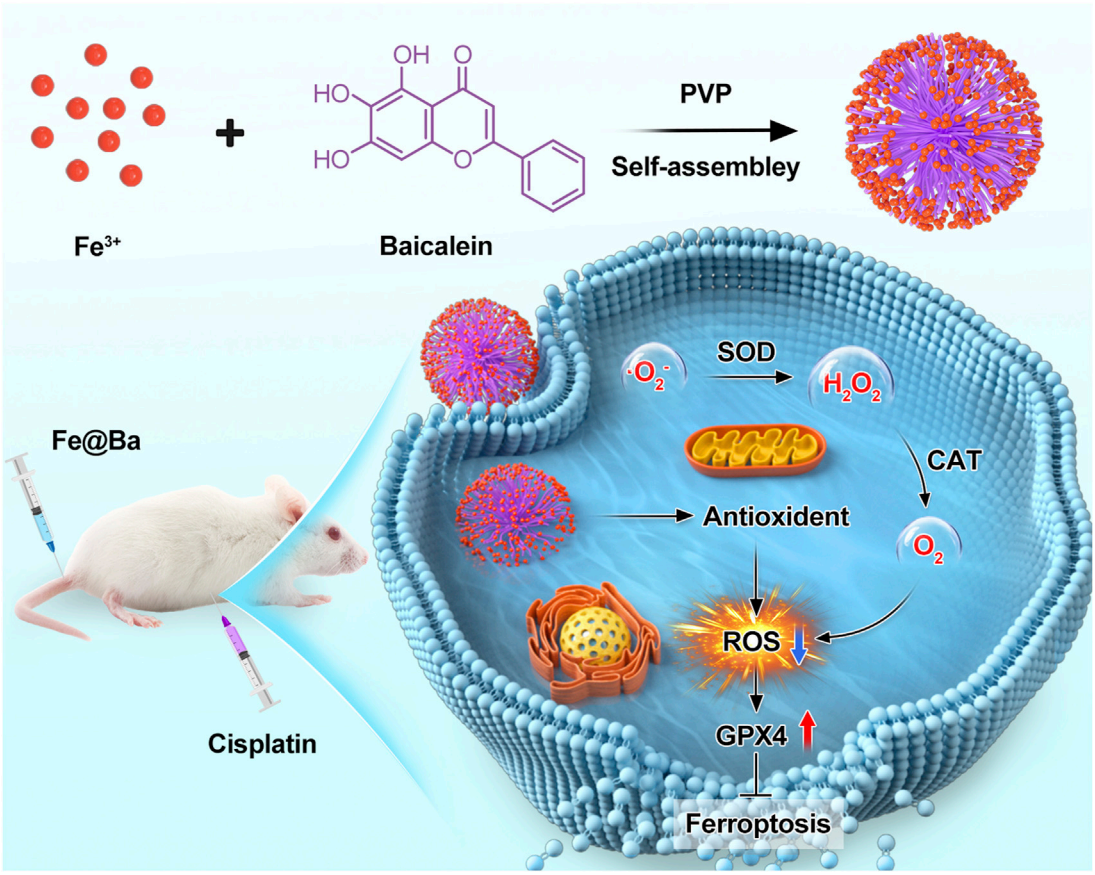

SCHEME 1
Schematic representation of the application of Fe@Ba nanozyme to inhibit ferroptosis in a cisplatin-induced AKI model.

has vacant orbitals. Therefore, the phenolic hydroxyl groups can effectively coordinate with the iron ions to form nanoparticles. Fe@Ba inhibits lipid peroxidation (LPO), a process that contributes to cell death known as ferroptosis, by neutralizing harmful ROS and activating the antioxidant properties of baicalein. Fe@Ba nanozyme mimics the functions of natural enzymes, CAT and SOD, to convert toxic superoxide anions ($\cdot O_2^-$) into harmless oxygen, thereby reducing inflammation and preventing ferroptosis. It also increases the expression of glutathione peroxidase 4 (GPX4), a key enzyme in the antioxidant defense system, further inhibiting ferroptosis. Fluorescence imaging reveals that the cyanine 5.5 (Cy5.5)-labeled Fe@Ba nanozyme effectively accumulates in the kidneys. Our *in vivo* experiments have shown that Fe@Ba can alleviate inflammation and improve survival rates in an AKI model, demonstrating its therapeutic potential. This research provides a proof-of-concept for the development of self-assembling nanozymes and offers new insights into the use of nanomedicine for treating AKI, highlighting their potential to mitigate the negative effects of inflammation.

Results and discussions

The synthesis of the Fe@Ba nanozyme was outlined in Scheme 1. We utilized a self-assembly method to combine Fe^{3+} ions with a metal-organic framework Ba in the presence of polyvinylpyrrolidone (PVP). As depicted in Figure 1A, the resulting Fe@Ba nanozyme, which was uniformly dispersed and approximately 50 nm in size, was directly visualized using transmission electron microscopy (TEM). The hydrodynamic size of the Fe@Ba nanozyme was measured with dynamic light scattering (DLS), as shown in Figure 1B. The zeta potential of Fe@Ba was −16.7 mV.

The high-angle annular dark-field scanning transmission electron microscopy (HAADF-STEM) images was employed to observed the element analysis (Supplementary Figure S1). Further analysis was conducted using X-ray photoelectron spectroscopy (XPS) to determine the oxidation states of iron and oxygen in the Fe@Ba nanozyme, with results presented in Figures 1D; Supplementary Figures S2, S3. The O 1s XPS spectrum revealed a peak at a binding energy of 531.4 eV, indicative of the presence of Fe-O bonds, as shown in Figure 1C. The high-resolution Fe 2p XPS spectrum split the Fe 2p peak into two components, corresponding to Fe^{3+} at 722.9 eV and Fe^{2+} at 710.1 eV, which are crucial for the nanozyme's catalytic activity. The X-ray powder diffraction (XRD) spectrum indicated no distinct crystal pattern, suggesting that the iron in the Fe@Ba nanozyme had poor crystallinity, as shown in Figure 1E. Raman spectroscopy was employed to assess the degree of crystallinity, with results in Supplementary Figure S4. Ultraviolet-visible (UV-vis) spectroscopy confirmed the successful assembly of Ba and Fe^{3+}, as illustrated in Figure 1F. Collectively, these findings confirmed the successful fabrication of the Fe@Ba nanozyme.

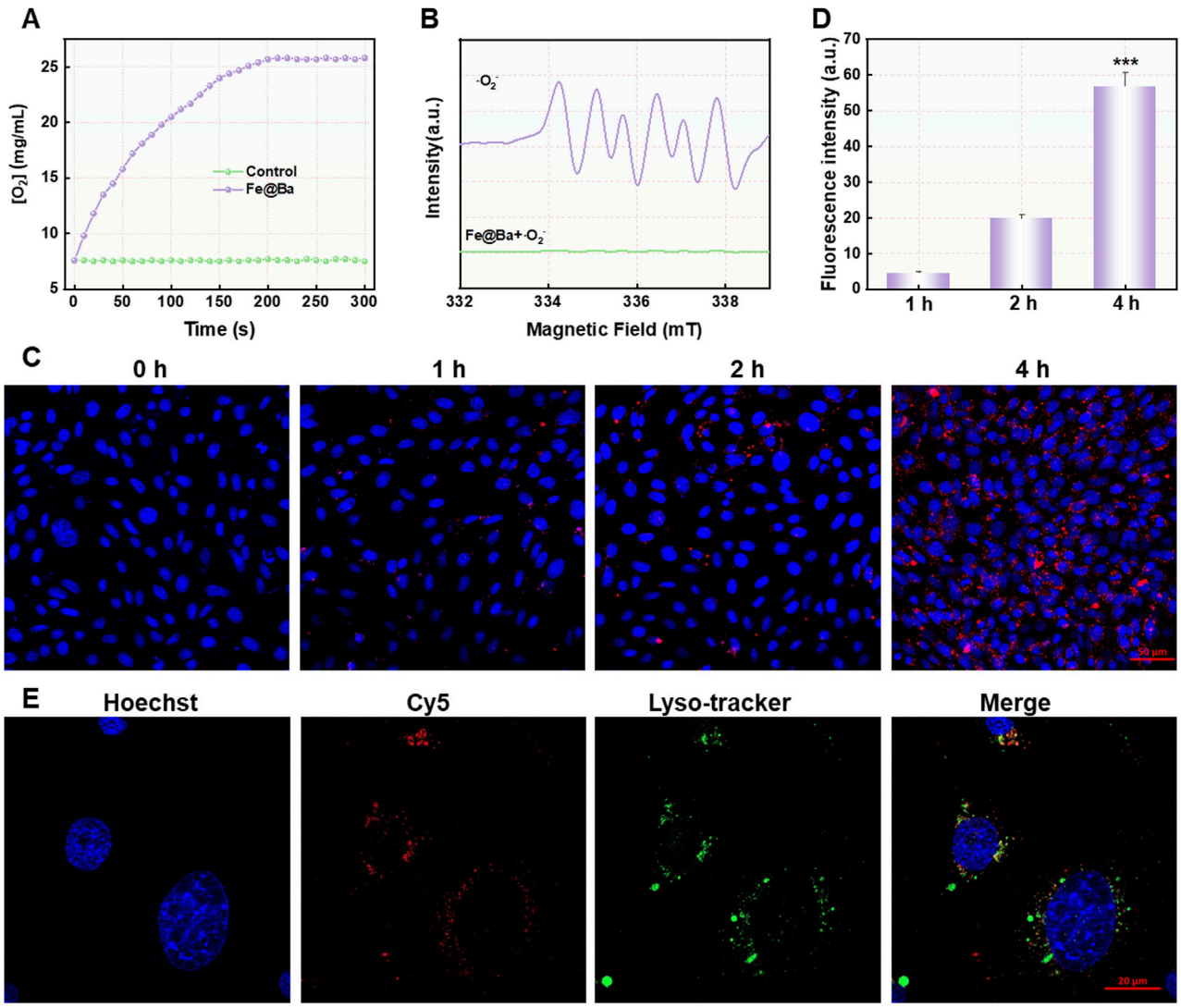

FIGURE 2
(A) The oxygen generation rate of H_2O_2 catalyzed by Fe@Ba nanozyme was assessed by dissolved oxygen analyzer. **(B)** ESR spectra of Fe@Ba nanozyme with DMPO as the spin trapper. **(C)** The CLSM images and **(D)** corresponding quantification of MTEC cells treated with Cy5.5-labeled Fe@Ba nanozyme. **(E)** The CLSM images revealed the colocalization of Cy5.5-labeled Fe@Ba nanozyme with the lysosomes of MTEC cells.

Motivated by the potential of multivalent iron elements, we investigated the catalytic capabilities of the Fe@Ba nanozyme. We assessed its catalase-like activity by measuring its ability to convert the highly toxic H_2O_2 into the non-toxic O_2, which helps to reduce oxidative stress caused by ROS, as shown in Figure 2A. Furthermore, we determined SOD-like activity of Fe@Ba nanozyme using electron spin resonance (ESR) analysis with the spin-trap reagent 5-tert-butyloxycarbonyl-5-methyl-1-pyrroline N-oxide (BMPO). The distinctive quadrupling peak for BMPO-OOH confirmed the effectiveness of Fe@Ba nanozyme in scavenging superoxide anions, demonstrating the strong SOD mimetic activity, as depicted in Figure 2B. These results confirmed the effectiveness of Fe@Ba nanozyme in reducing ROS and alleviating oxidative stress. AKI is a significant side effect of DDP treatment, closely linked to the accumulation of ROS due to an overactive oxidation system and a compromised antioxidant defense. To evaluate the cellular protective effects of the Fe@Ba nanozyme, we used confocal laser scanning microscopy (CLSM) to observe the uptake of Cy5.5-labeled Fe@Ba nanozyme by DDP-induced cells over time. The increasing red fluorescence signal indicated that the nanozyme had a favorable cellular affinity and could enter mouse tubular epithelial cells (MTEC) cells to exert its therapeutic effects, as seen in Figures 2C, D; Supplementary Figure S5. A colocalization assay revealed that some Fe@Ba nanozyme could escape from lysosomes into the cytoplasm, where it scavenged ROS and exhibited antioxidant capabilities (Figure 2E). These findings indicated that Fe@Ba nanozyme can effectively be internalized by MTEC cells.

The protective impact of the Fe@Ba nanozyme on cells was measured using a cell counting kit 8 (CCK-8), which showed that the nanozyme did not hinder the growth of MTEC cells and was associated with strong antioxidant effects and reduction of ROS, as illustrated in Figure 3A. Importantly, the CCK-8 assay indicated that the Fe@Ba nanozyme significantly improved the MTEC cell viability in a concentration-dependent way, as shown in Figure 3B.

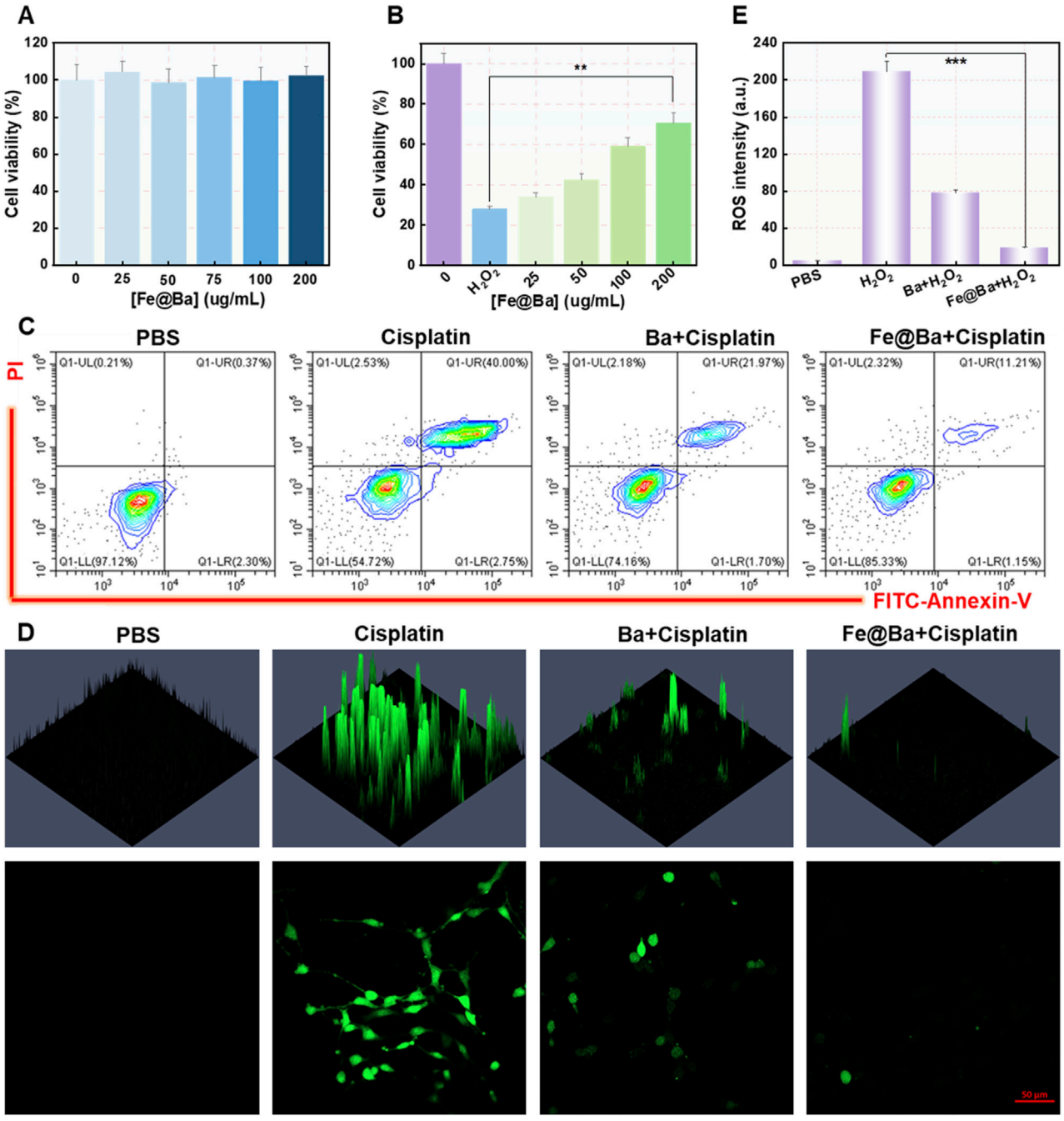

FIGURE 3
(A) Cell viability after a 24-h treatment with various concentrations of Fe@Ba nanozyme. **(B)** Cell viability after a 24-h treatment with various concentrations of Fe@Ba nanozyme in the presence of cisplatin. **(C)** Flow cytometry measurement of MTEC cells death rate following different treatments. **(D)** DCF fluorescence and **(E)** corresponding quantification of MTEC cells subjected to different treatments.

The cytoprotective effect of the Fe@Ba nanozyme was also evaluated visually through flow cytometry analysis, with results displayed in Figure 3C; Supplementary Figure S6. These analyses showed that the Fe@Ba nanozyme-treated group had a notably higher cell survival rate compared to groups treated with free baicalein or cisplatin, aligning with the findings from the CCK-8 assay. Moreover, cellular ROS levels were quantified using a ROS probe, 2′,7′-dichlorofluorescin diacetate (DCFH-DA), as illustrated in Figures 3D, E. CLSM revealed that the Fe@Ba nanozyme had a greater capacity to reduce ROS than baicalein alone, attributed to its robust catalytic activities and antioxidant properties. These results confirm that the Fe@Ba nanozyme can effectively lower cellular ROS levels and enhance cell viability.

To understand how the Fe@Ba nanozyme can prevent ferroptosis in MTEC cells, we used a fluorescence probe, 5,5′,6,6′-tetrachloro-1,1′,3,3′-tetraethyl-imidacarbocyanine iodide (JC-1), to assess changes in mitochondrial membrane potential (MMP). The fluorescence of probe shifts from green to red as

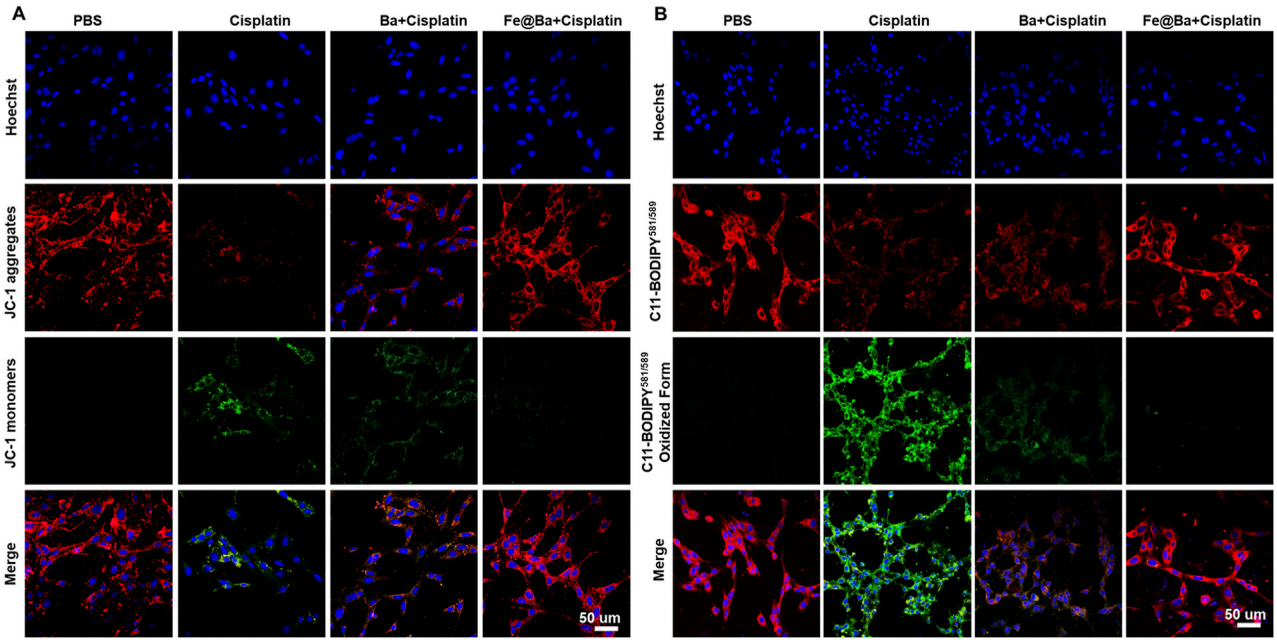

FIGURE 4
(A) Confocal images of MTEC cells stained with JC-1 kit following a 24-h treatment with different formulations. **(B)** Confocal images of MTEC cells stained with C11-BODIPY$^{581/589}$ following different formulations.

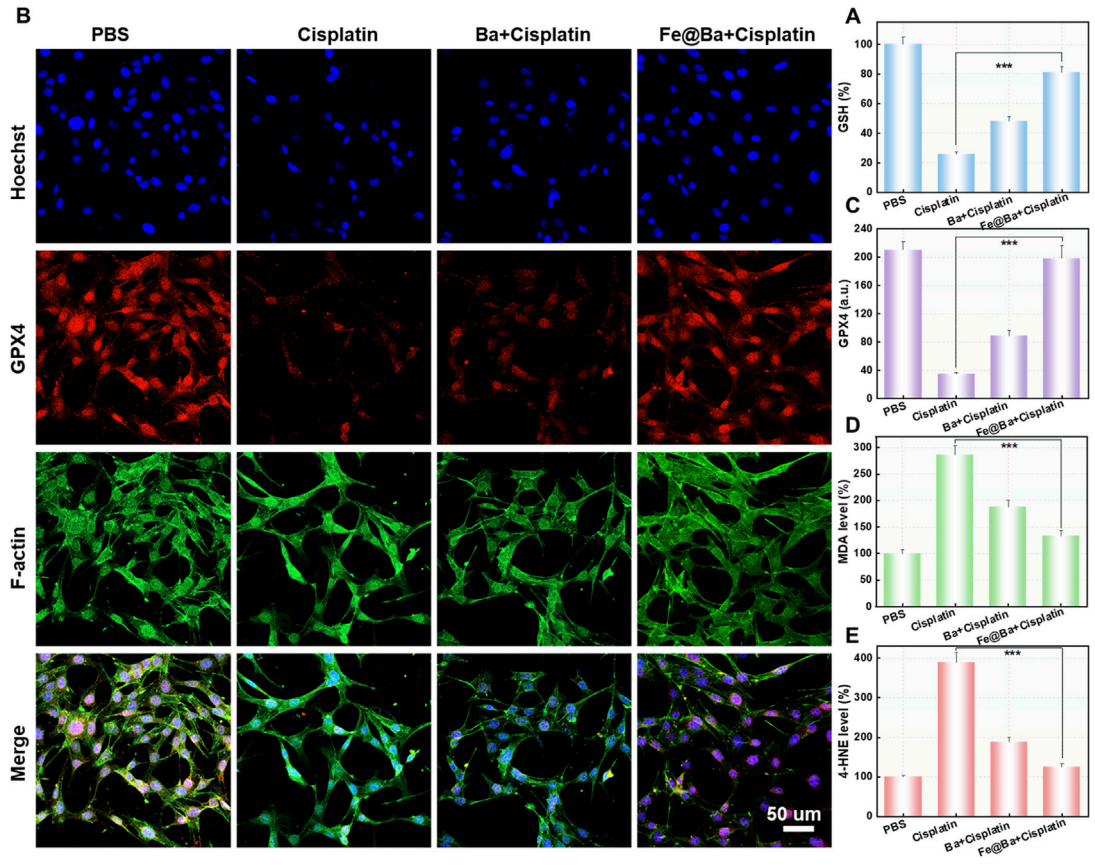

FIGURE 5
(A) The cellular levels of GSH after different treatments were measured using a DTNB assay kit. **(B)** Confocal images **(C)** and the corresponding quantification (f) of GPX4 expression in MTEC cells after different formulations. **(D)** Quantitative analysis of MDA **(E)** and 4-HNE levels following different formulations.

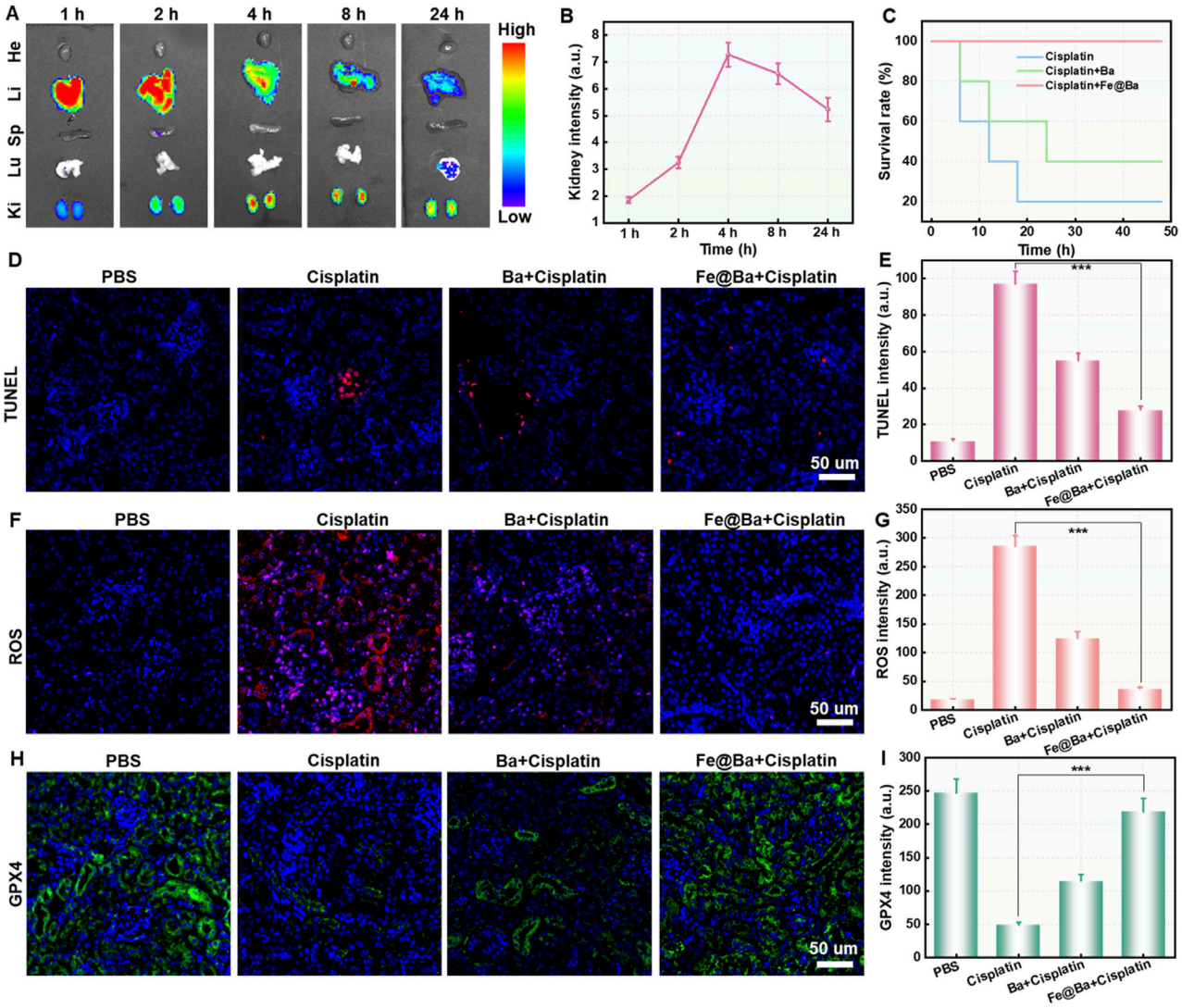

FIGURE 6
(A) Fluorescence images **(B)** corresponding quantification of cisplatin-induced AKI mice at different time points post-injection with Cy5.5-labeled Fe@Ba nanozyme. **(C)** Kaplan-Meier survival curves of mice following different treatments. **(D)** TUNEL staining of kidney slices and **(E)** the corresponding quantification from various groups following a 24-h treatment with different formulations. **(F)** ROS staining and **(G)** the corresponding quantification of kidney slices following various formulations. **(H)** Immunofluorescence staining and **(I)** the corresponding quantification of GPX4 in kidney slices following various formulations.

MMP decreases. CLSM images revealed a decrease in red fluorescence and an increase in green fluorescence in the DDP group, indicating MMP damage, as shown in Figure 4A. In contrast, the Fe@Ba nanozyme treatment resulted in a decrease in green fluorescence and an increase in red fluorescence, suggesting significant mitochondrial depolarization. Ferroptosis is marked by mitochondrial damage, and we used the fluorescent probe BODIPY $C11^{581/591}$ to measure lipid peroxide levels, which change from red to green fluorescence. CLSM images indicated that the Fe@Ba nanozyme significantly reduced green fluorescence and increased red fluorescence, as depicted in Figure 4B, suggesting a reduction in lipid peroxides and thus inhibiting LPO. Furthermore, the Fe@Ba nanozyme was found to enhance glutathione (GSH) levels, which in turn increases the expression of GPX4, a key enzyme that inhibits ferroptosis. Figure 5A shows that the Fe@Ba nanozyme substantially increased GSH levels due to its excellent enzymatic activities and antioxidant capabilities. An immunofluorescence assay was used to measure GPX4 expression, and Figures 5B, C shows that the Fe@Ba nanozyme upregulated GPX4 expression, likely due to its catalytic activities in raising GSH levels. We also measured additional indicators of ferroptosis, malondialdehyde (MDA) and 4-hydroxynonenal (4-HNE), to confirm the inhibitory effect of the Fe@Ba nanozyme on ferroptosis. Figures 5D, E demonstrate that MTEC cells treated with the Fe@Ba nanozyme significantly reduced the levels of these harmful byproducts. These findings suggest that the Fe@Ba nanozyme can effectively neutralize ROS and protect mitochondria from depolarization, potentially offering antioxidant protection in an AKI model. This provides strong evidence for the potential of Fe@Ba nanozyme as an effective inhibitor of ferroptosis.

The animal study protocol was approved by the Ethical Committee of Fujian Medical University (IACUC FJMU 2024-Y-0291). We used an IVIS imaging system to track the *in vivo* distribution of the Cy5.5-labeled Fe@Ba nanozyme. The imaging showed that the fluorescence signal at the kidney area increased over time, peaking 24 h after injection, which corresponds to ROS scavenging and ferroptosis inhibition effects of Fe@Ba nanozyme, as seen in Figures 6A, B. The mice were divided into four groups: PBS control, DDP treatment, DDP plus free Ba, and DDP plus Fe@Ba nanozyme. The results, as depicted in Figure 6C, indicated that the Fe@Ba nanozyme group had a significantly extended survival rate compared to the free Ba group, demonstrating the nanozyme's superior antioxidant performance. We have measured the serum creatinine and blood urea nitrogen of different treatment groups in mice *in vivo*. As shown in Supplementary Figures SS7, S8, Fe@Ba nanozyme can significantly decrease the levels of serum creatinine, blood urea nitrogen, and inflammatory factor. To further confirm the antioxidant effect of Fe@Ba nanozyme, we performed terminal deoxynucleotidyl transferase-mediated dUTP nick-end labeling (TUNEL) staining on kidney sections. Figures 6D, E; Supplementary Figure S9 show that kidneys treated with the Fe@Ba nanozyme experienced less damage than those treated with free Ba, indicating a significant therapeutic benefit. Immunofluorescence staining confirmed the inhibition of kidney ferroptosis, with notable reductions in ROS and increases in GPX4 expression observed directly in the kidney, as shown in Figures 6F–I and S10-S11. In conclusion, the Fe@Ba nanozyme reduced lipid peroxidation, decreased intracellular oxidative stress, and enhanced GPX4-mediated protection against ferroptosis. Blood biochemistry analysis of mice and H&E staining further confirmed the antioxidant ability of Fe@Ba nanozyme, significantly reducing the levels of blood urea nitrogen (BUN), creatinine (CREA), and renal injury (Supplementary Figures S12, S13). These findings underscore the potential of Fe@Ba nanozyme as an effective inhibitor of ferroptosis for the treatment of AKI.

Conclusion

We successfully developed a metal-polyphenol self-assembling nanozyme as a ROS scavenger for treating cisplatin-induced AKI. The Fe@Ba nanozyme was synthesized through the interaction between Fe^{3+} and the antioxidant compound Ba, derived from traditional Chinese medicine. This nanozyme effectively inhibited LPO, a key driver of ferroptosis, by scavenging highly reactive ROS and enhancing antioxidant properties of Ba. Fe@Ba nanozyme exhibited CAT- and SOD-like activities to convert toxic $\cdot O_2^-$ into harmless oxygen, thereby reducing inflammation and preventing ferroptosis. Additionally, Fe@Ba nanozyme upregulated the expression of GPX4, further inhibiting ferroptosis. Fluorescence imaging demonstrated that Cy5.5-labeled Fe@Ba nanozyme effectively accumulated in the kidneys. *In vivo* experiments confirmed that Fe@Ba nanozyme reduced inflammation and improved survival rates in an AKI model, showcasing its therapeutic potential. This research not only validated the concept of self-assembling nanozymes but also offered new insights into the use of nanomedicine for AKI treatment, emphasizing their ability to counteract inflammation-related damage.

Data availability statement

The original contributions presented in the study are included in the article/Supplementary Material, further inquiries can be directed to the corresponding authors.

Ethics statement

The animal study protocol was approved by the Ethical Committee of Fujian Medical University (IACUC FJMU 2024-Y-0291). The studies were conducted in accordance with the local legislation and institutional requirements. Written informed consent was obtained from the owners for the participation of their animals in this study.

Author contributions

YX: Writing – original draft, Writing – review and editing. HK: Conceptualization, Data curation, Formal Analysis, Investigation, Methodology, Project administration, Writing – original draft, Writing – review and editing. YR: Conceptualization, Writing – original draft, Writing – review and editing. XH: Data curation, Writing – original draft, Writing – review and editing. YZ: Supervision, Writing – original draft, Writing – review and editing. LW: Supervision, Writing – original draft, Writing – review and editing.

Funding

The author(s) declare that financial support was received for the research and/or publication of this article. This work was supported by the National Natural Science Foundation of China (82070727 to Lixin Wei), Joint Funds for the innovation of Science and Technology, Fujian province (2020Y9074 to Lixin Wei), and by Fujian provincial health technology project (2020QNA031 to Huimin Kang).

Conflict of interest

The authors declare that the research was conducted in the absence of any commercial or financial relationships that could be construed as a potential conflict of interest.

Generative AI statement

The author(s) declare that no Generative AI was used in the creation of this manuscript.

Publisher's note

All claims expressed in this article are solely those of the authors and do not necessarily represent those of their affiliated organizations, or those of the publisher, the editors and the reviewers. Any product that may be evaluated in this article, or claim that may be made by its manufacturer, is not guaranteed or endorsed by the publisher.

Supplementary material

The Supplementary Material for this article can be found online at: https://www.frontiersin.org/articles/10.3389/fphar.2025.1535969/full#supplementary-material

References

Chen, K., and Arnold, F. H. (2020). Engineering new catalytic activities in enzymes. *Nat. Catal.* 3 (3), 203–213. doi:10.1038/s41929-019-0385-5

Chen, Q., Nan, Y., Yang, Y., Xiao, Z., Liu, M., Huang, J., et al. (2023). Nanodrugs alleviate acute kidney injury: manipulate RONS at kidney. *Bioact. Mater.* 22, 141–167. doi:10.1016/j.bioactmat.2022.09.021

Dai, Y., Zhu, Y., Cheng, J., Shen, J., Huang, H., Liu, M., et al. (2020). Nitric oxide-releasing platinum(IV) prodrug efficiently inhibits proliferation and metastasis of cancer cells. *Chem. Commun.* 56 (90), 14051–14054. doi:10.1039/D0CC05422D

Huang, L., Chen, J., Gan, L., Wang, J., and Dong, S. (2019). Single-atom nanozymes. *Sci. Adv.* 5 (5), eaav5490. doi:10.1126/sciadv.aav5490

Huang, W., Tian, Y., Ma, J., Wei, P., Du, C., Zhang, X., et al. (2024). Neutrophil membrane-based biomimetic metal-polyphenol self-assembled nanozyme for the targeting treatment of early brain injury following subarachnoid hemorrhage. *Chem. Eng. J.* 498, 155643. doi:10.1016/j.cej.2024.155643

Jiang, D., Ni, D., Rosenkrans, Z. T., Huang, P., Yan, X., and Cai, W. (2019). Nanozyme: new horizons for responsive biomedical applications. *Chem. Soc. Rev.* 48 (14), 3683–3704. doi:10.1039/C8CS00718G

Jiang, W., Hou, X., Qi, Y., Wang, Z., Liu, Y., Gao, X. J., et al. (2024). pH-activatable pre-nanozyme mediated H2S delivery for endo-exogenous regulation of oxidative stress in acute kidney injury. *Adv. Sci.* 11 (18), 2303901. doi:10.1002/advs.202303901

Li, L., Liu, X., Liu, G., Xu, S., Hu, G., and Wang, L. (2024). Valence-engineered catalysis-selectivity regulation of molybdenum oxide nanozyme for acute kidney injury therapy and post-cure assessment. *Nat. Commun.* 15 (1), 8720. doi:10.1038/s41467-024-53047-1

Li, L., Shen, Y., Tang, Z., Yang, Y., Fu, Z., Ni, D., et al. (2023). Engineered nanodrug targeting oxidative stress for treatment of acute kidney injury. *Exploration* 3 (6), 20220148. doi:10.1002/EXP.20220148

Li, L., Zhu, Y., Liu, M., Jin, D., Zhang, L., Cheng, J., et al. (2021a). Conjugation of oxaliplatin with PEGylated-nanobody for enhancing tumor targeting and prolonging circulation. *J. Inorg. Biochem.* 223, 111553. doi:10.1016/j.jinorgbio.2021.111553

Li, L., Zhu, Y., Liu, M., Jin, D., Zhang, L., Cheng, J., et al. (2021b). Conjugation of oxaliplatin with PEGylated-nanobody for enhancing tumor targeting and prolonging circulation. *J. Inorg. Biochem.* 223, 111553. doi:10.1016/j.jinorgbio.2021.111553

Liang, X., Ding, L., Ma, J., Li, J., Cao, L., Liu, H., et al. (2024b). Enhanced mechanical strength and sustained drug release in carrier-free silver-coordinated anthraquinone natural antibacterial anti-inflammatory hydrogel for infectious wound healing. *Adv. Healthc. Mater.* 13 (23), 2400841. doi:10.1002/adhm.202400841

Liang, X., Liu, H., Chen, H., Peng, X., Li, Z., Teng, M., et al. (2024a). Rhein-based Pickering emulsion for hepatocellular carcinoma: shaping the metabolic signaling and immunoactivation in transarterial chemoembolization. *Aggregate* 5 (4), e552. doi:10.1002/agt2.552

Liu, D., Shu, G., Jin, F., Qi, J., Xu, X., Du, Y., et al. (2020). ROS-responsive chitosan-SS31 prodrug for AKI therapy via rapid distribution in the kidney and long-term retention in the renal tubule. *Sci. Adv.* 6 (41), eabb7422. doi:10.1126/sciadv.abb7422

Liu, L., Zhang, K., Sandoval, H., Yamamoto, S., Jaiswal, M., Sanz, E., et al. (2015). Glial lipid droplets and ROS induced by mitochondrial defects promote neurodegeneration. *Cell* 160 (1), 177–190. doi:10.1016/j.cell.2014.12.019

Liu, M., Zhu, Y., Jin, D., Li, L., Cheng, J., and Liu, Y. (2021). Hemin-caged ferritin acting as a peroxidase-like nanozyme for the selective detection of tumor cells. *Inorg. Chem.* 60 (19), 14515–14519. doi:10.1021/acs.inorgchem.1c01863

Magner, K., Ilin, J. V., Clark, E. G., Kong, J. W. Y., Davis, A., and Hiremath, S. (2022). Meta-analytic techniques to assess the association between N-acetylcysteine and acute kidney injury after contrast administration: a systematic review and meta-analysis. *JAMA Netw. Open* 5 (7), e2220671. doi:10.1001/jamanetworkopen.2022.20671

Meng, X.-M., Ren, G.-L., Gao, L., Yang, Q., Li, H.-D., Wu, W.-F., et al. (2018). NADPH oxidase 4 promotes cisplatin-induced acute kidney injury via ROS-mediated programmed cell death and inflammation. *Lab. Investig.* 98 (1), 63–78. doi:10.1038/labinvest.2017.120

Pan, Y., Cheng, J., Zhu, Y., Zhang, J., Fan, W., and Chen, X. (2024). Immunological nanomaterials to combat cancer metastasis. *Chem. Soc. Rev.* 53 (12), 6399–6444. doi:10.1039/D2CS00968D

Peng, C., Pang, R., Li, J., and Wang, E. (2024). Current advances on the single-atom nanozyme and its bioapplications. *Adv. Mater.* 36 (10), 2211724. doi:10.1002/adma.202211724

Scholz, H., Boivin, F. J., Schmidt-Ott, K. M., Bachmann, S., Eckardt, K.-U., Scholl, U. I., et al. (2021). Kidney physiology and susceptibility to acute kidney injury: implications for renoprotection. *Nat. Rev. Nephrol.* 17 (5), 335–349. doi:10.1038/s41581-021-00394-7

Tang, C., Livingston, M. J., Safirstein, R., and Dong, Z. (2023). Cisplatin nephrotoxicity: new insights and therapeutic implications. *Nat. Rev. Nephrol.* 19 (1), 53–72. doi:10.1038/s41581-022-00631-7

Wang, K., Zhang, Y., Mao, W., Feng, W., Lu, S., Wan, J., et al. (2022). Engineering ultrasmall ferroptosis-targeting and reactive oxygen/nitrogen species-scavenging nanozyme for alleviating acute kidney injury. *Adv. Funct. Mater.* 32 (10), 2109221. doi:10.1002/adfm.202109221

Xu, R., Zhang, S., Wang, P., Zhang, R., Lin, P., Wang, Y., et al. (2024). Nanozyme-based strategies for efficient theranostics of brain diseases. *Coord. Chem. Rev.* 501, 215519. doi:10.1016/j.ccr.2023.215519

Zhang, D.-Y., Liu, H., He, T., Younis, M. R., Tu, T., Yang, C., et al. (2021b). Biodegradable self-assembled ultrasmall nanodots as reactive oxygen/nitrogen species scavengers for theranostic application in acute kidney injury. *Small* 17 (8), 2005113. doi:10.1002/smll.202005113

Zhang, D.-Y., Liu, H., Younis, M. R., Lei, S., Yang, C., Lin, J., et al. (2021c). Ultrasmall platinum nanozymes as broad-spectrum antioxidants for theranostic application in acute kidney injury. *Chem. Eng. J.* 409, 127371. doi:10.1016/j.cej.2020.127371

Zhang, D.-Y., Younis, M. R., Liu, H., Lei, S., Wan, Y., Qu, J., et al. (2021a). Multi-enzyme mimetic ultrasmall iridium nanozymes as reactive oxygen/nitrogen species scavengers for acute kidney injury management. *Biomaterials* 271, 120706. doi:10.1016/j.biomaterials.2021.120706

Zhang, S., Li, Y., Sun, S., Liu, L., Mu, X., Liu, S., et al. (2022). Single-atom nanozymes catalytically surpassing naturally occurring enzymes as sustained stitching for brain trauma. *Nat. Commun.* 13 (1), 4744. doi:10.1038/s41467-022-32411-z

Zhao, M., Wang, Y., Li, L., Liu, S., Wang, C., Yuan, Y., et al. (2021). Mitochondrial ROS promote mitochondrial dysfunction and inflammation in ischemic acute kidney injury by disrupting TFAM-mediated mtDNA maintenance. *Theranostics* 11 (4), 1845–1863. doi:10.7150/thno.50905

Zhu, Y., Ding, C., Fang, W., Li, T., Yan, L., Tian, Y., et al. (2024b). Metal-polyphenol self-assembled nanodots for NIR-II fluorescence imaging-guided chemodynamic/photodynamic therapy-amplified ferroptosis. *Acta Biomater.* 185, 361–370. doi:10.1016/j.actbio.2024.07.017

Zhu, Y., Gong, P., Wang, J., Cheng, J., Wang, W., Cai, H., et al. (2023a). Amplification of lipid peroxidation by regulating cell membrane unsaturation to enhance chemodynamic therapy. *Angew. Chem. Int. Ed.* 62 (12), e202218407. doi:10.1002/anie.202218407

Zhu, Y., Jin, D., Liu, M., Dai, Y., Li, L., Zheng, X., et al. (2022). Oxygen self-supply engineering-ferritin for the relief of hypoxia in tumors and the enhancement of photodynamic therapy efficacy. *Small. 2022 2022/04/01* 18 (15), 2200116. doi:10.1002/smll.202200116

Zhu, Y., Liao, Y., Zou, J., Cheng, J., Pan, Y., Lin, L., et al. (2023c). Engineering single-atom nanozymes for catalytic biomedical applications. *Small. 2023 2023/07/01* 19 (30), 2300750. doi:10.1002/smll.202300750

Zhu, Y., Niu, X., Wu, T., Cheng, J., Zou, J., Pan, Y., et al. (2024a). Metal-phenolic nanocatalyst rewires metabolic vulnerability for catalytically amplified ferroptosis. *Chem. Eng. J.* 485, 150126. doi:10.1016/j.cej.2024.150126

Zhu, Y., Wang, W., Cheng, J., Qu, Y., Dai, Y., Liu, M., et al. (2021). Stimuli-Responsive manganese single-atom nanozyme for tumor therapy via integrated cascade reactions. *Angew. Chem. Int. Ed.* 60 (17), 9480–9488. doi:10.1002/anie.202017152

Zhu, Y., Wang, W., Gong, P., Zhao, Y., Pan, Y., Zou, J., et al. (2023b). Enhancing catalytic activity of a nickel single atom enzyme by polynary heteroatom doping for ferroptosis-based tumor therapy. *ACS Nano.* 17 (3), 3064–3076. doi:10.1021/acsnano.2c11923

frontiers | Frontiers in Cell and Developmental Biology

TYPE Original Research
PUBLISHED 03 April 2025
DOI 10.3389/fcell.2025.1532910

OPEN ACCESS

EDITED BY
Bilal ÇİĞ,
Ahi Evran University Medicine Faculty Department of Physiology, Türkiye

REVIEWED BY
Bavani Subramaniam,
Children's National Hospital, United States
Küçük Nihan,
Hittite University, Türkiye

*CORRESPONDENCE
Songjia Lai,
laisj5794@163.com

†These authors have contributed equally to this work and share first authorship

RECEIVED 22 November 2024
ACCEPTED 06 March 2025
PUBLISHED 03 April 2025

CITATION
Sun W, Ren H, Chen L, Zhang B, Mei L, Wen J, Zhang Y, Li J, Yan Y and Lai S (2025) *TAp73* modulates proliferation and ferroptosis in mammary epithelial cells.
Front. Cell Dev. Biol. 13:1532910.
doi: 10.3389/fcell.2025.1532910

TAp73 modulates proliferation and ferroptosis in mammary epithelial cells

Wenqiang Sun[1,2,3†], Hanjun Ren[1,2,3†], Le Chen[1,2,3], Bingfei Zhang[1,2,3], Liping Mei[1,2,3], Jiaqi Wen[1,2,3], Yilu Zhang[1,2,3], Jiaqi Li[1,2,3], Yongping Yan[1,2,3] and Songjia Lai[1,2,3*]

[1]Farm Animal Genetic Resources Exploration and Innovation Key Laboratory of Sichuan Province, Sichuan Agricultural University, Ya'an, China, [2]State Key Laboratory of Swine and Poultry Breeding Industry, College of Animal Science and Technology, Sichuan Agricultural University, Ya'an, China, [3]Key Laboratory of Livestock and Poultry Multi-Omics, Ministry of Agriculture and Rural Affairs, College of Animal Science and Technology, Sichuan Agricultural University, Ya'an, China

Introduction: *TAp73*, a transcriptionally active isoform of the *p73* gene, is essential for epithelial tissue development. Ferroptosis, a regulated form of cell death characterized by lipid peroxidation and reactive oxygen species (ROS) accumulation, has been increasingly studied in recent years. However, its role in epithelial cells and the regulatory function of *TAp73* in this context remain poorly understood.

Methods: We investigated the role of *TAp73* in epithelial cell proliferation and ferroptosis using ectopic overexpression and RNA interference approaches. Cell proliferation was assessed through colony formation and DNA synthesis assays. Ferroptosis was induced using RSL3, and the effects were evaluated by measuring cell viability, ROS levels, and the expression of ferroptosis-associated genes *PTGS2* and TFRC.

Results: *TAp73* overexpression significantly increased *p21* expression, suppressed colony formation and DNA synthesis, thereby inhibiting cell proliferation. In contrast, *TAp73* knockdown reduced *p21* levels and enhanced cell proliferation. RSL3 treatment induced a dose-dependent increase in cell death and ROS accumulation, confirming the susceptibility of epithelial cells to ferroptosis. Furthermore, *TAp73* overexpression enhanced RSL3-induced ferroptosis by upregulating *PTGS2* and *TFRC*, while *TAp73* knockdown diminished their expression, reducing oxidative stress and lipid peroxidation.

Conclusion: *TAp73* acts as a dual regulator of epithelial cell fate by inhibiting proliferation and promoting ferroptosis. These findings reveal a novel role for *TAp73* in epithelial cell biology and suggest potential therapeutic targets for diseases involving epithelial cell death.

KEYWORDS

***TAp73*, mammary epithelial cells, cell death, ferroptosis, proliferation**

Introduction

The mammary ducts, comprising two main cell populations—basal and luminal cells—the mammary gland undergoes dynamic structural remodeling throughout

the lactation cycle. In late pregnancy, luminal progenitors differentiate terminally to form secretory alveoli, which are specialized for milk biosynthesis and secretion (Macias and Hinck, 2012). Thus, understanding the dynamic development of mammary epithelial cells is crucial.

Previous studies have underscored the significance of specific genetic factors in mammary gland development. Zhang et al. established that conditional deletion of *TAp73* – the transcriptionally active isoform encoded by the *TP73* gene – in murine mammary epithelia disrupts alveolar morphogenesis. Notably, genetic ablation of the oncogenic Δ*Np73* isoform rescues morphological defects arising from PUMA or p21 deficiency, revealing an antagonistic interplay between *p73* isoforms during alveologenesis (Zhang et al., 2015). Yan et al. further reported that *TAp73* knockdown results in irregular, non-cavitary alveoli and induces epithelial-mesenchymal transition by modulating the expression of E-cadherin, β-catenin, and laminin (Zhang et al., 2012). These findings highlight the necessity of *p73* for normal mammary gland development.

Ferroptosis, an iron-dependent regulated cell death pathway driven by lipid peroxidation, has emerged as a key determinant of tissue homeostasis and disease pathogenesis (Dixon et al., 2012; Li et al., 2020). This process can be triggered by various factors and involves multiple signaling pathways. For instance, the inhibition of GPX4 activity reduces cellular antioxidant capacity, leading to increased intracellular ROS and the onset of ferroptosis (Ursini and Maiorino, 2020). However, it is still rarely reported whether mammary epithelial cells can undergo ferroptosis.

Central to this regulatory network, p53 acts as a key ferroptosis sensitizer by transcriptionally repressing SLC7A11, the cystine/glutamate antiporter, leading to glutathione depletion and facilitating lethal lipid peroxidation (Jiang et al., 2015). Structurally homologous to *p53*, *p73* participates in overlapping molecular networks governing proliferation and death, yet exhibits distinct context-dependent functionalities (Lokshin et al., 2007; Jost et al., 1997). The diverse isoforms of *p73*, resulting from selective promoter usage and alternative splicing, include *TAp73*, which exerts tumor-suppressive effects, and *ΔNp73*, which has oncogenic properties (Irwin et al., 2003). Research indicates that *TAp73* can induce ferroptosis in lung cancer cells by suppressing CDO1 expression, leading to increased ROS accumulation (Zhang et al., 2023). This functional conservation, coupled with mammary-specific *p73* expression patterns, strongly implicates p73 isoforms as putative modulators of ferroptotic signaling in lactating epithelia.

Although previous studies have focused on human mammary epithelial cells, our study employs bovine mammary epithelial cells (BMECs) as a model to investigate p73-mediated ferroptosis and proliferation. BMECs serve as a valuable model due to their physiological relevance in lactation biology and mammary gland development in livestock, which has direct implications for dairy production and animal health. Additionally, bovine models provide unique insights into mammary gland function in species with extended lactation cycles, making them particularly relevant for studying long-term epithelial cell dynamics.

Our study aims to investigate, for the first time, whether *TAp73* can regulate both the proliferation and ferroptosis of BMECs. By exploring the expression changes of ferroptosis-related genes and assessing cell proliferation and death under conditions of *TAp73* ectopic expression and knockdown, we seek to elucidate the role of *TAp73* in these fundamental cellular processes. This research could provide novel insights into the molecular mechanisms governing mammary gland development and function.

Materials and methods

Cell culture

The Bovine mammary epithelial cell line (BMECs, MAC-T), provided by Dr. Chunlei Zhang of Jiangsu Normal University (Xuzhou, China), was cultured in DMEM/F12 medium (Gibco, CA, United States) supplemented with 10% fetal bovine serum (FBS, Gibco, CA, United States). Cells were maintained at 37°C in a 5% CO_2 incubator. The cells were grown in T-75 cell culture flasks until they reached 70%–80% confluence and were sub-cultured using a 0.25% trypsin/EDTA solution (Gibco, CA, United States). For all experiments, cells from passages 5–6 were used to ensure consistency and optimal cell viability. Cell viability was assessed routinely using the Trypan Blue exclusion method, with viability consistently maintained above 95%. The culture duration for each experiment was approximately 24–48 h, depending on the experimental design. Additional culture conditions, such as media changes every 24–48 h, were strictly followed to ensure cell health and experimental reproducibility.

Plasmid construction

To overexpress TAp73, we engineered a mammalian expression vector, pcDNA3.1-TAp73, by subcloning the full-length bovine TAp73 cDNA, obtained from TSINGKE (China), into the pcDNA3.1 vector (Invitrogen, Shanghai, China).

Cell transfection

The TAp73 ectopic expression plasmid (pcDNA3.1-TAp73) or TAp73-targeting siRNA (final concentration of 20 nM) was transfected into cells using Lipofectamine 3000 (Invitrogen, Carlsbad, CA), following the manufacturer's instructions. Empty pcDNA3.1 vector and scrambled siRNA were used as respective controls. For ectopic expression experiments, cells were transfected with 2 μg of plasmid DNA per well and harvested 24 h post-transfection. In siRNA-mediated knockdown experiments, cells were maintained for 72 h, with the medium replaced every 24 h. To assess transfection efficiency, TAp73 mRNA levels were quantified by qRT-PCR, demonstrating over a 100-fold induction in the ectopic expression group and approximately 50% knockdown in siRNA-treated cells compared to controls. Furthermore, successful transfection was validated by analyzing p21 mRNA expression via qRT-PCR, as p21 is a well-established transcriptional target of TAp73.

Real-time quantitative PCR analysis

Total RNA was isolated from BEMCs using TRIzol reagent (Aidlab, Beijing, China) and quantified with a NanoDrop 2000

spectrophotometer (Thermo Scientific, Wilmington, DE, United States). After treating with DNase I to eliminate genomic DNA, cDNA synthesis was conducted using the PrimeScript RT Master Mix kit (Vazyme, Nanjing, China). RT-qPCR was then carried out on a ForeQuant F4 Sequence detection system with SYBR® Premix Ex Taq™ (Foregene, Chengdu, China). The PCR cycling protocol included an initial step at 95°C for 10 min, followed by 40 cycles at 95°C for 10 s and 60°C for 40 s, during which fluorescence signals were collected. All primer sequences can be found in Table 1. The expression levels of the genes were normalized to glyceraldehyde-3-phosphate dehydrogenase (GAPDH) and beta-actin (β-actin) and calculated using the $2^{-\Delta\Delta CT}$ method (Livak and Schmittgen, 2001).

5-Ethynyl-2′-deoxyuridine (EdU) assay

Cell proliferation was assessed using the BeyoClick™ EdU Cell Proliferation Kit with Alexa Fluor 555 (Beyotime, China). Cells were seeded in a 12-well plate and incubated with EdU working solution (1:1000 dilution) for 1 h at 37°C in a humidified atmosphere with 5% CO_2. After incubation, cells were fixed with methanol for 15 min and permeabilized with 0.5% Triton X-100 for 5 min. They were then incubated with Click reaction solution for 30 min and stained with DAPI for 10 min. Images were captured from at least 12 random fields per group using an Olympus IX73 microscope (Olympus, Tokyo, Japan). Cell counting was conducted using ImageJ software.

Colony formation assay

Control and pcDNA3.1-TAp7α or si-TAp73 cells were seeded in six-well plates (approximately 1000 cells per well, in triplicate) and cultured for 2 weeks. Colonies were fixed with a methanol/glacial acetic acid solution (7:1) and stained with crystal violet. Colony density was quantified using ImageJ software with the ColonyArea plugin, as described previously (Guzman et al., 2014).

Measurement of ROS levels

Reactive oxygen species (ROS) levels were measured using a commercially available ROS detection kit (Beyotime, China), following the manufacturer's instructions. Treated cells were incubated with the fluorescent probe DCFH-DA (1:1000 dilution) at 37°C for 30 min. Cells were then fixed with 4% paraformaldehyde for 10 min, washed three times with PBS, and stained with DAPI for 10 min. The stained cells were visualized under an Olympus IX73 microscope (Olympus, Tokyo, Japan).

CCK-8 assay

BMECs were seeded in 96-well plates and treated with RSL3. After the treatment, 10 μL of CCK-8 solution (Solarbio Life Sciences, Beijing, China) was added to each well, and the plates were incubated for 2 h. The optical density (OD) at 450 nm was measured using a Varioskan LUX spectrophotometer (Thermo Scientific, Waltham, MA, United States). The half-maximal inhibitory concentration (IC50) of RSL3 was then determined based on the CCK-8 assay results.

TABLE 1 Primer sequences.

Primer name	Sequence
GAPDH	GCGCCAAGAGGGTCATCATCTCTG CATAAGTCCCTCCACGATGCCAAAG
β-actin	GCCCATCTATGAGGGGTACGC CTCCTTGATGTCACGGACGATTTC
TFRC	TTGGATTTATGATTGGCTACTTGGG AATATGCGAGGTACTCCAGGGAGTTG
PTGS2	TCTTCCTCCTGTGCCTGATGACTGC ACATCAGATTTGTGCCCTGGGGATC
p73	ACCTCATCCGTGTGGAGGGCAAC CACCTGTCCGTCCCGTGTCTCC

LDH content

BMECs were treated with RSL3 for 24 h, while the control group received DMSO treatment. After incubation, the supernatant was collected by centrifugation at 1,000 g for 5 min, and lactate dehydrogenase (LDH) levels were measured using an LDH cytotoxicity assay kit (Solarbio Life Sciences, Beijing, China).

Statistical analysis

Data are presented as mean ± standard deviation (SD). For each experiment, the sample size is explicitly stated in the figure legends. Each experiment was repeated independently at least three times to ensure reproducibility. Normality of data distribution was assessed using the Shapiro-Wilk test. For comparisons between two groups, the student's t-test was applied when data met assumptions of normality and homogeneity of variance; For comparisons among more than two groups, one-way analysis of variance (ANOVA) with Tukey's *post hoc* test was performed for normally distributed data. Statistical significance was defined as $p < 0.05$. All analyses were conducted using SPSS 17.0 statistical software.

Results

Ectopic expression of TAp73 can inhibit BMECs proliferation

To investigate whether TAp73 can regulate BMECs, we ectopic expressionTAp73 and quantified its canonical transcriptional target p21 (Figure 1A). Our findings revealed that TAp73 significantly upregulates p21 expression (Figure 1B) ($p < 0.05$). Following this, we conducted colony formation and EdU assays to examine the effects on cell proliferation. The results showed that the colony formation assay demonstrated a substantial decrease in colony numbers in TAp73-overexpressing cells compared to control cells, indicating inhibited cell growth (Figure 1C). Similarly, the EdU assay, which measures DNA synthesis as an indicator of cell proliferation, showed a significant reduction in the number of proliferating cells upon TAp73 ectopic expression (Figures 1D,E). These findings collectively support the role of TAp73 in modulating cell cycle progression and proliferation in BMECs, highlighting its potential as a key regulatory factor in these cells.

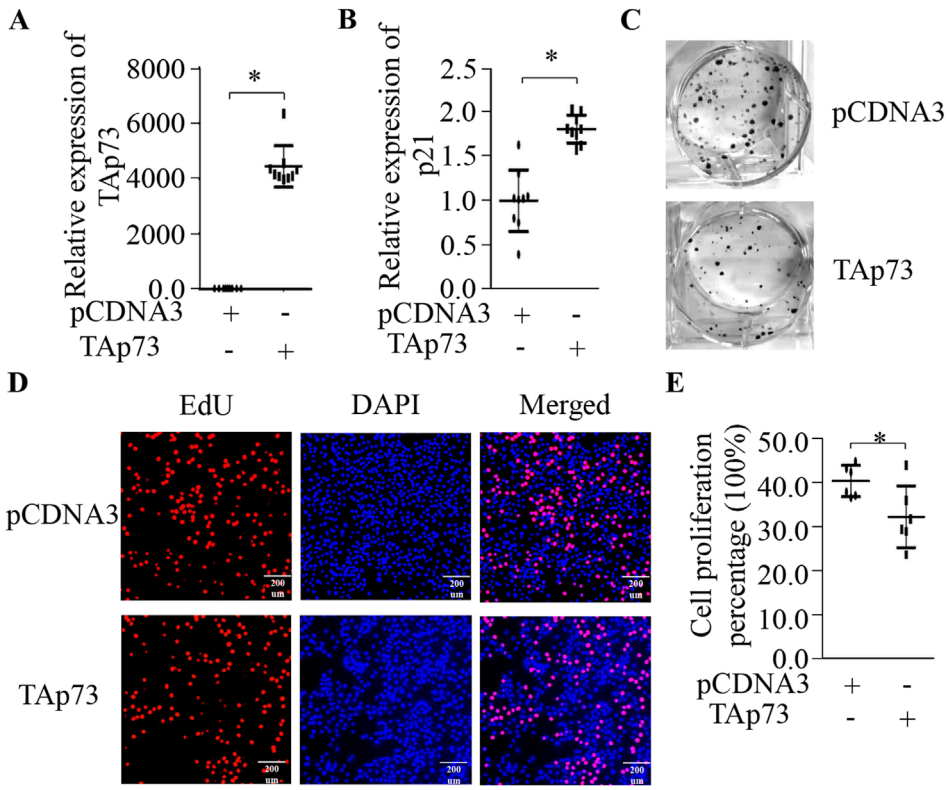

FIGURE 1
Effect of ectopic expression of TAp73 on BMECs proliferation. **(A)** Relative expression levels of TAp73 in BMECs following TAp73 plasmid transfection. **(B)** Relative expression levels of p21 in BMECs following TAp73 plasmid transfection **(C)** A colony formation assay was performed following TAp73 plasmid transfection. **(D, E)** EdU assay was performed following TAp73 plasmid transfection. Three biological replicates and three technical replicates were performed for the qPCR analysis. The colony formation and EdU assays were conducted with six replicates. Data are presented as mean ± SD.*$p < 0.05$.

Knock-down TAp73 can accelerates BMECs proliferation

To further validate the influence of TAp73 on BMECs proliferation, we performed transfection with TAp73 siRNA to suppress the expression of endogenous TAp73. RNAi-mediated TAp73 silencing (confirmed in Figure 2A, $p < 0.05$) reduced p21 expression ($p < 0.05$; Figure 2B), attenuating cell cycle constraints. We then conducted colony formation and EdU assays to assess the effects on cell proliferation. The colony formation assay showed a substantial increase in colony numbers in TAp73 knockdown cells compared to control cells, indicating promoted cell growth (Figure 2C). Similarly, the EdU assay demonstrated a significant increase in the number of proliferating cells upon TAp73 knockdown (Figures 2D,E). These findings further emphasize the role of TAp73 in modulating cell cycle progression and proliferation in BMECs, underscoring its potential as a key regulatory factor in these cells.

BMECs can induce ferroptosis

To explore the potential for ferroptosis in BMECs, we treated these cells with the classical ferroptosis inducer, RSL3. Our results demonstrated a dose-dependent increase in cell death following RSL3 treatment (Figure 3A). Notably, RSL3 treatment led to a significant, dose-dependent release of LDH, further confirming cell death (Figure 3B). The IC50 value for RSL3 in BMECs was calculated to be 6.315 μM (Supplementary Figure S1A). Additionally, there was a corresponding dose-dependent accumulation of reactive oxygen species (ROS) within the cells (Figure 3C), indicating that BMECs can undergo ferroptosis when induced by RSL3. Additionally, we assessed the expression of ferroptosis-related genes PTGS2 and TRFC, observing a significant elevation in their expression levels post-RSL3 treatment (Figures 3D,E) ($p < 0.05$). These findings collectively suggest that BMECs are capable of undergoing ferroptosis.

TAp73 is involved in the regulation of ferroptosis in BMECs

To explore whether TAp73 can regulate ferroptosis in BMECs, we first examined the expression of ferroptosis-related genes. Our findings revealed that ectopic expression of TAp73 significantly promotes the expression of PTGS2 and TRFC, which are key genes involved in the ferroptosis pathway (Figures 4A,B). This suggests that TAp73 might enhance the susceptibility of BMECs to ferroptosis. Conversely, knockdown of TAp73 resulted in a marked decrease in the expression levels of PTGS2 and TRFC (Figures 4C,D) ($p < 0.05$), indicating a potential protective effect

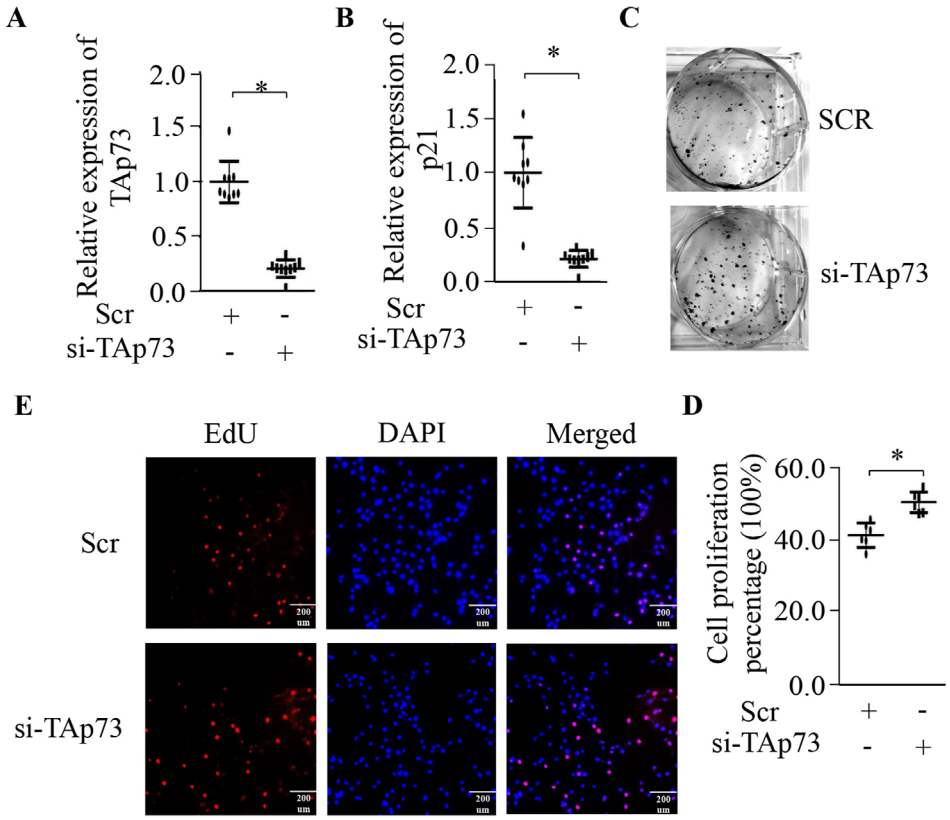

FIGURE 2
Effect of knockdown of TAp73 on BMECs proliferation. **(A)** Relative expression levels of TAp73 in BMECs following TAp73 siRNA transfection. **(B)** Relative expression levels of p21 in BMECs following TAp73 siRNA transfection. **(C)** A colony formation assay was performed following TAp73 siRNA transfection. **(D, E)** EdU assay was performed following TAp73 siRNA transfection. Three biological replicates and three technical replicates were performed for the qPCR analysis. The colony formation and EdU assays were conducted with six replicates. Data are presented as mean ± SD.*$p < 0.05$.

against ferroptosis. To further validate the role of TAp73 in ferroptosis, we treated BMECs with the ferroptosis inducer RSL3 while simultaneously knocking down TAp73 expression. The results demonstrated that TAp73 knockdown significantly attenuated RSL3-induced ferroptosis, as evidenced by reduced cell death and a decrease in ROS accumulation (Figures 3E,F). This indicates that TAp73 knockdown can mitigate the oxidative stress and cellular damage typically associated with ferroptosis. Additionally, the reduction in ROS levels upon TAp73 knockdown was accompanied by decreased lipid peroxidation. Further supporting the role of TAp73 in regulating ferroptosis in BMECs.

Discussion

Our investigation into the role of p73, a member of the p53 family, in regulating BMECs revealed significant insights. The TP73 gene encodes two functionally antagonistic isoforms, *TAp73* and *ΔNp73*, which are produced through alternative promoter usage and C-terminal splicing (Rufini et al., 2011). Functionally divergent, these isoforms govern opposing cellular outcomes: *TAp73*, a transcriptionally active p53 homolog mediating cell cycle arrest, whereas ΔNp73 acts as a dominant-negative regulator over TAp73, possessing its own distinct transcriptional activities (Jost et al., 1997; Irwin et al., 2003). Known for its dual role in tumor suppression and promotion, p73 is also critical in the development and differentiation of specific tissues and organs, such as neuronal differentiation, the development of the central nervous and olfactory systems, and is highly expressed in airway ciliated columnar cells and the myoepithelial and basal cells of the salivary gland (Rufini et al., 2011; Yang et al., 2000; Lee et al., 2007).

Previous studies have highlighted *TAp73*'s necessity for proper mammary epithelial acinar formation and its ability to suppress cell migration and invasion by regulating the expression of E-cadherin and other epithelial-mesenchymal transition (EMT) markers (Zhang et al., 2012). To interrogate its functional role in BMECs, we employed gain- and loss-of-function approaches targeting *TAp73*. Our findings showed that ectopic expression of *TAp73* significantly upregulates *p21* expression (Figure 1B) ($p < 0.05$). This upregulation was associated with a substantial decrease in colony formation and a significant reduction in DNA synthesis, as demonstrated by the EdU assay (Figures 1C–E). These results suggest that *TAp73* inhibits cell proliferation in BMECs, highlighting its potential as a key regulatory factor. Conversely, RNAi-mediated *TAp73* silencing suppressed *p21* expression (Figure 2B) ($p < 0.05$). The colony formation assay showed a substantial increase in colony numbers, and the EdU assay demonstrated a significant increase in the number of proliferating cells upon *TAp73* knockdown, indicating promoted

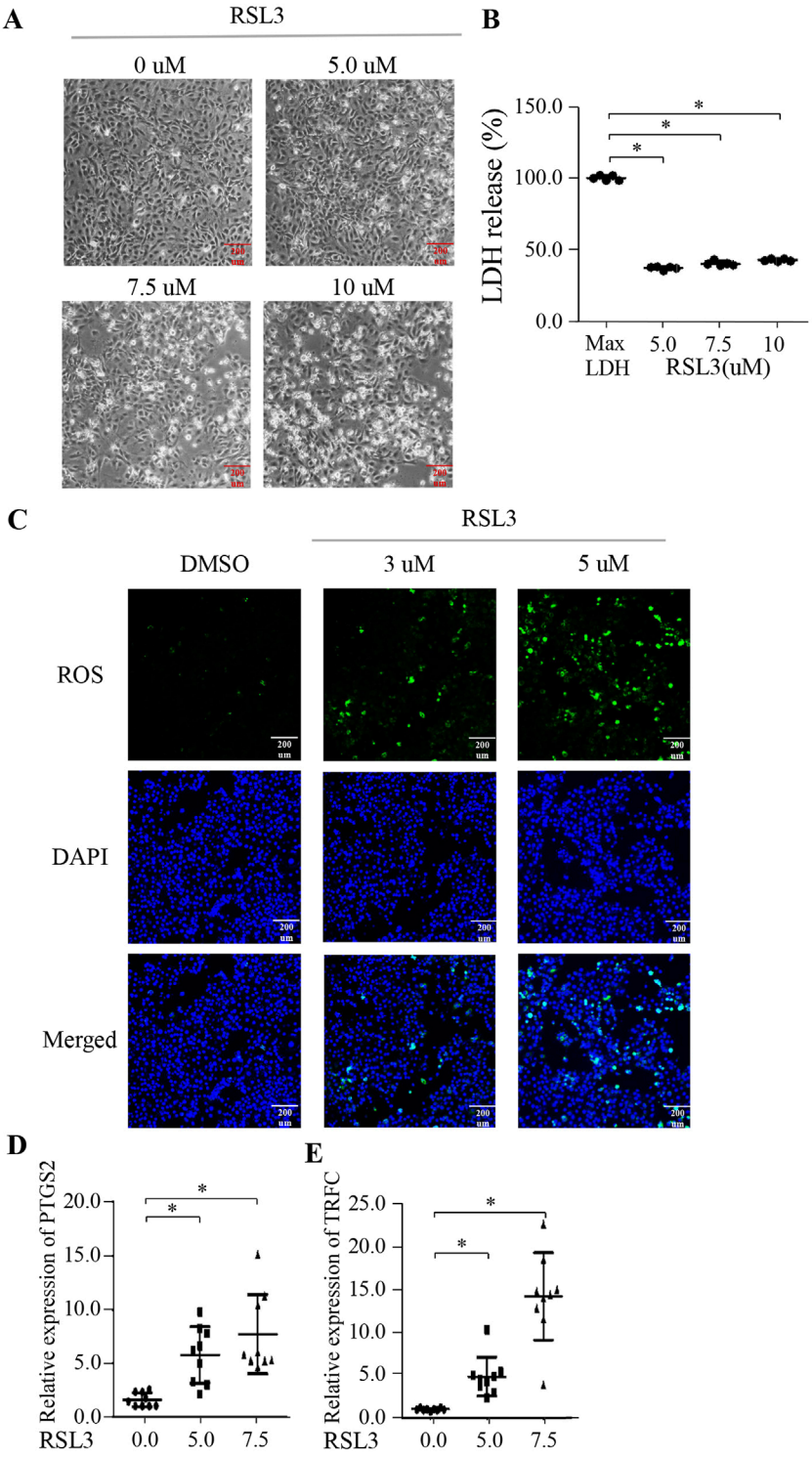

FIGURE 3
BMECs can undergo ferroptosis. **(A)** BMECs were treated with various concentrations of RSL3 (0, 5, 7.5, 10 μM) for 24 h, and representative microscopic images were taken to show cell morphology. **(B)** LDH content of BMECs cells treated with RSL3 (0, 5, 7.5, 10 μM) for 24 h. **(C)** Intracellular ROS levels were measured using the fluorescent probe DCFH-DA in BMECs cells treated with RSL3 (0, 3, 5 μM) for 24 h. **(D, E)** Relative expression levels of PTGS2 and TRFC in BMECs cells treated with RSL3 (0, 5, 7.5 μM) for 24 h. Three biological replicates and three technical replicates were performed for the qPCR analysis. The LDH, colony formation, and EdU assays were conducted with six biological replicates each. Data are presented as mean ± SD.*p < 0.05.

cell growth (Figures 2C–E). These findings further emphasize *TAp73*'s role in modulating cell cycle progression and proliferation in BMECs, underscoring its importance as a regulatory factor.

Ferroptosis, an iron-catalyzed form of regulated cell death driven by lethal lipid peroxidation (Ursini and Maiorino, 2020; Yang and Stockwell, 2016), has emerged as a pivotal mechanism

10.3389/fcell.2025.1532910

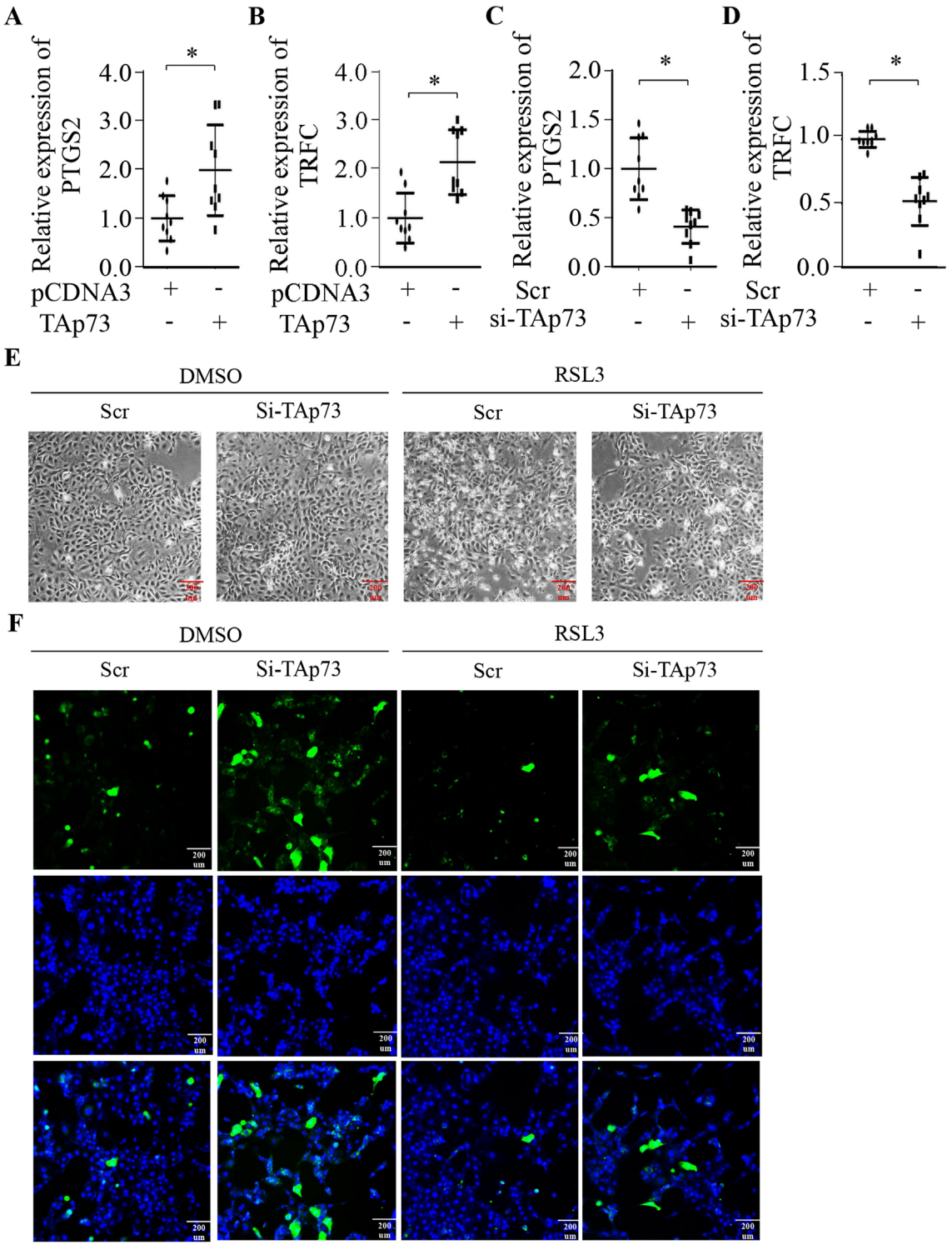

FIGURE 4
TAp73 is Involved in the Regulation of Ferroptosis in BEMCs. **(A, B)** Relative expression levels of PTGS2, and TRFC in BEMCs following TAp73 plasmid transfection. **(C, D)** Relative expression levels of PTGS2 and TRFC in BEMCs cells following si-TAp73 transfection. **(E)** BEMCs cells were treated with RSL3, si-TAp73, or their combination, and representative microscopic images were taken to show cell morphology. **(F)** Intracellular ROS levels were measured using the fluorescent probe DCFH-DA in BEMCs cells treated with RSL3, si-TAp73, or their combination. Three biological replicates and three technical replicates were employed in the qPCR analysis to ensure data reliability and reproducibility. Data are presented as mean ± SD.*$p < 0.05$.

implicated in various physiological and pathological processes, including cancer, neurodegeneration, and ischemia-reperfusion injury (Lei et al., 2022; Vitalakumar et al., 2021; Zhao et al., 2021). At the core of ferroptosis execution is the inactivation of glutathione peroxidase 4 (GPX4), which disrupts redox homeostasis by allowing lipid peroxide accumulation through Fenton chemistry (Shimada et al., 2016), ultimately culminating in membrane rupture and lytic cell death (Seibt et al., 2019). Although extensively studied in other cell types, the occurrence of ferroptosis in bovine mammary epithelial cells rarely explored.

Our study aimed to explore the potential for ferroptosis in BMECs by treating these cells with the classical ferroptosis inducer, RSL3 (Shintoku et al., 2017). The results demonstrated a dose-dependent increase in cell death following RSL3 treatment, indicating that BMECs are susceptible to ferroptosis induction. This was further supported by the corresponding dose-dependent accumulation of ROS within the cells, a hallmark of ferroptosis. Consistent with ferroptosis biomarkers, RSL3 treatment significantly upregulated PTGS2, a sensor of lipid peroxides, and TFRC, a key regulator of iron uptake (Chen et al., 2021; Feng et al., 2020), further confirming the occurrence of ferroptosis in BMECs. These findings collectively suggest that BMECs are capable of undergoing ferroptosis when exposed to appropriate inducers like RSL3. The ability of BMECs to undergo ferroptosis expands our understanding of the cellular responses in mammary epithelial cells and highlights the potential implications for dairy cow health.

Having established BMECs' ferroptotic susceptibility, we next interrogated whether TAp73 modulates this death pathway. Given its dual role in oxidative stress responses and cell fate determination, we hypothesized that TAp73 acts as a ferroptosis rheostat in mammary epithelia. TAp73 gain-of-function robustly upregulated PTGS2and TFRC ($p < 0.05$; Figures 4A,B), priming cells for lipid peroxidation. Conversely, TAp73 loss-of-function suppressed both markers (Figures 4C,D), attenuating ferroptotic priming. The increased expression of PTGS2 and TRFC in *TAp73*-overexpressing cells indicates a heightened state of oxidative stress and lipid peroxidation, which are hallmarks of ferroptosis. Conversely, knocking down *TAp73* resulted in a marked reduction in the expression levels of these ferroptosis-related genes, highlighting a potential protective role against ferroptosis. This downregulation of PTGS2 and TRFC suggests that the absence of *TAp73* may help maintain cellular homeostasis by mitigating oxidative stress and preventing the accumulation of toxic lipid peroxides. The observed decrease in these gene expressions upon *TAp73* knockdown underscores the importance of *TAp73* in the ferroptosis process. To further substantiate the involvement of *TAp73* in ferroptosis, we conducted experiments where BMECs were treated with the ferroptosis inducer RSL3 while simultaneously knocking down *TAp73* expression. The results were compelling: *TAp73* knockdown significantly alleviated RSL3-induced ferroptosis, as evidenced by a notable reduction in cell death and a decrease in ROS accumulation. This indicates that *TAp73* knockdown can effectively mitigate the oxidative stress and cellular damage typically associated with ferroptosis, thereby conferring a protective effect against this form of cell death. Moreover, the reduction in ROS levels observed upon *TAp73* knockdown was accompanied by decreased lipid peroxidation, further supporting the role of *TAp73* in regulating ferroptosis. The attenuation of lipid peroxidation is particularly significant, as it underscores the mechanism by which *TAp73* influences ferroptosis: by modulating the cellular oxidative state and lipid metabolism. These findings collectively highlight *TAp73* as a key regulatory factor in ferroptosis, modulating the susceptibility of BMECs to oxidative stress and lipid peroxidation.

Conclusion

This study underscores the critical role of *TAp73* in regulating both proliferation and ferroptosis in BMECs. Ectopic expression of *TAp73* significantly reducing cell proliferation, while *TAp73* knockdown increased cell growth. We confirmed that BMECs can undergo ferroptosis when treated with RSL3, with dose-dependent increases in cell death and ROS accumulation. Notably, *TAp73* modulates this process: its ectopic expression enhanced PTGS2 and TRFC expression, increasing susceptibility to ferroptosis, while its knockdown mitigated these effects, reducing oxidative stress and lipid peroxidation. These findings highlight *TAp73*'s dual regulatory role in BMECs, impacting both cell proliferation and ferroptosis. Understanding these mechanisms offers new therapeutic strategies for managing oxidative stress and enhancing dairy cow health and productivity.

Data availability statement

The original contributions presented in the study are included in the article/Supplementary Material, further inquiries can be directed to the corresponding author.

Ethics statement

Ethical approval was not required for the studies on animals in accordance with the local legislation and institutional requirements because only commercially available established cell lines were used.

Author contributions

WS: Conceptualization, Funding acquisition, Project administration, Supervision, Writing–original draft. HR: Data curation, Methodology, Software, Validation, Writing–original draft. LC: Data curation, Methodology, Software, Validation, Writing–review and editing. BZ: Data curation, Methodology, Software, Validation, Writing–review and editing. LM: Data curation, Methodology, Software, Validation, Writing–review and editing. JW: Data curation, Methodology, Software, Validation, Writing–review and editing. YZ: Data curation, Methodology, Software, Validation, Writing–review and editing. JL: Data curation, Methodology, Software, Validation, Writing–review and editing. YY: Data curation, Methodology, Software, Validation, Writing–review and editing. SL: Funding acquisition, Project administration, Supervision, Writing–review and editing.

Funding

The author(s) declare that financial support was received for the research and/or publication of this article. This research was

funded by National Natural Science Foundation of China Youth Science Foundation Project (32202670); The 74th Batch of General Grants for Postdoctoral Researchers in China (2023M742516); Sichuan innovation team of national modern agricultural industry technology system (SCCXTD-2023-13); Ya'an City Establishes National Modern Agriculture Industry Technology Innovation Center "Leading the Charge" Project (kczx2023-2025-02); College Student Innovation and Entrepreneurship Training Program (S202410626073).

Conflict of interest

The authors declare that the research was conducted in the absence of any commercial or financial relationships that could be construed as a potential conflict of interest.

Generative AI statement

The authors declare that Gen AI was used in the creation of this manuscript. During the preparation of this work we used ChatGPT in order to improve the readability and language of the manuscript. After using this tool/service, we reviewed and edited the content as needed and take full responsibility for the content of the published article.

Publisher's note

All claims expressed in this article are solely those of the authors and do not necessarily represent those of their affiliated organizations, or those of the publisher, the editors and the reviewers. Any product that may be evaluated in this article, or claim that may be made by its manufacturer, is not guaranteed or endorsed by the publisher.

Supplementary material

The Supplementary Material for this article can be found online at: https://www.frontiersin.org/articles/10.3389/fcell.2025.1532910/full#supplementary-material

References

Chen, X., Comish, P. B., Tang, D., and Kang, R. (2021). Characteristics and biomarkers of ferroptosis. *Front. Cell. Dev. Biol.* 9, 637162. Epub 2021/02/09. doi:10.3389/fcell.2021.637162

Dixon, S. J., Lemberg, K. M., Lamprecht, M. R., Skouta, R., Zaitsev, E. M., Gleason, C. E., et al. (2012). Ferroptosis: an iron-dependent form of nonapoptotic cell death. *Cell.* 149 (5), 1060–1072. Epub 2012/05/29. doi:10.1016/j.cell.2012.03.042

Feng, H., Schorpp, K., Jin, J., Yozwiak, C. E., Hoffstrom, B. G., Decker, A. M., et al. (2020). Transferrin receptor is a specific ferroptosis marker. *Cell. Rep.* 30 (10), 3411–3423. doi:10.1016/j.celrep.2020.02.049

Guzman, C., Bagga, M., Kaur, A., Westermarck, J., and Abankwa, D. (2014). Colonyarea: an imagej plugin to automatically quantify colony formation in clonogenic assays. *PLoS One* 9 (3), e92444. Epub 2014/03/22. doi:10.1371/journal.pone.0092444

Irwin, M. S., Kondo, K., Marin, M. C., Cheng, L. S., Hahn, W. C., and Kaelin, W. G., Jr (2003). Chemosensitivity linked to P73 function. *Cancer Cell.* 3 (4), 403–410. Epub 2003/05/03. doi:10.1016/s1535-6108(03)00078-3

Jiang, L., Kon, N., Li, T., Wang, S. J., Su, T., Hibshoosh, H., et al. (2015). Ferroptosis as a P53-mediated activity during tumour suppression. *Nature* 520 (7545), 57–62. Epub 2015/03/25. doi:10.1038/nature14344

Jost, C. A., Marin, M. C., and Jr, W. G. K. (1997). P73 is a human P53-related protein that can induce apoptosis. *Nature* 389 (6647), 191–194. doi:10.1038/38298

Lee, Y., Miron, A., Drapkin, R., Nucci, M., Medeiros, F., Saleemuddin, A., et al. (2007). A candidate precursor to serous carcinoma that originates in the distal fallopian tube. *J. Pathology A J. Pathological Soc. G. B. Irel.* 211 (1), 26–35. doi:10.1002/path.2091

Lei, G., Zhuang, L., and Gan, B. (2022). Targeting ferroptosis as a vulnerability in cancer. *Nat. Rev. Cancer* 22 (7), 381–396. doi:10.1038/s41568-022-00459-0

Li, J., Cao, F., Yin, H. L., Huang, Z. J., Lin, Z. T., Mao, N., et al. (2020). Ferroptosis: past, present and future. *Cell. Death Dis.* 11 (2), 88. Epub 2020/02/06. doi:10.1038/s41419-020-2298-2

Livak, K. J., and Schmittgen, T. D. (2001). Analysis of relative gene expression data using real-time quantitative pcr and the 2(-delta delta C(T)) method. *Methods* 25 (4), 402–408. Epub 2002/02/16. doi:10.1006/meth.2001.1262

Lokshin, M., Li, Y., Gaiddon, C., and Prives, C. (2007). P53 and P73 display common and distinct requirements for sequence specific binding to DNA. *Nucleic Acids Res.* 35 (1), 340–352. Epub 2006/12/16. doi:10.1093/nar/gkl1047

Macias, H., and Hinck, L. (2012). Mammary gland development. *Wiley Interdiscip. Rev. Dev. Biol.* 1 (4), 533–557. Epub 2012/07/31. doi:10.1002/wdev.35

Rufini, A., Agostini, M., Grespi, F., Tomasini, R., Sayan, B. S., Niklison-Chirou, M. V., et al. (2011). P73 in cancer. *Genes. Cancer* 2 (4), 491–502. Epub 2011/07/23. doi:10.1177/1947601911408890

Seibt, T. M., Proneth, B., and Conrad, M. (2019). Role of Gpx4 in ferroptosis and its pharmacological implication. *Free Radic. Biol. Med.* 133, 144–152. Epub 2018/09/17. doi:10.1016/j.freeradbiomed.2018.09.014

Shimada, K., Skouta, R., Kaplan, A., Yang, W. S., Hayano, M., Dixon, S. J., et al. (2016). Global survey of cell death mechanisms reveals metabolic regulation of ferroptosis. *Nat. Chem. Biol.* 12 (7), 497–503. Epub 2016/05/10. doi:10.1038/nchembio.2079

Shintoku, R., Takigawa, Y., Yamada, K., Kubota, C., Yoshimoto, Y., Takeuchi, T., et al. (2017). Lipoxygenase-mediated generation of lipid peroxides enhances ferroptosis induced by erastin and Rsl3. *Cancer Sci.* 108 (11), 2187–2194. Epub 2017/08/25. doi:10.1111/cas.13380

Ursini, F., and Maiorino, M. (2020). Lipid peroxidation and ferroptosis: the role of gsh and Gpx4. *Free Radic. Biol. Med.* 152, 175–185. Epub 2020/03/14. doi:10.1016/j.freeradbiomed.2020.02.027

Vitalakumar, D., Sharma, A., and Flora, S. J. S. (2021). Ferroptosis: a potential therapeutic target for neurodegenerative diseases. *J. Biochem. Mol. Toxicol.* 35 (8), e22830. Epub 2021/05/29. doi:10.1002/jbt.22830

Yang, A., Walker, N., Bronson, R., Kaghad, M., Oosterwegel, M., Bonnin, J., et al. (2000). P73-Deficient mice have neurological, pheromonal and inflammatory defects but lack spontaneous tumours. *Nature* 404 (6773), 99–103. doi:10.1038/35003607

Yang, W. S., and Stockwell, B. R. (2016). Ferroptosis: death by lipid peroxidation. *Trends Cell. Biol.* 26 (3), 165–176. Epub 2015/12/15. doi:10.1016/j.tcb.2015.10.014

Zhang, J., Sun, W., Yan, W., Kong, X., Shen, T., Laubach, K., et al. (2023). Tp73 isoform-specific disruption reveals a critical role of Tap73beta in growth suppression and inflammatory response. *Cell. Death Dis.* 14 (1), 14. Epub 2023/01/12. doi:10.1038/s41419-022-05529-7

Zhang, Y., Yan, W., Jung, Y. S., and Chen, X. (2012). Mammary epithelial cell polarity is regulated differentially by P73 isoforms via epithelial-to-mesenchymal transition. *J. Biol. Chem.* 287 (21), 17746–17753. Epub 2012/03/30. doi:10.1074/jbc.M112.358143

Zhang, Y., Young, A., Zhang, J., and Chen, X. (2015). P73 tumor suppressor and its targets, P21 and puma, are required for madin-darby canine kidney cell morphogenesis by maintaining an appropriate level of epithelial to mesenchymal transition. *Oncotarget* 6 (16), 13994–14004. Epub 2015/06/24. doi:10.18632/oncotarget.4374

Zhao, W. K., Zhou, Y., Xu, T. T., and Wu, Q. (2021). Ferroptosis: opportunities and challenges in myocardial ischemia-reperfusion injury. *Oxid. Med. Cell. Longev.* 2021, 9929687. Epub 2021/11/03. doi:10.1155/2021/9929687

Frontiers in
Cell and Developmental Biology

Explores the fundamental biological processes of life, covering intracellular and extracellular dynamics.

The world's most cited developmental biology journal, advancing our understanding of the fundamental processes of life. It explores a wide spectrum of cell and developmental biology, covering intracellular and extracellular dynamics.

Discover the latest Research Topics

See more →

Frontiers

Avenue du Tribunal-Fédéral 34
1005 Lausanne, Switzerland
frontiersin.org

Contact us

+41 (0)21 510 17 00
frontiersin.org/about/contact